



World Journal of Gastroenterology®


Supported by NSFC
2005-2006

Volume 11 Number 5
February 7, 2005



National Journal Award

Contents

REVIEW	617	Current research of hepatic cirrhosis in China <i>Yao XX, Jiang SL, Yao DM</i>
GASTRIC CANCER	623	Increased expression of mitogen-activated protein kinase and its upstream regulating signal in human gastric cancer <i>Liang B, Wang S, Zhu XG, Yu YX, Cui ZR, Yu YZ</i>
	629	Expression of Epstein-Barr virus genes in EBV-associated gastric carcinomas <i>Luo B, Wang Y, Wang XF, Liang H, Yan LP, Huang BH, Zhao P</i>
	634	Selection of optimal antisense accessible sites of survivin and its application in treatment of gastric cancer <i>Tong QS, Zheng LD, Chen FM, Zeng FQ, Wang L, Dong JH, Lu GC</i>
	641	Quantitative assessment model for gastric cancer screening <i>Chen K, Yu WP, Song L, Zhu YM</i>
COLORECTAL CANCER	645	Cytokeratins and carcinoembryonic antigen in diagnosis, staging and prognosis of colorectal adenocarcinoma <i>Fernandes LC, Kim SB, Matos D</i>
VIRAL HEPATITIS	649	<i>In vitro</i> resistance to interferon of hepatitis B virus with precore mutation <i>Wang Y, Wei L, Jiang D, Cong X, Fei R, Xiao J, Wang Y</i>
BASIC RESEARCH	656	Inhibition of p38 mitogen-activated protein kinase may decrease intestinal epithelial cell apoptosis and improve intestinal epithelial barrier function after ischemia-reperfusion injury <i>Zheng SY, Fu XB, Xu JG, Zhao JY, Sun TZ, Chen W</i>
	661	Differences in platelet endothelial cell adhesion molecule-1 expression between peripheral circulation and pancreatic microcirculation in cerulein-induced acute edematous pancreatitis <i>Gao HK, Zhou ZG, Han FH, Chen YQ, Yan WW, He T, Wang C, Wang Z</i>
	665	Toxicity of novel anti-hepatitis drug bicyclol: A preclinical study <i>Liu GT, Li Y, Wei HL, Lu H, Zhang H, Gao YG, Wang LZ</i>
	672	Effects of unsaturated fatty acids on calcium-activated potassium current in gastric myocytes of guinea pigs <i>Zheng HF, Li XL, Jin ZY, Sun JB, Li ZL, Xu WX</i>
	676	Hepato-cardiovascular response and its regulation <i>Li XN, Benjamin IS, Alexander B</i>
CLINICAL RESEARCH	681	Association between polymorphisms in the Toll-like receptor 4, CD14, and <i>CARD15/NOD2</i> and inflammatory bowel disease in the Greek population <i>Gazouli M, Mantzaris G, Kotsinas A, Zacharatos P, Papalambros E, Archimandritis A, Ikonopoulos J, Gorgoulis VG</i>

Contents

- CLINICAL RESEARCH** 686 Ultrastructural changes in non-specific duodenitis
Wang CX, Liu LJ, Guan J, Zhao XL
- BRIEF REPORTS**
- 690 Heme oxygenase-1 alleviates ischemia/reperfusion injury in aged liver
Wang XH, Wang K, Zhang F, Li XC, Li J, De W, Guo J, Qian XF, Fan Y
- 695 Enhanced production of leptin in gastric fundic mucosa with *Helicobacter pylori* infection
Nishi Y, Isomoto H, Uotani S, Wen CY, Shikuwa S, Ohnita K, Mizuta Y, Kawaguchi A, Inoue K, Kohno S
- 700 Tumor vaccine against recurrence of hepatocellular carcinoma
Peng BG, Liang LJ, He Q, Kuang M, Lia JM, Lu MD, Huang JF
- 705 Tiam1 gene expression and its significance in colorectal carcinoma
Liu L, Wu DH, Ding YQ
- 708 Value of portal hemodynamics and hypersplenism in cirrhosis staging
Shi BM, Wang XY, Mu QL, Wu TH, Xu J
- 712 Existence and significance of hepatitis B virus DNA in kidneys of IgA nephropathy
Wang NS, Wu ZL, Zhang YE, Liao LT
- 717 Pharmacokinetics of C-1027 in mice as determined by TCA-RA method
Liu YP, Li QS, Huang YR, Zhou MJ, Liu CX
- 721 Correlation between expression of gastrin, somatostatin and cell apoptosis regulation gene bcl-2/bax in large intestine carcinoma
Mao JD, Wu P, Xia XH, Hu JQ, Huang WB, Xu GQ
- 726 Effect of mutated I κ B α transfection on multidrug resistance in hilar cholangiocarcinoma cell lines
Chen RF, Li ZH, Kong XH, Chen JS
- 729 Treatment of pancreatic pseudocysts in line with D'Egidio's classification
Zhang AB, Zheng SS
- 733 Effect of glutamate on inflammatory responses of intestine and brain after focal cerebral ischemia
Xu L, Sun J, Lu R, Ji Q, Xu JG
- 737 Effects of psychological stress on small intestinal motility and expression of cholecystokinin and vasoactive intestinal polypeptide in plasma and small intestine in mice
Cao SG, Wu WC, Han Z, Wang MY
- 741 Tumor angiogenesis and its clinical significance in pediatric malignant liver tumor
Sun XY, Wu ZD, Liao XF, Yuan JY
- 744 Association of cyclin D1, p16 and retinoblastoma protein expressions with prognosis and metastasis of gallbladder carcinoma
Ma HB, Hu HT, Di ZL, Wang ZR, Shi JS, Wang XJ, Li Y
- 748 Metastasis of primary gallbladder carcinoma in lymph node and liver
Lin HT, Liu GJ, Wu D, Lou JY
- 752 Role of PGI₂ in the formation and maintenance of hyperdynamic circulatory state of portal hypertensive rats
Wu ZY, Chen XS, Qiu JF, Cao H
- 756 Knockdown of survivin gene expression by RNAi induces apoptosis in human hepatocellular carcinoma cell line SMMC-7721
Cheng SQ, Wang WL, Yan W, Li QL, Wang L, Wang WY

Contents		<i>World Journal of Gastroenterology</i> [®] Volume 11 Number 5 February 7, 2005
BRIEF REPORTS	760	Effect of bone marrow-derived monocytes transfected with RNA of mouse colon carcinoma on specific antitumor immunity <i>Chu XY, Chen LB, Zang J, Wang JH, Zhang Q, Geng HC</i>
CASE REPORTS	764	Acquired hepatocerebral degeneration: A case report <i>Chen WX, Wang P, Yan SX, Li YM, Yu CH, Jiang LL</i>
	767	Hematemesis as the initial complication of pancreatic adenocarcinoma directly invading the duodenum: A case report <i>Lin YH, Chen CY, Chen CP, Kuo TY, Chang FY, Lee SD</i>
ACKNOWLEDGEMENTS	770	Acknowledgements to reviewers for this issue
APPENDIX	1A	Meetings
	2A	Instructions to authors
	4A	<i>World Journal of Gastroenterology</i> standard of quantities and units
FLYLEAF	I-V	Editorial Board
INSIDE FRONT COVER		ISI journal citation reports 2003-GASTROENTEROLOGY AND HEPATOLOGY
INSIDE BACK COVER		E-journal of <i>World Journal of Gastroenterology</i>

Editorial Coordinator for this issue: Michelle Gabbe, PhD

World Journal of Gastroenterology[®]
World J Gastroenterol
Weekly
Founded with a name of *China National Journal of New Gastroenterology* on October 1, 1995
Renamed as *World Journal of Gastroenterology* on January 25, 1998
Publication date February 7, 2005
President and Editor-in-Chief
Lian-Sheng Ma
Editor-in-Chief
Bo-Rong Pan
Managing Director
Jing-Yun Ma
Associate Managing Editor
Jian-Zhong Zhang, Shi-Yu Guo
Typesetter Meng Li
Proofreaders Hong Li, Shi-Yu Guo

Edited by Editorial Board of *World Journal of Gastroenterology*, PO Box 2345, Beijing 100023, China
Published jointly by The WJG Press and Elsevier Inc.
For inquiries regarding distribution of the material in China, please contact The WJG Press; for inquiries regarding distribution elsewhere, please contact Elsevier Inc.
Subscriptions
Domestic Local Post Offices Code No. BM 82-261
Foreign Elsevier (Singapore) Pte Ltd, 3 Killiney Road #08-01, Winsland House I, Singapore 239519
Telephone: +65-6349 0200 **Fax:** +65-6733 1817
E-mail: r.garcia@elsevier.com
<http://asia.elsevierhealth.com>
Personal Price: USD700.00
Institutional Price: USD1 500.00
Online Submissions
<http://www.wjgnet.com/wjg/index.jsp>
Telephone: +86-(0)10-85381901 **Fax:** +86-(0)10-85381893
E-mail: wjg@wjgnet.com <http://www.wjgnet.com>

Indexed and Abstracted in: *Index Medicus*, MEDLINE, PubMed, Chemical Abstracts, EMBASE, Abstracts Journals, *Nature Clinical Practice Gastroenterology and Hepatology*, CAB Abstracts and Global Health. **ISI JCR 2000-2003:** IF = 0.993, 1.445, 2.532 and 3.318 respectively. A total of 687 articles published in WJG were cited by 389 ISI/SCI-covered journals distributed in 39 countries during January 1998 - March 2004. Supported by the National Natural Science Foundation of China, No. 30224801; Certificate of the 100 Outstanding Academic Journals of China 2002, National Journal Award, Journal of the Statistic Source of Papers on Science and Technology of China and Key Journals of China Science and Technology.

ISSN 1007-9327 CN 14-1219/R
Copyright © 2005 The WJG Press and Elsevier Inc.

Special Statement All articles published in this journal represent the viewpoints of the authors except where indicated otherwise.

World Journal of Gastroenterology®

Editorial Board

2004-2006



Published by The WJG Press and Elsevier Inc., PO Box 2345, Beijing 100023, China
Fax: +86-(0)10-85381893 E-mail: wjg@wjgnet.com <http://www.wjgnet.com>

HONORARY EDITORS-IN-CHIEF

Ke-Ji Chen, *Beijing*
Dai -Ming Fan, *Xi'an*
Zhi-Qiang Huang, *Beijing*
Nicholas F LaRusso, *Rochester*
Jie-Shou Li, *Nanjing*
Geng-Tao Liu, *Beijing*
Fa-Zu Qiu, *Wuhan*
Eamonn M Quigley, *Cork*
David S Rampton, *London*
Rudi Schmid, *California*
Nicholas Joseph Talley, *Rochester*
Zhao-You Tang, *Shanghai*
Guido NJ Tytgat, *Amsterdam*
Meng-Chao Wu, *Shanghai*
Xian-Zhong Wu, *Tianjin*
Hui Zhuang, *Beijing*
Jia-Yu Xu, *Shanghai*

PRESIDENT AND EDITOR-IN-CHIEF

Lian-Sheng Ma, *Beijing*

EDITOR-IN-CHIEF

Bo- Rong Pan, *Xi'an*

ASSOCIATE EDITORS-IN-CHIEF

Bruno Annibale, *Roma*
Henri Bismuth, *Villesuif*
Jordi Bruix, *Barcelona*

Roger William Chapman, *Oxford*
Alexander L Gerbes, *Munich*
Shou-Dong Lee, *Taipei*
Walter Edwin Longo, *New Haven*
You-Yong Lu, *Beijing*
Masao Omata, *Tokyo*
Harry H-X Xia, *Hong Kong*

MEMBERS OF THE EDITORIAL BOARD



Albania
Bashkim Resuli, *Tirana*



Algeria
Hocine Asselah, *Algiers*



Argentina
Julio Horacio Carri, *Córdoba*

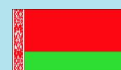


Australia
Darrell HG Crawford, *Brisbane*
Robert JL Fraser, *Daw Park*
Yik-Hong Ho, *Townsville*
Gerald J Holtmann, *Adelaide*
Michael Horowitz, *Adelaide*

Riordan SM, *Sydney*
IC Roberts-Thomson, *Adelaide*
James Toouli, *Adelaide*



Austria
Dragosics BA, *Vienna*
Peter Ferenci, *Vienna*
Alfred Gangl, *Vienna*
Michael Trauner, *Graz*
Harald Vogelsang, *Vienna*



Belarus
Yury K Marakhouski, *Minsk*



Belgium
Geerts AEC, *Brussels*
Cremer MC, *Brussels*
Yves J Horsmans, *Brussels*
Yvan Vandenplas, *Brussels*
Eddie Wisse, *Keerbergen*



Brazil
Heitor Rosa, *Goiania*

**Bulgaria**Zahariy Alexandrov Krastev, *Sofia***Canada**Wang-Xue Chen, *Ottawa*
Richard N Fedorak, *Edmonton*
Hugh James Freeman, *Vancouver*
Samuel S Lee, *Calgary*
Philip Martin Sherman, *Toronto*
Alan BR Thomson, *Edmonton*
Eric M Yoshida, *Vancouver***China**Francis KL Chan, *Hong Kong*
Xiao-Ping Chen, *Wuhan*
Jun Cheng, *Beijing*
Chi-Hin Cho, *Hong Kong*
Zong-Jie Cui, *Beijing*
Da-Jun Deng, *Beijing*
Er-Dan Dong, *Beijing*
Sheung-Tat Fan, *Hong Kong*
Xue-Gong Fan, *Changsha*
Jin Gu, *Beijing*
De-Wu Han, *Taiyuan*
Shao-Heng He, *Shantou*
Fu-Lian Hu, *Beijing*
Wayne HC Hu, *Hong Kong*
Ching Lung Lai, *Hong Kong*
Kam Chuen Lai, *Hong Kong*
Wai-Keung Leung, *Hong Kong*
Zhi-Hua Liu, *Beijing*
Ai-Ping Lu, *Beijing*
Jing-Yun Ma, *Beijing*
Lun-Xiu Qin, *Shanghai*
Yu-Gang Song, *Guangzhou*
Peng Shang, *Xi'an*
Qin Su, *Beijing*
Yuan Wang, *Shanghai*
Benjamin Wong, *Hong Kong*
Wai-Man Wong, *Hong Kong*
Hong Xiao, *Shanghai*
Dong-Liang Yang, *Wuhan*
Xue-Biao Yao, *Hefei*
Yuan Yuan, *Shenyang*
Man-Fung Yuen, *Hong Kong*
Jian-Zhong Zhang, *Beijing*
Zhi-Rong Zhang, *Chengdu*
Xiao-Hang Zhao, *Beijing*
Shu Zheng, *Hangzhou***Costa Rica**Edgar M Izquierdo, *San José***Croatia**Marko Duvnjak, *Zagreb***Denmark**Flemming Burcharth, *Herlev*
Peter Bytzer, *Copenhagen*
Hans Gregersen, *Aalborg***Egypt**Abdel-Rahman El-Zayadi, *Giza***Finland**Pentti Sipponen, *Espoo***France**Charles Paul Balabaud, *Bordeaux*
Jacques Belghiti, *Clichy*
Pierre Brissot, *Rennes*
Franck Carbonnel, *Besancon*
Bruno Clément, *Rennes*
Jacques Cosnes, *Paris*
Francoise Degos, *Clichy*
Francoise Lunel Fabian, *Angers*
Gérard Feldmann, *Paris*
Jean Fioramonti, *Toulouse*
Rene Lambert, *Lyon*
Didier Lebrec, *Clichy*
Francis Mégraud, *Bordeaux*
Richard Moreau, *Clichy*
Jose Sahel, *Marseille*
Jean-Yves Scoazec, *Lyon*
Jean-Pierre Henri Zarski, *Grenoble***Germany**HD Allescher, *Garmisch-Partenkirchen*
Rudolf Arnold, *Marburg*
Hubert Blum, *Freiburg*
Peter Born, *Muchen*
Heinz J Buhr, *Berlin*
Haussinger Dieter, *Düsseldorf*
Dietrich CF, *Bad Mergentheim*
Wolfram W Domschke, *Muenster*
Ulrich Robert Fölsch, *Kiel*
Peter R Galle, *Mainz*
Burkhard Göke, *Munich*
Axel M Gressner, *Aachen*
Eckhart Georg Hahn, *Erlangen*
Werner Hohenberger, *Erlangen*
RG Jakobs, *Ludwigshafen*
Joachim Labenz, *Siegen*
Ansgar W Lohse, *Hamburg*
Peter Malfertheiner, *Magdeburg*
Andrea Dinah May, *Wiesbaden*
Stephan Miehlke, *Dresden*
Gustav Paumgartner, *Munich*
Ulrich Ks Peitz, *Magdeburg*
Giuliano Ramadori, *Göttingen*
Tilman Sauerbruch, *Bonn*
Hans Seifert, *Oldenburg*
J Ruediger Siewert, *Munich*
Manfred V Singer, *Mannheim***Greece**Arvanitakis C, *Thessaloniki*
Elias A Kouroumalis, *Heraklion***Hungary**Simon A László, *Szekszárd*
János Papp, *Budapest***Iceland**Hallgrímur Gudjonsson, *Reykjavik***India**Sujit Kumar Bhattacharya, *Kolkata*
Chawla YK, *Chandigarh*
Radha Dhiman K, *Chandigarh*
Sri Prakash Misra, *Allahabad*
Kartar Singh, *Lucknow***Iran**Reza Malekzadeh, *Tehran***Israel**Abraham Rami Eliakim, *Haifa*
Yaron Niv, *Pardesia***Italy**Giovanni Addolorato, *Roma*
Alfredo Alberti, *Padova*
Annese V, *San Giovanni Rotondo*
Giovanni Barbara, *Bologna*
Gabrio Bassotti, *Perugia*
Franco Bazzoli, *Bologna*
Adolfo Francesco Attili, *Roma*
Antonio Benedetti, *Ancona*
Giovanni Cammarota, *Roma*
Antonino Cavallari, *Bologna*
Dario Conte, *Milano*
Gino Roberto Corazza, *Pavia*
Guido Costamagua, *Roma*
Antonio Craxi, *Palermo*
Fabio Farinati, *Padua*
Giovanni Gasbarrini, *Roma*
Paolo Gentilini, *Florence*
Eduardo G Giannini, *Genoa*

Paolo Gionchetti, *Bologna*
Roberto De Giorgio, *Bologna*
Mario Guslandi, *Milano*
Giovanni Maconi, *Milan*
Giulio Marchesini, *Bologna*
Giuseppe Montalto, *Palermo*
Luisi Pagliaro, *Palermo*
Fabrizio R Parente, *Milan*
Perri F, *San Giovanni Rotondo*
Raffaele Pezzilli, *Bologna*
Pilotto A, *San Giovanni Rotondo*
Massimo Pinzani, *Firenze*
Gabriele Bianchi Porro, *Milano*
Piero Portincasa, *Bari*
Giacomo Laffi, *Firenze*
Enrico Roda, *Bologna*
Massimo Rugge, *Padova*
Vincenzo Savarino, *Genova*
Vincenzo Stanghellini, *Bologna*
Calogero Surrenti, *Florence*
Roberto Testa, *Genoa*
Dino Vaira, *Bologna*



Japan

Kyoichi Adachi, *Izumo*
Takashi Aikou, *Kagoshima*
Taiji Akamatsu, *Matsumoto*
Takafumi Ando, *Nagoya*
Akira Andoh, *Otsu*
Taku Aoki, *Tokyo*
Masahiro Arai, *Tokyo*
Tetsuo Arakawa, *Osaka*
Yasuji Arase, *Tokyo*
Masahiro Asaka, *Sapporo*
Hitoshi Asakura, *Tokyo*
Yutaka Atomi, *Tokyo*
Takeshi Azuma, *Fuku*
Nobuyuki Enomoto, *Yamanashi*
Kazuma Fujimoto, *Saga*
Toshio Fujioka, *Oita*
Yoshihide Fujiyama, *Otsu*
Hiroyuki Hanai, *Hamamatsu*
Kazuhiro Hanazaki, *Nagano*
Naohiko Harada, *Fukuoka*
Makoto Hashizume, *Fukuoka*,
Tetsuo Hayakawa, *Nagoya*
Kazuhide Higuchi, *Osaka*
Ichiro Hirata, *Osaka*
Keiji Hirata, *Kitakyushu*
Takafumi Ichida, *Shizuoka*
Kenji Ikeda, *Tokyo*
Kohzoh Imai, *Sapporo*
Fumio Imazeki, *Chiba*
Masayasu Inoue, *Osaka*
Hiromi Ishibashi, *Nagasaki*
Shunji Ishihara, *Izumo*
Toru Ishikawa, *Niigata*
Kei Ito, *Sendai*
Masayoshi Ito, *Tokyo*
Hiroaki Itoh, *Akita*
Hiroshi Kaneko, *Aichi-Gun*
Shuichi Kaneko, *Kanazawa*
Takashi Kanematsu, *Nagasaki*

Junji Kato, *Sapporo*
Mototsugu Kato, *Sapporo*
Shinzo Kato, *Tokyo*
Sunao Kawano, *Osaka*
Yoshikazu Kinoshita, *Izumo*
Masaki Kitajima, *Tokyo*
Tsuneo Kitamura, *Chiba*
Seigo Kitano, *Oita*
Hironori Koga, *Kurume*
Satoshi Kondo, *Sapporo*
Shoji Kubo, *Osaka*
Shigeki Kuriyama, *Kagawa*
Masato Kusunoki, *Mie*
Takashi Maeda, *Fukuoka*
Shin Maeda, *Tokyo*
Osamu Matsui, *Kanazawa*
Yasushi Matsuzaki, *Tsukuba*
Hirotomo Miwa, *Hyogo*
Masashi Mizokami, *Nagoya*
Motowo Mizuno, *Hiroshima*
Morito Monden, *Suita*
Hisataka S Moriwaki, *Gifu*
Yoshiharu Motoo, *Kanazawa*
Akihiro Munakata, *Hirosaki*
Kazunari Murakami, *Oita*
Kunihiko Murase, *Tusima*
Masato Nagino, *Nagoya*
Yuji Naito, *Kyoto*
Hisato Nakajima, *Tokyo*
Hiroki Nakamura, *Yamaguchi*
Shotaro Nakamura, *Fukuoka*
Akimasa Nakao, *Nagoya*
Mikio Nishioka, *Niihama*
Susumu Ohmada, *Maebashi*
Masayuki Ohta, *Oita*
Tetsuo Ohta, *Kanazawa*
Susumu Okabe, *Kyoto*
Katsuhisa Omagari, *Nagasaki*
Saburo Onishi, *Nankoku*
Morikazu Onji, *Ehime*
Hiromitsu Saisho, *Chiba*
Hidetsugu Saito, *Tokyo*
Takafumi Saito, *Yamagata*
Isao Sakaida, *Yamaguchi*
Michie Sakamoto, *Tokyo*
Iwao Sasaki, *Sendai*
Motoko Sasaki, *Kanazawa*
Chifumi Sato, *Tokyo*
Shuichi Seki, *Osaka*
Hiroshi Shimada, *Yokohama*
Mitsuo Shimada, *Tokushima*
Hiroaki Shimizu, *Chiba*
Tooru Shimosegawa, *Sendai*
Tadashi Shimoyama, *Hirosaki*
Ken Shirabe, *Izuka City*
Yoshio Shirai, *Niigata*
Katsuya Shiraki, *Mie*
Yasushi Shiratori, *Okayama*
Yasuhiko Sugawara, *Tokyo*
Toshiro Sugiyama, *Toyama*
Kazuyuki Suzuki, *Morioka*
Hidekazu Suzuki, *Tokyo*
Tadatashi Takayama, *Tokyo*
Tadashi Takeda, *Osaka*

Koji Takeuchi, *Kyoto*
Kiichi Tamada, *Tochigi*
Akira Tanaka, *Kyoto*
Eiji Tanaka, *Matsumoto*
Noriaki Tanaka, *Okayama*
Shinji Tanaka, *Hiroshima*
Kyuichi Tanikawa, *Kurume*
Tadashi Terada, *Shizuoka*
Akira Terano, *Shimotsugagun*
Kazunari Tominaga, *Osaka*
Hidenori Toyoda, *Ogaki*
Akihito Tsubota, *Chiba*
Shingo Tsuji, *Osaka*
Takato Ueno, *Kurume*
Shinichi Wada, *Tochigi*
Hiroyuki Watanabe, *Kanazawa*
Sumio Watanabe, *Akita*
Toshio Watanabe, *Osaka*
Yuji Watanabe, *Ehime*
Chun-Yang Wen, *Nagasaki*
Koji Yamaguchi, *Fukuoka*
Takayuki Yamamoto, *Yokkaichi*
Takashi Yao, *Fukuoka*
Hiroshi Yoshida, *Tokyo*
Masashi Yoshida, *Tokyo*
Norimasa Yoshida, *Kyoto*
Kentaro Yoshika, *Toyooka*
Masahide Yoshikawa, *Kashihara*



Lithuania

Sasa Markovic, *Japljeva*



Macedonia

Vladimir Cirko Serafimovski, *Skopje*



Malaysia

Andrew Seng Boon Chua, *Ipah*
Jayaram Menon, *Sabah*
Khean-Lee Goh, *Kuala Lumpur*



Monaco

Patrick Rampal, *Monaco*



Netherlands

Louis MA Akkermans, *Utrecht*
Karel Van Erpecum, *Utrecht*
Albert K Groen, *Amsterdam*
Dirk Joan Gouma, *Amsterdam*
Jan BMJ Jansen, *Nijmegen*
Evan Anthony Jones, *Abcoude*
Ernst Johan Kuipers, *Rotterdam*
Chris JJ Mulder, *Amsterdam*
Michael Müller, *Wageningen*

Pena AS, *Amsterdam*
Andreas Smout, *Utrecht*
RW Stockbrugger, *Maastricht*
GP Vanberge-Henegouwen,
Utrecht



New Zealand

Ian David Wallace, *Auckland*



Norway

Trond Berg, *Oslo*
Helge Lyder Waldum, *Trondheim*



Pakistan

Muhammad S Khokhar, *Lahore*



Philippines

Eulenia Rasco Nolasco, *Manila*



Poland

Tomasz Brzozowski, *Cracow*
Andrzej Nowak, *Katowice*



Portugal

Miguel Carneiro De Moura, *Lisbon*



Russia

Vladimir T Ivashkin, *Moscow*
Leonid Lazebnik, *Moscow*
Vasily I Reshetnyak, *Moscow*



Singapore

Bow Ho, *Kent Ridge*
Francis Seow-Choen, *Singapore*



Slovakia

Anton Vavrecka, *Bratislava*



South Africa

Michael C Kew, *Parktown*



South Korea

Jin-Hong Kim, *Suwon*
Myung-Hwan Kim, *Seoul*
Yun-Soo Kim, *Seoul*
Yung-Il Min, *Seoul*

Jae-Gahb Park, *Seoul*
Dong Wan Seo, *Seoul*



Spain

Abraldes JG, *Barcelona*
Fernando Azpiroz, *Barcelona*
Ramon Bataller, *Barcelona*
Josep M Bordas, *Barcelona*
Maria Buti, *Barcelon*
Xavier Calvet, *Sabadell*
Antoni Castells, *Barcelona*
Manuel Daz-Rubio, *Madrid*
Juan C Garcia-Pagán, *Barcelona*
Genover JB, *Barcelona*
Javier P Gisbert, *Madrid*
Jaime Guardia, *Barcelona*
Angel Lanas, *Zaragoza*
Ricardo Moreno-Otero, *Madrid*
Julian Panes, *Barcelona*
Miguel Perez-Mateo, *Alicante*
Josep M Pique, *Barcelona*
Jesus Prieto, *Pamplona*
Luis Rodrigo, *Oviedo*



Sri Lanka

Janaka De Silva, *Ragama*



Swaziland

Gerd Kullak-Ublick, *Zurich*



Sweden

Lars Christer Olbe, *Molndal*
Curt Einarsson, *Huddinge*
Lars R Lundell, *Stockholm*
Xiao-Feng Sun, *Linkoping*



Switzerland

Christoph Beglinger, *Basel*
Michael W Fried, *Zurich*
Bruno Stieger, *Zurich*
Arthur Zimmermann, *Berne*



Turkey

Yusuf Bayraktar, *Ankara*
Figen Gurakan, *Ankara*
Cihan Yurdaydin, *Ankara*



United Kingdom

Axon ATR, *Leeds*
Paul Jonathan Ciclitira, *London*
Amar Paul Dhillon, *London*



United States

Firas H Ac-Kawas, *Washington*
Gianfranco D Alpini, *Temple*
Paul Angulo, *Rochester*
Jamie S Barkin, *Miami Beach*
Todd Baron, *Rochester*
Kim Elaine Barrett, *San Diego*
Jennifer D Black, *Buffalo*
Xu Cao, *Birmingham*
David L Carr-Locke, *Boston*
Marc F Catalano, *Milwaukee*
Xian-Ming Chen, *Rochester*
James M Church, *Cleveland*
Vincent Coghlan, *Beaverton*
James R Connor, *Hershey*
Pelayo Correa, *New Orleans*
John Cuppoletti, *Cincinnati*
Peter V Danenberg, *Los Angeles*
Kiron Moy Das, *New Brunswick*
Hala El-Zimaity, *Houston*
Ronnie Fass, *Tucson*
Emma E Furth, *Pennsylvania*
John Geibel, *New Haven*
Graham DY, *Houston*
Joel S Greenberger, *Pittsburgh*
Anna S Gukovskaya, *Los Angeles*
Gavin Harewood, *Rochester*
Atif Iqbal, *Omaha*
Hajime Isomoto, *Rochester*
Dennis M Jensen, *Los Angeles*
Leonard R Johnson, *Memphis*
Peter James Kahrilas, *Chicago*
Anthony Nicholas Kallou, *Baltimore*
Neil Kaplowitz, *Los Angeles*
Emmet B Keefe, *Palo Alto*
Joseph B Kirsner, *Chicago*
Burton I Korelitz, *New York*
Robert J Korst, *New York*
Richard A Kozarek, *Seattle*
Shiu-Ming Kuo, *Buffalo*
Frederick H Leibach, *Augusta*
Andreas Leodolter, *La Jolla*
Ming Li, *New Orleans*
Lenard M Lichtenberger, *Houston*
Gary R Lichtenstein, *Philadelphia*
Josep M Llovet, *New York*
Martin Lipkin, *New York*

Robin G Lorenz, *Birmingham*
James David Luketich, *Pittsburgh*
Henry Thomson Lynch, *Omaha*
Paul Martiw, *New York*
Richard W McCallum, *Kansas City*
Timothy H Moran, *Baltimore*
Hiroshi Nakagawa, *Philadelphia*
Douglas B Neison, *Minneapolis*
Juan J Nogueras, *Weston*
Curtis T Okamoto, *Los Angeles*
Pankaj Jay Pasricha, *Galveston*
Zhiheng Pei, *New York*
Pitchumoni CS, *New Brunswick*
Satish Rao, *Iowa City*
Adrian Reuben, *Charleston*

Victor E Reyes, *Galveston*
Richard E Sampliner, *Tucson*
Vijay H Shah, *Rochester*
Stuart Sherman, *Indianapolis*
Stuart Jon Spechler, *Dallas*
Michael Steer, *Boston*
Gary D Stoner, *Columbus*
Rakesh Kumar Tandon, *New Delhi*
Tchou-Wong KM, *New York*
Paul Joseph Thuluvath, *Baltimore*
Swan Nio Thung, *New York*
Travagli RA, *Baton Rouge-La*
Triadafilopoulos G, *Stanford*
David Hoffman Vanthiel, *Mequon*
Jian-Ying Wang, *Baltimore*

Kenneth Ke-Ning Wang, *Rochester*
Judy Van De Water, *Davis*
Steven David Wexner, *Weston*
Russell Harold Wiesner, *Rochester*
Keith Tucker Wilson, *Baltimore*
George Y Wu, *Farmington*
Jian Wu, *Sacramento*
Chung Shu Yang, *Piscataway*
David Yule, *Rochester*
Michael Zenilman, *Brooklyn*



Yugoslavia

Jovanovic DM, *Sremska Kamenica*

**Manuscript reviewers of
*World Journal of Gastroenterology***

Yogesh K Chawla, *Chandigarh*
Chiung-Yu Chen, *Tainan*
Gran-Hum Chen, *Taichung*
Li-Fang Chou, *Taipei*
Jennifer E Hardingham, *Woodville*
Ming-Liang He, *Hong Kong*
Li-Sung Hsu, *Taichung*
Guang-Cun Huang, *Shanghai*
Shinn-Jang Hwang, *Taipei*
Jia-Horng Kao, *Taipei*
Aydin Karabacakoglu, *Konya*
Sherif M Karam, *Al-Ain*
Tadashi Kondo, *Tsukiji*
Jong-Soo Lee, *Nam-yang-ju*
Lein-Ray Mo, *Tainan*
Kpozehouen P Randolph, *Shanghai*
Bin Ren, *Boston*
Tetsuji Sawada, *Osaka*
Cheng-Shyong Wu, *Cha-Yi*
Ming-Shiang Wu, *Taipei*
Wei-Guo Zhu, *Beijing*

Current research of hepatic cirrhosis in China

Xi-Xian Yao, Shu-Lin Jiang, Dong-Mei Yao

Xi-Xian Yao, Shu-Lin Jiang, Dong-Mei Yao, Second Hospital, Hebei Medical University, Shijiazhuang 050000, Hebei Province, China
Correspondence to: Professor Xi-Xian Yao, Department of Gastroenterology of Internal Medicine, Second Hospital, Hebei Medical University, Shijiazhuang 050000, Hebei Province, China. yaoxixian@163.com

Telephone: +86-311-7814356

Received: 2004-01-12 **Accepted:** 2004-05-15

Abstract

Hepatic cirrhosis is a common disease that poses a serious threat to public health, and is characterized by chronic, progressive and diffuse hepatic lesions preceded by hepatic fibrosis regardless of the exact etiologies. In recent years, considerable achievements have been made in China in research of the etiopathogenesis, diagnosis and especially the treatment of hepatic fibrosis, resulting in much improved prognosis of hepatic fibrosis and cirrhosis. In this paper, the authors review the current status of research in hepatic fibrosis, cirrhosis and their major complications.

© 2005 The WJG Press and Elsevier Inc. All rights reserved.

Key words: Hepatic cirrhosis; China

Yao XX, Jiang SL, Yao DM. Current research of hepatic cirrhosis in China. *World J Gastroenterol* 2005; 11(5): 617-622
<http://www.wjgnet.com/1007-9327/11/617.asp>

ETIOLOGY OF HEPATIC CIRRHOSIS

In China, virus hepatitis B and C remain the primary etiological factors for hepatic cirrhosis, and a recent increase in alcoholic cirrhosis has also been noted^[1,2]. But in the past years, approximately 25% to 40% of HBsAg-, antiHBc and antiHBe-positive cases failed to receive due attention^[3] for the potential risk of hepatic cirrhosis, and carcinoma in relatively rare cases. With the development of public hygiene, schistosomal liver cirrhosis has greatly decreased, and other etiologies such as biliary cirrhosis, hemochromatosis and Wilson's disease are now hardly seen.

STUDY ON HEPATIC FIBROSIS

Hepatic fibrosis is a reversible pathological process^[4] and chronic hepatic disease has become a widespread concern of researchers. Recently, significant results have been obtained in research of the pathogenesis of hepatic fibrosis in view of the role of hepatic stellate cells (HSCs)^[5-7], formation of extracellular matrix (ECM), hyperoxidation, cytokine network, Na⁺/H⁺ exchange pump and calcium channel.

Pathogenic mechanism of hepatic fibrosis

HSCs, the main source of ECM^[8,9], play important roles in the formation of hepatic fibrosis^[2,12-16]. Pathogenic research of hepatic fibrosis is now focused on the following respects:

peroxidation mechanism, cytokine network, signal transduction pathways, and cell apoptosis, as examined briefly in the following.

Peroxidation mechanism Chronic hepatic damage by inflammation, toxins, immunity, and malnutrition, *etc.*, can activate HSCs. The process of activation is closely related to peroxidation^[10-13]. It has been shown that lipid peroxidation occurs in injured hepatic cells^[14], which may further activate HSCs. In the event of hepatic inflammatory reaction, neutrophilic granulocytes are the main source of reactive oxygen species (ROS)^[15] that have been proved to be able to promote HSC activation and proliferation *in vitro*^[16]. Some anti-oxidants can inhibit the activation of HSCs, suggesting that peroxidation accompanies the progression of hepatic fibrosis.

Cytokine network Kupffer cells can initiate the progress of hepatic fibrosis^[17]. After being activated, Kupffer cells release a variety of cytokines closely related to hepatic fibrosis such as transforming growth factors (TGF) α and β , tumor necrosis factor (TNF) α , interleukin-1 (IL-1) and platelet-derived growth factor (PDGF). In addition, Kupffer cells, which can be regarded as important "coefficients", help maintain the kinetic equilibrium of hepatic fibrosis, and mediate the feedback mechanism of some biological messages during the progression of hepatic fibrosis. HSCs have both paracrine and autocrine functions, the activation of which can be triggered via a reaction cascade of cytokines and biochemical factors^[18-20]. Two major changes occur after the activation of HSC, that is, proliferation and phenotypic transition^[21]. PDGF and TGF β 1 play an important role in the proliferation and transformation of HSCs^[22]. The key role of PDGF, a most effective mitogen during the synthesis of HSC DNA^[23], is to convert HSC from G₀ to G₁ and S phases, whereas TGF β 1 promotes the synthesis of collagen and inhibitors of tissue metalloproteinases (TIMPs) in activated HSCs^[24]. Moreover, PDGF and TGF β 1 can interact with each other. PDGF is capable of inducing HSCs to express and secrete PDGF receptors. PDGF and TGF β 1 can also interact with IL-1 and TNF α ^[25], leading to the formation of cytokine network with HSCs at the crucial center.

Na⁺/H⁺ exchange pump and calcium/calmodulin Messages in cytokines could pass to HSC nuclei through the membrane or intracellular pathways. Svegliati Baroni *et al*^[14] found that the HSCs exposed for 24 h to the culture medium of hepatocytes subjected to oxidative stress could increase the proliferation of HSCs and accumulation of collagen I. The mechanism is related to the increased intracellular pH of HSCs and enhanced activation of Na⁺/H⁺ exchanger. Actually, Na⁺ influx is the key element that initiates the proliferative reaction^[26]. PDGF can activate Na⁺/H⁺ exchanger by activating IP₃-calcium/calmodulin and protein kinase C^[27]. Synthesis of ECM promoted by TGF β 1 may be modulated by the activity of calcium channel^[28]. Therefore, activation of IP₃-calcium/calmodulin-Na⁺/H⁺ exchanger in succession induces proliferation of HSCs and synthesis of ECM, which serves as the theoretical basis for therapy of hepatic fibrosis.

HSC apoptosis Concerning the apoptosis of HSCs, consensus has been reached over the occurrence of HSC apoptosis, which takes place in α -SMA-positive but not static HSCs, in parallel with phenotypic transition^[29]. CD95 (APO-1/Fas) receptor and

its ligand have been recognized for their important role in inducing HSC apoptosis^[30], and the therapeutic strategy against hepatic fibrosis is maneuvered to target at promoting the apoptosis of HSCs. Realization that activation is the premise of apoptosis of HSCs is not meant to confirm the seemingly natural cause-effect relationship between monophasic HSC activation and apoptosis, and the reversibility of phenotype transformation of HSCs is still worthy of further exploration.

Diagnosis of hepatic fibrosis

Currently, the diagnosis of hepatic cirrhosis depends mainly on needle biopsy of the liver, and ultrasonic examination can hardly define the degree of hepatic fibrosis. Through consistent effort, researchers have made encouraging progress in serological diagnosis of hepatic cirrhosis^[31-34].

Pathological diagnosis In May 1995, the *Prevention and Treatment of Virus Hepatitis* was revised at the 5th Congress of Parasite and Infectious Diseases, and chronic hepatitis was then classified into mild, moderate and severe degrees and pathologically graded into G0-G4 degrees and S0-S4 stages. Wang *et al*^[35], after observing 1 000 hepatic biopsy specimens, proposed a classification protocol of the inflammatory activity and fibrosis, which was an improved version of the criteria given by Knodell *et al*^[36] and Chevallier *et al*^[37]. This protocol has now been accepted in clinical practice.

Serological diagnosis Needle biopsy of the liver has its inherent limitations in diagnosis and curative effect assessment^[38]. Currently, great progress has been made in the serological diagnosis of hepatic fibrosis^[39,40]. Many useful indices have been set up to reflect the metabolism of ECM, including PCIII/PIIP, CIV, PIIP, and LN^[41,42], of which HA is the most sensitive. CIV, the main ingredient of basal membrane, was found to elevate during capillarization of the hepatic sinusoid. After comprehensive analysis, HA and CIV were established as the most significant indices during S3 and S4 stages^[38]. Our hospital developed a "quadruple detection" protocol combining CIV, PIIP, LN and HA, which proved to be highly specific and sensitive. However, its value should not be overemphasized while comprehensive judgment is still needed including that derived from biochemical examinations.

Treatment of hepatic fibrosis

So far, no satisfactory treatment protocol with western drugs is available for hepatic fibrosis because of their severe side effects. Meanwhile, we have obtained promising results with traditional Chinese medicines, and a number of drugs have been found to reverse the progression of hepatic fibrosis. Antifibrotic therapy targets at the inhibition of HSC proliferation^[43-46], cytokine activity^[47-49] and ECM degradation. Calmodulin antagonists belong to HSC proliferation inhibitors, working to inhibit the pathway of IP3-calcium/calmodulin-Na⁺/H⁺ exchangers, but relevant studies^[50-52] conducted in China have so far achieved no significant breakthrough in this aspect. The apoptosis of HSC was another interest of study in recent years^[31-33,53-55]. Gene therapies using antisense oligonucleotides, nucleases and gene carriers promise optimistic results of treatment, but the problems of gene targeting and expression modulation have yet to be solved. Studies have shown that traditional Chinese medicines can inhibit the deposition of collagen fibers^[56-63] and promote the reversion of fibrosis, which was also confirmed by experimental evidence that *Radix Salviae Miltiorrhizae*, *Radix Angelicae Sinensis*, *Radix Astragali seu Hedysari*, *Radix Paeoniae Rrbra*, *Semen Persicae*, *Hirudo*, *Flos Carthami*, *Radix Notoginseng*, *Rhizoma Sparganii*, *Rhizoma Zedoariae*, *etc* could obviously inhibit the formation of collagen fibers. The agent 861^[56,59], *Qianggan* capsule, *Fuzhenghuayu* 319^[58],

Dahuangzhechong pill^[59], *Yigan* infusion^[60], and the traditional Chinese medicinal formula *Xiaochaihu* decoction *etc.*, could eliminate clinical symptoms, improve liver function, decrease liver collagen content and improve the histologic picture of the liver without obvious side effects, all of which seem to suggest a bright future of traditional Chinese medicine in treating hepatic fibrosis. Problems, however, do exist in traditional Chinese medicines, in the standardization and purification methodology. Currently no standardized criteria are available to compensate for the geographical variation in the content of effective components of drugs, and the methods of harvest and refinement are also controversial. The methodology employed for animal experiments needs standardization, and strict double-blind, multi-center studies have yet to be performed.

STUDY OF LIVER CIRRHOSIS

In China, histological diagnosis of liver cirrhosis is not a universal practice and liver puncture is performed in a very small portion of patients suspected of the disease. The clinical diagnosis of liver cirrhosis still depends on the presence of enlarged and hardened liver and spleen, and manifestations of portal hypertension. Non-invasive B type ultrasound provides a convenient means for the diagnosis of liver cirrhosis, the typical manifestations of which include sharp or wave-like margins of the liver and disproportional right and left lobes of the liver with uneven echoes from the hepatic parenchyma. The indirect signs include enlarged spleen, dilated portal (>1.4 cm) or splenic veins (>0.9 cm) and ascites. The treatment of cirrhotic patients is directed against the complications including ascites, gastrointestinal bleeding, spontaneous bacterial peritonitis (SBP), hepatorenal syndrome, hepatic encephalopathy, cirrhosis-induced carcinoma and thrombosis, *etc*. Current interests of research are devoted predominantly to bleeding gastroesophageal varices, early diagnosis of SBP, recognition and treatment of subclinical hepatorenal syndrome, treatment of ascites especially refractory ascites, diagnosis of subclinical hepatoencephalopathy, early detection of liver cancer, and hypertensive gastrointestinal diseases.

Esophageal variceal bleeding (EVB)

Critical factors and prediction of EVB Degree of liver damage, size of varices, endoscopic red color signs and elevated portal vein pressure (PVP) or hepatic vein pressure gradient (HVPG) are the major risk factors for bleeding^[64]. In China, patients with PV \geq 1.70 cm, SPV \geq 1.20 cm and EV \geq 6.0 mm especially those with red color signs are at high risk for bleeding^[65]. Impaired liver function is the dominant factor threatening bleeding, as the blood flow rate in cases of extrahepatic hypertension with normal liver function, in spite of the presence of severe varices and higher PVPs, is decidedly lower than that in liver cirrhosis patients with portal hypertension^[66]. The more relevant factors are the red color signs on the varices seen on endoscopy and hemodynamic changes with portal pressure^[67]. Recently, much attention has been paid to bacterial infection for its potential to cause bleeding^[68-70], possibly because in patients with severe varices and a high esophageal wall tension, the release of endotoxin into the systemic circulation during the episodes of bacterial infection resulted in a further increase in the portal pressure induced by endothelin and possibly vasoconstrictive cyclo-oxygenase products. The subsequent contraction of HSC caused a rise in intrahepatic vascular resistance. Furthermore, endotoxin-induced nitric oxide and prostacyclin, and prostacyclin induced by endothelin could inhibit platelet aggregation, which may result in further deterioration of the already existent bleeding^[64].

Strategies of management Correct use of Sengstaken-Blakemore tube, knot and sclerosis of esophageal varices, and uses of new hemostatics such as somatostatin and thrombin, have improved the prognosis of EVB^[71-74]. The rebleeding and mortality rates have been greatly reduced by use of β -receptor blockers as the first-line drugs; the combination of β -receptor blockers, calmodulin antagonists, and nitroesters can enhance the efficacy; vasopressin should be used with nitroglycerin or to reduce the side effects, somatostatin and octreotide are better options than vasopressin and have no obvious side effects. Traditional Chinese herbal drugs such as *Radix Salviae Miltiorrhizae*, *Radix Angelicae Sinensis*, may promote the blood flow and remove blood stasis, and are effective for lowering the PVP and HVPG. The slow but relatively long-lasting effects of the herbal drugs help prevent bleeding^[75,76]. Sclerosis and knot of the varices also effectively prevent the primary bleeding and decrease the rate of rebleeding. Porto-systemic shunt, however, is not recommended for the prevention of the primary bleeding. TIPSS could prevent the primary bleeding, but the rebleeding rate and long-term effect need further assessment.

Refractory ascites and hepatorenal syndrome

The ascites in cirrhotic patients usually indicates the progression of the disease into the decompensatory stage. Patients with a small amount of ascites should receive active and adequate treatment when they respond favorably to diuretics and have sufficient renal function without electrolyte disturbance. Rest, restricted salt intake, protein-rich food or application of herbal drugs that promote blood flow, removing stasis, invigorating the spleen and refreshing *Qi* (such as *Rhizoma Alismatis*, *Polyporus Umbellatus*, *Semen Plantaginis* and the preparation of *Weiling* decoction), could help eliminate the ascites. For patients with a large amount of ascites that failed to be resolved by exclusive use of traditional Chinese drugs, spiro lactone should be given with short-term use of dihydrochlorothiazide. Diuretic abuse should be avoided for potential drastic reduction in systemic blood volume and development of hepatorenal syndrome. Close relationship has been identified between ascites and renal function. Patients with refractory ascites are often characterized by increased resistance index (RI) of the interlobar and cortical vessels in comparison with patients with responsive ascites. The RI decreases physiologically from the hilum of the kidney to the outer parenchyma in healthy subjects and patients with responsive ascites, but this difference vanishes in patients with refractory ascites^[76]. Examination of renal blood distribution may help identify hepatorenal syndrome at early stages and make correct therapeutic decisions on responsive ascites. In clinical practice, elimination of ascites should be considered in line with the evaluation of the renal function. Spontaneous ascites discharge with intravenous albumin^[77] or dextran infusion^[78] and ascites autoperfusion^[79] have achieved good results. Close monitoring of the renal function needs to be carried out when attempt is made to lower the portal pressure and eliminate the ascites. Radionuclide renal dynamic imaging can be performed for diagnosis of subclinical hepatorenal syndrome^[80], and a thorough understanding of the status of the renal blood dynamics and perfusion of the glomeruli may hold much significance for the prognosis of hepatorenal syndrome and refractory ascites.

Splanchnic hyperdynamics and SBP

Most cirrhotic patients suffer from disturbance of the intestinal flora. The overgrowth of aerobic Gram-negative bacteria may play an important role in endotoxemia^[81]. The diagnosis of SBP is based mainly on the results of cell counting, and differential

or bacterial culture of the ascites greatly helps the description of SBP. So far, the knowledge about endotoxemia, endothelin and NO has revealed a new scope of splanchnic hyperdynamics and SBP: endotoxin evokes the release of endothelin, which in turn increases the PVP, and promotes the synthesis of NO and other vasodilators such as VEGF^[82] derived from the residue cells induced by IL-1 and TNF α as well. These dilators cause the dilation of the splanchnic vascular beds, and the arterioles and microarteries are especially responsive to these substances, to result in the decreased blood RI followed by lowered blood pressure and increased heart output. This low RI and hyperdynamics, along with the high CI and low blood flow velocity^[76] at the portal system, are further deteriorated by SBP, resulting in variceal bleeding for more elevated PVP and heat shock or hepatorenal syndrome. Close relationship was found among the four episodes: SBP, portal hypertension with splanchnic hyperdynamics, esophageal venous bleeding and hepatorenal syndrome. For those who were not responsive to diuretics, diagnostic abdominocentesis and bacterial culture should be performed even in the absence of abdominal signs of SBP. The treatment of SBP include (1) strengthening the trophotherapy, (2) using antibiotics according to the bacterial culture, (3) treatment with intravenous antibiotics for more than 7 d or continuous use for 3-6 d after the abdominocentesis becomes negative, and (4) intravenous antibiotics combined with ascites discharge and intraperitoneal injection of drugs, which may produce better effect than exclusive use of intravenous antibiotics.

Hepatic encephalopathy

Severe liver diseases may lead to functional disturbance of the central nervous system with a high mortality rate, which can be relieved by early detection of the condition. In recent years, the diagnosis of subclinical hepatic encephalopathy has witnessed great improvement in China. The examination of nerve-evoked potentials offers a means of objective and sensitive diagnosis of the disease^[83]. Several factors may contribute to the occurrence of encephalopathy, including (1) blood accumulation in the intestines after bleeding or intake of substances containing nitrogen, (2) water and electrolyte disturbance for iatrogenic reasons, (3) endotoxemia and infections, (4) *Helicobacter pylori* (*H pylori*) infection, (5) use of anesthetics or sedatives, and (6) decompression of the portal vein such as by TIPSS or porto-systemic shunt. Elimination of these factors may reduce or even prevent the occurrence of encephalopathy. When the disease occurs, treatments with defecation and intestinal acidification, use of arginine or glutamate, branch-chain amino acids, and levodopa are often effective. Antibiotics for *H pylori* can be used to reduce the absorption of ammonia from the intestine for treatment of hepatic encephalopathy.

Others

Ultrasonic examination and AFP dynamic methods are reliable for early diagnosis of primary liver cancer. Hepatic arterial radiography, CT and needle biopsy should be used in suspected cases to raise the diagnostic accuracy. Gastrointestinal disease with portal hypertension is no longer a concept of simple pathology, but a disease with specific clinical and endoscopic presentations secondary to liver cirrhosis^[84-86]. Low blood oxygen capacity in liver cirrhosis, or hepatopulmonary syndrome, is closely related to the portopulmonary shunt, inflammation of the lungs, hydrothorax and atelectasis at the base of the lung^[87]. Hepatic hydrothorax is most often found on the right side of the pleural cavity, but so far its causes have not been fully understood. Hypoalbuminemia

could accelerate the formation of hydrothorax in cirrhotic cases. Budd-Chiari syndrome, which is found much more frequently than ever, is likely to be confused with liver cirrhosis. Color Doppler ultrasound or infravenacavography, if necessary, could identify most of the causes of the disease. It is worth noticing that splanchnic hyperdynamics and hypoalbuminemia may lead to hepatic myocardiopathy and heart insufficiency^[88].

We believe that the incidence of liver cirrhosis can be lowered with its prognosis improved, when more effort is made in research of the complex mechanism of fibrosis and cirrhosis and their molecular biology, serological diagnosis, complications in relation to liver cirrhosis, application of integrated Chinese and western medicine, and especially the study of the curative mechanism of Chinese herbs, their serological pharmacology and the extraction of effective components.

REFERENCES

- Friedman SL. Seminars in medicine of the Beth Israel Hospital, Boston. The cellular basis of hepatic fibrosis. Mechanisms and treatment strategies. *N Engl J Med* 1993; **328**: 1828-1835
- Zhang Y, Pu XX, Zhao JY, Ren SZ. The differences in cirrhosis and primary cancer of liver caused by ethanol, HCV and HBV. *Shijie Huaren Xiaohua Zazhi* 1999; **7**: 572
- Yao SK, Ying F. The diagnosis and treatment of liver cirrhosis. *Shijie Huaren Xiaohua Zazhi* 2000; **8**: 681-683
- Friedman SL. Molecular mechanisms of hepatic fibrosis and principles of therapy. *J Gastroenterol* 1997; **32**: 424-430
- Pinzani M. Novel insights into the biology and physiology of the Ito cell. *Pharmacol Ther* 1995; **66**: 387-412
- Hautekeete ML, Geerts A. The hepatic stellate (Ito) cell: its role in human liver disease. *Virchows Arch* 1997; **430**: 195-207
- Moshage H, Casini A, Lieber CS. Acetaldehyde selectively stimulates collagen production in cultured rat liver fat-storing cells but not in hepatocytes. *Hepatology* 1990; **12**: 511-518
- Friedman SL. Cellular sources of collagen and regulation of collagen production in liver. *Semin Liver Dis* 1990; **10**: 20-29
- Gressner AM, Bachem MG. Molecular mechanisms of liver fibrogenesis—a homage to the role of activated fat-storing cells. *Digestion* 1995; **56**: 335-346
- Gualdi R, Casalgrandi G, Montosi G, Ventura E, Pietrangelo A. Excess iron into hepatocytes is required for activation of collagen type I gene during experimental siderosis. *Gastroenterology* 1994; **107**: 1118-1124
- Pietrangelo A, Gualdi R, Casalgrandi G, Geerts A, De Bleser P, Montosi G, Ventura E. Enhanced hepatic collagen type I mRNA expression into fat-storing cells in a rodent model of hemochromatosis. *Hepatology* 1994; **19**: 714-721
- Niemela O, Parkkila S, Yla-Herttua S, Villanueva J, Ruebner B, Halsted CH. Sequential acetaldehyde production, lipid peroxidation, and fibrogenesis in micropig model of alcohol-induced liver disease. *Hepatology* 1995; **22**: 1208-1214
- Bedossa P, Hougum K, Trautwein C, Holstege A, Chojkier M. Stimulation of collagen alpha 1 (I) gene expression is associated with lipid peroxidation in hepatocellular injury: a link to tissue fibrosis? *Hepatology* 1994; **19**: 1262-1271
- Svegliati Baroni G, D'Ambrosio L, Ferretti G, Casini A, Di Sario A, Salzano R, Ridolfi F, Saccomanno S, Jezequel AM, Benedetti A. Fibrogenic effect of oxidative stress on rat hepatic stellate cells. *Hepatology* 1998; **27**: 720-726
- Nordmann R. Alcohol and antioxidant systems. *Alcohol Alcohol* 1994; **29**: 513-522
- Casini A, Ceni E, Salzano R, Biondi P, Parola M, Galli A, Foschi M, Caligiuri A, Pinzani M, Surrenti C. Neutrophil-derived superoxide anion induces lipid peroxidation and stimulates collagen synthesis in human hepatic stellate cells: role of nitric oxide. *Hepatology* 1997; **25**: 361-367
- Yang YX, Kang JY. The mechanism and serum diagnosis of liver cirrhosis. *Xin Xiaohuabingxue Zazhi* 1997; **5**: 119-120
- Pinzani M. Novel insights into the biology and physiology of the Ito cell. *Pharmacol Ther* 1995; **66**: 387-412
- Gressner AM, Bachem MG. Molecular mechanisms of liver fibrogenesis—a homage to the role of activated fat-storing cells. *Digestion* 1995; **56**: 335-346
- Wu YX. Cytokine and liver. *Zhonghua Xiaohua Zazhi* 1998; **18**: 166-170
- Baroni GS, D'Ambrosio L, Curto P, Casini A, Mancini R, Jezequel AM, Benedetti A. Interferon gamma decreases hepatic stellate cell activation and extracellular matrix deposition in rat liver fibrosis. *Hepatology* 1996; **23**: 1189-1199
- Matsuoka M, Tsukamoto H. Stimulation of hepatic lipocyte collagen production by Kupffer cell-derived transforming growth factor beta: implication for a pathogenetic role in alcoholic liver fibrogenesis. *Hepatology* 1990; **11**: 599-605
- Di Sario A, Baroni GS, Bendia E, D'Ambrosio L, Ridolfi F, Marileo JR, Jezequel AM, Benedetti A. Characterization of ion transport mechanisms regulating intracellular pH in hepatic stellate cells. *Am J Physiol* 1997; **273**: G39-G48
- Knittel T, Mehde M, Kobold D, Saile B, Dinter C, Ramadori G. Expression patterns of matrix metalloproteinases and their inhibitors in parenchymal and non-parenchymal cells of rat liver: regulation by TNF-alpha and TGF-beta1. *J Hepatol* 1999; **30**: 48-60
- Mauviel A, Heino J, Kahari VM, Hartmann DJ, Loyau G, Pujol JP, Vuorio E. Comparative effects of interleukin-1 and tumor necrosis factor-alpha on collagen production and corresponding procollagen mRNA levels in human dermal fibroblasts. *J Invest Dermatol* 1991; **96**: 243-249
- Vairo G, Argyriou S, Bordun AM, Gonda TJ, Cragoe EJ, Hamilton JA. Na⁺/H⁺ exchange involvement in colony-stimulating factor-1-stimulated macrophage proliferation. Evidence for a requirement during late G1 of the cell cycle but not for early growth factor responses. *J Biol Chem* 1990; **265**: 16929-16939
- Di Sario A, Bendia E, Svegliati Baroni G, Ridolfi F, Bolognini L, Feliciangeli G, Jezequel AM, Orlandi F, Benedetti A. Intracellular pathways mediating Na⁺/H⁺ exchange activation by platelet-derived growth factor in rat hepatic stellate cells. *Gastroenterology* 1999; **116**: 1155-1166
- Roth-Eichhorn S, Eberheim A, Bode HP, Gressner AM. Transformation-dependent calcium influx by voltage-operated calcium channels in stellate cells of rat liver. *J Hepatol* 1999; **30**: 612-620
- Gong W, Pecci A, Roth S, Lahme B, Beato M, Gressner AM. Transformation-dependent susceptibility of rat hepatic stellate cells to apoptosis induced by soluble Fas ligand. *Hepatology* 1998; **28**: 492-502
- Muschen M, Warskulat U, Douillard P, Gilbert E, Haussinger D. Regulation of CD95(APO-1/Fas) receptor and ligand expression by lipopolysaccharide and dexamethasone in parenchymal and nonparenchymal rat liver cells. *Hepatology* 1998; **27**: 200-208
- Sakaida I, Uchida K, Hironaka K, Okita K. Prolyl 4-hydroxylase inhibitor (HOE 077) prevents TIMP-1 gene expression in rat liver fibrosis. *J Gastroenterol* 1999; **34**: 376-377
- Murawaki Y, Yamada S, Ikuta Y, Kawasaki H. Clinical usefulness of serum matrix metalloproteinase-2 concentration in patients with chronic viral liver disease. *J Hepatol* 1999; **30**: 1090-1098
- Ueno T, Sujaku K, Tamaki S, Ogata R, Kin M, Nakamura T, Sakamoto M, Torimura T, Mitsuyama K, Sakisaka S, Sata M, Tanikawa K. OK-432 treatment increases matrix metalloproteinase-9 production and improves dimethylnitrosamine-induced liver cirrhosis in rats. *Int J Mol Med* 1999; **3**: 497-503
- Liu YL, Li DG, Lu HM, Jiang ZM, Xu QF. The subcellular study of calcium antagonists in treatment of hepatofibrosis. *Xin Xiaohuabingxue Zazhi* 1996; **4**: 3-5
- Wang TL, Liu X, Zhou YP, He JW, Zhang J, Li NZ, Duan ZP, Wang BE. A semiquantitative scoring system for assessment of hepatic inflammation and fibrosis in chronic viral hepatitis. *Zhonghua Ganzhangbing Zazhi* 1998; **6**: 195-197
- Knodell RG, Ishak KG, Black WC, Chen TS, Craig R, Kaplowitz N, Kiernan TW, Wollman J. Formulation and application of a

- numerical scoring system for assessing histological activity in asymptomatic chronic active hepatitis. *Hepatology* 1981; **1**: 431-435
- 37 **Chevallier M**, Guerret S, Chossegros P, Gerard F, Grimaud JA. A histological semiquantitative scoring system for evaluation of hepatic fibrosis in needle liver biopsy specimens: comparison with morphometric studies. *Hepatology* 1994; **20**: 349-355
- 38 **Wang BE**. The diagnosis and severity assessment of liver fibrosis. *Zhonghua Ganzangbing Zazhi* 1998; **6**: 193-194
- 39 **Wang Q**, Ren XD, Qi Z, Li ML, Song X. The values of the serum variables in patients with alcoholic cirrhosis. *Huaren Xiaohua Zazhi* 1998; **6**: 364
- 40 **Gu SW**, Zhang L, Hou JL, Feng XR, Luo KX, Weng JY. The clinic value of serum HA and hPC III in liver cirrhosis and fibrosis. *Shijie Huaren Xiaohua Zazhi* 1999; **7**: 1011-1012
- 41 **Luo JQ**, Chen SQ, Wang F, Ren Y. The clinical significance of serum HA, PCIII, LN in the diagnosis of liver cirrhosis. *Huaren Xiaohua Zazhi* 1998; **6**(Suppl 7): 444
- 42 **Nyberg A**, Engstrom-Laurent A, Loof L. Serum hyaluronate in primary biliary cirrhosis-a biochemical marker for progressive liver damage. *Hepatology* 1998; **8**: 142-146
- 43 **Iwamoto H**, Nakamuta M, Tada S, Sugimoto R, Enjoji M, Nawata H. A p160ROCK-specific inhibitor, Y-27632, attenuates rat hepatic stellate cell growth. *J Hepatol* 2000; **32**: 762-770
- 44 **Marra F**, Arrighi MC, Fazi M, Caligiuri A, Pinzani M, Romanelli RG, Efsen E, Laffi G, Gentilini P. Extracellular signal-regulated kinase activation differentially regulates platelet-derived growth factor's actions in hepatic stellate cells, and is induced by *in vivo* liver injury in the rat. *Hepatology* 1999; **30**: 951-958
- 45 **Tao J**, Mallat A, Gallois C, Belmadani S, Mery PF, Nhieu JT, Pavoine C, Lotersztajn S. Biological effects of C-type natriuretic peptide in human myofibroblastic hepatic stellate cells. *J Biol Chem* 1999; **274**: 23761-23769
- 46 **Svegliati-Baroni G**, Ridolfi F, Di Sario A, Casini A, Marucci L, Gaggiotti G, Orlandoni P, Macarri G, Perego L, Benedetti A, Folli F. Insulin and insulin-like growth factor-1 stimulate proliferation and type I collagen accumulation by human hepatic stellate cells: differential effects on signal transduction pathways. *Hepatology* 1999; **29**: 1743-1751
- 47 **Carloni V**, Pinzani M, Giusti S, Romanelli RG, Parola M, Bellomo G, Failli P, Hamilton AD, Sebt SM, Laffi G, Gentilini P. Tyrosine phosphorylation of focal adhesion kinase by PDGF is dependent on ras in human hepatic stellate cells. *Hepatology* 2000; **31**: 131-140
- 48 **Li D**, Friedman SL. Liver fibrogenesis and the role of hepatic stellate cells: new insights and prospects for therapy. *J Gastroenterol Hepatol* 1999; **14**: 618-633
- 49 **Qi Z**, Atsuchi N, Ooshima A, Takeshita A, Ueno H. Blockade of type beta transforming growth factor signaling prevents liver fibrosis and dysfunction in the rat. *Proc Natl Acad Sci USA* 1999; **96**: 2345-2349
- 50 **Diamantis I**, Luthi M, Hosli M, Reichen J. Cloning of the rat ADAMTS-1 gene and its down regulation in endothelial cells in cirrhotic rats. *Liver* 2000; **20**: 165-172
- 51 **Cho JJ**, Hochoer B, Herbst H, Jia JD, Ruehl M, Hahn EG, Riecken EO, Schuppan D. An oral endothelin-A receptor antagonist blocks collagen synthesis and deposition in advanced rat liver fibrosis. *Gastroenterology* 2000; **118**: 1169-1178
- 52 **Lichtinghagen R**, Huegel O, Seifert T, Haberkorn CI, Michels D, Flemming P, Bahr M, Boeker KH. Expression of matrix metalloproteinase-2 and -9 and their inhibitors in peripheral blood cells of patients with chronic hepatitis C. *Clin Chem* 2000; **46**: 183-192
- 53 **Jiang XL**, Quan QZ, Sun ZQ, Wang YJ. The development of study of calmodulin antagonist in treating liver fibrosis. *Xin Xiaohuabingxue Zazhi* 1995; **3**: 161-162
- 54 **Liu XS**, Li DG, Lu HM, Xu QF. Effects of tetrandrine and verapamil on fibroblastic growth and proliferation. *Xin Xiaohuabingxue Zazhi* 1997; **5**: 82-83
- 55 **Jiang SL**, Yao XX, Sun YF. Treatment of liver cirrhosis. *Huaren Xiaohua Zazhi* 2000; **8**: 684-686
- 56 **Xu RY**, Ling YB, Wang ZL, Qiu WC, Yang HZ. Gan-xian-fang treats post-hepatitis cirrhosis. *Shijie Huaren Xiaohua Zazhi* 1999; **7**: 866
- 57 **Li BS**, Wang J, Zhen YJ, Wang XG, Sun YH, Wang SQ, Wu ZQ. Blocking effect of Chinese herbs Yiganxian and PHGF on immunodamaged hepatic fibrosis in rats. *Huaren Xiaohua Zazhi* 1998; **6**: 786-788
- 58 **Hu YY**, Liu C, Liu P, Gu HT, Ji G, Wang XL. Anti-fibrosis and anti-peroxidation of lipid effects of Fuzhenghuayu decoction on rat liver induced by CCl₄. *Xin Xiaohuabingxue Zazhi* 1997; **5**: 485-486
- 59 **Sun KW**, Chu YY, Chen X, Xie FY, Liu WS. Experimental Study of Dahunag Zhechong Pill(DHZC) in Treatment of Liver Fibrosis. *Zhongxiyi Jiehe Ganbing Zazhi* 1997; **7**: 90-92
- 60 **Yao XX**, Fu YL, Li XL. A multi-central study of the effect of yigan-chong-ji in treating chronic hepatitis of 324 cases. *Hebei Yixueyuan Xuebao* 1989; **10**: 231-233
- 61 **Cheng ML**, Ding YS, Leng XK, Yang J, Luo TY, Luo YF, Tian M, Lu YY, Liu Q, Wu J. Radix Stepheniae Tetrandiae and Radix Salviae Miltiorrhiza. *Zhongyi Zazhi* 1997; **38**: 361-362
- 62 **Zhang GL**, Gao FA, Li M, Ji XY. The effect of Ruan Gan Yin on erythrocyte superoxide dismutase, plasma lipoeroxide, serum hyaluronic acid and serum laminin in patients with hepatocirrhosis. *Zhongxiyi Jiehe Ganbing Zazhi* 1996; **6**: 8-11
- 63 **Goullis J**, Patch D, Burroughs AK. Bacterial infection in the pathogenesis of variceal bleeding. *Lancet* 1999; **353**: 139-142
- 64 **Jing CC**, Fu B, Cheng WF. The forecast and prognosis of 42 cases of patients with liver cirrhosis and esophageal varice bleeding. *Xin Xiaohuabingxue Zazhi* 1995; **3**: 243
- 65 **Okuda K**, Kono K, Ohnishi K, Kimura K, Omata M, Koen H, Nakajima Y, Musha H, Hirashima T, Takashi M. Clinical study of eighty-six cases of idiopathic portal hypertension and comparison with cirrhosis with splenomegaly. *Gastroenterology* 1984; **86**: 600-610
- 66 **D'Amico G**, Pagliaro L, Bosch J. The treatment of portal hypertension: a meta-analytic review. *Hepatology* 1995; **22**: 332-354
- 67 **Bernard B**, Grange JD, Khac EN, Amiot X, Opolon P, Poynard T. Antibiotic prophylaxis for the prevention of bacterial infections in cirrhotic patients with gastrointestinal bleeding: a meta-analysis. *Hepatology* 1999; **29**: 1655-1661
- 68 **Goullis J**, Armonis A, Patch D, Sabin C, Greenslade L, Burroughs AK. Bacterial infection is independently associated with failure to control bleeding in cirrhotic patients with gastrointestinal hemorrhage. *Hepatology* 1998; **27**: 1207-1212
- 69 **Bernard B**, Cadranet JF, Valla D, Escolano S, Jarlier V, Opolon P. Prognostic significance of bacterial infection in bleeding cirrhotic patients: a prospective study. *Gastroenterology* 1995; **108**: 1828-1834
- 70 **Yao XX**. The situation and development of study of liver diseases and uppergastrointestinal bleeding. *Huaren Xiaohua Zazhi* 1998; **6**(Suppl 7): 36-38
- 71 **Su L**, Pan HZ, Hong MY. The comparison study of knot and sclerosis in treating esophageal varices. *Huaren Xiaohua Zazhi* 1998; **6**(Suppl 7): 356
- 72 **Zhou QL**, Kou XB, Shen GX, Fu YQ. Octritide treating esophageal varice bleeding in patients with liver cirrhosis. *Huaren Xiaohua Zazhi* 1998; **6**(Suppl 7): 354
- 73 **Cao P**, Li RM. Thrombin treating digestive tract bleeding under endoscopy. *Huaren Xiaohua Zazhi* 1998; **6**(Suppl 7): 344
- 74 **Yao XX**, Li XT, Li YW, Zhang XY. Clinical and experimental study of radix salviae miltiorrhiza and other Chinese herbs of blood-activating and stasis-eliminating effects on hemodynamics of portal hypertension. *Zhonghua Xiaohua Zazhi* 1998; **18**: 24-27
- 75 **Yao XX**, Cui DL, Sun YF, Li XT. Clinical and experimental study of effect of Raondix Salviae Miltiorrhiza and other blood-activating and stasis-eliminating Chinese herbs on hemodynamics of portal hypertension. *World J Gastroenterol* 1998; **4**: 439-442
- 76 **Rivolta R**, Maggi A, Cazzaniga M, Castagnone D, Panzeri A, Solenghi D, Lorenzano E, di Palo FQ, Salerno F. Reduction of renal cortical blood flow assessed by Doppler in cir-

- rhotic patients with refractory ascites. *Hepatology* 1998; **28**: 1235-1240
- 77 **Gong QT**, Liu F, Xia KW, Jiang HQ, Yao XX. The effect of paracentesis and intravenous albumin infusion on plasma ANF and RAA system in cirrhotics with ascites. *Xin Xiaohuabingxue Zazhi* 1997; **5**: 305-307
- 78 **Han QX**, Huang ZM, Lin XY. Treating refractory ascites in patients with liver cirrhosis by emitting ascites and intravenous dextran. *Xin Xiaohuabingxue Zazhi* 1997; **5**: 186
- 79 **Bruno S**, Borzio M, Romagnoni M, Battezzati PM, Rossi S, Chiesa A, Podda M. Comparison of spontaneous ascites filtration and reinfusion with total paracentesis with intravenous albumin infusion in cirrhotic patients with tense ascites. *BMJ* 1992; **304**: 1655-1658
- 80 **Yang H**, Li SJ, Zhao JH, Zhang W, Zhang CG. Radionuclide renal dynamic imaging in the diagnosis of subclinical hepatorenal syndrome. *Xin Xiaohuabingxue Zazhi* 1997; **5**: 86-87
- 81 **Hua J**, Li JQ, Zeng MD, Zhang DR, Dong XX. A study of intestinal flora in patients with cirrhosis. *Zhonghua Ganzangbing Zazhi* 1998; **6**: 79-81
- 82 **Perez-Ruiz M**, Ros J, Morales-Ruiz M, Navasa M, Colmenero J, Ruiz-del-Arbol L, Cejudo P, Claria J, Rivera F, Arroyo V, Rodes J, Jimenez W. Vascular endothelial growth factor production in peritoneal macrophages of cirrhotic patients: regulation by cytokines and bacterial lipopolysaccharide. *Hepatology* 1999; **29**: 1057-1063
- 83 **Sun ZQ**, Wang YJ, Quan QZ, Liu XF, Zhang ZJ. The significance of nervous evoked potentials in the diagnosis of subclinical hepatic encephalopathy in patients with liver cirrhosis. *Xin Xiaohuabingxue Zazhi* 1994; **2**: 217-218
- 84 **An ZY**, Xu DY, Wu HQ. Special complications in liver cirrhosis. *Xin Xiaohuabingxue Zazhi* 1996; **4**: 42-43
- 85 **Yang HQ**, Huang CY. Forty-eight cases of peptic ulcers in liver cirrhosis and portal hypertension. *Xin Xiaohuabingxue Zazhi* 1994; **2**: 119-120
- 86 **Wang Y**, Wang HT, Guo XN, Fan N. The endoscopic observations of colonic mucosa in liver cirrhosis and portal hypertension. *Xin Xiaohuabingxue Zazhi* 1994; **2**: 48
- 87 **Qiao ZN**, Miao JY. Forty cases of hepatopulmonary syndrome. *Xin Xiaohuabingxue Zazhi* 1996; **4**: 410
- 88 **Wang AY**, Hou PZ, Gao J. The heart damages caused by liver cirrhosis. *Zhonghua Xiaohua Zazhi* 1998; **18**: 184

Edited by Chen WW and Wang XL

• GASTRIC CANCER •

Increased expression of mitogen-activated protein kinase and its upstream regulating signal in human gastric cancer

Bin Liang, Shan Wang, Xue-Guang Zhu, Yong-Xiang Yu, Zhi-Rong Cui, You-Zhi Yu

Bin Liang, Xue-Guang Zhu, Yong-Xiang Yu, Zhi-Rong Cui, Shan Wang, Division of Surgical Oncology and Division of Gastrointestinal Surgery, Peking University People's Hospital, Beijing 100044, China
You-Zhi Yu, Division of Pathology, Peking University People's Hospital, Beijing 100044, China

Supported by Technology Foundation of Ministry of Education, China
Correspondence to: Professor Shan Wang, Mentor of Doctor, Division of Surgical Oncology and Division of Gastrointestinal Surgery, Peking University People's Hospital, Beijing 100044, China. liangbin_df@yahoo.com.cn

Telephone: +86-10-68792772 **Fax:** +86-10-68318386

Received: 2004-05-11 **Accepted:** 2004-06-17

Abstract

AIM: To investigate the expression of mitogen-activated protein kinases (MAPKs) and its upstream protein kinase in human gastric cancer and to evaluate the relationship between protein levels and clinicopathological parameters.

METHODS: Western blot was used to measure the expression of extracellular signal-regulated kinase (ERK)-1, ERK-2, ERK-3, p38 and mitogen or ERK activated protein kinase MEK-1 proteins in surgically resected gastric carcinoma, adjacent normal mucosa and metastatic lymph nodes from 42 patients. Immunohistochemistry was employed for their localization.

RESULTS: Compared with normal tissues, the protein levels of ERK-1 (integral optical density value $159\ 526 \pm 65\ 760$ vs $122\ 807 \pm 65\ 515$, $P = 0.001$), ERK-2 ($168\ 471 \pm 95\ 051$ vs $120\ 469 \pm 72\ 874$, $P < 0.001$), ERK-3 ($118\ 651 \pm 71\ 513$ vs $70\ 934 \pm 68\ 058$, $P < 0.001$), P38 ($104\ 776 \pm 51\ 650$ vs $82\ 930 \pm 40\ 392$, $P = 0.048$) and MEK-1 ($116\ 486 \pm 45\ 725$ vs $101\ 434 \pm 49\ 387$, $P = 0.027$) were increased in gastric cancer tissues. Overexpression of ERK-3 was correlated to TNM staging [average ratio of integral optic density (IOD)_{tumor}: IOD_{normal} in TNM I, II, III, IV tumors was 1.43 ± 0.34 , 5.08 ± 3.74 , 4.99 ± 1.08 , 1.44 ± 1.02 , $n = 42$, $P = 0.023$] and serosa invasion (4.31 ± 4.34 vs 2.00 ± 2.03 , $P = 0.037$). In poorly differentiated cancers ($n = 33$), the protein levels of ERK-1 and ERK-2 in stage III and IV tumors were higher than those in stage I and II tumors (2.64 ± 3.01 vs 1.01 ± 0.33 , $P = 0.022$; 2.05 ± 1.54 vs 1.24 ± 0.40 , $P = 0.030$). Gastric cancer tissues with either lymph node involvement (2.49 ± 2.91 vs 1.03 ± 0.36 , $P = 0.023$; 1.98 ± 1.49 vs 1.24 ± 0.44 , $P = 0.036$) or serosa invasion (2.39 ± 2.82 vs 1.01 ± 0.35 , $P = 0.022$; 1.95 ± 1.44 vs 1.14 ± 0.36 , $P = 0.015$) expressed higher protein levels of ERK-1 and ERK-2. In Borrmann II tumors, expression of ERK-2 and ERK-3 was increased compared with Borrmann III tumors (2.57 ± 1.86 vs 1.23 ± 0.60 , $P = 0.022$; 5.50 ± 5.05 vs 1.83 ± 1.21 , $P = 0.014$). Borrmann IV tumors expressed higher p38 protein levels. No statistically significant difference in expression of MAPKs was found when stratified to tumor size or histological grade ($P > 0.05$). Protein levels of ERK-2, ERK-3 and MEK-1 in metastatic lymph nodes were 2-7 folds higher than those in adjacent normal mucosa. The immunohistochemistry demonstrated

that ERK-1, ERK-2, ERK-3, p38 and MEK-1 proteins were mainly localized in cytoplasm. The expression of MEK-1 in gastric cancer cells metastasized to lymph nodes was higher than that of the primary site.

CONCLUSION: MAPKs, particularly ERK subclass are overexpressed in the majority of gastric cancers. Overexpression of ERKs is correlated to TNM staging, serosa invasion, and lymph node involvement. The overexpression of p38 most likely plays a prominent role in certain morphological subtypes of gastric cancers. MEK-1 is also overexpressed in gastric cancer, particularly in metastatic lymph nodes. Upregulation of MAPK signal transduction pathways may play an important role in tumorigenesis and metastatic potential of gastric cancer.

© 2005 The WJG Press and Elsevier Inc. All rights reserved.

Key words: Gastric cancer; Mitogen-activated protein kinase; Extracellular signal-regulated kinase; Signal transduction

Liang B, Wang S, Zhu XG, Yu YX, Cui ZR, Yu YZ. Increased expression of mitogen-activated protein kinase and its upstream regulating signal in human gastric cancer. *World J Gastroenterol* 2005; 11(5): 623-628
<http://www.wjgnet.com/1007-9327/11/623.asp>

INTRODUCTION

The incidence and mortality of gastric cancer have decreased markedly since 1930s^[1]. This decrease is mirrored worldwide, but it is comparatively higher in Japan, China, Chile, and Ireland. Gastric cancer still is the leading cause of cancer-related deaths in China^[2].

Surgical removal with resection of adjacent lymph nodes offers the only chance for cure, which is less than 33% of patients with gastric cancer. The five-year survival rate is 30-40% with a poorer prognosis of advanced tumors^[3-5]. Thus far, current treatments have largely been unsuccessful. Therefore it is critical to further elucidate the etiological factors and molecular mechanism for the pathogenesis of gastric cancer.

Mitogen-activated protein kinases (MAPKs) are serine/threonine kinases activated in response to a variety of external signals. Three major subclasses of MAPKs, namely, extracellular signal-regulated kinase (ERK), c-Jun NH₂-terminal kinase (JNK), and p38 have been identified^[6,7]. Various receptor tyrosine kinases, cytokine receptors, G proteins and oncogene products can activate MAPKs through phosphorylation by mitogen activated protein kinase or ERK-activated protein kinase (MEK)^[8-10]. Thus, MAPKs are proposed to be a critical integrator of various signaling transduction systems and involved in various cellular processes including cell proliferation, differentiation, apoptosis, and transformation^[6,7]. Constitutive activation of these signaling cascades has been noted in the malignant transformation of various cell lines^[11,12] and implicated in carcinogenesis and metastatic potential of

human cancers^[13-15]. The purpose of this study was to investigate the expression of MAPKs and its upstream regulating signals in human gastric cancer and to evaluate the relationship between protein levels and clinicopathological parameters.

MATERIALS AND METHODS

Materials

Immobilon PPVDF membranes for Western blot were purchased from Millipore (Bedford, MA), and X-ray film was purchased from Eastman Kodak (Rochester, NY). Antibodies to ERK-1 (sc-94), ERK-2 (sc-154), ERK-3 (sc-155), p38 (sc-535) and MEK-1 (sc-219) were purchased from Santa Cruz Biotechnology (Santa Cruz, CA). The enhanced chemiluminescence (ECL) system for Western immunoblot analysis was purchased from Amersham (Arlington Heights, IL). The concentrated protein assay dye reagent was purchased from Bio-Rad Laboratories (Hercules, CA). All other reagents were of molecular biology grade and purchased from either Sigma or Amresco (Solon, OH).

Tissue procurement and whole cell extracts

Primary gastric adenocarcinomas, adjacent (5 to 10 cm from the primary site) normal mucosa and metastatic lymph nodes were obtained from 42 continuously enrolled patients undergoing elective radical gastrectomy at the Peking University People's Hospital from July 1998 to January 2000. Resected tissues were immediately flash frozen with liquid nitrogen. Tumors were classified according to the histological subgroups recommended by the World Health Organization (WHO) and staged by the TNM system.

Tissues were homogenized on ice in RIPA lysis buffer (50 mmol/L NaCl, 50 mmol/L Tris, pH 7.4, 0.5% NP-40, 1 mmol/L EDTA, 1 mmol/L dithiothreitol, 1 mmol/L Na₃VO₄, 1 mmol/L phenylmethylsulfonyl fluoride, 1 mmol/L NaF, 1 µg/mL aprotinin, 1 µg/mL leupeptin). Cell extracts were then clarified by centrifugation (for 30 min at 12 000 g) and protein concentration was determined using the method of Bradford^[16].

Western blotting

Western blotting was performed as described previously^[17]. Briefly, whole cell lysates (50 µg) were denatured in SDS sample loading buffer (50 mmol/L Tris, pH 6.8, 100 mmol/L DTT, 2% SDS, 0.1% bromophenol blue, 10% glycerol) and fractionated on a 10% SDS-polyacrylamide gel. Proteins were electroblotted to Immobilon-P PVDF membranes. Filters were probed overnight at 4 °C in blocking solution (TBS containing 5% non-fat dried milk, 0.1% Tween 20) followed by an incubation for 3 h with the primary antibody. Filters were then washed in blocking solution and incubated with a horseradish peroxidase-conjugated donkey anti-rabbit immunoglobulin G (IgG) as a secondary antibody for 1 h. After 4 final washes, the immune complexes were visualized using ECL detection. ERK-1, ERK-2, ERK-3, p38 and MEK-1 expression in tumor and paired normal mucosae were quantitated by densitometry to obtain an integral optic density (IOD) value.

Immunohistochemical staining

In brief, sections (5 µm thick) placed on silane-coated slides (Muto Pure Chemicals, Sigma, Co. USA) were deparaffinized, rehydrated and then pretreated with 3% H₂O₂ in methanol for 20 min at 25 °C to quench the endogenous peroxidase activity. The sections were then placed in 10 mmol/L citrate buffer (pH 6.0) and heated in a microwave oven (400 W) for 10 min to facilitate antigen retrieval. Subsequently, the sections were incubated with 10% goat non-immune serum-3% BSA in PBS at room temperature for 60 min to block the nonspecific binding

and then incubated with primary antibodies for 1 h. The sections were then incubated at room temperature with the secondary antibodies (biotinylated goat anti-rabbit IgG; Dako, Denmark) followed by incubation with avidin-biotin-peroxidase complex (Dako, Denmark), labeled with peroxidase and colored with diaminobenzidine substrate. Sections of gastric adenocarcinoma, confirmed to overexpress the protein of interest, were used as positive controls. No primary antibody was used as negative control.

Statistical analysis

Paired-samples *t* test was used to analyze the difference in MAPKs expression between cancer tissues and normals. Either independent-sample *t* test or one-way ANOVA was used to analyze the relationships between IOD_{tumor}/IOD_{normal} ratios and clinicopathological characteristics. All analyses were performed with the SPSS statistical software (Ver. 9.0). *P* values less than 0.05 were considered statistically significant.

RESULTS

Expression of ERK-1, ERK-2, ERK-3, p38 and MEK-1 in gastric cancer

To determine whether ERK-1, ERK-2 or ERK-3 was overexpressed in gastric cancer, 42 gastric cancer tissues and adjacent normal mucosa were examined by Western blot. The protein levels of ERK-1, ERK-2 and ERK-3 were increased in gastric cancer tissues compared with adjacent normal mucosa (*P*<0.001, Table 1). ERK-1, ERK-2 and ERK-3 were overexpressed, as defined by an IOD_{tumor}/IOD_{normal} ratio >1.3, in 22, 22 and 27 cases of gastric cancer, respectively (Figure 1). The average protein levels of ERK-1, ERK-2 and ERK-3 in gastric cancer were 2.10, 2.04 and 3.85 folds higher than those in adjacent normal mucosa, respectively. Because parts of our samples were used up in previous experiments, the expressions of p38 and MEK-1 were detected in 30 gastric cancers. The protein levels of p38 (*P*=0.048) and MEK-1 (*P*=0.027, Table 1) were increased in gastric cancer tissues compared with adjacent normal mucosa. MEK-1 and p38 were overexpressed in 14 and 12 cases of gastric cancer, respectively (Figure 1). The average protein levels of p38 and MEK-1 in gastric cancer were 1.71 and 1.31 folds higher than those in adjacent normal mucosa, respectively.

Table 1 Integral optical density value of gastric cancer and adjacent normal mucosa (mean±SD)

Items	<i>n</i>	IOD value		<i>t</i>	<i>P</i>
		Gastric cancer	Normal mucosa		
ERK-1	42	159 526±65 760	122 807±65 515	3.658	0.001
ERK-2	42	168 471±95 051	120 469±72 874	4.758	<0.001
ERK-3	42	118 651±71 513	709 34±68 058	5.065	<0.001
p38	30	104 776±51 650	829 30±40 392	2.064	0.048
MEK-1	30	116 486±45 725	101 434±49 387	2.160	0.027

Relationships between expressions of ERK-1, ERK-2, ERK-3, p38, MEK-1 and clinicopathological characteristics

When stratified to clinicopathological parameters, expression of ERK-2 and ERK-3 was increased in Borrmann II tumors in comparison to Borrmann III or Borrmann IV tumors (2.57±1.86 vs 1.23±0.60, *P*=0.022; 5.50±5.05 vs 1.83±1.21, *P*=0.014). The protein levels of ERK-3 were higher in stage II and stage III tumors than those in stage I and IV tumors (average ratio of IOD_{tumor}:IOD_{normal} in TNM I, II, III, IV tumors was 1.43±0.34, 5.08±3.74, 4.99±1.08, 1.44±1.02, *n*=42, *P*=0.023). Stage III tumors trended to express higher levels of ERK-1 and ERK-2 proteins, but no statistically significant difference was found (*P*>0.05). Gastric cancer tissues with serosa invasion expressed higher protein levels of ERK-3 (4.31±4.34 vs 2.00±2.03, *P*=0.037).

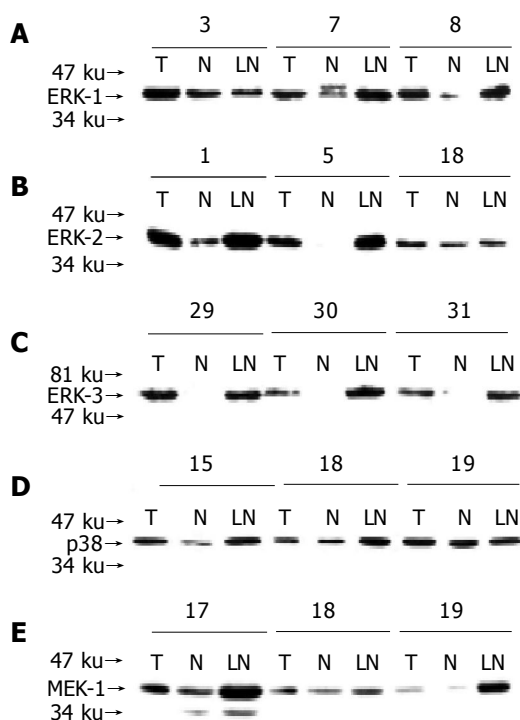


Figure 1 Assessment of ERK-1, ERK-2, ERK-3, p38 and MEK-1 expression by Western blot. A: Expression of ERK-1 in gastric carcinoma; B: Expression of ERK-2 in gastric carcinoma; C: Expression of ERK-3 in gastric carcinoma; D: Expression of p38 in gastric carcinoma; E: Expression of MEK-1 in gastric carcinoma. Rabbit polyclonal anti-ERK-1, anti-ERK-2, anti-ERK-3, anti-p38 and anti-MEK-1 antibodies were used to recognize the 44 ku, 42 ku, 63 ku, 41 ku, and 41 ku isoforms respectively.

Interestingly, in 33 cases of poorly differentiated cancer, the protein levels of ERK-1 and ERK-2 in stage III and IV tumors were higher than those in stage I and II tumors (Table 2, $P < 0.05$).

Table 2 Relationship between ERK1/2 expression and clinicopathological characteristics in poorly differentiated gastric cancers (mean±SD)

Items	n	ERK1			ERK2		
		T:N ratio ¹	F (t)	P	T:N ratio ¹	F (t)	P
TNM stage							
I, II	11	1.01±0.33	2.505	0.022	1.24±0.40	2.297	0.030
III, IV	22	2.64±3.01			2.05±1.54		
Lymph node involvement							
+	24	2.49±2.91	2.421	0.023	1.98±1.49	2.191	0.036
-	9	1.03±0.36			1.24±0.44		
Serosa invasion							
+	26	2.39±2.82	2.428	0.022	1.95±1.44	2.585	0.015
-	7	1.01±0.35			1.14±0.36		
Tumor size							
<5 cm	19	1.97±2.30	0.323	0.749	1.72±1.31	0.309	0.760
>5 cm	14	2.27±2.96			1.86±1.39		
Borrmann classification							
I	5	1.27±0.53	1.420	0.257	0.96±0.22	1.169	0.338
II	22	2.17±1.64			2.96±3.27		
III	12	1.30±0.68			1.02±0.37		
IV	3	1.38±0.19			1.59±0.20		

¹ Average ratio of IOD_{tumor}: IOD_{normals}.

Gastric cancer tissues with either lymph node metastasis or serosa invasion expressed higher protein levels of ERK-1 and ERK-2 ($P < 0.05$). No statistically significant difference in ERK expression was found when stratified to tumor size or histological grade ($P > 0.05$).

No statistically significant association was found between the IOD_{tumor}/IOD_{normal} ratio of p38 or MEK-1 proteins when stratified to age, sex, histological classification, or TNM staging of patients. However in Borrmann IV cancers, there was an increase in p38 expression compared with Borrmann II (3.83 ± 4.43 vs 1.64 ± 1.21 , $P = 0.039$) and Borrmann III tumors (3.83 ± 4.43 vs 1.19 ± 0.89 , $P = 0.019$), as defined by the average ratio of IOD_{tumor}: IOD_{normal}.

Expression of MAPKs and MEK-1 in metastatic lymph nodes

Although the cellular content of metastatic lymph nodes was heterogenous, we found that the overall expression of ERK-2, and ERK-3 was still increased (Figure 1 and Table 3). The average protein levels of ERK-2 and ERK-3 in metastatic lymph nodes were 1.68 and 6.89 folds higher than those in adjacent normal mucosa in 14 paired samples, respectively.

Metastatic lymph nodes expressed higher levels of MEK-1 protein when compared with normal mucosa and primary sites ($P < 0.05$, Figure 1 and Table 3). The average protein level of MEK-1 in metastatic lymph nodes was 2.09 folds higher than that in adjacent normal mucosa in 12 paired samples. The protein level of p38 was not increased in metastatic lymph nodes in comparison to normal mucosa or primary sites ($P > 0.05$).

Immunohistochemical staining

Immunohistochemistry of gastric carcinomas and normal mucosa demonstrated that ERK-1, ERK-2, ERK-3, p38 and MEK1 proteins were localized in the cytoplasm. Gastric cancer cells expressed higher levels of these proteins compared with adjacent normal mucosa. In particular, the expression of MEK-1 in metastatic gastric cancer cells localized in lymph nodes was higher than that of the primary sites (Figures 2A-D).

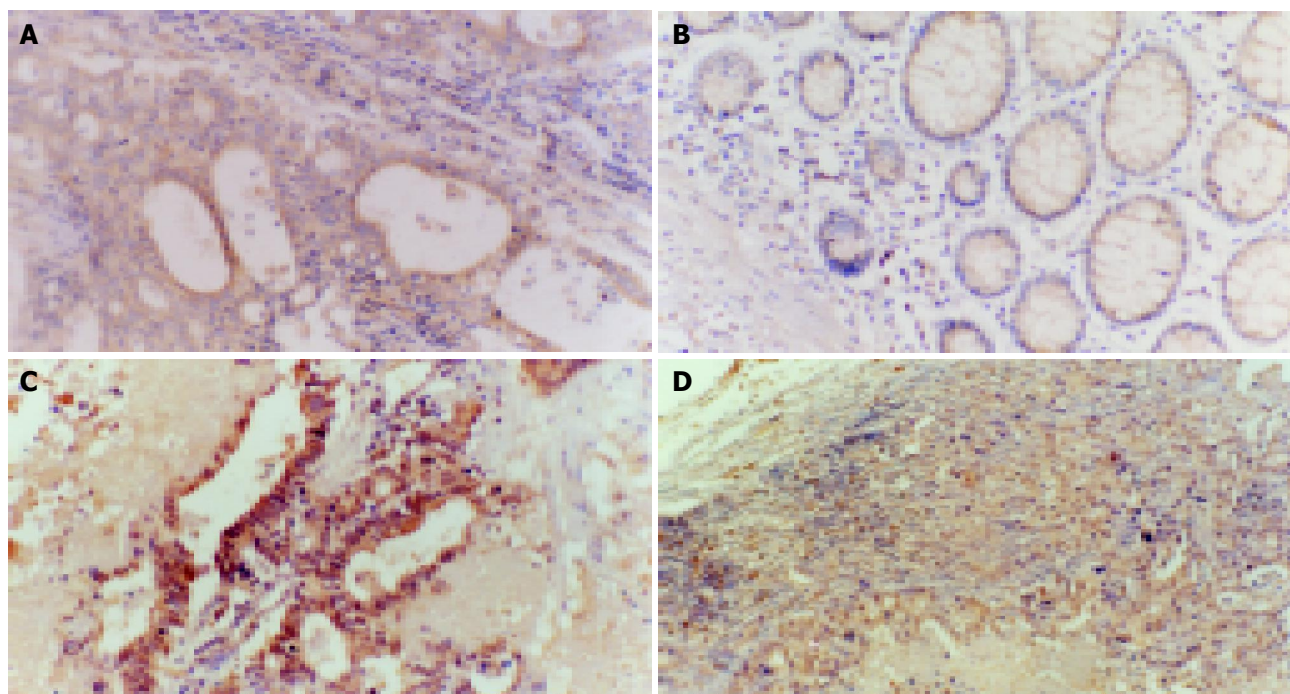


Figure 2 Assessment of MEK-1 expression in human gastric cancer, adjacent normal mucosa, and metastatic lymph nodes by immunohistochemical staining. Magnification, A-C, $\times 200$; D, $\times 100$. A: Expression of MEK-1 in primary sites; B: Expression of MEK-1 in normal mucosa; C, D: Expression of MEK-1 in metastatic lymph nodes.

Table 3 Expression of ERK-1, ERK-2, ERK-3, p38 and MEK-1 in metastatic lymph nodes (mean \pm SD)

Items	<i>n</i>	IOD value	<i>t</i>	<i>P</i>
ERK-1				
Metastatic lymph nodes	14	195 734.7 \pm 70 508.8		
Primary site		210 423.7 \pm 74 207.3	0.608	0.554 ^b
Normal mucosa		155 862.3 \pm 79 052.8	1.453	0.170 ^a
ERK-2				
Metastatic lymph nodes	14	186 959.5 \pm 80 801.8		
Primary site		211 155.1 \pm 64 116.8	0.893	0.388 ^b
Normal mucosa		127 092.4 \pm 56 585.6	2.579	0.023 ^a
ERK-3				
Metastatic lymph nodes	14	140 323.2 \pm 120 532.0		
Primary site		98 732.1 \pm 54 021.3	1.261	0.230 ^b
Normal mucosa		50 032.9 \pm 58 937.8	3.116	<0.001 ^a
P38				
Metastatic lymph nodes	12	96 866.8 \pm 76 857.3		
Primary site		99 740.6 \pm 38 279.6	0.202	0.844 ^b
Normal mucosa		77 784.4 \pm 30 367.0	0.797	0.442 ^a
MEK-1				
Metastatic lymph nodes	12	133 353.9 \pm 42 374.3		
Primary site		101 112.5 \pm 39 124.0	2.203	0.05 ^b
Normal mucosa		77 431.9 \pm 31 282.1	4.235	<0.001 ^a

^a $P < 0.05$ vs normal mucosa; ^b $P > 0.05$ vs primary site.

DISCUSSION

Mitogen-activated protein kinase is a key molecule in intracellular signal transducing pathways that transport extracellular stimuli from cell surface to nuclei. MAPK pathway has been revealed to be involved in the physiological proliferation of mammalian cells and also to potentiate them to transform^[6,7]. With regard to human gastric carcinoma, investigations of alterations in expression and activity of components of the MAPK cascade will help to understand the mechanisms of malignant behaviors of gastric cancer cells.

In the present report, the expression of MAPKs was examined by Western blot in 42 gastric cancer tissues and adjacent normal mucosa. Our results demonstrate that the protein levels of ERK-1, ERK-2 and ERK-3 are increased in gastric cancer tissues compared with adjacent normal mucosa. The average protein levels of ERK-1, ERK-2 and ERK-3 in gastric cancers are 2.10, 2.04 and 3.85 folds higher than those in adjacent normal mucosa, respectively. In a previous report^[18], we showed an increase of phosphorylated ERK1/2 in gastric adenocarcinoma compared to normals and the consistency of

ERK1/2 activity and expression. Therefore, our results suggest that ERK hyperexpression and increased activation may contribute to the determination of the constitutive activation of MAPK/ERK pathways in gastric carcinoma. Iwase *et al.*^[19] found that upregulation of ERK pathway could contribute to proliferation and transformation of gastric mucosa cells. Thus constitutive activation of MAPK/ERK pathways may play an important role in tumorigenesis of gastric cancer.

Cancer development is thought to be regulated by the integration of distinct signals. It has been reported that ERK-3 is structurally related to the better characterized ERK-1 and ERK-2 with 43% overall homology^[20], however little is known about its cellular function. Recent studies have shown that activation of ERK-3 may participate in recovery of malignant behaviors of colon HD3 cell line, including tumorigenesis in nude mice^[21]. Wang *et al.*^[22] found that the activation of ERK-3 was increased in colon cancer, but the relationship between ERK-3 activation and clinicopathological characteristics remains to be identified. Our results demonstrate that overexpression of ERK-3 is noted in 64.3% samples, and increased protein levels of ERK-3 are found in TNM stage II and III tumors or Borrmann II tumors. The exact roles of ERK-3 in human cancer carcinogenesis has not been identified. Its upstream and downstream molecular targets are also unidentified. Our data show that ERK-3 is associated with the progression of gastric cancer, but the role is unclear. ERK-3 could be activated in certain morphological subtypes of gastric cancer, and might play an important role in a certain stage. Future investigation will provide the necessary information to shed lights on these points.

The ERK signaling pathway is associated with progression and metastatic potential of tumors. When we analyzed the relationship between ERK-1 and ERK-2 expression and clinicopathological characteristics of the patients, overexpression of these proteins was positively correlated with later TNM staging, lymph node involvement, and serosa invasion in poorly differentiated gastric carcinomas. Lengye *et al.*^[23] suggested the role of ERK pathway in regulation of urokinase-type plasminogen activator expression in NIH3T3 cells. Shibata *et al.*^[24] found that Ras signaling was required for enhanced matrix metalloproteinase 9 secretions induced by fibronectin in ovarian cancer cells. Taken together, our data show that overexpression of ERK-1 and ERK-2 is part of its upregulation in gastric cancer. Upregulation of ERKs may therefore play an important role in the progression and metastatic potential of gastric cancer.

Several recent studies have demonstrated that tumor cell invasion is associated with p38 MAPK signaling pathway^[25,26]. Huang *et al.*^[25] showed that endogenous p38 MAPK activity correlated well with breast carcinoma cell invasiveness. They have suggested that p38 MAPK signaling pathway is important for the maintenance of BT549 breast cancer cell invasive phenotype by promoting the stabilities of uPA and uPAR mRNA. In our study, the expression of p38 protein in gastric cancer was also increased. No statistically significant association was found between the IOD_{tumor}/IOD_{normal} ratio of p38 protein with age, sex, histological classification, or TNM staging of patients. However in Borrmann IV cancers, there was an increase in p38 expression compared with Borrmann II and III tumors. Our data may shed lights on the possible role of p38 in gastric cancer tumorigenesis. Further work will focus on the p38 activity in gastric cancer and the role of p38 pathway in gastric cancer tumorigenesis and metastasis.

Alterations in the upstream signals could lead to subsequent alterations within the intracellular phosphorylation cascade. Our data show that the protein level of MEK-1 is increased in

gastric cancer tissues and consistent with that of ERKs, suggesting that up regulated upstream signals are amplified through intracellular phosphorylation cascade and could lead to constitutive activation of MAPK signaling pathway.

Although the cellular content of metastatic lymph nodes was heterogeneous, we found that in metastatic lymph nodes, the expression of ERK-2, ERK-3, and MEK-1 was increased. Immunohistochemical data also show that the expression of MEK-1 in gastric cancer cells metastasized to lymph nodes is higher than that of the primary sites (Figures 2A-C). Sivaraman *et al.*^[27] used *in situ* RT-PCR to detect the expression of ERK mRNA in breast cancer cells metastasized to involved lymph nodes and found intense staining in the metastatic cancer cells, but not in the surrounding stromal cells within the lymph node. Webb *et al.*^[28] also found that the activity of ERK in metastatic NIH3T3 transformed cells was higher than that in parent cells. Their data suggest that overexpression of MAP kinase may potentiate metastases. All in all, upregulation of the MAP kinase pathway might be associated with malignant potential in gastric cancer and can potentiate metastases.

In conclusion, upregulation of ERK pathway rather than p38, plays a more important role in cancer tumorigenesis, aggressiveness and metastases. Future studies are required to better delineate the effectors that mediate the malignant phenotype. Studies, which assess resected human samples, are essential to our better understanding of the signaling mechanisms underlying the regulation of gastric carcinogenesis.

REFERENCES

- 1 Greenlee RT, Murray T, Bolden S, Wingo PA. Cancer statistics, 2000. *CA Cancer J Clin* 2000; **50**: 7-33
- 2 Guo HQ, Guan P, Shi HL, Zhang X, Zhou BS, Yuan Y. Prospective cohort study of comprehensive prevention to gastric cancer. *World J Gastroenterol* 2003; **9**: 432-436
- 3 Fuchs CS, Mayer RJ. Gastric carcinoma. *N Engl J Med* 1995; **333**: 32-41
- 4 Jatzko GR, Lisborg PH, Denk H, Klimpfinger M, Stettner HM. A 10-year experience with Japanese-type radical lymph node dissection for gastric cancer outside of Japan. *Cancer* 1995; **76**: 1302-1312
- 5 Bremers AJ, Rutgers EJ, van de Velde CJ. Cancer surgery: the last 25 years. *Cancer Treat Rev* 1999; **25**: 333-353
- 6 Whitmarsh AJ, Davis RJ. Transcription factor AP-1 regulation by mitogen-activated protein kinase signal transduction pathways. *J Mol Med (Berl)* 1996; **74**: 589-607
- 7 Seger R, Krebs EG. The MAPK signaling cascade. *FASEB J* 1995; **9**: 726-735
- 8 Zheng CF, Guan KL. Cloning and characterization of two distinct human extracellular signal-regulated kinase activator kinases, MEK1 and MEK2. *J Biol Chem* 1993; **268**: 11435-11439
- 9 Lenormand P, Sardet C, Pages G, L'Allemain G, Brunet A, Pouyssegur J. Growth factors induce nuclear translocation of MAP kinases (p42mapk and p44mapk) but not of their activator MAP kinase kinase (p45mapkk) in fibroblasts. *J Cell Biol* 1993; **122**: 1079-1088
- 10 Tibbles LA, Woodgett JR. The stress-activated protein kinase pathways. *Cell Mol Life Sci* 1999; **55**: 1230-1254
- 11 Manni A, Wechter R, Gilmour S, Verderame MF, Mauger D, Demers LM. Ornithine decarboxylase over-expression stimulates mitogen-activated protein kinase and anchorage-independent growth of human breast epithelial cells. *Int J Cancer* 1997; **70**: 175-182
- 12 Mansour SJ, Matten WT, Hermann AS, Candia JM, Rong S, Fukasawa K, Vande Woude GF, Ahn NG. Transformation of mammalian cells by constitutively active MAP kinase kinase. *Science* 1994; **265**: 966-970
- 13 Salh B, Marotta A, Matthewson C, Ahluwalia M, Flint J, Owen D, Pelech S. Investigation of the Mek-MAP kinase-Rsk pathway in human breast cancer. *Anticancer Res* 1999; **19**: 731-740

- 14 **Ito Y**, Sasaki Y, Horimoto M, Wada S, Tanaka Y, Kasahara A, Ueki T, Hirano T, Yamamoto H, Fujimoto J, Okamoto E, Hayashi N, Hori M. Activation of mitogen-activated protein kinases/extracellular signal-regulated kinases in human hepatocellular carcinoma. *Hepatology* 1998; **27**: 951-958
- 15 **Leav I**, Galluzzi CM, Ziar J, Stork PJ, Ho SM, Loda M. Mitogen-activated protein kinase and mitogen-activated kinase phosphatase-1 expression in the Noble rat model of sex hormone-induced prostatic dysplasia and carcinoma. *Lab Invest* 1996; **75**: 361-370
- 16 **Bradford MM**. A rapid and sensitive method for the quantitation of microgram quantities of protein utilizing the principle of protein-dye binding. *Anal Biochem* 1976; **72**: 248-254
- 17 **Wang S**, Evers BM. Caco-2 cell differentiation is associated with a decrease in stat protein levels and binding. *J Gastrointest Surg* 1999; **3**: 200-207
- 18 **Liang B**, Wang S, Zhu XG, Yu YX, Cui ZR, Jiang KW, Wang ZZ, Yu YZ. Increased expression of extracellular signal-regulated kinase in human gastric cancer. *Zhonghua Putong Waike Zazhi* 2001; **16**: 409-412
- 19 **Iwase T**, Tanaka M, Suzuki M, Naito Y, Sugimura H, Kino I. Identification of protein-tyrosine kinase genes preferentially expressed in embryo stomach and gastric cancer. *Biochem Biophys Res Commun* 1993; **194**: 698-705
- 20 **Gonzalez FA**, Raden DL, Rigby MR, Davis RJ. Heterogeneous expression of four MAP kinase isoforms in human tissues. *FEBS Lett* 1992; **304**: 170-178
- 21 **Sauma S**, Friedman E. Increased expression of protein kinase C beta activates ERK3. *J Biol Chem* 1996; **271**: 11422-11426
- 22 **Wang Q**, Ding Q, Dong Z, Ehlers RA, Evers BM. Downregulation of mitogen-activated protein kinases in human colon cancers. *Anticancer Res* 2000; **20**: 75-83
- 23 **Lengye E**, Singh B, Gum R, Nerlov C, Sabichi A, Birrer M, Boyd D. Regulation of urokinase-type plasminogen activator expression by the v-mos oncogene. *Oncogene* 1995; **11**: 2639-2648
- 24 **Shibata K**, Kikkawa F, Nawa A, Thant AA, Naruse K, Mizutani S, Hamaguchi M. Both focal adhesion kinase and c-Ras are required for the enhanced matrix metalloproteinase 9 secretion by fibronectin in ovarian cancer cells. *Cancer Res* 1998; **58**: 900-903
- 25 **Huang S**, New L, Pan Z, Han J, Nemerow GR. Urokinase plasminogen activator/urokinase-specific surface receptor expression and matrix invasion by breast cancer cells requires constitutive p38 alpha mitogen-activated protein kinase activity. *J Biol Chem* 2000; **275**: 12266-12272
- 26 **Miki H**, Yamada H, Mitamura K. Involvement of p38 MAP kinase in apoptotic and proliferative alteration in human colorectal cancers. *Anticancer Res* 1999; **19**: 5283-5291
- 27 **Sivaraman VS**, Wang H, Nuovo GJ, Malbon CC. Hyperexpression of mitogen-activated protein kinase in human breast cancer. *J Clin Invest* 1997; **99**: 1478-1483
- 28 **Webb CP**, Van Aelst L, Wigler MH, Vande Woude GF. Signaling pathways in Ras-mediated tumorigenicity and metastasis. *Proc Natl Acad Sci USA* 1998; **95**: 8773-8778

Assistant Editor Guo SY Edited by Wang XL

Expression of Epstein-Barr virus genes in EBV-associated gastric carcinomas

Bing Luo, Yun Wang, Xiao-Feng Wang, Hua Liang, Li-Ping Yan, Bao-Hua Huang, Peng Zhao

Bing Luo, Yun Wang, Xiao-Feng Wang, Hua Liang, Li-Ping Yan, Department of Microbiology, Qingdao University Medical College, Qingdao 266021, Shandong Province, China

Bao-Hua Huang, Department of Oncology, Yantai Yuhuangding Hospital, Yantai 264002, Shandong Province, China

Peng Zhao, Department of Pathology, Affiliated Hospital of Qingdao University Medical College, Qingdao 266003, Shandong Province, China

Supported by National Natural Science Foundation of China, No 30371618

Correspondence to: Professor Bing Luo, Department of Microbiology, Qingdao University Medical College, Number 38 of Dengzhou Road, Qingdao 266021, Shandong Province, China. qingdaoluobing@yahoo.com

Telephone: +86-532-3812423

Received: 2004-03-11 **Accepted:** 2004-04-20

Abstract

AIM: To understand the expression of latent and lytic genes of Epstein-Barr virus (EBV) in EBV-associated gastric carcinoma (EBVaGC) and to explore the relationship between EBV-encoded genes and development of EBVaGC at molecular level.

METHODS: One hundred and seventy-two gastric carcinoma tissues and 172 corresponding para-carcinoma tissues were tested for EBV genome by polymerase chain reaction (PCR)-Southern blotting. EBV-encoded small RNA (EBER) 1 of the PCR positive specimens was detected by *in situ* hybridization (ISH). Gastric carcinomas with positive EBER1 signals were classified as EBVaGCs. RT-PCR and Southern hybridization were applied to the detection of expression of nuclear antigen (EBNA) promoters (Qp, Wp and Cp), EBNA 1 and EBNA 2, latent membrane proteins (LMP) 1, 2A and 2B and lytic genes (immediate early genes BZLF1 and BRLF1, early genes BARF1 and BHRF1, late genes BcLF1 and BLLF1) in EBVaGCs.

RESULTS: Eleven EBV positive samples existed in gastric carcinoma tissues (6.39%). No EBV positive sample was found in corresponding para-carcinoma tissues. The difference between EBV positivity in carcinoma tissues and corresponding para-carcinoma tissues was significant ($\chi^2 = 9.0909$, $P = 0.0026$). Transcripts of Qp and EBNA1 were detected in all the 11 EBVaGCs, while both Wp and Cp were silent. EBNA2, LMP1 and LMP2B mRNA were absent in all the cases, while LMP2A mRNA was detected in 4 of the 11 cases. Of the 11 EBVaGCs, 7 exhibited BcLF1 transcripts and 2 exhibited BHRF1 transcripts. The transcripts of BZLF1 and BARF1 were detected in 5 cases, respectively. No BLLF1 and BRLF1 mRNA were detected.

CONCLUSION: The latent pattern of EBV in gastric carcinoma corresponds to the latency I/II. Some lytic infection genes are expressed in EBVaGCs tissues. BARF1 and BHRF1 genes may play an important role in tumorigenesis of gastric carcinoma.

© 2005 The WJG Press and Elsevier Inc. All rights reserved.

Key words: Gastric carcinomas; Epstein-Barr virus; Gene expression

Luo B, Wang Y, Wang XF, Liang H, Yan LP, Huang BH, Zhao P. Expression of Epstein-Barr virus genes in EBV-associated gastric carcinomas. *World J Gastroenterol* 2005; 11(5): 629-633

<http://www.wjgnet.com/1007-9327/11/629.asp>

INTRODUCTION

Epstein-Barr virus (EBV) is a tumor-related virus and EBV genome exists in many human malignant tumors, such as Burkitt's lymphoma (BL), nasopharyngeal carcinoma (NPC), Hodgkin's disease (HD) and B lymphocyte carcinoma in immunodeficiency patients. In recent years, EBV has also been reported to be associated with the development of gastric carcinoma. EBV has been found in most cases of rare gastric lymphoepithelioma-like carcinomas and in a small but significant proportion of common gastric adenocarcinomas. EBV-associated gastric carcinoma (EBVaGC) is observed in various histological types, such as well moderately and poorly differentiated adenocarcinomas, signet ring carcinomas^[1,2]. Latent infection is a characteristic of EBV infection. It is generally thought that EBV-carrying tumors express latent infection genes but not lytic infection genes. Studies about Burkitt's lymphoma and nasopharyngeal carcinoma (NPC) have shown that the expression of EBV genes is different in different types of malignancies and that lytic genes are also expressed^[3,4]. The pathogenic role of EBV in gastric carcinomas still remains undefined. In order to identify the role of EBV in oncogenesis, the form of EBV and expression of EBV genes in tumor tissues must be understood. The aims of the present study were to understand the expression of EBV latent and lytic genes in EBVaGCs at transcriptional level, and to investigate the relationship between EBV-encoded genes and development and progress of gastric carcinomas at molecular level.

MATERIALS AND METHODS

Specimens and extraction of DNA and RNA

Tumor tissues and corresponding para-carcinoma tissues were dissected from the stomachs removed at surgery from 172 patients with gastric carcinoma in the Affiliated Hospital of Qingdao University Medical College, Qingdao Municipal Hospital and Yantai Yuhuangding Hospital. DNA was extracted by the standard proteinase K-sodium dodecyl sulfate (SDS) method, followed by phenol-chloroform purification. Total RNA was extracted with TRIzol reagent (Gibco BRL, Gaithersburg MD, USA) following the manufacturer's instructions.

PCR-Southern blotting for EBV DNA

EBV DNA was detected by PCR and Southern hybridization analysis as previously described^[5].

In situ hybridization for EBV-encoded small RNA (EBER) 1

EBER1 of the PCR positive specimens was detected by *in situ* hybridization (ISH) to confirm EBV infection. ISH was carried out as previously described^[6]. Briefly, paraffin-embedded sections were deparaffinized with xylene, hydrated with ethanol, and predigested with proteinase K. Then the sections were hybridized with digoxigenin (DIG)-labeled oligonucleotide probes (antisense probe: 5'-AGACACCGTCCTCACCACCCGGGACTTGTA-3'; senseprobe: 5'-TCTGTGGCAGGAGTGGTG-GGCCCTGAACAT-3') overnight at 37 °C. DIG-labeled probes were visualized by alkaline phosphatase (AP) conjugated anti-DIG antibodies.

NBT/BCIP (Roche Diagnostics, Germany) was used as a substrate for AP. EBER1 sense probe was used to confirm the specificity of hybridization.

RT-PCR analysis for EBV gene expression

Details of the sequences and genome coordinates of primers and probes used to detect EBV transcripts are given in Table 1^[1,7-11]. The probes were labeled with DIG-ddUTP by DIG oligonucleotide 3'-end labeling kit (Roche Diagnostics, Germany). Approximately 1 µg RNA of EBV-positive samples was subjected to cDNA synthesis with a reverse transcription system (Promega, USA).

Table 1 Sequences and coordinates of primers and probes for RT-PCR analysis

Transcript	Oligonucleotide sequence (5'-3')	Product size (bp)	Genome coordinate
Wp	5'primer CAGGAGATCTGGAGTCCACACAAATCCT	131/136	14 396-14 556
	5'primer GAGGAGATCTGGAGTCCACACAAATGGG		14 396-14 561
	3'primer ACTGAAGCTTGACCGGTGCCTTCTTAGGAG probe GAGACCGAAGTGAAGGCCCTGGACCAACCC		14 735-14 716 14 561-14 590
Cp	5'primer TGTAGATCTGATGGCATAGAGAC	285/290	11 342-11 355
	3'primer ACTGAAGCTTGACCGGTGCCTTCTTAGGAG probe AAGGACACCGAAGACCCAGAG		14 735-14 716 11 356-11 378
	5'primer ATATGAGCTCGTGCCTACCGGATGGCG		62 441-62 457
Qp	3'primer GATCGAATCCATTTCCAGGTCCTGTACCT probe GGTAATCTGCTCCCAGGTC	255	107 987-107 967 67 628-67 609
	5'primer GATGAGCGTTGGGAGAGCTGATTCTGCA		67 510-67 539
EBNA1	3'primer TCCTCGTCCATGGTTATCAC probe AGACCTGGGAGCAGATTAC	273	108 075-108 056 67 608-67 627
	5'primer GCTGCTACGCATTAGAGACC		47 892-47 911
EBNA2	3'primer TCCTGGTAGGGATTCCGAGGG probe CAGCACTGGCGTGTGACGTGGTGTAAAGTT	339	48 616-48 597 48 391-48 420
	5'primer TCCTCCTCTGGCGCTACTG		169 383-169 364
LMP1	3'primer TCATCACTGTGTGCTGTGCC probe GAACAGCACAAATCCAAGGAACAATGCCTG	490	168 740-168 759 169 061-169 090
	5'primer ATGACTCATCTCAACACATA		166 874-166 893
LMP2A	3'primer CATGTTAGGCAAATTGCAA probe ATCCAGTATGCCTGCCTGTA	280	380-361 62-81
	5'primer CAGTGTAATCTGCACAAAGA		169 819-169 838
LMP2B	3'primer CATGTTAGGCAAATTGCAAA probe ATCCAGTATGCCTGCCTGTA	325	380-361 62-81
	5'primer ATTGCACCTTGCCGCCACCTTTG		103 194-103 180
BZLF1	3'primer CGGCATTTTCTGGAAGCCACCCGA probe CACTGCTGCTGCTGTTGAACAGT	608	102 486-102 463 102 772-102 795
	5'primer ACCATACAGGACACAACACCTC		106 166-106 145
BRLF1	3'primer GATGTTGAGCGTGGCCATTAGC probe GTTAGCCTCAGAAAGTCTTCCAAGCCATCC	266	104 959-104 980 105 140-105 169
	5'primer GGCTGTCACCGCTTTCTTGG		165 560-165 579
BARF1	3'primer AGGTGTTGGCACTTCTGTGG probe CTGGTTAAACTGGGCCAGGAGAGAGCA	203	165 762-165 743 165 644-165 673
	5'primer GTCAAGGTTTCGTCTGTGTG		53 830-53 849
BHRF1	3'primer TTCTCTTGCTGCTAGCTCCA probe ATGCACACGACTGTCCCCTATACAC	211	54 480-54 461 54 435-54 411
	5'primer TGCCCAATCCCAAGTACACGACC		136 229-136 207
BcLF1	3'primer CAGCAGGTCATAATTGGACGGG probe GAGAGCATTCTGTAGGTTAAACGCGAGGA	377	135 853-135 874 136 099-136 128
	5'primer CCTACCTGAATACAACCTGG		90 860-90 841
BLLF1	3'primer TGACGCTTGGCTGGTGGTGC probe TGGTGACATCCGCGGTGGAT	309	89 961-89 980 90 731-90 750

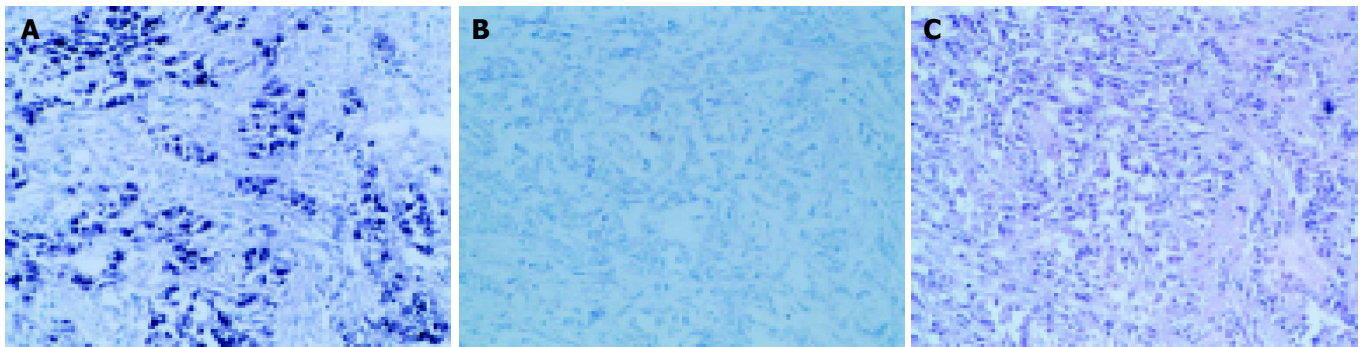


Figure 1 *In situ* hybridization for EBER1 in gastric carcinoma tissue. A: *In situ* EBER1 hybridization with antisense probes. Strong signals were observed in the nuclei of all tumor cells; B: *In situ* EBER1 hybridization with sense probes; C: Hematoxylin/eosin (H&E) staining in the adjacent pair of EBER1 *in situ* hybridization. original magnification $\times 200$.

Three microliters of cDNA was added into a solution containing 200 $\mu\text{mol/L}$ dNTPs, 500 $\mu\text{mol/L}$ each primer, 1.5 mmol/L MgCl_2 and 1 U Taq DNA polymerase (Promega, USA) in a total volume of 30 μL . PCR was carried out under the following conditions: first denaturation at 94 $^\circ\text{C}$ for 5 min, then denaturation for 45 s at 94 $^\circ\text{C}$, annealing for 45 s at 55 $^\circ\text{C}$, extension for 1 min at 72 $^\circ\text{C}$ in 35 amplification cycles, and finally extension for 5 min at 72 $^\circ\text{C}$. The amplified products were electrophoresed in 2% agarose gel, transferred onto a Hybond N⁺ nylon membrane (Amersham Pharmacia Biotech, Ireland) and subjected to hybridization with 3'-end-DIG-labeled oligonucleotide probes. The hybridized signals were detected by alkaline phosphatase (AP) conjugated anti-DIG antibodies. The substrate of AP was CSPD (Roche Diagnostics, Germany). cDNAs from EBV-immortalized lymphoblastoid cell lines (LCL) were used as positive controls, and those from EBV-negative Ramos cells as negative controls. The integrity of RNA was checked by the parallel amplification of glyceraldehyde-3-phosphate dehydrogenase (GAPDH)mRNA.

Statistical analysis

Software SAS 6.12 was employed to process the data with fourfold table χ^2 test.

RESULTS

Detection of EBVaGC

One hundred and seventy-two gastric carcinoma tissues and corresponding para-carcinoma tissues were tested for EBV genome by PCR-Southern blotting. EBER1 of the PCR positive specimens was detected by ISH to confirm EBV infection. Eleven EBV positive samples were found in gastric carcinomas (6.39%). No EBV positive sample was found in corresponding para-carcinoma tissues. The difference in EBV positivity was significant between carcinoma and corresponding para-carcinoma tissues ($\chi^2 = 9.0909$, $P = 0.0026$). Tumor cell nuclei of EBER1-positive cells were stained dark blue (Figure 1). Of the 11 EBVaGCs, 10 expressed EBER1 in almost all carcinoma cells, only one case expressed EBER1 in a proportion of tumor cells.

Expression of EBNA promoters

RT-PCR and Southern hybridization were performed with exon-specific primers of Qp, Wp and Cp. Transcripts of Qp were detected in all the 11 EBVaGCs, while neither Wp nor Cp transcripts were detected. The transcripts were also detected in LCL cells but not in Ramos cells (Figure 2). GAPDH mRNA was amplified to check pertinent RNA extraction. The result showed the integrity of RNA.

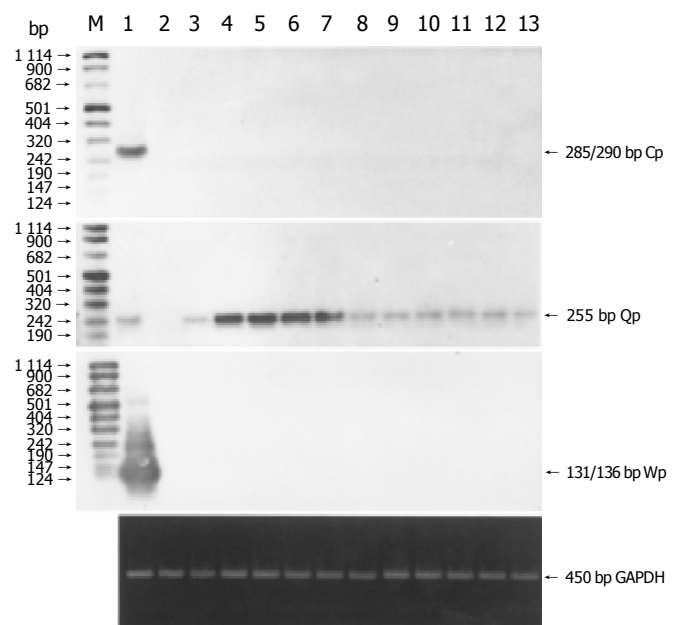


Figure 2 RT-PCR and Southern hybridization analysis of EBNA gene transcription using promoters. M: DIG-labeled DNA molecular weight marker VIII (Roche). Lane 1: EBV-positive LCL (positive control); lane 2: EBV-negative Ramos cells (negative control); lanes 3-13: EBV-positive gastric carcinoma samples. GAPDH mRNA was amplified to check pertinent RNA extraction and results were shown by EB staining.

Expression of EBV latent infection genes

We investigated the expression of latent infection genes in 11 EBVaGCs with RT-PCR and Southern blotting (Figure 3A). EBNA1 mRNA was detected in all the cases, while EBNA2 mRNA was not detected, which was consistent with the Qp utilization for EBNA1 mRNA. LMP2A mRNA was found in 4 of the 11 cases, but neither LMP1 nor LMP2B mRNA was found in any of the cases.

Expression of EBV lytic infection genes

To characterize the EBV lytic cycles in EBVaGCs, transcription of EBV immediate-early genes BZLF1 and BRLF1, early genes BARF1 and BHRF1 and late genes BcLF1 and BLLF1 were analyzed by RT-PCR and Southern blotting (Figure 3B). Of the 11 EBVaGCs, 7 exhibited BcLF1 transcripts and 2 exhibited BHRF1 transcripts. The transcripts of BZLF1 and BARF1 were detected respectively. No BLLF1 and BRLF1 mRNA were detected in the 11 EBVaGCs.

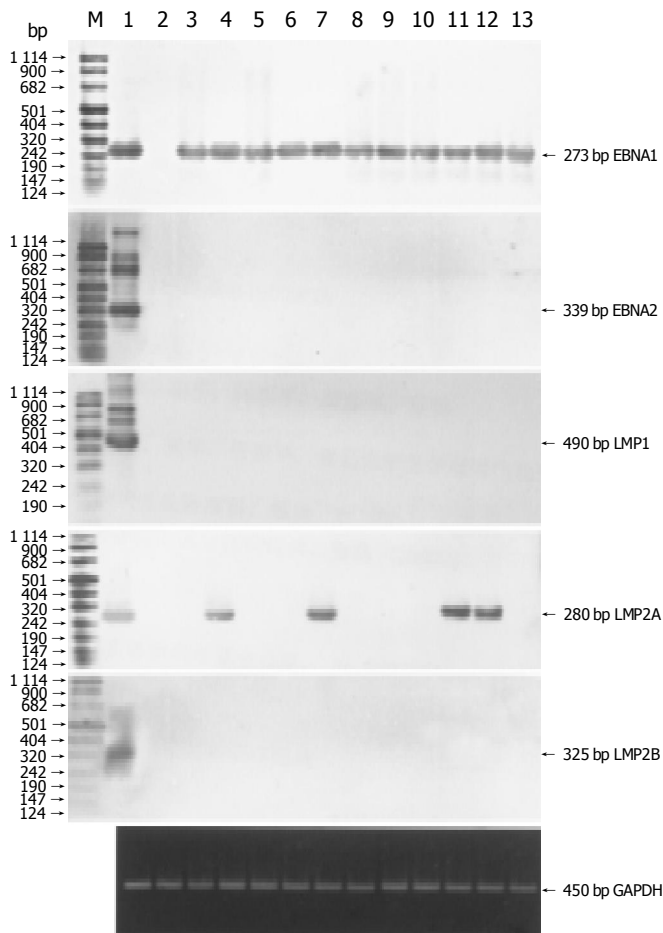


Figure 3 Detection of EBV latent gene expression (A) and EBV lytic gene expression (B) by RT-PCR and Southern hybridization. M: DIG-labeled DNA molecular weight marker VIII (Roche). Lane 1: EBV-positive LCL (positive control); lane 2: EBV-negative Ramos cells (negative control); lanes 3-13: EBV-positive gastric carcinoma samples. GAPDH mRNA was amplified to check pertinent RNA extraction and results were shown by EB staining.

DISCUSSION

Recently, great attention has been paid to the association of EBV infection and gastric carcinoma. In the present study, 11 EBVaGCs (6.39%) were confirmed, while no EBV positive sample was found from corresponding para-carcinoma tissues ($P < 0.01$). These results are consistent with previous reports on EBV positivity in gastric carcinoma^[1,2]. Ten of the 11 EBVaGCs expressed EBER1 in almost all carcinoma cells, suggesting that EBV infection occurs early in oncogenesis with a subsequent clonal expansion of EBV-containing tumor cells as shown by other investigators using molecular genetic techniques^[7,12]. One EBVaGC expressed EBER1 in a small number of gastric carcinoma cells with focal EBER1 staining, indicating that EBV infection occurs after the neoplastic transformation.

The expression of EBNA promoter genes was investigated in 11 EBVaGC tissues. Qp was clearly detected in all the cases, whereas Cp and Wp were not detected in all EBVaGCs, indicating that Qp, but not Cp or Wp, mediates EBNA transcription in EBVaGC tissues. Activation of Qp only resulted in expression of EBNA1 gene but not other EBNA genes. EBNA1 mRNA was transcribed from Qp in 11 EBVaGCs. EBNA2, LMP1 and LMP2B mRNA were not detected. Four of 11 cases exhibited LMP2A mRNA. These results are consistent with previous reports on

EBVaGC^[7,8]. The pattern of viral gene expression is not like the latency I of Burkitt's lymphoma (BL) or the latency II of NPC, but corresponds to the unique latency I/II of EBV infection.

EBNA and LMP1 are essential genes for transformation of cells. Since EBNA1 is commonly expressed in 3 types of latency, it may play a similar pathogenic role in different types of tumors. Several *in vitro* studies have demonstrated that LMP1 can transform rodent fibroblasts and human keratinocytes, inhibit differentiation of human epithelial cells, and induce expression of epidermal growth factor receptors. These important findings strongly support that they play crucial roles in the development of non-lymphoid cell carcinomas, for example, the positivity of NPC LMP1 exceeds 80% of the NPC cases^[13-15]. In the present study, EBNA1 mRNA was detected in all of the EBVaGCs, suggesting that the pathogenic role of EBNA1 is similar in EBVaGCs, NPC and BL. The absence of LMP1 expression in EBVaGCs implies that LMP1 may not be necessary for the tumors, at least not necessary for sustaining its already established malignant state. Rather, LMP1 might participate in the earlier stage of tumor development and is down-regulated thereafter. Alternatively, the lack of LMP1 may reflect the result of clonal selection of LMP1-negative tumor cells by immunological pressure because EBV-specific cytotoxic T cells are potentially directed against the viral latent membrane proteins rather than EBNA1. In fact, patients with EBVaGC normally retain virus-specific immune T-cell responses, in contrast to NPC patients^[8]. It has been reported that LMP2A is involved in blocking B-cell specific signaling pathways and calcium mobilization, which might be advantageous for maintaining latent patterns of EBV infection and inhibiting EBV reactivation^[16]. However, the functions of LMP2A in epithelial cells have not been analyzed yet. Serological studies have shown that NPC patients have elevated titers of antibody to both LMP2A and LMP2B, suggesting that LMP2A and LMP2B are expressed during the progression of the disease^[17]. The pathogenic roles of LMP2A in the development and progression of gastric carcinoma remain to be determined.

In our study, the expression of lytic infection genes in 11 EBVaGC tissues was detected by RT-PCR analysis. We demonstrated EBV replication in part of the samples. Four cases simultaneously exhibited BZLF1, BARF1 and BcLF1 mRNA. Immediate-early genes BZLF1 and BRLF1 were necessary and sufficient to orchestrate the switch from latency to lytic replication and expression of early and late genes. BRLF1 mRNA was not detected in 11 EBVaGCs, whereas BZLF1 mRNA was detected in 5 of 11 cases. We therefore assume that BZLF1 gene activates EBV lytic replication. Early gene BHRF1 showed partial sequence homologous to human bcl-2 proto-oncogene, a gene involved in inhibiting cell apoptosis. BHRF1 protein could inhibit apoptosis of B lymphocytes and epithelial cells, and promote cell growth and transformation^[18,19]. BARF1 is able to immortalize epithelial cells and fibroblast cells *in vitro*. Furthermore, it could activate the expression of bcl-2^[1,20]. We demonstrated that 5 of 11 EBVaGCs exhibited BARF1 mRNA and 2 exhibited BHRF1 mRNA. Because EBVaGC lacks the expression of LMP1^[1,7,8], BARF1 and BHRF1 genes might be the viral oncogenes in EBVaGC. Late gene BLLF1 encodes envelope glycoprotein gp320/220, which is the most abundant protein synthesized during lytic replication of EBV. The infection of B lymphocytes is mediated by adsorption of EBV gp320/220 to the receptor, CD21. In our study, BLLF1 mRNA was not found in 11 EBVaGCs. It can be proposed that EBV infects gastric epithelial cells by CD21-independent pathways.

In lytic lymphocytes, transcripts of all known EBV lytic genes have been detected. In our study, BLLF1 and BRLF1 mRNA were not detected in EBVaGC. The expression of lytic genes

varied among the individual tumors analyzed. These results suggest that EBV lytic infection occurs in a small portion of EBV-infected carcinoma cells and the productive cycle is often incomplete. The same results have been reported previously^[7]. Because EBER1-positive cells are detected only in carcinoma cells but not in infiltrated lymphocytes in tumor tissues, we could deny the possibility that EBV lytic infection occurs in other cells (such as infiltrated lymphocytes in tumor tissues) but not in carcinoma cells. Many studies have shown that the pattern of viral gene expression corresponds to latency I/II of EBV infection in EBVaGC. However, reports on the expression of lytic infection genes in EBVaGC are very few and have disparate results. For example, Sugiura *et al*^[8] did not detect BZLF1 mRNA in EBVaGCs, whereas Hoshikawa *et al*^[7] detected BZLF1, BRLF1, BLLF1 and BcLF1 mRNA in EBVaGCs.

In conclusion, the latent pattern of EBV corresponds to latency I/II and EBV lytic infection occurs in EBVaGC. BARF1 and BHRF1 may play important roles in tumorigenesis of EBVaGC. However, the mechanism by which EBV lytic infection regulates the pathogenesis and development of gastric carcinoma remains to be determined.

REFERENCES

- zur Hausen A, Brink AA, Craanen ME, Middeldorp JM, Meijer CJ, van den Brule AJ. Unique transcription pattern of Epstein-Barr virus (EBV) in EBV-carrying gastric adenocarcinomas: expression of the transforming *BARF1* gene. *Cancer Res* 2000; **60**: 2745-2748
- Imai S, Koizumi S, Sugiura M, Tokunaga M, Uemura Y, Yamamoto N, Tanaka S, Sato E, Osato T. Gastric carcinoma: monoclonal epithelial malignant cells expressing Epstein-Barr virus latent infection protein. *Proc Natl Acad Sci USA* 1994; **91**: 9131-9135
- Martel-Renoir D, Grunewald V, Touitou R, Schwaab G, Joab I. Qualitative analysis of the expression of Epstein-Barr virus lytic genes in nasopharyngeal carcinoma biopsies. *J Gen Virol* 1995; **76** (Pt 6): 1401-1408
- Bashir R, Luka J, Cheloha K, Chamberlain M, Hochberg F. Expression of Epstein-Barr virus proteins in primary CNS lymphoma in AIDS patients. *Neurology* 1993; **43**: 2358-2362
- Ikuta K, Satoh Y, Hoshikawa Y, Sairenji T. Detection of Epstein-Barr virus in salivas and throat washings in healthy adults and children. *Microbes Infect* 2000; **2**: 115-120
- Tokunaga M, Uemura Y, Tokudome T, Ishidate T, Masuda H, Okazaki E, Kaneko K, Naoe S, Ito M, Okamura A. Epstein-Barr virus related gastric cancer in Japan: a molecular patho-epidemiological study. *Acta Pathol Jpn* 1993; **43**: 574-581
- Hoshikawa Y, Satoh Y, Murakami M, Maeta M, Kaibara N, Ito H, Kurata T, Sairenji T. Evidence of lytic infection of Epstein-Barr virus (EBV) in EBV-positive gastric carcinoma. *J Med Virol* 2002; **66**: 351-359
- Sugiura M, Imai S, Tokunaga M, Koizumi S, Uchizawa M, Okamoto K, Osato T. Transcriptional analysis of Epstein-Barr virus gene expression in EBV-positive gastric carcinoma: unique viral latency in the tumour cells. *Br J Cancer* 1996; **74**: 625-631
- Oudejans JJ, van den Brule AJ, Jiwa NM, de Bruin PC, Ossenkuppele GJ, van der Valk P, Walboomers JM, Meijer CJ. BHRF1, the Epstein-Barr virus (EBV) homologue of the BCL-2 protooncogene, is transcribed in EBV associated B-cell lymphomas and in reactive lymphocytes. *Blood* 1995; **86**: 1893-1902
- Kelleher CA, Paterson RK, Dreyfus DH, Streib JE, Xu JW, Takase K, Jones JF, Gelfand EW. Epstein-Barr virus replicative gene transcription during de novo infection of human thymocytes: simultaneous early expression of BZLF-1 and its repressor RAZ. *Virology* 1995; **208**: 685-695
- Prang NS, Hornef MW, Jager M, Wagner HJ, Wolf H, Schwarzmann FM. Lytic replication of Epstein-Barr virus in the peripheral blood: analysis of viral gene expression in B lymphocytes during infectious mononucleosis and in the normal carrier state. *Blood* 1997; **89**: 1665-1677
- Gulley ML, Pulitzer DR, Eagan PA, Schneider BG. Epstein-Barr virus infection is an early event in gastric carcinogenesis and is independent of bcl-2 expression and p53 accumulation. *Hum Pathol* 1996; **27**: 20-27
- Levitskaya J, Coram M, Levitsky V, Imreh S, Steigerwald-Mullen PM, Klein G, Kurilla MG, Masucci MG. Inhibition of antigen processing by the internal repeat region of the Epstein-Barr virus nuclear antigen-1. *Nature* 1995; **375**: 685-688
- Miller WE, Earp HS, Raab-Traub N. The Epstein-Barr virus latent membrane protein 1 induces expression of the epidermal growth factor receptor. *J Virol* 1995; **69**: 4390-4398
- Chen F, Hu LF, Ernberg I, Klein G, Winberg G. Coupled transcription of Epstein-Barr virus latent membrane protein (LMP)-1 and LMP-2B genes in nasopharyngeal carcinomas. *J Gen Virol* 1995; **76** (Pt 1): 131-138
- Miller CL, Lee JH, Kieff E, Longnecker R. An integral membrane protein (LMP2) blocks reactivation of Epstein-Barr virus from latency following surface immunoglobulin crosslinking. *Proc Natl Acad Sci USA* 1994; **91**: 772-776
- Lenette ET, Winberg G, Yadav M, Enblad G, Klein G. Antibodies to LMP2A/2B in EBV-carrying malignancies. *Eur J Cancer* 1995; **31A**: 1875-1878
- Dawson CW, Dawson J, Jones R, Ward K, Young LS. Functional differences between BHRF1, the Epstein-Barr virus-encoded Bcl-2 homologue, and Bcl-2 in human epithelial cells. *J Virol* 1998; **72**: 9016-9024
- Huang Q, Petros AM, Virgin HW, Fesik SW, Olejniczak ET. Solution structure of the BHRF1 protein from Epstein-Barr virus, a homolog of human Bcl-2. *J Mol Biol* 2003; **332**: 1123-1130
- Sheng W, Decaussin G, Sumner S, Ooka T. N-terminal domain of BARF1 gene encoded by Epstein-Barr virus is essential for malignant transformation of rodent fibroblasts and activation of BCL-2. *Oncogene* 2001; **20**: 1176-1185

Assistant Editor Li WZ Edited by Zhu LH and Wang XL

Selection of optimal antisense accessible sites of survivin and its application in treatment of gastric cancer

Qiang-Song Tong, Li-Duan Zheng, Fang-Min Chen, Fu-Qing Zeng, Liang Wang, Ji-Hua Dong, Gong-Cheng Lu

Qiang-Song Tong, Fang-Min Chen, Fu-Qing Zeng, Liang Wang, Gong-Cheng Lu, Department of Surgery, Union Hospital of Tongji Medical College, Huazhong University of Science and Technology, Wuhan 430022, Hubei Province, China

Li-Duan Zheng, Department of Pathology, Union Hospital of Tongji Medical College, Huazhong University of Science and Technology, Wuhan 430022, Hubei Province, China

Ji-Hua Dong, Department of Central Laboratory, Union Hospital of Tongji Medical College, Huazhong University of Science and Technology, Wuhan 430022, Hubei Province, China

Supported by National Natural Science Foundation of China, No. 30200284 and Science Foundation of Huazhong University of Science and Technology

Correspondence to: Dr. Qiang-Song Tong, Department of Surgery, Union Hospital of Tongji Medical College, Huazhong University of Science and Technology, Wuhan 430022, Hubei Province, China. qs_tong@hotmail.com

Telephone: +86-27- 85991567

Received: 2004-02-23 Accepted: 2004-04-13

Abstract

AIM: To select the optimal antisense accessible sites of survivin, a highly expressed gene in tumor tissues, in order to explore a novel approach to improve biological therapy of gastric cancer.

METHODS: The 20 mer random oligonucleotide library was synthesized, hybridized with *in vitro* transcribed total survivin cRNA, then digested by RNase H. After primer extension and autoradiography, the antisense accessible sites (AAS) of survivin were selected. Then RNADraw software was used to analyze and choose the AAS with obvious stem-loop structures, according to which the complementary antisense oligonucleotides (AS-ODNs) were synthesized and transferred into survivin highly-expressing gastric cancer cell line MKN-45. Survivin expression was detected by RT-PCR and Western Blotting. Cellular growth activities were assayed by tetrazolium bromide (MTT) colorimetry. Cellular ultrastructure was observed by electronic microscopy, while apoptosis was detected by annexin V-FITC and propidium iodide staining flow cytometry.

RESULTS: Thirteen AAS of survivin were selected *in vitro*. Four AAS with stem-loop structures were chosen, locating at 207-226 bp, 187-206 bp, 126-145 bp and 44-63 bp of survivin cDNA respectively. When compared with non-transfection controls, their corresponding AS-ODNs (AS-ODN₁, AS-ODN₂, AS-ODN₃ and AS-ODN₄) could reduce Survivin mRNA levels in MKN-45 cells by 54.3±1.1% ($t = 6.12, P < 0.01$), 86.1±1.0% ($t = 5.27, P < 0.01$), 32.2±1.3% ($t = 7.34, P < 0.01$) and 56.2±0.9% ($t = 6.45, P < 0.01$) respectively, while survivin protein levels were decreased by 42.2±2.5% ($t = 6.26, P < 0.01$), 75.4±3.1% ($t = 7.11, P < 0.01$), 28.3±2.0% ($t = 6.04, P < 0.01$) and 45.8±1.2% ($t = 6.38, P < 0.01$) respectively. After transfection with 600 nmol/L AS-ODN₁~AS-ODN₄ for 24 h, cell growth was inhibited by 28.12±1.54% ($t = 7.62, P < 0.01$), 38.42±3.12% ($t = 7.75, P < 0.01$), 21.46±2.63%

($t = 5.94, P < 0.01$) and 32.12±1.77% ($t = 6.17, P < 0.01$) respectively. Partial cancer cells presented the characteristic morphological changes of apoptosis, with apoptotic rates being 19.31±1.16% ($t = 7.16, P < 0.01$), 29.24±1.94% ($t = 8.15, P < 0.01$), 11.87±0.68% ($t = 6.68, P < 0.01$) and 21.68±2.14% ($t = 7.53, P < 0.01$) respectively.

CONCLUSION: The AAS of survivin could be effectively selected *in vitro* by random oligonucleotide library/RNase H cleavage method combined with computer software analysis, this has important reference values for further studying survivin-targeted therapy strategies for gastric cancer.

© 2005 The WJG Press and Elsevier Inc. All rights reserved.

Key words: Gastric cancer; Survivin; Antisense accessible sites; Gene expression

Tong QS, Zheng LD, Chen FM, Zeng FQ, Wang L, Dong JH, Lu GC. Selection of optimal antisense accessible sites of survivin and its application in treatment of gastric cancer. *World J Gastroenterol* 2005; 11(5): 634-640
<http://www.wjgnet.com/1007-9327/11/634.asp>

INTRODUCTION

Survivin is a novel member of inhibitors of apoptosis (IAPs) family, which expresses during human embryonal development and in most of tumor tissues, whereas lacks of expression in terminally differentiated normal tissues^[1-4]. A series of studies indicate that survivin has a double function in blocking cell apoptosis and regulating cell proliferation, its overexpression correlates with occurrence and development of gastric cancer^[5,6]. Antisense technique has become an efficient therapeutic method for gastric cancer through blocking gene expression and biological function of survivin^[7]. However, since the target sequence is always folded into secondary and tertiary structures, resulting in the blocking effects on antisense accessible sites, which leads to the low inhibition activities of antisense oligonucleotides designed only by computer software, it is an attractive research focus on how to select optimal antisense accessible sites of targeted sequence^[8-11]. In this research, the antisense accessible sites of survivin were selected *in vitro* through random oligonucleotide library/RNase H cleavage method combined with computer analysis software, in order to establish an experimental basis for further exploring the survivin-targeted therapy strategies for gastric cancer.

MATERIALS AND METHODS

Design and synthesis of random oligonucleotide library

According to literature^[12], random oligonucleotide library was synthesized, with the following required standards: a length of 20 bp, a mixture of phosphoramidites at a ratio of 1.5:1.25:1.15:1.0 (A:C:G:U/T), and a sequence of 5'-mmmmmmmmmmmmmmmmmm-

3'. G, A, T and C denote four kinds of deoxynucleotides, m denotes the methylation, n denotes random deoxynucleotides. Random oligonucleotide library was synthesized and purified by Shanghai Sangon Company.

Transcription of target gene *in vitro*

The plasmid pcDNA-SVV including full length of survivin cDNA was a kind gift from the Walter and Eliza Hall Institute of Medical Research (Australia). The plasmid was linearized by digestion with restriction enzyme *Nhe* I (Takara Biology Company) and transcribed into cRNA *in vitro* using a T₇ transcription kit (Promega Biology Company). The total reaction volume was 50 μ L, and incubated at 37 °C for 2 h. Then the DNA template was removed by digestion with DNase I for 30 min. The products were extracted with phenol: chloroform: isoamyl alcohol (V/V 25:24: 1), precipitated with 100% ethanol, washed with 70% ethanol and dissolved in DEPC H₂O after drying at room temperature. The cRNA concentrations were measured with UV spectro- photometer, and determined with 1% agarose gel electrophoresis. The cRNA was preserved at -70 °C.

RNase H cleavage reaction

The total volume for hybridization reaction between random oligonucleotide library and cRNA was 200 μ L. The oligonucleotide library (60 μ L, 300 nmol/L) was denatured at 95 °C for 5 min, kept on ice for 5 min, added with cRNA 3 μ L (30 pmol/L), 5 \times Tris buffer (200 mmol/L Tris, pH 8.0, 20 mmol/L MgCl₂, 5 mmol/L DTT) 40 μ L, 10 U/ μ L RNase H (Takara Biology Company) 2 μ L and 1% DEPC H₂O 95 μ L. The reaction was conducted at 30 °C for 1h. Then the product was extracted with phenol: chloroform: isoamyl alcohol (V/V 25:24:1), added with 1/10 volume 3 mol/L NaAc and 2.5 volume 100% ethanol, precipitated at -20 °C for 30 min, washed with 70% ethanol and dissolved with DEPC H₂O.

Primer extension and selection of antisense accessible sites

According to human survivin cDNA sequence (429 bp) and protocol of the primer extension kit (Promega Corporation), two extension primers were designed with Primer 5.0 software: P₁ 5'-CCAAGGGTAAATCTTCAAACCTGCTTC-3', P₂ 5'-CCAAGTCTGGCTCGTTCTCAGTGGGGCAGT-3', which were synthesized by Shanghai Genebase Company and diluted with double distilled H₂O into 150 nmol/L. Primers and PhiX174 Hinf I DNA marker were labeled with ³²P-ATP (Beijing Furui Biology Corporation) with T₄ polynucleotide kinase. The 5' end primer extension reaction was conducted on the RNase H cleaved products with each labeled primer, and reaction volume was 20 μ L. The reaction was continued at 42 °C for 30 min, terminated by adding 20 μ L loading dye, then analyzed on 8% denaturing polyacrylamide gel. The gel was fixed with 8% acetic acid for 10 min at room temperature, dried up in vacuum at 80 °C for 1 h, exposed to X-ray film overnight at -70 °C for autoradiography. The secondary structures of full-length survivin cDNA were predicted with RNADraw software. The antisense accessible sites (AAS) with obvious stem-loop structure domains, were selected with results of random oligonucleotide libraries/RNase H cleavage *in vitro* combined with RNADraw analysis. Their complementary antisense oligonucleotides (AS-ODNs) were synthesized by Shanghai Gene-base Company.

Design of control AS-ODN

According to the secondary structure of survivin cDNA predicted by RNADraw, the antisense accessible site containing two stem-loop domains (4-23 bp) was selected (Figure 1). Its complementary antisense oligonucleotide, named as AS-ODN₀

(sequence: 5'-GGGGGCAACGTCGGGGCACC-3'), was synthesized as a control.

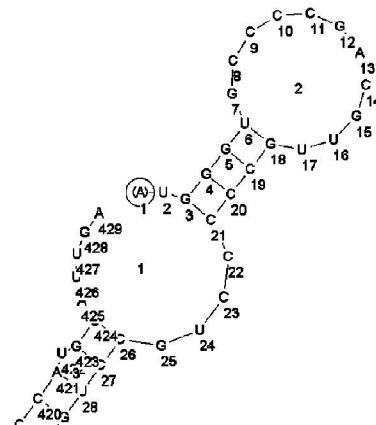


Figure 1 Secondary structure of antisense accessible sites (4-23 bp) of survivin designed only with RNADraw software.

Cell culture and gene transfection

The gastric cancer cell line MKN-45, a highly expressing survivin gene, was purchased from American Type Culture Collection (ATCC), and incubated in RPMI 1640 medium supplemented with penicillin/ streptomycin (100 U/mL and 100 μ g/mL respectively) and 10% fetal bovine serum at 37 °C in a humidified atmosphere of 50 mL/L CO₂ and passaged every three days. MKN-45 cells at exponential phases of growth were inoculated into 24-well plates. The procedure for transfection of AS-ODN₀ and AS-ODNs was conducted according to the protocol of Lipofectamine 2000 kit (Gibco Company).

Survivin mRNA expression detection

Reverse transcription polymerase chain reaction (RT-PCR) was used. Eighteen hours after gene transfection, total RNA was extracted from cells of each group. Reverse transcription reaction was carried out using the following mixture containing 1 μ L 10 mmol/L 4 \times dNTP, 1 μ L 1 U/ μ L RNase inhibitor, 1 μ L 0.5 μ g/ μ L Oligo dT primer, 0.5 μ L AMV reverse transcriptase, 4 μ L 5 \times AMV buffer, 4 μ L RNA template, 8.5 μ L ddH₂O. The reaction was conducted at 42 °C for 30 min, heated to 99 °C for 5 min to inactivate AMV reverse transcriptase and kept at 5 °C for 10 min. In reference to survivin cDNA sequence in GenBank (accession number: U75285), the primer pairs for survivin fragments were designed with Primer Premier 5.0 software: forward primer: 5'-CACCGCATCTCTACATTCAA-3', reverse primer: 5'-CACTTTCTTCGAGTTTCCT-3'. The anticipated product was 345 bp in length. The primers for α -tubulin, including forward primer: 5'-CCGTCCTTCCACTCA-3' and reverse primer: 5'-GTAATCT CGGCAACAC-3', served as an inner control with a product of 410 bp. PCR amplification was conducted in following condition: pre-denaturation at 95 °C for 5 min, denaturation at 95 °C for 1 min, annealing at 60 °C for 1 min, and extension at 72 °C for 90 s. After 30 amplification cycles the products were extended at 72 °C for 10 min. The PCR products were separated with electrophoresis on 1% agarose gel and photographed under ultraviolet radiation light.

Survivin protein expression assay

Western blotting was used. The total cellular protein was extracted and determined according to the Molecular Cloning Manual. Western blot was conducted. Blots were incubated sequentially with 1% fat free dry milk, rabbit polyclonal anti-survivin antibody (Santa Cruz Company) and peroxidase-conjugated second antibody, and evaluated using ECL Western blotting kit. Survivin

protein band intensities were determined densitometrically using the CMIASWIN computer imaging system.

Cell growth assay

The 3-(4,5-dimethylthiazol-2-yl)-2,5-dimethyl tetrazolium bromide (MTT) colorimetry method was used. MKN-45 cells were seeded at a density of $3 \times 10^3/100 \mu\text{L}$ into 96-well chamber slides. The non-transfection controls, 600 nmol/L AS-ODN₀ transfection and 600 nmol/L AS-ODN transfection groups were designed, with each group having five wells. After transfected for 6, 12, 18 and 24 h, each well was added with 0.5% MTT 20 μL and incubated for another 4 h. The supernates were discarded, then DMSO 100 μL was added. When the crystals were dissolved, the optical density *A* values of the slides were read on enzyme-labeled minireader II at the wavelength of 490 nm. Cell growth inhibition rate (%) = (1 - average *A* value of experimental group/ average *A* value of non-transfection control group) $\times 100\%$.

Cellular ultrastructure observation

Cancer cells from three groups were collected, rinsed with PBS and fixed using 2.5% glutaraldehyde for 30 min, then washed with PBS. After routine embedding and sectioning, cells were observed under electronic microscope.

Cell apoptosis detection

Apoptosis was detected by annexin V-FITC and propidium iodide staining flow cytometry. Cells were collected, washed twice with cold PBS, resuspended with 100 μL binding buffer (10 mmol/L HEPES, 140 mmol/L NaCl, 2.5 mmol/L CaCl₂, pH 7.4) to $2-5 \times 10^5/\text{mL}$, and incubated with annexin V-FITC at room temperature for 10 min. After washed with binding buffer, cells were resuspended with 400 μL binding buffer containing 10 μL PI (20 $\mu\text{g}/\text{mL}$) and incubated on ice for 15 min. Apoptosis was analyzed by flow cytometry (BD Company, USA) at the wavelength of 488 nm.

Statistical analysis

Data were expressed as mean \pm SD and analyzed by SPSS10.0

statistical software.

RESULTS

In vitro selection of antisense accessible sites of survivin

As shown in Figure 2, after survivin cRNA was mixed with the random oligonucleotide library and digested by RNase H, there were obvious products on autoradiography through primer extension of P₁ and P₂, which were targeting coding regions of survivin mRNA. Thirteen antisense accessible sites were selected. Their product size of primer extension, 3' end cleaving sites by RNase H and corresponding antisense accessible sites are shown in Table 1. Secondary structures of these thirteen sites were analyzed with RNADraw software. As shown in Figure 3, four sites were found to have obvious stem-loop structures (at 207-226 bp, 187-206 bp, 126-145 bp, 44-63 bp of survivin cDNA respectively). The antisense oligonucleotides AS-ODN₁-AS-ODN₄, complementary to these four sites, were synthesized (Table 2).

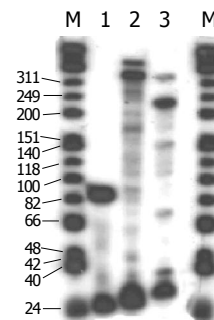


Figure 2 Primer extension analysis for the selection of antisense accessible sites of survivin by random oligonucleotide library/RNase H cleavage method. M: PhiX174 HinI DNA marker. Lane 1: Primer extension positive control; lanes 2-3: Primer extension products of P₁ and P₂.

Table 1 Antisense accessible regions of survivin mRNA shown by primer extension analysis

Primer name	Product size of primer extension (bp)	3' end site of primer extension (bp)	3' end site of RNase H cleavage (bp)	Antisense accessible sites (bp)
P ₁	42	255	254	235-254
	60	237	236	217-236
	70	227	226	207-226
	82	215	214	195-214
	90	207	206	187-206
	104	193	192	173-192
	118	179	178	159-178
	151	146	145	126-145
P ₂	40	124	123	104-123
	70	94	93	74-93
	100	64	63	44-63
	118	46	45	26-45
	140	24	23	4-23

Table 2 Antisense accessible sites and their complementary oligonucleotide sequences selected by random oligonucleotide library/RNase H cleavage combined with RNADraw analysis

Serial number	Base sequence	Origination-end sites	Base pair
ODN ₁	AGATGACGACCCCATAGAGG	207-226	20 bp
AS-ODN ₁	CCTCTATGGGGTCGTCATCT		
ODN ₂	GAGCTGGAAGGCTGGGAGCC	187-206	20 bp
AS-ODN ₂	GGCTCCCAGCCTTCCAGCTC		
ODN ₃	CTTCATCCACTGCCCACTG	126-145	20 bp
AS-ODN ₃	CAGTGGGGCAGTGGATGAAG		
ODN ₄	AGGACCACGCATCTCTACA	44-63	20 bp
AS-ODN ₄	TGTAGAGATGCGGTGGTCCT		

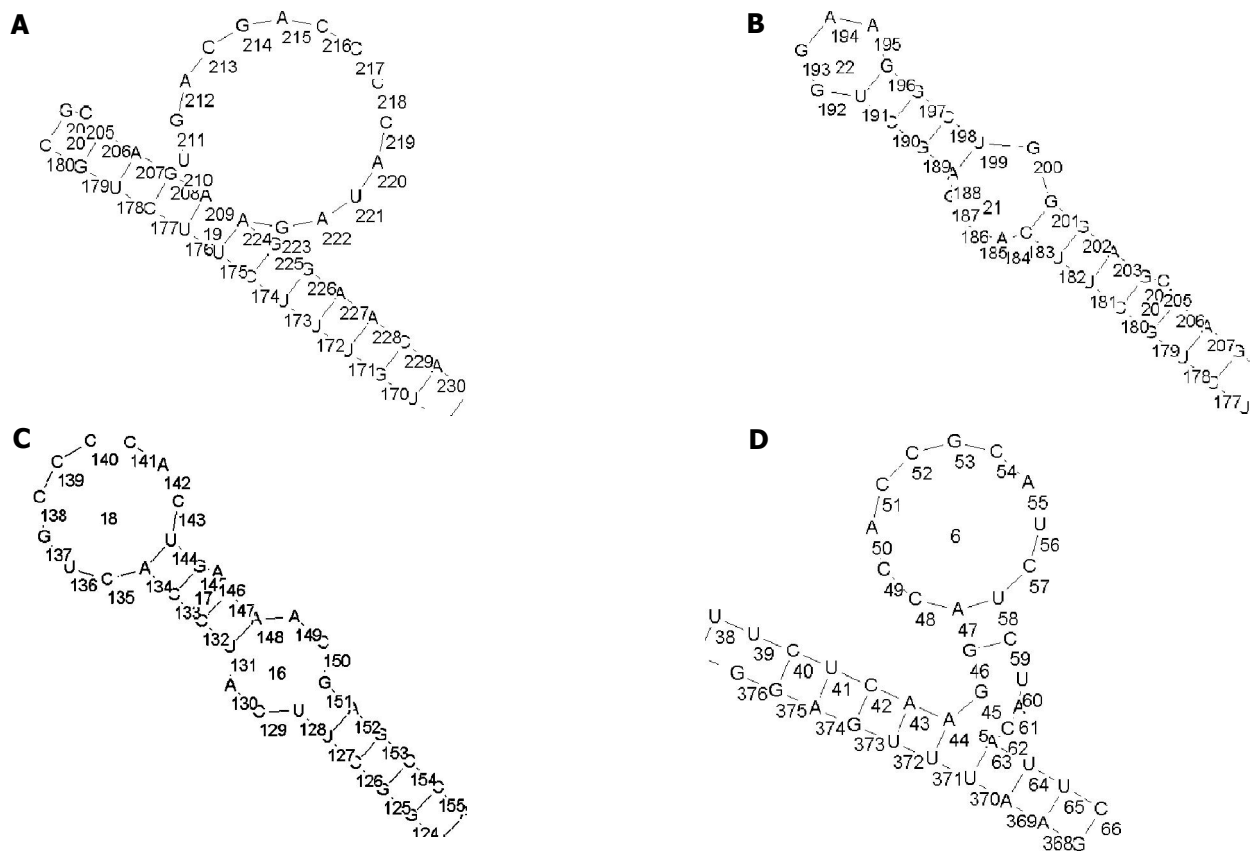


Figure 3 Four secondary structures of antisense accessible sites predicted by RNADraw software. A: ODN₁ (207-226 bp); B: ODN₂ (187-206 bp); C: ODN₃ (126-145 bp); D: ODN₄ (44-63 bp).

Blocking effects of antisense oligonucleotides on gene expression

The ratio of survivin/ α -tubulin in non-transfection group was 0.918 ± 0.006 . Eighteen hours after transfection with AS-ODN₀ and AS-ODN₁-AS-ODN₄, the survivin/ α -tubulin ratios were 0.749 ± 0.006 , 0.419 ± 0.011 , 0.128 ± 0.009 , 0.622 ± 0.012 and 0.402 ± 0.008 respectively (Figure 4A). Their inhibitory rates on survivin mRNA expression were $18.4 \pm 0.6\%$ ($t = 5.02$, $P < 0.05$), $54.3 \pm 1.1\%$ ($t = 6.12$, $P < 0.01$), $86.1 \pm 1.0\%$ ($t = 5.27$, $P < 0.01$), $32.2 \pm 1.3\%$ ($t = 7.34$, $P < 0.01$) and $56.2 \pm 0.9\%$ ($t = 6.45$, $P < 0.01$) respectively. As shown in Figure 4B, Western blotting detection found obvious 16.5 KD protein bands in non-transfected MKN-45 cells. Computer imaging system demonstrated that the inhibitory efficiencies of AS-ODN₀ and AS-ODN₁-AS-ODN₄ on survivin

protein expression were $12.6 \pm 1.1\%$ ($t = 4.05$, $P < 0.05$), $42.2 \pm 2.5\%$ ($t = 6.26$, $P < 0.01$), $75.4 \pm 3.1\%$ ($t = 7.11$, $P < 0.01$), $28.3 \pm 2.0\%$ ($t = 6.04$, $P < 0.01$) and $45.8 \pm 1.2\%$ ($t = 6.38$, $P < 0.01$), respectively. The blocking effect of AS-ODN₂ was the highest among all these antisense oligonucleotides.

Cell growth inhibition

After treatment with 600 nmol/L AS-ODN₀ and AS-ODN₁-AS-ODN₄, the growth activities of MKN-45 cells were reduced in a time dependent manner. Twenty-four hours after transfection, their growth inhibition rates on MKN-45 cells were $15.24 \pm 1.85\%$ ($t = 5.44$, $P < 0.01$), $28.12 \pm 1.54\%$ ($t = 7.62$, $P < 0.01$), $38.42 \pm 3.12\%$ ($t = 7.75$, $P < 0.01$), $21.46 \pm 2.63\%$ ($t = 5.94$, $P < 0.01$) and $32.12 \pm 1.77\%$ ($t = 6.17$, $P < 0.01$) respectively. The growth inhibition effect of AS-ODN₂ was the highest in all antisense oligonucleotides (Figure 5).

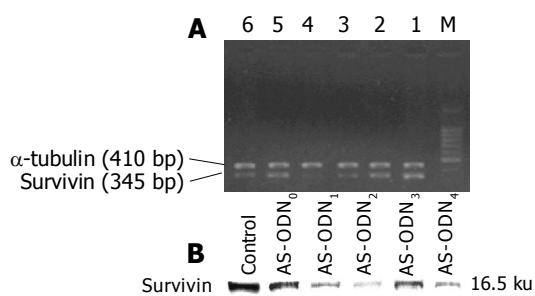


Figure 4 RT-PCR and Western blotting detection of the blocking effects of various antisense oligonucleotides on survivin mRNA and protein expression of MKN-45 cells. A: RT-PCR detection of the blocking effects of various antisense oligonucleotides on survivin mRNA expression of MKN-45 cells M: PCR marker (100-1 000 bp). Lane 1: Non-transfection Control; lane 2: AS-ODN₀; lane 3: AS-ODN₁; lane 4: AS-ODN₂; lane 5: AS-ODN₃; lane 6: AS-ODN₄; B: Western blotting detection of the blocking effects of various antisense oligonucleotides on survivin protein expression of MKN-45 cells.

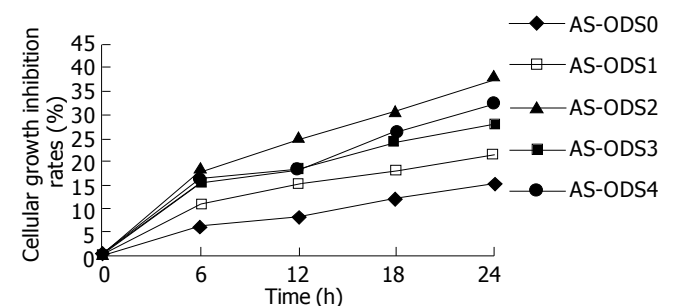


Figure 5 Growth inhibitory effects of various antisense oligonucleotides on MKN-45 cells.

Cell morphological features

Cancer cells in non-transfection control group grew rapidly, with a regular polygon shape. After transfection with 600 nmol/L AS-

ODNS₁₋₄, some cells presented reduced size, irregular shape, and mostly round profile. Under electronic microscope, some cells had characteristic morphological changes of apoptosis such as nuclear shrinkage, chromatin congregation around nuclear membranes, reduction of cell volume and integrity of nuclear membranes (Figure 6).

Induction of cell apoptosis

The apoptotic rate of MKN-45 cells in non-transfection group was $0.92 \pm 0.12\%$. After treatment with 600 nmol/LAS-ODN₀ and AS-ODNS₁₋₄ for 24 h, the apoptotic rates of MKN-45 cells were $5.02 \pm 0.26\%$ ($t = 4.17, P < 0.05$), $19.31 \pm 1.16\%$ ($t = 7.16, P < 0.01$), $29.24 \pm 1.94\%$ ($t = 8.15, P < 0.01$), $11.87 \pm 0.68\%$ ($t = 6.68, P < 0.01$) and $21.68 \pm 2.14\%$ ($t = 7.53, P < 0.01$) respectively. The apoptosis-inducing effect of AS-ODN₂ was the highest in all antisense oligonucleotides (Figure 7).

DISCUSSION

Gastric cancer is a common malignant neoplasm of the alimentary tract, its incidence is among the leading three kinds of cancers in different regions of China and has an increasing tendency^[13-15]. It is one of the research focuses to explore effective methods for early prevention and treatment of gastric cancer. Survivin is a novel member of the apoptosis inhibitor gene family, which was identified by hybridization screening of human genome libraries with cDNA of effector cell protease receptor-1 (EPR-1)

by Altieri *et al*^[16] at Yale University in 1997. Interestingly, survivin expresses during embryonal development and in most human tumor tissues. It also expresses in many transformed cell lines, whereas lacks of expression in normal adult tissues^[17], indicating that survivin participates in occurrence and development of neoplasms through inhibiting apoptosis, promoting cell proliferation and regulating mitosis and angiogenesis. These findings indicate that survivin is a potential neoplasm marker correlated with prognosis^[18]. A series of researches demonstrate that both mRNA and protein levels of survivin in gastric cancer tissues are significantly higher than those in adjacent non-tumor gastric tissues, indicating that it can serve as a novel target for early diagnosis and treatment of gastric cancer^[19,20]. Tu *et al*^[7] stably transferred the antisense RNA vector for survivin into gastric cancer cells and found that cell growth was decreased with an increased rate of apoptosis, while these cells also exhibited decreased *de novo* gastric tumor formation and reduced angiogenesis.

In recent years, antisense oligonucleotide has been used to explore gene function, and exhibits a great potential in prevention and treatment of neoplasms^[21-23]. Because the secondary or tertiary structure of target gene is found in its regions inaccessible to their complementary nucleic acids through base partnership, the selection of optimal antisense accessible sites of targeted sequence is one of the key factors influencing the blocking effects of antisense nucleic acids^[24,25].

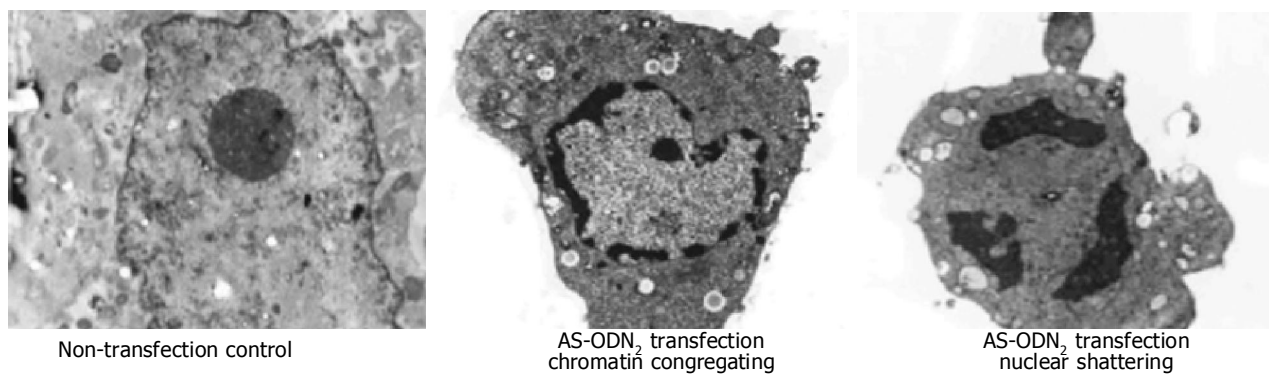


Figure 6 Morphological observation of gastric cancer cells after transfection with antisense oligonucleotides targeting survivin by electronic microscopy.

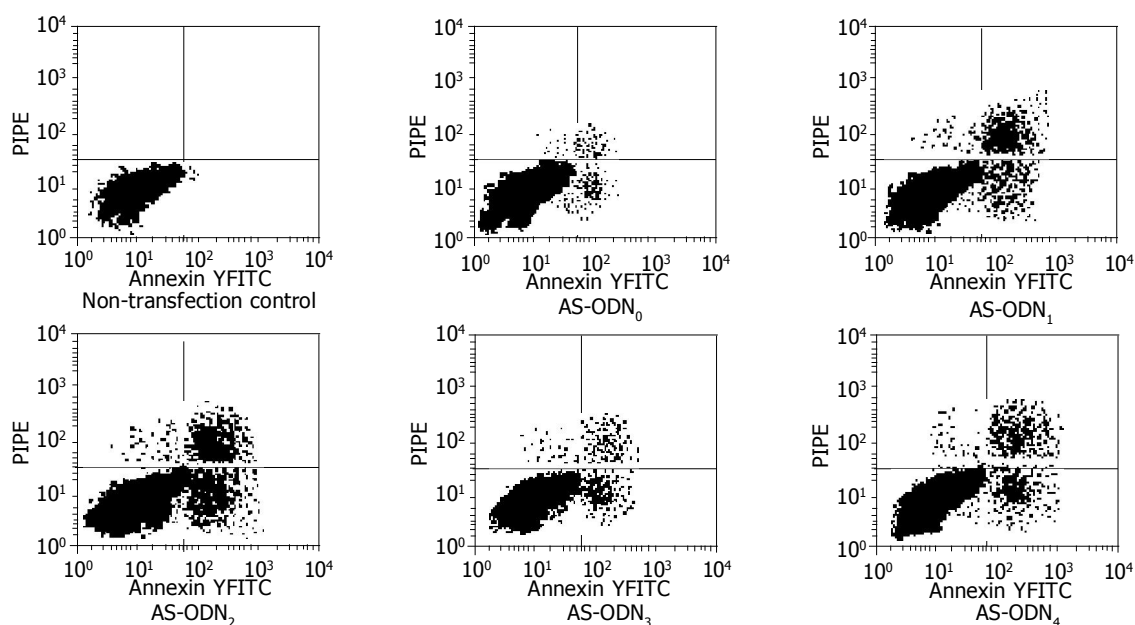


Figure 7 Flow cytometry detection of apoptosis-inducing effects of various antisense oligonucleotides on MKN-45 cells.

Random shooting method has been widely used to select antisense nucleic acids, in which a series of oligonucleotides (usually 50-100 pieces) targeting different regions of a special mRNA were synthesized and evaluated for their antisense activities or accessibilities to targeted sites. But generally only 2-5% antisense oligonucleotides are efficient. Moreover, this method can not determine all accessible sites of targeted mRNA^[26]. By computer- predicting method, RNA secondary structures can be predicted through RNA fold softwares, such as MFOLD. Though it has been used for 25 years, it is not sufficient to design antisense oligonucleotides, except for few successful examples. The reason is that computer software can form different structures with similar free energies, which makes it difficult to determine folded structures^[27-29]. Antisense hybridization screening was once considered as an efficient way to select antisense oligonucleotides, by which a large number of oligonucleotides could be synthesized and fixed in solid medium for preparation of screen-array, while corresponding analysis softwares for hybridization are also required. So, it costs a large amount of research expenditure^[30].

In 1996, based on the fact that RNase H could specifically hydrolyze the phosphodiester backbone of the RNA strand in RNA-DNA duplex hybrid, Siew *et al* firstly brought forward a brand-new conception for the *in vitro* selection of antisense accessible sites by random oligonucleotide libraries/RNase H cleavage method. Firstly, a set of random oligonucleotide libraries, which were fixed in length and composed of possible sequences, were synthesized and incubated with targeted mRNA. Oligonucleotides, which were complementary to accessible sites in libraries, could form hybridization duplex with targeted mRNA. After RNase H cleavage, the sizes and sites of the cleaved products are determined by 5' end primer extension reaction, then the accessible sites of targeted sequence are selected^[12]. This method does not require a complex resource of molecular biology and has full consideration of the blocking effects of thermodynamics on secondary or tertiary structure of mRNA. Using this method, Siew *et al* successfully selected 22 antisense accessible sites of human MDR-1 mRNA, and the maximal blocking rate of synthesized complementary antisense oligonucleotides to MDR-1 expression reached 95 percent. In order to explore the effects of random oligonucleotide libraries on selection of antisense accessible sites, Lloyd *et al*^[31] introduced four kinds of random oligonucleotide libraries including 8, 12, 16 and 20 mer, and selected 34 antisense accessible sites of TNF α mRNA, in which the 20 mer library has the highest selection efficiency. Vickers *et al*^[32] compared this method with RNAi (RNA interference) technique, and found the blocking effect of antisense oligonucleotides designed and synthesized by this method was close to that of siRNA.

In this study, thirteen antisense accessible sites of survivin were selected *in vitro* by the random oligonucleotide libraries/RNase H cleavage method, then analyzed by RNADraw software. Four sites with obvious stem-loop structures were chosen to synthesize their complementary oligonucleotides. The results of cell transfection indicate that these four antisense oligonucleotides have significantly higher blocking effects on gene expression of survivin than that of simply designed by computer software. AS-ODN₂ against 187-206 bp region of survivin cDNA, had the best blocking effects. After transfected with 600 nmol/L AS-ODN₂, the growth activities of gastric cancer cells were significantly inhibited with obvious apoptotic cells. This demonstrates that the selected antisense oligonucleotides can block the biological function of survivin. This research establishes a basis for further exploring the roles of survivin in biological behaviors of gastric cancer and its regulation mechanisms. Meanwhile, it also provides a brand-new field of

vision and an important method for the targeted therapy of gastric cancer, through antisense technology against survivin genes to carry biological therapeutic drugs^[33,34].

REFERENCES

- 1 Altieri DC. Survivin, versatile modulation of cell division and apoptosis in cancer. *Oncogene* 2003; **22**: 8581-8589
- 2 Chiou SK, Jones MK, Tarnawski AS. Survivin-an anti-apoptosis protein: its biological roles and implications for cancer and beyond. *Med Sci Monit* 2003; **9**: P125-P129
- 3 Andersen MH, Thor SP. Survivin-a universal tumor antigen. *Histol Histopathol* 2002; **17**: 669-675
- 4 Yamamoto T, Tanigawa N. The role of survivin as a new target of diagnosis and treatment in human cancer. *Med Electron Microsc* 2001; **34**: 207-212
- 5 Altieri DC. Survivin in apoptosis control and cell cycle regulation in cancer. *Prog Cell Cycle Res* 2003; **5**: 447-452
- 6 Miyachi K, Sasaki K, Onodera S, Taguchi T, Nagamachi M, Kaneko H, Sunagawa M. Correlation between survivin mRNA expression and lymph node metastasis in gastric cancer. *Gastric Cancer* 2003; **6**: 217-224
- 7 Tu SP, Jiang XH, Lin MC, Cui JT, Yang Y, Lum CT, Zou B, Zhu YB, Jiang SH, Wong WM, Chan AO, Yuen MF, Lam SK, Kung HF, Wong BC. Suppression of survivin expression inhibits *in vivo* tumorigenicity and angiogenesis in gastric cancer. *Cancer Res* 2003; **63**: 7724-7732
- 8 Sohail M, Southern EM. Selecting optimal antisense reagents. *Adv Drug Deliv Rev* 2000; **44**: 23-34
- 9 Scherr M, Rossi JJ, Sczakiel G, Patzel V. RNA accessibility prediction: a theoretical approach is consistent with experimental studies in cell extracts. *Nucleic Acids Res* 2000; **28**: 2455-2461
- 10 Lehmann MJ, Patzel V, Sczakiel G. Theoretical design of antisense genes with statistically increased efficacy. *Nucleic Acids Res* 2000; **28**: 2597-2604
- 11 Pan WH, Devlin HF, Kelley C, Isom HC, Clawson GA. A selection system for identifying accessible sites in target RNAs. *RNA* 2001; **7**: 610-621
- 12 Ho SP, Britton DH, Stone BA, Behrens DL, Leffet LM, Hobbs FW, Miller JA, Trainor GL. Potent antisense oligonucleotides to the human multidrug resistance-1 mRNA are rationally selected by mapping RNA-accessible sites with oligonucleotide libraries. *Nucleic Acids Res* 1996; **24**: 1901-1907
- 13 Yin T, Ji XL, Shen MS. Relationship between lymph node sinuses with blood and lymphatic metastasis of gastric cancer. *World J Gastroenterol* 2003; **9**: 40-43
- 14 Karatzas G, Kouskos E, Kouraklis G, Mantas D, Papachristodoulou A. Gastrointestinal carcinoid tumors: 10-year experience of a general surgical department. *Int Surg* 2004; **89**: 21-26
- 15 Correa P, Piazuelo MB, Camargo MC. The future of gastric cancer prevention. *Gastric Cancer* 2004; **7**: 9-16
- 16 Ambrosini G, Adida C, Altieri DC. A novel anti-apoptosis gene, survivin, expressed in cancer and lymphoma. *Nat Med* 1997; **3**: 917-921
- 17 Altieri DC. Validating survivin as a cancer therapeutic target. *Nat Rev Cancer* 2003; **3**: 46-54
- 18 Nasu S, Yagihashi A, Izawa A, Saito K, Asanuma K, Nakamura M, Kobayashi D, Okazaki M, Watanabe N. Survivin mRNA expression in patients with breast cancer. *Anticancer Res* 2002; **22**: 1839-1843
- 19 Kania J, Konturek SJ, Marlicz K, Hahn EG, Konturek PC. Expression of survivin and caspase-3 in gastric cancer. *Dig Dis Sci* 2003; **48**: 266-271
- 20 Yu J, Leung WK, Ebert MP, Ng EK, Go MY, Wang HB, Chung SC, Malfertheiner P, Sung JJ. Increased expression of survivin in gastric cancer patients and in first degree relatives. *Br J Cancer* 2002; **87**: 91-97
- 21 Dean NM, Bennett CF. Antisense oligonucleotide-based therapeutics for cancer. *Oncogene* 2003; **22**: 9087-9096
- 22 Biroccio A, Leonetti C, Zupi G. The future of antisense therapy: combination with anticancer treatments. *Oncogene* 2003; **22**:

- 6579-6588
- 23 **Lavery KS**, King TH. Antisense and RNAi: powerful tools in drug target discovery and validation. *Curr Opin Drug Discov Devel* 2003; **6**: 561-569
- 24 **Giddings MC**, Shah AA, Freier S, Atkins JF, Gesteland RF, Matveeva OV. Artificial neural network prediction of antisense oligodeoxynucleotide activity. *Nucleic Acids Res* 2002; **30**: 4295-4304
- 25 **Ho SP**, Britton DH, Bao Y, Scully MS. RNA mapping: selection of potent oligonucleotide sequences for antisense experiments. *Methods Enzymol* 2000; **314**: 168-183
- 26 **Toulme JJ**, Tinevez RL, Brossalina E. Targeting RNA structures by antisense oligonucleotides. *Biochimie* 1996; **78**: 663-673
- 27 **'t Hoen PA**, Out R, Commandeur JN, Vermeulen NP, van Batenburg FH, Manoharan M, van Berkel TJ, Biessen EA, Bijsterbosch MK. Selection of antisense oligodeoxynucleotides against glutathione S-transferase Mu. *RNA* 2002; **8**: 1572-1583
- 28 **Smith L**, Andersen KB, Hovgaard L, Jaroszewski JW. Rational selection of antisense oligonucleotide sequences. *Eur J Pharm Sci* 2000; **11**: 191-198
- 29 **Matveeva OV**, Tsodikov AD, Giddings M, Freier SM, Wyatt JR, Spiridonov AN, Shabalina SA, Gesteland RF, Atkins JF. Identification of sequence motifs in oligonucleotides whose presence is correlated with antisense activity. *Nucleic Acids Res* 2000; **28**: 2862-2865
- 30 **Patzel V**, Steidl U, Kronenwett R, Haas R, Sczakiel G. A theoretical approach to select effective antisense oligodeoxyribonucleotides at high statistical probability. *Nucleic Acids Res* 1999; **27**: 4328-4334
- 31 **Lloyd BH**, Giles RV, Spiller DG, Grzybowski J, Tidd DM, Sibson DR. Determination of optimal sites of antisense oligonucleotide cleavage within TNFalpha mRNA. *Nucleic Acids Res* 2001; **29**: 3664-3673
- 32 **Vickers TA**, Koo S, Bennett CF, Croke ST, Dean NM, Baker BF. Efficient reduction of target RNAs by small interfering RNA and RNase H-dependent antisense agents. A comparative analysis. *J Biol Chem* 2003; **278**: 7108-7118
- 33 **Ma Z**, Taylor JS. Nucleic acid triggered catalytic drug and probe release: a new concept for the design of chemotherapeutic and diagnostic agents. *Bioorg Med Chem* 2001; **9**: 2501-2510
- 34 **Ma Z**, Taylor JS. Nucleic acid-triggered catalytic drug release. *Proc Natl Acad Sci USA* 2000; **97**: 11159-11163

Assistant Editor Guo SY Edited by Zhu LH and Wang XL

Quantitative assessment model for gastric cancer screening

Kun Chen, Wei-Ping Yu, Liang Song, Yi-Min Zhu

Kun Chen, Wei-Ping Yu, Liang Song, Yi-Min Zhu, School of Medicine, Zhejiang University, Hangzhou 310031, Zhejiang Province, China
Supported by National Nature Science Foundation of China, No. 30170828

Correspondence to: Kun Chen, M.D., Department of Epidemiology, School of Medicine, Zhejiang University, 353 Yan-an Road, Hangzhou 310031, Zhejiang Province, China. ck@zjuem.zju.edu.cn

Telephone: +86-571-87217190 **Fax:** +86-571-87217184

Received: 2004-03-03 **Accepted:** 2004-04-13

Abstract

AIM: To set up a mathematic model for gastric cancer screening and to evaluate its function in mass screening for gastric cancer.

METHODS: A case control study was carried on in 66 patients and 198 normal people, then the risk and protective factors of gastric cancer were determined, including heavy manual work, foods such as small yellow-fin tuna, dried small shrimps, squills, crabs, mothers suffering from gastric diseases, spouse alive, use of refrigerators and hot food, etc. According to some principles and methods of probability and fuzzy mathematics, a quantitative assessment model was established as follows: first, we selected some factors significant in statistics, and calculated weight coefficient for each one by two different methods; second, population space was divided into gastric cancer fuzzy subset and non gastric cancer fuzzy subset, then a mathematic model for each subset was established, we got a mathematic expression of attribute degree (AD).

RESULTS: Based on the data of 63 patients and 693 normal people, AD of each subject was calculated. Considering the sensitivity and specificity, the thresholds of AD values calculated were configured with 0.20 and 0.17, respectively. According to these thresholds, the sensitivity and specificity of the quantitative model were about 69% and 63%. Moreover, statistical test showed that the identification outcomes of these two different calculation methods were identical ($P > 0.05$).

CONCLUSION: The validity of this method is satisfactory. It is convenient, feasible, economic and can be used to determine individual and population risks of gastric cancer.

© 2005 The WJG Press and Elsevier Inc. All rights reserved.

Key words: Gastric cancer; Mass screening; Quantitative assessment model

Chen K, Yu WP, Song L, Zhu YM. Quantitative assessment model for gastric cancer screening. *World J Gastroenterol* 2005; 11(5): 641-644

<http://www.wjgnet.com/1007-9327/11/641.asp>

INTRODUCTION

Gastric cancer is the second most common cause of cancer

deaths in the world, and China is one of the high-risk areas^[1]. Population screening is an effective program for providing early diagnosis and subsequent treatment of gastric cancer at its curable stage. Whatever screening method is used, the most important thing is that the method should be convenient, feasible, and acceptable to the target population^[2]. At present, the methods used to find and diagnose gastric cancer at early time are complicated, or their sensitivity and specificity are dissatisfactory. Based on a population case-control study, a mathematic model was established for determining individual and population risks of gastric cancer in this paper. An assessment of its practical application was also carried out to determine its validity.

MATERIALS AND METHODS

Case-control study

To study the risk factors for gastric cancer, a case-control study including 66 patients and 198 normal people, was carried out in 1999. Factors involving demographic variables, diet, drinking water source, individual habits, disease history and family history of gastric cancer were investigated in this study. Risk and protective factors for gastric cancer were determined by the fast epidemiology assessment method^[3]. At the level of $\alpha = 0.10$, gastric cancer risk factors included heavy manual work (>2 h/d), foods such as small yellow-fin tuna, dried small shrimps, squills, crabs, and mothers suffering from gastric diseases. In contrast, spouse alive, use of refrigerators and hot food were the protective factors against gastric cancer.

Mathematic expression

Based on the case-control study, a quantitative assessment method was put forward by selecting some factors significant in statistics, including risk factors and protective factors, with application of some theories and approaches of fuzzy and probability mathematics. The method was set up as follows. Population characteristic space was divided into gastric cancer fuzzy subset and non gastric cancer fuzzy subset, respectively. Which subset each subject belonged to was determined by attribute function, and the determination probability should be maximal, or its error probability should be minimum. \tilde{A} was configured as a fuzzy subset suffering from gastric cancer. First, for setting up a fuzzy mathematical model, a group of standard factors should be determined, that was U_i . Weight sum (P) of U_i was configured as following:

$$P_{\tilde{A}} = \sum_{j=1}^n \alpha_j C_j \cdots \cdots (1)$$

In the expression (1), $j = 1, 2, 3, \dots, n$, and n is the number of the factors selected. C_j is an identification score of each factor, that is C_j equals 1 when a subject has a factor of F_i , no matter that F_i is a risk factor or not. α_j is an attribute coefficient of F_i , thereof P is weight sum of all factors (F_i).

$P_{\tilde{A}}$ is representative of weight sum of a subject when he (or she) has some or all factors, that is:

$$P_{\tilde{A}} = \sum_{j=1}^n \alpha_j C_j \cdots \cdots (2) \quad (j = 1, 2, 3, \dots, n)$$

In the expression (2), α_j is the attribute coefficient of each

F_i , and when a subject has a certain F_i , C_j equals C_j if F_i is a risk factor. On the contrary, C_j equals 0 or 1 if a subject has no F_i . An attribute function (individual or population) can be set up with $P_{\hat{A}}$ and $P_{\bar{A}}$:

$$\mu_{\hat{A}}(U_i) = \frac{P_{\hat{A}}}{P_{\bar{A}}} \dots \dots (3)$$

In the expression (3), $\mu_{\hat{A}}(U_i)$ is the expression of attribute function of \hat{A} . A specific value ranging from 0 to 1 can be calculated by the expression for each subject, that is AD.

Determination of weight coefficient for each factor

α_i in the expressions (1) and (2) was calculated by two different methods. In method 1, OR for each F_i is taken as the weight coefficient of each F_i (if F_i is a protective factor, its weight coefficient equals 1/OR), that is $\alpha_i = \frac{OR_i(or 1/OR_i)}{\sum OR_i}$. A weight

coefficient was calculated using the conditional probability and entropy of each F_i , which is $\alpha_i = \frac{H(F_i/D)}{H(F_i/D) + H(F_i/\bar{D})}$ in method 2.

In the expression, $H(F_i/D)$ is the entropy of F_i in the condition of patients, and $H(F_i/\bar{D})$ is entropy of F_i in the condition of normal people.

$$H(F_i/D) = -P(F_i/D) \log_2 P(F_i/D)$$

$$H(F_i/\bar{D}) = -P(F_i/\bar{D}) \log_2 P(F_i/\bar{D})$$

Weight coefficients of all factors are illustrated in Table 1.

Assessment of quantitative method

AD values of 63 patients and 693 normal people were calculated with the expression (3), based on the quantitative assessment of individual risk and population screening of gastric cancer. The variational trend of sensitivity, specificity and Youden indexes were identical, which are illustrated in Figure 1, though calculation methods were different.

Because AD is a continuous variable, the identification threshold could be determined based on actual needs. The threshold could be reduced a little in order to increase the positive rate while trying to check out more patients. Moreover, the threshold could be raised to increase the specificity and reduce the rate of false diagnosis in detective diagnosis (Figure 1).

In order to get the maximal Youden indexes, the thresholds of AD values were configured with 0.20 and 0.17, considering the sensitivity and specificity of population screening for gastric cancer. Diagnostic value of different calculation methods of weight coefficients are summarized in Table 2, and significance test showed that these Youden indexes had no statistical significance ($P > 0.05$). Thus we could see the outcomes tended to be identical.

DISCUSSION

Gastric cancer, the most common fatal malignancy in the world, causes more than 750 000 deaths annually^[4]. To the year of 2005, the mortality of gastric cancer is about to reach 26.3/100 000 per year in china^[5]. Early finding, diagnosis and treatment are the keys to reduce the mortality of gastric cancer, to raise the survival rate and improve the life quality of patients.

Table 1 OR values, confidence limits and weight coefficients of risk factors and protective factors of gastric cancer

Variable	OR _i	95% C.I.	α_i (method 1)	α_i (method 2)
Time of heavy manual work (>2 h/d)	2.00	1.14-3.54	0.084	0.439
Eating small yellow-fin tuna frequently	1.52	1.10-2.09	0.064	0.490
Often eating squills (dry)	6.12	1.15-32.66	0.257	0.782
Eating dried small shrimps frequently	1.26	0.99-1.60	0.053	0.462
Often eating squills (fresh)	1.70	0.92-3.13	0.071	0.429
Eating crabs frequently	1.76	1.00-3.09	0.074	0.451
Mother suffering tummy bug	5.51	0.95-32.06	0.231	0.774
Eating shortly after anger	2.07	1.31-3.27	0.087	0.522
Spouse alive	0.89	0.81-0.99	0.047	0.819
Using refrigerators	0.47	0.19-1.15	0.089	0.399
Often eating hot food	0.52	0.28-0.97	0.081	0.438

Table 2 Diagnosis value of different calculation method of weight coefficient

α_j	AD	Patients (n/N)	Normal people (n/N)	Sensitivity (%)	Specificity (%)	Youden index
Method 1	≥ 0.20	44/64	440/693	69.8	63.5	0.333
Method 2	≥ 0.17	43/63	435/693	68.3	62.8	0.311

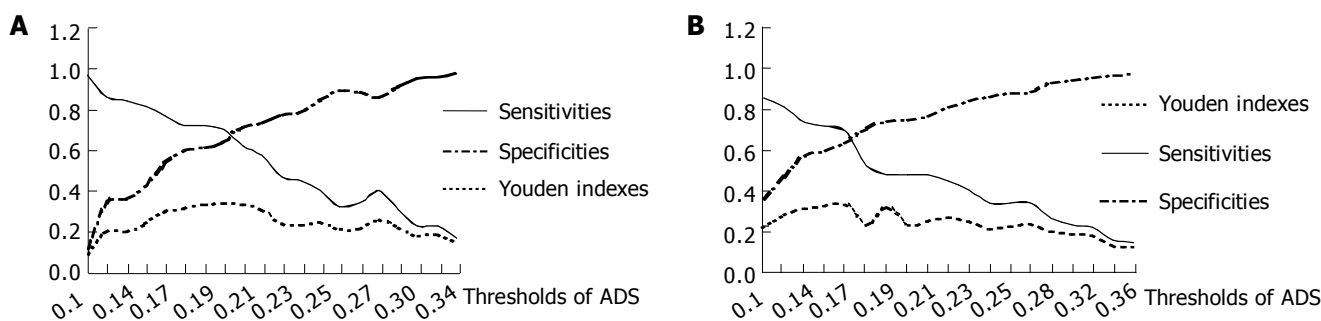


Figure 1 Diagnostic value of risk assessment for gastric cancer by method 1 (A) and method 2 (B).

In early gastric cancer, the 5-year survival rate is greater than 90% if treated by experienced hands^[6]. It has important significance to develop a simple and feasible screening method to find high risk populations or early gastric cancer.

Up to now various methods for gastric cancer screening have been developed. X-ray examination^[7,8], endoscopy^[9,10], *Helicobacter pylori* screening^[11], power Doppler imaging^[12] and photo fluorography^[13] are used in gastric cancer screening. In addition, gastric occult blood bead test^[14], serum pepsinogen concentration measure^[15] and fecal carcinoembryonic antigen measurement^[16], are also used in screening gastric cancer. The efficacy of some methods has reached an ideal level^[15-17]. Except for the methods mentioned above, some gene alterations, such as hMLH1 methylation^[18], BAT-26 mutation localized in intron 5 of hMSH2 gene^[19], E-cadherin germline mutations^[20], cyclin overexpression, microsatellite instability, P53 mutation^[21] are useful molecular markers for gastric cancer.

Quantitative method has rarely been applied to gastric cancer screening either at home or at abroad. Qiu *et al*^[22] studied the application of pattern recognition method in 1994. A computer program was designed according to the principle of pattern recognition and risk factors for gastric cancer. Its detection rate was 1.54/1 000 in a study of 51 735 males aged 45-64 years.

Though the accuracy of some screening methods is ideal, they have obvious disadvantages in practice. Endoscopy and biopsy could make subjects discomfort. Many suspicious patients tend to refuse these kinds of examinations. Another shortcoming is the high cost. Some molecular biology marker tests cost subjects too much due to expensive reagents, some of them are invasive because gastric juice must be collected before tests. In addition, the pattern recognition method reported by Qiu *et al*^[22] was complicated and high-cost, because 61 indexes must be questioned to subjects. Moreover, the principle of pattern recognition is difficult to be mastered by subjects and inquirers, and the workload is heavy. Therefore, a conclusion may be reached that these methods are not suitable for application in China.

Compared with these methods, the quantitative assessment model is simple, economic, non-invasive and feasible. Identification can be run as long as each subject fills in a simple questionnaire, and calculation method is simpler than traditional mathematic methods such as regression identification. Furthermore, the diagnostic value of this quantitative method is relatively high. Its sensitivity and specificity are about 69% and 63%. Given the factors just outlined, this quantitative screening method for gastric cancer can be applied to a large population in China.

Formerly, quantitative methods were mostly applied to differential diagnosis in clinic^[23]. There have been some methods for assessing health hazard/health risk based on epidemic study of population since 1980s^[24]. In the 1990s, a quantitatively scored cancer-risk assessment model^[25] was developed to promote cancer prevention and screening in America. Subsequently quantitative models are widely used in the diagnosis, treatment and prevention of diseases, such as multi-stage lung cancer^[26], assessment of cancer death in elderly patients^[27], quantitative model for early diagnosis of colorectal cancer^[28] and efficacy evaluation of intervention experiments^[29]. In the late 1980s, Chen *et al*^[30] reported a mathematic model for mass screening of colorectal cancer, which was subsequently proved to be a convenient, effective and economic screening method. In recent years, the mathematic model has been applied to screening other diseases, including coronary heart disease and stroke^[31], lung cancer^[32]. These studies show that the model has good efficacy. However, there are two points to which attention must be paid. One is how to identify threshold values. In our study,

the threshold could be defined with practical application because AD is a continuous variable. However, further follow-up is needed to increase its precision in screening other diseases, because causes of different diseases are complicated. The other is the low Youden index^[30,31]. The reasons why many factors are associated with these diseases are still unclear.

In short, the quantitative method can be regarded as the front line method for assessing risks of gastric cancer. Occurrence of gastric cancer is the outcome of many influential factors, which are possibly different in different areas and populations, that combining with actual status is very important. Further studies are needed to testify whether this screening method can contribute to the decrease of gastric cancer mortality.

REFERENCES

- 1 **Correa P**, Piazuolo MB, Camargo MC. The future of gastric cancer prevention. *Gastric Cancer* 2004; **7**: 9-16
- 2 **Tan ZH**. Modern epidemiology. 1st ed. Beijing: People's Medical Publishing House 2001: 162
- 3 **Zhu YM**, Chen K, Zhang Y, Zhu YP, Liu XY, Chen XX, Xu ZZ, Chen JH. Analysis on risk factors of gastric cancer in island residents. *Zhongguo Gonggong Weisheng* 2000; **16**: 916
- 4 **Xia HH**, Wong BC, Lam SK. Chemoprevention of gastric cancer: current status. *Chin Med J* 2003; **116**: 5-10
- 5 **Sun XD**, Mu R, Zhou YS, Dai XD, Zhang SW, XM, Sun J, Li LD, Lu FZ, Qiao YL. Analysis of mortality rate of stomach cancer and its trend in twenty years in China. *Zhonghua Zhongliu Zazhi* 2004; **26**: 4-9
- 6 **Hohenberger P**, Gretschel S. Gastric cancer. *Lancet* 2003; **362**: 305-315
- 7 **Inaba S**, Hirayama H, Nagata C, Kurisu Y, Takatsuka N, Kawakami N, Shimizu H. Evaluation of a screening program on reduction of gastric cancer mortality in Japan: preliminary results from a cohort study. *Prev Med* 1999; **29**: 102-106
- 8 **Sasagawa Y**, Sasagawa T, Takasaki K. Mass screening for gastric cancer performed in Costa Rica. *Shokakibyō Gakkai Zasshi* 2002; **99**: 577-583
- 9 **Han JY**, Son H, Lee WC, Choi BG. The correlation between gastric cancer screening method and the clinicopathologic features of gastric cancer. *Med Oncol* 2003; **20**: 265-269
- 10 **Riecken B**, Pfeiffer R, Ma JL, Jin ML, Li JY, Liu WD, Zhang L, Chang YS, Gail MH, You WC. No impact of repeated endoscopic screens on gastric cancer mortality in a prospectively followed Chinese population at high risk. *Prev Med* 2002; **34**: 22-28
- 11 **Roderick P**, Davies R, Raftery J, Crabbe D, Pearce R, Patel P, Bhandari P. Cost-effectiveness of population screening for *Helicobacter pylori* in preventing gastric cancer and peptic ulcer disease, using simulation. *J Med Screen* 2003; **10**: 148-156
- 12 **Kawasaki T**, Ueo T, Itani T, Shibatohege M, Mimura J, Komori H, Todo A, Kudo M. Vascularity of advanced gastric carcinoma: evaluation by using power Doppler imaging. *J Gastroenterol Hepatol* 2001; **16**: 149-153
- 13 **Portnoi LM**, Kazantseva IA, Isakov VA, Nefedova VI, Gaganov LE. Gastric cancer screening in selected population of Moscow region: retrospective evaluation. *Eur Radiol* 1999; **9**: 701-705
- 14 **Zhou L**, Yu H, Zheng S. The value of "occult blood bead" in detection of upper digestive tract disorders with bleeding. *Zhonghua Zhongliu Zazhi* 1999; **21**: 48-50
- 15 **Kitahara F**, Kobayashi K, Sato T, Kojima Y, Araki T, Fujino MA. Accuracy of screening for gastric cancer using serum pepsinogen concentrations. *Gut* 1999; **44**: 693-697
- 16 **Kim Y**, Lee S, Park S, Jeon H, Lee W, Kim JK, Cho M, Kim M, Lim J, Kang CS, Han K. Gastrointestinal tract cancer screening using fecal carcinoembryonic antigen. *Ann Clin Lab Sci* 2003; **33**: 32-38
- 17 **Kubota H**, Kotoh T, Masunaga R, Dhar DK, Shibakita M, Tachibana M, Kohno H, Nagasue N. Impact of screening survey of gastric cancer on clinicopathological features and survival: retrospective study at a single institution. *Surgery* 2000; **128**: 41-47
- 18 **Waki T**, Tamura G, Tsuchiya T, Sato K, Nishizuka S, Motoyama

- T. Promoter methylation status of E-cadherin, hMLH1, and p16 genes in nonneoplastic gastric epithelia. *Am J Pathol* 2002; **161**: 399-403
- 19 **Wu MS**, Lee CW, Sheu JC, Shun CT, Wang HP, Hong RL, Lee WJ, Lin JT. Alterations of BAT-26 identify a subset of gastric cancer with distinct clinicopathologic features and better post-operative prognosis. *Hepatogastroenterology* 2002; **49**: 285-289
- 20 **Graziano F**, Ruzzo AM, Bearzi I, Testa E, Lai V, Magnani M. Screening E-cadherin germline mutations in Italian patients with familial diffuse gastric cancer: an analysis in the District of Urbino, Region Marche, Central Italy. *Tumori* 2003; **89**: 255-258
- 21 **Lam SK**. 9th Seah Cheng Siang Memorial Lecture: gastric cancer--where are we now? *Ann Acad Med Singapore* 1999; **28**: 881-889
- 22 **Qiu XY**, Shi QX, Shi R, Tu JT, Chen HQ. Mass screening of gastric cancer-establishment of pattern recognition method and its application. *Zhongguo Weisheng Tongji* 1994; **11**: 47-50
- 23 **Zhou HW**, Sun WM. Metrological medicine of clinic. 1st ed. Shanghai: Publishing House of Shanghai Medical University 1999: 51-72
- 24 **Wagner EH**, Beery WL, Schoenbach VJ, Graham RM. An assessment of health hazard/health risk appraisal. *Am J Public Health* 1982; **72**: 347-352
- 25 **Lippman SM**, Bassford TL, Meyskens FL. A quantitatively scored cancer-risk assessment tool: its development and use. *J Cancer Educ* 1992; **7**: 15-36
- 26 **Dawson SV**, Alexeeff GV. Multi-stage model estimates of lung cancer risk from exposure to diesel exhaust, based on a U.S. railroad worker cohort. *Risk Anal* 2001; **21**: 1-18
- 27 **Walter LC**, Covinsky KE. Cancer screening in elderly patients: a framework for individualized decision making. *JAMA* 2001; **285**: 2750-2756
- 28 **Jin W**, Gao MQ, Lin ZW, Yang DX. Multiple biomarkers of colorectal tumor in a differential diagnosis model: a quantitative study. *World J Gastroenterol* 2004; **10**: 439-442
- 29 **Wilcox S**, Parra-Medina D, Thompson-Robinson M, Will J. Nutrition and physical activity interventions to reduce cardiovascular disease risk in health care settings: a quantitative review with a focus on women. *Nutr Rev* 2001; **59**: 197-214
- 30 **Chen K**. A quantitative method for mass screening of colorectal cancer. *Zhejiang Yike Daxue Xuebao* 1988; **17**: 49-52
- 31 **Chen K**, Zhu YM, Fang SY, Chen YY. Quantitative method for mass screening of coronary heart disease (CHD) and stroke. *Jibing Kongzhi Zazhi* 1997; **1**: 15-17
- 32 **Zhou BS**, He AG, Liu KL, Sun J, Shi HL, Gu DY, Gu HC. Quantitative scored lung cancer risk assessment. *Zhongguo Weisheng Tongji* 1996; **13**: 19-22

Edited by Wang XL and Kumar M

• COLORECTAL CANCER •

Cytokeratins and carcinoembryonic antigen in diagnosis, staging and prognosis of colorectal adenocarcinoma

Luís C. Fernandes, Su B. Kim, Delcio Matos

Luís C. Fernandes, Su B. Kim, Delcio Matos, Coloproctology Sector of Surgical Gastroenterology Department, UNIFESP - Escola Paulista de Medicina, São Paulo, Brazil

Supported by Foundation for Research Support of the State of São Paulo

Correspondence to: Dr. Luís C. Fernandes, Al. Santos, 211, cj.304, Paraíso São Paulo -SP, 01419-000, Brazil. luisfernandes@terra.com.br

Telephone: +55-11-287-7231 Fax: +55 -11-251-1662

Received: 2004-05-01 Accepted: 2004-06-29

Abstract

AIM: To evaluate the serum levels of cytokeratins and carcinoembryonic antigen (CEA) in diagnosis, staging and prognosis of patients with colorectal adenocarcinoma.

METHODS: The sample consisted of 169 patients. One hundred blood donors formed the control group. Radical surgery was performed on 120 patients, with an average follow-up duration of 22.3 mo. Relapses occurred in 23 individuals after an average of 18.09 mo. CEA was assayed via the Delfia® method with a limit of 5 ng/mL. Cytokeratins were assayed via the LIA-mat® TPA-M Prolifigen® method with a limit of 72 U/L.

RESULTS: In the diagnosis of patients with colorectal adenocarcinoma, CEA showed a sensitivity of 56%, a specificity of 95%, a positive predictive value of 94%, a negative predictive value of 50% and an accuracy of 76.8%. TPA-M had a sensitivity of 70%, a specificity of 96%, a positive predictive value of 97%, a negative predictive value of 66% and an accuracy of 93.6%. The elevation of one of the markers was shown to have a sensitivity of 76.9%, a specificity of 91%, a positive predictive value of 93.5%, a negative predictive value of 70% and an accuracy of 83.6%. There was no variation in the levels of the markers according to the degree of cell differentiation while there was an elevation in their concentrations in accordance with the increase in neoplastic dissemination. There was a statistically significant difference between the patients with stage IV lesions and those with stages I, II and III tumors. With regard to CEA, the average level was 14.2 ng/mL in patients with stage I lesions, 8.5 ng/mL in patients with stage II lesions, 8.0 ng/mL in patients with stage III lesions and 87.7 ng/mL in patients with stage IV lesions. In relation to TPA-M, the levels were 153.1 U/L in patients with stage I tumors, 106.5 U/L in patients with stage II tumors, 136.3 U/L in patients with stage III tumors and 464.3 U/L in patients with stage IV tumors. There was a statistical difference in patients with a high CEA level in relation to a shorter survival ($P < 0.05$). However, there was no correlation between patients with high TPA-M levels and prognostic indices of patients undergoing radical surgery.

CONCLUSION: Cytokeratins demonstrate a greater sensitivity than CEA in the diagnosis of colorectal adenocarcinoma. There is an increase in the sensitivity of the markers with

tumor dissemination. Cytokeratins cannot identify the worse prognosis in patients undergoing radical surgery. Cytokeratins constitute an advance in the direction of a perfect tumor marker in the treatment of patients with colorectal cancer.

© 2005 The WJG Press and Elsevier Inc. All rights reserved.

Key words: Colorectal adenocarcinoma; Cytokeratins; Carcinoembryonic antigen

Fernandes LC, Kim SB, Matos D. Cytokeratins and carcinoembryonic antigen in diagnosis, staging and prognosis of colorectal adenocarcinoma. *World J Gastroenterol* 2005; 11(5): 645-648

<http://www.wjgnet.com/1007-9327/11/645.asp>

INTRODUCTION

Colorectal cancer is the third most frequent cancer in the world, with a high incidence rate in North America, Western Europe, Australia, New Zealand and France^[1,2]. The general survival rate of colorectal patients does not exceed 40%^[3,4].

The average five-year survival rate of patients with lesions diagnosed at early stages (stage I) is approximately 70%, and is 6% in cases of advanced disease (stage IV)^[5]. Better public awareness has assisted in diagnosing lesions at initial stages. Nonetheless, patients are commonly found to have the disease at advanced stages with extremely poor results. Sometimes palliative surgery or interventions are performed in which tumor resection is not achieved^[6,7].

It is in this context that the use of serum tumor markers has its place. These substances, which can be detected in peripheral blood indicate the existence of developing neoplasm in the body^[8]. In colorectal adenocarcinoma, CEA^[9] has become distinguished as a tumor marker in the diagnosis^[10-12], staging^[10-12], and prognosis^[13-15] of patients with colorectal carcinoma, and in the detection of its recurrence^[16-19].

Other markers have been developed such as CA 19-9^[20,21], CA 242^[21], CA 72-4^[22], cytokeratins^[23,24], VEGF^[25], and p53^[26,27]. Of these, cytokeratins merit attention.

Tissue polypeptide antigen (TPA) was the first developed for detecting cytokeratins in 1978^[23]. This evolved into tissue polypeptide specific antigen (TPS) in 1992^[28,29]. Subsequent to this, monoclonal tissue polypeptide antigen (TPA-M) was developed in 1994. Its utilization has been analyzed with regard to the diagnosis of colorectal adenocarcinoma^[30,31] and neoplasms in other organs, such as the prostate^[32], ovaries^[33], lungs^[34], bladder^[35] and breast^[36].

A comparison between cytokeratins and CEA would be useful for determining whether they have clinical advantages in the diagnosis, staging and prognosis of colon or rectal cancer patients.

MATERIALS AND METHODS

A study was made in 169 patients (n) with colorectal

adenocarcinoma undergoing surgical treatment. The study was conducted in accordance with international standards (Helsinki Declaration)^[37], and approved by the Institutional Ethics Committee. Patients who had a previous neoplasm history were excluded. A control group of 100 individuals was recruited among blood donors at the General Hospital, São Paulo.

The patients were informed that the study period would consist of the surgical phase and a postoperative follow-up period of 6, 12, 18, 24, 36, 48 and 60 mo. The preoperative staging was achieved via clinical evaluation, colonoscopy, computerized tomography (CT) of the abdomen and pelvis, and chest radiography. Opaque enema, nuclear magnetic resonance (NMR) and bone scintigraphy were performed in accordance with the clinical indications of each case.

Blood samples were centrifuged and the peripheral serum was frozen at -20 °C. The patients were periodically followed up during the postoperative period by means of clinical evaluation and performing the examinations mentioned. In the control group, peripheral blood samples were collected via procedures similar to those used for the patients.

With regard to ethnicity, 69.2% of the patients were whites, 20.1% brown-skinned, 7.7% yellow-skinned and 3% blacks. With regard to gender, 43.2% were males. At the time of diagnosis, the average age was 62.2 years, ranging from 19 to 89 years. Fifty-four point four percent of the lesion locations were in the rectum, 18.9% in the left colon, 3.6% in the transverse colon and 23.1% in the right colon. The average diameter of the neoplasms was 6.1 cm, ranging from 1 to 17 cm.

Of the initial 169 patients, 120 underwent curative surgery (71%). The average time of follow-up was 22.3 mo.

Follow-up was lost in 3 patients (1.8%). Of the 120 patients undergoing radical surgery, 81 (67.5%) completed the follow.

Among the 120 patients undergoing radical surgery, 23 (19.2%) presented neoplastic relapse at an average of 18.1 mo after the initial surgery.

The control group was composed of 100 blood donors at the General Hospital, São Paulo (HGSP). Forty-five percent of the donors were whites, 39% brown-skinned, 12% blacks and 4% yellow-skinned. Fifty-four were males. At the time of blood donation, their average age was 42.5 years, ranging from 18 to 60 years.

A single professional at the Clinical Analysis Laboratory of Hospital São Paulo, Federal University of São Paulo - Escola Paulista de Medicina, performed the serum assays for tumor markers. The CEA level was determined via the Delfia® method, using the Cobas Mira Plus® automatic analyzer from Roche®, and the limit for normality was considered to be 5 ng/mL^[10,11,18]. The cytokeratin levels were determined via the LIA-mat TPA-M Prolifigen® method from the AB Sangtec Medical® Laboratory, using the Lumat LB 9501® Luminometer from EG&G Berthold, and the reference value of 72 U/L.

The following were utilized in the statistical analysis: ROC curve^[38], kappa statistic analysis (κ)^[39], variance analysis^[40], Student's *t* test (*t*)^[41] and survival analysis^[41] via the Kaplan-Meier curves. $P < 0.05$ was considered statistically significant.

RESULTS

Diagnosis

In the diagnosis of colorectal adenocarcinoma, CEA demonstrated a sensitivity of 56%, a specificity of 95%, a positive predictive value of 94%, a negative predictive value of 50% and an accuracy of 76.8%. TPA-M presented a sensitivity of 70%, a specificity of 96%, a positive predictive value of 97%, a negative predictive value of 66% and an accuracy of 93.6% (Figure 1).

The elevation of one of the markers was shown to have a sensitivity of 76.9%, a specificity of 91%, a positive predictive value of 93.5%, a negative predictive value of 70% and an

accuracy of 83.6%. The reagents had independent action modes in samples from the patients.

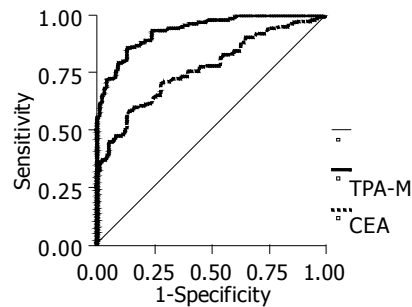


Figure 1 Receiver operating characteristic curve obtained in analysis of CEA and TPA-M in patients with colorectal cancer and individuals of the control group.

Staging

There was no variation in the levels of the markers according to the degree of cell differentiation while there was an elevation in their concentrations in accordance with the neoplastic dissemination. There was a statistically significant difference between the patients with stage IV lesions and those with stages I, II and III tumors.

With regard to CEA, the average level was 14.2 ng/mL in patients with stage I lesions, 8.5 ng/mL in patients with stage II lesions, 8.0 ng/mL in patients with stage III lesions and 87.7 ng/mL in patients with stage IV lesions. In relation to TPA-M, the levels were 153.1 U/L in patients with stage I tumors, 106.5 U/L in patients with stage II tumors, 136.3 U/L in patients with stage III tumors and 464.3 U/L in patients with stage IV tumors.

The sensitivity of each marker or its association with stages I, II, III and IV of the TNM classification is described in Table 1.

Table 1 Sensitivity of CEA and TPA-M in patients with colorectal cancer according to the staging of the TNM classification

	Sensitivity at different stages (%)			
	I	II	III	IV
CEA	35.0	23.3	34.1	69.0
TPA-M	75.0	53.3	61.0	82.8
Increased CEA or TPA-M	77.5	60.0	68.3	91.4

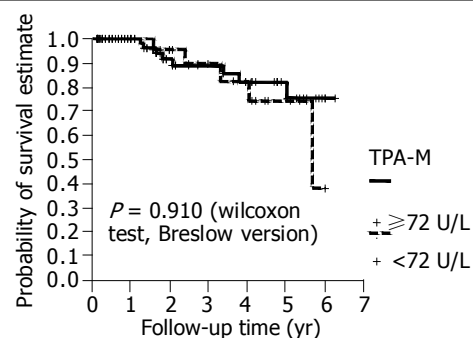


Figure 2 Preoperative TPA-M and survival of patients with colorectal cancer undergoing radical surgical treatment.

Prognosis

There was a statistical difference in patients with a high CEA level in relation to a shorter survival. However, there was no statistical difference between patients with high TPA-M levels in relation to a shorter survival (Figure 2). Even when higher

cut-off values for TPA-M were adopted (216 U/L, three times higher than the maximum value were considered to be normal), no significant differences were discovered.

DISCUSSION

The exclusion criteria for patients with a prior history of benign or malignant neoplasms were appropriate, because they could have an increase in the levels of the serum tumor markers analyzed not due to the colorectal neoplasm present. For the control group, blood donors present colorectal neoplasm were used as the healthy population sample as in other studies of the same nature^[30,31].

CEA presented unsatisfactory results when the diagnosis of colorectal neoplasia was made, with a diagnostic rate of about 40%^[10-12]. In this study, the sensitivity was approximately 50%, confirming that this marker should, therefore not be utilized for the diagnosis of lesions^[42-44]. The cytokeratins assayed via TPA-M showed a sensitivity of about 70%. Correale *et al.*^[30] found a sensitivity of 48% with a cut-off point of 70 U/L. Plebani *et al.*^[31] by using TPA-M with a cut-off value of 46 U/L, identified a sensitivity of 58%. The rates obtained in the present investigation appear to be promising. Additional studies are necessary for verifying the real sensitivity of TPA-M in colorectal cancer patients.

Plebani *et al.*^[31] foresaw the advantages in utilizing cytokeratins in combination with CEA in the diagnosis of colorectal neoplastic lesions. On the basis of the data from the present research, the utilization of cytokeratins and CEA was attractive, with a sensitivity of 77%.

Perhaps the use of TPA-M in combination with CEA will make it possible to detect colorectal neoplasms in populations at risk at a reasonable cost, especially when its ease of execution and elevated sensitivity are considered.

With such a sensitivity, TPA-M may have some usefulness, even in terms of diagnosis, of the lesions that have the macroscopic characteristics of neoplasm in endoscopic or radiological examinations but without confirmation of the malignant nature from the anatomopathological examination. Increased use of TPA-M in combination with CEA may constitute an additional element for indicating surgical interventions.

The association between quantification of these tumor markers and staging of patients is relative. Carriquiry and Piñeyro^[10] studied 209 patients, and identified an average preoperative CEA level of 4.25 ng/mL in patients with stage I tumors, 7.49 ng/mL in patients with stage II tumors, 6.42 ng/mL in patients with stage III tumors, and 241.88 ng/mL in patients with stage IV tumors. The percentage of increased CEA at each stage was 21%, 31%, 36% and 92% in patients with stages I, II, III and IV tumors, respectively.

Correale *et al.*^[30] studied TPA-M assays taken from 98 patients with malignant colorectal tumors using a cut-off point of 57 U/L, and found the sensitivity 33%, 35%, 59% and 73% in patients with stages I, II, III, and IV tumors, respectively. Plebani *et al.*^[31] reported a statistically significant variation in TPA-M levels only in patients with stage IV colorectal neoplasm, in relation to those with other stage tumors.

In this research, the sensitivity of CEA and TPA-M presented a statistically significant difference between stage IV and the other stage tumors. Larger samples would perhaps be able to find evidence for other differences. However, it is possible that elevation in serum levels of tumor markers might only be provoked by lesions that extend beyond the colon or rectum. In any event, preoperative assay of the markers would show some value in the staging, and should be done for all patients. Several studies demonstrated lower levels on the survival curves for patients with elevated CEA assays during the preoperative

period, such as the studies by Carriquiry and Piñeyro^[10], Wang *et al.*^[14] and Wiratkapun *et al.*^[15].

No studies are available regarding the correlation between preoperative TPA-M levels above or below 72 U/L and prognostic indices such as disease-free intervals and relapse, in patients with colon or rectum cancer.

In the present study, no statistical difference was identified in the disease-free interval and survival of patients with preoperative concentrations of TPA-M above or below the level of 72 U/L. In the same way, with cut-off value three times greater than normal, as calculated by Forones *et al.*^[13] and Wiratkapun *et al.*^[15] for CEA, there was no difference in patient survival for TPA-M. This does not, however, necessarily signify that there is no difference between the groups of individuals with normal or elevated pre-surgical levels of this tumor marker. It is possible that the patient sample did not have medical follow-up for a sufficient period of time for a statistical difference to emerge between the groups in relation to the marker studied. In this research, the average patient follow-up time was 22.3 mo. Other investigations^[10,14,15] did have a longer follow-up, with a statistical difference identified in survival. TPA-M can demonstrate prognostic importance in studies with a longer follow-up time.

The peripheral serum level of CEA during the preoperative period reached the status of a relevant prognostic variable. At present, the preoperative staging of colorectal cancer includes CEA assay with the following classification: CX - undetermined CEA level, C0 - level less than 5 ng/mL, and C1 - level greater than 5 ng/mL^[45].

What are the intrinsic characteristics that would define an ideal tumor marker? The level of such a marker would rise in the presence of the smallest neoplastic lesions, and would increase only with the existence of tumors. The marker would be produced by all neoplastic cells, thus making it possible to correlate between marker levels and tumor extent. All patients would generate such a marker. For the public, the examination must have an accessible cost, be minimally invasive and can be performed in any location. The marker should precisely indicate the diagnosis, staging, prognosis and occurrence of neoplastic relapse. There is a consensus on the fact that the ideal tumor marker does not exist^[8,46].

Cytokeratins constitute an advance in the direction of a perfect tumor marker, and their association with CEA is useful in offering a better approach towards patients with colorectal cancer.

REFERENCES

- 1 Hoel DG, Davis DL, Miller AB, Sondik EJ, Swerdlow AJ. Trends in cancer mortality in 15 industrialized countries, 1969-1986. *J Natl Cancer Inst* 1992; **84**: 313-320
- 2 Colonna M, Grosclaude P, Launoy G, Tretarre B, Arveux P, Raverdy N, Benhamiche AM, Herbert C, Faivre J. Estimation of colorectal cancer prevalence in France. *Eur J Cancer* 2001; **37**: 93-96
- 3 Wilmink AB. Overview of the epidemiology of colorectal cancer. *Dis Colon Rectum* 1997; **40**: 483-493
- 4 Wang HZ, Huang XF, Wang Y, Ji JF, Gu J. Clinical features, diagnosis, treatment and prognosis of multiple primary colorectal carcinoma. *World J Gastroenterol* 2004; **10**: 2136-2139
- 5 Zinkin LD. A critical review of the classifications and staging of colorectal cancer. *Dis Colon Rectum* 1983; **26**: 37-43
- 6 Hurst R, Stamos M, Wilmoth G, Lin C. Rectal carcinoma: are we making a difference? *Am Surg* 1996; **62**: 806-810
- 7 Theile DE, Cohen JR, Holt J, Davis NC. Mortality and complications of large-bowel resection for carcinoma. *Aust N Z J Surg* 1979; **49**: 62-66
- 8 Bates SE. Clinical applications of serum tumor markers. *Ann Intern Med* 1991; **115**: 623-638
- 9 Gold P, Freedman SO. Demonstration of tumor-specific antigens in human colonic carcinomata by immunological toler-

- ance and absorption techniques. *J Exp Med* 1965; **121**: 439-462
- 10 **Carriquiry LA**, Piñeyro A. Should carcinoembryonic antigen be used in the management of patients with colorectal cancer? *Dis Colon Rectum* 1999; **42**: 921-929
- 11 **Li Destri G**, Greco S, Rinzivillo C, Racalbuto A, Curreri R, Di Cataldo A. Monitoring carcinoembryonic antigen in colorectal cancer: is it still useful? *Surg Today* 1998; **28**: 1233-1236
- 12 **Engarås B**, Kewenter J, Nilsson O, Wedel H, Hafstrom L. CEA, CA 50 and CA 242 in patients surviving colorectal cancer without recurrent disease. *Eur J Surg Oncol* 2001; **27**: 43-48
- 13 **Forones NM**, Tanaka M, Falcão JB. CEA as a prognostic index in colorectal cancer. *Sao Paulo Med J* 1997; **115**: 1589-1592
- 14 **Wang WS**, Lin JK, Chiou TJ, Liu JH, Fan FS, Yen CC, Lin TC, Jiang JK, Yang SH, Wang HS, Chen PM. Preoperative carcinoembryonic antigen level as an independent prognostic factor in colorectal cancer: Taiwan experience. *Jpn J Clin Oncol* 2000; **30**: 12-16
- 15 **Wiratkapun S**, Kraemer M, Seow-Choen F, Ho YH, Eu KW. High preoperative serum carcinoembryonic antigen predicts metastatic recurrence in potentially curative colonic cancer: results of a five-year study. *Dis Colon Rectum* 2001; **44**: 231-235
- 16 **Steele G**, Zamcheck N, Wilson R, Mayer R, Lokich J, Rau P, Maltz J. Results of CEA-initiated second-look surgery for recurrent colorectal cancer. *Am J Surg* 1980; **139**: 544-548
- 17 **Minton JP**, Hoehn JL, Gerber DM, Horsley JS, Connolly DP, Salwan F, Fletcher WS, Cruz AB, Gatchell FG, Oviedo M. Results of a 400-patient carcinoembryonic antigen second-look colorectal cancer study. *Cancer* 1985; **55**: 1284-1290
- 18 **Lucha PA**, Rosen L, Olenwine JA, Reed JF, Riether RD, Stasik JJ, Khubchandani IT. Value of carcinoembryonic antigen monitoring in curative surgery for recurrent colorectal carcinoma. *Dis Colon Rectum* 1997; **40**: 145-149
- 19 **Wichmann MW**, Müller C, Lau-Werner U, Strauss T, Lang RA, Hornung HM, Stieber P, Schildberg FW. The role of carcinoembryonic antigen for the detection of recurrent disease following curative resection of large-bowel cancer. *Langenbecks Arch Surg* 2000; **385**: 271-275
- 20 **Nakayama T**, Watanabe M, Teramoto T, Kitajima M. CA 19-9 as a predictor of recurrence in patients with colorectal cancer. *J Surg Oncol* 1997; **66**: 238-243
- 21 **Nilsson O**, Johansson C, Glimelius B, Persson B, Norgaard-Pedersen B, Andren-Sandberg A, Lindholm L. Sensitivity and specificity of CA242 in gastro-intestinal cancer. A comparison with CEA, CA50 and CA 19-9. *Br J Cancer* 1992; **65**: 215-221
- 22 **Fernández-Fernández L**, Tejero E, Tieso A. Significance of CA 72-4 in colorectal carcinoma. Comparison with CEA and CA 19-9. *Eur J Surg Oncol* 1995; **21**: 388-390
- 23 **Björklund B**. Tissue polypeptide antigen (TPA): Biology, biochemistry, improved assay methodology, clinical significance in cancer and other conditions, and future outlook. *Antibiot Chemother (1971)* 1978; **22**: 16-31
- 24 **Moll R**, Franke WW, Schiller DL, Geiger B, Krepler R. The catalog of human cytokeratins: patterns of expression in normal epithelia, tumors and cultured cells. *Cell* 1982; **31**: 11-24
- 25 **Broll R**, Erdmann H, Duchrow M, Oevermann E, Schwandner O, Markert U, Bruch HP, Windhovel U. Vascular endothelial growth factor (VEGF)--a valuable serum tumour marker in patients with colorectal cancer? *Eur J Surg Oncol* 2001; **27**: 37-42
- 26 **Shiota G**, Ishida M, Noguchi N, Oyama K, Takano Y, Okubo M, Katayama S, Tomie Y, Harada K, Hori K, Ashida K, Kishimoto Y, Hosoda A, Suou T, Kanbe T, Tanaka K, Nosaka K, Tanida O, Kojo H, Miura K, Ito H, Kaibara N, Kawasaki H. Circulating p53 antibody in patients with colorectal cancer: relation to clinicopathologic features and survival. *Dig Dis Sci* 2000; **45**: 122-128
- 27 **Hammel P**, Soussi T. Serum p53 antibody assay: evaluation in colorectal cancer. *Rev Med Interne* 2000; **21**: 167-173
- 28 **Lindmark G**, Bergstrom R, Pählman L, Glimelius B. The association of preoperative serum tumour markers with Dukes' stage and survival in colorectal cancer. *Br J Cancer* 1995; **71**: 1090-1094
- 29 **Carpelan-Holmström M**, Haglund C, Lundin J, Alfthan H, Stenman UH, Roberts PJ. Independent prognostic value of preoperative serum markers CA 242, specific tissue polypeptide antigen and human chorionic gonadotrophin beta, but not of carcinoembryonic antigen or tissue polypeptide antigen in colorectal cancer. *Br J Cancer* 1996; **74**: 925-929
- 30 **Correale M**, Arnberg H, Blockx P, Bombardieri E, Castelli M, Encabo G, Gion M, Klapdor R, Martin M, Nilsson S. Clinical profile of a new monoclonal antibody-based immunoassay for tissue polypeptide antigen. *Int J Biol Markers* 1994; **9**: 231-238
- 31 **Plebani M**, De Paoli M, Basso D, Roveroni G, Giacomini A, Galeotti F, Corsini A. Serum tumor markers in colorectal cancer staging, grading, and follow-up. *J Surg Oncol* 1996; **62**: 239-244
- 32 **Lewenhaupt A**, Ekman P, Eneroth P, Nilsson B, Nordström L. Tissue polypeptide antigen (TPA) as a prognostic aid in human prostatic carcinoma. *Prostate* 1985; **6**: 285-291
- 33 **Panza N**, Pacilio G, Campanella L, Peluso G, Battista C, Amoriello A, Utech W, Vacca C, Lombardi G. Cancer antigen 125, tissue polypeptide antigen, carcinoembryonic antigen, and beta-chain human chorionic gonadotropin as serum markers of epithelial ovarian carcinoma. *Cancer* 1988; **61**: 76-83
- 34 **Gronowitz JS**, Bergström R, Nöu E, Pählman S, Brodin O, Nilsson S, Kallander CF. Clinical and serologic markers of stage and prognosis in small cell lung cancer. A multivariate analysis. *Cancer* 1990; **66**: 722-732
- 35 **Tizzani A**, Casetta G, Cavallini A, Piana P, Piantino P. Blood and urine determinations of tissue polypeptide antigen in patients with bladder carcinoma. *Minerva Urol Nefrol* 1990; **42**: 69-71
- 36 **Barak M**, Steiner M, Finkel B, Abrahamson J, Antal S, Gruener N. CA-15.3, TPA and MCA as markers for breast cancer. *Eur J Cancer* 1990; **26**: 577-580
- 37 **Annas GJ**. The changing landscape of human experimentation: Nuremberg, Helsinki and beyond. *Health Matrix Cleve* 1992; **2**: 119-140
- 38 **Fletcher RH**, Fletcher SW, Wagner EW. *Epidemiologia Clínica*. Porto Alegre: *Artes Médicas* 1989
- 39 **Agresti A**. *Categorical Data Analysis*. New York: *Wiley Interscience* 1990
- 40 **Neter J**, Kutner MH, Nachtsheim CJ, Wasserman W. *Applied linear statistical models*. 4th ed. Boston: *Irwin* 1996
- 41 **Kalbfleisch JD**, Prentice RL. *The statistical analysis of time failure data*. New York: *John Wiley and Sons* 1980
- 42 **Fletcher RH**. Carcinoembryonic antigen. *Ann Intern Med* 1986; **104**: 66-73
- 43 **Trillet-Lenoir V**, Freyer G. Advantage of using tumor markers in colorectal and breast cancers. Guidelines of the American Society of Clinical Oncology (ASCO). *Bull Cancer* 1997; **84**: 767-768
- 44 **Bast RC**, Ravdin P, Hayes DF, Bates S, Fritsche H, Jessup JM, Kemeny N, Locker GY, Mennel RG, Somerfield MR. 2000 update of recommendations for the use of tumor markers in breast and colorectal cancer: clinical practice guidelines of the American Society of Clinical Oncology. *J Clin Oncol* 2001; **19**: 1865-1878
- 45 **Compton C**, Fenoglio-Preiser CM, Pettigrew N, Fielding LP. American Joint Committee on Cancer Prognostic Factors Consensus Conference: Colorectal Working Group. *Cancer* 2000; **88**: 1739-1757
- 46 **Fernandes LC**, Matos D. Marcadores tumorais no câncer colorretal. *Rev Col Bras Cir* 2002; **29**: 106-111

***In vitro* resistance to interferon of hepatitis B virus with precore mutation**

Yan Wang, Lai Wei, Dong Jiang, Xu Cong, Ran Fei, Jiang Xiao, Yu Wang

Yan Wang, Lai Wei, Dong Jiang, Xu Cong, Ran Fei, Jiang Xiao, Yu Wang, Hepatology Institute, Peking University People's Hospital, Beijing 100044, China

Supported by the Major State Basic Research Development Program of China (973 Program), No. G1999054106

Correspondence to: Dr. Lai Wei, Hepatology Institute, Peking University People's Hospital, No.11 Xizhimen South Street, Beijing 100044, China. w1114@hotmail.com

Telephone: +86-10-68314422-5730 Fax: +86-10-68318386

Received: 2004-04-09 Accepted: 2004-05-24

Abstract

AIM: Chronic hepatitis B virus (HBV) infection is predominantly treated with interferon alpha (IFN- α), which results in an efficient reduction of the viral load only in 20-40% of treated patients. Mutations at HBV precore prevail in different clinical status of HBV infection. The roles of precore mutation in the progression of chronic hepatitis and interferon sensitivity are still unknown. The aim of this study was to explore if there was any relationship between HBV precore mutation and sensitivity to interferon *in vitro*.

METHODS: HBV replication-competent recombinant constructs with different patterns of precore mutations were developed. Then the recombinants were transiently transfected into hepatoma cell line (Huh7) by calcium phosphate transfection method. With or without IFN, viral products in culture medium were collected and quantified 3 d after transfection.

RESULTS: We obtained 4 recombinant constructs by orientation-cloning 1.2-fold-overlength HBV genome into pUC18 vector via the *EcoRI* and *HindIII* and PCR mediated site-directed mutagenesis method. All the recombinants contained mutations within precore region. Huh7 cells transfected with recombinants secreted HBSAg and HBV particles into the cell culture medium, indicating that all the recombinants were replication-competent. By comparing the amount of HBV DNA in the medium, we found that HBV DNA in medium reflecting HBV replication efficiency was different in different recombinants. Recombinants containing precore mutation had fewer HBV DNAs in culture medium than wild type. This result showed that recombinants containing precore mutation had lower replication efficiency than wild type. HBV DNA was decreased in pUC18-HBV1.2-WT recombinants after IFN was added while others with precore mutations were not, indicating that HBV harboring precore mutation was less sensitive to IFN in cell culture system.

CONCLUSION: These data indicate that HBV harboring precore mutation may be resistant to IFN *in vitro*.

© 2005 The WJG Press and Elsevier Inc. All rights reserved.

Key words: Hepatitis B virus; Mutation; Interferon; Viral resistance

Wang Y, Wei L, Jiang D, Cong X, Fei R, Xiao J, Wang Y. *In vitro* resistance to interferon of hepatitis B virus with precore mutation. *World J Gastroenterol* 2005; 11(5): 649-655
<http://www.wjgnet.com/1007-9327/11/649.asp>

INTRODUCTION

Hepatitis B virus (HBV) is a small, partially double-stranded DNA (dsDNA) virus that causes acute and chronic hepatitis in humans. HBV infection is a global health problem. Current estimates are that 2 billion people are infected with HBV worldwide, 360 million of them suffer from chronic HBV infection resulting in over 520 000 deaths each year (52 000 from acute hepatitis B and 470 000 from cirrhosis or liver cancer)^[1]. Transient infections may lead to serious illness, and approximately 0.5% are terminated in fatal, fulminant hepatitis. Chronic infections may also have serious consequences, nearly 25% are terminated in untreatable liver cancer^[2]. Chronic HBV infection is predominantly treated with IFN alpha, which could reduce the viral load in only 20-40% of treated patients with low-level viremia and evidence of active liver disease^[3,4]. It is known that IFN alpha reduces viremia in responding patients by modulation of immunological responses and/or by direct induction of an intracellular antiviral state in infected cells. So far, drug-induced intracellular antiviral mechanisms against HBV have mostly been examined by use of hepatoma cell lines and transgenic mice with integrated HBV DNA, since cell lines permissive for HBV infection are not available. Studies have shown that treatment of various stable HBV-expressing hepatoma cell lines with IFN- α could lead to intracellular inhibition of synthesis of one or several HBV products, depending on the type of cells and systems used^[5-7].

HBV sequence variability has been increasingly recognized as a factor that modulates the course and outcome of HBV infection. Variants with disturbed hepatitis B e antigen (HBeAg) synthesis, large deletions in the nucleocapsid gene, or mutations in the basic core promoter (BCP) have been found to be associated with severe liver diseases and might be related to the sensitivity of interferon therapy^[8]. There have been many studies on HBV replication and IFN sensitivity, but the results are inconclusive. The significance of mutations of HBV precore/core antigen in causing persistent infection and subsequent liver diseases is debatable. Therefore the roles of precore mutations in the progression of chronic hepatitis are still unknown. G to A transition at nt1896 in the precore (preC) region terminates translation of the HBeAg precursor and results in HBeAg-minus HBV. Although A1896 mutation was reported previously to be associated with severe forms of chronic liver diseases^[9], the real significance of A1896 mutation in the course of hepatitis is still controversial^[10,11].

In addition, there are a few works about HBV mutation and IFN sensitivity *in vitro*. HBV genome is a condensed structure, the open reading frames are overlapped. Therefore mutation at one site may alter transcription or translation of more than one viral gene. Most previous studies focused on HBV subgenomic fragments, nevertheless, there are a few researches on the full

Table 1 Sequences of primers for mutagenesis reaction

Primer	Direction	Length	Position (nt)	5'-sequence-3'
A1762/G1764For	+	34	1 748-1 781	aggagattagttaa agg tctttgtactaggaggc
1896/1899Rev	-	20	1 895-1 876	aaagccaccaaggcagc
A1896For	+	31	1 876-1 906	gctgtgccttgggtggc tttag ggcatggac
A1899For	+	34	1 876-1 909	gctgtgccttgggtggc ttggg acatggacatt
A1896A1899For	+	34	1 876-1 909	gctgtgccttgggtggc tttag acatggacatt
PS5For	+	20	1 260-1 279	gccgatccatactcggaac
PS4Rev	-	20	2 386-2 405	gagaccttgcctgcgaggc

length of HBV. Therefore we introduced recombinant constructs harboring more than one copy of HBV genome into hepatoma cell line by transient transfection. Since the recombinants contained different mutations at the precore region, we could study the relationship of these mutations and interferon sensitivity *in vitro*.

MATERIALS AND METHODS

Construction of plasmids

Cloning of plasmid constructs used in transfection experiments was performed by standard techniques^[12]. Mutagenesis reactions were performed through polymerase chain reaction (PCR)-mediated site-directed mutagenesis with the designed mutagenetic primers (Table 1). For the calculation of the nucleotide (ntd.) positions, the first thymine of the putative *EcoRI* site of HBV was defined as position 1 and then anti-clockwise was counted (GenBank accession number is AY040627, genotype C). Different kinds of mutations were introduced by amplification with Pwo-Taq DNA polymerase mix (expand high fidelity PCR system, Roche Molecular Biochemical, Germany).

First, pUC18-HBV1.2-TA was constructed. Plasmid pUC18-HBV1.2-TA was derived from pALTER-HBV1.2 containing a 1.2×HBV full length (T1762/A1764 mutant type). The 1.2×HBV full length from pALTER-HBV1.2 and linearized pUC18 vector were obtained by restrictive endonuclease *EcoRI* and *Hind* III digestion. Both of them were purified by QIAquick gel extraction kit (Qiagen, Germany). Then the 1.2×HBV full length was orientally subcloned into the linearized vector pUC18 to acquire pUC18-HBV1.2-TA (T1762/A1764).

Second, we constructed wild type recombinants. Plasmid pUC18-HBV1.2-WT was produced by the large primer PCR method. In brief, fragments which were prepared by expand high fidelity PCR system (Roche) were used as large primers. In the PCR system, pUC18-HBV1.2-TA was used as a template with repair primer (wild type) A1762/G1764For and primer PS4Rev. The PCR products were purified by QIAGEN gel extraction kit and then used as large primers. The large primers and primer PS5For were used to amplify template pUC18-HBV1.2-TA to obtain the wild type fragments of HBV which were ascertained by sequencing. The PCR products and pUC18-HBV1.2-TA were both digested by restrictive endonucleases *EcoRI* and *Xmn* I respectively. After ligation and subcloning, the fragments between *EcoRI* and *Xmn* I in pUC18-HBV1.2-TA were replaced by corresponding fragments derived from PCR products, then wild type constructs of pUC18-HBV1.2-WT were produced which had a wild type A1762/G1764 instead of a mutant type T1762A1764.

Third, we constructed 1896/1899 recombinants. One segment, designated as segment A was prepared by PCR using pUC18-HBV1.2 as template with the primers PS5For and 1896/1899Rev, this fragment was used as a common segment for all next round amplifications. Segment B was prepared with

the primers A1896For and PS4Rev, while segment C was prepared with primers A1899For and PS4Rev and segment D with primers A1896A1899For and PS4Rev. Then A1896 mutated fragments were obtained by PCR using segments A and B as templates with primers PS4 and PS5. Restrictive endonucleases *EcoRI* and *Xmn* I were used to digest PCR products and pUC18-HBV1.2-WT, then fragments between *EcoRI* and *Xmn* I were exchanged between pUC18-HBV1.2-WT and PCR products by subcloning as described above. Plasmids containing the mutated site A1896 were obtained and named as pUC18-HBV1.2-A1896. Accordingly, plasmids pUC18-HBV1.2-A1899 and pUC18-HBV1.2-AA were obtained later. The detailed mutation patterns of all the produced plasmids are shown in Table 2 and Figure 1. Correctly introduced nucleotides were verified by sequencing.

Table 2 Mutation patterns of the 4 recombinant constructs

Number	Recombinant constructs	Mutation pattern	
		A1896	A1899
1	pUC18-HBV1.2-WT	-	-
2	pUC18-HBV1.2-A1896	+	-
3	pUC18-HBV1.2-A1899	-	+
4	pUC18-HBV1.2-AA	+	+

Note: "+" indicates the construct containing the corresponding mutation, "-" indicates the constructs containing no corresponding mutation instead of wild type.

Determination of the most optimum concentration of interferon- α *in vitro*

Huh7 cells were seeded at a density of 6×10^5 /well in six-well plates (10 cm² per well, Falcon) in Dulbecco's modified Eagle's medium supplemented with 10% fetal calf serum and cultured at 37 °C in 5 mL/L CO₂ 1 d before transfection. The medium was changed 4 h before transfection. Five μ g plasmid was transfected into nearly confluent Huh7 cells. Sixteen hours after transfection, Huh7 cells were shocked with 15% glycerol solution, and then incubated with a fresh culture medium for 24 h. To determine the most optimal concentration of interferon *in vitro*, different concentrations of interferon α -2b were added to the culture medium. The concentrations of IFN- α (Intron A, Schering-Plough Research Institute) used in the experiment were 62.5 IU/mL, 125 IU/mL, 250 IU/mL, 500 IU/mL, 1 000 IU/mL, 2 000 IU/mL, 4 000 IU/mL, 8 000 IU/mL. Three days after transfection, cell medium was collected to detect HBsAg, HBeAg and HBV DNA. By comparing the amount of HBsAg, HBeAg and HBV DNA secreted to the medium, we selected the concentration of interferon which could inhibit HBV most.

Transfection of HBV DNA by calcium phosphate precipitation

All plasmid DNAs were prepared and purified by QIAGEN

EndoFree maxi kit (EndoFree™ Plasmid Mega Kit, Qiagen, Germany). The DNA was then quantified spectrophotometrically (a ratio of the optical density at 260 nm to that at 280 nm of 1.7 to 1.8).

Transfection was performed by the calcium phosphate precipitation method (Promega ProFectin® mammalian transfection system-calcium phosphate) according to the supplied protocol. Human hepatoma cell line Huh7 was grown as a monolayer in Dulbecco's modified Eagle's medium supplemented with 10% fetal calf serum at 37 °C in 5 mL/L CO₂. Huh7 cells were plated at a density of 3.0×10⁶ cells per Petri dish (Falcon) 1 d before transfection to reach 80% confluence at transfection. The medium was changed 4 h before transfection. Twenty µg corresponding HBV replication-competent plasmid was mixed with CaCl₂ solution, then added dropwise to 2× HEPES-buffered saline (pH 7.05), and transfected into confluent Huh7 cells. Sixteen hours after transfection Huh7 cells were shocked with 15% glycerol solution, and then incubated with a fresh culture medium for 24 h. Medium with or without 1000 IU/mL IFN-α (interferon alfa-2b, Intron A, Schering-Plough Research Institute) was then added and the culture medium was harvested 3 d after transfection.

Transfection efficiency was measured by cotransfection of 1.0 µg of reporter plasmid pSEAP2-Control-SV40 (Clontech) expressing secretable alkaline phosphatase under the control of the SV40 early promoter and the SV40 enhancer^[13,14]. The SEAP coding sequence was followed by the SV40 late polyadenylation signal to ensure proper and efficient processing of the SEAP transcript in eukaryotic cells. The secreted SEAP enzyme was assayed directly from the culture medium. The reporter plasmid served as an internal control to monitor transfection efficiency and potential IFN-α-mediated cytotoxic effects or nonspecific inhibitory effects. Transfection efficiency in each cell culture plate was carefully controlled by determination of the SEAP enzymatic activity in the cell culture medium before addition of IFN-α, and was found to vary by less than 10% (data not shown).

The SEAP activity of the culture media was measured 24 h after transfection by performing a colorimetric assay according to the recommendation^[13]. Briefly, twenty microliters of heat-treated (at 65 °C for 5 min) medium was adjusted to 1×SEAP assay buffer (1.0 mol/L diethanolamine pH9.8, 0.5 mmol/L MgCl₂, 10 mmol/L L-homoarginine) in a final volume of 200 µL and prewarmed to 37 °C for 10 min in a 96-well flat-bottom culture dish. Twenty microlitres of prewarmed 120 mmol/L p-nitrophenylphosphate (pNPP) dissolved in 1×SEAP assay buffer was then added and mixed. A405 of the reaction mixture was read in a microplate reader at 5-min intervals. The change in absorbance was plotted and the maximum linear reaction rate was determined. The SEAP activity was expressed in A405 (data not shown). The amount of both HBsAg and HBV DNA was corrected by the SEAP activities.

Detection for HBsAg secreted to cell culture medium

The amount of HBV surface antigen (HBsAg) secreted into the cell culture medium was determined by enzyme-linked immunosorbent assay (ELISA, Hepanostika HBsAg Uni-Form II, Biomérieux by, Netherlands) after removal of cell debris and stored at -20 °C until analysis. Total amount of HBsAg was calculated by comparison with a standard HBsAg-positive human serum and negative control sera provided by the manufacturer. If the A₄₅₀ for HBsAg was more than 3.0, a 1:10 dilution of culture medium was made for further assay.

Real-time quantitative PCR to detect HBV DNA secreted to culture medium

Cell culture medium was collected 3 d after transfection and centrifuged at 14 000 r/m rpm 10 min at 4 °C to remove cell debris. The supernatant was adjusted to 10 mmol/L MgCl₂ and treated with 100 µg/mL DNase I for 60 min at 37 °C to remove the remaining recombinants. The reaction was stopped by adding EDTA to a final concentration of 25 mmol/L. HBV DNA in the cell medium was detected by fluorescent real-time quantitative PCR (commercially available assay kit, Roche Light cycler).

RESULTS

Replication-competent constructs containing HBV genome with mutations at precore region

By PCR-mediated site-directed mutagenesis method and molecular cloning, we obtained different HBV fragments containing varied mutations with different mutagenetic primers. The agarose gel electrophoresis of different HBV fragments is shown in Figure 1. Finally we acquired four kinds of replication-competent constructs containing HBV genome with mutations at the precore region. All the mutated sites were ascertained by sequencing. The sequences were analyzed by Chromas and Bioedit software. Therefore the desired mutations instead of the unrelated mutations were introduced. Part of the sequencing results at the mutation site are shown in Figure 2.

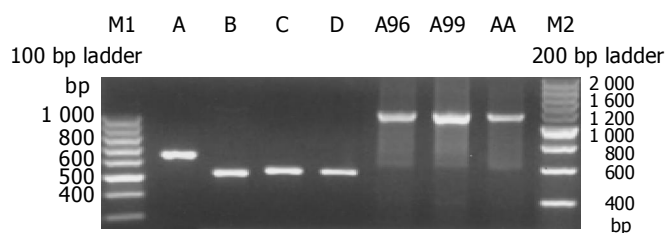


Figure 1 Electrophoresis of mutagenesis PCR product. Lanes A-D: Different HBV fragments using different mutated primers, Lanes E-G: The second round PCR products.

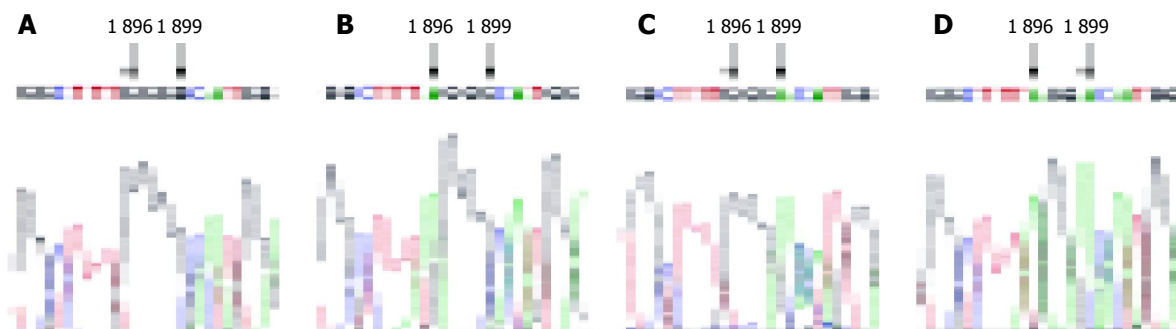


Figure 2 Local sequences of mutagenesis sites of 4 recombinants. Arrowhead indicates the mutated nucleosides. A: pUC18-HBV1.2-WT; B: pUC18-HBV1.2-A1896; C: pUC18-HBV1.2-A1899; D: pUC18-HBV1.2-AA.

Table 3 HBsAg and HBV DNA secreted into cell culture medium with or without IFN (mean±SD)

Recombinants	HBsAg (A_{450})		HBV DNA (realtime PCR, log10)	
	Without IFN	With IFN	Without IFN	With IFN
Puc18-HBV1.2-WT	2.63±0.1 ^c	1.96±0.07 ^c	5.02±0.06 ^{ac}	4.86±0.07 ^c
Puc18-HBV1.2-A1896	1.43±0.05	1.46±0.07	4.43±0.09 ^{ac}	5.53±0.07 ^c
Puc18-HBV1.2-A1899	1.97±0.15	1.96±0.12	4.80±0.05	4.90±0.06
Puc18-HBV1.2-AA	2.6±0.05	2.5±0.06	4.06±0.07 ^{ac}	4.46±0.05 ^c

$n = 3$, ^a $P < 0.05$ (WT in comparison with MT without IFN), ^c $P < 0.05$ (without IFN in comparison with with IFN). WT: wild type, MT: mutated type.

HBV reconstructs were named as pHBV1.2 containing a 1.2-fold-overlength genome of HBV, genotype C, with a 5' terminal redundancy encompassing enhancers I and II, the origin of replication (direct repeats DR1 and DR2), the X- and pregenomic/core promoter regions, the transcription initiation site of the pregenomic RNA, the unique polyadenylation site, and the entire X open reading frame as depicted in Figure 3. Such a recombinant was proven to initiate HBV replication efficiently and with high liver specificity in transfection experiments and in transgenic mice^[15]. In this research, we obtained 4 recombinant constructs by orientation-cloning and PCR-mediated site-directed mutagenesis. As shown in Figure 3, the 4 constructs contained different combinations of mutations at HBV precore region.

Dose-dependent sensitivity to interferon *in vitro*

As described in Materials and Methods, the plasmid containing wild type HBV was transfected to Huh7 in six-well plates. Different concentrations of interferon- α (62.5 IU/mL, 125 IU/mL, 250 IU/mL, 500 IU/mL, 1 000 IU/mL, 2 000 IU/mL, 4 000 IU/mL, 8 000 IU/mL) were added and cell medium was collected 3 d after transfection. As shown in Figure 4, different concentrations of interferon- α had different effects on HBV antigen expression and viral replication. Along with increase of interferon- α concentration, HBsAg and HBeAg secretion decreased almost in the same extent in general. The results showed that interferon- α with 2 000 IU/mL medium *in vitro* could inhibit HBV antigen expression to the highest extent. For the viral DNA secreted to the medium, the realtime PCR was used to detect HBV DNA. With different concentrations of interferon- α in cell medium, the amounts of secreted viral DNA were also different. HBV DNA decreased most in the medium with 1 000 IU/mL interferon- α . According to previous reports and our experimental results,

we selected the concentration 1 000 IU/mL of interferon- α as the concentration of experiments *in vitro*.

Precore mutation decreased HBV replication

All the different recombinants were introduced into hepatoma cell Huh7 by calcium phosphate transient transfection method. Cell culture medium was collected 3 d after transfection and HBV DNA was detected by fluorescent real-time quantitative PCR. HBV DNA in the cell medium was given as viral copies per milliliter. As shown in Table 3 and Figure 4, all the recombinants could produce and secrete HBV DNA to the cell medium. When the amounts of HBV DNA in the medium were compared, replication efficiency was different in different recombinants. Recombinants containing precore mutations had lower replication efficiency than wild type. The recombinant containing the A1896 and A1899 double mutations had lower replication efficiency than the recombinant containing A1896 or A1899 single mutations.

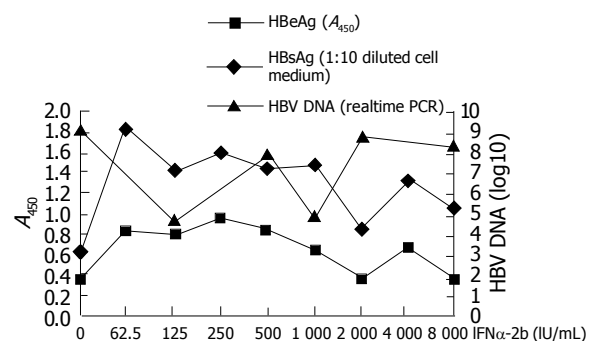


Figure 4 Detection of HBsAg, HBeAg, HBV DNA secreted to the cell medium with different concentrations of interferon.

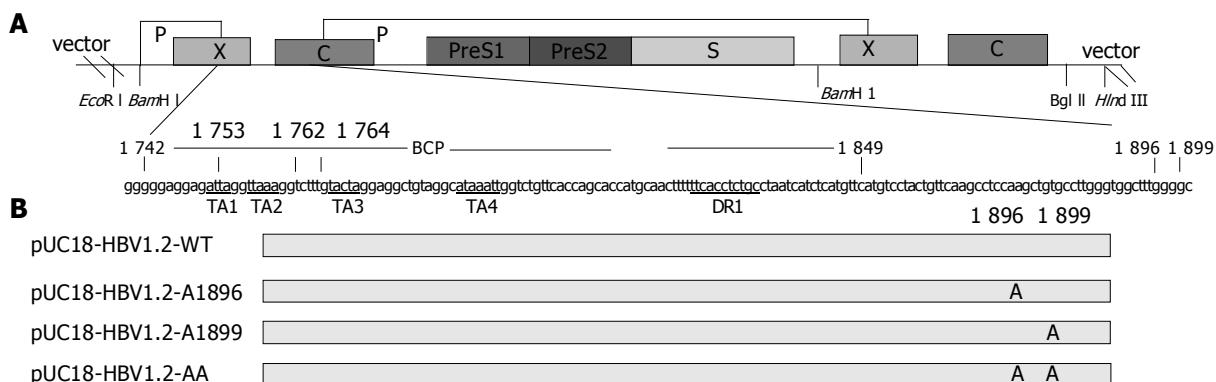


Figure 3 Sketch map of structure of plasmid pUC-HBV1.2 and the mutation sites of all constructed plasmids. Panel A: Upper line and box figure indicate the 1.2 copy HBV genome cloned into pUC18 *EcoRI* and *HindIII* sites. Different open reading frames are indicated with corresponding box. Lower letters indicate HBV BCP and precore region sequence, TA rich region and DR region are underlined. Scheduled nucleosides to be mutated are indicated with numeral; Panel B: Recombinant constructs and their corresponding mutation sites. The constructs are listed at left, long gray box indicate consensus sequences, mutation nucleosides and their sites are indicated.

Precore mutation exerted no effect on expression of HBsAg

Cell culture medium was collected 3 d after transfection with recombinant constructs. The amount of hepatitis B virus surface antigen (HBsAg) secreted into the cell culture medium was determined by ELISA. All the recombinants could express and secrete HBsAg into cell medium. When the relative amount of HBsAg was compared (Table 3), a slight difference was found among all the recombinants containing different precore mutation combinations. But there was no significant difference by statistic analysis ($P > 0.05$). The result indicated that precore mutation might have no effect on expression of HBsAg.

Recombinants containing precore mutation were resistant to interferon

Sixteen hours after transfection, Huh7 cells were shocked with 15% glycerol solution, and then incubated with fresh culture medium for 24 h. Fresh complete medium with and without 1 000 IU/mL IFN- α was added and the culture medium was harvested 3 d after transfection. HBV DNA in the cell medium was detected by fluorescent real-time quantitative PCR. By comparing HBV DNA in the cell medium with or without addition of IFN, we could know the sensitivity to IFN of different recombinants. The level of HBV DNA was decreased in pUC18-HBV1.2-WT recombinants after IFN was added while others with precore mutations were not. HBV DNA in the medium from the recombinants containing HBV precore mutations such as A1896 and/or A1899 did not decrease in amount after IFN was added. Thus recombinants containing precore mutations were resistant to interferon, precore mutations might be one indicator of HBV resistance to IFN.

Effect of IFN on secretion of HBsAg

As shown in Table 3, HBsAg secreted to the medium was slightly decreased in recombinants with HBV wild type after IFN was added. While after interferon was added, HBsAg in the medium of recombinants with HBV precore mutations did not decrease.

DISCUSSION

Chronic HBV infection remains a major public health problem worldwide as well as a therapeutic challenge. Despite a high rate of viral clearance in immunocompetent adults and the availability of efficient vaccines, a large proportion of the world's population (400 million) are chronically infected with HBV. This is due to the fact that vertical transmission of HBV in neonates leads to a chronic infection in 90% of cases. Chronic HBV infection may result in a wide spectrum of liver diseases including acute self-limiting hepatitis or chronic infection. There are still 250 000 deaths each year resulted from hepatitis B. While HBV is generally regarded as noncytotoxic, HBV-induced liver diseases are mediated by cytotoxic T-lymphocyte (CTL) lysis of infected hepatocytes^[16,17]. Nevertheless, activity of HBV-induced liver diseases may also relate to viral factors. The coexistence of repeated cycles of HBV replication and immune lysis of infected hepatocytes are associated with fibrosis, cirrhosis, and hepatocellular carcinoma.

Current strategies for treating hepatitis B are focused on clearance of active HBV infection through suppression of viral replication. Interferon- α (IFN- α) and nucleoside analogs (lamivudine and adefovir) have been approved for their clinical use by FDA. The sustained virological response rate to IFN- α , however, ranges between 20% and 40%^[3,4]. The actual rate of sustained response in non selected patients is supposed to be lower. The resistance to antiviral treatment by some viruses is due to positive selection of variants harboring mutations that

confer resistance^[18]. Variations at the precore region have been reported to be associated with the response to IFN therapy^[19]. The mutation G to A switch at position 1896 of the pre-core region of the HBV genome that leads to a translational stop codon in the leader sequence of HBeAg protein could result in the inhibition of protein synthesis^[20]. Such variants selected during seroconversion from HBeAg to anti-HBe are responsible for HBeAg-negative chronic hepatitis B, which represents up to 50-95% of the chronic hepatitis B cases followed up in liver units in Europe and has an increasing prevalence from north to south^[21]. Recently a total of 694 consecutive chronic HBV-infected patients seen in 17 liver centers in the US during a one-year period were enrolled^[22]. Precore variants are found in 27% of chronic hepatitis B (CHB) patients and more common in hepatitis B e antigen (HBeAg)-negative patients than in HBeAg-positive patients (38% vs 9%, $P < 0.001$). The precore stop codon variants are detected in a median of 60% (range 0-100%) of HBeAg-negative patients, 92% in the Mediterranean, 50% in Asia Pacific and 24% in the USA and Northern Europe^[23]. Anti-hepatitis e antigen-positive chronic hepatitis B is a progressive liver disease associated with precore mutants and poor response to interferon. It is still unknown why this variant is related to IFN responsiveness, and whether it is IFN-sensitive or resistant, or whether it is directly or causally related to responsiveness. Previous studies have not fully answered these questions and the results are contradictory^[10].

Some studies have shown that mutant-type diseases (anti-HBe-positive/HBeAg-negative) are less responsive to IFN given for 6-12 mo while wild-type responds relatively well to IFN treatment. Naoumov *et al.*^[24] sequenced precore/core region in 46 serum samples obtained before, during, and after interferon treatment of 12 patients. No significant changes occurred in the precore/core regions in responders after seroconversion to anti-hepatitis B e antigen, but multiple variations persisted in nonresponders during treatment and new mutations occurred with the relapse of hepatitis. Other studies had contradictory results. Shindo *et al.*^[25] investigated 93 patients with chronic hepatitis B treated with IFN alpha. The results suggest that the precore wild type and mutant have similar sensitivity to IFN. Schepis *et al.*^[26] found core gene variability did not seem to be involved either in the outcome of infection or in the responses to IFN treatment in children with chronic HBV infection. Zampino *et al.*^[27] showed that G1896A precore stop codon mutation was not detected before, during and after interferon treatment in young Caucasian cancer survivors who acquired HBV infection during chemotherapy for malignancies. Some researchers^[10] have found that precore mutant HBV could influence the response to interferon when it reaches significant serum levels ($> 20\%$ of total viremia).

For the study of HBV infection, no permissive cell line or small animals are available. Stable cell lines with integrated HBV genomes, e.g., HepG2.2.15 cells^[28], are commonly used for assessing the action of drugs on HBV replication. HBV-transgenic mice have been proved to be very useful for immunological studies^[29]. However, stable cell lines as well as transgenic mice have the disadvantage that, unlike in natural infection, HBV replicates from an integrated genome which cannot be eliminated. In contrast to almost all previous studies with cell lines containing chromosomally integrated HBV DNA or transfection of cells with subgenomic HBV fragments^[5,30-32], we developed recombinant constructs in which 1.2-fold-overlength HBV containing precore mutations were inserted. All the different recombinants were introduced into hepatoma cell line Huh7 by calcium phosphate transient transfection method. The constructs efficiently initiated virus replication and antigen expression in transiently transfected hepatoma cell line Huh7, which could be demonstrated by measuring

HBsAg and HBV DNA secreted to the cell culture medium. All the recombinant constructs were replication-competent. By comparing the amount of HBV DNA into the medium, we found that the replication efficiency was different in different recombinants. Whether HBV harboring single A1896 and A1899 precore mutations affects replication efficiency or not is still uncertain.

Interferons exert their cellular activities by binding to specific membrane receptors on the cell surface. Once bound to the cell membrane, interferons initiate a complex sequence of intracellular events including induction of certain enzymes, suppression of cell proliferation, immunomodulating activities such as enhancement of the phagocytic activity of macrophages and augmentation of the specific cytotoxicity of lymphocytes for target cells, and inhibition of virus replication in virus-infected cells. It has been reported that type I interferons have immunomodulatory properties as well as direct antiviral activity^[33]. Previous results obtained in *in vivo* studies could not show whether precore mutation of HBV is directly related to between IFN responsiveness. We used an *in vitro* system by hepatoma cell lines (as described before) to investigate the relationship between precore mutation and IFN responsiveness. By comparing HBV DNA in the cell medium, we found that the production of HBV DNA was decreased in HBV wild type after adding IFN but not in HBV precore mutations. It demonstrates that IFN could directly suppress viral replication in Huh7 cells transiently transfected with wild type HBV DNA *in vitro*. These *in vitro* experiment results indicate that the mechanism of IFN's antiviral effect is not only by immune regulation but also by direct or indirect suppression of viral replication. IFN can not suppress viral replication in Huh7 cells transiently transfected with mutant type HBV DNA *in vitro* while it suppresses wild type. Meanwhile our results imply that the antiviral effect of IFN *in vitro* is dose-dependent. Based on the above results, we conclude that interferon has direct anti-viral effects, HBV harboring precore mutations influences the sensitivity of IFN. Therefore precore mutations might at least partly affect the response of IFN *in vivo*.

As discussed before, IFN might have direct antiviral effects on HBV. HBsAg secreted to the medium was slightly decreased in recombinants with HBV wild type after adding IFN while HBsAg did not decrease in recombinants with precore mutations. The results imply that the antiviral mechanism of IFN is not only by affecting viral replication but also by affecting viral antigen expression of HBV wild type. Precore mutations might hamper this mechanism. These results are similar to previous studies. Recent studies in chimpanzees have shown that in the initial phase of acute HBV-infection a non-cytolytic downregulation of HBV-replication takes place before cytotoxic T-cell mediated destruction of HBV-antigen^[34]. Various *in vitro* studies have examined the inhibitory effects of IFN- α/β on HBV replication. Rang *et al*^[35] showed that IFN- α might reduce the stability of HBV RNA in transiently transfected Huh7-cells and Caselmann *et al*^[6] observed a decrease of pregenomic HBV RNA in HepG2 cells stably transfected with the HBV-genome when they were treated with IFN- β . Hamasaki *et al*^[36] demonstrated a reduction of HBs-antigen mRNA-levels by IFN- α in hepatoma cells with integrated HBV-DNA. Thus type I IFNs inhibit HBV replication and protein production by a variety of mechanisms.

Our experiments indicate that HBV with precore stop mutation is resistant to IFN treatment *in vitro*. The result has been ascertained by some studies *in vivo*. The anti-viral mechanisms of IFN are very complicated. Further studies are needed to explore the mechanisms of HBV precore mutation resistance to IFN therapy. The pathogenicity and the treatment

of HBV precore mutation remain to be investigated.

REFERENCES

- 1 de Franchis R, Hadengue A, Lau G, Lavanchy D, Lok A, McIntyre N, Mele A, Paumgartner G, Pietrangelo A, Rodes J, Rosenberg W, Valla D. EASL International Consensus Conference on Hepatitis B. 13-14 September, 2002 Geneva, Switzerland. Consensus statement (long version). *J Hepatol* 2003; **39** Suppl 1: S3-25
- 2 Seeger C, Mason WS. Hepatitis B virus biology. *Microbiol Mol Biol Rev* 2000; **64**: 51-68
- 3 Niederau C, Heintges T, Lange S, Goldmann G, Niederau CM, Mohr L, Haussinger D. Long-term follow-up of HBeAg-positive patients treated with interferon alfa for chronic hepatitis B. *N Engl J Med* 1996; **334**: 1422-1427
- 4 Zuckerman AJ, Lavanchy D. Treatment options for chronic hepatitis. Antivirals look promising. *BMJ* 1999; **319**: 799-800
- 5 Hayashi Y, Koike K. Interferon inhibits hepatitis B virus replication in a stable expression system of transfected viral DNA. *J Virol* 1989; **63**: 2936-2940
- 6 Caselmann WH, Meyer M, Scholz S, Hofschneider PH, Koshy R. Type I interferons inhibit hepatitis B virus replication and induce hepatocellular gene expression in cultured liver cells. *J Infect Dis* 1992; **166**: 966-971
- 7 Davis MG, Jansen RW. Inhibition of hepatitis B virus in tissue culture by alpha interferon. *Antimicrob Agents Chemother* 1994; **38**: 2921-2924
- 8 Marrone A, Zampino R, Luongo G, Utili R, Karayiannis P, Ruggiero G. Low HBeAg serum levels correlate with the presence of the double A1762T/G1764A core promoter mutation and a positive response to interferon in patients with chronic hepatitis B virus infection. *Intervirology* 2003; **46**: 222-226
- 9 Raimondo G, Schneider R, Stemler M, Smedile V, Rodino G, Will H. A new hepatitis B virus variant in a chronic carrier with multiple episodes of viral reactivation and acute hepatitis. *Virology* 1990; **179**: 64-68
- 10 Brunetto MR, Giarin M, Saracco G, Oliveri F, Calvo P, Capra G, Randone A, Abate ML, Manzini P, Capalbo M. Hepatitis B virus unable to secrete e antigen and response to interferon in chronic hepatitis B. *Gastroenterology* 1993; **105**: 845-850
- 11 Brunetto MR, Oliveri F, Rocca G, Criscuolo D, Chiaberge E, Capalbo M, David E, Verme G, Bonino F. Natural course and response to interferon of chronic hepatitis B accompanied by antibody to hepatitis B e antigen. *Hepatology* 1989; **10**: 198-202
- 12 Sambrook J, Fritsch EF, Maniatis T. Molecular cloning: A Laboratory Manual, 2nd ed. New York: Cold Spring Harbor Laboratory Press 1989
- 13 Berger J, Hauber R, Geiger R, Cullen BR. Secreted placental alkaline phosphatase: a powerful new quantitative indicator of gene expression in eukaryotic cells. *Gene* 1988; **66**: 1-10
- 14 Cullen BR, Malim MH. Secreted placental alkaline phosphatase as a eukaryotic reporter gene. *Methods Enzymol* 1992; **216**: 362-368
- 15 Guidotti LG, Matzke B, Schaller H, Chisari FV. High-level hepatitis B virus replication in transgenic mice. *J Virol* 1995; **69**: 6158-6169
- 16 Chisari FV, Ferrari C, Mondelli MU. Hepatitis B virus structure and biology. *Microb Pathog* 1989; **6**: 311-325
- 17 Suri D, Schilling R, Lopes AR, Mullerova I, Colucci G, Williams R, Naoumov NV. Non-cytolytic inhibition of hepatitis B virus replication in human hepatocytes. *J Hepatol* 2001; **35**: 790-797
- 18 Carman W, Thomas H, Domingo E. Viral genetic variation: hepatitis B virus as a clinical example. *Lancet* 1993; **341**: 349-353
- 19 Fattovich G, McIntyre G, Thursz M, Colman K, Giuliano G, Alberti A, Thomas HC, Carman WF. Hepatitis B virus precore/core variation and interferon therapy. *Hepatology* 1995; **22**: 1355-1362
- 20 Carman WF, Jacyna MR, Hadziyannis S, Karayiannis P, McGarvey MJ, Makris A, Thomas HC. Mutation preventing formation of hepatitis B e antigen in patients with chronic hepatitis B infection. *Lancet* 1989; **2**: 588-591

- 21 **Zoulim F**, Tong S, Trepo C. Study of HBV replication capacity in relation to sequence variation in the precore and core promoter regions. *Methods Mol Med* 2004; **95**: 235-246
- 22 **Chu CJ**, Keeffe EB, Han SH, Perrillo RP, Min AD, Soldevila-Pico C, Carey W, Brown RS, Luketic VA, Terrault N, Lok AS. Prevalence of HBV precore/core promoter variants in the United States. *Hepatology* 2003; **38**: 619-628
- 23 **Funk ML**, Rosenberg DM, Lok AS. World-wide epidemiology of HBeAg-negative chronic hepatitis B and associated precore and core promoter variants. *J Viral Hepat* 2002; **9**: 52-61
- 24 **Naoumov NV**, Thomas MG, Mason AL, Chokshi S, Bodicky CJ, Farzaneh F, Williams R, Perrillo RP. Genomic variations in the hepatitis B core gene: a possible factor influencing response to interferon alfa treatment. *Gastroenterology* 1995; **108**: 505-514
- 25 **Shindo M**, Hamada K, Koya S, Sokawa Y, Okuno T. The clinical significance of core promoter and precore mutations during the natural course and interferon therapy in patients with chronic hepatitis B. *Am J Gastroenterol* 1999; **94**: 2237-2245
- 26 **Schepis F**, Verucchi G, Pollicino T, Attard L, Brancatelli S, Longo G, Raimondo G. Outcome of liver disease and response to interferon treatment are not influenced by hepatitis B virus core gene variability in children with chronic type B hepatitis. *J Hepatol* 1997; **26**: 765-770
- 27 **Zampino R**, Marrone A, Cirillo G, del Giudice EM, Utili R, Karayiannis P, Liang TJ, Ruggiero G. Sequential analysis of hepatitis B virus core promoter and precore regions in cancer survivor patients with chronic hepatitis B before, during and after interferon treatment. *J Viral Hepat* 2002; **9**: 183-188
- 28 **Sells MA**, Chen ML, Acs G. Production of hepatitis B virus particles in Hep G2 cells transfected with cloned hepatitis B virus DNA. *Proc Natl Acad Sci USA* 1987; **84**: 1005-1009
- 29 **Guidotti LG**, Borrow P, Hobbs MV, Matzke B, Gresser I, Oldstone MB, Chisari FV. Viral cross talk: intracellular inactivation of the hepatitis B virus during an unrelated viral infection of the liver. *Proc Natl Acad Sci USA* 1996; **93**: 4589-4594
- 30 **Tur-Kaspa R**, Teicher L, Laub O, Itin A, Dagan D, Bloom BR, Shafritz DA. Alpha interferon suppresses hepatitis B virus enhancer activity and reduces viral gene transcription. *J Virol* 1990; **64**: 1821-1824
- 31 **Berthillon P**, Crance JM, Leveque F, Jouan A, Petit MA, Deloince R, Trepo C. Inhibition of the expression of hepatitis A and B viruses (HAV and HBV) proteins by interferon in a human hepatocarcinoma cell line (PLC/PRF/5). *J Hepatol* 1996; **25**: 15-19
- 32 **Romero R**, Lavine JE. Cytokine inhibition of the hepatitis B virus core promoter. *Hepatology* 1996; **23**: 17-23
- 33 **Pfeffer LM**, Dinarello CA, Herberman RB, Williams BR, Borden EC, Bordens R, Walter MR, Nagabhushan TL, Trotta PP, Pestka S. Biological properties of recombinant alpha-interferons: 40th anniversary of the discovery of interferons. *Cancer Res* 1998; **58**: 2489-2499
- 34 **Guidotti LG**, Rochford R, Chung J, Shapiro M, Purcell R, Chisari FV. Viral clearance without destruction of infected cells during acute HBV infection. *Science* 1999; **284**: 825-829
- 35 **Rang A**, Günther S, Will H. Effect of interferon alpha on hepatitis B virus replication and gene expression in transiently transfected human hepatoma cells. *J Hepatol* 1999; **31**: 791-799
- 36 **Hamasaki K**, Nakata K, Nakao K, Mitsuoka S, Tsutsumi T, Kato Y, Shima M, Ishii N, Tamaoki T, Nagataki S. Interaction of interferon-alpha with interleukin-1 beta or tumor necrosis factor-alpha on hepatitis B virus enhancer activity. *Biochem Biophys Res Commun* 1992; **183**: 904-909

Edited by Wang XL and Zhu LH

• BASIC RESEARCH •

Inhibition of p38 mitogen-activated protein kinase may decrease intestinal epithelial cell apoptosis and improve intestinal epithelial barrier function after ischemia-reperfusion injury

Shu-Yun Zheng, Xiao-Bing Fu, Jian-Guo Xu, Jing-Yu Zhao, Tong-Zhu Sun, Wei Chen

Shu-Yun Zheng, Xiao-Bing Fu, Jing-Yu Zhao, Tong-Zhu Sun, Wei Chen, Wound Healing and Cell Biology Laboratory, Burns Institute, 304 Medical Department, The General Hospital of PLA, Trauma Center of Postgraduate Medical College, Beijing 100037, China
Shu-Yun Zheng, Central Hospital of Jinghua City, Jinghua 321000, Zhejiang Province, China

Jian-Guo Xu, Jinling Hospital, School of Medicine, Nanjing University, Nanjing 210002, Jiangsu Province, China

Supported by the National Basic Science and Development Programme (973 Programme), No.G1999054204; National Natural Science Foundation of China, No. 30170966, 30230370; and National High-Technology Programme (863 Programme), No. 2001AA215131

Correspondence to: Xiao-Bing Fu, MD, Wound Healing and Cell Biology Laboratory, Burns Institute, 304 Medical Department, The General Hospital of PLA, Trauma Center of Postgraduate Medical College, 51 Fu Cheng Road, Beijing 100037, China. fuxb@cgw.net.cn
Telephone: +86-10-66867396 **Fax:** +86-10-88416390

Received: 2004-03-23 **Accepted:** 2004-04-16

Key words: Intestines; Ischemia-reperfusion injury; p38 mitogen-activated protein kinase; Apoptosis

Zheng SY, Fu XB, Xu JG, Zhao JY, Sun TZ, Chen W. Inhibition of p38 mitogen-activated protein kinase may decrease intestinal epithelial cell apoptosis and improve intestinal epithelial barrier function after ischemia-reperfusion injury. *World J Gastroenterol* 2005; 11(5): 656-660

<http://www.wjgnet.com/1007-9327/11/656.asp>

INTRODUCTION

Growing evidence from both animal experiments and clinical observations indicates that apoptosis, a form of cell death that is distinct from necrosis, plays a key role in intestinal ischemia-reperfusion injury^[1,2]. The signal transduction pathway that leads to this post-ischemic intestinal apoptosis, however, remains unclear. Recently, cell biology studies have demonstrated that *c-Jun N-terminal kinase* (JNKs)/stress-activated protein kinase (SAPK) and p38 mitogen-activated protein kinase (MAPK), two members of the MAPK family, are activated by a variety of cellular stresses^[3,4] and that their activations result in apoptosis and cell death^[5-11]. It has also been known recently that intestinal I/R, an extreme pathological stress to the gut, activates p38 MAPK^[12]. However, whether activation of p38 MAPK plays a role in intestinal I/R apoptosis has not been determined. The objectives of the present studies were to determine the time course of p38 MAPK activation *in vivo* in I/R rat model, establish a direct link between p38 MAPK activation and intestinal epithelial cell apoptosis after intestinal I/R, and define the effects of inhibition of p38MAPK activation and I/R-induced cell apoptosis by specific pharmacological agents on intestinal epithelial barrier functional damage.

MATERIALS AND METHODS

Animal model and experimental design

Ninety healthy male Wistar rats weighing 220±20 g (Animal Centre, Chinese Academy of Military Medical Science, Beijing) were used in this study. Rats were housed in wire-bottomed cages placed in a room illuminated from 08:00 AM to 20:00 PM (12:12 h light-dark cycle) and maintained at 21±1 °C. Rats were allowed access to water and chow *ad libitum*. After they were anesthetized by 30 g/L sodium pentobarbital (40 mg/kg), and a laparotomy was performed. The superior mesenteric artery (SMA) was identified and freed by blunt dissection. A micro-bulldog clamp was placed at the root of SMA to induce complete cessation of blood flow for 45 min, and thereafter the clamp was loosened to form reperfusion injury^[13]. The animals were randomly divided into sham-operation group (C), I/R vehicle group (R) and SB 203580 pre-treated group (S). According to different periods after reperfusion, groups R and S were further divided into 0.25, 0.5, 1, 2, 6, 12 and 24 h subgroups. In group R and S, 0.15 mL saline or 0.15 mL saline plus SB 203580 (250 µg/rat)

Abstract

AIM: To investigate the role of p38 mitogen-activated protein kinase in rat small intestine after ischemia-reperfusion (I/R) insult and the relationship between activation of p38 MAPK and apoptotic cell death of intestine.

METHODS: Ninety Wistar rats were divided randomly into three groups, namely sham-operated group (C), I/R vehicle group (R) and SB203580 pre-treated group (S). In groups R and S, the superior mesenteric artery (SMA) was separated and occluded for 45 min, then released for reperfusion for 0.25, 0.5, 1, 2, 6, 12 and 24 h. In group C, SMA was separated without occlusion. Plasma *D*-lactate levels were examined and histological changes were observed under a light microscope. The activity of p38 MAPK was determined by Western immunoblotting and apoptotic cells were detected by the terminal deoxynucleotidyl transferase (TdT)-mediated dUDP-biotin nick end labeling (TUNEL).

RESULTS: Intestinal ischemia followed by reperfusion activated p38 MAPK, and the maximal level of activation (7.3-fold *vs* sham-operated group) was reached 30 min after I/R. Treatment with SB 203580, a p38 MAPK inhibitor, reduced intestinal apoptosis (26.72±3.39% *vs* 62.50±3.08% in I/R vehicle, *P*<0.01) and decreased plasma *D*-lactate level (0.78±0.15 mmol/L in I/R vehicle *vs* 0.42±0.17 mmol/L in SB-treated group) and improved post-ischemic intestinal histological damage.

CONCLUSION: p38 MAPK plays a crucial role in the signal transduction pathway mediating post-ischemic intestinal apoptosis, and inhibition of p38 MAPK may attenuate ischemia-reperfusion injury.

was injected right before SMA occlusion via tail vein for pre-treatment. In group C, SMA was separated but without occlusion, and samples were taken after exposure to SMA for 45 min. In groups R and S, rats were sacrificed at different time points after reperfusion, and blood samples and intestinal tissue biopsies were taken. Blood samples were centrifuged and serum was frozen to measure plasma *D*-lactate. A small piece of tissue samples was fixed with 100 g/L neutral buffered formalin for immunohistochemical detection of intestinal epithelial apoptosis. The rest of tissue samples were placed in liquid nitrogen for Western immunoblotting detection of p38 MAPK activities.

Measurement of plasma *D*-lactate

The level of plasma *D*-lactate was measured with modified Brandt's method. Briefly, heparinized blood was centrifuged at 3 200 r/min for 10 min and 2 mL of the plasma was deproteinized with 0.2 mL perchloric acid (PCA) (1/10 vol), mixed and kept in an ice bath for 10 min. The denatured protein solution was centrifuged at 3200 r/min for 10 min and the supernatant was removed. To 1.4 mL of supernatant, 0.12 mL KOH was added and mixed for 20 s. Precipitant KClO₄ was removed by centrifugation at 3200 r/min for 10 min. The supernatant and neutralized-protein-free plasma were used to measure the absorbency at 304 nm. Plasma *D*-lactate concentration was expressed as mmol/L.

Histological staining

Formalin-fixed, paraffin-embedded intestinal samples were also cut into 5- μ m thick sections, deparaffinized in xylene, rehydrated in graded ethanol, and then stained with haematoxylin-eosin (HE) for histological observation under light microscope.

In situ detection of cell death

The apoptotic cells of post-ischemic intestinal tissue were detected by the terminal deoxynucleotidyl transferase (TdT)-mediated dUDP-biotin nick end labeling (TUNEL) method^[14]. *In situ* cell death detection kit (POD) was purchased from Roche Inc., USA. Specimens were dewaxed and immersed in phosphate-buffered saline containing 3 g/L hydrogen peroxide for 10 min at room temperature and then incubated with 20 μ g/mL proteinase K for 15 min at room temperature. Seventy-five microliters of equilibration buffer was applied directly onto the specimens for 10 min at room temperature, followed by incubation with 55 μ L of TdT enzyme at 37 °C for 1 h. The reaction was terminated by transferring the slides to prewarmed stop/wash buffer for 30 min at 37 °C. The specimens were covered with a few drops of rabbit serum and incubated for 20 min at room temperature and then covered with 55 μ L of anti-digoxigenin peroxidase and incubated for 30 min at room temperature. Specimens were then soaked in Tris buffer containing 0.2 g/L diaminobenzidine and 0.2 g/L hydrogen peroxide for 1 min to achieve color development. Finally, the specimens were counterstained by immersion in hematoxylin. The cells with clear nuclear labeling were defined as TUNEL-positive cells. The apoptotic cell rate (apoptotic index) was calculated as percentage of TUNEL-positive cells using the following formula: the number of TUNEL-positive cell nuclei / (number of TUNEL-positive cell nuclei + the number of total cell nuclei) \times 100.

p38 MAP kinase activity assay

p38 MAP kinase activity assay was performed using a P38 MAPK assay kit (cell signaling technology) according to the manufacturer's instructions. In brief, intestinal tissue (100 mg) was homogenized in 1 mL ice-cold cell lysis buffer (20 mmol/L

Tris, pH 7.5, 150 mmol/L NaCl, 1 mmol/L EDTA, 1 mmol/L EGTA, 1% Triton x-100, 2.5 mmol/L sodium pyrophosphate, 1 mmol/L β -glycerolphosphate, 1 mmol/L Na₃VO₄, 1 mg/mL Leupeptin, 1 mmol/L PMSF). The lysates were then sonicated on ice and centrifuged at 15 000 g for 10 min at 4 °C. Immunoprecipitation was performed by adding 20 μ L of resuspended immobilized monoclonal antibody against phospho-p38 MAP kinase (Thr 180/Tyr 182) to 200 μ L cell lysate containing 200 μ g protein. The mixture was incubated with gentle rocking overnight at 4 °C. After centrifugation at 10 000 g for 2 min, the pellets were washed twice with lysis buffer and twice with kinase buffer (25 mmol/L Tris, pH 7.5, 5 mmol/L β -glycerolphosphate, 2 mmol/L DTT, 0.1 mmol/L Na₃VO₄, 10 mmol/L MgCl₂). Kinase reactions were carried out in the presence of 200 μ mol/L of ATP and 2 μ g of ATF-2 fusion protein at 30 °C for 30 min. After incubation, the samples were separated by SDS-PAGE, and ATF-2 phosphorylation was measured by Western immunoblotting using a monoclonal antibody against phosphorylated ATF-2, followed by an enhanced chemiluminescent detection.

Statistical analysis

All values were expressed as mean \pm SE. The statistical significance was determined by one-way analysis of variance (ANOVA), followed by the Student Newman-Keuls multiple comparison test. $P < 0.05$ was considered as statistically significant.

RESULTS

Ischemia - reperfusion activation of p38 MAPK and its blockade by SB 203580

Effect of *in vivo* intestinal I/R on p38 MAPK activity and its inhibition by SB 203580 were determined using a p38 MAPK assay kit. The data showed that p38 MAPK was markedly activated in intestinal epithelial cells subjected to I/R. A 3.8-fold increase in p38 MAPK activity was observed at 15 min after reperfusion. After 30 min of reperfusion, p38 MAPK activity reached a peak level of 7.3-fold increase and gradually returned to control level thereafter. Treatment with SB 203580 at the dose regime selected virtually abolished p38 MAPK activation and brought p38 MAPK activity to a level that was not statistically different from those seen in intestinal epithelia subjected to sham intestinal I/R (Figures 1A, B). These results demonstrated that p38 MAPK was activated by I/R, and its activation could be inhibited by SB 203580 at the dose regime selected in the present experiment.

In situ determination of apoptotic intestinal cells in I/R and its inhibition by SB 203580

The immunohistochemical staining of small intestinal tissue before and after I/R was evaluated and summarized. Before I/R, few TUNEL-positive cells were observed at the villus surface. However, when ischemic intestinal tissue was reperfused, TUNEL-positive cells of the villus were markedly increased compared with the sham-operation group ($P < 0.05$). The number of TUNEL-positive cells increased 5-fold and 6.7-fold at 30 min and 60 min after I/R (29.83 \pm 3.43% vs 5.83 \pm 1.47% at 30 min and 39.33 \pm 4.32% vs 5.83 \pm 1.47% at 60 min, $P < 0.05$), and reached its peak value at 12 h after I/R, which was an increase of 10.72-fold as compared with those in sham-operation group (62.50 \pm 3.08% vs 5.83 \pm 1.47%, $P < 0.01$). Treatment with SB 203580 abolished p38 MAPK activity, the number of TUNEL-positive cells significantly reduced to 26.72 \pm 2.39% in SB 203580 pre-treated group compared with 62.50 \pm 3.08% in I/R vehicle group at 12 h after I/R ($P < 0.05$, Figures 2A, B).

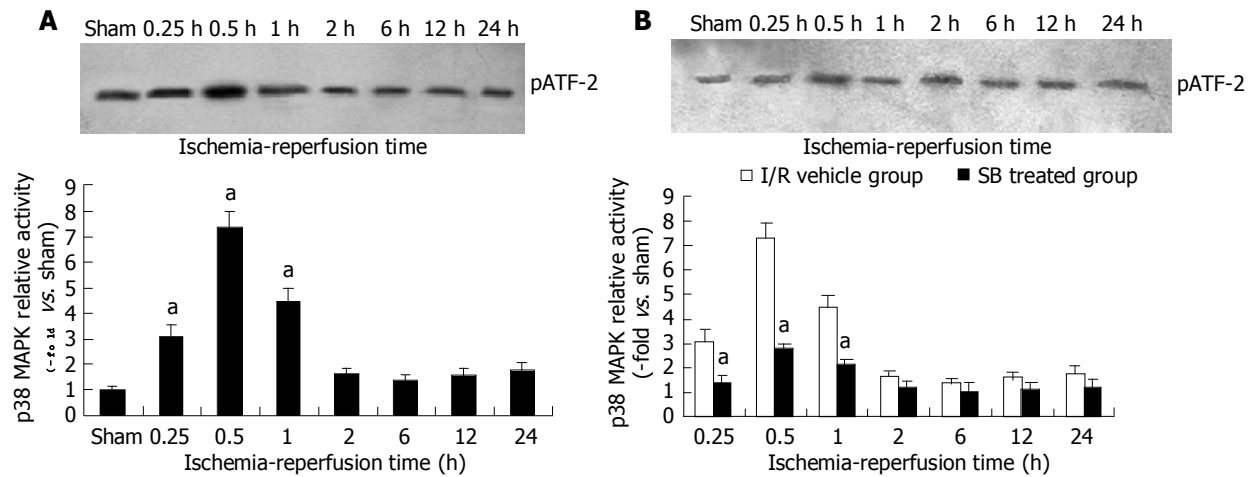


Figure 1 Changes of p38 mitogen-activated protein kinase activities in intestinal tissue after I/R (A) and of different groups after I/R (B). ^a $P < 0.05$ vs I/R vehicle group.

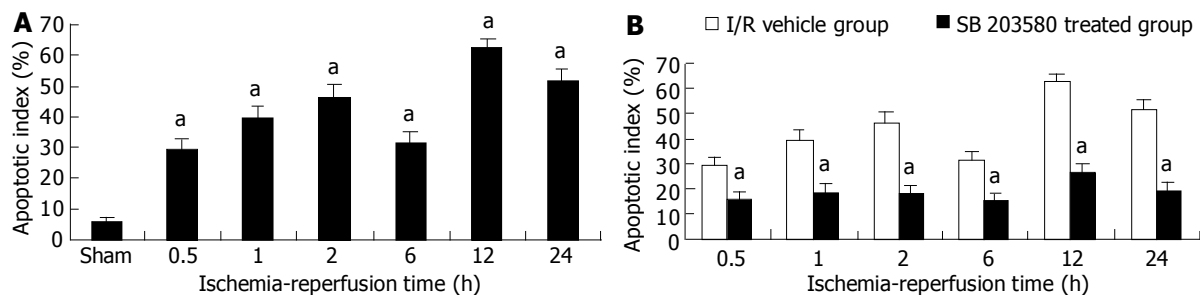


Figure 2 Apoptotic cell rate in intestinal tissue after I/R in I/R vehicle group (A) and apoptotic cells rate in intestinal tissue after I/R in I/R vehicle and SB 203580 treated groups (B). ^a $P < 0.05$ vs I/R vehicle group.

Effect of p38 MAPK inhibition on intestinal histological damage and plasma D-lactate level after I/R

As shown in Figure 3, 45 min after intestinal ischemia followed by reperfusion resulted in significant intestinal histological damage and plasma D-lactate level elevation. Plasma D-lactate level elevated from 15 min after reperfusion in I/R vehicle group, and reached its peak at 12 h, which was an increase of 6-fold as compared with those in sham-operation group (0.78 ± 0.15 mmol/L vs 0.13 ± 0.06 mmol/L, $P < 0.05$), and then gradually decreased. This increased plasma D-lactate level in I/R vehicle group was significantly decreased by treatment with SB 203580 (0.42 ± 0.17 mmol/L vs 0.78 ± 0.15 mmol/L, $P < 0.05$). HE staining showed the damage of intestinal epithelial cells, hemorrhage and necrosis accompanied by inflammatory cell infiltration into the intestinal wall. However, histological structure of intestinal mucosa was significantly improved after treatment with SB 203580 (Figures 4 A-C).

DISCUSSION

Intestinal ischemia-reperfusion injury may cause significant structural alteration of the intestinal wall including disruption of intestinal epithelial barrier by inducing intestinal epithelial programmed cell death^[15,16]. Recently, several mechanisms have been proposed for ischemia-reperfusion injury. The first event is an influx of calcium into cells and a redistribution of intracellular calcium pools with an increase of the free form (biologically active) in the cytosol^[17,18]. The increased calcium level manifests its toxic effects on cells by altering mitochondrial respiratory function and energy metabolism, resulting in serious damage

to cells. The second event is the generation of oxygen free radicals. Free radicals and calcium work in concert to destroy lipids and thereby destroy membrane structures including both the cell membrane and mitochondrial membrane^[19]. The third event is a "no reflow" phenomenon. This condition may contribute to increased neutrophil adherence to damaged endothelium, and expression of P-selectin as well as intercellular adhesion molecule-1 (ICAM-1), promoting microcirculation disturbance, which is thought to be a major mechanism of ischemia-reperfusion injury.

Although it is well known that intestinal epithelial cells are highly sensitive to ischemia-reperfusion injury, the relationship between ischemia-reperfusion induced apoptosis and the injury mechanisms involved in the signal transduction remains largely unclear. Some studies demonstrate that MAPK family plays an important role in intracellular signal transduction in response to extracellular stimuli^[20-22], such as, ischemia-reperfusion. MAPK family members are activated by dual phosphorylation of tyrosine and threonine in response to extracellular stimuli. Once activated, these kinases are translocated to nuclei, where they phosphorylate and activate different transcription factors and transactivate target genes. In this group of kinases, classical extracellular signal-regulated kinase is mainly stimulated by growth factors, and is associated with proliferation. On the other hand, p38 MAPK and JNK have been reported to be activated by a variety of cellular stresses, such as inflammatory cytokines, lipopolysaccharides, heat shock, osmotic stress, and ischemia-reperfusion^[23,24].

The ischemia-reperfusion process differentially activates MAPK. In hepatic ischemia-reperfusion, p38 MAPK and JNK

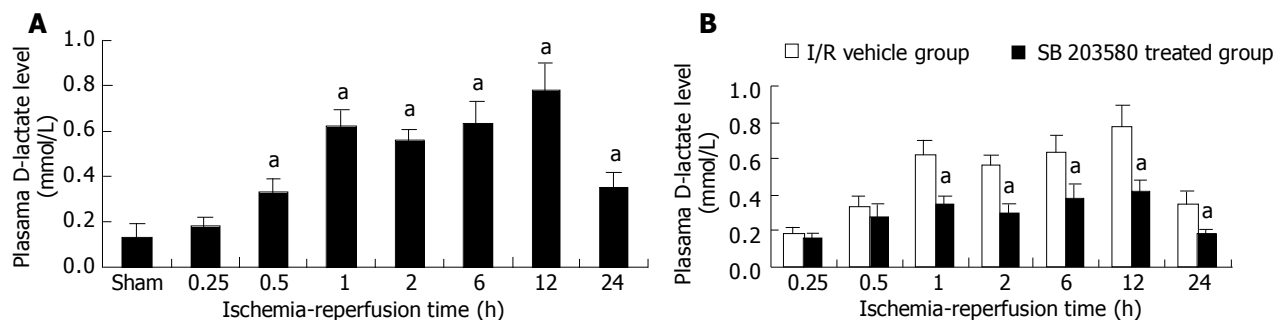


Figure 3 Plasma *D*-lactate level in intestinal tissue after I/R in I/R vehicle group (A) and plasma *D*-lactate level in intestinal tissue after I/R in I/R vehicle and SB 203580 treated groups (B). ^a $P < 0.05$ vs I/R vehicle group.

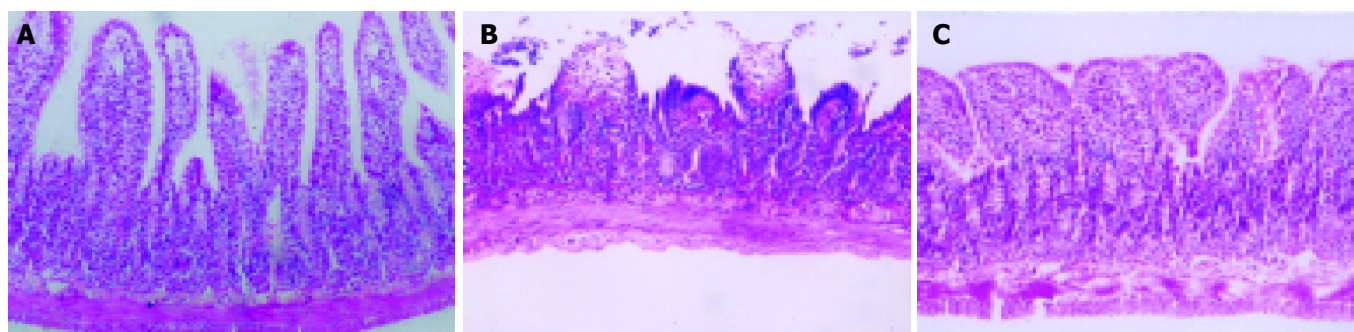


Figure 4 Villus structure. A: Before I/R in sham-operation group; B: Structural changes of the villus after I/R in I/R vehicle group; C: Structural changes of the villus after I/R in SB 203580 treated group.

are activated by reperfusion after ischemia. Ma *et al.*^[25] reported that the administration of SB 203580 decreased myocardial apoptosis and improved cardiac function after myocardial ischemia-reperfusion by inhibiting p38 MAPK. In our study, ischemia followed by reperfusion resulted in marked activation of p38 MAPK, with 7.3-fold activation achieved 30 min after ischemia-reperfusion. These results also lead us to hypothesize that the strong activation of p38 MAPK by reperfusion might play a more significant role in subsequent intestinal injury than previously realized.

Another important discovery from the present study is that administration of a p38 MAPK inhibitor, SB 203580, markedly reduced post-ischemic intestinal apoptosis. Although previous studies have demonstrated that p38 MAPK plays a key role in apoptosis in a variety of cell culture systems^[26], and that ischemia-reperfusion activates p38 MAPK in animal models^[27]. Whether or not p38 MAPK activation in ischemic intestinal tissue is involved in post-ischemic intestinal cell apoptosis has not been directly determined. Our results provide the evidence that p38 MAPK is a key factor in signal transduction leading to intestinal apoptosis after ischemia-reperfusion. However, it should be noted that although administration of SB 203580 blocked p38 MAPK activation, it failed to induce complete inhibition of apoptosis caused by ischemia-reperfusion. These results suggest that other signal transduction pathways, such as JNK/SAPK, may also contribute to post-ischemic intestinal cell apoptosis.

In addition, we also demonstrated that administration of SB 203580 significantly attenuated post-ischemic intestinal histological structural damage and decreased plasma *D*-lactate level. *D*-lactate is the stereoisomer of mammalian *L* (+)-lactate and is produced by bacterial fermentation. Since mammals do not produce *D*-lactate and possess the enzyme system to rapidly metabolize *D*-lactate^[28,29], the released *D*-lactate will pass through the gut barrier and liver in an unchanged form and

appears in the peripheral blood. As intestinal ischemia injury causes mucosal injury and subsequent bacterial proliferation, *D*-lactate is released from gut into the circulation. Thus, the changes of serum *D*-lactate are used as a predictor of intestinal ischemia reperfusion injury. In this study, serum *D*-lactate level elevation and intestinal mucosal damage were observed after ischemia reperfusion, and inhibition of p38 MAPK by SB 203580, *D*-lactate was not significantly increased and intestinal mucosal histological damage was improved, indicating that inhibition of p38 MAPK might exert an important protective effect on the mucosal barrier and decrease the permeability.

In summary, intestinal ischemia-reperfusion, a real pathological stress to the gut, results in significant activation of p38 MAPK. This provides the direct evidence that activation of p38 MAPK plays a key role in the signal transduction pathway mediating intestinal apoptosis after ischemia-reperfusion. Inhibiting p38 MAPK, which reduces intestinal apoptosis associated with p38 MAPK activation, significantly improves post-ischemic intestinal epithelial barrier functional recovery.

REFERENCES

- 1 Fu XB, Jiang LX, Yang YH, Sun TZ, Wang YP, Zou BT, Sheng ZY. Induction of gut mucosa necrosis and apoptosis after ischemia-reperfusion and the effects of fibroblast growth factor. *Zhongguo Weizhongbing Jijiu Yixue* 1998; **10**: 455-458
- 2 Fu XB, Yang YH, Sun TZ, Jiang LX, Sheng ZY. Bcl-2 gen expression and its effect on apoptosis in intestine after ischemia-reperfusion in rats. *Zhongguo Weizhongbing Jijiu Yixue* 1999; **11**: 459-461
- 3 Kyriakis JM, Avruch J. Protein kinase cascades activated by stress and inflammatory cytokines. *Bioessays* 1996; **18**: 567-577
- 4 Yue TL, Wang X, Loudon CS, Gupta S, Pillarisetti K, Gu JL, Hart TK, Lysko PG, Feuerstein GZ. 2-Methoxyestradiol, an endogenous estrogen metabolite, induces apoptosis in endothelial cells and inhibits angiogenesis: possible role for stress-

- activated protein kinase signaling pathway and Fas expression. *Mol Pharmacol* 1997; **51**: 951-962
- 5 **Ichijo H**, Nishida E, Irie K, ten Dijke P, Saitoh M, Moriguchi T, Takagi M, Matsumoto K, Miyazono K, Gotoh Y. Induction of apoptosis by ASK1, a mammalian MAPKKK that activates SAPK/JNK and p38 signaling pathways. *Science* 1997; **275**: 90-94
- 6 **Brenner B**, Koppenhofer U, Weinstock C, Linderkamp O, Lang F, Gulbins E. Fas- or ceramide-induced apoptosis is mediated by a Rac1-regulated activation of Jun N-terminal kinase/p38 kinases and GADD153. *J Biol Chem* 1997; **272**: 22173-22181
- 7 **Juo P**, Kuo CJ, Reynolds SE, Konz RF, Raingeaud J, Davis RJ, Biemann HP, Blenis J. Fas activation of the p38 mitogen-activated protein kinase signalling pathway requires ICE/CED-3 family proteases. *Mol Cell Biol* 1997; **17**: 24-35
- 8 **Chauhan D**, Kharbanda S, Ogata A, Urashima M, Teoh G, Robertson M, Kufe DW, Anderson KC. Interleukin-6 inhibits Fas- induced apoptosis and stress-activated protein kinase activation in multiple myeloma cells. *Blood* 1997; **89**: 227-234
- 9 **Xia Z**, Dickens M, Raingeaud J, Davis RJ, Greenberg ME. Opposing effects of ERK and JNK-p38 MAP Kinases on apoptosis. *Science* 1995; **270**: 1326-1331
- 10 **Kummer JL**, Rao PK, Heidenreich KA. Apoptosis induced by withdrawal of trophic factors is mediated by p38 mitogen-activated protein kinase. *J Biol Chem* 1997; **272**: 20490-20494
- 11 **Schwenger P**, Bellosta P, Vietor I, Basilico C, Skolnik EY, Vilcek J. Sodium salicylate induces apoptosis via p38 mitogen-activated protein kinase but inhibits tumor necrosis factor-induced c-Jun N-terminal kinase/stress-activated protein kinase activation. *Proc Natl Acad Sci USA* 1997; **94**: 2869-2873
- 12 **Fu XB**, Xing F, Yang YH, Sun TZ, Guo BC. Activation of phosphorylating-p38 mitogen-activated protein kinase and its relationship with localization of intestinal stem cells in rats after ischemia-reperfusion injury. *World J Gastroenterol* 2003; **9**: 2036-2039
- 13 **Fu X**, Sheng Z, Wang Y, Ye Y, Xu M, Sun T, Zhou B. Basic fibroblast growth factor reduces the gut and liver morphologic and functional injuries after ischemia and reperfusion. *J Trauma* 1997; **42**: 1080-1085
- 14 **Gavrieli Y**, Sherman Y, Ben-Sasson SA. Identification of programmed cell death in situ via specific labeling of nuclear DNA fragmentation. *J Cell Biol* 1992; **119**: 493-501
- 15 **Yang YH**, Fu XB, Sun TZ, Jiang LX, Gu XM. The effect of exogenous basic fibroblast growth factor on hepatic endogenous basic fibroblast growth factor and fibroblast growth factor receptor expression after intestinal ischemia-reperfusion injury. *Zhongguo Weizhongbing Jijiu Yixue* 1999; **11**: 734-736
- 16 **Fu XB**, Yang YH, Sun TZ, Sun XQ, Gu XM, Chang GY, Sheng ZY. Effect of inhibition or anti-endogenous basic fibroblast growth factor on functional changes in intestine, liver and kidneys in rats after gut ischemia-reperfusion injury. *Zhongguo Weizhongbing Jijiu Yixue* 2000; **12**: 465-468
- 17 **Humes HD**. Role of calcium in pathogenesis of acute renal failure. *Am J Physiol* 1986; **250**: F579-F589
- 18 **Schrier RW**, Arnold PE, Van Putten VJ, Burke TJ. Cellular calcium in ischemic acute renal failure: role of calcium entry blockers. *Kidney Int* 1987; **32**: 313-321
- 19 **Granger DN**, Hollwarth ME, Parks DA. Ischemia-reperfusion injury: role of oxygen-derived free radicals. *Acta Physiol Scand Suppl* 1986; **548**: 47-63
- 20 **Bogoyevitch MA**, Ketterman AJ, Sugden PH. Cellular stresses differentially activate c-Jun N-terminal protein kinases and extracellular signal-regulated protein kinases in cultured ventricular myocytes. *J Biol Chem* 1995; **270**: 29710-29717
- 21 **Seth A**, Gonzalez FA, Gupta S, Raden DL, Davis RJ. Signal transduction within the nucleus by mitogen-activated protein kinase. *J Biol Chem* 1992; **267**: 24796-24804
- 22 **Han J**, Lee JD, Bibbs L, Ulevitch RJ. A MAP kinase targeted by endotoxin and hyperosmolarity in mammalian cells. *Science* 1994; **265**: 808-811
- 23 **Clerk A**, Fuller SJ, Michael A, Sugden PH. Stimulation of "stress-regulated" mitogen-activated protein kinases (stress-activated protein kinases/c-Jun N-terminal kinases and p38-mitogen-activated protein kinases) in perfused rat hearts by oxidative and other stresses. *J Biol Chem* 1998; **273**: 7228-7234
- 24 **De Silva H**, Cioffi C, Yin T, Sandhu G, Webb RL, Whelan J. Identification of a novel stress activated kinase in kidney and heart. *Biochem Biophys Res Commun* 1998; **250**: 647-652
- 25 **Ma XL**, Kumar S, Gao F, Loudon CS, Lopez BL, Christopher TA, Wang C, Lee JC, Feuerstein GZ, Yue TL. Inhibition of p38 mitogen-activated protein kinase decreases cardiomyocyte apoptosis and improves cardiac function after myocardial ischemia and reperfusion. *Circulation* 1999; **99**: 1685-1691
- 26 **Kawasaki H**, Morooka T, Shimohama S, Kimura J, Hirano T, Gotoh Y, Nishida E. Activation and involvement of p38 mitogen-activated protein kinase in glutamate-induced apoptosis in rat cerebellar granule cells. *J Biol Chem* 1997; **272**: 18518-18521
- 27 **Bogoyevitch MA**, Gillespie-Brown J, Ketterman AJ, Fuller SJ, Ben-Levy R, Ashworth A, Marshall CJ, Sugden PH. Stimulation of the stress-activated mitogen-activated protein kinase subfamilies in perfused heart. p38/RK mitogen-activated protein kinases and c-Jun N-terminal kinases are activated by ischemia/reperfusion. *Circ Res* 1996; **79**: 162-173
- 28 **Murray MJ**, Barbose JJ, Cobb CF. Serum D(-)-lactate levels as a predictor of acute intestinal ischemia in a rat model. *J Surg Res* 1993; **54**: 507-509
- 29 **Murray MJ**, Gonze MD, Nowak LR, Cobb CF. Serum D(-)-lactate levels as an aid to diagnosing acute intestinal ischemia. *Am J Surg* 1994; **167**: 575-578

Edited by Kumar M and Wang XL Proofread by Zhu LH

• BASIC RESEARCH •

Differences in platelet endothelial cell adhesion molecule-1 expression between peripheral circulation and pancreatic microcirculation in cerulein-induced acute edematous pancreatitis

Hong-Kai Gao, Zong-Guang Zhou, Fang-Hai Han, You-Qin Chen, Wen-Wei Yan, Tao He, Cun Wang, Zhao Wang

Hong-Kai Gao, Zong-Guang Zhou, Wen-Wei Yan, Tao He, Cun Wang, Zhao Wang, Department of General Surgery & Division of Digestive Surgery and Organ-Microcirculation, West China Hospital, Sichuan University, Chengdu 610041, Sichuan Province, China

Fang-Hai Han, Department of Gastrointestinal Surgery, First Affiliated Hospital, Zhongshan University, Guangzhou 510120, Guangdong Province, China

You-Qin Chen, Cardiovascular Biology, Oklahoma Medical Research Foundation, Oklahoma City, OK 73104, USA

Supported by National Natural Science Foundation of China, No. 39925032

Correspondence to: Dr. Zong-Guang Zhou, Department of General Surgery & Division of Digestive Surgery and Organ-Microcirculation, West China Hospital, Sichuan University, Chengdu 610041, Sichuan Province, China. zhou767@21cn.com

Telephone: +86-28-85422525 **Fax:** +86-28-85422484

Received: 2003-11-22 **Accepted:** 2004-03-02

Abstract

AIM: To investigate the changes of platelet endothelial cell adhesion molecule-1 (PECAM-1) expression on polymorphonuclear leukocytes (PMNs) in peripheral circulation and pancreatic microcirculation in cerulein-induced acute edematous pancreatitis (AEP).

METHODS: Fifty Wistar rats were randomly divided into control group ($n = 10$) and AEP group ($n = 40$). A model of AEP was established by subcutaneous injection of cerulein 5.5 and 7.5 $\mu\text{g}/\text{kg}$ at 0 and 1 h after the beginning of experiment respectively. PECAM-1 expression on PMNs from splenic vein and inferior vena cava was determined by RT-PCR at mRNA level and determined by flow cytometry at protein level.

RESULTS: In experimental rats, an increased PECAM-1 mRNA expression was seen from 4 to 8 h of AEP in peripheral circulation ($0.77 \pm 0.25\%$, $0.76 \pm 0.28\%$, $0.89 \pm 0.30\%$, $1.00 \pm 0.21\%$), while in pancreatic microcirculation, expression decreased from 2 h and reached the lowest level at 6 h of AEP ($0.78 \pm 0.29\%$, $0.75 \pm 0.26\%$, $0.62 \pm 0.28\%$, $0.66 \pm 0.20\%$). There were significant differences at 8-h time point of AEP between peripheral circulation and pancreatic microcirculation ($1.00 \pm 0.21\%$ vs $0.66 \pm 0.20\%$, $P < 0.05$). Meanwhile, the difference at protein level was also found.

CONCLUSION: A reverse expression of PECAM-1 on PMNs was found between peripheral circulation and pancreatic microcirculation, suggesting that inhibition of PECAM-1 expression may improve the pathological change of AEP.

© 2005 The WJG Press and Elsevier Inc. All rights reserved.

Key words: Pancreatitis; Platelet endothelial cell adhesion molecule-1; Microcirculation; Cerulein

Gao HK, Zhou ZG, Han FH, Chen YQ, Yan WW, He T, Wang C, Wang Z. Differences in platelet endothelial cell adhesion molecule-1 expression between peripheral circulation and pancreatic microcirculation in cerulein-induced acute edematous pancreatitis. *World J Gastroenterol* 2005; 11(5): 661-664
<http://www.wjgnet.com/1007-9327/11/661.asp>

INTRODUCTION

Acute pancreatitis (AP) is a potentially lethal disease and characterized by acinar cell necrosis, extensive interstitial edema, and migration of neutrophils to the damaged gland. However, the development and etiology of AP remain poorly understood.

Cerulein-induced acute edematous pancreatitis (AEP) is a widely used model in investigating the pathophysiological events of the disease. In this regard, rapid induction of mild disease with a highly reproducible course and easily detected changes of acute interstitial pancreatitis have made this secretagogue-induced model favorable for the investigation of the pathogenesis of the disease.

Platelet endothelial cell adhesion molecule-1 (PECAM-1, CD31) is a cell adhesion molecule that belongs to the Ig superfamily expressed on endothelial cells as well as circulating leukocytes including neutrophils^[1,2], monocytes and NK cells^[3,4]. The homophilic interaction of neutrophil or monocyte PECAM-1 with endothelial PECAM-1 is very important to neutrophil and monocyte transendothelial migration as demonstrated in studies in several different laboratories^[5-9]. The interaction may be mediated by interdigitating PECAM-1 molecules from neutrophils or monocytes and endothelial cells, forming a zipper which promotes their adhesion^[10-12].

Recently, several studies have demonstrated that AP is frequently associated with sequestration of inflammatory cells, particularly leukocytes^[13-15]. However, the expression of PECAM-1 on leukocytes and the role of PECAM-1 in pancreatic injury in AP are not very clear. Therefore, we conducted this study to investigate the expression of PECAM-1 on PMNs and the role of PECAM-1 in microcirculatory injury in AEP.

MATERIALS AND METHODS

Animals

Male Wistar rats (250-350 g) were provided by the Center of Experimental Animals, Sichuan University (Chengdu, China). All animals were fasted for 12 h before the experiments but had free access to water. They were treated in accordance with the protocols approved by the local Animal Use and Care Committee and executed according to the National Animal Welfare Law.

Induction of acute pancreatitis

All experimental rats were given subcutaneous injection of cerulein (Sigma Co, USA) 5.5 and 7.5 $\mu\text{g}/\text{kg}$ at 0 and 1 h after the

beginning of experiment respectively, while control rats were given subcutaneous injection of 0.9% saline solution.

Experimental protocols

The rats were randomly assigned into control group ($n = 10$) and AEP group ($n = 40$). Rats in AEP group were sacrificed at 2 ($n = 10$), 4 ($n = 10$), 6 ($n = 10$) and 8 h ($n = 10$) after induction of AEP.

Collection of samples

At different time points (2, 4, 6, and 8 h) after induction of AEP, the experimental animals underwent laparotomy under anesthesia by intraperitoneal injection of 50 mg/kg sodium pentobarbital (Sanofi, Libourne, France). Blood samples were immediately obtained from splenic vein by retrograde catheterization from portal vein and inferior vena cava and samples of pancreatic head were taken immediately after the animals were killed. Control animals underwent laparotomy and were sampled in the same fashion as animals with AEP.

Amylase measurement

Serum amylase levels were measured at 37 °C by an enzymatic assay with a spectrophotometer according to the manufacturer's instructions. All serum samples were assayed in duplicate, and the results were averaged at the end of the experiment.

Edema assessment

Pancreatic edema was evaluated by measuring the wet-to-dry weight ratio. A segment of the pancreas was trimmed of fat and weighed. The water content was determined by calculating the wet-to-dry weight ratio from the initial weight (wet weight) and its weight after incubation at 160 °C for 24 h (dry weight).

Reverse transcriptase-polymerase chain reaction

Total RNA was isolated from blood using TRIzol® reagent kits (Gibco BRL, USA). RT-PCR was performed with the Access RT-PCR kit (Takara, Japan) according to the manufacturer's protocol. The primer for rat PECAM-1 was constructed based on published human and mouse PECAM-1 nucleotide sequences and synthesized by Life Technology (Hong Kong, China). We obtained two different bands from RT-PCR corresponding to the splice variants. The band densities of the two splice variants behaved in the same manner. The primers are indicated in Table 1. RT-PCR reactions were performed in 50 µL reaction volume and run in GeneAmp 9600 machine (Perkin-Elmer, USA). The conditions of RT-PCR were as follows: 1 cycle for 30 min at 50 °C; 1 cycle for 2 min at 94 °C; 30 cycles for 30 s at 94 °C, for 30 s at 55 °C, for 30 s at 72 °C; 1 cycle for 10 min at 72 °C. The PCR products were separated by electrophoresis in 2% agarose gels and stained with ethidium bromide. The densities of cDNA bands were analyzed by scanning densitometry using GelDoc 2000 (Bio-Rad, USA). The band densities were normalized to the β-actin band densities and the results were expressed as ratio.

Neutrophils preparation

Blood was immediately mixed with heparin (50 U/mL) and

centrifuged in a discontinuous Percoll gradient to yield a fraction of approximately 97% purity. Rat PMNs were isolated by a modification of the technique. Cell viabilities, as assessed by trypan blue exclusion, were above 96% under all experimental conditions.

Flow cytometry

To determine PECAM-1 protein expression, rat PMNs were incubated with phycoerythrin (PE)-anti-PECAM-1 monoclonal antibody (BD PharMingen, USA) at 4 °C in the dark for 20 min. After washing with PBS and fixed in 0.5% paraformaldehyde in phosphate-buffered saline, cells were resuspended and mean fluorescence intensity was measured by flow cytometry (ELITE ESP, Coulter, USA).

Statistical analysis

The results were expressed as mean±SE, individual comparisons of group means were performed with one-way ANOVA, $P < 0.05$ was considered statistically significant.

RESULTS

Serum amylase

After induction of acute pancreatitis by subcutaneous injection of cerulein as shown in Table 2, serum amylase increased sharply and reached the peak at 4-h time point, then dropped slightly at 8-h time point. Compared to control rats, all AEP rats demonstrated hyperamylasemia ($P < 0.05$).

Wet-to-dry weight ratio

As shown in Table 3, subcutaneous injection of cerulein resulted in an increase in the wet/dry weight ratio in AEP rats. Compared to control rats, all AEP rats had a significant increase in the wet/dry weight ratio ($P < 0.05$).

RT-PCR demonstration of PECAM-1 expression on PMNs

To determine the role of PECAM-1 in AEP, we evaluated the PECAM-1 mRNA expression on PMNs by RT-PCR. As shown in Figure 1, in experimental rats, the PECAM-1 mRNA expression slightly increased from 4 to 8-h time points of AEP in peripheral circulation, while in pancreatic microcirculation, the expression decreased from 2 h and reached the lowest level at 6-h time point of AEP and the PECAM-1 mRNA expression difference became significant between peripheral circulation and pancreatic microcirculation at 8-h time point of AEP ($P < 0.05$).

Flow cytometry demonstration of PECAM-1 expression on PMNs

At protein level, we analyzed the PECAM-1 expression on the surface of PMNs by flow cytometry. As shown in Figure 2, in experimental rats, the expression of PECAM-1 on PMNs had no significant difference between peripheral circulation and pancreatic microcirculation at 2 and 4-h time points of AEP. Then from 4 to 8-h time points, the expression of PECAM-1 was up-regulated in peripheral circulation, while it was down-regulated in pancreatic microcirculation. As a result, the expression had a significant difference between peripheral circulation and pancreatic microcirculation at 8-h time point of AEP ($P < 0.05$).

Table 1 Primer list of RT-PCR

mRNA	Upper primer	Lower primer	Fragment size
β-actin	5'-GATGGTGGGTATGGGTAGAA-3'	5'-CTAGGAGCCAGGGCAGTAATC-3'	346 bp
PECAM-1	5'-AGGGCTCATTGCGGTGGTTGTCAT-3'	5'-TAAGGGAGCCTTCCGTTCTAGAGT-3'	348, 404 bp

PECAM-1: platelet endothelial cell adhesion molecule-1.

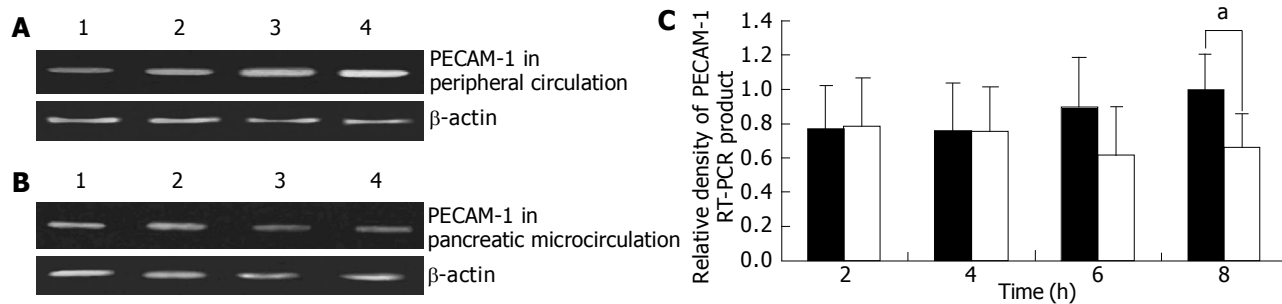


Figure 1 RT-PCR analysis of PMNs PECAM-1. A: Expression of on PMNs PECAM-1 mRNA in peripheral circulation. Lanes 1, 2, 3 and 4: PECAM-1 cDNA after amplification from RNA of PMNs from inferior vena cava at 2, 4, 6 and 8-h time points of AEP respectively; B: Expression of on PMNs PECAM-1 mRNA on in pancreatic microcirculation. Lanes 1, 2, 3 and 4: PECAM-1 cDNA after amplification from RNA of PMNs from splenic vein at 2, 4, 6 and 8-h time points of AEP respectively; C: Values of the density of PECAM-1 RT-PCR product normalized to that of β -actin in the same RNA sample. Symbols are: (■) peripheral circulation; (□) pancreatic microcirculation. $^aP < 0.05$, by one-way ANOVA.

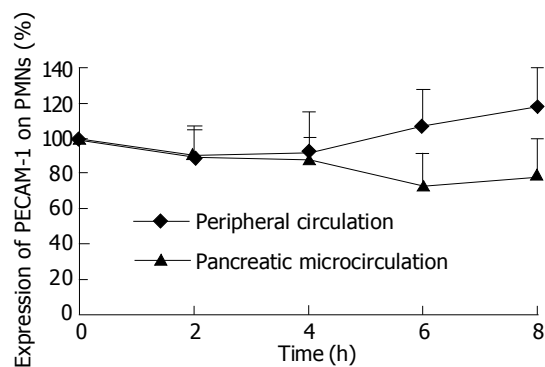


Figure 2 Flow cytometry analysis of PECAM-1 on PMNs. $^aP < 0.05$ vs peripheral circulation values.

Table 2 Serum amylase level in AEP (mean \pm SE)

Group	Serum amylase (IU/L)
Control	319.5 \pm 78.7
AEP 2 h	1 493.3 \pm 308.9 ^a
AEP 4 h	2 095 \pm 956.7 ^b
AEP 6 h	1 662.7 \pm 544.6 ^a
AEP 8 h	1 514.2 \pm 634.2 ^a

$^aP < 0.05$ vs control group; $^bP < 0.001$ vs control group.

Table 3 Wet/dry pancreatic weight ratio in AEP (mean \pm SE)

Group	Wet/dry weight ratio (%)
Control	3.4 \pm 0.2
AEP 2 h	3.9 \pm 0.3 ^a
AEP 4 h	4.0 \pm 0.3 ^a
AEP 6 h	4.3 \pm 0.4 ^a
AEP 8 h	4.1 \pm 0.5 ^a

$^aP < 0.05$ vs control group.

DISCUSSION

This study demonstrates that PECAM-1 mRNA expression on PMNs between peripheral circulation and pancreatic microcirculation is in a reverse pattern in cerulein-induced AEP. In peripheral circulation, the PECAM-1 mRNA expression is up-regulated, while it is down-regulated in pancreatic microcirculation, especially in the late stage of AEP. Moreover, PECAM-1 gene activation is in good correlation with its protein expression.

Since the concept of autodigestion is accepted generally, considerable progress has been made in the understanding of pathogenesis of AEP. In recent years, basic researches on the morphology of pancreatic microcirculation have revealed that intralobular arterioles could be considered as 'end-arteries'. Furthermore, they have no anastomosis with adjacent intralobular arterioles and their branches. This anatomic feature makes pancreas susceptible to the pancreatic microcirculatory impairment. However, the key factors for local microcirculatory disturbance remain obscure.

Several lines of evidence have shown that PECAM-1 is required for leukocyte transmigration through endothelial cell monolayer^[16-18] and PMNs play an important role in microcirculatory injury during inflammation^[19,20]. But these researches mainly focused on the expression of PECAM-1 on leukocytes in peripheral circulation and rarely investigated its expression in microcirculation. Moreover, the expression of PECAM-1 and its role in pancreatic injury *in vivo* have been ambiguous. Therefore, we examined the PECAM-1 expression on PMNs in pancreatic microcirculation and peripheral circulation during AEP.

PECAM-1, expressed on the surface of most leukocytes and endothelial cells, can up-regulate leukocyte integrin affinity by homophilic engagement of PECAM-1 molecules between circulating leukocytes and the underlying endothelial cell monolayer, facilitating leukocyte transmigration subsequently^[20-22]. Neutralized antibodies to PECAM-1 could inhibit neutrophil and monocyte transendothelial migration by 80% *in vitro* and *in vivo*. The anti-PECAM-1 antibodies could inhibit tissue recruitment of neutrophils and monocytes *in vivo* by inhibiting the transmigration of neutrophils and monocytes between endothelial cells^[23]. Studies using intravital videomicroscopy have demonstrated that anti-PECAM-1 antibodies do not inhibit other steps in neutrophil or monocyte recruitment such as rolling on endothelium or activation-dependent adhesion to endothelium^[24]. In our experiments, we found that PECAM-1 expression on PMNs in pancreatic microcirculation was significantly down-regulated, in comparison with its expression in peripheral circulation in AEP. In addition, the more the serum amylase and wet/dry weight ratio increased, the more the PECAM-1 expression decreased on PMNs in pancreatic microcirculation, suggesting that PECAM-1 expression on PMNs in pancreatic microcirculation is correlated with the development of AEP. It is possible that the up-regulation of PECAM-1 may prepare PMNs for transmigration through the monolayer of endothelial cells in microvessels, and down-regulation of PECAM-1 may reflect the activation of PMNs. While the activated PMNs go through pancreas, they can swim from the

microvessel lumen, across the endothelium, to the inflammatory tissue more easily, causing the deterioration of pancreatic injury. Thus we hypothesize that inhibition of PECAM-1 expression on PMNs may block the interaction between endothelial cells and PMNs, thereby preventing PMNs' transmigration.

In conclusion, our study is the first to investigate the expression of PECAM-1 mRNA and protein on PMNs in pancreatic microcirculation and peripheral circulation. PECAM-1 expression on PMNs between peripheral circulation and pancreatic microcirculation is in a reverse direction in AEP. Furthermore, down-regulation of PECAM-1 expression may be one of the most important parameters of pancreatic microcirculatory injury and inhibition of PECAM-1 expression may alleviate the pathological changes of AEP.

REFERENCES

- 1 **Wakayama T**, Hamada K, Yamamoto M, Suda T, Iseki S. The expression of platelet endothelial cell adhesion molecule-1 in mouse primordial germ cells during their migration and early gonadal formation. *Histochem Cell Biol* 2003; **119**: 355-362
- 2 **Mamdouh Z**, Chen X, Pierini LM, Maxfield FR, Muller WA. Targeted recycling of PECAM from endothelial surface-connected compartments during diapedesis. *Nature* 2003; **421**: 748-753
- 3 **Pu FR**, Williams RL, Markkula TK, Hunt JA. Expression of leukocyte-endothelial cell adhesion molecules on monocyte adhesion to human endothelial cells on plasma treated PET and PTFE *in vitro*. *Biomaterials* 2002; **23**: 4705-4718
- 4 **Kawabata K**, Nakai S, Miwa M, Sugiura T, Otsuka Y, Shinzato T, Hiki N, Tomimatsu I, Ushida Y, Hosono F, Maeda K. CD31 expression on leukocytes is downregulated *in vivo* during hemodialysis. *Nephron* 2001; **89**: 153-160
- 5 **Zaremba J**, Losy J. sPECAM-1 in serum and CSF of acute ischaemic stroke patients. *Acta Neurol Scand* 2002; **106**: 292-298
- 6 **Luscinskas FW**, Ma S, Nusrat A, Parkos CA, Shaw SK. Leukocyte transendothelial migration: a junctional affair. *Semin Immunol* 2002; **14**: 105-113
- 7 **Radi ZA**, Kehrli ME, Ackermann MR. Cell adhesion molecules, leukocyte trafficking, and strategies to reduce leukocyte infiltration. *J Vet Intern Med* 2001; **15**: 516-529
- 8 **Neubauer K**, Ritzel A, Saile B, Ramadori G. Decrease of platelet-endothelial cell adhesion molecule 1-gene-expression in inflammatory cells and in endothelial cells in the rat liver following CCl(4)-administration and *in vitro* after treatment with TNFalpha. *Immunol Lett* 2000; **74**: 153-164
- 9 **Neubauer K**, Wilfling T, Ritzel A, Ramadori G. Platelet-endothelial cell adhesion molecule-1 gene expression in liver sinusoidal endothelial cells during liver injury and repair. *J Hepatol* 2000; **32**: 921-932
- 10 **Lefer AM**. Role of the beta2-integrins and immunoglobulin superfamily members in myocardial ischemia-reperfusion. *Ann Thorac Surg* 1999; **68**: 1920-1923
- 11 **Nakada MT**, Amin K, Christofidou-Solomidou M, O'Brien CD, Sun J, Gurubhagavatula I, Heavner GA, Taylor AH, Paddock C, Sun QH, Zehnder JL, Newman PJ, Albelda SM, DeLisser HM. Antibodies against the first Ig-like domain of human platelet endothelial cell adhesion molecule-1 (PECAM-1) that inhibit PECAM-1-dependent homophilic adhesion block *in vivo* neutrophil recruitment. *J Immunol* 2000; **164**: 452-462
- 12 **Muller WA**, Randolph GJ. Migration of leukocytes across endothelium and beyond: molecules involved in the transmigration and fate of monocytes. *J Leukoc Biol* 1999; **66**: 698-704
- 13 **de Dios I**, Perez M, de La Mano A, Sevillano S, Orfao A, Ramudo L, Manso MA. Contribution of circulating leukocytes to cytokine production in pancreatic duct obstruction-induced acute pancreatitis in rats. *Cytokine* 2002; **20**: 295-303
- 14 **Bhatnagar A**, Wig JD, Majumdar S. Immunological findings in acute and chronic pancreatitis. *ANZ J Surg* 2003; **73**: 59-64
- 15 **Mann DV**, Kalu P, Foulds S, Edwards R, Glazer G. Neutrophil activation and hyperamylasaemia after endoscopic retrograde cholangiopancreatography: potential role for the leukocyte in the pathogenesis of acute pancreatitis. *Endoscopy* 2001; **33**: 448-453
- 16 **Solowiej A**, Biswas P, Graesser D, Madri JA. Lack of platelet endothelial cell adhesion molecule-1 attenuates foreign body inflammation because of decreased angiogenesis. *Am J Pathol* 2003; **162**: 953-962
- 17 **O'Brien CD**, Lim P, Sun J, Albelda SM. PECAM-1-dependent neutrophil transmigration is independent of monolayer PECAM-1 signaling or localization. *Blood* 2003; **101**: 2816-2825
- 18 **Thompson RD**, Noble KE, Larbi KY, Dewar A, Duncan GS, Mak TW, Nourshargh S. Platelet-endothelial cell adhesion molecule-1 (PECAM-1)-deficient mice demonstrate a transient and cytokine-specific role for PECAM-1 in leukocyte migration through the perivascular basement membrane. *Blood* 2001; **97**: 1854-1860
- 19 **Dangerfield J**, Larbi KY, Huang MT, Dewar A, Nourshargh S. PECAM-1 (CD31) homophilic interaction up-regulates alpha6beta1 on transmigrated neutrophils *in vivo* and plays a functional role in the ability of alpha6 integrins to mediate leukocyte migration through the perivascular basement membrane. *J Exp Med* 2002; **196**: 1201-1211
- 20 **Okouchi M**, Okayama N, Shimizu M, Omi H, Fukutomi T, Itoh M. High insulin exacerbates neutrophil-endothelial cell adhesion through endothelial surface expression of intercellular adhesion molecule-1 via activation of protein kinase C and mitogen-activated protein kinase. *Diabetologia* 2002; **45**: 556-559
- 21 **Thompson RD**, Wakelin MW, Larbi KY, Dewar A, Asimakopoulos G, Horton MA, Nakada MT, Nourshargh S. Divergent effects of platelet-endothelial cell adhesion molecule-1 and beta 3 integrin blockade on leukocyte transmigration *in vivo*. *J Immunol* 2000; **165**: 426-434
- 22 **Cid MC**, Cebrian M, Font C, Coll-Vinent B, Hernandez-Rodriguez J, Esparza J, Urbano-Marquez A, Grau JM. Cell adhesion molecules in the development of inflammatory infiltrates in giant cell arteritis: inflammation-induced angiogenesis as the preferential site of leukocyte-endothelial cell interactions. *Arthritis Rheum* 2000; **43**: 184-194
- 23 **Su WH**, Chen HI, Jen CJ. Differential movements of VE-cadherin and PECAM-1 during transmigration of polymorphonuclear leukocytes through human umbilical vein endothelium. *Blood* 2002; **100**: 3597-3603
- 24 **Sun Z**, Wang X, Lasson A, Bojesson A, Annborn M, Andersson R. Effects of inhibition of PAF, ICAM-1 and PECAM-1 on gut barrier failure caused by intestinal ischemia and reperfusion. *Scand J Gastroenterol* 2001; **36**: 55-65

Toxicity of novel anti-hepatitis drug bicyclol: A preclinical study

Geng-Tao Liu, Yan Li, Huai-Ling Wei, Hong Lu, Hui Zhang, Yu-Gui Gao, Ling-Zhi Wang

Geng-Tao Liu, Yan Li, Huai-Ling Wei, Hong Lu, Hui Zhang, Yu-Gui Gao, Ling-Zhi Wang, Department of Pharmacology, Institute of Materia Medica, Chinese Academy of Medical Sciences and Peking Union Medical College, Beijing 100050, China

Supported by the Grant From Ministry of Sciences and Technology of China, No.96-901-01-45

Correspondence to: Professor Geng-Tao Liu, Department of Pharmacology, Institute of Materia Medica, Chinese Academy of Medical Sciences, 1 Xian Nong Tan St, Beijing 100050, China. liugt@imm.ac.cn

Telephone: +86-10-63165178 **Fax:** +86-10-63017757

Received: 2004-07-23 **Accepted:** 2004-09-04

Abstract

AIM: To study the toxicity of bicyclol to animals.

METHODS: Acute toxicity test was performed in Kunming strain mice that were orally given bicyclol at the doses of 3 and 5 g/kg body weight, respectively. Wistar rats were orally administered bicyclol at a dose of 5 g/kg body weight. Death and clinical symptoms of animals were recorded within 7 d. Sub-acute toxicity test was carried out in rats that were treated with various doses of bicyclol (150, 300, 600 mg/kg) once daily for 14 d. Animal behaviors, blood biochemical markers, blood and urine pictures were examined. Chronic toxicity test was conducted in 80 Wistar rats of both sexes. The animals were orally administered with various doses of bicyclol [150, 300, 600 mg/kg, 100-400 folds corresponding to the proposed therapeutic dose (1.5 mg/(kg·d)) of bicyclol for patients] once daily for 6 mo except for Sunday. The control group was given the same volume of 0.2% sodium carboxyl methylcellulose (Na-CMC). Twenty-one beagle dogs received bicyclol (25, 75, 225 mg/kg, 16.6, 50, 150 folds corresponding to the proposed therapeutic dose of bicyclol for patients) once a day for 6 mo except for Sunday. The body weight, food intake, urine and feces, blood picture, blood biochemical markers, and pathological examination of main organs were determined. Mutagenicity and teratogenicity were determined. Mutagenicity assay included Ames's test, chromosome aberration test in CHL cells and micronucleus test in mice. For the teratogenicity assay, pregnant Wistar rats weighing 200-250 g were treated with 0.2, 1.0 g/kg bicyclol once daily from the 7th d of gestation for 10 d.

RESULTS: The oral LD₅₀ of bicyclol was over 5 g/kg in mice and rats. No noticeable alterations in subacute and chronic toxicity of rats and dogs were demonstrated. No mutagenicity and teratogenicity of bicyclol were found.

CONCLUSION: Bicyclol has no detectable chronic toxicity as well as mutagenicity and teratogenicity in animals.

© 2005 The WJG Press and Elsevier Inc. All rights reserved.

Key words: Bicyclol; Antiviral agents; Toxicity test

Liu GT, Li Y, Wei HL, Lu H, Zhang H, Gao YG, Wang LZ. Toxicity of novel anti-hepatitis drug bicyclol: A preclinical study. *World J Gastroenterol* 2005; 11(5): 665-671

<http://www.wjgnet.com/1007-9327/11/665.asp>

INTRODUCTION

Chronic viral hepatitis is a worldwide disease. The incidence of chronic viral hepatitis B (CHB) in China is the highest in the world. Although many drugs have been used in the treatment of CHB and chronic viral hepatitis C (CHC) patients, no satisfactory drug is available. The long-term therapeutic efficacy of interferon-2 α and lamivudine on CHB patients is still limited^[1,2]. Therefore, it is necessary to develop effective and safe new drugs for the treatment of chronic viral hepatitis.

In order to develop effective and safe drugs against viral hepatitis, Professor Chun-Zhen Zhang in our institute has synthesized a series of derivatives of 4, 4'-dimethoxy-5, 6, 5', 6'-dimethylene-dioxy-2, 2'-dicarboxylate biphenyl (DDB), a widely used hepatoprotectant in China and foreign countries^[3-5]. 4, 4'-dimethoxy-5, 6, 5', 6'-dimethylene-dioxy-2-hydroxymethyl-2'-carbonyl biphenyl (bicyclol) has anti-liver injury, anti-liver fibrosis and anti-hepatitis B virus effects in animal models^[6-8]. In order to carry out the clinical trial of bicyclol in viral hepatitis patients, the toxicity of bicyclol was studied in animals. The results are described in this paper with its chemical structure shown in Figure 1.

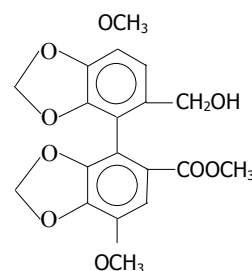


Figure 1 Chemical structure of bicyclol.

MATERIALS AND METHODS

Animals

Both sexes of Kunming strain mice weighing 18-22 g and Wistar rats weighing 50-70 g or 150-250 g were obtained from the Animal Center of Chinese Academy of Medical Sciences. The animals were fed laboratory chow and water *ad libitum* and maintained in an air-conditioned environment (23±1 °C, 50±5% humidity) in a 12 h light/dark cycle. Both sexes of beagle dogs weighing 8-12 kg (10 males, 11 females) were obtained from the Animal Center of Chinese Academy of Military Medical Sciences. All animals received care in compliance with the guidelines of Beijing Animal Control Center.

Drug

Bicyclol, a non-water soluble white powder with 99% purity, was kindly provided by Professor Chun-Zhen Zhang. Bicyclol was suspended in 0.2% sodium carboxyl methylcellulose (Na-CMC) for oral administration.

Acute toxicity test in mice and rats

Twenty mice were randomly divided into two groups, 10 (5 males and 5 females) each group. One group of mice received 3 g/(10 mL·kg) body weight of bicyclol by gavage, and the other group was given 5 g/kg of bicyclol. Ten rats weighing 150-200 g (5 males, 5 females) were orally administered 5 g/kg of bicyclol. Animal behavior and death were recorded within 7 d.

Subcutaneous injection toxicity test in mice

Ten mice (5 males, 5 females) were subcutaneously injected 2 g/kg of bicyclol. Animal behavior and death were observed within 7 d.

Subacute toxicity test in rats

Sixty-four rats were randomly divided into 4 groups, 16 each group. Bicyclol (150, 300, 600 mg/(10 mL·kg)) was administered by gavage to rats once a day for 14 d. Control group was given a corresponding volume of 0.2% Na-CMC vehicle. The intake of water and food, and body weight of each group rats were recorded every 2 d. All rats were sacrificed by decapitation 14 d after treatment with bicyclol. Animal general behavior and their serum ALP, GOT, BUN, LDH, TRIG, GLU, GPT, CHOL, TP, ALB, BIL, HB, WRC and RBC were determined. Pathological examination of main organs (heart, liver, kidney, lung, spleen, thymus, pituitary, adrenal, uterus, ovary, testis, prostate and seminal vesicle) was performed by microscopy.

Chronic toxicity test in rats

Eighty rats of both sexes weighing 50-70 g were equally divided into four groups (10 males and 10 females each group). Three groups of rats were administered 150, 300, 600 mg/(10 mL·kg) of bicyclol, respectively, once daily for 6 mo except for Sunday. The control group was given the same volume of 0.2% Na-CMC vehicle. On the next day after the last administration of bicyclol, all rats were decapitated. Blood and main organs of each rat were collected for pathological examination.

Chronic toxicity test in beagle dogs

Beagle dogs were placed in individual cages. The room temperature was kept at 16-22°C. Twenty-one beagle dogs were divided into four groups, 5 (2 females, 3 males) in control group, 5 (3 females, 2 males) in 25 mg/kg bicyclol group, 5 (2 females, 3 males) in 75 mg/kg bicyclol group, and 6 (4 females, 2 males) in 225 mg/kg bicyclol group. Bicyclol was mixed with a small piece of beef and given to each dog every day for 6 consecutive months before food was fed. One male dog from control group and 2 dogs (1 male and 1 female) from high dose (225 mg/kg) bicyclol group were sacrificed for biochemical and pathological examinations 3 mo after treatment. The remaining dogs in each group were continuously treated with bicyclol till to the end of 6 mo. Half of the dogs in each group were sacrificed 6 mo after bicyclol treatment, and the remaining dogs of each group were killed 1 mo after withdrawal of bicyclol medication.

General behavior, food intake and defecation of the animals were recorded every day. The dogs were weighed every 2 wk. Blood picture, biochemical parameters and urine were determined twice before bicyclol administration, and every 1.5 mo after bicyclol medication and 1 mo after withdrawal of bicyclol treatment. EKG (I, II, III, AVR, AVL, and ALF) was detected one time before and 1.5, 3, 6 mo after administration of bicyclol. The main organs including heart, liver, lung, kidney, spleen, brain, spinal cord, thymus, thyroid, pituitary, pancreas, stomach, jejunum, colon, mesentery, bladder, adrenal, uterus, ovary and testis were all removed for pathological examination.

Mutagenicity assay

The assay was carried out on TA97 and TA102 bacterial strains according to the classical method of Ames test. Both activating

and non-activating system were used. Briefly, 0.1 mL of TA 97 or TA 102 cultured at 37°C for 12 h was mixed with 0.1 mL of various concentrations of bicyclol (10, 100, 500, 1 000, 5 000 µg/plate) and 0.5 mL of phosphate buffer or S9 mixture. The above mixture was incubated at 37°C for 12 min, then added on the agar plate and incubated for another 48 h. The number of revertants on each plate was counted.

Micronucleus assay in mice

Male mice (3 each group) weighing 22-25 g were used in preliminary test. In brief, 3.0 g/kg bicyclol was orally administered to mice, and then the mice were sacrificed by decapitation at 18, 24, 30, 48 and 72 h after administration of bicyclol. The leg bone marrow of each mouse was removed for sliding smears. The smears were fixed with methanol and stained with 10% Giemsa. The number of micronucleus polychromatic erythrocytes (MNPCE) per 1 000 cells was counted under a light microscope. Male mice (6 each group) weighing 22-25g were used in regular test. Cyclophosphamide (50 mg/kg, i.p) was used as a positive control drug. Different doses of bicyclol (0.75, 1.5, 3.0 g/kg) were orally administered to mice. The mice were sacrificed by decapitation 24 h after drug treatment. The rest procedure was the same as described in preliminary test.

Chromosome aberration test of bicyclol

Chinese hamster lung (CHL) cells (10^6 cells/plate) were pre-incubated for 24 h. The test compounds were added to the plates and incubated for another 24 h. The cells were harvested and stained with 0.5% trepan blue. The survived cells of 100 cells per plate were counted and 50% inhibition rate of cell survival was calculated. The concentration of 50% inhibition rate of bicyclol on cell growth was 200 µg/mL.

The cultured medium contained RPMI 16 40, 10% fetal bovine serum, penicillin and streptomycin. Chinese hamster lung (CHL) cells were preincubated for 24 h. The non-metabolic activation group (-S9) was incubated with test compound for another 24 h. The metabolic activation group was incubated with test compound for 6 h in the absence of fetal bovine serum, then the incubation mixture was replaced by fresh medium and incubated for 48 h. Bicyclol was dissolved in PEG 400 and a same volume of PEG 400 was added onto the control plate. Colchicum (1 µg) was added to all groups and incubated for 3 h. The cells were harvested, centrifuged, fixed, sliced and stained with 10% Giemsa for 10 min. One hundred metaphase cells dispersed freely were examined for chromosome structure aberration and the incidence rate of mitiploids was determined under microscope.

Teratogenicity assay

Both sexes of Wistar rats (20 each group) weighing 200-250 g were used. Every early morning, the sperms were examined by vaginal smear for determination of pregnancy (d 0) after female and male rats were put into an animal cage at 2:1 ratio. Bicyclol (100, 1 000 mg/kg) was orally administered once a day from d 7 for 10 d. Control group was given a same volume of 0.2% Na-CMC.

Pregnant rats were weighed every 3 d. The rats were sacrificed by dislocation on d 20 (1 d before delivery). The living fetuses were taken from uterus and the number of corpora luteum, absorbed fetuses, dead and living fetuses was recorded, respectively. Meanwhile, the sex status and outside appearance of fetus were also observed. The fetuses were fixed with Bouin's solution and 95% ethanol for morphological examination of organs and bones.

Statistical analysis

All data were expressed as mean±SD and analyzed by Student's *t* test or χ^2 test between control and bicyclol-treated groups.

Table 1 Effect of bicyclol on blood picture and biochemical markers in rats (mean±SD)

Group (mg/kg)	Sex	Blood picture				Classification of leukocytes, RET and PT				
		RBC (10 ⁴ /mm ³)	WBC (/mm ³)	Hb (g/dL)	HCT (%)	Leukocytes (%)			RET (%)	Platelet (1×10 ⁹ /L)
						Neutrophil	Lymphocyte	Reticulocyte		
Control	M	713.8±95.8	14 400±3 969	17.3±1.4	37.5±5.2	39.3±7.05	58.6±4.32	4.5±2.06	1.55±0.99	900.75±136.07
Bicyclol 150		753.7±55.0	14 102±3 531	17.1±0.8	38.8±3.6	39.0±8.12	58.6±6.97	2.0±0.89	0.86±0.26	837.60±155.62
300		609.1±109	15 850±5 813	15.4±5.3	31.7±11	29.6±9.22	68.4±9.07	2.0±0.63	1.14±0.91	905.60±106.10
600		593.2±86.8 ^a	11 477±1 919	14.7±1.5 ^a	29.7±3.8	-	-	-	-	-
Control	F	681.9±104	13 230±3 671	16.8±1.99	35.1±5.0	29.4±13.47	67.8±13.9	2.4±2.5	1.04±0.62	763.20±144.50
Bicyclol 150		620.1±104	13 220±2 721	15.7±1.25	31.3±3.7	33.4±10.07	65.4±11.7	1.0±0.9	0.74±0.37	715.60±76.20
300		626.9±70	12 656±1 461	15.3±1.52	34.6±3.9	45.0±8.7	53.4±8.7	1.6±1.6	0.92±0.55	831.6±82.20
600		622.9±80	10 777±4 355	14.7±1.51	34.1±4.4	42.0±15.6	54.4±14.6	3.6±2.9	0.70±0.49	562.4±273.30

^aP<0.05 vs control group.

RESULTS

Acute toxicity test in mice and rats

No death and clinical symptoms of mice and rats treated with 3, 6, and 5 g/kg of bicyclol were observed within 7 d. Two mice and 2 rats from bicyclol treated groups were sacrificed and dissected on d 8. No abnormal changes of organs were observed by gross necropsy. The results suggested that the oral LD₅₀ of bicyclol was at least greater than 5 g/kg.

Subcutaneous injection toxicity test in mice

Subcutaneous injection of 2 g/kg bicyclol to mice did not induce death and abnormal changes in general behavior of mice within 7 d. Two mice were sacrificed and dissected for observation of lung, heart, liver, kidney and spleen by gross necropsy. No abnormal changes of the main organs were observed.

Subacute toxicity test in rats

After 14 d treatment of rats with 150, 300 and 600 mg/kg bicyclol, the general behavior and serum ALP, GOT, BUN, LDH, TRIG, GLU, GPT, CHOL, TP, ALB, BIL, HB, WRC, RBC values were all in normal range. The pathological observations of heart, liver, kidney, lung, spleen, thymus, pituitary, adrenal, uterus, ovary, testis, prostate and seminal vesicle were also normal under microscope (data not shown).

Chronic toxicity test in rats

For observation of chronic toxicity of bicyclol in rats, 4 groups of rats weighing 50–70 g were treated with 150, 300, 600 mg/kg bicyclol once a day for 6 mo. Four months after bicyclol treatment, 10 rats (5 males, 5 females) from bicyclol (600 mg/kg) group and 10 rats from control group were sacrificed by decapitation. The remaining rats in each group were given bicyclol for another 2 mo and then killed by decapitation. The following indexes were observed for toxicity assay: general behaviors including activity, fur color, feces, body weight and food intake; blood picture including RBC, WBC, Hb, HCT, classification of leukocytes (neutrophils, lymphocyte, reticulocyte), platelet, RET count; blood biochemical markers including GPT, GOT, ALP, LAP, total cholesterol triglyceride, D-bilirubin, total bilirubin, total protein, albumin, A/G ratio, glucose, BUN, creatine; urine test including glucose, protein, ketone body, and occult blood; pathological examination including heart, liver, lung, kidney, spleen, thymus, pituitary, adrenal, uterus, ovary, testis, seminal vesicle, prostate 6 mo after bicyclol treatment.

No toxic effect of bicyclol and no pathological changes in main organs were observed, although some variations in certain parameters were demonstrated (Tables 1–3), suggesting that bicyclol had no noticeable toxicity to rats at the test dosages.

Table 2 Effect of bicyclol on organ weight in rats (n = 10, mean±SD)

Organ weight mg/100g BW	Sex	Control	Bicyclol (mg/kg)		
			150	300	600
Heart	M	308±38	300±42	310±74	360±70
Liver		2 960±310	3 120±610	3 200±810	3 300±700
Lung		570±120	620±280	580±160	700±180
Kidney		670±70	660±120	700±180	580±270
Spleen		160±30	170±40	170±43	140±45
Thymus		60±20	60±20	60±17	45±18
Pituitary		3±4	2±1	2±1	2±1
Adrenal		20±10	24±30	14±3	16±4
Prostate		110±30	120±30	109±29	110±40
Seminal		250±80	240±80	250±55	260±66
Testis		1150±160	1 120±180	1 040±301	1 130±296
Heart	F	350±40	360±38	380±40	370±41
Liver		3 200±330	3 300±220	3 300±210	3 300±290
Lung		970±320	890±280	700±80	680±291
Kidney		810±110	820±100	810±140	770±130
Spleen		220±44	210±36	240±34	320±54 ^b
Thymus		102±36	67±23 ^b	53±24 ^b	120±88
Pituitary		5±2	3±1	5±2	12±15
Adrenal		29±4	26±4	29±3	51±8
Uterus		173±50	147±48	163±31	158±57
Ovary		39±19	34±24	37±3	47±25

^bP<0.01 vs control group.

Chronic toxicity test in beagle dogs

The criteria of toxicology study were essentially the same as in chronic toxicity test in rats. Serum GPT, GOT, ALP, glucose, total cholesterol, total protein, total-bilirubin, albumin, creatine and BUN, RBC, WBC, Hb, RET, platelet (PLT) polymorphonuclear leukocyte, lymphocyte, monocyte and prothrombin (capillary method) and urine glucose, protein, ketone body, occult blood, pH were determined. Pathological examination of main organs included morphological change of organs by gross necropsy and light microscopy, weight of main organs and organ index. The results were as follows.

The body weight, stool, water and food intake of dogs treated with bicyclol were normal, except for 2 dogs in high dose (225 mg/kg) bicyclol group having less food intake in the first few days. No abnormal changes in heart rate and waveform from 6 leads were observed after bicyclol treatment. Most parameters of blood picture assay were in normal range. Although variations in certain parameters (Hb, lymphocytes, PLT, etc.) were demonstrated, there was no significant difference between control and bicyclol groups. Some changes in blood biochemical parameters such as total protein (TP) and albumin (ALB) increased, while T-BIL decreased in bicyclol-treated groups. However, there was no significant difference between control and bicyclol groups before and after bicyclol treatment (Tables 4–6).

Table 3 Effect of bicyclol on blood biochemical markers in rats ($n = 10$, mean \pm SD)

Parameter	Control	Bicyclol (mg/kg)		
		150	300	600
Male rats				
TP 10 g/L	6.68 \pm 0.31	6.30 \pm 0.63	7.30 \pm 0.61	6.47 \pm 0.41
ALB 10 g/L	3.82 \pm 0.22	3.55 \pm 0.29	3.79 \pm 0.42	3.68 \pm 0.21
GLB 10 g/L	2.86 \pm 0.22	2.75 \pm 0.43	3.51 \pm 0.38	2.80 \pm 0.32
A/G	1.34 \pm 0.13	1.31 \pm 0.17	1.09 \pm 0.15	1.33 \pm 0.17
SGOT IU/L	391 \pm 74	411 \pm 57	406 \pm 50	431 \pm 76
SGPT IU/L	63 \pm 10	50 \pm 8	46 \pm 8	62 \pm 10
ALP IU/L	293 \pm 42	255 \pm 53	303 \pm 67	285 \pm 68
LAP IU/L	63 \pm 5	62 \pm 7	69 \pm 8	65 \pm 5
T-CHO 10 mg/L	73.6 \pm 6.68	65.7 \pm 8.26	72.1 \pm 9.51	69.3 \pm 5.87
TG 10 mg/L	107.4 \pm 33.7	109.9 \pm 30.6	97.1 \pm 15.1	106.7 \pm 25.8
GLU 10 mg/L	4.2 \pm 5.33	2.2 \pm 1.87	8.5 \pm 12.7	8.2 \pm 8.8
D-BIL 10 mg/L	0.14 \pm 0.03	0.16 \pm 0.07	0.18 \pm 0.08	0.18 \pm 0.06
T-BIL 10 mg/L	1.33 \pm 0.22	1.32 \pm 0.71	1.58 \pm 0.67	1.68 \pm 0.53
BUN 10 mg/L	20.7 \pm 4.8	18.3 \pm 4.7	18.4 \pm 2.7	17.0 \pm 5.8
Creat 10 mg/L	1.14 \pm 0.19	1.13 \pm 0.16	1.13 \pm 0.23	0.97 \pm 2.2
Female rats				
TP 10 g/L	6.53 \pm 0.78	6.58 \pm 0.75	6.93 \pm 0.64	6.73 \pm 0.44
ALB 10 g/L	3.55 \pm 0.57	3.58 \pm 0.46	3.97 \pm 0.36	4.06 \pm 0.36
GLB 10 g/L	2.99 \pm 0.53	2.99 \pm 0.45	2.96 \pm 0.45	2.68 \pm 0.40
A/G	1.22 \pm 0.26	1.22 \pm 0.19	1.37 \pm 0.21	1.55 \pm 0.30
sGOT IU/L	439 \pm 95	403 \pm 70	520 \pm 119	433 \pm 100
sGPT IU/L	59 \pm 31	38 \pm 11	49 \pm 16	46 \pm 10
ALP IU/L	227 \pm 170	203 \pm 156	189 \pm 46	151 \pm 26
LAP IU/L	59 \pm 18	59 \pm 5	69 \pm 7	69 \pm 6
T-CHO 10 mg/L	66.4 \pm 14.5	63.2 \pm 10.5	63.5 \pm 4.20	60.4 \pm 9.2
TG 10 mg/L	108.6 \pm 49.5	117.5 \pm 58.7	121.9 \pm 23.1	120.8 \pm 4.3
GLU 10 mg/L	7.4 \pm 4.8	6.1 \pm 5.5	8.2 \pm 4.0	16.3 \pm 12.0
D-BIL 10 mg/L	0.36 \pm 0.45	0.27 \pm 0.09	0.19 \pm 0.05	0.16 \pm 0.08
T-BIL 10 mg/L	2.84 \pm 3.03	2.35 \pm 0.65	1.79 \pm 0.54	1.57 \pm 0.77
BUN 10 mg/L	23.0 \pm 7.2	32.7 \pm 16.7	24.6 \pm 9.6	23.5 \pm 4.5
Creat 10 mg/L	0.90 \pm 0.14	1.06 \pm 0.25	0.98 \pm 0.18	0.81 \pm 0.28

Table 4 Blood test of female and male beagle dogs in control group before and after bicyclol treatment (mean \pm SD)

Parameter	Before treatment	After treatment (mo)				
		1.5	3	4.5	6	7 ($n = 1$)
Female ($n = 2$)						
RBC $\times 10^{12}$ /L	9.2 \pm 0.5	9.2 \pm 0.5	7.3 \pm 2.2	8.2 \pm 0.9	9.8 \pm 2.0	8.4
Hb g/L	140 \pm 14	140 \pm 7	145 \pm 7	143 \pm 11	148 \pm 11	140
RET (%)	0.9 \pm 0.3	0.8 \pm 0.3	0.9 \pm 0.3	0.7 \pm 0.3	0.8 \pm 0.1	0.6
PLT $\times 10^9$ /L	200 \pm 14	205 \pm 21	215 \pm 35	370 \pm 14 ^a	265 \pm 78	240
WBC $\times 10^9$ /L	14.6 \pm 2.2	13.7 \pm 2.0	15.2 \pm 3.7	13.6 \pm 2.6	16.2 \pm 7.2	14.5
Lymphocyte (%)	55 \pm 11	55 \pm 12	62 \pm 14	61 \pm 12	69 \pm 8	74
Polymorphonuclear leukocyte (%)	41 \pm 7	41 \pm 13	36 \pm 13	34 \pm 9	28 \pm 4	21
Monocyte (%)	5.5 \pm 2.1	5.0 \pm 1.4	2.5 \pm 0.7	4.0 \pm 1.4	3.5 \pm 0.7	5
Male ($n = 3$)						
RBC $\times 10^{12}$ /L	8.7 \pm 1.7	7.3 \pm 0.6	8.7 \pm 2.1	8.5 \pm 1.6	7.9 \pm 1.1	8.6
Hb g/L	135 \pm 10	140 \pm 5	135 \pm 9	145 \pm 7	150 \pm 7	140
RET (%)	0.9 \pm 0.4	0.6 \pm 0.1	0.6 \pm 0.2	0.9 \pm 0.4	0.8 \pm 0.4	0.8
PLT $\times 10^9$ /L	223 \pm 38	250 \pm 26	197 \pm 32	260 \pm 85	290 \pm 28	312
WBC $\times 10^9$ /L	12.1 \pm 3.1	12.7 \pm 0.8	10.6 \pm 2.3	11.9 \pm 2.1	12.2 \pm 1.6	20.1
Lymphocyte (%)	52 \pm 12	57 \pm 11	48 \pm 11	69 \pm 4	67 \pm 8	66
Polymorphonuclear leukocyte (%)	45 \pm 11	39 \pm 13	47 \pm 10	28 \pm 4	26 \pm 1	26
Monocyte (%)	3.7 \pm 0.6	3.3 \pm 1.5	2.7 \pm 0.6	3.5 \pm 0.7	7.0 \pm 1.4 ^a	8

^a $P < 0.05$ vs before dosing.

There were no abnormal changes in urine and prothrombin test 6 mo after bicyclol treatment. No abnormal changes of the main organs were observed by gross necropsy and light microscopy.

In a word, oral administration of bicyclol (25, 75, 225 mg/(kg·d)) for 6 mo, 16.6-150 folds corresponding to the proposed therapeutic dose of bicyclol for clinical use) to both sexes of beagle dogs had no detectable toxicity.

Mutagenicity test of bicyclol

The results of Ames test of bicyclol (reverse mutation test) in bacteria indicated that the positive mutagens induced a significant increase of revertants, whereas bicyclol showed no detectable mutagenicity in bacterial strains (Table 7).

Micronucleus test of bicyclol in mice

The results of preliminary test showed that there was no

Table 5 Blood test of female and male beagle dogs before and after treatment with 225 mg/kg bicyclol (mean±SD)

Parameter	Before treatment	After treatment (mo)				
		1.5	3	4.5	6	7 (n = 1)
Female (n = 4)						
RBC ×10 ¹² /L	8.9±2.1	9.0±2.5	8.1±1.6	10.0±0.8	9.0±2.3	8.8
Hb g/L	141±9	151±9	141±6	153±12	165±13 ^a	155
RET (%)	1.0±0.2	0.6±0.1	0.8±0.2	0.7±0.1	0.8±0.2	0.8
PLT ×10 ⁹ /L	195±55	230±37	217±29	237±15	313±25 ^a	368
WBC ×10 ⁹ /L	10.6±2.2	10.2±0.7	12.2±3.2	10.5±2.4	12.2±3.0	10.9
Lymphocyte (%)	51±6	52±8	60±11	59±11	59±10	63
Polymorphonuclear						
Leukocyte (%)	44±6	43±8	37±6	39±9	36±8	31
Monocyt (%)	3.8±1.3	4.5±0.6	3.0±1.2	2.0±2.0	5.3±3.1	6
Male (n = 2)						
RBC ×10 ¹² /L	8.9±0.3	10.4±0.0 ^a	9.9±1.6	7.4	7.9	7.5
Hb g/L	140±14	142±9	140±7	155	160	145
RET (%)	1.1±0.1	0.9±0.2	1.0±0.4	0.9	0.8	0.6
PLT ×10 ⁹ /L	215±7	290±0 ^a	138±23 ^a	210	260	248
WBC ×10 ⁹ /L	9.3±0.6	9.5±0.7	11.2±1.9	6.9	12.8	14.4
Lymphocyte (%)	55±4	51±11	52±6	48	55	67
Polymorphonuclear						
Leukocyte (%)	41±3	46±11	46±6	48	40	26
Monocyt (%)	3.5±0.7	3.0±0.0	4.0±1.4	4	5	7

^aP<0.05 vs before dosing.**Table 6** Blood biochemical parameters of female and male beagle dogs 6 mo after bicyclol treatment (mean±SD)

Parameter	Control	Bicyclol (mg/kg)		
		25	75	225
Female				
Glu mmol/L	4.94±0.83	6.06±0.38	5.60±0.08	6.36±0.62
T-CHO mmol/L	2.56±1.08	2.82±0.60	2.97±1.02	3.43±1.39
TP g/L	71.3±0.2	74.3±4.2 ^a	73.5±3.3	76.1±6.2
ALB g/L	37.0±0.9	39.9±1.7	41.0±3.7	44.0±4.1
Crea μmol/L	119±28	138±10	145±42	143±27
BUN mmol/L	4.25±0.05	3.51±0.24	4.22±0.29	3.60±0.78
T-BIL μmol/L	2.80±1.70	4.00±2.26	3.60±0.57	1.20±0.40
SGPT 10 U/L	26.2±1.3	28.3±15.0	12.8±8.9	25.2±8.1
SGOT 10 U/L	61.8±14.9	41.3±14.6	45.1±8.0	45.8±23.8
ALP 10 U/L	2.65±1.51	1.95±0.39	2.55±0.38	3.14±1.12
Male				
Glu mmol/L	5.79±0.29	5.19±0.44	5.58±0.88	4.65
T-CHO mmol/L	2.37±0.35	2.82±0.60	2.39±0.06	2.65
TP g/L	74.2±5.2	71.6±9.8	79.1±12.2	70.6
ALB g/L	34.9±1.6	38.7±1.5	42.4±7.5	33.4
Crea μmol/L	136±10	136±9.8	165±39	105
BUN mmol/L	3.43±0.63	3.94±0.58	2.95±0.34	3.20
T-BIL μmol/L	4.40±0.57	4.00±0.00	3.20±0.80	2.80
SGPT 10 U/L	34.6±9.9	23.1±6.9	25.7±9.9	36.0
SGOT 10 U/L	57.9±11.6	37.9±5.8	54.5±7.3	53.3
ALP 10 U/L	2.51±0.46	5.41±4.59	2.23±1.16	1.94

^aP<0.05 vs control group.

significant alteration in the number of micronucleated polychromatic erythrocytes (MNPCE) per 1 000 cells in mice after treatment with 3 g/kg bicyclol. Then, the regular test was performed in mice treated with different doses of bicyclol (0.75, 1.5, 3.0 g/kg, P.O.) or cyclophosphamide (50 mg/kg, i.p). The results showed that bicyclol exhibited no mutagenicity in micronucleus test (Table 8) while cyclophosphamide induced remarkable mutagenicity of MNPCE.

Chromosome aberration test of bicyclol

The results indicated that there was no significant difference in chromosome aberrations between control and bicyclol-treated cells (χ^2 test). The positive control compounds, carboplatin and cyclophosphamide, induced significant chromosome aberrations in CHL (Table 9).

Teratogenicity test of bicyclol

No abortion, premature labor and other toxic effects of bicyclol

were found in pregnant rats except for a pregnant rat in high dose group died of pneumonia on d 10 (Table 10).

There were no significant differences in body height and weight, ratio of sex, outward appearance, living and dead fetus between control and bicyclol treatment groups, suggesting that bicyclol had no toxic effect on embryonic development and fetus (Tables 11, 12).

Bicyclol had no effect on the development of occipital, cervical, sacral bones and coccyx. Defect of sternum was observed in all groups.

No abnormal changes in development of bones were observed in all groups, except for multi-rib in high dose bicyclol group rats (Tables 13, 14). Bicyclol had no effect on development of main organs of fetus.

In a word, the results indicated that when bicyclol (200, 1000 mg/kg) was given orally once daily from the 7th d for 10 d, no significant effects on pregnant rats, development of embryo, skeleton and organs of fetuses were observed.

Table 7 Mutagenicity of bicyclol in bacteria (revertants/plate) (mean±SD)

(µg/plate)	TA97		TA102	
	-S9	+S9	-S9	+S9
Bicyclol 0	86±15	130±15	227±15	272±12
10	68±8	111±1	237±13	230±10
100	80±1	116±20	259±33	304±40
500	57±14	120±6	236±16	279±5
1 000	88±8	140±4	237±35	344±18
5 000	80±4	88±1	259±23	153±2
9-aminoacridine 0.2	938±10			
2AF 10		1 736±509		
DMC 20				
MMS 2 µL			1 606±48	
Vp16 1 mg				1 270±37

Table 8 Mutagenicity in mice after bicyclol treatment

Group	Dosage (mg/kg)	n	MNPCE (‰)	P/N value	P
Control		6	2.2±0.04	100/56	1.8
Bicyclol	750	6	1.8±0.09	135/65	2.1
	1 500	6	2.5±0.14	126/74	1.7
	3 000	6	1.7±0.08	130/70	1.9
Cyclophosphamide	50	6	38.2±3.0	100/250	0.4

Table 9 Chromosome aberrations in mice after bicyclol treatment

Dosage (µg/kg)	-S9		+S9	
	Aberration (%)	P	Aberration (%)	P
Control (DMSO) 100	100	2	100	3
Bicyclol 50	100	2	100	2
	100	3	100	3
	200	2	100	3
Carboplatin 100	50	84		
CY 100			50	66

Table 10 Effect of bicyclol on pregnant rats (mean±SD)

Group	n	Number of pregnancies	Death	Body weight (g)		
				D 0	D 9	D 18
Control	20	15	0	251.9±6.8	271.0±6.8	337.7±8.2
Bicyclol 200 mg/kg	20	15	1	253.5±5.4	295.4±5.5	373.3±6.7
Bicyclol 1 000 mg/kg	20	17	0	258.2±5.7	277.4±5.64	352.9±7.5

Table 11 Effect of bicyclol on embryonic development

Dosage (mg/kg)	n	Corpus luteum	Living fetus(%)	Dead fetus (%)	Resorption (%)
Control	15	177	171 (96.6)	0	6 (3.4)
Bicyclol 200	15	181	155 (93.3)	6 (3.6)	5 (3.0)
Bicyclol 1 000	17	225	203 (97.1)	1 (0.5)	5 (2.4)

Even though defect of sternum was observed in high dose bicyclol group, no significant difference in the development of skeleton between control and bicyclol groups was found by χ^2 test. The multi-rib in individual fetuses was considered to be normal variation.

DISCUSSION

The acute, chronic and special toxicity of any new drug should be studied before recommended for clinical trial. Acute toxicity is mainly to determine the lethal dose (LD_{50}) of a drug to induce 50% death of experimental animals. Results of the present study indicated that 5 g/kg bicyclol given orally to mice and rats did not induce clinical intoxication and death, suggesting that the LD_{50} of bicyclol is at least greater than 5 g/kg body weight. In general, if the LD_{50} of a single drug is over 5 g/kg, it may be regarded as a low toxicity drug. Bicyclol belongs to this kind of

drugs. Chronic toxicity test should be performed in 2 species of animals and 3 doses should be tested. One of the doses should be the effective dosage in pharmacology, and the biggest dose should be large enough to produce toxicity in animals. In the study of chronic toxicity, 3 doses of bicyclol (150, 300 and 600 mg/kg) were used. Among the 3 doses of bicyclol tested, 150 mg/kg was the pharmacologically effective dose, and 600 mg/kg was 400 folds higher than the proposed therapeutic dose of bicyclol (1.5 mg/(kg·d)) for patients. As a result, the 3 doses of bicyclol given for 6 mo have no detectable toxic effects on rats. All parameters obtained from blood picture, urine, blood biochemistry and pathological examinations of main organs were in normal range. In chronic toxicity test of beagle dogs for 6 mo, 25, 75 and 225 mg/kg of bicyclol were used. The highest dose of 225 mg/kg was 150 folds corresponding to the proposed therapeutic dose of bicyclol for patients. Like the results of chronic toxicity in rats, bicyclol

Table 12 Effect of bicyclol on fetus (mean±SD)

Dosage (mg/kg)	Brood number (X)	BW (g)	Height (cm)	Tail length (cm)	Sex ratio (F/M)
Control	39.9±4.1	3.5±0.01	3.4±0.02	1.28±0.02	89/82
Bicyclol 200	43.3±3.1	4.3±0.08	3.4±0.02	1.26±0.01	81/74
Bicyclol 1 000	47.7±2.2	4.0±0.09	3.3±0.02	1.17±0.01	97/106

Table 13 Effect of bicyclol on ossification of fetus, *n* (%)

Dosage (mg/kg)	<i>n</i>	Ossification of sternum		
		Defect of the 5th and 6th sternums	Defect of the 6th sternum	Number of sternum defects
Control	87	0	8 (9.2)	79 (91.0)
Bicyclol 200	77	1 (1.3)	6 (7.8)	70 (90.9)
Bicyclol 1 000	108	9 (8.3)	1 (0.9)	94 (87.0)

Table 14 Effect of skeleton development of fetus

Dosage (mg/kg)	<i>n</i>	Cervical -rib	Defect of the 13th rib	Defect of the 14th rib
Control	87	0	0	0
Bicyclol 200	77	0	0	0
Bicyclol 1 000	108	0	0	4 (3.7%)

also had no noticeable toxic effects on all biochemical indices and pathological examinations of the main organs, although there were variations of certain parameters before and after bicyclol treatment, there were no statistically significant difference between control and bicyclol groups, suggesting that bicyclol is a low toxicity drug.

The purposes of specific toxicity tests including mutagenicity, teratogenicity and carcinogenesis are to study whether the tested drug would induce fetal deformation and mutation or carcinogenesis. Mutagenicity test includes the classical Ames test, chromosome aberrations in Chinese hamster lung (CHL) cells and micronucleus assay. In Ames test, the biggest dose of any test drug should reach 5 000 µg/plate. For chromosome aberration assay, the concentration of 50% inhibition rate of test compound on growth of CHL cells should be tested. In both Ames and chromosome aberration assays, positive mutagenic compounds should also be used as control in presence and absence of liver microsomes (S9 mixtures). In micronucleus assay, 1/2 LD₅₀ of test drug should be used. The data of our current study show that bicyclol at doses of 5 000 µg/plate in Ames test, 200 µg/mL (IC₅₀) in chromosome aberration assay and 3 g/kg in mice all have no mutagenic effect, while the positive control compounds all induce mutation. In other word, bicyclol has no mutagenicity.

The purpose of teratogenicity assay is to evaluate whether the test drug induces fetal deformation of pregnant patients who take the tried drug. As shown in the present study, bicyclol at a rather high dose of 1 g/kg, which was 667 folds of the proposed therapeutic dose (1.5 mg/(kg·d)) for patients, did not induce fetal deformation. All the above results indicate that bicyclol is a low toxicity drug. This conclusion is supported by the results of clinical trial of bicyclol on chronic viral hepatitis. More than 2 000 chronic hepatitis B patients were treated with bicyclol for 6 mo. As a result, bicyclol significantly normalized the elevated serum transaminases (ALT and AST) by about 50%, and also turned positive virus markers such as HBeAg to negative by about 20%. Side effects such as headache and skin eruption occurred in only about 1% of these patients^[9,10]. No other noticeable side effects were observed. It was reported that adverse effects (influenza-like syndrome) occur frequently during treatment with interferons^[11], and that lamivudine can

induce mitochondrial toxicity^[12]. The side effect and toxicity of bicyclol are lower than those of interferon-2α and lamivudine.

REFERENCES

- 1 **Lok AS.** Hepatitis B infection: pathogenesis and management. *J Hepatol* 2000; **32**: 89-97
- 2 **Liaw YF, Chien RN, Yeh CT, Tsai SL, Chu CM.** Acute exacerbation and hepatitis B virus clearance after emergence of YMDD motif mutation during lamivudine therapy. *Hepatology* 1999; **30**: 567-572
- 3 **Liu GT.** Therapeutic effects of biphenyl dimethyl dicarboxylate (DDB) on chronic viral hepatitis B. *Proc Chin Acad Med Sci Peking Union Med Coll* 1987; **2**: 228-233
- 4 **Liu GT.** From *Fructus Schizandrae* to biphenyl dimethyl dicarboxylate (DDB), a new hepatoprotector for hepatitis. In: Zhou JH, Liu GZ, eds. *Recent Advances in Chinese Herbal Drugs-Actions and Uses*. Beijing: Science Press, Beijing China & S.A.T.A.S. Belgium 1991: 112-125
- 5 **Fu TB, Liu GT.** Protective effects of dimethyle-4,4'-dimethoxy-5,6,5',6'-dimethylene dioxybiphenyl-2,2'-dicarboxylate on damages of isolated rat hepatocytes induced by carbon tetrachloride and D-galactosamine. *Biome Environ Sci* 1992; 5185-5194
- 6 **Liu GT.** The anti-virus and hepatoprotective effect of bicyclol and its mechanism of action. *Zhongguo Xinyao Zazhi* 2001; **10**: 325-327
- 7 **Li Y, Dai GW, Li Y, Liu GT.** Effect of bicyclol on acetaminophen-induced hepatotoxicity: energetic metabolism and mitochondrial injury in acetaminophen-intoxicated mice. *Yaoxue Xuebao* 2001; **36**: 723-726
- 8 **Gu XJ.** The efficacy of bicyclol in treatment of chronic hepatitis B. *Zhongguo Xinyao Zazhi* 2004; **13**: 940-942
- 9 **Yao GB, Ji YY, Wang QH, Zhou XQ, Xu DZ, Chen XY.** A randomized double-blind controlled trial of bicyclol in treatment of chronic viral hepatitis. *Zhongguo Xinyao Linchuang Zazhi* 2002; **21**: 457-461
- 10 **Yin H.** Results of phase IV clinical trial of bicyclol on chronic viral hepatitis. *China Prescription Drug* 2004; **9**: 25-27
- 11 **Haria M, Benfield P.** Interferon-alpha-2a. A review of its pharmacological properties and therapeutic use in the management of viral hepatitis. *Drugs* 1995; **50**: 873-896
- 12 **Kakuda TN.** Pharmacology of nucleoside and nucleotide reverse transcriptase inhibitor-induced mitochondrial toxicity. *Clin Ther* 2000; **22**: 685-708

Effects of unsaturated fatty acids on calcium-activated potassium current in gastric myocytes of guinea pigs

Hai-Feng Zheng, Xiang-Lan Li, Zheng-Yuan Jin, Jia-Bin Sun, Zai-Liu Li, Wen-Xie Xu

Hai-Feng Zheng, Xiang-Lan Li, Zheng-Yuan Jin, Jia-Bin Sun, Zai-Liu Li, Department of Physiology, Yanbian University College of Medicine, Yanji 133000, Jilin Province, China

Wen-Xie Xu, Department of Physiology, Shanghai Jiaotong University School of Medicine, Shanghai 200030, China

Supported by the National Natural Science Foundation of China, No. 30160028

Correspondence to: Professor Wen-Xie Xu, Shanghai Jiaotong University School of Medicine, Shanghai 200030, China. wenxiexu@sjtu.edu.cn

Telephone: +86-21-62932910 **Fax:** +86-21-62832528

Received: 2004-01-10 **Accepted:** 2004-03-18

Abstract

AIM: To investigate the effects of exogenous unsaturated fatty acids on calcium-activated potassium current [$I_{K(Ca)}$] in gastric antral circular myocytes of guinea pigs.

METHODS: Gastric myocytes were isolated by collagenase from the antral circular layer of guinea pig stomach. The whole-cell patch clamp technique was used to record $I_{K(Ca)}$ in the isolated single smooth muscle cells with or without different concentrations of arachidonic acid (AA), linoleic acid (LA), and oleic acid (OA).

RESULTS: AA at concentrations of 2,5 and 10 $\mu\text{mol/L}$ markedly increased $I_{K(Ca)}$ in a dose-dependent manner. LA at concentrations of 5, 10 and 20 $\mu\text{mol/L}$ also enhanced $I_{K(Ca)}$ in a dose-dependent manner. The increasing potency of AA, LA, and oleic acid (OA) on $I_{K(Ca)}$ at the same concentration (10 $\mu\text{mol/L}$) was in the order of AA>LA>OA. AA (10 $\mu\text{mol/L}$)-induced increase of $I_{K(Ca)}$ was not blocked by H-7 (10 $\mu\text{mol/L}$), an inhibitor of protein kinase C (PKC), or indomethacin (10 $\mu\text{mol/L}$), an inhibitor of the cyclooxygenase pathway, and 17-octadecynoic acid (10 $\mu\text{mol/L}$), an inhibitor of the cytochrome P450 pathway, but weakened by nordihydroguaiaretic acid (10 $\mu\text{mol/L}$), an inhibitor of the lipoxygenase pathway.

CONCLUSION: Unsaturated fatty acids markedly increase $I_{K(Ca)}$, and the enhancing potencies are related to the number of double bonds in the fatty acid chain. The lipoxygenase pathway of unsaturated fatty acid metabolism is involved in the unsaturated fatty acid-induced increase of $I_{K(Ca)}$ in gastric antral circular myocytes of guinea pigs.

© 2005 The WJG Press and Elsevier Inc. All rights reserved.

Key words: Gastric myocytes; Calcium-activated potassium channel; Unsaturated fatty acids

Zheng HF, Li XL, Jin ZY, Sun JB, Li ZL, Xu WX. Effects of unsaturated fatty acids on calcium-activated potassium current in gastric myocytes of guinea pigs. *World J Gastroenterol* 2005; 11(5): 672-675

<http://www.wjgnet.com/1007-9327/11/672.asp>

INTRODUCTION

Unsaturated fatty acids are the major components of membrane lipids and they are mainly released by stimulation of phospholipase A₂. Arachidonic acid (AA) and other unsaturated fatty acids modulate the activities of various ion channels^[1-3] through direct or indirect pathways. The direct effects are mediated by the interaction between fatty acids and ion channel proteins or through the interference with plasma membranes. The indirect actions on ion channels result from cyclo-oxygenase, lipoxygenase, and epoxygenase metabolites or cellular signal transduction pathways^[4]. For example, AA directly affects the activities of cloned human potassium channels mainly existing in heart and brain^[5] and Ca²⁺-activated K⁺ channels in rabbit coronary smooth muscle cells^[6]. In addition, AA has been shown to modulate ion transient receptor potential channels as a second messenger^[7] and to enhance voltage-dependent calcium channels in vascular smooth muscle cells through cytochrome P450 metabolites^[8].

The Ca²⁺-activated potassium channel [$I_{K(Ca)}$] has been considered to play an important role in excitability and functional regulation in excitable cells^[9]. Agonists of $I_{K(Ca)}$, such as carbon monoxide and bradykinin, which change the activity of the Ca²⁺-activated potassium channels, can affect the membrane potential and contractility in smooth muscle cells^[10,11]. We have shown that NO relaxes gastric antral smooth muscle of the guinea pig through increase of $I_{K(Ca)}$ ^[12]. It has been reported that AA affects $I_{K(Ca)}$ in many cells. It inhibits $I_{K(Ca)}$ in T84 cells^[13], activates $I_{K(Ca)}$ in vascular smooth muscles^[14] and GH(3) cells^[15]. In our previous study, we have reported that AA and other unsaturated fatty acids directly inhibit calcium current (I_{Ca})^[16], chloride current (I_{Cl})^[17] and muscarinic current (I_{CCh})^[18] in gastric myocytes of guinea pigs. But the effects of AA and other unsaturated fatty acids on $I_{K(Ca)}$ in gastric myocytes have not yet been reported. In the present study, we investigated the effect of AA and other unsaturated fatty acids on $I_{K(Ca)}$ in gastric antral circular myocytes of guinea pigs.

MATERIALS AND METHODS

Preparation of cells

Gastric myocytes were isolated enzymatically from the antral circular layer of guinea pig stomachs as described previously^[15]. Briefly, EWG/B guinea pigs (obtained from the Experimental Animal Department of Jilin University Clinical College, Certificate No 10-6004) of either sex weighing 300-350 g were euthanized by a lethal dose of IV sodium pentobarbital (50 mg/kg). The antral part of the stomach was dissected from the longitudinal layer using fine scissors and then cut into small segments (2-3 mm). The tissue chunks were then incubated at 36 °C for 25-30 min in a digestion medium consisting of 4 mL Ca²⁺-free physiology solution containing 8 mg bovine serum albumin, 4.5 mg trypsin inhibitor, 4 mg collagenase type II, and 4 mg dithioerythritol. Single myocytes were kept at 4 °C until use.

Electrophysiological recordings

The isolated cells were transferred to a small chamber (0.1 mL) on the stage of an inverted microscope (IX-70 Olympus, Japan)

for 10–15 min to settle down. The cells were superfused continuously with isosmotic solution. An 8-channel perfusion system (L/M-sps-8, List Electronics, Germany) was used to change the solution. Experiments were performed at 20–25 °C and the whole-cell configuration of the patch-clamp technique was applied. Patch-clamp pipettes were manufactured from borosilicate glass capillaries (GC150T-7.5, Clark Electromedical Instruments, UK) by a two-stage puller (PP-83, Narishige, Japan). The resistance of the patch pipettes was 3–5 M Ω when being filled with pipette solution. Liquid junction potentials were compensated prior to seal formation. The whole-cell holding currents were recorded with an Axopatch 1-D patch-clamp amplifier (Axon Instrument, USA) and an EPC-10 amplifier (HEKA Instrument, Germany).

Drugs and solutions

All drugs were purchased from Sigma Chemical Co, USA. Tyrode's solution contained NaCl 147, KCl 4, CaCl₂·2H₂O 2, MgCl₂·6H₂O 1.05, NaH₂PO₄·2H₂O 0.42, Na₂HPO₄·2H₂O 1.81 and glucose 5.5 mmol/L, pH was adjusted to 7.35 with NaOH. PSS contained NaCl 134.8, KCl 4.5, MgCl₂·6H₂O 1.0, CaCl₂·2H₂O 2.0, glucose 5.0 and HEPES 10.0 mmol/L, and pH was adjusted to 7.4 by using Tris. In Ca²⁺-free PSS, 2.0 mmol/L CaCl₂·2H₂O was omitted from PSS. The pH of modified Kraft-Bruhe solution containing 0.5 mmol/L egtazic acid, 10 mmol/L HEPES, MgCl₂·6H₂O 3 mmol/L, 50 mmol/L KCl, 10 mmol/L glucose, 50 mmol/L L-glutamata, 20 mmol/L taurine and 20 mmol/L KH₂PO₄, was adjusted to 7.40 with KOH 1 mmol/L. The pipette solution contained 110 mmol/L potassium-aspartic acid, 5 mmol/L Mg-ATP, 5 mmol/L HEPES, 1.0 mmol/L MgCl₂·6H₂O, 20 mmol/L KCl, 0.1 mmol/L egtazic acid, 2.5 mmol/L di-*tris*-creatine phosphate and 2.5 mmol/L disodium-creatine phosphate, pH was adjusted to 7.30 with Tris. AA, LA and OA were separately prepared at 1 mmol/L. All unsaturated fatty acids were added in external perfusing solution. Indomethacin, 17-octadecynoic acid, nordihydroguaiaretic acid and H-7 were prepared at 1 mmol/L.

Statistical analysis

This experiment was consubstantially compared. The current before perfusion with fatty acids served as controls. All values were expressed as mean \pm SD. Statistical significance was evaluated by *t*-test.

RESULTS

Effects of unsaturated fatty acids on $I_{K(Ca)}$

Under the whole-cell configuration, the membrane potential was clamped at -60 mV, and $I_{K(Ca)}$ was elicited by step voltage command pulse from -40 mV to 100 mV for 440 ms with a 20 mV increment at 10 s intervals. AA, an unsaturated fatty acid (with 4 double bonds) significantly increased $I_{K(Ca)}$ in a dose-dependent manner. AA increased $I_{K(Ca)}$ by (15.9 \pm 3.6)%, (31.9 \pm 7.0)% and (46.3 \pm 10.4)% at the concentrations of 2, 5 and 10 μ mol/L at +60 mV, respectively ($n = 8$, Figure 1 C). Under the whole-cell patch-clamp mode the membrane potential was clamped at -20 mV, the spontaneous transient outward currents (STOCs) due to activation of calcium-activated potassium^[19] were then recorded. AA markedly increased STOCs at 10 μ mol/L (Figure 1 D). Another unsaturated fatty acid LA (with 2 double bonds) also increased $I_{K(Ca)}$ by (27.8 \pm 4.8)%, (37.9 \pm 13.9)% and (70.8 \pm 19.9)% at the concentrations of 5, 10 and 20 μ mol/L at +60 mV, respectively ($n = 8$, Figure 1F-G).

Comparison of the effects among different unsaturated fatty acids on $I_{K(Ca)}$

To determine the enhancing potency of unsaturated fatty acids,

the effects of different unsaturated fatty acids on $I_{K(Ca)}$ were observed. Under the whole-cell configuration, AA, LA, and OA (with one double bond) at the same concentration (10 μ mol/L) increased $I_{K(Ca)}$ by (46.3 \pm 10.4)%, (37.9 \pm 13.9)% and (13.5 \pm 5.1)% at +60 mV, respectively ($n = 8$, Figure 2). Among them, the increasing potency was in the order of AA (C20: 4, *cis*-5, 8, 11, 14) > LA (C18: 2, *cis*-9, 12) > OA (C18: 1, *cis*-9). The increasing potency of unsaturated fatty acids was in accordance with the number of double bonds in the fatty acid chain.

Effects of PKC inhibitor and oxygenase inhibitor on AA-induced increase of $I_{K(Ca)}$

To determine whether unsaturated fatty acids induced increase of $I_{K(Ca)}$ directly or indirectly, the effect of AA on $I_{K(Ca)}$ was observed after pretreatment with indomethacin (indocin, cyclo-oxygenase inhibitor), nordihydroguaiaretic acid (NDGA, lipoxygenase inhibitor), 17-octadecynoic acid (17-ODA, cytochrome P450 inhibitor) and H-7 (protein kinase C inhibitor), which were added in external perfusing solution for about 10–15 min. H-7 (10 μ mol/L), indocin (10 μ mol/L) and 17-ODA (10 μ mol/L) could not block AA-induced increase of $I_{K(Ca)}$, and AA still increased $I_{K(Ca)}$ by (41.8 \pm 3.7)%, (42.9 \pm 10.8)% and (40.8 \pm 6.8)% at +60 mV, respectively (Figure 3). There was no significant difference between the two groups before and after pretreatment with H-7 and oxygenase inhibitors ($P < 0.05$, $n = 8$). But after pretreatment with NDGA 10 μ mol/L, AA-induced increase of $I_{K(Ca)}$ was diminished from 46.3 \pm 10.4% of control to (11.3 \pm 4.3)% (Figure 3). There was a significant difference between the two groups before and after pretreatment with NDGA ($P > 0.05$, $n = 8$).

DISCUSSION

In this study, it was found that unsaturated fatty acids increased $I_{K(Ca)}$ in a dose-dependent manner and AA increased STOCs also. AA-induced increase of $I_{K(Ca)}$ was not blocked by H-7, indocin and 17-ODA, but was markedly weakened by NDGA. Many experiments have shown that AA and other unsaturated fatty acids enhance $I_{K(Ca)}$. It has been described that AA could directly increase $I_{K(Ca)}$ in human mesangial cells^[20] through lipoxygenase metabolites in rat pituitary tumor cells^[21] and cytochrome p-450 epoxygenase products in smooth muscle cells of rat cerebral arteries^[22]. The results described here show that unsaturated fatty acids increase $I_{K(Ca)}$ and the more double bonds they have, the more potent their enhancing effect on $I_{K(Ca)}$ in gastric antral smooth muscle cells of guinea pigs is. Our previous studies have shown that more double bonds lead to more inhibitory potency on I_{Ca} ^[16], and I_{Ch} ^[18] in gastric antral smooth muscle cells of guinea pigs; however, saturated fatty acids have no effect on I_{Cl} ^[17]. Horimoto *et al.*^[23] also reported only fatty acids having more than two double bonds activated the K⁺ channels in freshly dissociated neurons of 10- to 20-day-old rat visual cortex. These data show that double bonds must be satisfied for a given fatty acid to affect ion channels. The double bonds of unsaturated fatty acids might be easily oxidized to form reactive oxygen species or make unsaturated fatty acids to form barrette-like structures, which may optimize the possibility of binding to ion channels to modulate $I_{K(Ca)}$ ^[15].

The indirect effects of AA on ion channels require the metabolite transformation of AA^[20,21] and activation of PKC^[24]. In this study, the lipoxygenase metabolism pathway was involved in AA-induced increase of $I_{K(Ca)}$, since NDGA markedly diminished AA-induced increase of $I_{K(Ca)}$, but H-7, indocin and 17-ODA had no effect. Many studies have demonstrated that AA exerts physiological function via lipoxygenase metabolism pathway by modulating ion channels. It has been reported that

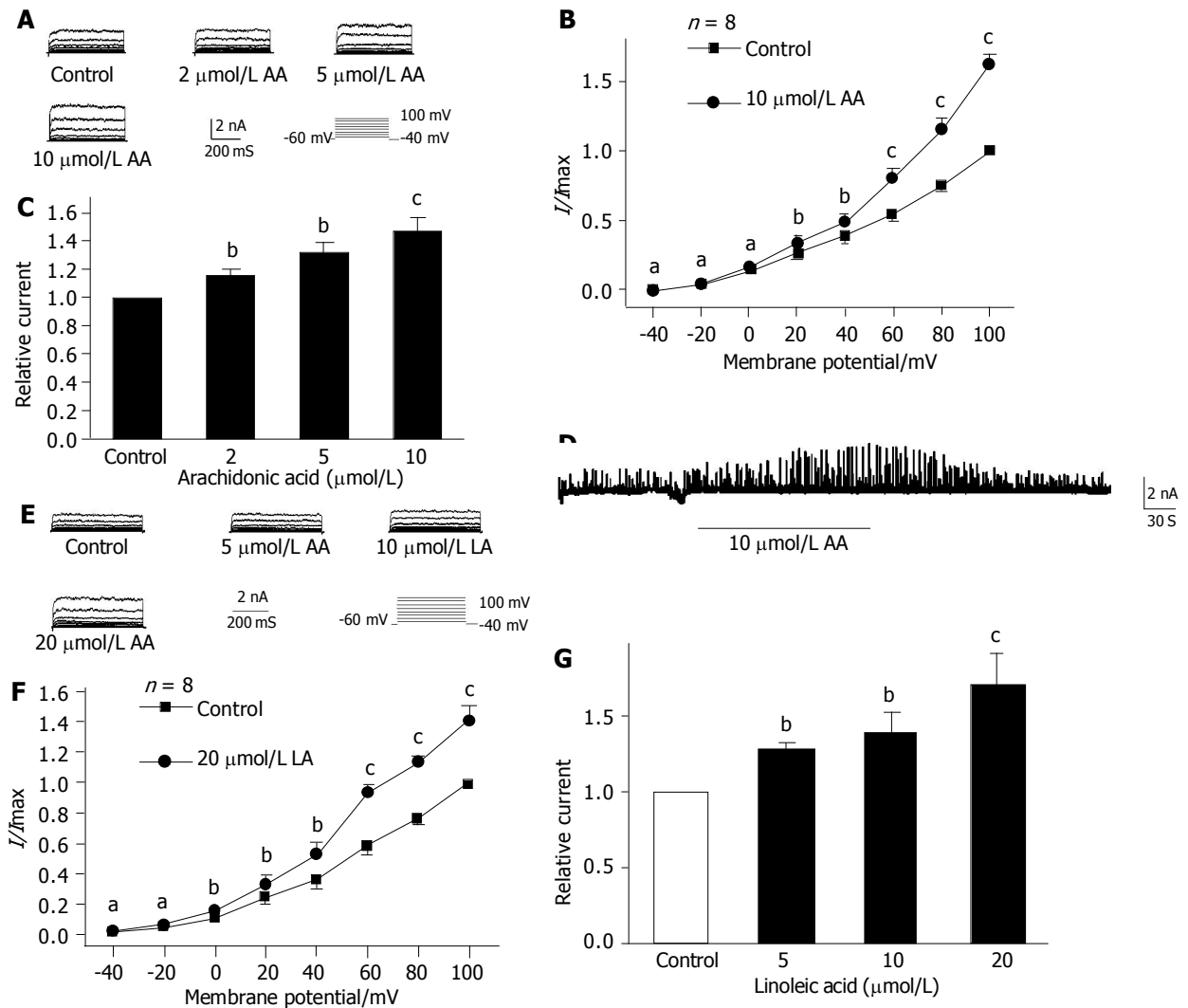


Figure 1 Effects of AA and LA on $I_{K(Ca)}$. A: Raw traces of AA on $I_{K(Ca)}$ at different concentrations; B: I/V relationship of AA on $I_{K(Ca)}$. Peak values were normalized to the values obtained at 100mV under control condition ($n = 8$, $^aP > 0.05$, $^cP < 0.05$, $^bP < 0.01$ vs control); C: Dose-dependent increase of AA on $I_{K(Ca)}$ ($n = 8$, $^cP < 0.05$, $^bP < 0.01$ vs control); D: Increase of AA on STOCs; E: Raw traces of LA on $I_{K(Ca)}$ at different concentrations; F: I/V relationship of LA on $I_{K(Ca)}$ ($n = 8$, $^aP > 0.05$, $^cP < 0.05$, $^bP < 0.01$ vs control); G: Dose-dependent increase of LA on $I_{K(Ca)}$ ($n = 8$, $^aP < 0.05$, $^bP < 0.01$ vs control).

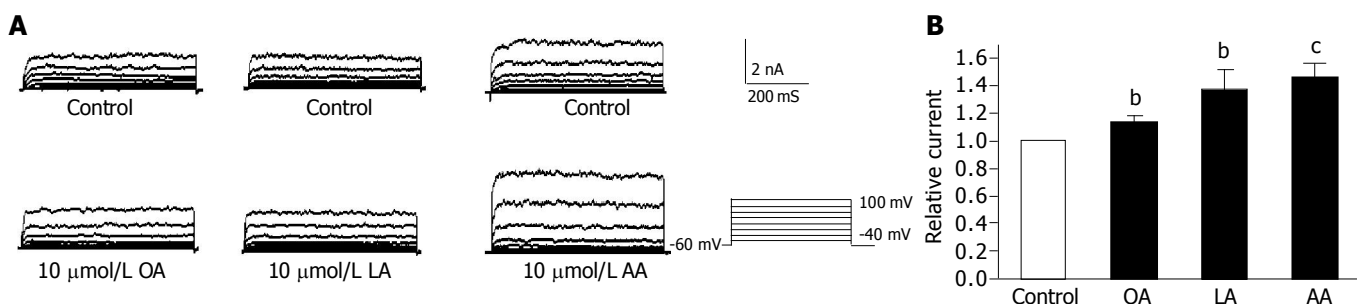


Figure 2 Comparison of different unsaturated fatty acids on $I_{K(Ca)}$. A: Raw traces of 10 μmol/L OA, LA and AA on $I_{K(Ca)}$; B: Increased effect of different unsaturated fatty acids on $I_{K(Ca)}$ ($n = 8$, $^aP < 0.05$, $^bP < 0.01$ vs control).

the lipoxygenase pathway mediates AA-induced vasodilation through a K^+ channel-dependent mechanism in rat small mesenteric arteries and rat basilar arteries. The effect of AA by lipoxygenase metabolites on $I_{K(Ca)}$ might play an important role in regulating secretory function of adrenal chromaffin cells in bovine. However, we can not exclude the direct effect of AA on $I_{K(Ca)}$, since NDGA could not abolish entirely AA-induced

increase of $I_{K(Ca)}$. Unsaturated fatty acids may directly or/and indirectly modulate $I_{K(Ca)}$.

In summary, $I_{K(Ca)}$ is increased by unsaturated fatty acids in a dose-dependent manner. There is a correlation between the degree of *cis* unsaturation and the increasing potency on $I_{K(Ca)}$. Lipoxygenase metabolism pathway is involved in unsaturated fatty acid-induced increase of $I_{K(Ca)}$.

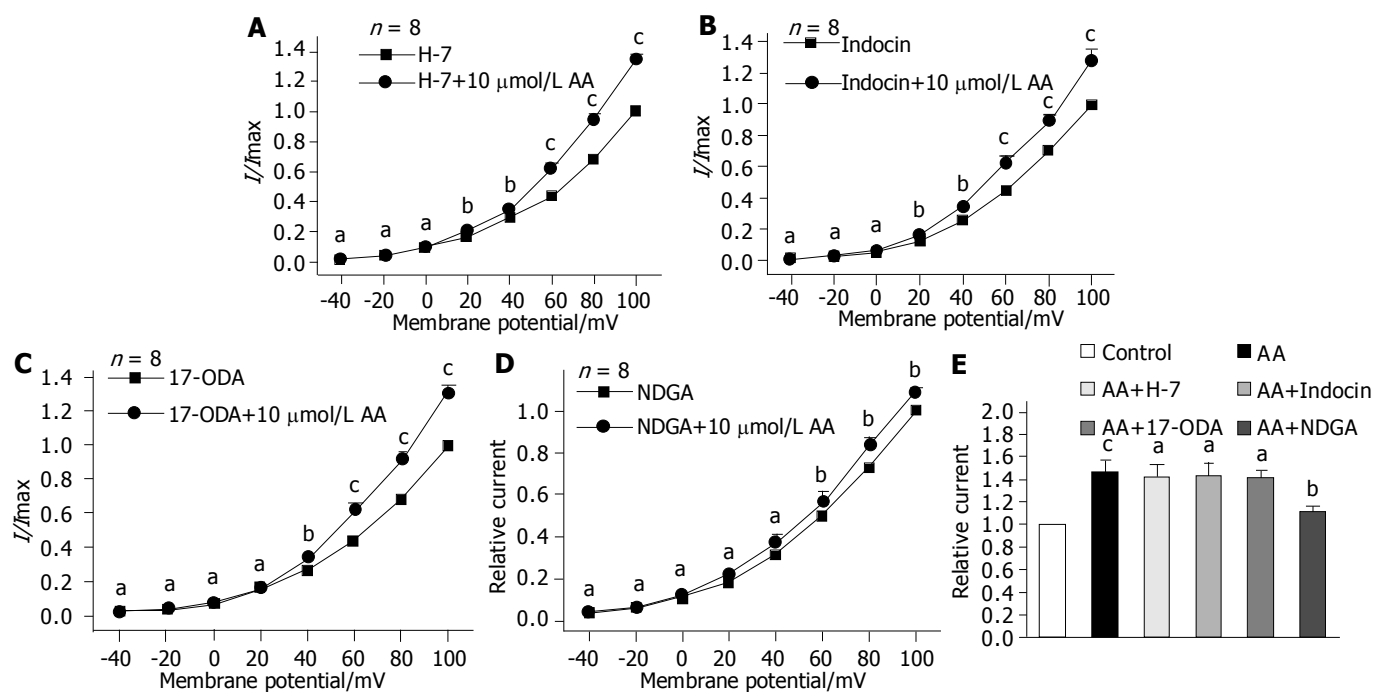


Figure 3 Effects of PKC inhibitor and oxygenase inhibitor on AA-induced increase of $I_{K(Ca)}$. A, B, C and D: Effects of AA on $I_{K(Ca)}$ after pretreatment with H-7, indomethacin, 17-octadecynoic acid and nordihydroguaiaretic acid, respectively ($n = 8$, $^aP > 0.05$, $^cP < 0.05$, $^bP < 0.01$ vs control); E: Comparison of AA on $I_{K(Ca)}$ before and after pretreatment with H-7, indomethacin, 17-octadecynoic acid and nordihydroguaiaretic acid, respectively ($n = 8$, $^bP < 0.01$ vs control, $^aP > 0.05$, $^cP < 0.05$ vs AA).

REFERENCES

- Kang JX, Leaf A. Evidence that free polyunsaturated fatty acids modify Na^+ channels by directly binding to the channel proteins. *Proc Natl Acad Sci USA* 1996; **93**: 3542-3546
- Petit-Jacques J, Hartzell HC. Effect of arachidonic acid on the L-type calcium current in frog cardiac myocytes. *J Physiol* 1996; **493**(Pt 1): 67-81
- Kim D, Pleumsamran A. Cytoplasmic unsaturated free fatty acids inhibit ATP-dependent gating of the G protein-gated K⁺ channel. *J Gen Physiol* 2000; **115**: 287-304
- Ordway RW, Singer JJ, Walsh JV. Direct regulation of ion channels by fatty acids. *Trends Neurosci* 1991; **14**: 96-100
- Liu Y, Liu D, Heath L, Meyers DM, Krafte DS, Wagoner PK, Silvia CP, Yu W, Curran ME. Direct activation of an inwardly rectifying potassium channel by arachidonic acid. *Mol Pharmacol* 2001; **59**: 1061-1068
- Ahn DS, Kim YB, Lee YH, Kang BS, Kang DH. Fatty acids directly increase the activity of Ca^{2+} -activated K^+ channels in rabbit coronary smooth muscle cells. *Yonsei Med J* 1994; **35**: 10-24
- Hardie RC. Regulation of TRP channels via lipid second messengers. *Annu Rev Physiol* 2003; **65**: 735-759
- Fang X, Weintraub NL, Stoll LL, Spector AA. Epoxyeicosatrienoic acids increase intracellular calcium concentration in vascular smooth muscle cells. *Hypertension* 1999; **34**: 1242-1246
- Lingle CJ. Setting the stage for molecular dissection of the regulatory components of BK channels. *J Gen Physiol* 2002; **120**: 261-265
- Wang R, Wang Z, Wu L. Carbon monoxide-induced vasorelaxation and the underlying mechanisms. *Br J Pharmacol* 1997; **121**: 927-934
- Mazzucco TL, Andre E, Calixto JB. Contribution of nitric oxide, prostanoids and Ca^{2+} -activated K^+ channels to the relaxant response of bradykinin in the guinea pig bronchus *in vitro*. *Naunyn Schmiedeberg's Arch Pharmacol* 2000; **361**: 383-390
- Li Y, Xu WX, Li ZL. Effects of nitroprusside, 3-morpholino-sydnnonimine, and spermine on calcium-sensitive potassium currents in gastric antral circular myocytes of guinea pig. *Acta Pharmacol Sin* 2000; **21**: 571-576
- Devor DC, Frizzell RA. Modulation of K^+ channels by arachidonic acid in T84 cells. I. Inhibition of the Ca^{2+} -dependent K^+ channel. *Am J Physiol* 1998; **274**: C138-C148
- Quignard JF, Chataigneau T, Corriu C, Edwards G, Weston A, Feletou M, Vanhoutte PM. Endothelium-dependent hyperpolarization to acetylcholine in carotid artery of guinea pig: role of lipoxygenase. *J Cardiovasc Pharmacol* 2002; **40**: 467-477
- Denson DD, Wang X, Worrell RT, Eaton DC. Effects of fatty acids on BK channels in GH (3) cells. *Am J Physiol Cell Physiol* 2000; **279**: C1211-1219
- Xu WX, Kim SJ, So I, Suh SH, Kim KW. Effects of Arachidonic acid on the calcium channel current (IBa) and on the osmotic stretch-induced increase of IBa in guinea pig gastric myocytes. *Korea J physiol pharmacol* 1997; **1**: 435-443
- Xu WX, Kim SJ, So I, Kang TM, Rhee JC, Kim KW. Volume-sensitive chloride current activated by hyposmotic swelling in antral gastric myocytes of the guinea-pig. *Pflugers Arch* 1997; **435**: 9-19
- Cui YF, Jin H, Guo HS, Li L, Yu YC, Xu WX. Effect of unsaturated fatty acid on muscarinic current in guinea pig gastric antral circular myocytes. *Acta Pharmacol Sin* 2003; **24**: 283-288
- Zhuge R, Fogarty KE, Tuft RA, Walsh JV. Spontaneous transient outward currents arise from microdomains where BK channels are exposed to a mean Ca^{2+} concentration on the order of 10 μM during a Ca^{2+} spark. *J Gen Physiol* 2002; **120**: 15-27
- Stockand JD, Silverman M, Hall D, Derr T, Kuback B, Sansom SC. Arachidonic acid potentiates the feedback response of mesangial BKCa channels to angiotensin II. *Am J Physiol* 1998; **274**: F658-F664
- Duerson K, White RE, Jiang F, Schonbrunn A, Armstrong DL. Somatostatin stimulates BKCa channels in rat pituitary tumor cells through lipoxygenase metabolites of arachidonic acid. *Neuropharmacology* 1996; **35**: 949-961
- Lauterbach B, Barbosa-Sicard E, Wang MH, Honeck H, Kargel E, Theuer J, Schwartzman ML, Haller H, Luft FC, Gollasch M, Schunck WH. Cytochrome P450-dependent eicosapentaenoic acid metabolites are novel BK channel activators. *Hypertension* 2002; **39**: 609-613
- Horimoto N, Nabekura J, Ogawa T. Arachidonic acid activation of potassium channels in rat visual cortex neurons. *Neuroscience* 1997; **77**: 661-671
- Smirnov SV, Aaronson PI. Modulatory effects of arachidonic acid on the delayed rectifier K^+ current in rat pulmonary arterial myocytes. Structural aspects and involvement of protein kinase C. *Circ Res* 1996; **79**: 20-31

Hepato-cardiovascular response and its regulation

Xiang-Nong Li, Irving S Benjamin, Barry Alexander

Xiang-Nong Li, Department of General Surgery, Affiliated Hospital of Xuzhou Medical College, Xuzhou 221002, Jiangsu Province, China

Irving S Benjamin, Barry Alexander, Liver Sciences Unit, Academic Department of Surgery, St Thomas's Hospital, The Guy's, King's and St Thomas's School of Medicine, London SE1 7EH, UK
Supported by the Medical Science and Technology Development Foundation of Health Department of Jiangsu Province, China. No. H200204

Correspondence to: Xiang-Nong Li, Department of General Surgery, Affiliated Hospital of Xuzhou Medical College, 99 West Huaihai Road, Xuzhou 221002, Jiangsu Province, China. xnl2002@yahoo.com.cn

Telephone: +86-516-5802009 **Fax:** +86-516-5601529

Received: 2004-04-24 **Accepted:** 2004-05-09

Abstract

AIM: To determine the possible existence of a hepato-cardiovascular response and its regulatory mechanism in normal rats.

METHODS: Systemic hemodynamic changes following intraportal injection of latex microspheres were studied in two modified rat models of hepatic circulation, in which the extrahepatic splanchnic circulation was excluded by evisceration and the liver was perfused by systemic blood via either the portal vein (model 1) or hepatic artery (model 2) *in vivo*.

RESULTS: In model 1, intraportal injection of two sized microspheres (15- μ m and 80- μ m) induced a similar decrease in mean arterial pressure, while extrahepatic portal venous occlusion induced an immediate increase in mean arterial pressure. In model 2, microsphere injection again induced a significant reduction in mean arterial pressure, aortic blood flow and aortic resistance. There were no significant differences in these parameters between liver-innervated rats and liver-denervated rats. The degrees of microsphere-induced reduction in mean arterial pressure (-38.1 \pm 1.9% in liver-innervated rats and -35.4 \pm 2.1% in liver-denervated rats, respectively) were similar to those obtained by withdrawal of 2.0 mL of blood via the jugular vein (-33.3 \pm 2.1%) ($P>0.05$). Injection of 2.0 mL Haemaccel in microsphere-treated rats, to compensate for the reduced effective circulating blood volume, led to a hyperdynamic state which, as compared with basal values and unlike control rats, was characterised by increased aortic blood flow (+21.6 \pm 3.3%), decreased aortic resistance (-38.1 \pm 3.5%) and reduced mean arterial pressure (-9.7 \pm 2.8%).

CONCLUSION: A hepato-cardiovascular response exists in normal rats. It acts through a humoral mechanism leading to systemic vasodilatation, and may be involved in the hemodynamic disturbances associated with acute and chronic liver diseases.

Key words: Hepato-cardiovascular response; Hemodynamics

Li XN, Benjamin IS, Alexander B. Hepato-cardiovascular response and its regulation. *World J Gastroenterol* 2005; 11(5): 676-680

<http://www.wjgnet.com/1007-9327/11/676.asp>

INTRODUCTION

Several mechanisms are involved in the regulation of hepatic hemodynamics, which include distensible hepatic resistance^[1], changeable hepatic blood volume^[2], hepatic arterial buffer response^[3] and intrahepatic portal systemic shunts^[4-6]. However, a direct hemodynamic relationship between the liver and the cardiovascular system has not been described.

In our previous studies, it was found that intrahepatic portal block by microspheres induced an acute reduction in systemic blood pressure^[4-6]. Originally this was attributed to mesenteric pooling of portal venous blood^[4-6], but subsequent studies have suggested that this might be due to a hepato-cardiovascular response^[7,8]. To further confirm such a response, the present study used eviscerated rats to exclude extrahepatic splanchnic circulation, and the liver was perfused with systemic blood via either the portal vein or hepatic artery *in vivo*. Thus, if an autoregulatory response mechanism exists between the liver and the systemic circulation, this could be activated directly following appropriate stimulation to the liver. The aims of the present study were to determine whether: (1) intraportal injection of latex microspheres would result in hemodynamic changes in the systemic circulation; (2) different-sized microspheres affected changes in systemic hemodynamics; (3) systemic circulatory responses to the microsphere injection could be induced in the absence of portal flow to the liver; and (4) denervation of the liver altered microsphere-induced responses in systemic hemodynamics.

MATERIALS AND METHODS

Animals and surgical procedures

Male Wistar rats (350-400 g) were anaesthetized with fentanyl/fluanisone (0.3 mL/kg subcutaneously) and midazolam (0.3 mL/kg subcutaneously). The left carotid artery was cannulated for measurement of mean arterial pressure (MAP). Another cannula was inserted into the right jugular vein and advanced 2-3 cm to reach the superior vena cava for measurement of central venous pressure (CVP).

The abdomen was then opened via a midline incision. The gastric artery, splenic artery and superior mesenteric artery were exposed and ligated, and the stomach, intestines and spleen were subsequently removed.

After evisceration, the liver was perfused either by aortic blood via the portal vein *in vivo* (model 1) or by hepatic arterial blood *in vivo* (model 2). In model 1, the hepatic artery was carefully dissected and ligated. The main portal vein was divided so that a complete evisceration could be achieved. To re-construct the portal venous supply to the liver, the abdominal aorta was ligated and divided just above its bifurcation and the

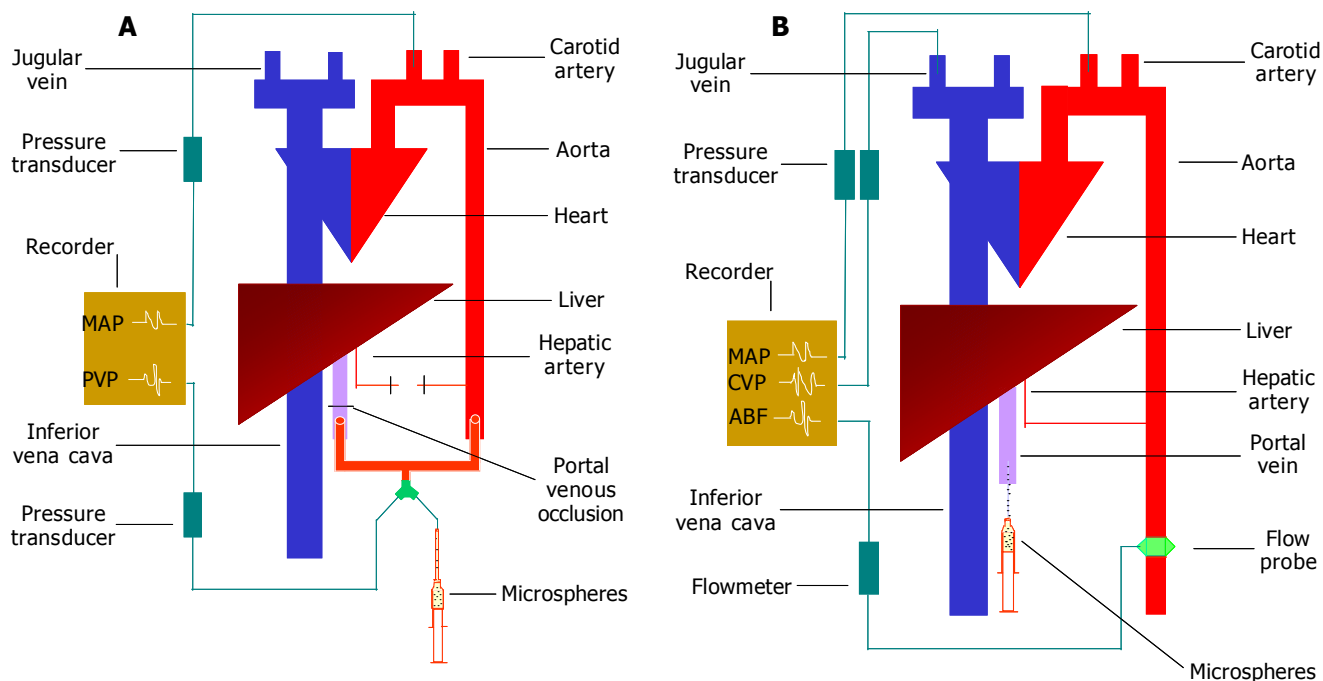


Figure 1 Diagram of experimental models. Rats in both models were eviscerated. In model 1, the hepatic artery was divided and the liver was then perfused only by aortic blood via the portal vein (A). In model 2, the liver was perfused only by the hepatic artery (B). Latex microspheres were injected intraportally and the resultant changes in mean arterial pressure (MAP), central venous pressure (CVP) and portal venous pressure (PVP) were monitored by the cannulae in the carotid artery, jugular vein and portal vein, respectively. Aortic blood flow (ABF) was measured by an electric magnetic flow probe placed around the abdominal aorta.

cephalad end of the aorta was connected to the hepatic end of the portal vein by a T-type connector. The third arm of the connector was used for measurement of portal venous pressure (PVP) and injection of microspheres (Figure 1A). In model 2, the liver was supplied only by the hepatic artery. The portal vein was also divided, and the hepatic remnant cannulated for injection of microspheres (Figure 1B).

Experimental design

Experiment 1 After a 20-min stabilization period, a vascular clamp was applied to the portal vein in model 1 (Figure 1A) for 2–3 min and the pressures recorded as a measurement of the maximum attainable portal venous pressure^[4,5]. Five minutes after releasing the vascular clamp, rats were given intraportally via four equal injections (0.2 mL/injection) with a total of 2.2×10^7 15- μ m diameter microspheres (group 1, $n = 6$), or 3.6×10^5 80- μ m diameter microspheres (group 2, $n = 6$)^[4,5]. Identical volumes of saline were given intraportally to controls (group 3, $n = 6$) during the same time course. When steady-state portal venous pressure was obtained, portal venous occlusion (PVO) was performed again. The resultant changes in MAP and PVP were continuously monitored. Because the liver was perfused by aortic blood with high pressure, which might have enlarged the hepatic sinusoids and/or opened intrahepatic portal-systemic shunts^[4–6] to lead to pulmonary embolization with a large number of microspheres, an additional group of rats ($n = 6$) was, therefore, used for measurement of intrahepatic shunting by using 15- μ m diameter ⁵¹Cr labeled microspheres^[6,9].

Experiment 2 In model 2 (Figure 1B), 5.6×10^6 15- μ m diameter microspheres or equivalent volumes of saline (0.2 mL) were injected intraportally, and the resultant changes in MAP, CVP and aortic blood flow (ABF) were measured in liver-innervated rats (group 1, $n = 8$), liver-denervated rats^[10] (group 2, $n = 8$) and control rats (group 3, $n = 8$) respectively. ABF was measured by using an electromagnetic flow transducer that was placed around the abdominal aorta between the celiac axis and renal arteries.

Results obtained were compared with that of group 4 ($n = 6$) which underwent sequential blood withdrawals and subsequent Haemacel injections via the jugular vein (0.5 mL/withdrawal or injection, both up to 6 times). The microsphere-induced hypovolemia, secondary to vasodilatation (see below), was then identified, and an appropriate volume of Haemacel was given via the jugular vein to rats pre-treated with 15- μ m diameter microspheres (5.6×10^6) injected intraportally (group 5, $n = 8$).

Statistical analysis

Aortic blood flow was measured as mL/(min · 100 g) body weight. Aortic resistance (AR) was calculated as kPa/aortic blood flow. Intrahepatic shunting was calculated from injection of 15- μ m diameter ⁵¹Cr labeled microspheres as follows^[9]: Intrahepatic shunting (%) = lung radioactivity (cpm) × 100 / (liver radioactivity (cpm) + lung radioactivity (cpm)). The results were expressed as mean ± SE. Statistical comparisons were performed using *t* test and factorial ANOVA where appropriate unless otherwise stated. Results were considered statistically significant when a *P* value was <0.05.

RESULTS

MAP, PVP and intrahepatic shunting in experiment 1

Basal MAP and PVP were significantly increased by PVO to a similar level, which returned to basal values immediately after release of PVO (Table 1, Figure 2). In contrast, although microsphere injections in groups 1 and 2 gradually increased PVP due to increased intrahepatic portal resistance, MAP was significantly decreased following the first injection of microspheres in both groups, and showed no further significant changes following the subsequent 3 injections. There were no significant differences in MAP reduction between group 1 and group 2. PVO, following microsphere injections, induced a significantly smaller increase in MAP and PVP than PVO prior to injection of microspheres (Table 1, Figure 2). There were no

significant changes in control rats given saline.

Although the liver was perfused via the portal vein by aortic blood with high pressure, intrahepatic shunting was negligible with a mean value of $(0.06 \pm 0.04)\%$ ($0.03-0.10\%$).

Table 1 Changes in MAP and PVP during PVO, intraportal injection of microspheres and re-PVO after microsphere injections in experiment 1 (mean \pm SE)

	Basal	PVO	Microsphere injection	Re-PVO
MAP (kPa)				
Group 1	11.6 \pm 0.4	13.0 \pm 0.3 ^a	8.8 \pm 0.4 ^a	9.0 \pm 0.4 ^c
Group 2	11.2 \pm 0.3	13.2 \pm 0.5 ^a	8.5 \pm 0.3 ^a	9.3 \pm 0.3 ^c
Group 3	11.4 \pm 0.4	12.6 \pm 0.3 ^a	11.5 \pm 3.9	12.4 \pm 0.3
PVP (kPa)				
Group 1	4.1 \pm 0.3	13.0 \pm 0.3 ^b	4.5 \pm 0.3 ^a	8.4 \pm 0.3 ^c
Group 2	4.5 \pm 0.2	13.2 \pm 0.4 ^b	5.1 \pm 0.2 ^a	9.2 \pm 0.2 ^c
Group 3	4.2 \pm 0.2	12.6 \pm 0.3 ^b	4.2 \pm 0.2	12.4 \pm 0.3

Group 1: 15 μ m microspheres; group 2: 80 μ m microspheres; group 3: saline control. MAP, mean arterial pressure; PVP, portal venous pressure; PVO, portal venous occlusion. ^a $P < 0.05$; ^b $P < 0.01$ vs Basal. ^c $P < 0.05$ vs PVO.

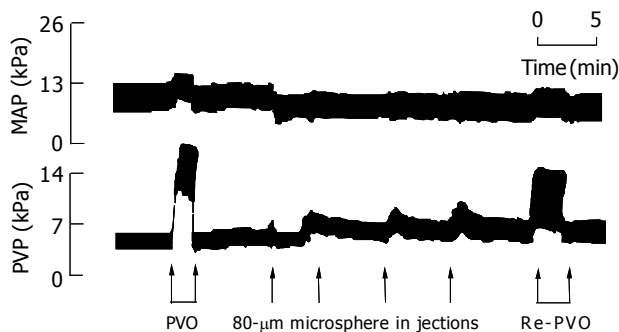


Figure 2 Mean arterial pressure (MAP) and portal venous pressure (PVP) recordings from a rat in group 2 of experiment 1 during portal venous occlusion (PVO), intraportal injection of 80- μ m diameter microspheres and re-PVO after microsphere injection.

Systemic hemodynamics in experiment 2

Intraportal injection of microspheres resulted in significant reductions in MAP, ABF and AR, 60-90 s after microsphere injection (Table 2, Figure 3). CVP showed no significant changes following microsphere injection. There were no significant differences in these parameters between liver-innervated rats (group 1) and liver-denervated rats (group 2). No significant changes were observed in control group given saline.

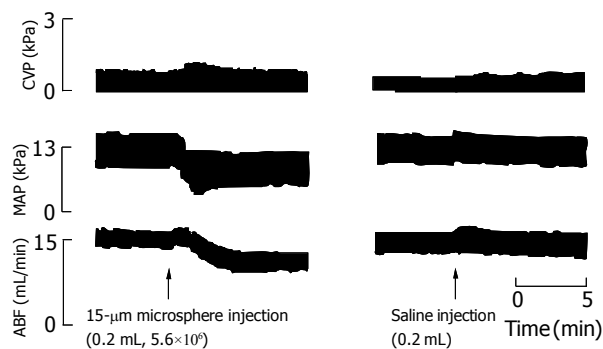


Figure 3 Central venous pressure (CVP), mean arterial pressure (MAP) and aortic blood flow (ABF) recordings from experiment 2 after intraportal injection of 15- μ m diameter microspheres in a liver-innervated rat (group 1) and saline injection in a control rat (group 3).

Table 2 Changes in CVP, MAP, ABF and AR before and after intraportal injection of microspheres in experiment 2 (mean \pm SE)

	Pre-injection	Post-injection	Change (%)
CVP (kPa)			
Group 1	0.43 \pm 0.07	0.39 \pm 0.06	-6.9 \pm 0.72
Group 2	0.40 \pm 0.08	0.38 \pm 0.59	-5.5 \pm 0.66
Group 3	0.34 \pm 0.06	0.35 \pm 0.08	1.3 \pm 0.22
MAP (kPa)			
Group 1	12.7 \pm 0.4	7.9 \pm 0.4 ^a	-38.1 \pm 1.9
Group 2	12.9 \pm 0.6	8.4 \pm 0.5 ^a	-35.4 \pm 2.1
Group 3	12.9 \pm 0.4	13.1 \pm 0.4	1.5 \pm 0.2
ABF (mL/min/100 g BW)			
Group 1	4.2 \pm 0.3	3.4 \pm 0.3 ^a	-21.3 \pm 2.6
Group 2	3.7 \pm 0.2	3.1 \pm 0.2 ^a	-16.8 \pm 2.5
Group 3	4.1 \pm 0.3	4.2 \pm 0.3	2.1 \pm 0.1
AR (kPa/mL/min/100 g BW)			
Group 1	3.1 \pm 0.1	2.4 \pm 0.1 ^a	-21.0 \pm 2.3
Group 2	3.5 \pm 0.1	2.7 \pm 0.1 ^a	-21.7 \pm 2.3
Group 3	3.3 \pm 0.2	3.2 \pm 0.2	-0.4 \pm 0.1

Group 1: liver-innervated rats; group 2: liver-denervated rats; and group 3: control rats. CVP, central venous pressure; MAP, mean arterial pressure; ABF, aortic blood flow; AR, aortic resistance. ^a $P < 0.05$ vs pre-injection.

Sequential blood withdrawal in group 4 caused a parallel decrease in MAP and ABF, which, after subsequent Haemacel injections, completely returned to basal values. Microsphere-induced MAP reductions in liver-innervated rats (7.9 ± 0.4 kPa) and liver-denervated rats (8.4 ± 0.5 kPa) were comparable to those obtained by withdrawal of 2.0 mL blood via the jugular vein in group 4 (8.3 ± 0.5 kPa) ($P > 0.05$). Therefore 2.0 mL of Haemacel was infused in microsphere-treated rats in group 5, to compensate for the reduced effective circulating blood volume. This led to a hyperdynamic state which, as compared with the basal values and unlike rats in group 4, was characterized by increased ABF, decreased AR and reduced MAP (Table 3, Figures 4, 5).

Table 3 Changes in MAP, ABF and AR following intraportal injection of microspheres (5.6×10^6) and infusion of Haemacel (2 mL) via the jugular vein in group 5 of experiment 2

	Basal	Microsphere injection	Haemacel injection
MAP (kPa)	12.8 \pm 0.5	7.6 \pm 0.3 ^b	11.6 \pm 0.4 ^{a,d}
ABF (mL/min/100 g body weight)	4.4 \pm 0.2	3.4 \pm 0.2 ^b	5.6 \pm 0.4 ^{b,d}
AR (kPa/mL/min/100 g body weight)	2.9 \pm 0.1	2.3 \pm 0.1 ^b	2.1 \pm 0.1 ^b

MAP, mean arterial pressure; ABF, aortic blood flow; AR, aortic resistance. ^a $P < 0.05$; ^b $P < 0.01$ vs Basal. ^d $P < 0.01$ vs Microsphere injection.

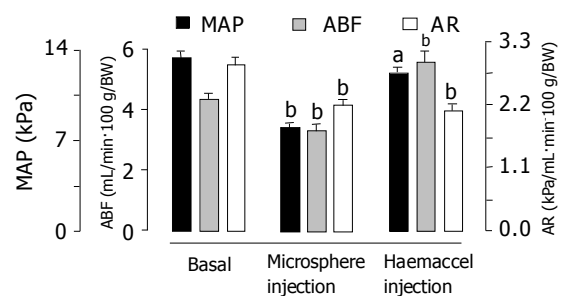


Figure 4 Mean arterial pressure (MAP), aortic blood flow (ABF) and aortic resistance (AR) after intraportal injection of 15- μ m diameter microspheres and subsequent Haemacel injection in group 5 of experiment 2. ^a $P < 0.05$, ^b $P < 0.01$ vs Basal.

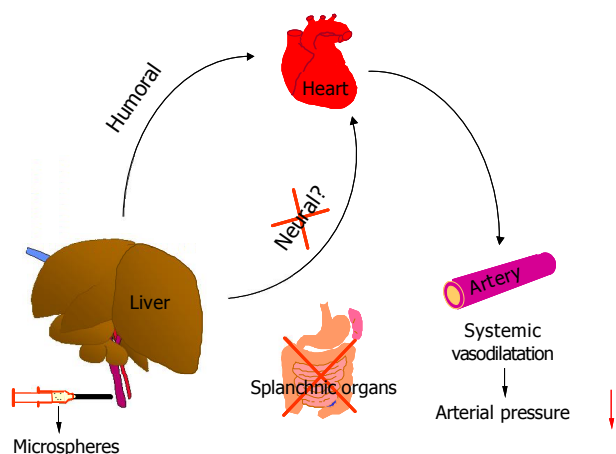


Figure 5 Illustration of the hepato-cardiovascular response and its regulatory mechanism. Intrahepatic stimulation induced by microspheres led to release of humoral mediator (s) from the liver, which, in turn, caused systemic vasodilatation and subsequently the reduction in arterial blood pressure.

DISCUSSION

The present study established two modified rat models of hepatic circulation, in which the extrahepatic splanchnic circulation was excluded by evisceration and the liver was perfused by systemic blood via either the portal vein (model 1) or hepatic artery (model 2) *in vivo*. Therefore, the possible hemodynamic relationship between the liver and the cardiovascular system could be easily observed. Results showed that intraportal injection of microspheres induced a significant reduction in MAP in both models, thus supporting our previous hypothesis that there exists a hepato-cardiovascular response in normal rats^[7,8].

In model 1, the liver was only supplied by aortic blood via the portal vein (Figure 1A). It was expected that in this model, either intraportal injection of microspheres or PVO should increase the resistance to aortic blood that was flowing through the portal vasculature, thus leading to elevations in both MAP and PVP. As expected, PVO prior to injection of microspheres, induced an immediate increase in mean arterial pressure. However, injection of microspheres into the liver induced an immediate decrease in MAP. Furthermore, PVO following microsphere injections induced a significantly smaller increase in MAP.

The reduction in MAP might be a result of a major shunting of microspheres into the pulmonary circulation, due to enlarged sinusoids and opened intrahepatic portal-systemic shunts^[4,5] caused by a high portal venous perfusion pressure. However, we showed that the percentage of intrahepatic shunting, measured with 15- μ m diameter labeled microspheres, was negligible (<0.1%). This is consistent with our recent findings that intrahepatic shunts in the normal rat liver are predominantly small with diameters less than 15- μ m^[6].

The liver is characterized by a high degree of compliance. Therefore the microsphere-induced reductions in MAP could also result from intrahepatic blood pooling, secondary to portal block by the injected microspheres. If so, MAP should decrease progressively with increasing numbers and sizes (diameters) of microspheres as more sinusoids would become occluded in the liver, but this was not observed. In fact, a similar and sustained reduction in MAP was observed in groups 1 and 2 of experiment 1, following the first injection of 15- μ m and 80- μ m microspheres, respectively. Moreover, significant intrahepatic portal pooling could not occur because the opening of intrahepatic

portal systemic shunts (<15- μ m) can permit 70% of the basal portal venous blood to bypass the hepatic sinusoids^[6]. We, therefore, hypothesize that the reduction in MAP is possibly due to an autoregulatory response elicited by the effects of injected microspheres in the liver.

This hypothesis is supported by the results from the subsequent experiments with model 2, in which the absence of portal flow excluded portal venous pooling as the cause. Again, significant reductions in MAP, aortic blood flow and aortic resistance were induced by intraportal injection of microspheres. These changes strongly suggest a significant systemic vasodilatation leading to reductions in effective circulating blood volume. Furthermore, the microsphere-induced hemodynamic responses are different from those seen in acute toxic liver injury, in which vasodilatation develops over hours or days^[11], not in seconds as observed in the present study. It is, therefore, suggested that a hepato-cardiovascular response exists in normal rats, by which the systemic circulation may quickly respond to intrahepatic portal block by injected microspheres.

The fact that denervation of the liver does not eliminate this response suggests that a humoral mechanism is involved in the hepato-cardiovascular response, and that, following microsphere injection, the liver releases substance (s) which may exert a potent vasodilator action on the systemic circulation. Although we did not perform humoral measurements as this is beyond the scope of the present study, it is well known that the liver can produce many vasodilators such as nitric oxide^[12]. The systemic responses in model 1, in which a large quantity of aortic blood flows through the liver via the portal vein with low resistance, occurred immediately, while in model 2 there was a delay of 60-90 s. This is consistent with rapid flushing of humoral factors into the systemic circulation in model 1.

Microsphere-induced acute systemic vasodilatation resulted in a state of relative hypovolemia and thus a reduction in MAP comparable to withdrawal of 2.0 mL of blood via the jugular vein. Infusion of 2.0 mL Haemaccel, to compensate for the reduced effective circulating blood volume in microsphere-treated rats, led to a hyperdynamic circulation, characterized by increased aortic blood flow, decreased aortic resistance and reduced MAP. Such circulatory disturbances are similar to those observed following acute^[11] or chronic liver injuries^[13], and consistent with the hypothesis that the combination of vasodilatation and expanded plasma volume is necessary for full expression of the hyperdynamic state^[14]. However, the initiating factor for the hyperdynamic circulation appears to be the development of vasodilatation, which evokes an increase in blood volume and cardiac output as a compensatory response^[15]. Although the mechanisms underlying the vasodilatation are still not fully understood, we have shown here, for the first time, a direct hemodynamic response between the liver and the cardiovascular system. It is suggested that this response may play a role in the development of vasodilatation observed in acute and chronic liver diseases such as severe hepatitis and cirrhosis, where the mechanical stimulation to the liver, similar to that induced by microsphere injections, is a common feature which results from leukocyte accumulation^[16], endothelial oedema^[17], Kupffer cell swelling^[16], and portal occlusion or compression by scar tissue and regenerative hyperplastic nodules^[18,19].

In conclusion, this study demonstrates the existence of a hepato-cardiovascular response in normal rats. This response acts through a humoral mechanism and leads to systemic vasodilatation, and may be involved in the hemodynamic disturbances associated with acute and chronic liver diseases.

REFERENCES

- 1 Lautt WW, Legare DJ. Passive autoregulation of portal venous

- pressure: distensible hepatic resistance. *Am J Physiol* 1992; **263**: G702-G708
- 2 **Lautt WW**, Brown LC, Durham JS. Active and passive control of hepatic blood volume responses to hemorrhage at normal and raised hepatic venous pressure in cats. *Can J Physiol Pharmacol* 1980; **58**: 1049-1057
 - 3 **Lautt WW**. Mechanism and role of intrinsic regulation of hepatic arterial blood flow: hepatic arterial buffer response. *Am J Physiol* 1985; **249**: G549-G556
 - 4 **Li XN**, Benjamin I, Alexander B. A new rat model of portal hypertension induced by intraportal injection of microspheres. *World J Gastroenterol* 1998; **4**: 66-69
 - 5 **Li X**, Benjamin IS, Alexander B. The relationship between intrahepatic portal systemic shunts and microsphere induced portal hypertension in the rat liver. *Gut* 1998; **42**: 276-282
 - 6 **Li X**, Benjamin IS, Naftalin R, Alexander B. Location and function of intrahepatic shunts in anaesthetised rats. *Gut* 2003; **52**: 1339-1346
 - 7 **Li X**, Benjamin IS, Alexander B. Evidence for a hepato-cardiovascular reflex in the rat. *Hepatogastroenterology* 1999; **46**(Suppl II): 1419
 - 8 **Li X**, Benjamin IS, Alexander B. Further evidence for a hepato-cardiovascular reflex: demonstrated in a rat model of hepatic circulation in the absence of portal flow *in vivo*. *Hepatogastroenterology* 1999; **46**(Suppl II): 1448
 - 9 **Groszmann RJ**, Vorobioff J, Riley E. Splanchnic hemodynamics in portal hypertensive rats: measurement with gamma-labeled microspheres. *Am J Physiol* 1982; **242**: G156-G160
 - 10 **Holmin T**, Ekelund M, Kullendorff CM, Lindfeldt J. A microsurgical method for denervation of the liver in the rat. *Eur Surg Res* 1984; **16**: 288-293
 - 11 **Makin AJ**, Hughes RD, Williams R. Systemic and hepatic hemodynamic changes in acute liver injury. *Am J Physiol* 1997; **272**: G617-G625
 - 12 **Li X**, Benjamin IS, Alexander B. The role of nitric oxide in systemic and hepatic haemodynamics in the rat *in vivo*. *Naunyn Schmiedebergs Arch Pharmacol* 2003; **368**: 142-149
 - 13 **Bosch J**, Enriquez R, Groszmann RJ, Storer EH. Chronic bile duct ligation in the dog: hemodynamic characterization of a portal hypertensive model. *Hepatology* 1983; **3**: 1002-1007
 - 14 **Colombato LA**, Albillos A, Groszmann RJ. Temporal relationship of peripheral vasodilatation, plasma volume expansion and the hyperdynamic circulatory state in portal hypertensive rats. *Hepatology* 1992; **15**: 323-328
 - 15 **Schrier RW**, Arroyo V, Bernardi M, Epstein M, Henriksen JH, Rodes J. Peripheral arterial vasodilation hypothesis: a proposal for the initiation of renal sodium and water retention in cirrhosis. *Hepatology* 1988; **8**: 1151-1157
 - 16 **Jaeschke H**, Smith CW. Cell adhesion and migration. III. Leukocyte adhesion and transmigration in the liver vasculature. *Am J Physiol* 1997; **273**: G1169-G1173
 - 17 **Vollmar B**, Glasz J, Leiderer R, Post S, Menger MD. Hepatic microcirculatory perfusion failure is a determinant of liver dysfunction in warm ischemia-reperfusion. *Am J Pathol* 1994; **145**: 1421-1431
 - 18 **Li X**, Benjamin IS, Alexander B. Reproducible production of thioacetamide-induced macronodular cirrhosis in the rat with no mortality. *J Hepatol* 2002; **36**: 488-493
 - 19 **Li XN**, Huang CT, Wang XH, Leng XS, Du RY, Chen YF, Hou X. Changes of blood humoral substances in experimental cirrhosis and their effects on portal hemodynamics. *Chin Med J (Engl)* 1990; **103**: 970-977

Edited by Xia HHX Proofread by Zhu LH

• CLINICAL RESEARCH •

Association between polymorphisms in the Toll-like receptor 4, CD14, and *CARD15/NOD2* and inflammatory bowel disease in the Greek population

Maria Gazouli, Gerassimos Mantzaris, Athanassios Kotsinas, Panayotis Zacharatos, Efstathios Papalambros, Athanassios Archimandritis, John Ikonomopoulos, Vassilis G Gorgoulis

Maria Gazouli, Athanassios Kotsinas, Panayotis Zacharatos, Vassilis G Gorgoulis, Department of Histology-Embryology, School of Medicine, University of Athens, 11527 Athens, Greece
Gerassimos Mantzaris, Department of Gastroenterology, "Evangelismos" Hospital, 11521 Athens, Greece
Efstathios Papalambros, First Department of Surgery, Laikon Hospital, School of Medicine, University of Athens, 11527 Athens, Greece
Athanassios Archimandritis, Department of Pathophysiology, Gastroenterology Section, School of Medicine, University of Athens, "Hippocraton" Hospital, 11527 Athens, Greece
John Ikonomopoulos, Agricultural University of Athens, Department of Anatomy-Physiology, Faculty of Animal Science, 11855 Athens, Greece
Supported by the EU Project "Sacrohn" N. QLK2-CT-2000-00928
Correspondence to: Dr. Vassilis G Gorgoulis, Department of Histology-Embryology, 53 Antaiou St. Ano Patisia, 11146 Athens, Greece. histoclub@ath.forthnet.gr
Fax: +302106535894
Received: 2004-05-25 **Accepted:** 2004-07-27

CONCLUSION: Our results indicate that co-existence of a mutation in either the TLR4 or CD14 gene, and in *NOD2/CARD15* is associated with an increased susceptibility to developing CD compared to UC, and to developing either CD or UC compared to healthy individuals.

© 2005 The WJG Press and Elsevier Inc. All rights reserved.

Key words: Inflammatory bowel disease; *CARD15/NOD2* gene; Toll-like receptor 4; CD14 Antigen

Gazouli M, Mantzaris G, Kotsinas A, Zacharatos P, Papalambros E, Archimandritis A, Ikonomopoulos J, Gorgoulis VG. Association between polymorphisms in the Toll-like receptor 4, CD14, and *CARD15/NOD2* and inflammatory bowel disease in the Greek population. *World J Gastroenterol* 2005; 11(5): 681-685
<http://www.wjgnet.com/1007-9327/11/681.asp>

Abstract

AIM: Crohn's disease (CD) and ulcerative colitis (UC) are multifactorial diseases with a significant genetic background. Apart from *CARD15/NOD2* gene, evidence is accumulating that molecules related to the innate immune response such as CD14 or Toll-like receptor 4 (TLR4), are involved in their pathogenesis. In further exploring the genetic background of these diseases, we investigated the variations in the *CARD15/NOD2* gene (Arg702Trp, Gly908Arg and Leu1007fsinsC), and polymorphisms in the TLR4 gene (Asp299Gly and Thr399Ile) as well as in the promoter of the CD14 gene (T/C at position -159) in Greek patients with CD and UC.

METHODS: DNA was obtained from 120 patients with CD, 85 with UC and 100 healthy individuals. Genotyping was performed by allele specific PCR or by PCR-RFLP analysis.

RESULTS: The 299Gly allele frequency of the TLR4 gene and the T allele and TT genotype frequencies of the CD14 promoter were significantly higher in CD patients only compared to healthy individuals ($P = 0.026 < 0.05$; $P = 0.0048 < 0.01$ and $P = 0.047 < 0.05$ respectively). Concerning the *NOD2/CARD15* mutations the overall presence in CD patients was significantly higher than that in UC patients or in controls. Additionally, 51.67% of the CD patients were carriers of a TLR4 and/or CD14 polymorphic allele and at least one variant of the *NOD2/CARD15*, compared to 27% of the UC patients. It should be pointed out that both frequencies significantly increased as compared with the 10% frequency of multiple carriers found in healthy controls. A possible interaction of the *NOD2/CARD15* with TLR4 and especially CD14, increased the risk of developing inflammatory bowel disease (IBD).

INTRODUCTION

Inflammatory bowel diseases (IBD), Crohn's disease (CD) and ulcerative colitis (UC) are multifactorial disorders characterized by failure to limit the inflammatory response to luminal antigens. Genetic predisposition to IBD has been well established through epidemiological studies and genome wide linkage analyses, but little is known about the accountable genes^[1]. Animal models have demonstrated that genes involved in the regulation of the immune response are likely to play a crucial role in the genetic predisposition to IBD^[2].

The innate immune response represents the first defense line in preventing systemic infection with bacteria. Several host receptors interact with endotoxins and mediate cytokine production of macrophages. Lipopolysaccharides (LPS) are the main endotoxins derived from Gram-negative bacteria, and their pivotal role in the pathogenesis of a variety of infectious and allergic diseases has been suggested^[3,4]. *CARD15/NOD2*, a cytosolic protein expressed in monocytes, is involved in the innate immune response to LPS and peptidoglycans (PGN)^[5].

The association between mutations in the *CARD15/NOD2* gene and CD has been described recently^[6,7]. The 3 major variants Gly908Arg, Arg702Trp, and Leu1007fsinsC are associated with a deficit in NF- κ B activation in response to bacterial components, providing a unifying mechanism for the major CD-associated *CARD15/NOD2* variants^[5].

The question arises as to how *CARD15/NOD2* mutations and impaired NF- κ B activation confer susceptibility to CD. It has been suggested that the answer most likely lies within the leucine-rich repeats (LRR) of the *CARD15/NOD2* gene and the family of Toll-like receptors. These receptors recognize pathogen-associated molecular patterns and activate signal transduction pathways of the innate immune response genes including inflammatory cytokines and the NF- κ B signaling

pathway^[8]. Therefore, one could speculate that extracellular Toll-like receptors and intracellular *CARD15/NOD2* participate as pattern-recognition receptors in the regulation of mucosal innate immune responses to intestinal microbes. Among the Toll-like receptors, Toll-like receptor 4 (TLR4) was found to be strongly up-regulated in both UC and CD^[9]. TLR4 binds to LPS together with CD14 and by internalization prevents inappropriate NF- κ B activation^[10].

Very recently, Arbour *et al*^[11] reported that the Asp299Gly and Thr399Ile polymorphisms of human TLR4 determine, in concert with other genetic changes, the airway responsiveness to inhaled LPS in humans. In addition, Klein *et al*^[12] have demonstrated an association of CD with a functional relevant single nucleotide polymorphism in the promoter of the CD14 gene (T/C at position -159) and suggested that the interaction of the *CARD15/NOD2* and CD14 genes increases the risk for developing CD^[13].

In order to evaluate whether the above mentioned polymorphisms in TLR4 and CD14 genes contributed to the predisposition to IBD, as well as whether the interaction of *CARD15/NOD2*, TLR4 and CD14 genes could increase the risk for IBD in a Greek population, we genotyped 120 patients with CD, 85 patients with UC and 100 healthy controls for the Asp299Gly and Thr399Ile polymorphisms of the TLR4 gene and the promoter of the CD14 gene (T/C at position -159).

MATERIALS AND METHODS

Materials

Blood samples from 120 patients with CD, 85 patients with UC and 100 age and sex-matched healthy individuals were collected at the IBD Outpatient Clinic between September 2002 and February 2003. The diagnosis of either CD or UC was based on standard clinical, endoscopic, radiological, and histological criteria^[14]. Before commencement of the study, the Ethics Committee at the participating centers approved the recruitment protocols. All participants were informed of the study. DNA was isolated from blood with the NucleoSpin Blood Kit (Macherey-Nagel, Germany).

Methods

Genotyping for the TLR4 Asp299Gly and TLR4 Thr399Ile polymorphisms was performed using PCR-RFLP as previously described^[15]. Specifically, primers for TLR4 Asp299Gly were forward (5' GATTAGCATACTTAGACTACTACCTCCATG 3') and reverse (5' GATCAACTTCTGAAAAGCATTCCCAC 3'). Primers for TLR4 Thr399Ile were forward (5' GGTGCTGTTCTCAAAGTGATTTTGGGAGAA 3') and reverse (5' CCTGAAGA CTGGAGAGTGAGTTAAATGCT 3'). The underlined bases in both forward primers indicate the altered nucleotide to create a *Nco*I (TLR4 Asp299Gly) and a *Hinf*I (TLR4 Thr399Ile) restriction site, respectively. PCR reactions were run at 95 °C for 5 min followed by 35 cycles at 95 °C for 30 s, at 55 °C for 30 s, at 72 °C for 30 s, and a final incubation at 72 °C for 5 min. A 15- μ L aliquot of the product was digested with the appropriate restriction enzyme and electrophoresed in a 3% agarose gel to identify the TLR4 alleles on the basis of the respective allele size. After digestion, fragment sizes for carriers of the polymorphic allele decreased from 249 bp (wild-type) to 223 bp for the 299 residue, and from 406 bp (wild-type) to 377 bp for the 399 residue.

Genotyping for -159(C/T) of the CD14 gene was performed using the method described by Hubacek *et al*^[16]. In brief, the promoter of the CD14 receptor gene was amplified by the primers CDP-1 (5' TTGGTGCCAACAGATGAGGTTTCAC 3'), and CDP-2 (5' TTCTTTCCTACACAGCGGCACCC 3') under the following conditions: an initial denaturation at 95 °C for 5 min,

followed by 35 cycles at 92 °C for 40 s, at 62 °C for 35 s, and at 72 °C for 50 s. The final extension step was prolonged to 5 min. The 561 bp PCR product was digested with the restriction enzyme *Hae*III, into the fragments of 204, 201 and 156 bp in length in the presence of the wild-type allele. The variant allele showed a loss of one *Hae*III cleavage site, resulting in the presence of fragments 360 and 201 bp in length.

The cytosine insertion mutation was genotyped by a PCR amplification of specific allele assay using two allele-specific forward primers L1007fsinsCWTF: 5' CAGAAGCCCTCCTGCA GGCCCT 3' for the wild-type allele and L1007fsinsCMUTF: 5' CAGAAGCCCTCCTGCAGGCCCT 3' for the L1007fsinsC mutant allele, in combination with a common primer L1007fsinsCR: 5' TCTTCAACCACATCCCCATT 3', in two separate PCR reactions. The 3'-ends of the forward primers, were able to anneal to regions that differed between the two alleles. The PCR profile was as follows: initial denaturation at 95 °C for 5 min, followed by 35 cycles of denaturing at 94 °C for 45 s, annealing at 65 °C for 40 s and extension at 72 °C for 30 s and a final incubation at 72 °C for 10 min. The missense mutation R702W was genotyped by a PCR amplification of specific allele assay using two allele-specific forward primers R702WWTF: 5' ATCTGAGAAGGCCCTGCTCC 3' for the wild-type allele and R702WMUTF: 5' ATCTGAGAAGGCCCTGCTCT 3' for the R702W mutant allele, in combination with a common primer R702WR: 5' CCCACACTTAGCCTTGATG 3', in two separate PCR reactions. The 3'-ends of the forward primers, were able to anneal to regions that differed between the two alleles. The PCR profile was as follows: initial denaturation at 95 °C for 5 min, followed by 35 cycles of denaturing at 94 °C for 45 s, annealing at 53 °C for 40 s and extension at 72 °C for 30 s and a final incubation at 72 °C for 10 min. The missense mutation G908R created a restriction site for *Hha*I and was genotyped by a PCR-RFLP method (5' CCCAGCTCCTCCCTCTTC 3' and 5' AAGTCTGTAATGTAAAGCCAC 3'). The presence of a wild-type allele resulted in an intact 380 bp band, whereas the RFLP profile of the G908R variant was characterized by two bands of 138 bp and 242 bp. The PCR conditions were as follows: initial denaturation at 95 °C for 5 min, followed by 35 cycles of denaturing at 94 °C for 45 s, annealing at 53 °C for 40 s, extension at 72 °C for 30 s, and a final incubation at 72 °C for 10 min. All PCR assays were performed in a 50 μ L volume reaction containing 10 mmol/L Tris-HCl, pH 8.3, 50 mmol/L KCl, 2 mmol/L MgCl₂, 250 μ mol/L dNTPs, 0.20 μ mol/L concentration of each primer, 200 ng of genomic DNA and 2.5 U of Taq DNA polymerase (Promega). PCR products were electrophoresed on an agarose gel and visualized by ethidium bromide staining.

Statistical analysis

Odds ratios (OR) were calculated with the corresponding 95% confidence intervals (CI_{95%}). Frequencies and susceptibilities of mutations among CD, UC and controls were compared based on χ^2 distribution. All tests were 2-tailed with significance at $P < 0.05$. Inference was aided by GraphPad InStat (version 3.00, GraphPad Software Inc., San Diego, CA).

RESULTS

TLR4 Asp299Gly and Thr399Ile genotype carrier frequencies are summarized in Table 1. The 299Gly allele frequencies were 7.92%, 3.53%, and 3% in CD, UC and healthy controls, respectively. The frequency of the 299Gly allele was significantly higher in CD patients than in controls ($P = 0.026 < 0.05$, OR = 2.78 CI_{95%}: 1.088-7.103). The 299Gly allele was not found to be significantly associated with UC ($P = 0.77$, OR = 1.18 CI_{95%}: 0.37-3.74). No significant difference was found in the frequencies of the 399Ile polymorphism among CD or UC

patients and controls.

Allele and genotype frequencies of the polymorphism -159 (C/T) of the CD14 gene are presented in Table 2. T allele and TT genotype frequencies were increased in CD patients only compared to controls ($P = 0.0048 < 0.01$, OR = 1.73, CI_{95%}: 1.18-2.54 and $P = 0.047 < 0.05$, OR = 1.93, CI_{95%}: 1.00-3.72, respectively).

Concerning the *NOD2/CARD15* mutations, the overall presence in CD patients (81.7%; 98/120) was significantly higher than that in UC patients (47%; 40/85) ($P < 0.0001 < 0.01$, OR = 5.01, CI_{95%}: 2.67-9.38) or in healthy control individuals (21%; 21/100) ($P < 0.0001 < 0.01$, OR = 16.76 CI_{95%}: 8.60- 32.67) (Table 3). A significant association was found between ileal disease and possession of one or more variant alleles. For each *NOD2/CARD15* variant, allele frequencies for overall ileal involvement (ileal disease and ileocolitis) were significantly different from non-ileal diseases (R702W ileal 8.3%, non-ileal 1.7%, $P = 0.014 < 0.05$; G908R ileal 12.1%, non-ileal 2%, $P < 0.0001 < 0.01$; and L007fsincC ileal 17.1%, non-ileal 0.83% $P < 0.0001 < 0.01$).

Co-existence of the TLR4 polymorphic allele and the T allele of the polymorphism -159 (C/T) of the CD14 gene was observed in 12 CD patients (10%), in 5 UC patients (5.88%) and in 4 healthy controls (4%). Notably, there was a higher percentage of mutated allele coexistence in CD patients compared to UC or healthy subjects, suggesting that coexistence might increase the susceptibility to CD. However the χ^2 of CD *versus* the

controls was marginal ($P = 0.08$) and that of UC *versus* the controls was not significant.

Among the 98 CD patients harboring *NOD2/CARD15* variants, 9 (9.2%) were found to carry also a TLR4 polymorphic allele, whereas among the 40 UC patients harboring *NOD2/CARD15* variants, 5 (12.5%) were found to carry also a TLR4 polymorphic allele. None of the 21 healthy controls harboring *NOD2/CARD15* variants was found carrying a TLR4 polymorphic allele. This indicated that coexistence of mutations in these genes could also increase the risk for IBD. However, there was no significantly increased risk of association with the disease.

As indicated in Table 4, the TT genotype and T allele frequencies of the -159(C/T) polymorphism in the CD14 gene increased in CD patients harboring at least one variant of the *NOD2/CARD15*, compared to controls. The odds of developing CD significantly increased in either case ($P = 0.012 < 0.05$, OR = 9.4 CI_{95%}: 1.18-74.40, and $P = 0.003 < 0.01$, OR = 1.45 CI_{95%}: 1.48-6.81, for the T genotype and TT allele respectively).

Four of the CD patients (3.3%), 3 of the UC patients (3.5%) and none of the healthy controls were found to carry simultaneously a polymorphic allele of all the genes tested.

Additionally, 62 out of 120 (51.67%) of the CD patients were carriers of a TLR4 and/or CD14 polymorphic allele and at least one variant of the *NOD2/CARD15*, compared to 23 out of 85 (27%) of the UC patients ($P = 0.0004 < 0.01$, OR = 2.88 CI_{95%}:

Table 1 TLR4 Asp299Gly and Thr399Ile genotype carriers in CD and UC patients and healthy individuals

Group	TLR4 Asp299Gly genotype					TLR4 Thr399Ile genotype				
	Asp/Asp	Asp/Gly	Gly/Gly	299Gly allele frequencies (%)	OR	Thr/Thr	Thr/Ile	Ile/Ile	399Ile allele frequencies (%)	OR
CD	103	15	2	7.92	2.78 ^a	119	1	0	0.42	0.41 ^a
UC	79	6	0	3.53	1.18	82	3	0	1.76	1.78
Controls	95	4	1	3	98	2	0	1		

^a $P < 0.05$ vs control group.

Table 2 Allele and genotype frequencies of the promoter polymorphism at position -159 of the CD14 gene in CD and UC patients and healthy controls

Group	Alleles				Genotypes				
	C	T	T allele frequencies (%)	OR	CC	CT	TT	TT genotype frequencies (%)	OR
CD	119	121	50.42	1.73 ^b	33	53	34	28.33	1.93 ^a
UC	102	68	40	1.13	32	38	15	17.65	1.046
Controls	126	74	37		43	40	17	17	

^a $P < 0.05$, ^b $P < 0.01$, vs control group.

Table 3 *NOD2/CARD15* mutant allele frequencies in Crohn's disease (CD) patients, in ulcerative colitis (UC) patients and controls

Samples		Genotype			Allele frequency (%)	OR
		1	2	3		
R702W	CD	96	24	0	10	11.05 ^b
	UC	73	12	0	7.1	7.52 ^b
	Control	98	2	0	1	
G908R	CD	87	32	1	14.2	4.51 ^b
	UC	63	21	1	13.5	4.31 ^b
	Control	93	7	0	3.5	
L1007fsincC	CD	79	39	2	17.9	3.42 ^b
	UC	79	6	0	3.5	0.57
	Control	88	12	0	6	

1: homozygous wild-type; 2: heterozygous; 3: homozygous mutant, ^b $P < 0.01$ vs UC group and control group.

Table 4 Allele and genotype frequencies of the promoter polymorphism at position -159 of the CD14 gene

CD14 genotypes	Genotyped for the <i>CARD15/NOD2</i> gene					
	CD		UC		Controls	
	No variant (n = 47)	At least one variant (n = 73)	No variant (n = 49)	At least one variant (n = 36)	No variant (n = 81)	At least one variant (n = 19)
CC	17	16	18	14	34	9
CT	21	32	23	15	31	9
TT, n (%)	9 (19.1)	25 (34.2) (P = 0.012) ^a	8 (16.3)	7 (19.4) (P = 0.156)	16 (19.7)	1 (5.3)
CD14 Alleles						
C, n (%)	55 (58.5)	64 (43.8)	59 (60.2)	43 (59.7)	99 (61.1)	27 (71)
T, n (%)	39 (41.5)	82 (56.2) (P = 0.003) ^b	39 (39.8)	29 (40.3) (P = 0.24)	63 (38.8)	11 (28.9)

^aP<0.05, ^bP<0.01 vs control group.

1.88-5.24). It should be pointed out that both frequencies significantly increased in CD and UC as compared to the 10% frequency of multiple carriers found in healthy controls ($P<0.0001<0.01$, OR=9.62 CI_{95%}: 4.56-20.27 and $P=0.002<0.01$, OR= 3.34, CI_{95%}: 1.48-7.50, for CD and UC respectively). Consequently, the co-existence of a mutation in either the TLR4 or CD14 gene and in *NOD2/CARD15* increased the risk for developing CD.

DISCUSSION

Crohn's disease and ulcerative colitis are multifactorial diseases with a polygenic nature. Despite both being chronic disorders of the gastrointestinal tract with unknown etiology, an abnormal inflammatory response directed against the enteric microflora in a genetically susceptible host has been postulated as a possible explanation^[17]. In human system, the TLR4.MD2.CD14 complex has been demonstrated to serve as a surface receptor for LPS^[18]. In addition to the cell surface TLR4 complex, there is evidence that mammalian cells have an intracellular receptor that could detect LPS in the cytoplasm of infected cells^[19]. These data suggest that TLRs and members of the NOD family represent another innate immune system for the recognition of a wide array of pathogen products^[20].

Our study dealt with the relationship between the major mutations in TLR4, CD14 and *CARD15/NOD2* genes singularly and in combination, and IBD in a Greek population.

Regarding the TLR4, Cario and Podolsky^[9] recently showed that TLR4 was strongly up-regulated in CD and UC, which may be caused by an exaggerated host defense reaction of the intestinal epithelium to endogenous luminal bacterial flora. It was intriguing to hypothesize that the Asp299Gly allele of the TLR4 gene could be related to such an imbalanced reaction. Our findings indicate that the frequency of the 299Gly allele was significantly higher in CD patients compared to UC patients and controls and support the hypothesis that innate immunity may play a role in Crohn's disease pathogenesis. Our results differ from those of a recent study in 86 UC patients of Japanese population in whom this mutation could not be detected^[21]; however, our results are in accordance with those of recent studies in European patients^[22,23]. Nevertheless, it is well known that the frequency of the mutations varies in different populations^[24,25].

Concerning the CD14 gene, functional relevance between T allele and increased expression of CD14, has been demonstrated previously^[26]. A significant increase of the T allele and the TT genotype was found exclusively among CD patients. Our results are in agreement with those from a recent study by Klein *et al*^[12] but differ from those of a cohort in a Japanese population^[27]. However, they demonstrated a

significant association of the T allele and TT genotype frequencies with UC^[27].

Regarding *NOD2/CARD15*, all the three risk alleles were more common in patients with IBD than in the control Greek population. The frequencies of the R702W and L1007fsinsC mutations were significantly higher in CD patients compared to UC patients and controls, whereas the frequency of the G908R mutation was similar in CD and UC patients but significantly higher compared to controls. Our results concerning the presence of L1007fsinsC in Greek population differ from those of a recent study in a Cretan population whose incidence was only 5.3%^[28]. This inconsistency may be attributed to the fact that Crete is an isolated geographic region with a homogenous population dispersed over a small geographic area where this mutation does not seem to predispose to the disease or to the relatively small size of the examined sample^[28]. Collectively our study confirmed previous studies, which reported, increased mutation carrier frequencies of one of the three variant alleles in CD patients compared to UC patients or healthy controls^[6,29]. However, in contrary to the previously mentioned European studies, which reported that mutation frequencies in UC patients are comparable with those found in healthy controls. The allelic frequencies of R702W and G908R appeared to be higher in our UC patients than those found in healthy individuals. Interestingly, very recently Andriulli *et al*^[30] reported a significant association between the L1007fsincC mutation and UC, although at a lower frequency in comparison with that observed in CD patients, suggesting a possible involvement of the *NOD2/CARD15* also in UC patients^[30]. Our findings may indicate the contribution of *NOD2/CARD15* variants to the pathogenesis of UC in our population as well, or may reflect the well known difficulty to classify correctly from the onset in all the patients with inflammatory bowel disease.

Co-existence of TLR4 and CD14 mutated alleles was higher in CD patients compared to UC or healthy subjects, but this association was not significant. Additionally, there was no significantly increased risk of IBD related to the coexistence of mutations in TLR4 and in *CARD15/NOD2*. On the contrary, it is of interest that the T allele in the TT genotype appeared to increase the relative risk for developing CD in combination with at least one variation in the *CARD15/NOD2* gene. These results, are in accordance with a recent study by Klein *et al*^[13], suggesting that as both CD14 and *CARD15/NOD2* genes are involved in the recognition of LPS and subsequent activation of NFκ-B, disturbed activation of the innate immune system by bacterial antigens may be crucial in some patients with CD.

Co-existence of mutations in all the three genes was found in only a small fraction of the CD or UC patients. But as mentioned earlier, the extracellular complex TLR4.MD2.CD14

and the intracellular *CARD15/NOD2* might participate in the regulation of innate immune responses to intestinal microflora. This seemed to point to the danger of IBD development in patients with at least one mutated allele in TLR4 and/or CD14 and at least one variant of *CARD15/NOD2*. Our results indicate that, co-existence of a mutation in either the TLR4 or CD14 gene and in *NOD2/CARD15* is associated with an increased susceptibility to CD or UC.

In conclusion, the Greek population suffering from IBD most likely carry polymorphisms in one or more of the genes related to the innate immune system. However, further research in larger and diverse populations is needed to elucidate the biological mechanism behind IBD susceptibility. Understanding the influence of predisposing genes can lead to a more precise diagnosis and permit the development of personalized medicines.

REFERENCES

- Hugot JP, Thomas G. Genome-wide scanning in inflammatory bowel diseases. *Dig Dis* 1998; **16**: 364-369
- Strober W, Ludviksson BR, Fuss IJ. The pathogenesis of mucosal inflammation in murine models of inflammatory bowel disease and Crohn disease. *Ann Intern Med* 1998; **128**: 848-856
- Heumann D, Glauser MP, Calandra T. Molecular basis of host-pathogen interaction in septic shock. *Curr Opin Microbiol* 1998; **1**: 49-55
- Herz U, Lacy P, Renz H, Erb K. The influence of infections on the development and severity of allergic disorders. *Curr Opin Immunol* 2000; **12**: 632-640
- Bonen DK, Ogura Y, Nicolae DL, Inohara N, Saab L, Tanabe T, Chen FF, Foster SJ, Duerr RH, Brant SR, Cho JH, Nunez G. Crohn's disease-associated NOD2 variants share a signaling defect in response to lipopolysaccharide and peptidoglycan. *Gastroenterology* 2003; **124**: 140-146
- Hugot JP, Chamaillard M, Zouali H, Lesage S, Cezard JP, Belaiche J, Almer S, Tysk C, O'Morain CA, Gassull M, Binder V, Finkel Y, Cortot A, Modigliani R, Laurent-Puig P, Gower-Rousseau C, Macry J, Colombel JF, Sahbatou M, Thomas G. Association of NOD2 leucine-rich repeat variants with susceptibility to Crohn's disease. *Nature* 2001; **411**: 599-603
- Ogura Y, Bonen DK, Inohara N, Nicolae DL, Chen FF, Ramos R, Britton H, Moran T, Karaliuskas R, Duerr RH, Achkar JP, Brant SR, Bayless TM, Kirschner BS, Hanauer SB, Nunez G, Cho JH. A frameshift mutation in NOD2 associated with susceptibility to Crohn's disease. *Nature* 2001; **411**: 603-606
- Medzhitov R, Janeway CA. Innate immunity: impact on the adaptive immune response. *Curr Opin Immunol* 1997; **9**: 4-9
- Cario E, Podolsky DK. Differential alteration in intestinal epithelial cell expression of toll-like receptor 3 (TLR3) and TLR4 in inflammatory bowel disease. *Infect Immun* 2000; **68**: 7010-7017
- Kopp EB, Medzhitov R. The Toll-receptor family and control of innate-immunity. *Curr Opin Immunol* 1999; **11**: 13-18
- Arbour NC, Lorenz E, Schutte BC, Zabner J, Kline JN, Jones M, Frees K, Watt JL, Schwartz DA. TLR4 mutations are associated with endotoxin hyporesponsiveness in humans. *Nat Genet* 2000; **25**: 187-191
- Klein W, Tromm A, Griga T, Fricke H, Folwaczny C, Hocke M, Eitner K, Marx M, Duerig N, Epplen JT. A polymorphism in the CD14 gene is associated with Crohn disease. *Scand J Gastroenterol* 2002; **37**: 189-191
- Klein W, Tromm A, Griga T, Folwaczny C, Hocke M, Eitner K, Marx M, Duerig N, Epplen JT. Interaction of polymorphisms in the CARD15 and CD14 genes in patients with Crohn disease. *Scand J Gastroenterol* 2003; **38**: 834-836
- Podolsky DK. Inflammatory bowel disease (1). *N Engl J Med* 1991; **325**: 928-937
- Lorenz E, Hallman M, Marttila R, Haataja R, Schwartz DA. Association between the Asp299Gly polymorphisms in the Toll-like receptor 4 and premature births in the Finnish population. *Pediatr Res* 2002; **52**: 373-376
- Hubacek JA, Rothe G, Pit'ha J, Skodova Z, Stanek V, Poledne R, Schmitz G. C(-260)--&T polymorphism in the promoter of the CD14 monocyte receptor gene as a risk factor for myocardial infarction. *Circulation* 1999; **99**: 3218-3220
- Fiocchi C. Inflammatory bowel disease: etiology and pathogenesis. *Gastroenterology* 1998; **115**: 182-205
- Aderem A, Ulevitch RJ. Toll-like receptors in the induction of the innate immune response. *Nature* 2000; **406**: 782-787
- Philpott DJ, Yamaoka S, Israel A, Sansonetti PJ. Invasive *Shigella flexneri* activates NF-kappa B through a lipopolysaccharide-dependent innate intracellular response and leads to IL-8 expression in epithelial cells. *J Immunol* 2000; **165**: 903-914
- Inohara N, Ogura Y, Chen FF, Muto A, Nunez G. Human Human Nod1 confers responsiveness to bacterial lipopolysaccharides. *J Biol Chem* 2001; **276**: 2551-2554
- Okayama N, Fujimura K, Suehiro Y, Hamanaka Y, Fujiwara M, Matsubara T, Maekawa T, Hazama S, Oka M, Nohara H, Kayano K, Okita K, Hinoda Y. Simple genotype analysis of the Asp299Gly polymorphism of the Toll-like receptor-4 gene that is associated with lipopolysaccharide hyporesponsiveness. *J Clin Lab Anal* 2002; **16**: 56-58
- Franchimont D, Vermeire S, El Housni H, Pierik M, Van Steen K, Gustot T, Quertinmont E, Abramowicz M, Van Gossum A, Deviere J, Rutgeerts P. Deficient host-bacteria interactions in inflammatory bowel disease? The toll-like receptor (TLR)-4 Asp299gly polymorphism is associated with Crohn's disease and ulcerative colitis. *Gut* 2004; **53**: 987-992
- Torok HP, Glas J, Tonenchi L, Mussack T, Folwaczny C. Polymorphisms of the lipopolysaccharide-signaling complex in inflammatory bowel disease: association of a mutation in the Toll-like receptor 4 gene with ulcerative colitis. *Clin Immunol* 2004; **112**: 85-91
- Pena AS. Genetics of inflammatory bowel diseases--past, present, and future. *Dig Dis* 2003; **21**: 85-90
- Arnott ID, Nimmo ER, Drummond HE, Fennell J, Smith BR, MacKinlay E, Morecroft J, Anderson N, Kelleher D, O'Sullivan M, McManus R, Satsangi J. NOD2/CARD15, TLR4 and CD14 mutations in Scottish and Irish Crohn's disease patients: evidence for genetic heterogeneity within Europe? *Genes Immun* 2004; **5**: 417-425
- Baldini M, Lohman IC, Halonen M, Erickson RP, Holt PG, Martinez FD. A Polymorphism* in the 5' flanking region of the CD14 gene is associated with circulating soluble CD14 levels and with total serum immunoglobulin E. *Am J Respir Cell Mol Biol* 1999; **20**: 976-983
- Obana N, Takahashi S, Kinouchi Y, Negoro K, Takagi S, Hiwatashi N, Shimosegawa T. Ulcerative colitis is associated with a promoter polymorphism of lipopolysaccharide receptor gene, CD14. *Scand J Gastroenterol* 2002; **37**: 699-704
- Roussomoustakaki M, Koutroubakis I, Vardas EM, Dimoulios P, Kouroumalis EA, Baritaki S, Koutsoudakis G, Krambovitis E. NOD2 insertion mutation in a Cretan Crohn's disease population. *Gastroenterology* 2003; **124**: 272-273; author reply 273-274
- Ahmad T, Armuzzi A, Bunce M, Mulcahy-Hawes K, Marshall SE, Orchard TR, Crawshaw J, Large O, de Silva A, Cook JT, Barnardo M, Cullen S, Welsh KI, Jewell DP. The molecular classification of the clinical manifestations of Crohn's disease. *Gastroenterology* 2002; **122**: 854-866
- Andriulli A, Annese V, Latiano A, Palmieri O, Fortina P, Ardizzone S, Cottone M, D'Inca R, Riegler G. The frame-shift mutation of the NOD2/CARD15 gene is significantly increased in ulcerative colitis: an *IG-IBD study. *Gastroenterology* 2004; **126**: 625-627

Ultrastructural changes in non-specific duodenitis

Cheng-Xin Wang, Li-Jiang Liu, Jing Guan, Xiao-Ling Zhao

Cheng-Xin Wang, Li-Jiang Liu, Jing Guan, Xiao-Ling Zhao, Department of Pathology and Pathophysiology, School of Medicine and Life Sciences, Jiangnan University, Wuhan 430056, Hubei Province, China

Correspondence to: Cheng-Xin Wang, Department of Pathology and Pathophysiology, School of Medicine and Life Sciences, Jiangnan University, Wuhan 430056, Hubei Province, China. wangchengxin2000@yahoo.com.cn

Telephone: +86-27-82411803 **Fax:** +86-27-82411803

Received: 2004-02-21 **Accepted:** 2004-04-05

Abstract

AIM: To investigate the ultrastructural and morphological changes of non-specific duodenitis (NSD) in an attempt to grade them according to the extent of the lesions.

METHODS: Biopsies were taken from the mucosa of duodenal bulb of 44 patients selected from the patients undergoing upper gastrointestinal endoscopy for epigastric discomforts. From each patient, two pinch biopsies on the same area were obtained from duodenal bulb. One was for scanning electron microscopy and the other was stained with hematoxylin-eosin, Warthin-Starry silver and both were then examined under light microscope. A total of 12 specimens (three from each degree of the normal and I-III of NSD diagnosed and graded by histology) selected from the 44 patients were dehydrated, critical point dried, coated with gold palladium and examined under a JEOL JSM-30 scanning electron microscope (SEM) at 20 kV.

RESULTS: According to the ultrastructural morphologic changes, non-specific duodenitis was divided into normal (as control group), mild, moderate and severe degrees according to results of SEM. The normal villi of duodenal bulb were less than 0.2 mm. There were inflammation cells, occasionally red blood cells and macrophages on the mucosal epithelial surface. Erosion and desquamation of epithelium could be seen. Three cases (25%, 3/12) had gastric metaplasia and *Helicobacter pylori* (*H. pylori*) infection could be found in 5 cases (41.67%, 5/12) in duodenal bulb mucosa. The most distinctive feature was the ulcer-like defect on the surface of epithelial cells.

CONCLUSION: Non-specific duodenitis is a separate entity disease caused by different factors. SEM is of value as an aid in the diagnosis of mucosal diseases of duodenum.

© 2005 The WJG Press and Elsevier Inc. All rights reserved.

Key words: Non-specific duodenitis; Intestinal Mucosa; Ultrastructural organization

Wang CX, Liu LJ, Guan J, Zhao XL. Ultrastructural changes in non-specific duodenitis. *World J Gastroenterol* 2005; 11(5): 686-689

<http://www.wjgnet.com/1007-9327/11/686.asp>

INTRODUCTION

Chronic duodenitis is a common disease which might be a separate entity or accompanied with duodenal ulceration and also a common clinical symptom of dyspepsia^[1,2]. Chronic duodenitis could be divided into three types according to their endoscopic, histological, and etiologic findings^[3]. Histologically chronic duodenitis was divided into two principal forms: primary (non-specific duodenitis, NSD) form which is usually restricted to the duodenal bulb and the first part of duodenum^[4], and secondary (specific) form which has been found in association with various other disorders such as Crohn's disease, sarcoidosis, aspirin ingestion and stress^[3]. The diagnosis of NSD is frequently made both endoscopically and histopathologically and many research articles have documented it^[3-13]. Ultrastructural morphological study of NSD with scanning electron microscope has been seldom reported. Therefore, we carried out the present study on the ultrastructural changes of non-specific duodenitis.

MATERIALS AND METHODS

Materials

Multiple biopsies from 44 patients selected from the patients who underwent routine upper gastrointestinal endoscopy for a variety of reasons including epigastric pain or discomforts, heartburn *etc.* were taken from the mucosa duodenal bulb. Patients with active duodenitis and duodenal ulcers were excluded from this study. Specimens for SEM were obtained from 12 of 44 patients, five women and seven men with an age range of 19-62 years and an average age of 37.0±12.9 years. No attempt was made to match the morphologic changes with the clinical symptoms.

Methods

Biopsies were obtained through endoscopic biopsy forceps directly at the endoscopically abnormal mucosa in each area or randomly at the site if the mucosa appeared normal from the duodenal bulb. At each endoscopy two pinch biopsies on the same area were obtained from the duodenal bulb mucosa. One was for SEM, the other for light microscopy. Each biopsy specimen was then oriented.

The material used for light microscopy was immediately fixed in 40 g/L formaldehyde, dehydrated in a graded series of ethyl alcohol solution, embedded in paraffin and cut into 3-4 μm thick sections. These specimens were stained with hematoxylin-eosin, Warthin-Starry silver (for the identification of the *H. pylori* infection) and then examined with light microscopy. All histological evaluations were performed blindly regardless of the endoscopic diagnosis by one pathologist. According to the extent of lesions, non-specific duodenitis was divided into normal (as control group), mild, moderate and severe degrees respectively referring to the Whitehead's classification and literature^[1-3,5-7].

A total of 12 specimens (three from each degree of NSD diagnosed and graded by histology) selected for SEM were placed immediately into 25 g/L glutaraldehyde in phosphate buffer, pH 7.4. After post-fixation and mucus removal, tissues

were dehydrated in a graded series of acetone, critical point dried using liquid carbon dioxide as an exchange medium. After mounted onto stubs by means of quick drying silver paint, the specimens were sputter coated with gold palladium to a thickness of approximately 25 nm and examined under a JEOL JSM-30 scanning electron microscope at 20 kV.

RESULTS

The morphologic changes of mucosal biopsies from the duodenal bulb showed various patterns. Ultrastructural alterations in NSD were restricted to the surface epithelial cells. Corresponding to the degrees of histological and endoscopic examination, NSD was also divided into the normal, mild, moderate and severe degrees. The details were as follows. The specimens taken from the normal duodenal bulb mucosa showed the villi in uniform shapes and sizes such as leaf-like or fingerlike villous patterns with no surface exudates and intraluminal cells adhered to the surface (Figure 1A). The majority of villi (over 90%) were less than 0.2 mm. The epithelial cells were related to five to seven adjacent cells. Each cell surface was therefore five-seven sided but the sides were not equal in length. There were no gaps between adjacent cells. Mild degree of NSD had

deformed and enlarged villi and its surface epithelial cells exhibited minor alterations with some exudates on the surface of the duodenal mucosa (Figure 1B). The villi were adhered and integrated. Parts of villi were greater than 0.2 mm but less than 0.3 mm. Moderate degree of NSD, had broader, swollen, lodging, shorter and flattened villi with convoluted or cerebroid patterns, and the minority of villi were greater than 0.4 mm (Figure 1C). Some areas of the duodenal mucosa were covered with mucus, which was mass or band-like secreted from the crypts. The most distinctive morphologic alteration was the ulcer-like defect on the surface of epithelial cells of villi (Figure 1D). The edge of the defect was abrupt and the bottom was rugged. In the defect there were inflammatory cells just as there were inflammatory cells and intraepithelial cells found in light microscopy. Epithelial cells around the defect were relatively normal. Severe degree of NSD had subtotal or total villous atrophy and severe erosion, in large areas of the mucosa covered with mucous exudates and hemorrhage and accompanied desquamation of epithelial cells (Figure 1E).

In degrees I-III of NSD, there were cells on the epithelial surface of the villi which had the SEM features of lymphocytes, red blood cells and a few macrophages, neutrophils (Figure 1F). The epithelial cells of gastric metaplasia (manifested as replacement

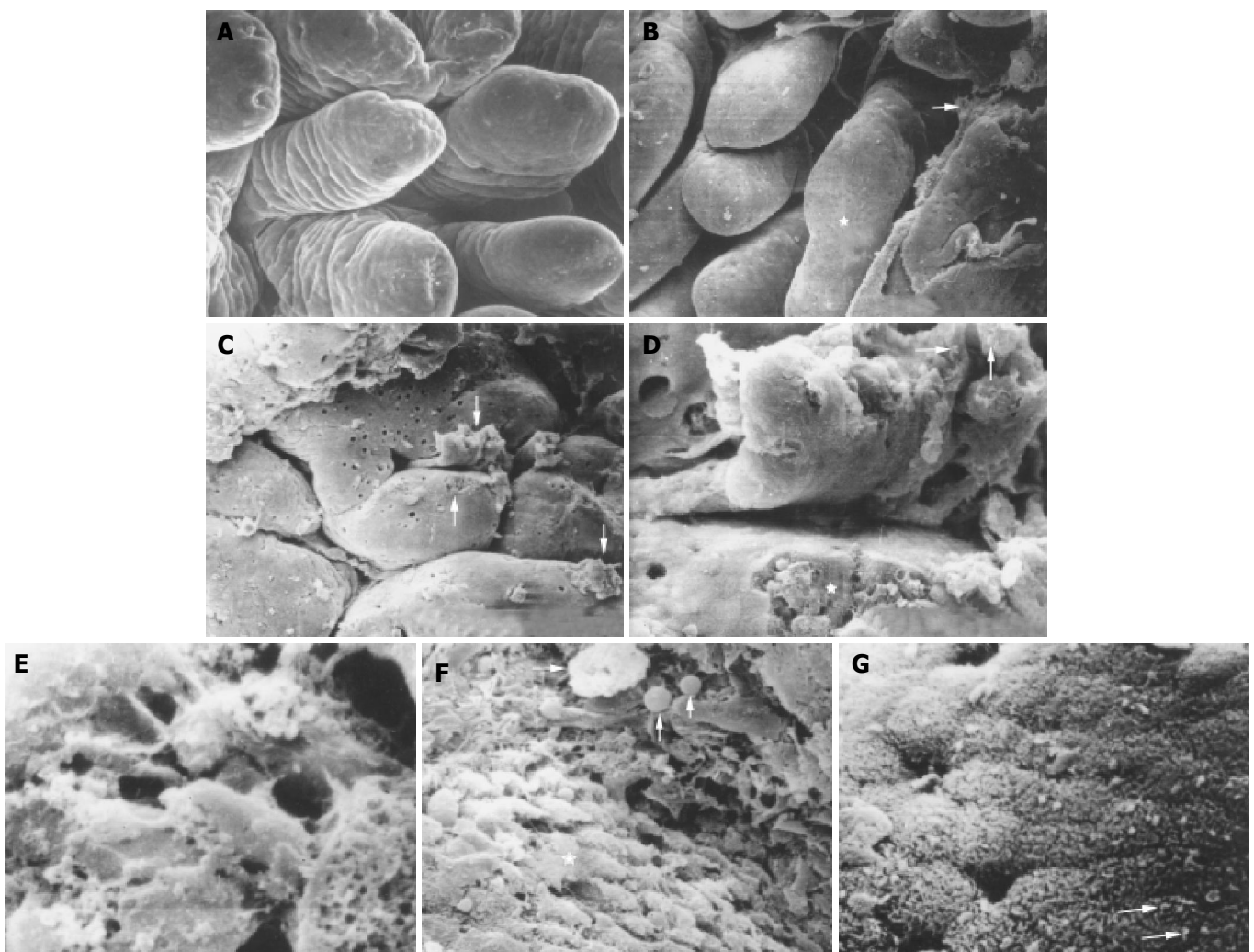


Figure 1 Photomicrograph of scanning electron microscopy of non-specific duodenitis. A: Villi in uniform shapes of leaf-like or fingerlike pattern of normal duodenal bulb mucosa. $\times 200$; B: Deformed and integrated villi (asterisk) and exudates (arrow) in degree II of NSD. $\times 100$; C: Broadened, flattened, convoluted or cerebroid villi, masses or band-like mucus (arrows), ulcer-like defect on the surface of a villus (long arrow) in degree II of NSD. $\times 100$; D: Ulcer-like defect (asterisk) and a few of *H. pylori* (arrows) in mucus. $\times 2\,500$; E: Mucus and severe erosion on the surface of mucosa in degree III of NSD. $\times 500$; F: Macrophages (long arrow) and inflammatory cells (arrows) on the surface of mucosa and gastric metoplasia cells (asterisk). $\times 2\,200$; G: *H. pylori* in S-shape on the microvilli of epithelial cells (arrows). $\times 3\,200$.

of the enterocytes of the villi by cells resembling the mucus-secreting surface cells of the stomach) with dome-shaped surface (Figure 1F) could also be found on the mucosa of three out of twelve patients (25%, 3/12). They were loosely arranged, and there were gaps between adjacent cells and a single cell loss or desquamation could be seen (Figure 1F). These might be the results of inflammatory edema due to inflammatory cells related to these gaps and the epithelial cell surface. A few bacteria were found on the microvilli of epithelial cells mainly on gastric metaplasia type, occasionally on intestinal type and luminal surface of the mucus (Figures 1D, G). Bacteria were found on the surface of five out of the twelve patients with NSD. According to the bacterial morphologic features curved in their long axis or S-shaped type found in SEM and based on the result of Warthin-Starry silver staining, the bacteria belonged to *H pylori*. No *H pylori* L-form was found in this study as reported by Wang *et al*^[14]. The incidence of *H pylori* on the mucosa of NSD in this limited sample was 41.67% (5/12), which was higher than that from literature reports^[8,13] and lower than that from the report of Qian *et al*^[15]. *H pylori* infection was not found in non-ulcer dyspepsia patients^[13]. This difference might result from different methods. Of course the most sensitive and accurate method was PCR for the diagnosis of *H pylori* infection^[16].

DISCUSSION

Endoscopic and histological changes of inflammation often occurring in the mucosa of duodenal bulb in association with peptic ulcer and similar change in the absence of frank ulceration are termed non-specific duodenitis and common duodenitis, chronic duodenitis, peptic duodenitis, gastroduodenitis, *etc.*

There are different methods of classification of NSD, including clinical, endoscopic and histologic classifications. As for grading the NSD according to SEM there are few reports in the literature, except for a few papers which describe the surface morphological characteristics of villi, and the bacteria on the epithelial surface of gastroduodenal mucosa^[7,17,18]. The grading of NSD by light microscopy is based on the inflammatory cell counts^[6,7], whereas the grading of NSD by scanning electron microscopy is based on the surface morphologic alterations of the duodenal bulb mucosa as revealed in this study.

The controversy as to whether NSD is a separate entity or whether it is only a stage of ulcer disease has been confused by the contradictory observations that in some patients duodenitis progressed to duodenal ulceration while in others it did not. Scott *et al*^[6] did contrast study of 16 pairs of patients with and without duodenal ulcer, which exactly matched for grade of duodenitis and the results supported the similarity of the two conditions. Our another study of NDS with inflammatory cell counts of lamina propria showed a significant change in degrees I-III of NSD compared with the normal. This article shows that NSD could also be divided into the normal and degrees I-III by SEM. These results could confirm the opinion that NSD is a separate entity disease based on ultrastructural morphology.

As its name implies, the cause of NSD is not very clear. There is evidence that the condition could be a part of the duodenal ulcer. Because of the coexistence of DU and duodenitis in surgical specimens, some authors^[3,6,11] suggest that increased acid secretion and ethanol might have an important role in the pathogenesis of NSD based on the histological changes and the response to cimetidine therapy which would initially cause duodenitis. After prolonged exposure duodenal ulcer, *H pylori* infection could also play a key role in the pathogenesis for gastroduodenal disease^[8,19-22] and is an independent risk factor of chronic inflammation in duodenal

bulb^[8]. Since *H pylori* was first isolated in 1983, *H pylori* related diseases have become the hot spot of gastroenterological studies^[17,23-26]. This organism infection not only relates to gastroduodenitis and most peptic ulcer^[13,20,24,26] but also closely relates to gastric carcinomas and mucosa-associated lymphoid tissue lymphoma. *H pylori* previously named *Compylobacter Pylori*, has a lot of characteristics such as the typical s-shape, the corkscrew-like movement and the powerful urease enzyme. These allow a rapid movement through the mucous layer to adhere directly to the membranes of the surface mucous cells. Under certain unfavorable conditions *H pylori* could transform into L-form by which it can escape the body's immune response^[14]. Some metabolic products of the bacteria have chemotactic properties that could cause an intense inflammation and some products of *H pylori* have immunosuppressive effects on prolonging the infection^[14]. White blood cells are attracted towards the chemotaxins, adhere to the vascular endothelium, emigrate between the endothelial cell junctions by amoeboid movement through venule into the mucosal surface^[27] as indicated by the photomicrograph in this study. *H pylori* could be phagocytosed by invading polymorphonuclear leukocytes, macrophages and worsened inflammatory response^[7,19,27], inducing several ultrastructural alterations such as edema of mucosa, architectural distortion of villi, epithelial damage, erosion, necrotic lesion and ulcer-like defect on the epithelium. These observations clearly demonstrate that pathological alterations in the ultrastructural level are induced mainly by *H pylori* with the result of disrupted mucosal barrier of duodenal bulb. *H pylori* was found on either gastric metaplasia epithelial cells or intestinal type cells in our study which differs from Steer's^[18] report that *H pylori* only existed on the surface of the gastric-type epithelial cells. The diagnosis of *H pylori* with SEM should be one of the gold standards. As for gastric metaplasia it might be normal. However, most observers consider it as a sign of severe duodenitis. As to the relationship between *H pylori* and gastric metaplasia, some authors^[18,25] hold that *H pylori* closely relates to gastric metaplasia, others suggest that *H pylori* has no major role in the development of gastric metaplasia in duodenal bulb, which is more common in DU patients^[13,23,24,26,28]. The present study indicates that NSD is a separate entity disease caused by multiple factors such as toxic dietary components, hyperacidity, ethanol, nonsteroidal anti-inflammatory drugs and especially *H pylori* infection^[3,8,22]. If the pathogenetic factors remain, duodenal ulceration may ensue on the basis of severe inflammation, desquamation, erosion, necrosis and the ulcer-like defect on the epithelial surface of duodenal bulb. The detailed relations between NSD, *H pylori* infection and gastric metaplasia still remain to be studied.

In conclusion, SEM is of value as an aid in the diagnosis of mucosal biopsies of duodenum and can improve the diagnostic criteria of NSD.

ACKNOWLEDGEMENTS

We are grateful to Professor Xiao-Nan You, Faculty of Foreign Studies, Hubei University, for her kind assistance in linguistic instruction of this article.

REFERENCES

- 1 Rosai J. Ackerman's Surgical Pathology. Trans. Hui YZ. 8th ed, Vol. one, Shenyang, Liaoning Edu Pub 1999: 619-620
- 2 Toukan AU, Kamal MF, Amr SS, Arnaout MA, Abu-Romiyeh AS. Gastroduodenal inflammation in patients with non-ulcer dyspepsia. A controlled endoscopic and morphometric study. *Dig Dis Sci* 1985; **30**: 313-320
- 3 Konorev MR, Litviakov AM, Matveenkov ME, Krylov IuV, Kovalev AV, Riashchikov AA. Principles of current classifica-

- tion of duodenitis. *Klin Med (Mosk)* 2003; **81**: 15-20
- 4 **Gong LB**, Yang X, Zhang WW, Li SL, Sun SY. Study on the content of serum epidermal growth factor, gastric acid secretion and serum gastrin in duodenitis. *China Nati J New Gastroenterol* 1996; **2**: 228-229
 - 5 **Elta GH**, Appelman HD, Behler EM, Wilson JA, Nostrant TJ. A study of the correlation between endoscopic and histological diagnoses in gastroduodenitis. *Am J Gastroenterol* 1987; **82**: 749-753
 - 6 **Scott BB**, Goodall A, Stephenson P, Jenkins D. Duodenal bulb plasma cells in duodenitis and duodenal ulceration. *Gut* 1985; **26**: 1032-1037
 - 7 **Hasan M**, Hay F, Sircus W, Ferguson A. Nature of the inflammatory cell infiltrate in duodenitis. *J Clin Pathol* 1983; **36**: 280-288
 - 8 **Voutilainen M**, Juhola M, Farkkila M, Sipponen P. Gastric metaplasia and chronic inflammation at the duodenal bulb mucosa. *Dig Liver Dis* 2003; **35**: 94-98
 - 9 **White NA**, Tyler DE, Blackwell RB, Allen D. Hemorrhagic fibrinonecrotic duodenitis-proximal jejunitis in horses: 20 cases (1977-1984). *J Am Vet Med Assoc* 1987; **190**: 311-315
 - 10 **Shklyayev AE**, Nikitin EN, Malakhova IG. Electrokinetic properties of cells in chronic duodenal diseases. *Klin Lab Diagn* 2003; **12**: 33-35
 - 11 **Tang HF**, Chen XX, Gu WZ, Ye HY, Ou BY. Histopathological changes of duodenal salami ulcer in children. *Zhonghua Erke Zazhi* 2003; **41**: 849-851
 - 12 **Zhou J**, Zhang J, Xu C, He L. *cagA* genotype and variants in Chinese *Helicobacter pylori* strains and relationship to gastroduodenal diseases. *J Med Microbiol* 2004; **53**: 231-235
 - 13 **Hsu CT**, Yeh C, Cheng HH. *Helicobacter pylori*, gastritis and duodenitis in the healing process of duodenal ulcer. *J Formos Med Assoc* 1992; **91**: 81-84
 - 14 **Wang KX**, Chen L. *Helicobacter pylori* L-form and patients with chronic gastritis. *World J Gastroenterol* 2004; **10**: 1306-1309
 - 15 **Qian XQ**, Peng MS, Zhang SY, Bei RR. *Helicobacter pylori* with *CagA* gene strain and gastroduodenal diseases. *Huaren Xiaohua Zazhi* 1998; **6**(Suppl 7): tk366c
 - 16 **Vilaichone RK**, Mahachai V, Tumwasorn S, Nunthapisud P, Wisedopas N, Kullavanijaya P. Duodenal *Helicobacter pylori* associated duodenal ulcer depend on gastric *Helicobacter pylori* status. *J Med Assoc Thai* 2002; **85** Suppl 1: S97-102
 - 17 **Siew S**, Goldstein ML. Scanning electron microscopy of mucosal biopsies of the human upper gastrointestinal tract. *Scan Electron Microsc* 1981; **4**: 173-181
 - 18 **Steer HW**. Surface morphology of the gastroduodenal mucosa in duodenal ulceration. *Gut* 1984; **25**: 1203-1210
 - 19 **Bode G**, Malfertheiner P, Ditschuneit H. Pathogenetic implications of ultrastructural findings in *Campylobacter pylori* related gastroduodenal disease. *Scand J Gastroenterol Suppl* 1988; **142**: 25-39
 - 20 **Yang H**, Dixon MF, Zuo J, Fong F, Zhou D, Corthesy I, Blum A. *Helicobacter pylori* infection and gastric metaplasia in the duodenum in China. *J Clin Gastroenterol* 1995; **20**: 110-112
 - 21 **Chattopadhyay G**, Basu K, Mukherjee S, Hazra BR. Gastroduodenal mucosa in peptic ulcer: endoscopic and histological assessment. *Trop Gastroenterol* 1997; **18**: 156-159
 - 22 **Peura DA**, Malfertheiner P. Chairmen's summary: dichotomies and directions in acid-related disorders. *Aliment Pharmacol Ther* 2004; **19** Suppl 1:77-80
 - 23 **Bago J**, Kranjcec D, Strinic D, Petrovic Z, Kucisec N, Bevanda M, Bilic A, Eljuga D. Relationship of gastric metaplasia and age, sex, smoking and *Helicobacter pylori* infection in patients with duodenal ulcer and duodenitis. *Coll Antropol* 2000; **24**: 157-165
 - 24 **Bakka AS**, El-Gariani AB, AbouGhrara FM, Salih BA. Frequency of *Helicobacter pylori* infection in dyspeptic patients in Libya. *Saudi Med J* 2002; **23**: 1261-1265
 - 25 **Ciancio G**, Nuti M, Orsini B, Iovi F, Ortolani M, Palomba A, Amorosi A, Surrenti E, Ilani SM, Surrenti C. Regression of duodenal gastric metaplasia in *Helicobacter pylori* positive patients with duodenal ulcer disease. *Dig Liver Dis* 2002; **34**: 16-21
 - 26 **Tovey FI**, Hobsley M, Kaushik SP, Pandey R, Kurian G, Singh K, Sood A, Jehangir E. Duodenal gastric metaplasia and *Helicobacter pylori* infection in high and low duodenal ulcer-prevalent areas in India. *J Gastroenterol Hepatol* 2004; **19**: 497-505
 - 27 **Li YL**. Pathology. 6th ed. Beijing: People's Medical Publishing House 2003: 74-82
 - 28 **Heikkinen M**, Pikkarainen P, Vornanen M, Hollmen S, Julkunen R. Prevalence of gastric metaplasia in the duodenal bulb is low in *Helicobacter pylori* positive non-ulcer dyspepsia patients. *Dig Liver Dis* 2001; **33**: 459-463

Edited by Wang XL Proofread by Ma JY

Heme oxygenase-1 alleviates ischemia/reperfusion injury in aged liver

Xue-Hao Wang, Ke Wang, Feng Zhang, Xiang-Cheng Li, Jun Li, Wei De, Jun Guo, Xiao-Feng Qian, Ye Fan

Xue-Hao Wang, Ke Wang, Feng Zhang, Xiang-Cheng Li, Jun Li, Xiao-Feng Qian, Ye Fan, The Liver Transplantation Center of the First Affiliated Hospital, Nanjing Medical University, Nanjing 210029, Jiangsu Province, China

Wei De, Jun Guo, Department of Biochemistry, Nanjing Medical University, Nanjing 210029, Jiangsu Province, China

Supported by the "135" Medical Project of Jiangsu, No. 135-10

Co-first-authors: Xue-Hao Wang and Ke Wang

Correspondence to: Dr. Ke Wang, the Liver Transplantation Center of the First Affiliated Hospital, Nanjing Medical University, 300 Guangzhou road, Nanjing 210029, Jiangsu province, China. skylancet@hotmail.com

Telephone: +86-25-83718836-6476 **Fax:** +86-25-86660751

Received: 2004-04-19 **Accepted:** 2004-05-13

protection against cold I/R injury. This effect depends, at least in part, on HO-1-mediated inhibition of antiapoptotic mechanism.

© 2005 The WJG Press and Elsevier Inc. All rights reserved.

Key words: Aged liver; Ischemia-reperfusion injury; Heme oxygenase-1

Wang XH, Wang K, Zhang F, Li XC, Li J, De W, Guo J, Qian XF, Fan Y. Heme oxygenase-1 alleviates ischemia/reperfusion injury in aged liver. *World J Gastroenterol* 2005; 11(5): 690-694
<http://www.wjgnet.com/1007-9327/11/690.asp>

Abstract

AIM: To investigate if ischemia/reperfusion (I/R) injury in aged liver could be alleviated by heme oxygenase-1 (HO-1).

METHODS: Three groups of SD rats (16 mo old) were studied. Group 1: control donors received physiological saline 24 h before their livers were harvested; group 2: donors were pretreated with hemin 24 h before their livers were harvested; and group 3: donors received hemin 24 h before their livers were harvested and zinc protoporphyrin (ZnPP, HO-1 inhibitor) was given to recipients at reperfusion. The harvested livers were stored in University of Wisconsin solution (4 °C) for 6 h, and then transplanted to syngeneic rats. Serum glutamic oxaloacetic transaminase (SGOT), apoptotic cells, and apoptotic gene were measured 3, 6, 12, 24, 48 h after reperfusion. We measured the apoptotic index by TUNEL, determined the expression of antiapoptotic Bcl-2 and proapoptotic (caspase-3) gene products by Western blot.

RESULTS: After 3, 6, 12, 24, and 48 h of reperfusion, the SGOT levels (584.4±85.8 u/L, 999.2±125.2 u/L, 423.4±161.3 u/L, 257.8±95.8 u/L, and 122.4±26.4 u/L) in hemin group were significantly (all $P < 0.05$) lower than those in saline group (1082.2±101.2 u/L, 1775.2±328.3 u/L, 840.4±137.8 u/L, 448.6±74.3 u/L, and 306.2±49.3 u/L). Liver HO-1 enzymatic activity correlated with beneficial effects of hemin and deleterious effects of adjunctive ZnPP treatment. Markedly less apoptotic (TUNEL+) liver cells 3, 6, 12, 24, and 48 h after reperfusion (5.16±0.73, 10.2±0.67, 9.28±0.78, 7.14±1.12, and 4.78±0.65) ($P < 0.05$) could be detected in hemin liver grafts, as compared to controls (7.82±1.05, 15.94±1.82, 11.67±1.59, 8.28±1.09, and 6.36±0.67). We detected the increased levels of Bcl-2 (1.5-fold) expression and compared with saline controls. These differences were most pronounced at 12 h after transplantation. In contrast, an active form of proapoptotic caspase-3 (p20) protein was found to be 2.9-fold lower at 24 h in hemin-pretreated group, as compared to saline liver transplant controls.

CONCLUSION: HO-1 overexpression can provide potent

INTRODUCTION

Orthotopic liver transplantation (OLT) has become an effective therapeutic modality for end-stage liver diseases. Advances in surgical procedures and immunosuppression protocols have considerably improved patient survival after liver transplantation. One problem associated with OLT is the disparity between the increasing number of potential recipients and the inferior number of eligible liver donors. The necessity to expand the donor population has attracted attention to the possible use of aged donor livers, which are frequently discarded because of their primary nonfunction. Ischemia/reperfusion (I/R) injury, an antigen-independent component of "harvesting" injury, is one of the most critical events leading to nonfunction or early dysfunction of aged liver grafts^[1,2]. Reversible liver impairment or severe injury resulting in cell death and ultimate liver failure is dependent on the extent of liver damage caused by I/R.

Heme oxygenases (HOs) are ubiquitous enzymes that catalyze the initial and rate-limiting steps in oxidative degradation of heme to bilirubin. HOs cleave a mesocarbon of the heme molecule, producing equimolar quantities of biliverdin, iron, and carbon monoxide (CO)^[3]. Biliverdin is reduced to bilirubin by bilirubin reductase, and free iron is used in intracellular metabolism or sequestered in ferritin. Three HO isoforms have been identified. HO-1, an inducible heat shock protein 32, is highly induced and confers protective effects on oxidative stress response both *in vivo* and *in vitro*. The mechanism by which HO-1 confers protection against oxidative stress has not yet been defined. It is believed that byproducts derived from the catalysis of heme by HO, namely biliverdin and ferritin accumulated from released iron, and finally CO, may mediate the physiological effects of HO-1. Both biliverdin and bilirubin possess antioxidant properties^[4], whereas iron released during heme catabolism can stimulate ferritin synthesis^[5]. Attention has been centered on the biological effects of reaction products that potentially possess important antioxidant, anti-inflammatory, antiapoptotic, and possible immune modulatory functions^[6-11]. However, putative mechanisms by which HO-1 induction may lead to cytoprotection during I/R insults before transplantation remain unclear. Since HO-1 may play a cytoprotective role through an antiapoptotic pathway *in vitro*, we hypothesize

that one possible pathway by which HO-1 confers protection against oxidant injury is via its ability to impart antiapoptotic activity. Thus, the present study was designed to examine whether attenuation of I/R injury by prior treatment with hemin, an HO-1 inducer, might indeed involve the antiapoptotic pathway in rat hearts undergoing a cold I/R insult.

MATERIALS AND METHODS

Animals

Aged male SD rats were obtained from the Laboratory Animal Center of Jiangsu Province. Animals were fed a standard rodent diet and water according to the guidelines approved by the China Association of Laboratory Animal Care.

Study design

Syngeneic liver transplantation was performed using livers that were harvested from aged rats and stored for 6 h at 4 °C in University of Wisconsin solution before transplanted into recipients with revascularization without hepatic artery reconstruction^[12,13]. In group 1, prospective liver donors ($n = 25$) were given 9 g/L saline (5 mL/kg s c) 24 h before their livers were harvested; group 2, donors ($n = 25$) received hemin (40 $\mu\text{mol/kg s c}$) in 24 h before procurement. After a 6-h storage at 4 °C in University of Wisconsin solution, livers in both groups were transplanted into rats. In group 3, donors ($n = 10$) were treated with hemin 24 h before their livers were harvested. After a 6-h cold storage, livers were transplanted into rats, which were then infused with ZnPP (1.5 mg/kg I v), at the end of surgery after the vessels were unclamped. Separate groups of rats ($n = 5$ group) were killed at 3, 6, 12, 24 and 48 h after their vessels were unclamped. Serum glutamic oxaloacetic transaminase (SGOT) levels were detected and liver samples were collected for further analysis.

Enzymatic assay for HO-1 activity

To determine HO-1 activity, liver isografts were removed and homogenized on ice in Tris-HCl lysis buffer (pH 7.4) containing 5 mL/L Triton X-100 and protease inhibitors. Samples were frozen in small aliquots until use. Graft homogenates were mixed with 0.8 mmol/L reduced form of nicotinamide-adenine dinucleotide phosphate (NADPH), 0.8 mmol/L glucose-6-phosphate, 1.0 U of G-60P dehydrogenase, 1 mmol/L MgCl_2 , and 10 mL of purified rat liver biliverdin reductase at 4 °C. The reaction was initiated by addition of hemin (final concentration 0.25 mmol/L). The reaction mixture was incubated at 37 °C in the dark for 15 min. At the end of the incubation period, all insoluble materials were removed by centrifugation, and supernatants were analyzed for bilirubin concentration. An extinction coefficient of 40 $\text{mmol/L}^{-1} \text{cm}^{-1}$ at $A_{460-530}$ nm was used to calculate the amount of bilirubin formed. Controls included naive samples in the absence of the NADPH generating system and all the ingredients of the reaction mixture in the absence of graft homogenates. Biliverdin reductase was purified from rat livers as previously described^[14].

Detection of apoptosis

Some of the specimens were immediately fixed in 4 °C buffered formalin and embedded in paraffin. In all cases, conventional histologic examination was performed on 4 μm thick sections of paraffin-embedded tissue. Terminal deoxynucleotidyl transferase-mediated dUTP nick-end labeling (TUNEL) assay was performed essentially according to the instructions of the commercial kit (ApopTag, Intergen Co., NY). Nuclear counterstaining was performed with methyl green. Negative and positive control reactions were performed for each reaction

step. Negative controls were obtained by omission of terminal deoxynucleotidyl transferase. All the negative controls showed no positive signal. Positive controls included sections that were pretreated by DNAase I. All the positive controls were positive. Morphometric analysis of the cells in tissue stained by the TUNEL method was performed under the high-power magnification ($\times 400$) in a blind fashion. Thirty random fields were counted for each TUNEL-stained tissue sample. The number of hepatocytes was counted and expressed as a percentage of the total number of respective liver cells counted. Hepatocytes were clearly identified as a specific population of cells. However, sinusoidal endothelial cells (SLCs) included endothelial cells, Kupffer cells, and possibly adherent neutrophils. All nucleated cells lining the sinusoids were evaluated.

Western blot analysis of Bcl-2 and caspase-3 expressions

Protein was extracted from liver tissue samples with PBSTDS buffer (50 mmol/L Tris, 150 mmol/L NaCl, 1 g/L sodium dodecyl sulfate [SDS], 10 g/L sodium deoxycholate, and 10 mL/L Triton X-100, pH 7.2). Proteins (30 g/sample) in SDS loading buffer (50 mmol/L Tris, pH 7.6, 100 g/L glycerol, and 10 g/L SDS) were subjected to 120 g/L SDS-polyacrylamide gel electrophoresis and transferred to nitrocellulose membranes (Bio-Rad, Hercules, CA). The gel was then stained with Coomassie blue to document equal protein loading. The membrane was blocked with 3% dry milk and 1 mL/L Tween 20 (USB, Cleveland, OH) in PBS and incubated with primary antibody against Bcl-2 or caspase-3 and actin. The filters were washed and then incubated with horseradish peroxidase donkey anti-rabbit antibody (Amersham, Arlington Heights, IL). Relative quantities of protein were determined using a densitometer (Kodak Digital Science 1D Analysis Software, Rochester, NY).

Statistical analysis

Results were expressed as mean \pm SD. Statistical comparisons between the groups were done using unpaired two-tailed Student's *t* test. *P* values less than 0.05 were considered statistically significant.

RESULTS

Alleviation of ischemia/reperfusion injury induced by HO-1

The SGOT release was a well-established marker of hepatocellular injury after ischemia/reperfusion. We measured SGOT levels at 3, 6, 12, 24 and 48 h after reperfusion. The SGOT level in hemin group was significantly lower than that in saline and hemin+ZnPP groups at any time point after reperfusion ($P < 0.05$, Figure 1).

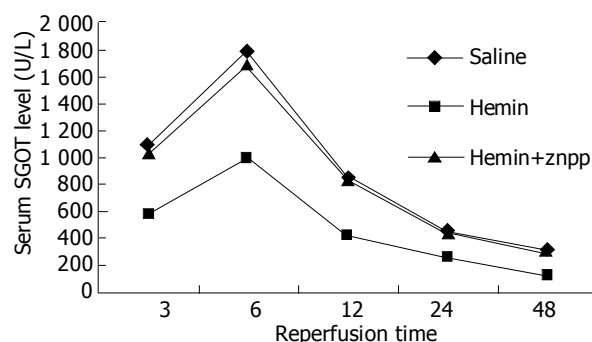


Figure 1 Comparison of serum SGOT levels in hemin group and in saline and hemin+ZnPP groups ($P < 0.05$). there was no difference between the two groups. After a 6-h reperfusion, the serum SGOT level was the highest.

Enhancement of HO-1 enzyme activity after hemin treatment

We analyzed HO-1 enzyme activity in aged rat liver and isograft samples [nmol of bilirubin/(mg protein min)]. As shown in Table 1 and Figure 2 pretreatment with hemin significantly increased HO-1 liver activity after transplantation (2.13±0.04 vs 1.09±0.03, 2.17±0.04 vs 1.20±0.03, 2.22±0.05 vs 1.27±0.04, 2.03±0.04 vs 1.15±0.03, and 1.94±0.03 vs 1.05±0.03 in controls at 3, 6, 12, 24, and 48 h, respectively, $P < 0.05$). Adjuvant ZnPP given during reperfusion inhibited HO-1 activity in liver isografts.

Table 1 Apoptotic index after reperfusion (mean±SD)

Group	3 h (%)	6 h (%)	12 h (%)	24 h (%)	48 h (%)
Saline	7.82±1.05	15.94±1.82	11.67±1.59	8.28±1.09	6.36±0.67
Hemin	5.16±0.73	10.2±0.67	9.28±0.78	7.14±1.12	4.78±0.65
Hemin+Znpp	7.8±0.83	15.94±1.58	11.68±1.59	8.76±0.88	6.48±0.70

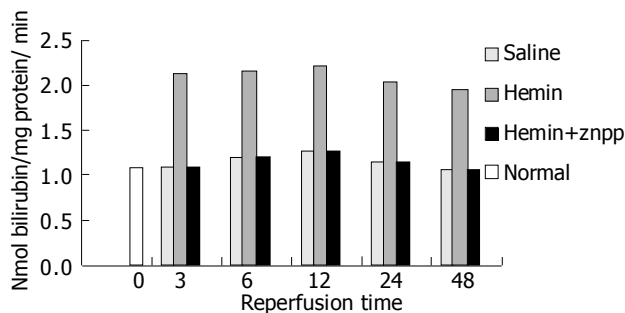


Figure 2 Enzymatic assay for HO-1 activity.

Depression of liver apoptotic cell death by HO-1 overexpression

To detect apoptotic cells, we performed TUNEL labeling in liver isografts that underwent cold I/R insults before transplantation. Classic TUNEL positivity was characterized by focal nuclear staining; the nuclear and cell membranes in apoptotic cells were intact. Results of TUNEL staining of liver isografts subjected to 3, 6, 12, 24 and 48 h of reperfusion after 24 h of cold preservation are shown in Figure 3. The frequency of TUNEL+ cells in liver myocytes was diminished in sections from rats pretreated with hemin (Figure 3A), as compared to saline-treated controls or those after adjuvant hemin plus ZnPP therapy. Consequently, an apoptotic index, calculated as the percentage of TUNEL-nuclei divided by the counterstained-nuclei, significantly diminished in the treated hemin group as compared to saline or hemin+ ZnPP-treated group.

Enhancement of Bcl-2 and depression of Caspase-3 expression by HO-1 overexpression

To evaluate whether hemin therapy affected the intragraft

apoptotic networks, we assessed the expression of antiapoptotic Bcl-2 and proapoptotic (caspase-3) gene products in orthotopic liver transplants by Western blot (Figure 4). In agreement with increased HO enzymatic activity in the liver treated with hemin, we detected increased levels of Bcl-2 (1.5-fold) expression, as compared to saline controls. These differences were most pronounced at 12 h after transplantation. In contrast, an active form of the proapoptotic caspase-3 (p20) protein was found to be 2.9 folds lower at 24 h in hemin-pretreated group, as compared to saline controls.

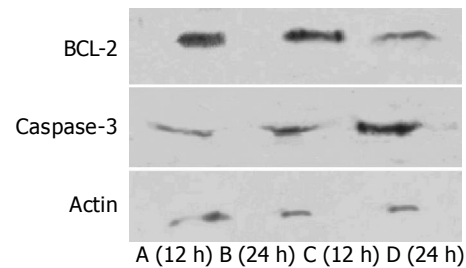


Figure 4 Western blot analyses of Bcl-2 and caspase-3 in orthotopic liver transplants at 12 h (lanes A and C) and 24 h (lanes B and D) after transplantation. At 12 and 24 h, higher levels of antiapoptotic Bcl-2 were found in hemin-treated livers (lanes A and B) as compared to saline controls (lanes C and D). Proapoptotic caspase-3 decreased in hemin-treated livers (lanes A and B) as compared to saline controls (lanes C and D).

DISCUSSION

The principal findings of this work are as follows. Hemin prevents I/R insults in aged rat livers with cold ischemia followed by reperfusion. Hemin-induced HO-1 overexpression, as determined by enzymatic assays, decreases hepatocellular apoptosis. Treatment with ZnPP, abolishes these beneficial effects, documenting the direct involvement of HO-1 in the protection against I/R injury in aged rat livers.

HO-1 activity, is considered as one of the most sensitive indicators of cellular stress^[15,16]. Being analogous to heat shock regulation, HO-1 overexpression may represent an endogenous adaptive mechanism protecting cells from stress after radiation, heat shock, inflammation, and ischemia. Indeed, hemin-induced HO-1 overexpression in our present study prevented or significantly decreased aged liver injury in a clinically relevant model of 6 h cold I/R injury after syngeneic transplantation. Unlike saline-pretreated controls, which had high serum levels of SGOT, aged livers harvested from hemin-pre treated donors had low levels of SGOT. ZnPP-mediated inhibition of HO-1 activity had negative effects after hemin treatment, which endorses the hypothesis that the mechanism underlying

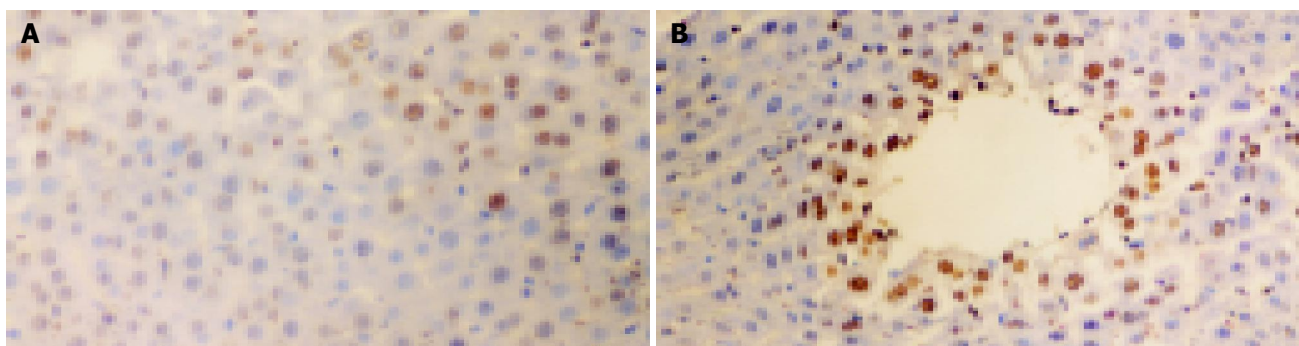


Figure 3 TUNEL-positive cells in (A) and saline-pretreated group (B) hemin-pretreated group (A) and (×200).

protection against liver I/R injury involves HO-1 induction rather than modulation of other biochemical pathways that may protect livers from oxidative injury.

Studies have shown that up-regulation of HO-1 expression could exert strikingly important adaptive antioxidant and anti-inflammatory functions to protect cells from pathophysiological conditions, including graft rejection and I/R injury^[17-22]. But the mechanisms underlying the beneficial effects of HO-1 on I/R injury have to be elucidated.

The exact mechanisms underlying the fulminant I/R insults by free radicals, calcium entry, or inflammation are currently unknown, although cell apoptosis has been suggested as a key early event^[23-25]. Thus, inhibition of the apoptotic pathway seems to be a rational therapeutic strategy to reduce the risk of preservation injury in transplanted organs. Up-regulation for HO-1 could inhibit apoptosis both *in vitro* and *in vivo*^[10,26], consistent with our present TUNEL-based findings of the decreased frequency of apoptotic cells in hemin-pretreated liver isografts as compared to controls. The cellular and physiological mechanisms by which HO-1 exerts its cytoprotective functions against I/R injury at the graft site might involve antiapoptotic protein expression. Indeed, adjuvant treatment with ZnPP, prevented the expression of Bcl-2 and promoted the activation of caspase-3 in this study. Caspase-3 activation is a key step in apoptosis. Bcl-2 could prevent release of apoptogenic factors such as cytochrome C and apoptosis-inducing factors from mitochondria into cytosols^[27,28]. Moreover, Bcl-2 could interact with apoptosis-related family members such as Bax, and several non-family member proteins including Raf-1 and Bag-1. Bag-1 could cooperate with Bcl-2 to suppress apoptosis^[29]. In this study, the up-regulation of antiapoptotic Bcl-2 occurred 3 h after the vessels were unclamped. Bcl-2 overexpression could block cell death in a caspase-independent manner, preserve mitochondrial integrity during hypoxia, and promote ATP generation even in the absence of glucose, and utilize respiratory substrates during reoxygenation^[30].

The mechanism by which HO-1 influences the production of antiapoptotic proteins remains to be elucidated. It has been shown that HO-1-induced antiapoptotic effects might be mediated via CO or p38 mitogen-activated protein kinase (MAPK) signaling transduction pathways^[26]. CO generation could prevent xenograft rejection via its ability to suppress endothelial cell apoptosis *in vivo*^[31], whereas low CO concentrations have been identified as the key factor in HO-1-induced protection against apoptosis induced by tumor necrosis factor -induced apoptosis in cultured fibroblasts^[10] as well as endothelial cells^[26] *in vitro*. Moreover, animals exposed to CO *in vivo* exhibit a significant attenuation of hyperoxia-induced lung apoptosis, at least in part via the anti-inflammatory mitogen-activated protein kinase-3 (MKK3)/p38 mitogen-activated protein kinase (p38 MAPK) pathway^[32]. Three major MAPKs in cardiomyocytes subjected to I/R and the endoplasmic reticulum kinase (ERK) pathway may be critical for the survival of cells by protecting them from programmed cell death caused by stress-induced activation of p38 and c-jun N-terminal kinase (JNK)^[33].

In summary, HO-1 up-regulation can provide potent protection against cold ischemia and reperfusion injury in aged rat livers. This beneficial effect depends, at least in part, on HO-1 modulation of the antiapoptotic pathway. HO-1-inducing agents could be used in preventing I/R injury of marginal donors.

REFERENCES

- 1 Deschenes M, Forbes C, Tchervenkov J, Barkun J, Metrakos P, Tector J, Alpert E. Use of older donor livers is associated with more extensive ischemic damage on intraoperative biopsies during liver transplantation. *Liver Transpl Surg* 1999; **5**: 357-361
- 2 Busquets J, Xiol X, Figueras J, Jaurrieta E, Torras J, Ramos E, Rafecas A, Fabregat J, Lama C, Ibanez L, Llado L, Ramon JM. The impact of donor age on liver transplantation: influence of donor age on early liver function and on subsequent patient and graft survival. *Transplantation* 2001; **71**: 1765-1771
- 3 Maines MD. The heme oxygenase system: a regulator of second messenger gases. *Annu Rev Pharmacol Toxicol* 1997; **37**: 517-554
- 4 Baranano DE, Rao M, Ferris CD, Snyder SH. Biliverdin reductase: a major physiologic cytoprotectant. *Proc Natl Acad Sci USA* 2002; **99**: 16093-16098
- 5 Balla G, Jacob HS, Balla J, Rosenberg M, Nath K, Apple F, Eaton JW, Vercellotti GM. Ferritin: a cytoprotective antioxidant strategem of endothelium. *J Biol Chem* 1992; **267**: 18148-18153
- 6 Oztecan S, Kirgiz B, Unlucerci Y, Dogru-Abbasoglu S, Bilge H, Uysal M, Aykac-Toker G. Heme oxygenase induction protects liver against oxidative stress in x-irradiated aged rats. *Biogerontology* 2004; **5**: 99-105
- 7 Vicente AM, Guillen MI, Habib A, Alcaraz MJ. Beneficial effects of heme oxygenase-1 up-regulation in the development of experimental inflammation induced by zymosan. *J Pharmacol Exp Ther* 2003; **307**: 1030-1037
- 8 Soares MP, Lin Y, Anrather J, Csizmadia E, Takigami K, Sato K, Grey ST, Colvin RB, Choi AM, Poss KD, Bach FH. Expression of heme oxygenase-1 can determine cardiac xenograft survival. *Nat Med* 1998; **4**: 1073-1077
- 9 Katori M, Busuttil RW, Kupiec-Weglinski JW. Heme oxygenase-1 system in organ transplantation. *Transplantation* 2002; **74**: 905-912
- 10 Petrache I, Otterbein LE, Alam J, Wiegand GW, Choi AM. Heme oxygenase-1 inhibits TNF-alpha-induced apoptosis in cultured fibroblasts. *Am J Physiol Lung Cell Mol Physiol* 2000; **278**: L312-L319
- 11 Thom SR, Fisher D, Xu YA, Notarfrancesco K, Ischiropoulos H. Adaptive responses and apoptosis in endothelial cells exposed to carbon monoxide. *Proc Natl Acad Sci USA* 2000; **97**: 1305-1310
- 12 Amersi F, Buelow R, Kato H, Ke B, Coito AJ, Shen XD, Zhao D, Zaky J, Melinek J, Lassman CR, Kolls JK, Alam J, Ritter T, Volk HD, Farmer DG, Ghobrial RM, Busuttil RW, Kupiec-Weglinski JW. Upregulation of heme oxygenase-1 protects genetically fat Zucker rat livers from ischemia/reperfusion injury. *J Clin Invest* 1999; **104**: 1631-1639
- 13 Kato H, Amersi F, Buelow R, Melinek J, Coito AJ, Ke B, Busuttil RW, Kupiec-Weglinski JW. Heme oxygenase-1 overexpression protects rat livers from ischemia/reperfusion injury with extended cold preservation. *Am J Transplant* 2001; **1**: 121-128
- 14 Kutty RK, Maines MD. Purification and characterization of biliverdin reductase from rat liver. *J Biol Chem* 1981; **256**: 3956-3962
- 15 Bonnell MR, Visner GA, Zander DS, Mandalapu S, Kazemfar K, Spears L, Beaver TM. Heme-oxygenase-1 expression correlates with severity of acute cellular rejection in lung transplantation. *J Am Coll Surg* 2004; **198**: 945-952
- 16 Lakkisto P, Palojoki E, Backlund T, Saraste A, Tikkanen I, Voipio-Pulkki LM, Pulkki K. Expression of heme oxygenase-1 in response to myocardial infarction in rats. *J Mol Cell Cardiol* 2002; **34**: 1357-1365
- 17 Attuwaybi BO, Kozar RA, Moore-Olufemi SD, Sato N, Hassoun HT, Weisbrodt NW, Moore FA. Heme oxygenase-1 induction by hemin protects against gut ischemia/reperfusion injury. *J Surg Res* 2004; **118**: 53-57
- 18 Ito K, Ozasa H, Kojima N, Miura M, Iwa T, Senoo H, Horikawa S. Pharmacological preconditioning protects lung injury induced by intestinal ischemia/reperfusion in rat. *Shock* 2003; **19**: 462-468
- 19 Braudeau C, Bouchet D, Tesson L, Iyer S, Remy S, Buelow R, Anegon I, Chauveau C. Induction of long-term cardiac allograft survival by heme oxygenase-1 gene transfer. *Gene Ther* 2004; **11**: 701-710
- 20 Amersi F, Buelow R, Kato H, Ke B, Coito AJ, Shen XD, Zhao D,

- Zaky J, Melinek J, Lassman CR, Kolls JK, Alam J, Ritter T, Volk HD, Farmer DG, Ghobrial RM, Busuttill RW, Kupiec-Weglinski JW. Upregulation of heme oxygenase-1 protects genetically fat Zucker rat livers from ischemia/reperfusion injury. *J Clin Invest* 1999; **104**: 1631-1639
- 21 **Hangaishi M**, Ishizaka N, Aizawa T, Kurihara Y, Taguchi J, Nagai R, Kimura S, Ohno M. Induction of heme oxygenase-1 can act protectively against cardiac ischemia/reperfusion *in vivo*. *Biochem Biophys Res Commun* 2000; **279**: 582-588
- 22 **Squiers EC**, Bruch D, Buelow R, Tice DG. Pretreatment of small bowel isograft donors with cobalt-protoporphyrin decreases preservation injury. *Transplant Proc* 1999; **31**: 585-586
- 23 **Liu X**, Drognitz O, Neeff H, Benz S, Hopt UT. Apoptosis is caused by prolonged organ preservation and blocked by apoptosis inhibitor in experimental rat pancreatic grafts. *Transplant Proc* 2004; **36**: 1209-1210
- 24 **Huet PM**, Nagaoka MR, Desbiens G, Tarrab E, Brault A, Bralet MP, Bilodeau M. Sinusoidal endothelial cell and hepatocyte death following cold ischemia-warm reperfusion of the rat liver. *Hepatology* 2004; **39**: 1110-1119
- 25 **Zhao ZQ**, Nakamura M, Wang NP, Wilcox JN, Shearer S, Ronson RS, Guyton RA, Vinten-Johansen J. Reperfusion induces myocardial apoptotic cell death. *Cardiovasc Res* 2000; **45**: 651-660
- 26 **Brouard S**, Otterbein LE, Anrather J, Tobiasch E, Bach FH, Choi AM, Soares MP. Carbon monoxide generated by heme oxygenase 1 suppresses endothelial cell apoptosis. *J Exp Med* 2000; **192**: 1015-1026
- 27 **Susin SA**, Zamzami N, Castedo M, Hirsch T, Marchetti P, Macho A, Daugas E, Geuskens M, Kroemer G. Bcl-2 inhibits the mitochondrial release of an apoptogenic protease. *J Exp Med* 1996; **184**: 1331-1341
- 28 **Kluck RM**, Bossy-Wetzel E, Green DR, Newmeyer DD. The release of cytochrome c from mitochondria: a primary site for Bcl-2 regulation of apoptosis. *Science* 1997; **275**: 1132-1136
- 29 **Wang HG**, Takayama S, Rapp UR, Reed JC. Bcl-2 interacting protein, BAG-1, binds to and activates the kinase Raf-1. *Proc Natl Acad Sci USA* 1996; **93**: 7063-7068
- 30 **Saikumar P**, Dong Z, Patel Y, Hall K, Hopfer U, Weinberg JM, Venkatachalam MA. Role of hypoxia-induced Bax translocation and cytochrome c release in reoxygenation injury. *Oncogene* 1998; **17**: 3401-3415
- 31 **Sato K**, Balla J, Otterbein L, Smith RN, Brouard S, Lin Y, Csizmadia E, Seigny J, Robson SC, Vercellotti G, Choi AM, Bach FH, Soares MP. Carbon monoxide generated by heme oxygenase-1 suppresses the rejection of mouse-to-rat cardiac transplants. *J Immunol* 2001; **166**: 4185-4194
- 32 **Otterbein LE**, Bach FH, Alam J, Soares M, Tao Lu H, Wysk M, Davis RJ, Flavell RA, Choi AM. Carbon monoxide has anti-inflammatory effects involving the mitogen-activated protein kinase pathway. *Nat Med* 2000; **6**: 422-428
- 33 **Yue TL**, Wang C, Gu JL, Ma XL, Kumar S, Lee JC, Feuerstein GZ, Thomas H, Maleeff B, Ohlstein EH. Inhibition of extracellular signal-regulated kinase enhances Ischemia/Reoxygenation-induced apoptosis in cultured cardiac myocytes and exaggerates reperfusion injury in isolated perfused heart. *Circ Res* 2000; **86**: 692-699

Edited by Wang XL and Kumar M

Enhanced production of leptin in gastric fundic mucosa with *Helicobacter pylori* infection

Yoshito Nishi, Hajime Isomoto, Shigeo Uotani, Chun Yang Wen, Saburo Shikuwa, Ken Ohnita, Yohei Mizuta, Akio Kawaguchi, Kenichiro Inoue, Shigeru Kohno

Yoshito Nishi, Hajime Isomoto, Ken Ohnita, Yohei Mizuta, Shigeru Kohno, Second Department of Internal Medicine, Nagasaki University School of Medicine, Sakamoto 1-7-1, Nagasaki, Japan
Shigeo Uotani, First Department of Internal Medicine, Nagasaki University School of Medicine, Sakamoto 1-7-1, Nagasaki, Japan
Chun Yang Wen, Department of Molecular Pathology, Atomic Bomb Disease Institute, Nagasaki University Graduate School of Biomedical Sciences, Sakamoto 1-12-4, Nagasaki 852-8523, Japan
Chun Yang Wen, Department of Digestive Disease, Nanjing Drum Tower Hospital, Medical School of Nanjing University, Nanjing 210008, Jiangsu Province, China
Saburo Shikuwa, Department of Endoscopy, National Nagasaki Medical Center, 1001-1 Kubara, Omura, Japan
Akio Kawaguchi, Kenichiro Inoue, Shunkaikai Inoue Hospital, Takaramachi 8-9, Nagasaki, Japan
Correspondence to: Dr. Hajime Isomoto, Second Department of Internal Medicine, Nagasaki University School of Medicine, 1-7-1 Sakamoto, Nagasaki 852-8501, Japan. hajime2002@yahoo.co.jp
Telephone: +81-95-849-7281 **Fax:** +81-95-849-7285
Received: 2004-06-19 **Accepted:** 2004-07-27

Abstract

AIM: To determine the concentrations of leptin in plasma and gastric fundic mucosa in humans, with reference to *Helicobacter pylori* (*H pylori*) infection, and their association with gastric mucosal levels of interleukin (IL)-1 β , IL-6 and IL-8.

METHODS: Plasma leptin concentrations were determined in 135 outpatients with non-ulcer dyspepsia, consisting of 95 *H pylori*-infected and 40 uninfected subjects, and 13 patients before and after cure of the infection with anti-*H pylori* regimen. Using biopsy samples that were endoscopically obtained from the middle corpus along the greater curvature, gastric leptin contents were measured by radioimmunoassay and the mucosal concentrations of IL-1 β , IL-6 and IL-8 were measured by enzyme linked immunosorbent assay. We also analysed the expression of leptin in the fundic mucosa by reverse transcriptase-polymerase chain reaction (RT-PCR) and immunohistochemistry.

RESULTS: The mucosal levels of leptin in the fundic mucosa of *H pylori*-infected patients were significantly higher than those of uninfected patients. The amount of gastric leptin correlated positively with the mucosal levels of IL-1 β and IL-6, but not IL-8. Circulating leptin correlated with body mass index, but not with *H pylori* status, and there was no change in plasma leptin levels following cure of the infection. Leptin immunoreactive cells were noted in the lower half of the fundic glands, and its expression of messenger ribonucleic acid in the oxyntic mucosa was detected by RT-PCR.

CONCLUSION: Leptin production is enhanced in *H pylori*-infected gastric mucosa. Gastric leptin may be involved in immune and inflammatory response during *H pylori* infection, through interaction with proinflammatory cytokines.

© 2005 The WJG Press and Elsevier Inc. All rights reserved.

Key words: *Helicobacter pylori* infection; Gastric fundic mucosa; Leptin

Nishi Y, Isomoto H, Uotani S, Wen CY, Shikuwa S, Ohnita K, Mizuta Y, Kawaguchi A, Inoue K, Kohno S. Enhanced production of leptin in gastric fundic mucosa with *Helicobacter pylori* infection. *World J Gastroenterol* 2005; 11(5): 695-699
<http://www.wjgnet.com/1007-9327/11/695.asp>

INTRODUCTION

Leptin is a 16-kDa protein synthesized mainly by the adipose tissue and plays a crucial role in homeostasis of body weight by reducing appetite and increasing energy expenditure^[1,2]. Originally thought to be a satiety factor, leptin is a pleiotropic bioactive molecule^[3,4]. Recent evidence demonstrates that leptin regulates immune functions and inhibits gastric acid secretion^[3-7]. Contrary to initial reports, leptin production is not restricted to adipocytes. It is also detected in human placenta, muscles and gastric chief cells^[3,4,8-10].

Helicobacter pylori (*H pylori*) is the major cause of chronic gastritis and peptic ulcer diseases^[11,12]. Chronic infection leads to atrophic gastritis, which increases the risk of gastric adenocarcinoma^[12]. It is well documented that *H pylori*-associated gastritis, which is characterized by intense infiltration of polynuclear and mononuclear cells, affects various cell types in gastric wall including chief cells^[13-15]. Studies from our laboratories and those of other investigators have documented the presence of high concentrations of various proinflammatory cytokines and chemokines in gastric mucosa infected with *H pylori*^[16-20]. Ghrelin, a novel endogenous ligand for growth hormone secretagogue receptor, not only exerts potent growth hormone releasing activity but also influences appetite, energy balance, gastric motility and acid secretion^[21]. This hormone is primarily produced by X/A-like neuroendocrine cells in the oxyntic gland^[21]. To date, conflicting results have been reported regarding the influence of *H pylori* status on ghrelin dynamics^[22-24]. In terms of the relationship between *H pylori* infection and leptin, recent studies have shown that gastric leptin contents are higher in *H pylori*-infected than in uninfected subjects, whereas the serum levels are not always different between the two groups^[9,13].

The present study was designed to determine the influence of *H pylori* status on plasma and gastric levels of leptin. We detected the presence of leptin messenger ribonucleic acid (mRNA) and protein in the gastric mucosa by reverse transcriptase-polymerase chain reaction (RT-PCR) and immunohistochemistry, respectively. In addition, we assessed the relationship between gastric leptin contents and levels of representative proinflammatory cytokines and chemokines including interleukin (IL)-1 β , IL-6 and IL-8.

MATERIALS AND METHODS

Patients

The study subjects were 135 outpatients, who were referred for

upper gastrointestinal endoscopy and diagnosed as having non-ulcer dyspepsia, between April 2000 and March 2003. The study was approved by Nagasaki University Human Ethics Committee. All samples were obtained with written informed consent of the patients prior to their inclusion, in accordance with the Helsinki Declaration. The exclusion criteria were: age <18 or >80 years, pregnancy, body mass index (BMI) > 30 kg/m², diabetes mellitus, systemic infection, thyroid and liver diseases, renal impairment, use of medications effective against *H pylori* during the preceding 3 mo, alcohol abuse, drug addiction, and long-term corticosteroid or nonsteroidal anti-inflammatory drug use. None had undergone gastrointestinal surgery.

During endoscopy, one biopsy specimen was obtained from the middle portion of the corpus along the greater curvature for the measurement of gastric leptin contents and cytokines, snap-frozen in an ethanol-dry ice mixture and then stored at -80 °C until use. Two additional biopsies were endoscopically taken from the antrum within 2 cm of the pyloric ring and the corpus along the greater curvature; one was for the rapid urease test (Helicocheck, Otsuka Pharmaceutical Co., Tokushima, Japan) and another for histopathological examination. In some cases, additional biopsy samples were obtained from the fundic gland mucosa for RT-PCR and immunohistochemical analysis.

We treated 13 *H pylori*-positive patients with 7-d triple therapy consisting of rabeprazole, amoxicillin and clarithromycin^[21]. Four weeks after cessation of the treatment, fasting plasma samples were also collected.

Plasma leptin concentrations

On the day of endoscopy, blood samples were taken between 9 and 11 a.m. after an overnight fast, transferred into chilled tubes containing ethylenediaminetetraacetic acid-2Na and aprotinin, stored on ice during collection, centrifuged, plasma separated, and stored at -80 °C until assay. Plasma leptin concentrations were measured in duplicate by a commercial radioimmunoassay (RIA) kit (Linco Research Co., St. Charles, USA), based on the protocol provided by the manufacturer.

Measurement of gastric mucosal levels of leptin and cytokines

As described previously^[16,17,26], biopsy samples were homogenized in phosphate-buffered saline (PBS) and aliquots of homogenate supernatants obtained by centrifugation (10 000 g for 10 min), were assayed for total protein by a modified Lowry method. The supernatants diluted to 0.50 mg/mL total protein concentration in PBS, were frozen at -80 °C until assay. Gastric leptin contents were measured by RIA (Linco Research). Mucosal levels of IL-1 β , IL-6 and IL-8 were measured using commercially available assay kits (Research and Diagnostics Co., Minneapolis, MN, USA), which employ the quantitative immunometric sandwich enzyme immunoassay technique. These assays were performed in duplicate according to the instructions provided by each manufacturer. The concentrations of leptin and cytokines were expressed in ng/mg protein and pg/mg protein, respectively.

Detection of *H pylori* infection

H pylori status was assessed by anti-*H pylori* immunoglobulin G antibody (HEL-p TEST, an enzyme linked immunosorbent assay kit, AMRAD Co., Melbourne, Australia) using the stored plasma, ¹³C-urea breath test (UBiT, Otsuka Pharmaceutical Co.) and rapid urease test using endoscopic biopsy samples. Patients were considered to be positive for *H pylori* infection when two of these examinations yielded positive results. On the other hand, patients were defined as *H pylori*-negative if all test results were negative^[27]. Eradication of *H pylori* was considered successful when ¹³C-urea breath test became negative^[25].

Histopathological examination

The sections were stained with hematoxylin and eosin. The grades of histological gastritis including activity (neutrophils) and chronic inflammation (mononuclear cells), was scored into 0, 1, 2 or 3 corresponding to none, mild, moderate or severe in accordance with the Sydney system^[16].

Immunohistochemistry

Immunohistochemical staining was performed with the streptavidin-biotin-peroxidase-complex method (Histofine SAB-PO[®] kit, Nichirei Co., Tokyo, Japan) as described previously^[16,17,26]. The following steps were performed at room temperature unless otherwise specified. Paraffin-embedded biopsy specimens were sectioned at 4- μ m thickness, deparaffinized and rehydrated. After inhibition of endogenous peroxidase activity for 30 min with methanol containing 0.3% H₂O₂, the sections were reacted for 20 min with 10% normal goat serum to prevent non-specific binding. They were then incubated overnight with the rabbit polyclonal anti-leptin antibody (diluted 1:100, Santa Cruz Biotechnologies Inc., Santa Cruz, CA, USA) at 4 °C. On the next day, the sections were washed in 0.01 M PBS and incubated for 20 min with 10 mg/mL biotinylated goat anti-rabbit immunoglobulins (Nichirei Co.). After washed in PBS, the sections were re-incubated for 20 min with 100 μ g/mL horseradish peroxidase (HRP)-conjugated streptavidin (Nichirei Co.) and stained with 0.02% 3,3'-diaminobenzidine tetrahydrochloride (Dojindo Co., Kumamoto, Japan) in 0.05 mol/L Tris-HCl buffer containing 0.03% H₂O₂. The sections were finally washed in PBS and counterstained with hematoxylin. Control studies were performed with normal rabbit serum or anti-leptin antiserum (Santa Cruz Biotechnologies Inc.).

We calculated the leptin-labelling index, which was the numbers of immunoreactive cells for leptin per total numbers of cells within the fundic gland area (percentage). The calculation was performed by two investigators without knowledge of the experimental results.

RT-PCR

Total RNA from each biopsy sample was extracted using a commercial kit according to the instructions provided by the supplier (ISOGEN, Nippon Gene Co., Toyama, Japan). Equivalent amounts of RNA were monitored by absorption at 260 nm and by monitoring the density of 28S and 18S RNA detected after electrophoresis. One μ g of total RNA was reverse transcribed into complementary deoxyribonucleic acid (cDNA) in a volume of 25 μ L with MuLV reverse transcriptase and random hexamers (both from PE Applied Biosystems, Warrington, UK). According to a previous report^[10] with a slight modification, the target sequence for leptin mRNA was amplified in 40 cycles, each consisting of 1 min at 94 °C for denaturation, 1 min at 62 °C for annealing and 1 min at 72 °C for extension, followed by a final extension for 10 min at 72 °C using a RT-PCR kit (Takara Shuzo Co., Otsu, Japan). Two primers, 5'-CCTGACCTTATCCAAGATG G-3', (forward) and 5'-GAGTAGCCTGAAGCTTCCAG (reverse), were used for amplification of a 224 bp product^[16]. A 10 μ L aliquot of each PCR product was analysed by electrophoresis on 2% agarose gel containing ethidium bromide, and the bands were examined under ultraviolet light for the presence of amplified DNA. Glyceraldehyde-3-phosphate dehydrogenase (G3PDH) gene transcript was routinely amplified as described previously^[24] and used as an internal control of the processed RNA for each preparation.

Statistical analysis

Statistical analyses were performed using Fisher's exact, χ^2 , Student's *t*, Mann-Whitney U, Kruskal-Wallis, Spearman rank

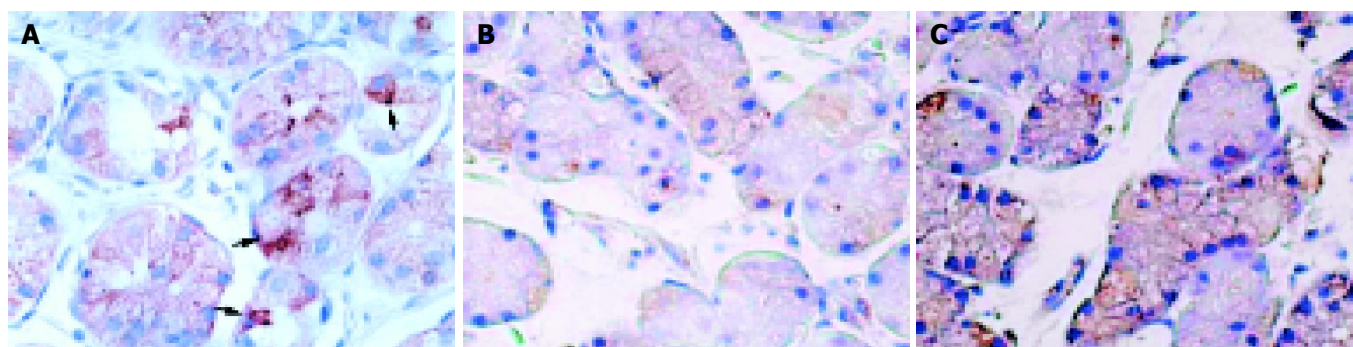


Figure 1 Leptin immunoreactive cells localized in the lower half of oxyntic glands (arrow head, magnification $\times 650$). A: Patients with *H pylori* infection; B: Uninfected subjects; C: Patients who had successful eradication.

and Wilcoxon signed ranks tests, as appropriate. A *P* value less than 0.05 was accepted as statistically significant. Data were expressed as mean \pm SD.

RESULTS

Patient demographics

The study population consisted of 69 men and 66 women, with a mean age of 54 years (range, 19-80). They consisted of 95 *H pylori*-infected and 40 uninfected subjects. There were no significant differences in age, sex, alcohol intake, smoking habit, BMI in terms of *H pylori* status.

Plasma concentrations of leptin and *H pylori* status

There was no significant difference in plasma leptin concentrations between *H pylori*-positive than -negative subjects (5.0 ± 3.5 and 4.8 ± 2.8 ng/mL, respectively). Successful eradication of the organism was confirmed in all of the 13 patients treated with anti-*H pylori* regimen. There was no significant difference in the leptin levels before and after cure of the infection (4.8 ± 3.3 and 4.7 ± 2.5 ng/mL, respectively).

Gastric mucosal levels of leptin, IL-1 β , IL-6 and IL-8 in relation to *H pylori* status

Gastric leptin contents in patients with *H pylori* infection were significantly higher than those in uninfected subjects ($P < 0.05$, Table 1). In addition, there were significant differences in the mucosal levels of IL-6 and IL-8 between *H pylori*-positive and -negative groups ($P < 0.0001$ and $P < 0.0005$, respectively, Table 1). The mucosal IL-1 β concentrations in *H pylori*-infected patients tended to be higher than those in uninfected subjects, though the difference was insignificant (Table 1). There were no relationships between these cytokines and circulating leptin concentrations.

Table 1 Gastric mucosal levels of leptin, interleukin 1 β , interleukin 6 and interleukin 8 in terms to *H pylori* status (mean \pm SD)

	<i>H pylori</i> -infected (<i>n</i> = 95)	Uninfected (<i>n</i> = 40)	<i>P</i>
Leptin(ng/mg protein)	0.18 \pm 0.13	0.14 \pm 0.15	<0.05
Interleukin 1 β (pg/mg protein)	43.38 \pm 33.03	33.27 \pm 24.61	NS
Interleukin 6 (pg/mg protein)	1.26 \pm 0.57	0.75 \pm 0.57	<0.0001
Interleukin 8 (pg/mg protein)	70.42 \pm 66.12	1.3 \pm 0.13	<0.0005

Correlation between gastric mucosal levels of leptin and cytokines

Gastric leptin contents correlated positively with the mucosal levels of IL-1 β (correlation coefficient, $r = 0.600$, $P < 0.0001$) and IL-6 ($r = 0.475$, $P < 0.0005$), but not the mucosal levels of IL-8 ($r = 0.168$).

Correlation between gastric mucosal levels of leptin and activity and chronic inflammation

Gastric leptin contents correlated positively with grading scores of chronic inflammation of gastritis (correlation coefficient, $r = 0.258$, $P < 0.05$), but not the scores of activity ($r = 0.111$).

Correlation between plasma and gastric leptin levels and baseline parameters

Concentrations of leptin in plasma, but not in gastric mucosa, correlated positively with BMI ($r = 0.548$, $P < 0.0001$). Other baseline characteristics including age, sex, alcohol intake and smoking habit did not correlate with circulating and gastric leptin concentrations.

Expression of leptin mRNA and protein in gastric mucosa

Using RT-PCR, leptin mRNA was identified in the fundic gland mucosa, albeit the band intensities of the gastric mucosa from patients with and without *H pylori* infection were much weaker compared to that of omental fatty tissue (Figure 1).

In gastric biopsy specimens, leptin immunoreactive cells were detected in the lower half of the fundic glands (Figure 1). The leptin-labelling indices of *H pylori*-infected patients tended to be higher than those of uninfected subjects (22.4 ± 14.3 and 18.1 ± 13.9 , respectively, $P < 0.10$).

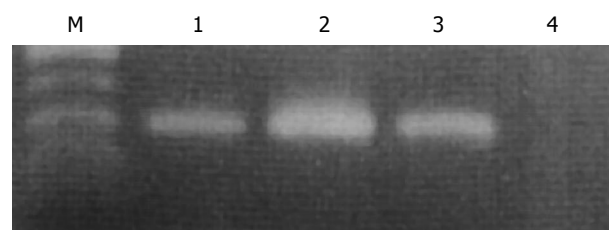


Figure 2 Reverse transcriptase-polymerase chain reaction. M; size marker. Lane 1: *H pylori*-uninfected gastric biopsy sample; lane 2: omental adipose tissue sample; lane 3: *H pylori*-infected gastric biopsy sample; lane 4: non-template negative control.

DISCUSSION

Bado and co-workers^[29] were the first group to report the presence of leptin mRNA and protein in the fundic glands of rat stomachs, and that the chief cells were mainly immunoreactive for leptin^[8].

Earlier studies failed to identify leptin mRNA in human gastric mucosa whereas the fundic epithelium exhibited the presence of immunoreactive leptin. Thus, it is suggested that leptin itself detected in gastric mucosa originates from the uptake of circulating one rather than representing local biosynthesis. However, we demonstrated here the expression of both leptin mRNA and its protein, providing further support for the recent results that leptin was a stomach-derived hormone in humans^[9,10].

In our study, gastric leptin contents in *H pylori*-infected patients were significantly higher than those in uninfected patients. Using quantitative RT-PCR, Azuma *et al*^[9] demonstrated that *H pylori* infection significantly increased the expression of leptin mRNA expression, and that cure of the infection significantly reduced it. Considered together, *H pylori* infection seems to enhance local biosynthesis of leptin as well as its release into gastric juice in response to cholecystokinin or meal^[7]. The finding that leptin was localized in the oxyntic gland area^[8-10], which is rarely colonized by the organism^[13], suggests that *H pylori* itself may not affect gastric leptin levels.

Our results demonstrated significantly positive correlations between gastric leptin contents and the mucosal concentrations of IL-1 β and IL-6. In fact, there is evidence for the expression of functional leptin receptor (Ob-R) in mononuclear cells^[3,4,10,29,30]. Ob-R is homologous to members of class I cytokine receptor (gp130) superfamily including IL-6^[3,4,31]. Several lines of evidence demonstrate that leptin could stimulate monocytes to produce IL-1, IL-6 and tumour necrosis factor α (TNF- α)^[5,6]. In turn, these cytokines could increase systemic leptin levels *in vivo*^[32]. It has been reported that IL-1 β and IL-6 are elevated in gastric mucosa infected with *H pylori*^[18-20], in line with this study. Thus, leptin released locally may be implicated in the immune and inflammatory responses to *H pylori* infection, through interaction with proinflammatory cytokines. Moreover, it not only modulates the activation and proliferation of T lymphocytes but also skews cytokine responses towards a Th 1 phenotype by enhancing production of IL-2 and interferon γ ^[33,34]. It has been well accepted that mucosal cytokine profiles during *H pylori* infection can imply Th1 predominance in human adults^[13]. Considered together, these findings highlight the possible role of leptin as an immunomodulator in *H pylori*-associated gastritis.

In our study, circulating leptin concentrations were not associated with *H pylori* status and there was no significant alteration in their levels following cure of the infection, consistent with previous reports^[19,35]. Gastric leptin may have a local rather than a systemic action, exerting paracrine effects within the gastric mucosa. On the other hand, plasma leptin concentrations significantly correlated with BMI, as the primary contributor of circulating leptin is exclusively the adipose tissue^[1,2].

In conclusion, we showed a significantly enhanced production of leptin in *H pylori*-infected than uninfected gastric mucosa. The amount of gastric leptin correlated positively with the mucosal concentrations of IL-1 β and IL-6, suggesting that local overproduction of leptin is likely to be involved in immune and inflammatory response during *H pylori* infection.

REFERENCES

- Zhang Y, Proenca R, Maffei M, Barone M, Leopold L, Friedman JM. Positional cloning of the mouse *obese* gene and its human homologue. *Nature* 1994; **372**: 425-432
- Coleman DL. Obese and diabetes: two mutant genes causing diabetes-obesity syndromes in mice. *Diabetologia* 1978; **14**: 141-148
- Faggioni R, Feingold KR, Grunfeld C. Leptin regulation of the immune response and the immunodeficiency of malnutrition. *FASEB J* 2001; **15**: 2565-2571
- Sanchez-Margalet V, Martin-Romero C, Santos-Alvarez J,

- Goberna R, Najib S, Gonzalez-Yanes C. Role of leptin as an immunomodulator of blood mononuclear cells: mechanisms of action. *Clin Exp Immunol* 2003; **133**: 11-19
- Santos-Alvarez J, Goberna R, Sanchez-Margalet V. Human leptin stimulates proliferation and activation of human circulating monocytes. *Cell Immunol* 1999; **194**: 6-11
- Zarkesh-Esfahani H, Pockley G, Metcalfe RA, Bidlingmaier M, Wu Z, Ajami A, Weetman AP, Strasburger CJ, Ross RJ. High-dose leptin activates human leukocytes via receptor expression on monocytes. *J Immunol* 2001; **167**: 4593-4599
- Konturek JW, Konturek SJ, Kwicien N, Bielanski W, Pawlik T, Rembiazk K, Domschke W. Leptin in the control of gastric secretion and gut hormones in humans infected with *Helicobacter pylori*. *Scand J Gastroenterol* 2001; **36**: 1148-1154
- Bado A, Levasseur S, Attoub S, Kermorgant S, Laigneau JP, Bortoluzzi MN, Moizo L, Lehy T, Guerre-Millo M, Le Marchand-Brustel Y, Lewin MJ. The stomach is a source of leptin. *Nature* 1998; **394**: 790-793
- Azuma T, Suto H, Ito Y, Ohtani M, Dojo M, Kuriyama M, Kato T. Gastric leptin and *Helicobacter pylori* infection. *Gut* 2001; **49**: 324-329
- Sobhani I, Bado A, Vissuzaine C, Buyse M, Kermorgant S, Laigneau JP, Attoub S, Lehy T, Henin D, Mignon M, Lewin MJ. Leptin secretion and leptin receptor in the human stomach. *Gut* 2000; **47**: 178-183
- Blaser MJ. *Helicobacter pylori* and the pathogenesis of gastroduodenal inflammation. *J Infect Dis* 1990; **161**: 626-633
- Ernst PB, Gold BD. The disease spectrum of *Helicobacter pylori*: the immunopathogenesis of gastroduodenal ulcer and gastric cancer. *Annu Rev Microbiol* 2000; **54**: 615-640
- Blaser MJ, Atherton JC. *Helicobacter pylori* persistence: biology and disease. *J Clin Invest* 2004; **113**: 321-333
- Beales IL, Calam J. Interleukin 1 beta and tumour necrosis factor alpha inhibit acid secretion in cultured rabbit parietal cells by multiple pathways. *Gut* 1998; **42**: 227-234
- Moss SF, Legon S, Bishop AE, Polak JM, Calam J. Effect of *Helicobacter pylori* on gastric somatostatin in duodenal ulcer disease. *Lancet* 1992; **340**: 930-932
- Isomoto H, Mizuta Y, Miyazaki M, Takeshima F, Omagari K, Murase K, Nishiyama T, Inoue K, Murata I, Kohno S. Implication of NF-kappaB in *Helicobacter pylori*-associated gastritis. *Am J Gastroenterol* 2000; **95**: 2768-2776
- Isomoto H, Miyazaki M, Mizuta Y, Takeshima F, Murase K, Inoue K, Yamasaki K, Murata I, Koji T, Kohno S. Expression of nuclear factor-kappaB in *Helicobacter pylori*-infected gastric mucosa detected with southwestern histochemistry. *Scand J Gastroenterol* 2000; **35**: 247-254
- Crabtree JE, Shallcross TM, Heatley RV, Wyatt JI. Mucosal tumour necrosis factor alpha and interleukin-6 in patients with *Helicobacter pylori* associated gastritis. *Gut* 1991; **32**: 1473-1477
- Noach LA, Bosma NB, Jansen J, Hoek FJ, van Deventer SJ, Tytgat GN. Mucosal tumor necrosis factor-alpha, interleukin-1 beta, and interleukin-8 production in patients with *Helicobacter pylori* infection. *Scand J Gastroenterol* 1994; **29**: 425-429
- Yamaoka Y, Kita M, Kodama T, Sawai N, Imanishi J. *Helicobacter pylori* cagA gene and expression of cytokine messenger RNA in gastric mucosa. *Gastroenterology* 1996; **110**: 1744-1752
- Murray CD, Kamm MA, Bloom SR, Emmanuel AV. Ghrelin for the gastroenterologist: history and potential. *Gastroenterology* 2003; **125**: 1492-1502
- Gokcel A, Gumurdulu Y, Kayaselcuk F, Serin E, Ozer B, Ozsahin AK, Guvener N. *Helicobacter pylori* has no effect on plasma ghrelin levels. *Eur J Endocrinol* 2003; **148**: 423-426
- Nwokolo CU, Freshwater DA, O'Hare P, Randevo HS. Plasma ghrelin following cure of *Helicobacter pylori*. *Gut* 2003; **52**: 637-640
- Suzuki H, Masaoka T, Hosoda H, Ota T, Minegishi Y, Nomura S, Kangawa K, Ishii H. *Helicobacter pylori* infection modifies gastric and plasma ghrelin dynamics in Mongolian gerbils. *Gut* 2004; **53**: 187-194
- Isomoto H, Furusu H, Morikawa T, Mizuta Y, Nishiyama T, Omagari K, Murase K, Inoue K, Murata I, Kohno S. 5-day vs. 7-day triple therapy with rabeprazole, clarithromycin and

- amoxicillin for *Helicobacter pylori* eradication. *Aliment Pharmacol Ther* 2000; **14**: 1619-1623
- 26 **Isomoto H**, Wang A, Mizuta Y, Akazawa Y, Ohba K, Omagari K, Miyazaki M, Murase K, Hayashi T, Inoue K, Murata I, Kohno S. Elevated levels of chemokines in esophageal mucosa of patients with reflux esophagitis. *Am J Gastroenterol* 2003; **98**: 551-556
- 27 **Isomoto H**, Inoue K, Furusu H, Nishiyama H, Shikuwa S, Omagari K, Mizuta Y, Murase K, Murata I, Kohno S. Lafutidine, a novel histamine H₂-receptor antagonist, *vs* lansoprazole in combination with amoxicillin and clarithromycin for eradication of *Helicobacter pylori*. *Helicobacter* 2003; **8**: 111-119
- 28 **Ohara H**, Isomoto H, Wen CY, Ejima C, Murata M, Miyazaki M, Takeshima F, Mizuta Y, Murata I, Koji T, Nagura H, Kohno S. Expression of mucosal addressin cell adhesion molecule 1 on vascular endothelium of gastric mucosa in patients with nodular gastritis. *World J Gastroenterol* 2003; **9**: 2701-2705
- 29 **Breidert M**, Miehlke S, Glasow A, Orban Z, Stolte M, Ehninger G, Bayerdorffer E, Nettesheim O, Halm U, Haidan A, Bornstein SR. Leptin and its receptor in normal human gastric mucosa and in *Helicobacter pylori*-associated gastritis. *Scand J Gastroenterol* 1999; **34**: 954-961
- 30 **Madej T**, Boguski MS, Bryant SH. Threading analysis suggests that the obese gene product may be a helical cytokine. *FEBS Lett* 1995; **373**: 13-18
- 31 **Tartaglia LA**, Dembski M, Weng X, Deng N, Culpepper J, Devos R, Richards GJ, Campfield LA, Clark FT, Deeds J, Muir C, Sanker S, Moriarty A, Moore KJ, Smutko JS, Mays GG, Wool EA, Monroe CA, Tepper RI. Identification and expression cloning of a leptin receptor, OB-R. *Cell* 1995; **83**: 1263-1271
- 32 **Sarraf P**, Frederich RC, Turner EM, Ma G, Jaskowiak NT, Rivet DJ, Flier JS, Lowell BB, Fraker DL, Alexander HR. Multiple cytokines and acute inflammation raise mouse leptin levels: potential role in inflammatory anorexia. *J Exp Med* 1997; **185**: 171-175
- 33 **Lord GM**, Matarese G, Howard JK, Bloom SR, Lechler RI. Leptin inhibits the anti-CD3-driven proliferation of peripheral blood T cells but enhances the production of proinflammatory cytokines. *J Leukoc Biol* 2002; **72**: 330-338
- 34 **Picker LJ**, Singh MK, Zdraveski Z, Treer JR, Waldrop SL, Bergstresser PR, Maino VC. Direct demonstration of cytokine synthesis heterogeneity among human memory/effector T cells by flow cytometry. *Blood* 1995; **86**: 1408-1419
- 35 **Shimzu T**, Satoh Y, Yamashiro Y. Serum leptin and body mass index in children with *H pylori* infection. *Gut* 2002; **51**: 142

Edited by Wang XL

Tumor vaccine against recurrence of hepatocellular carcinoma

Bao-Gang Peng, Li-Jiang Liang, Qiang He, Ming Kuang, Jia-Ming Lia, Ming-De Lu, Jie-Fu Huang

Bao-Gang Peng, Li-Jiang Liang, Qiang He, Ming Kuang, Jia-Ming Lia, Ming-De Lu, Jie-Fu Huang, Hepatobiliary Surgery Department, The First Affiliated Hospital, Sun Yat-Sen University, Guangzhou 510080, Guangdong Province, China

Supported by the Natural Science Foundation of Guangdong Province, No. 021889

Correspondence to: Bao-Gang Peng, Hepatobiliary Surgery Department, The First Affiliated Hospital, Sun Yat-Sen University, Guangzhou 510080, Guangdong Province, China. pengbaogang@163.net

Telephone: +86-20-87755766-8096 **Fax:** +86-20-87755766-8663

Received: 2004-02-02 **Accepted:** 2004-02-21

Abstract

AIM: To investigate the effects of autologous tumor vaccine on recurrence of hepatocellular carcinoma (HCC).

METHODS: Sixty patients with HCC who had undergone curative resection, were randomly divided into HCC vaccine group and control group. Three vaccinations at 2-wk intervals were performed after curative hepatic resection. Delayed-type- hypersensitivity (DTH) test was performed before and after vaccination. Primary endpoints were the time of recurrence.

RESULTS: Four patients in control group and 6 patients in HCC vaccine group were withdrawn from the study. The vaccine containing human autologous HCC fragments showed no essential adverse effect in a phase II clinical trial and 17 of 24 patients developed a DTH response against the fragments. Three of 17 DTH-positive response patients and 5 of 7 DTH- negative response patients had recurrences after curative resection. After the operation, 1-, 2- and 3-year recurrence rates of HCC vaccine group were 16.7%, 29.2% and 33.3%, respectively. But, 1-, 2- and 3-year recurrence rates of the control group were 30.8%, 53.8% and 61.5%, respectively. The time before the first recurrence in the vaccinated patients was significantly longer than that in the control patients ($P < 0.05$).

CONCLUSION: Autologous tumor vaccine is of promise in decreasing recurrence of human HCC.

© 2005 The WJG Press and Elsevier Inc. All rights reserved.

Key words: Hepatocellular carcinoma; HCC vaccine; Recurrence

Peng BG, Liang LJ, He Q, Kuang M, Lia JM, Lu MD, Huang JF. Tumor vaccine against recurrence of hepatocellular carcinoma. *World J Gastroenterol* 2005; 11(5): 700-704
<http://www.wjgnet.com/1007-9327/11/700.asp>

INTRODUCTION

Hepatocellular carcinoma (HCC) is one of the most common cancers worldwide, and its incidence is increasing^[1,2]. Although curative treatments such as hepatic resection, orthotopic liver transplantation or percutaneous regional treatments offer the

only chances of cure, the long-term results are still disappointed because of the high frequency of postoperative recurrence^[3-9]. Recurrence control is the primary goal of novel approaches for HCC treatment. Active specific immunotherapy using the patient's own tumor to elicit a long-term cell-mediated immune response has been successfully applied to melanoma, renal carcinoma and colon cancer^[10].

Tumor vaccines have been used to enhance T-cell responses in many forms^[11-16], such as whole tumor cells, tumor cell lysates, genetically modified tumor cells and peptide-pulsed autologous dendritic cells. Tumor cells themselves might be used as immunogens because it is believed that tumor cells could express a set of tumor-specific peptide-MHC complexes recognized by cytotoxic T lymphocytes (CTL). It has been reported that highly specific autologous CTL are induced from peripheral blood on formalin-fixed paraffin-embedded tumor sections^[17,18]. Using a formalin-fixed autologous tumor cell line as target cells, CTL could continuously amplify. When T lymphocytes are stimulated with formalin-fixed primary target cells derived from glioblastoma multiformis as tumor antigens, human tumor-specific CTL are expanded *in vitro*. HLA-A-2402-restricted and carcinoembryonic-antigen (CEA)-specific CTL could be induced by culturing human peripheral blood mononuclear cells (PBMC) with autologous formalin-fixed adhesive PBMC pre-loaded with CEA-bound latex beads^[19]. These observations have led us to propose that solid antigens in the size able to be phagocytosed by antigen presenting cells (APC) is one of the efficient tumor vaccines^[20]. We here reported a HCC vaccine against HCC recurrence.

MATERIALS AND METHODS

Patients

The following protocol was approved by the ethical authorities of the First Affiliated Hospital of Sun Yat-Sen University. All patients were histologically confirmed as HCC and underwent hepatectomy. Eligibility criteria included International Union Against Cancer (UICC) (1997, 5th edition) clinical tumor-node-metastasis (TNM) groupings of stages I, II, or IIIA. No patient received any immunosuppressive drugs including steroids within one month prior to receiving the vaccine. Furthermore, patients who had adequate hematologic, hepatic, and renal functions (hepatic function Child-Pugh class A or B, white cell count $> 3 \times 10^9/L$, platelets $> 5 \times 10^{10}/L$, and creatinine $< 88.4 \mu\text{mol}/L$) were enrolled, but those with any severe cardiac or psychiatric disease or distant metastases were excluded, after written informed consent was obtained. Exclusion criteria included evidence of extra-hepatic metastases (stage III-B or IV), hepatic function Child-Pugh C, other malignancies or history of other malignancies in the past five years, postoperative dysfunction of any organ for more than 2 wk, systemic active infections, autoimmune diseases at any period of study, systematic steroid therapy within one month prior to the vaccination and chemotherapy, radiation therapy or biological therapy within one month prior to the vaccination. Sixty patients with HCC underwent curative resection between January 2000 and June 2003, 7 of them received left lateral lobectomy, 15 left hepatectomy, 6 right hepatectomy and 32 irregular hepatectomy. All patients were randomly assigned into two groups. Thirty patients served as control group with no adjuvant treatment but with regular

follow-up observation in our hospital, and thirty patients treated with HCC vaccination served as treatment group.

Preparation of tumor vaccine and method for injection

Lecithin solution was prepared by adding 0.5 mL of 99.5% ethanol into 2.0 grams of lecithin, then dissolved at 45 °C in a water bath for approximately 1 h and filtered with 0.22 µm pore-size Millex-GV filters. α -tocopherol was dissolved at 45 °C in a water bath for less than 30 min and filtered with Steradisc 13 γ -ray sterile 0.45 µm filters. The two solutions were mixed. Cholesterol solution was prepared by dissolving 25 mg of cholesterol in 2 mL of 99.5% ethanol. Twenty-four microliters of cholesterol solution was added to 0.6 mL mixture solution of the α -tocopherol and lecithin, and then vortexed thoroughly to mix the solution. Then 0.1 mL of 10^7 IU/mL human IL-2 and human GM-CSF solution was added to 0.6 mL of the solution, and mixed.

Resected and neutral formalin-fixed HCC tissues (2 g or more) were homogenized. The fragments were filtered through 40 µm nylon meshes, washed and sterilized with 70% alcohol, then incubated in RPMI-1640 medium at 37 °C for 2 d. The tumor fragments were washed three times with saline, aliquoted into 50 mL per Eppendorf tube and stored at -80 °C until use.

HCC vaccine consisted of Vac-1 and Vac-2. Vac-1 contained (doses per injected site) 10 µL of fixed HCC fragments, 1 000 IU of hGM-CSF, 1 000 IU of hIL-2 and 0.05 µg of tuberculin. Vac-2 cytokine-grease contained 6 000 IU of hGM-CSF and 6 000 IU of hIL-2. Vac-1 (0.1 mL) was immunized by intradermal injection into the upper arm per injected site. After thirty minutes, 0.1 mL of Vac-2 was injected exactly into the Vac-1-injected site. One month after hepatic operation, eligible patients had the first vaccination. Autologous HCC vaccine was injected intradermally into the upper arm at a dose of 0.1 mL/site to 5 separate sites. The patients received three vaccinations at two-week intervals.

Delayed-type hypersensitivity (DTH) test

Patients who underwent curative hepatic resection were submitted to DTH test-1 before the first vaccination and to DTH test-2 two weeks after the final vaccine injection. Peripheral blood for PBMC preparation (10 mL) was taken for flow cytometry, and then, a suspension (0.1 mL in saline) of the autologous tumor fragments was injected intra-dermally into the left forearm. Forty-eight hours later, if erythema and induration shared a skin-area of more than 10 mm in diameter, it was defined positive. Slight responses (5-10 mm in diameter) though definitely observable, were recorded as weakly positive.

Follow up

Hepatic ultrasonography and serum alpha-fetoprotein (AFP) two weeks after DTH test-2 injection and then every two months, computed tomography (CT) scan and chest radiography at every six months after operations were performed. The protective effects of postoperative vaccine therapy on recurrence of HCC included the time to the first recurrence after operation, recurrence-free survival and overall survival. Once the recurrence was confirmed, follow-up was stopped, and routine treatments such as second hepatic resection, ultrasound-guided intratumoral ablation, transcatheter chemoembolisation (TACE) or systemic chemotherapy were performed.

Evaluation of adverse events

Although safety was confirmed in the preceding phase I study^[20], when any of the following events happened during the vaccination period, severe toxicity was considered. Using WHO grading of acute and sub-acute toxicity for reference^[21], the evaluation standards for toxicity of vaccine therapy were as follows. The toxicity to some main organs, such as heart, liver or kidney, reached

grade 3 or grade 4 of WHO standards, and the toxicity to skin reached grade 3 or grade 4 of WHO standards in two of three injections, acute fulminant hepatitis or any kind of autoimmune diseases was established.

Flow cytometry

Suspended cells (1×10^6 cells/mL) were washed three times with phosphate-buffered solution (PBS) (-), stained with monoclonal antibodies for 30 min, and FITC-labeled goat anti-mouse IgG polyclonal antibody for 5 min. The cells were again washed with PBS(-) containing 4% fibrinogens in fetal bovine serum (FBS), re-suspended in the same buffer at a concentration of 1×10^6 cells/mL and immediately analyzed by fluorescence-activated cell sorter (FACS) (Becton Dickinson, Co.) as previously described^[22]. The proportion of CD3+, CD4+, CD8+, CD16+, and CD56+ cells was determined using mouse anti-human monoclonal antibodies.

Statistical analysis

The *F*-test was used to analyze the data using Excel software. The prognostic relevance data of HCC tumor vaccine therapy were analyzed using log-rank test. *P* value less than 0.05 was considered statistically significant.

RESULTS

Base-line data of HCC patients

Four patients in the control group and 6 patients in the HCC vaccine group were withdrawn from the study, because they gave up tumor vaccine therapy or lost follow-up. Base-line data of 26 control patients and 24 vaccinated patients are shown in Table 1. No essential difference in the base-line data was observed between the vaccinated and control patients. Age, cause of liver injury, Child-Pugh classes, serum alanine-aminotransferase level, percentage of patients with cirrhosis, operation, American Joint Commission for Cancer (AJCC) stages, blood loss and transfusion in the operation were all in proximity. The major axis of resected tumor was 63 ± 22 mm and 56 ± 36 mm in the vaccinated and control patients, respectively.

Table 1 Base-line data of vaccinated and control patients (mean \pm SD)

	Vaccinated (<i>n</i> = 24, %)	Control (<i>n</i> = 26, %)
Age (yr)	53 \pm 9	49 \pm 15
Male	22 (92)	21 (81)
Female	2 (8)	5 (19)
Cause of liver injury		
Hepatitis B	19 (79.1)	18 (69.2)
Hepatitis C	1 (4.2)	2 (7.7)
Unknown	4 (16.7)	6 (23.1)
Child-Pugh class A	23 (96)	24 (92)
Child-Pugh class B	1 (4)	2 (8)
Alanine aminotransferase (U/L)	75 \pm 35	50 \pm 95
Cirrhosis	16 (67)	16 (62)
α -fetoprotein		
\geq 400 µg/L	17 (71.3)	16 (61.5)
<400 µg/L	7 (28.7)	10 (38.5)
Tumor size (major axis, mm)	63 \pm 22	56 \pm 36
AJCC stage I	4 (17)	2 (8)
AJCC stage II	20 (83)	24 (92)
Style of operation		
Left lateral lobectomy	3	4
Left hepatectomy	8	5
Right hepatectomy	2	3
Irregular hepatectomy	11	14
Blood loss during operation (mL)	812 \pm 536	769 \pm 620
Blood transfusion during operation (mL)	542 \pm 521	638 \pm 612

Adverse events in patients

The ultimate aim of this study was to detect toxicity. The vaccination was well tolerated and no severe adverse effect was observed in all patients. Erythema, dry desquamation and pruritus at the vaccinated sites were observed after each vaccination. These adverse effects disappeared 2 wk later and required no medical intervention. No exacerbation of cutaneous toxicities such as moist desquamation, ulceration or necrosis were observed. Lymphadenopathy and systemic reactions such as fever or chills, or vaccination-related impairments of the function of vital organs such as liver, kidney and bone marrow were not found. Occurrence of autoimmune diseases and skin toxicity was not observed. No patient withdrew from the study because of the adverse effects.

DTH responses induced by HCC vaccine

Delayed-type hypersensitivity (DTH) test was performed before vaccination and two weeks after the third vaccination. Negative responses were observed in all patients before vaccination. All patients demonstrated DTH responses two weeks after the third vaccination. Seventeen of 24 patients had delayed-type hypersensitivity (DTH) response to the HCC fragments, three weak-positive responses and fourteen positive responses were observed in the vaccinated patients. Seven patients showed a negative DTH response.

Tumor vaccine against recurrence of HCC

After three vaccinations at 2 wk intervals, seventeen of 24 patients had delayed-type hypersensitivity (DTH) response against the fragments. Three of 17-DTH positive response patients had HCC recurrence 13, 15 and 16 mo after curative resection. Five of 7-DTH negative response patients had HCC recurrence 8, 9, 10, 10, and 16 mo after operation. After the operation, the 1-, 2- and 3-year recurrence rates in HCC vaccine group were 16.7%, 29.2% and 33.3%, respectively. But the 1-, 2- and 3-year recurrence rates in the control group were 30.8%, 53.8% and 61.5%, respectively. The time before the first recurrence in the vaccinated patients was significantly longer than that in the control patients ($P < 0.05$). The recurrence-free HCC patients with or without tumor vaccine therapy is shown in Figure 1. The difference of the two curves was statistically significant (log-rank test, $P < 0.05$). These data suggested that vaccination of HCC patients with the autologous vaccine was a well-tolerated treatment and could induce tumor fragment-specific immunity.

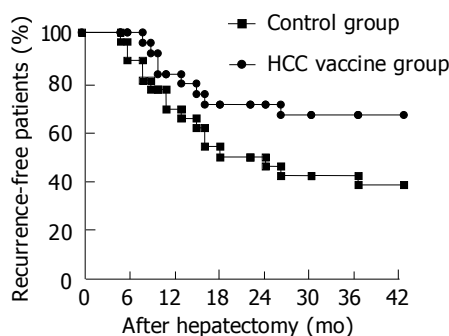


Figure 1 Recurrence-free HCC patients with or without tumor vaccine therapy (Kaplan-Meier curves).

Flow cytometric evaluation of surface phenotypes of peripheral blood lymphocytes

Twenty-four HCC patients who received the tumor vaccine were analyzed for surface phenotypes of peripheral blood

lymphocytes before and after vaccination. After tumor vaccination, the patients had a significantly higher number of CD3+ CD8+ positive lymphocytes and number of CD4+/CD8+ significantly lower ($P < 0.05$ Table 2).

Table 2 Surface phenotypes of peripheral blood lymphocytes (mean \pm SD)

	Control (n=26)	Before vaccination (n=24)	After vaccination (n=24)
CD3+	73.5 \pm 5.8	70.4 \pm 7.2	71.9 \pm 6.5
CD3+CD4+	45.2 \pm 9.7	48.3 \pm 7.6	49.0 \pm 9.2
CD3+CD8+	29.3 \pm 9.8 ^a	27.9 \pm 7.5 ^a	39.9 \pm 10.5 ^a
CD4+/CD8+	2.02 \pm 0.39 ^c	2.15 \pm 0.98 ^c	1.03 \pm 1.13 ^c
CD3-CD16+56+	18.5 \pm 3.9	16.9 \pm 8.3	19.7 \pm 9.3

^a $P < 0.05$, ^c $P < 0.05$ after tumor vaccination *vs* control or before tumor vaccination.

DISCUSSION

The present results suggest that a vaccine comprised of fixed HCC tissue fragments, cytokine controlled-release formulation, and adjuvant could elicit anti-tumor immune responses in human phase II clinical trials. The vaccine containing autologously fixed HCC fragments has no essential adverse effect; the time to the first recurrence in the vaccinated patients, especially in the DTH-positive response patients, is significantly longer than that in the control group (Figure 1).

In the clinical trial, we used DTH reaction, a monitoring method, for detecting antigen-specific immunity. Vaccination of patients with HCC fragments combined with hGM-CSF/hIL-2 controlled-release formulation and tuberculin was capable of inducing antitumor cellular immune response. We investigated DTH response to tumor fragments, which were processed by APC for effective presentation to effector T cells. After three vaccinations, 17 of 24 patients demonstrated positive DTH response. Furthermore, anti-hepatocellular carcinoma immune reaction was found to inhibit the recurrence. The results suggest that fixed HCC vaccination is well tolerated and is able to induce antitumor immunity, and should be considered for further clinical evaluation to define its potential therapeutic efficacy.

The major advantage of the present human HCC vaccine is that it contains personalized and very stable tumor antigens. HCC vaccine consisted unidentified autologous tumour antigens in fixed tumor tissues that can be preferably used in many medical institutions where vaccine is prepared with MHC-matched peptides and complicated recombinant techniques. Compared to the tumor vaccine containing live dendritic cells, which are considered the essential component, non-live cell-containing stable vaccines are easy to handle at bedside, thus increasing its use.

Active immunotherapy can induce tumor-specific cytotoxic T lymphocytes (CTL) and achieve a long-term antitumor immune response^[10,11,22]. AFP, a HCC-associated antigen, could serve as a target for T-cell immunotherapy in animals^[23,24], but patients carrying matched major histocompatibility complex (MHC) alleles could benefit from tumor-associated antigen-based vaccine^[12]. Antigen pre-loaded dendritic cells (DCs) could elicit strong antitumor immune response^[25,26], but DC-based approaches are cumbersome and expensive, and unsuitable for large-scale clinical trials. Until HCC-specific antigens are identified, the tumor cell itself is still the best source of tumor antigen. With autologous formalin-fixed paraffin-embedded tumor sections, we successfully induced tumor-specific cytotoxic T lymphocytes (CTL) from the peripheral blood of

tumor-bearing patients. From the present results, precise mechanisms of the anti-tumor immune response are obscure. However, we prepared fixed HCC as a fragment suspension in the vaccine. Phagocytosis of the particular antigen might be an important pathway to present the antigenic peptide on MHC-class I molecules^[27-30]. The present results suggest that antigens in a particular form could elicit CD8⁺ MHC class I-restricted CTL response (Table 2). Soluble antigens could elicit responses of CD4⁺ MHC class II-restricted lymphocytes^[31]. CD4⁺ T cells could then transfer their immune information to stimulate antibody production. Therefore, direct induction of CTL against soluble antigens is difficult, except when the antigenic peptide is loaded on the antigen presenting dendritic cells^[32]. However, studies have also reported that macrophages could efficiently induce CTL response *in vitro* when particular carriers are used to deliver antigenic short peptides^[33]. In our hypothesis, fixed tumor tissue can provide many tumor antigens that are recognized by the immune system of patients and elicit a specific antitumor response. Local use of hGM-CSF could activate dermal antigen-presenting cells (APC), hIL-2 could expand the proliferation of induced CTL, and the elicited antitumor immune response is then amplified. Slow release of these cytokines from cytokine controlled release formulation could maintain long-term stimulation of the immune system and induce persistent antitumor immunity.

Considering the simplicity in preparation, bed-side handling of the tumor vaccine is one of the most important factors. In this respect, vaccines including live cells in the formulation are disadvantageous because of the complicated preparation techniques. Tumor-associated antigenic peptides, DNA vaccines, and tumor cell lysate, are therefore the attractive alternatives. Unfortunately, peptides are only effective on patients carrying matched major histocompatibility complex (MHC) alleles^[12]. Peptides and tumor cell lysate are also rather weak immunogens. Antigen pre-loaded dendritic cells might be a promising vaccine^[34], which also require live cell handling. DNA vaccines could provide a definite amount of antigens^[14].

In conclusion, HCC vaccine can significantly control early post-operative recurrence of HCC and improve overall survival. This cell-free immunization mode should be recommended for a large-scale use in patients with HCC.

REFERENCES

- Peto J. Cancer epidemiology in the last century and the next decade. *Nature* 2001; **411**: 390-395
- El-Serag HB, Mason AC. Rising incidence of hepatocellular carcinoma in the United States. *N Engl J Med* 1999; **340**: 745-750
- Schafer DF, Sorrell MF. Hepatocellular carcinoma. *Lancet* 1999; **353**: 1253-1257
- Zhou XD, Tang ZY, Yang BH, Lin ZY, Ma ZC, Ye SL, Wu ZQ, Fan J, Qin LX, Zheng BH. Experience of 1000 patients who underwent hepatectomy for small hepatocellular carcinoma. *Cancer* 2001; **91**: 1479-1486
- Poon RT, Fan ST, Lo CM, Liu CL, Wong J. Long-term survival and pattern of recurrence after resection of small hepatocellular carcinoma in patients with preserved liver function: implications for a strategy of salvage transplantation. *Ann Surg* 2002; **235**: 373-382
- Bruix J, Llovet JM. Prognostic prediction and treatment strategy in hepatocellular carcinoma. *Hepatology* 2002; **35**: 519-524
- Fong Y, Sun RL, Jarnagin W, Blumgart LH. An analysis of 412 cases of hepatocellular carcinoma at a Western center. *Ann Surg* 1999; **229**: 790-799; discussion 799-800.
- Yao FY, Ferrell L, Bass NM, Watson JJ, Bacchetti P, Venook A, Ascher NL, Roberts JP. Liver transplantation for hepatocellular carcinoma: expansion of the tumor size limits does not adversely impact survival. *Hepatology* 2001; **33**: 1394-1403
- Lee WC, Jeng LB, Chen MF. Estimation of prognosis after hepatectomy for hepatocellular carcinoma. *Br J Surg* 2002; **89**: 311-316
- Vermorken JB, Claessen AM, van Tinteren H, Gall HE, Ezinga R, Meijer S, Scheper RJ, Meijer CJ, Bloemena E, Ransom JH, Hanna MG, Pinedo HM. Active specific immunotherapy for stage II and stage III human colon cancer: a randomised trial. *Lancet* 1999; **353**: 345-350
- Soiffer R, Lynch T, Mihm M, Jung K, Rhuda C, Schmollinger JC, Hodi FS, Liebster L, Lam P, Mentzer S, Singer S, Tanabe KK, Cosimi AB, Duda R, Sober A, Bhan A, Daley J, Neuberger D, Parry G, Rokovich J, Richards L, Drayer J, Berns A, Clift S, Cohen LK, Mulligan RC, Dranoff G. Vaccination with irradiated autologous melanoma cells engineered to secrete human granulocyte-macrophage colony-stimulating factor generates potent antitumor immunity in patients with metastatic melanoma. *Proc Natl Acad Sci USA* 1998; **95**: 13141-13146
- Protti MP, Bellone M. Immunotherapy: natural versus synthetic peptides. *Immunol Today* 1998; **19**: 98
- Gong J, Chen D, Kashiwaba M, Kufe D. Induction of antitumor activity by immunization with fusions of dendritic and carcinoma cells. *Nat Med* 1997; **3**: 558-561
- Pardoll DM. Cancer vaccines. *Nat Med* 1998; **4**: 525-531
- Zhang J, Zhang JK, Zhuo SH, Chen HB. Effect of a cancer vaccine prepared by fusions of hepatocarcinoma cells with dendritic cells. *World J Gastroenterol* 2001; **7**: 690-694
- Guo Y, Wu M, Chen H, Wang X, Liu G, Li G, Ma J, Sy MS. Effective tumor vaccine generated by fusion of hepatoma cells with activated B cells. *Science* 1994; **263**: 518-520
- Liu SQ, Saijo K, Todoroki T, Ohno T. Induction of human autologous cytotoxic T lymphocytes on formalin-fixed and paraffin-embedded tumour sections. *Nat Med* 1995; **1**: 267-271
- Liu SQ, Shiraiwa H, Kawai K, Hayashi H, Akaza H, Kim BS, Oki A, Nishida M, Kubo T, Hashizaki K, Saijo K, Ohno T. Tumor-specific autologous cytotoxic T lymphocytes from tissue sections. *Nat Med* 1996; **2**: 1283
- Kim C, Matsumura M, Saijo K, Ohno T. *In vitro* induction of HLA-A2402-restricted and carcinoembryonic-antigen-specific cytotoxic T lymphocytes on fixed autologous peripheral blood cells. *Cancer Immunol Immunother* 1998; **47**: 90-96
- Peng BG, Liu SQ, Kuang M, He Q, Totsuka S, Huang L, Huang J, Lu MD, Liang LJ, Leong KW, Ohno T. Autologous fixed tumor vaccine: A formulation with cytokine-microparticles for protective immunity against recurrence of human hepatocellular carcinoma. *Jpn J Cancer Res* 2002; **93**: 363-368
- Miller AB, Hoogstraten B, Staquet M, Winkler A. Reporting results of cancer treatment. *Cancer* 1981; **47**: 207-214
- McCune CS, O'Donnell RW, Marquis DM, Sahasrabudhe DM. Renal cell carcinoma treated by vaccines for active specific immunotherapy: correlation of survival with skin testing by autologous tumor cells. *Cancer Immunol Immunother* 1990; **32**: 62-66
- Vollmer CM, Eilber FC, Butterfield LH, Ribas A, Dissette VB, Koh A, Montejo LD, Lee MC, Andrews KJ, McBride WH, Glaspy JA, Economou JS. Alpha-fetoprotein-specific genetic immunotherapy for hepatocellular carcinoma. *Cancer Res* 1999; **59**: 3064-3067
- Meng WS, Butterfield LH, Ribas A, Dissette VB, Heller JB, Miranda GA, Glaspy JA, McBride WH, Economou JS. alpha-Fetoprotein-specific tumor immunity induced by plasmid prime-adenovirus boost genetic vaccination. *Cancer Res* 2001; **61**: 8782-8786
- Nestle FO, Banchereau J, Hart D. Dendritic cells: On the move from bench to bedside. *Nat Med* 2001; **7**: 761-765
- Homma S, Toda G, Gong J, Kufe D, Ohno T. Preventive antitumor activity against hepatocellular carcinoma (HCC) induced by immunization with fusions of dendritic cells and HCC cells in mice. *J Gastroenterol* 2001; **36**: 764-771
- Albert ML, Pearce SF, Francisco LM, Sauter B, Roy P, Silverstein RL, Bhardwaj N. Immature dendritic cells phagocytose apoptotic cells via alphavbeta5 and CD36, and cross-present

- antigens to cytotoxic T lymphocytes. *J Exp Med* 1998; **188**: 1359-1368
- 28 **Gallucci S**, Lolkema M, Matzinger P. Natural adjuvants: endogenous activators of dendritic cells. *Nat Med* 1999; **5**: 1249-1255
- 29 **Falo LD**, Kovacsics-Bankowski M, Thompson K, Rock KL. Targeting antigen into the phagocytic pathway *in vivo* induces protective tumour immunity. *Nat Med* 1995; **1**: 649-653
- 30 **Harding CV**, Song R. Phagocytic processing of exogenous particulate antigens by macrophages for presentation by class I MHC molecules. *J Immunol* 1994; **153**: 4925-4933
- 31 **Rock KL**, Clark K. Analysis of the role of MHC class II presentation in the stimulation of cytotoxic T lymphocytes by antigens targeted into the exogenous antigen-MHC class I presentation pathway. *J Immunol* 1996; **156**: 3721-3726
- 32 **De Bruijn ML**, Jackson MR, Peterson PA. Phagocyte-induced antigen-specific activation of unprimed CD8+ T cells *in vitro*. *Eur J Immunol* 1995; **25**: 1274-1285
- 33 **De Bruijn ML**, Peterson PA, Jackson MR. Induction of heat-stable antigen expression by phagocytosis is involved in *in vitro* activation of unprimed CTL by macrophages. *J Immunol* 1996; **156**: 2686-2692
- 34 **Mayordomo JI**, Zorina T, Storkus WJ, Zitvogel L, Celluzzi C, Falo LD, Melief CJ, Ildstad ST, Kast WM, Deleo AB. Bone marrow-derived dendritic cells pulsed with synthetic tumour peptides elicit protective and therapeutic antitumour immunity. *Nat Med* 1995; **1**: 1297-1302

Edited by Kumar M and Wang XL

Tiam1 gene expression and its significance in colorectal carcinoma

Li Liu, De-Hua Wu, Yan-Qing Ding

Li Liu, Yan-Qing Ding, Department of Pathology, First Military Medical University, Guangzhou 510515, Guangdong Province, China
De-Hua Wu, Department of Radiation Oncology, Nanfang Hospital, First Military Medical University, Guangzhou 510515, Guangdong Province, China

Supported by the National Natural Science Foundation of China, No. 30370649

Correspondence to: Dr. Yan-Qing Ding, Department of Pathology, First Military Medical University, Guangzhou 510515, Guangdong Province, China. dyq@fimmu.com

Telephone: +86-20-61642148 **Fax:** +86-20-61642148

Received: 2004-02-14 **Accepted:** 2004-03-02

Abstract

AIM: To explore the expression of Tiam1 gene in colorectal carcinoma and its correlation with tumor metastasis.

METHODS: Expressions of Tiam1 gene in 8 colorectal carcinoma cell lines were detected by reverse transcriptase-polymerase chain reaction. *In vitro* invasiveness was determined by means of Matrigel invasion assay. The correlation of Tiam1 expression with the invasive ability was also analyzed.

RESULTS: Tiam1 gene was highly expressed in LoVo and SW620, which were established from metastatic colorectal carcinomas in comparison with LS174T, SW480, HCT116, LST, HRT-18 and Hee8693, which were established from primary colorectal carcinomas. *In vitro* cell invasion demonstrated that LoVo and SW620 had a higher invasive ability than LS174T, SW480, HCT116, LST, HRT-18 and Hee8693. The expression of Tiam1 gene was highly related to the metastatic potential of colorectal carcinoma cells.

CONCLUSION: Tiam1 gene may play an important role in invasion and metastasis of colorectal carcinoma and is a metastasis-related gene.

© 2005 The WJG Press and Elsevier Inc. All rights reserved.

Key words: Colorectal carcinoma; Tiam1 gene; Gene expression; Tumor metastasis

Liu L, Wu DH, Ding YQ. Tiam1 gene expression and its significance in colorectal carcinoma. *World J Gastroenterol* 2005; 11(5): 705-707

<http://www.wjgnet.com/1007-9327/11/705.asp>

INTRODUCTION

Colorectal carcinoma is one of the most common malignancies. The majority of colorectal carcinomas arise from a series of somatic genetic changes that involve activation of oncogenes and inactivation of tumor suppressor genes. The delineation of molecular genetic and biological changes that accompany the pathogenesis of colorectal carcinoma will hopefully improve the outcome of patients in the future. Unfortunately, the overwhelming majority of patients with colorectal carcinoma would die of metastatic disease, that is to say, metastasis is the

major cause of mortality in the human population^[1]. Unlike the molecular events described for the pathogenesis of primary colorectal carcinomas, genes responsible for metastasis in these tumors have not been well characterized. Exploring metastasis-related genes is significantly important in the prevention of tumor metastasis and prolongation of the life expectancy of patients.

A gene designated Tiam1 was originally identified as the invasion- and metastasis-inducing gene by proviral tagging in combination with *in vitro* selection for invasiveness^[2]. Transfection of truncated Tiam1 cDNAs into noninvasive cells can make these cells invasive. Tiam1 protein contains a Dbl homologous (DH) domain and two pleckstrin homologous (PH) domains. DH domain is present in guanine nucleotide exchange factors (GEFs) that activate the Rho-like GTPases^[3]. PH domain, present in many signaling proteins, has been reported to be involved in protein-protein and protein-phospholipid interactions and might play a role in translocation of these proteins to membranes^[4]. Tiam1 is one of the GEFs and can specifically activate Rac *in vitro* as well as *in vivo*^[5]. Tiam1 has been implicated to directly bind to a plethora of different cytoplasmic and membrane-associated proteins, which couple Tiam1-Rac activity to specific signaling pathways^[6,7]. Interestingly, proteins such as Src^[8], Myc^[9], CD44^[10] and nm23^[11], claimed to interact with Tiam1 are well known players in the field of cancer. Tiam1 activation has also been shown to be stimulated by certain serum-derived growth activators such as S1P^[12] and LPA^[13] during cell spreading and motility.

Recent evidence suggests that Tiam1 could influence Rac GTPase signaling specificity in addition to promoting their activation^[14]. That is why Tiam1 has a different effect on different cancers. For example, activation of Tiam1 in breast cancer and T-lymphoma cell lines, produces specific structural changes in plasma membrane-cytoskeleton reorganization leading to membrane ruffling, lamellipodia, filopodia, and stresses fiber formation^[15,16]. These changes are prerequisite for invasion and metastasis. Conversely, in renal cell carcinoma cell lines, Tiam1 potentiates homotypic cell-cell adhesion and inhibits invasion^[17]. In epithelial MDCK cells, Tiam1-Rac1 signaling plays an invasion-suppressor role in Ras-transformed MDCK cells^[18]. A Tiam1 knock-out mouse is relatively resistant to chemical induction of skin tumors but paradoxically more prone to malignant histologic progression of those tumors^[19].

Tiam1 has been studied in breast cancer^[15], renal carcinoma^[17], chondrosarcoma^[20], T-lymphoma^[16], etc. However, it is not known at present whether there is any relationship between Tiam1 and colorectal carcinoma. Here we showed the expression of Tiam1 in 8 colorectal carcinoma cell lines, and analyzed its correlation with tumor metastasis. Our observations suggest that Tiam1 has a close relationship with metastasis of colorectal carcinoma and may be required for colorectal carcinoma cell invasion and migration.

MATERIALS AND METHODS

Cell lines and culture conditions

HRT-18 and Hee8693 cell lines were a kind gift from Cancer Research Institute in Xiangya Medical School of Central South University. LST cell line was a generous gift from Digestive Department in Nanfang Hospital. LoVo, LS174T, HCT116, SW480

and SW620 were obtained from America Type Culture Collection. LoVo, LS174T, LST, HRT-18, HCT116 and Hee8693 cell lines were cultured in RPMI-1640 medium. SW480 and SW620 were cultured in Dulbecco's modified Eagle's medium. All mediums supplemented with 10% heat-inactivated fetal bovine serum (FBS) and 100 U/mL penicillin/streptomycin. Cultured cells were grown in a 37 °C humidified incubator with 50 mL/L CO₂.

Total RNA extraction

Total RNA was extracted from the cell lines using TRIzol reagent (Invitrogen Corporation). Then DNase I was used to remove genomic DNA from total RNA. Concentration and purity of the RNA samples were examined by a spectrophotometer. Two oligonucleotides, 5'-AATCCCATCACCATTCTTCCA-3' and 5'-CCTGCTTCACCACCTTCTTG-3', designated GAPDH (a housekeeping gene), were utilized as primers to perform polymerase chain reaction (PCR) in order to check whether the RNA was contaminated with trace genomic DNA.

Reverse transcriptase-polymerase chain reaction (RT-PCR)

Reverse transcriptase (RT) was performed using an access RT-PCR system (Promega Corporation) according to the manufacturer's protocol. Total RNA in the amount of 1 µg was used in each RT reaction to synthesize cDNA. For PCR, we used the forward primer 5'-AAGACGTACTCAGGCCATGTCC-3' and reverse primer 5'-GACCCAAATGTCGAGTCAG-3', which were designed by primer premier 5.0 software, to amplify human Tiam1 (NM_003253 from GeneBank). And human GAPDH primers were utilized as an internal control. Thirty cycles of reactions were carried out, each at 94 °C for 45 s, at 58 °C for 45 s, at 72 °C for 45 s. PCR products were electrophoresed in 2% agarose gel and sequenced by Bioasia Biological Corporation. Electrophoretogram was taken by a pickup camera under UV light and analyzed by 1-D advanced software.

In vitro invasion assay

This assay was based on the principle of Boyden chamber^[21]. The top and bottom of Boyden chamber (corning company) were separated by a polycarbonate filter with 8 µm pore size. The top chamber was prepared by coating the filter with 50 µg of diluted Matrigel and incubated for 30 min. A single cell suspension of 10 000 tumor cells in serum-free medium was inoculated in the upper chamber, after 5% FBS was added into the bottom chamber as a chemoattractant. After 24 h incubation, noninvasive cells were removed with a cotton swab. The cells migrated through the membrane and stuck to the lower surface of the membrane were fixed with methanol and stained with hematoxylin. Tumor cell invasiveness was determined by counting all tumor cells in five randomly selected counting fields at ×200.

Statistical analysis

Relationship between expression of Tiam1 and invasive ability was analyzed by bivariate correlation using SPSS 10.0 Software.

RESULTS

Expression of Tiam1 in colorectal carcinoma cell lines

Total RNA extracted from eight colorectal carcinoma cell lines was confirmed to have no degradation by agarose gel electrophoresis (Figure 1). In order to detect whether the RNA was contaminated with gDNA, we used the RNA digested with DNase I and RNA not digested with DNase I as templates to amplify the housekeeping gene, GAPDH. The results showed that the RNA we extracted was not contaminated with gDNA (Figure 2).

RT-PCR detection of Tiam1 expression in eight colorectal carcinoma cell lines was heterogeneous (Figure 3). Analyzed by 1-D Advanced software, relative Tiam1 expression was calculated as the ratio of the densitometry of the Tiam1 band:

GAPDH band on RT-PCR. We found that Tiam1 was abundantly expressed in metastatic colorectal carcinoma cell lines, LoVo and SW620, 1.19 and 0.96 respectively. In primary colorectal carcinoma cell lines, SW480 (0.57), LS174T (0.32), LST (0.44), HCT116 (0.60), HRT-18 (0.52) and Hee8693 (0.55) were moderately and lowly expressed. The product of RT-PCR, Tiam1, was confirmed by sequence analysis (date was not shown).

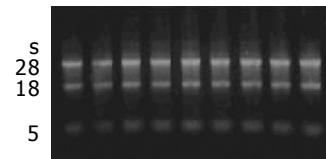


Figure 1 Agarose gel electrophoresis of total RNA from colorectal carcinoma cell lines.

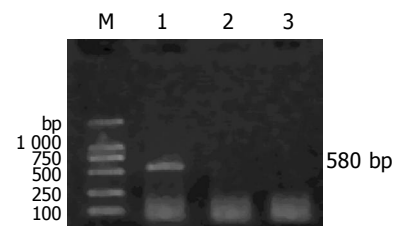


Figure 2 2% agarose gel electrophoresis of the product of PCR (580 bp). M: Marker; lane 1: Templates were the RNAs not digested with DNase I, GAPDH was amplified; lanes 2, 3: Templates were the RNAs digested with DNase I, no product was amplified.

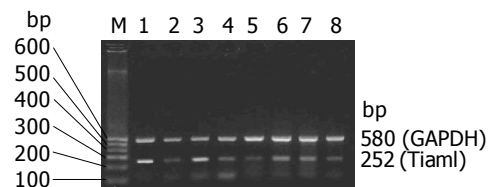


Figure 3 Expression of Tiam1 in 8 colorectal carcinoma cell lines by RT-PCR. M: Marker; lane 1: LoVo; lane 2: SW480; lane 3: SW620; lane 4: HCT116; lane 5: LS174T; lane 6: LST; lane 7: HRT-18; lane 8: Hee8693.

In vitro invasive assay

In vitro cell invasive assay was performed based on the principle of the Boyden chamber assay. Matrigel matrix served as a reconstituted basement membrane *in vitro*. The number of cells migrating through the Matrigel matrix was counted. The result indicated that LoVo (145) and SW620 (130) had a higher invasive ability than SW480 (91), HCT116 (89), LS174T (64), LST (79), HRT-18 (87) and Hee8693 (90).

Correlation analysis

We used the SPSS 10.0 to analysis the correlation between the expression of Tiam1 and invasive ability. The results showed that the both are highly correlative ($r = 0.995$, $P < 0.01$).

DISCUSSION

Tumor invasion is a complex biological process, during which tumor cells detach from the primary tumor and infiltrate its surrounding tissues. This process requires loss of cell contacts between tumor cells, active cell migration, adhesion to the extracellular matrix (ECM) and proteolytic degradation of

ECM^[22]. At the molecular level, a number of different molecules, including cadherins, integrins, proteases, and growth factors, have been implicated in the regulation of tumor cell invasiveness^[23].

It has been found that Tiam1 is capable of activating Rac1 as a ubiquitous guanine nucleotide exchange factor and inducing membrane cytoskeleton-mediated cell shape changes, cell adhesion, and cell motility^[24-26]. Rac1 could act on downstream of Tiam1 signaling and regulate the function of several cell adhesion molecules such as laminin receptor, integrin^[27], E-cadherin^[18], and the hyaluronan receptor, CD44.

In the past, to search new metastasis-associated genes, we prepared cDNA microarray which is highly sensitive and applicable in examining gene expression profile. Then metastatic colorectal carcinoma microarray gene expression data were mined by literature profiling, based on the analysis of literature profiles generated by extracting the frequencies of certain terms from MEDLINE. We found that Tiam1 gene had a potential relation to metastatic colorectal carcinoma.

In this study, we investigated the relation between Tiam1 expression and metastasis in colorectal carcinoma. LoVo cell line was derived from human colonic adenocarcinoma established from the metastatic nodule. SW480 was isolated from a high-grade primary colonic tumor, and SW620 was isolated from a metastatic lymph node from the same patient 1-year later at the time of clinical relapse. LS174T, LST and HCT116 were isolated from primary colonic carcinomas. HRT-18 was isolated from primary rectal cancer and Hee8693 from primary cecal cancer. We found that the expression of Tiam1 in cell lines established from metastatic colorectal carcinomas was much higher than that in cell lines established from primary colorectal carcinomas. We also found that the invasiveness and metastasis in cell lines established from metastatic colorectal carcinomas were much stronger than those in cell lines established from primary colorectal carcinomas. We identified that Tiam1 was highly correlated with invasiveness and metastasis ($P < 0.01$). These data indicate that enhanced expression of Tiam1 is associated with increased invasive ability.

In a word, our results suggest that Tiam1 might be a metastasis-related gene in colorectal carcinoma. In the future research, we will study the effect of Tiam1 gene on invasion and metastasis in colorectal carcinoma *in vivo* and *in vitro* through stable Tiam1 gene transfection or RNA interfering. The two-dimensional electrophoresis and mass spectrum analysis will be used to study the possible mechanism of Tiam1 gene and its signal transduction.

REFERENCES

- 1 **Budenholzer B.** Screening for colorectal cancer. *CMAJ* 2001; **164**: 965-966; author reply 967-968
- 2 **Habets GG, Scholtes EH, Zuydgeest D, van der Kammen RA, Stam JC, Berns A, Collard JG.** Identification of an invasion-inducing gene, Tiam-1, that encodes a protein with homology to GDP-GTP exchangers for Rho-like proteins. *Cell* 1994; **77**: 537-549
- 3 **Robbe K, Otto-Bruc A, Chardin P, Antony B.** Dissociation of GDP dissociation inhibitor and membrane translocation are required for efficient activation of Rac by the Dbl homology-pleckstrin homology region of Tiam. *J Biol Chem* 2003; **278**: 4756-4762
- 4 **Crompton AM, Foley LH, Wood A, Roscoe W, Stokoe D, McCormick F, Symons M, Bollag G.** Regulation of Tiam1 nucleotide exchange activity by pleckstrin domain binding ligands. *J Biol Chem* 2000; **275**: 25751-25759
- 5 **Lambert JM, Lambert QT, Reuther GW, Malliri A, Siderovski DP, Sondek J, Collard JG, Der CJ.** Tiam1 mediates Ras activation of Rac by a PI(3)K-independent mechanism. *Nat Cell Biol* 2002; **4**: 621-625
- 6 **Buchsbaum RJ, Connolly BA, Feig LA.** Interaction of Rac exchange factors Tiam1 and Ras-GRF1 with a scaffold for the p38 mitogen-activated protein kinase cascade. *Mol Cell Biol* 2002; **22**: 4073-4085
- 7 **Buchsbaum RJ, Connolly BA, Feig LA.** Regulation of p70 S6 kinase by complex formation between the Rac guanine nucleotide exchange factor (Rac-GEF) Tiam1 and the scaffold spinophilin. *J Biol Chem* 2003; **278**: 18833-18841
- 8 **Servtija JM, Marinissen MJ, Sodhi A, Bustelo XR, Gutkind JS.** Rac1 function is required for Src-induced transformation. Evidence of a role for Tiam1 and Vav2 in Rac activation by Src. *J Biol Chem* 2003; **278**: 34339-34346
- 9 **Otsuki Y, Tanaka M, Kamo T, Kitanaka C, Kuchino Y, Sugimura H.** Guanine nucleotide exchange factor, Tiam1, directly binds to c-Myc and interferes with c-Myc-mediated apoptosis in rat-1 fibroblasts. *J Biol Chem* 2003; **278**: 5132-5140
- 10 **Bourguignon LY.** CD44-mediated oncogenic signaling and cytoskeleton activation during mammary tumor progression. *J Mammary Gland Biol Neoplasia* 2001; **6**: 287-297
- 11 **Otsuki Y, Tanaka M, Yoshii S, Kawazoe N, Nakaya K, Sugimura H.** Tumor metastasis suppressor nm23H1 regulates Rac1 GTPase by interaction with Tiam1. *Proc Natl Acad Sci USA* 2001; **98**: 4385-4390
- 12 **Buchanan FG, Elliot CM, Gibbs M, Exton JH.** Translocation of the Rac1 guanine nucleotide exchange factor Tiam1 induced by platelet-derived growth factor and lysophosphatidic acid. *J Biol Chem* 2000; **275**: 9742-9748
- 13 **Van Leeuwen FN, Olivo C, Grivell S, Giepmans BN, Collard JG, Moolenaar WH.** Rac activation by lysophosphatidic acid LPA1 receptors through the guanine nucleotide exchange factor Tiam1. *J Biol Chem* 2003; **278**: 400-406
- 14 **Mertens AE, Roovers RC, Collard JG.** Regulation of Tiam1-Rac signalling. *FEBS Lett* 2003; **546**: 11-16
- 15 **Bourguignon LY, Zhu H, Shao L, Chen YW.** Ankyrin-Tiam1 interaction promotes Rac1 signaling and metastatic breast tumor cell invasion and migration. *J Cell Biol* 2000; **150**: 177-191
- 16 **Stam JC, Michiels F, van der Kammen RA, Moolenaar WH, Collard JG.** Invasion of T-lymphoma cells: cooperation between Rho family GTPases and lysophospholipid receptor signaling. *EMBO J* 1998; **17**: 4066-4074
- 17 **Engers R, Springer E, Michiels F, Collard JG, Gabbert HE.** Rac affects invasion of human renal cell carcinomas by up-regulating tissue inhibitor of metalloproteinases (TIMP)-1 and TIMP-2 expression. *J Biol Chem* 2001; **276**: 41889-41897
- 18 **Hordijk PL, ten Klooster JP, van der Kammen RA, Michiels F, Oomen LC, Collard JG.** Inhibition of invasion of epithelial cells by Tiam1-Rac signaling. *Science* 1997; **278**: 1464-1466
- 19 **Malliri A, van der Kammen RA, Clark K, van der Valk M, Michiels F, Collard JG.** Mice deficient in the Rac activator Tiam1 are resistant to Ras-induced skin tumours. *Nature* 2002; **417**: 867-871
- 20 **Karjalainen HM, Sironen RK, Elo MA, Kaarniranta K, Takigawa M, Helminen HJ, Lammi MJ.** Gene expression profiles in chondrosarcoma cells subjected to cyclic stretching and hydrostatic pressure. A cDNA array study. *Biorheology* 2003; **40**: 93-100
- 21 **Itoh F, Yamamoto H, Hinoda Y, Imai K.** Enhanced secretion and activation of matrilysin during malignant conversion of human colorectal epithelium and its relationship with invasive potential of colon cancer cells. *Cancer* 1996; **77**: 1717-1721
- 22 **Engers R, Gabbert HE.** Mechanisms of tumor metastasis: cell biological aspects and clinical implications. *J Cancer Res Clin Oncol* 2000; **126**: 682-692
- 23 **Takeda A, Stoeltzing O, Ahmad SA, Reinmuth N, Liu W, Parikh A, Fan F, Akagi M, Ellis LM.** Role of angiogenesis in the development and growth of liver metastasis. *Ann Surg Oncol* 2002; **9**: 610-616
- 24 **Michiels F, Habets GG, Stam JC, van der Kammen RA, Collard JG.** A role for Rac in Tiam1-induced membrane ruffling and invasion. *Nature* 1995; **375**: 338-340
- 25 **Sander EE, van Delft S, ten Klooster JP, Reid T, van der Kammen RA, Michiels F, Collard JG.** Matrix-dependent Tiam1/Rac signaling in epithelial cells promotes either cell-cell adhesion or cell migration and is regulated by phosphatidylinositol 3-kinase. *J Cell Biol* 1998; **143**: 1385-1398
- 26 **Michiels F, Collard JG.** Rho-like GTPases: their role in cell adhesion and invasion. *Biochem Soc Symp* 1999; **65**: 125-146
- 27 **Leeuwen FN, Kain HE, Kammen RA, Michiels F, Kranenburg OW, Collard JG.** The guanine nucleotide exchange factor Tiam1 affects neuronal morphology; opposing roles for the small GTPases Rac and Rho. *J Cell Biol* 1997; **139**: 797-807

Value of portal hemodynamics and hypersplenism in cirrhosis staging

Bao-Min Shi, Xiu-Yan Wang, Qing-Ling Mu, Tai-Huang Wu, Jian Xu

Bao-Min Shi, Qing-Ling Mu, Tai-Huang Wu, Jian Xu, Department of General Surgery, Shandong Provincial Hospital, Jinan 250021, Shandong Province, China

Xiu-Yan Wang, Center of Ultrasonography, Shandong Provincial Hospital, Jinan 250021, Shandong Province, China

Supported by the National Science Fund or Foundation for Postdoctoral Fellows in China, No. 2001.6; the Medical Science Found of Shandong Province, No. 1999CA2BJBA1

Correspondence to: Dr. Bao-Min Shi, Department of General Surgery, Shandong Provincial Hospital, Clinical College of Shandong University, 324 Jingwu Road, Jinan 250021, Shandong Province, China. baomins@tom.com

Telephone: +86-531-7938911-2363 **Fax:** +86-531-7937741

Received: 2004-02-28 **Accepted:** 2004-07-11

Abstract

AIM: To determine the correlation between portal hemodynamics and spleen function among different grades of cirrhosis and verify its significance in cirrhosis staging.

METHODS: The portal and splenic vein hemodynamics and spleen size were investigated by ultrasonography in consecutive 38 cirrhotic patients with cirrhosis (Child's grades A to C) and 20 normal controls. The differences were compared in portal vein diameter and flow velocity between patients with and without ascites and between patients with mild and severe esophageal varices. The correlation between peripheral blood cell counts and Child's grades was also determined.

RESULTS: The portal flow velocity and volume were significantly lower in patients with Child's C (12.25 ± 1.67 cm/s vs 788.59 ± 234 mm/min, respectively) cirrhosis compared to controls (19.55 ± 3.28 cm/s vs 1254.03 ± 410 mm/min, respectively) and those with Child's A (18.5 ± 3.02 cm/s vs 1358.48 ± 384 mm/min, respectively) and Child's B (16.0 ± 3.89 cm/s vs 1142.23 ± 390 mm/min, respectively) cirrhosis. Patients with ascites had much lower portal flow velocity and volume (13.0 ± 1.72 cm/s vs 1078 ± 533 mm/min) than those without ascites (18.6 ± 2.60 cm/s vs 1394 ± 354 mm/min). There was no statistical difference between patients with mild and severe esophageal varices. The portal vein diameter was not significantly different among the above groups. There were significant differences in splenic vein diameter, flow velocity and white blood cell count, but not in spleen size, red blood cell and platelet counts among the various grades of cirrhosis. The spleen size was negatively correlated with red blood cell and platelet counts ($r = -0.620$ and $r = -0.834$, respectively).

CONCLUSION: An optimal system that includes parameters representing the portal hemodynamics and spleen function should be proposed for cirrhosis staging.

© 2005 The WJG Press and Elsevier Inc. All rights reserved.

Key words: Liver cirrhosis; Portal vein; Splenic vein; Hemodynamics; Hypersplenism

Shi BM, Wang XY, Mu QL, Wu TH, Xu J. Value of portal hemodynamics and hypersplenism in cirrhosis staging. *World J Gastroenterol* 2005; 11(5): 708-711

<http://www.wjgnet.com/1007-9327/11/708.asp>

INTRODUCTION

Liver cirrhosis due to various causes is a very common and irreversible state. In China, there are hundreds of thousands of new cases annually, most of which are developed from chronic hepatitis^[1]. The diagnosis and prognosis in cirrhosis of liver mostly depend upon the Child's grading system or the modified Child-Pugh system, which takes into account the severity of jaundice, ascites, hypoalbuminemia, encephalopathy, and prothrombin time^[2]. Other liver function tests and biochemical markers are also reported to correlate with the prognosis and severity of liver cirrhosis^[3-5]. However, the most common clinical signs and symptoms of cirrhosis include three aspects: liver dysfunction, portal hypertension and hypersplenism, and the major causes of death for the patients with cirrhosis are hepatic failure, gastrointestinal hemorrhage and secondary infection. The criteria of the Child-Pugh system are all reflections of hepatocyte function, but not of portal hemodynamics and spleen. Therefore, a comprehensive evaluation for the cirrhosis staging should cover hepatocyte function, portal hemodynamics and spleen function. Several studies have shown that portal hemodynamics is closely related to the Child's scores and liver fibrosis^[2]. There are also published papers concerning the relationship among spleen size, hemodynamics of splenic vein, esophageal varices and Child's scores^[5-9]. To verify the correlation between portal hemodynamics, splenomegaly and various Child's scores and clarify the significance of portal hemodynamics and spleen function in cirrhosis staging, we studied retrospectively a group of patients with cirrhosis.

MATERIALS AND METHODS

Patients

Thirty-eight consecutive patients with cirrhosis (22 Child's grade A, 8 Child's grade B, and 8 Child's grade C) and 20 age- and sex-matched (authors) normal healthy controls were enrolled in this study. The diagnosis of cirrhosis was established by a combination of clinical, biochemical, surgical and pathological investigations. Child's grading was done by the modified Child-Pugh scoring method. All patients with cirrhosis underwent an upper gastrointestinal endoscopy within three months prior to the study, to determine esophageal varices and the varix degree if present, according to the Japanese Classification.

The exclusion criteria were 1, patients with gastrointestinal bleeding in the previous four weeks; 2, those who were taking portal pressure-lowering drugs such as β -blockers; 3, those with encephalopathy grade II or more; 4, those with portal or splenic vein thrombosis; and 5, those with a previous history of sclerotherapy or banding for esophageal varices.

Methods

A color Doppler US system BK3535 (BK Medical, Copenhagen,

Denmark) was used. All measurements were performed by the same examiner without knowledge of the clinical information of subjects. All patients and controls were kept fasting overnight prior to the sonography. Portal trunk was scanned longitudinally with the sector scanner. The 3 mm sampling marker was shifted to the corner of the lumen at 1.5-2.5 cm before the bifurcation of right and left branches, and the angle of insonation was kept below 60 °C. The portal vein diameter was measured directly at this point. The portal flow velocity (PFV) in centimeters per second (cm/s) was averaged by Doppler traces of 2-3 cardiac cycles. The portal blood flow rate (PBF) in milliliters per minute (mL/min) was obtained by the formula: PBF = PFV × A × 60, (A as cross-sectional area of portal vein in square centimeters).

The spleen maximal length, transverse diameter, and thickness at the hilum were measured. These were then multiplied together, and a further factor of 0.6 was included to obtain an approximation of volume. The diameter and flow velocity of the splenic vein were obtained at 1.0-1.5 cm before bifurcation. Peripheral blood routine test was also performed for each patient to evaluate the grade of hypersplenism.

Statistical analysis

All the data were analyzed with SAS10.0 software. Differences in mean values of Doppler US parameters between the normal control subjects and patients with cirrhosis were tested by Student's *t* test and univariate analysis. Correlation among variables was assessed by linear regression analysis. The results were expressed as mean ± SD, and the difference was considered statistically significant when $P < 0.05$.

RESULTS

Correlation between portal hemodynamics and Child's grade

There was no difference in the portal vein diameter between the controls and the patients with different grades of cirrhosis (Table 1). The portal flow velocity and volume were significantly lower in Child's C cirrhosis compared to controls, and Child's A and B cirrhotics. The portal flow velocity was also lower in Child's B cirrhotics than in Child's A cirrhotics ($P < 0.05$). However, there was no difference in the portal blood volume between patients with Child's A and B cirrhosis and the controls (Table 1). With increasing Child's grades of severity, the portal flow velocity and volume decreased significantly.

Table 1 Portal hemodynamics in patients with various grades of Child's cirrhosis (mean ± SD)

	Cases	Diameters (cm)	Flow velocity (cm/s)	Flow volume (mL/min)
Control	20	1.17 ± 0.13	19.55 ± 3.28	1 254.03 ± 410
Child A	22	1.23 ± 0.17	18.5 ± 3.02	1 358.48 ± 384
Child B	8	1.24 ± 0.15	16.0 ± 3.89 ^a	1 142.23 ± 390
Child C	8	1.16 ± 0.20	12.25 ± 1.67 ^b	788.59 ± 234 ^{bc}

^a $P < 0.05$, ^b $P < 0.01$ vs Child's A; ^c $P < 0.05$ vs Child's B.

The difference was not significantly in portal vein diameter between patients with and without ascites. However, both portal flow velocity and volume of the patients with ascites were statistically lower than those without ascites (Table 2).

There was no significant difference in portal flow velocity and volume between patients with mild varices and those with severe varices (Table 3).

Table 2 Portal hemodynamics between cirrhotics with and without ascites (mean ± SD)

	Number	Diameter (cm)	Velocity (cm/s)	Volume (mL/min)
With ascites	8	1.32 ± 0.17	13.0 ± 1.72	1 078 ± 533
Without ascites	30	1.20 ± 0.21	18.6 ± 2.60	1 394 ± 354
<i>P</i>		>0.05	<0.01	<0.05

Table 3 Portal hemodynamics between cirrhotics with mild and severe varices (mean ± SD)

	Number	Diameter (cm)	Velocity (cm/s)
Mild varices	21	1.20 ± 0.14	18.0 ± 3.92
Severe varices	17	1.26 ± 0.21	19.50 ± 3.93
<i>P</i>		>0.05	>0.05

Splenic hemodynamics and Child's grading

There were significant differences in splenic vein diameter, splenic flow velocity, peripheral white blood cell count among patients with various grades of Child's score. With the development of cirrhosis from Child's A to B and C, the splenic vein diameter increased correspondingly, while splenic flow velocity and white blood cell count decreased significantly. There was no statistical difference in peripheral red blood cell and platelet count among patients with various grades of cirrhosis (Table 4). The spleen volume negatively correlated with red blood ($R = -0.620$, $P < 0.05$) and platelet counting ($R = -0.834$, $P < 0.001$). Peripheral platelet count positively correlated with red blood cell count ($R = 0.583$, $P < 0.001$).

Table 4 Univariate analysis of parameters for hypersplenism among patients with various Child's grades

Parameters	<i>F</i>	<i>P</i>
Splenic diameter	4.832	0.014
Splenic velocity	4.873	0.013
Spleen size	4.136	0.024
WBC	5.286	0.010
RBC	1.746	0.189
Platelet	1.935	0.159

DISCUSSION

Cirrhosis is defined as a chronic disease of the liver in which diffuse destruction and regeneration of hepatic parenchymal cells have occurred, and in which a diffuse increase in connective tissues has resulted in disorganization of the lobular and vascular architecture. The principal pathologic features of cirrhosis include hepatic parenchymal necrosis, regeneration, and scarring. Clinically, distortion of the vascular architecture causes the most serious complications, portal hypertension with resulting ascites, variceal hemorrhage and hypersplenism^[10].

There are many factors that can cause liver cirrhosis and portal hypertension such as viral hepatitis, alcohol abuse, sclerosing cholangitis, schistosomiasis, and common inborn errors of metabolism including Wilson disease, hemochromatosis and α -antitrypsin deficiency. There are differences both in pathology and in clinical signs and symptoms among individual patients. Even in the same patient, there are different pathological and clinical characteristics at different stages. Accordingly, the treatment is very specific for each patient at different stages. Therefore, a clear and correct staging system for cirrhosis is required^[11].

However, there has been no optimal staging system so far to give a comprehensive stage analysis for cirrhosis. Warren *et al*^[12] once classified portal hypertension into four stages according to the degree of interference with portal flow to the liver, i.e., stage I (normal or only slightly restricted portal flow, hepatopetal portal flow), stage II (moderate reduction, hepatopetal or bi-directional portal flow), stage III (severe restriction of flow, bi-directional or hepatofugal portal flow), stage IV (lack of opacification of the portal vein by radiographic study), hepatofugal flow. But what they included was only portal flow direction not hepatocyte function. The most commonly used system to assess the severity of cirrhosis is still Child's score or Child-Pugh's score, which takes into account the jaundice, ascites, hypoalbuminemia, encephalopathy and prothrombin time. Biochemical markers are also reported to be helpful for Child's score^[13,14]. But all the parameters included are those for the hepatocyte function, but not for portal blood flow and spleen function.

Ultrasonography provides not only liver hemodynamics by color Doppler flow imaging, but also valuable information on the morphological changes of the liver^[15-19]. It has been reported that evaluating liver hemodynamics and morphology in patients with cirrhosis and portal hypertension is of immense value for the estimation of severity and prognosis of the disease^[20-22]. There also have been reports on the relationship between the hemodynamic changes of portal vein and the histological changes in chronic hepatitis^[19,22-24]. Aube *et al*^[22] observed that the decrease of portal venous velocity closely correlated with the histological degree of fibrosis. Similar to other studies^[2,6-8], our study showed a significant decrease in portal flow velocity and volume with increasing Child's grades of severity. In fact, portal flow velocity is a better parameter to reflect the portal pressure gradient and more useful for the diagnosis of portal hypertension. Therefore, the portal hemodynamics is very helpful in the assessment of the real status of cirrhosis and in finding the choice of the optimal therapy.

In contrast to the portal flow velocity, there was no significant difference in portal vein diameter among various Child's grades suggesting that portal vein diameter does not correlate with the high portal pressure and the severity of cirrhosis.

Our study also demonstrated that cirrhotics with ascites had a significantly lower portal flow velocity and volume compared to those without ascites, which confirms that ascites is a sign of liver function decompensation. However, there was no significant difference in portal flow velocity and volume between patients with mild and severe varices, indicating that the mechanisms of varices in cirrhosis are very complicated. They are not only the consequences of high portal pressure but also of formation of regional collaterals.

Splenomegaly is a cardinal feature of hepatic cirrhosis complicated by portal hypertension. The prevalence of splenomegaly in cirrhosis varies from 36-92%^[24,25]. Various mechanisms underlying the development of hypersplenism in portal hypertension have been proposed, including increased pooling and increased destruction of blood cells in the spleen, the dilutional effects of increased blood volume, and humoral factors. Hypersplenism can be regarded as the association of one or more of anemias, leukopenia, and thrombocytopenia with splenomegaly, and a normal or hypercellular bone marrow. Hypersplenism is a vital pathophysiological change in portal hypertension, and should be considered as a parameter in cirrhosis staging. In our study, although the splenic flow velocity and splenic vein diameter correlated with Child's grades as others reported, peripheral red blood cell and platelet count did not correlate with them. Furthermore, thrombocytopenia is the most common manifestation of hypersplenism in cirrhosis

and portal hypertension^[26,27]. Similar to previous studies^[26-28], we also observed a negative correlation between the platelet count and spleen volume. Therefore, peripheral blood cell count represents the severity of hypersplenism, and should also be taken into consideration in cirrhosis staging.

In conclusion, an optimal system that includes parameters representing the portal hemodynamics and spleen function should be proposed for cirrhosis staging.

REFERENCES

- 1 **Zhang CP**, Tian ZB, Liu XS, Zhao QX, Wu J, Liang YX. Effects of Zhaoyangwan on chronic hepatitis B and posthepatic cirrhosis. *World J Gastroenterol* 2004; **10**: 295-298
- 2 **Chawla Y**, Santa N, Dhiman RK, Dilawari JB. Portal hemodynamics by duplex Doppler sonography in different grades of cirrhosis. *Dig Dis Sci* 1998; **43**: 354-357
- 3 **Herold C**, Heinz R, Radespiel-Troger M, Schneider HT, Schuppan D, Hahn EG. Quantitative testing of liver function in patients with cirrhosis due to chronic hepatitis C to assess disease severity. *Liver* 2001; **21**: 26-30
- 4 **Herold C**, Heinz R, Niedobitek G, Schneider T, Hahn EG, Schuppan D. Quantitative testing of liver function in relation to fibrosis in patients with chronic hepatitis B and C. *Liver* 2001; **21**: 260-265
- 5 **Wehler M**, Kokoska J, Reulbach U, Hahn EG, Strauss R. Short-term prognosis in critically ill patients with cirrhosis assessed by prognostic scoring systems. *Hepatology* 2001; **34**: 255-261
- 6 **Nakano R**, Iwao T, Oho K, Toyonaga A, Tanikawa K. Splanchnic hemodynamic pattern and liver function in patients with cirrhosis and esophageal or gastric varices. *Am J Gastroenterol* 1997; **92**: 2085-2089
- 7 **Iwao T**, Toyonaga A, Oho K, Tayama C, Masumoto H, Sakai T, Sato M, Tanikawa K. Value of Doppler ultrasound parameters of portal vein and hepatic artery in the diagnosis of cirrhosis and portal hypertension. *Am J Gastroenterol* 1997; **92**: 1012-1017
- 8 **Shah SH**, Hayes PC, Allan PL, Nicoll J, Finlayson ND. Measurement of spleen size and its relation to hypersplenism and portal hemodynamics in portal hypertension due to hepatic cirrhosis. *Am J Gastroenterol* 1996; **91**: 2580-2583
- 9 **Angermayr B**, Cejna M, Karnel F, Gschwantler M, Koenig F, Pidlich J, Mendel H, Pichler L, Wichlas M, Kreil A, Schmid M, Ferlitsch A, Lipinski E, Brunner H, Lammer J, Ferenci P, Gangl A, Peck-Radosavljevic M. Child-Pugh versus MELD score in predicting survival in patients undergoing transjugular intrahepatic portosystemic shunt. *Gut* 2003; **52**: 879-885
- 10 **Nakaji M**, Hayashi Y, Ninomiya T, Yano Y, Yoon S, Seo Y, Nagano H, Komori H, Hashimoto K, Orino A, Shirane H, Yokozaki H, Kasuga M. Histological grading and staging in chronic hepatitis: its practical correlation. *Pathol Int* 2002; **52**: 683-690
- 11 **Zhou GW**, Tao ZY, Peng CH, Li HW. Reasonable choice of surgical procedures for patients with portal hypertension. *Hepatobiliary Pancreat Dis Int* 2003; **2**: 330-333
- 12 **Warren WD**, Fomon JJ, Viamonte M, Zeppa R. Preoperative assessment of portal hypertension. *Ann Surg* 1967; **165**: 999-1012
- 13 **Korner T**, Kropf J, Kosche B, Kristahl H, Jaspersen D, Gressner AM. Improvement of prognostic power of the Child-Pugh classification of liver cirrhosis by hyaluronan. *J Hepatol* 2003; **39**: 947-953
- 14 **Myers RP**, De Torres M, Imbert-Bismut F, Ratziu V, Charlotte F, Poynard T. Biochemical markers of fibrosis in patients with chronic hepatitis C: a comparison with prothrombin time, platelet count, and age-platelet index. *Dig Dis Sci* 2003; **48**: 146-153
- 15 **Tchelepi H**, Ralls PW, Radin R, Grant E. Sonography of diffuse liver disease. *J Ultrasound Med* 2002; **21**: 1023-1032; quiz 1033-1034
- 16 **Martinez-Noguera A**, Montserrat E, Torrubia S, Villalba J. Doppler in hepatic cirrhosis and chronic hepatitis. *Semin Ultra-*

- sound CT MR 2002; **23**: 19-36
- 17 **Arda K**, Ofelli M, Calikoglu U, Olcer T, Cumhuri T. Hepatic vein Doppler waveform changes in early stage (Child-Pugh A) chronic parenchymal liver disease. *J Clin Ultrasound* 1997; **25**: 15-19
 - 18 **Gorka W**, al Mulla A, al Sebayel M, Altraif I, Gorka TS. Qualitative hepatic venous Doppler sonography versus portal flowmetry in predicting the severity of esophageal varices in hepatitis C cirrhosis. *AJR Am J Roentgenol* 1997; **169**: 511-515
 - 19 **Nagata N**, Miyachi H, Nakano A, Nanri K, Kobayashi H, Matsuzaki S. Sonographic evaluation of the anterior liver surface in chronic liver diseases using a 7.5-MHz annular-array transducer: correlation with laparoscopic and histopathologic findings. *J Clin Ultrasound* 2003; **31**: 393-400
 - 20 **Li XH**, Wang L, Fang YW, Lu YK. Color Doppler evaluation for the hemodynamics of portal hypertension in liver cirrhosis. *Shijie Huaren Xiaohua Zazhi* 1999; **7**: 453-454
 - 21 **Ohta M**, Hashizume M, Kawanaka H, Akazawa K, Tomikawa M, Higashi H, Kishihara F, Tanoue K, Sugimachi K. Prognostic significance of hepatic vein waveform by Doppler ultrasonography in cirrhotic patients with portal hypertension. *Am J Gastroenterol* 1995; **90**: 1853-1857
 - 22 **Aube C**, Oberti F, Korali N, Namour MA, Loisel D, Tanguy JY, Valsesia E, Pilette C, Rousselet MC, Bedossa P, Rifflet H, Maiga MY, Penneau-Fontbonne D, Caron C, Cales P. Ultrasonographic diagnosis of hepatic fibrosis or cirrhosis. *J Hepatol* 1999; **30**: 472-478
 - 23 **Koda M**, Murawaki Y, Kawasaki H, Ikawa S. Portal blood velocity and portal blood flow in patients with chronic viral hepatitis: relation to histological liver fibrosis. *Hepatogastroenterology* 1996; **43**: 199-202
 - 24 **Mutchnick MG**, Lerner E, Conn HO. Effect of portacaval anastomosis on hypersplenism. *Dig Dis Sci* 1980; **25**: 929-938
 - 25 **Liangpunsakul S**, Ulmer BJ, Chalasani N. Predictors and implications of severe hypersplenism in patients with cirrhosis. *Am J Med Sci* 2003; **326**: 111-116
 - 26 **Bolognesi M**, Merkel C, Sacerdoti D, Nava V, Gatta A. Role of spleen enlargement in cirrhosis with portal hypertension. *Dig Liver Dis* 2002; **34**: 144-150
 - 27 **el-Khishen MA**, Henderson JM, Millikan WJ, Kutner MH, Warren WD. Splenectomy is contraindicated for thrombocytopenia secondary to portal hypertension. *Surg Gynecol Obstet* 1985; **160**: 233-238
 - 28 **Luo JC**, Hwang SJ, Chang FY, Chu CW, Lai CR, Wang YJ, Lee PC, Tsay SH, Lee SD. Simple blood tests can predict compensated liver cirrhosis in patients with chronic hepatitis C. *Hepatogastroenterology* 2002; **49**: 478-481

Assistant Editor Guo SY Edited by Xia HHX and Wang XL
Proofread by Ma JY

Existence and significance of hepatitis B virus DNA in kidneys of IgA nephropathy

Nian-Song Wang, Zhao-Long Wu, Yue-E Zhang, Lu-Tan Liao

Nian-Song Wang, Department of Nephrology, The Sixth Affiliated Hospital of Shanghai Jiaotong University, 600 Yushan Road, Shanghai 200233, China

Zhao-Long Wu, Lu-Tan Liao, Department of Nephrology, Zhong Shan Hospital, Fudan University, 180 Fenglin Road, Shanghai 200032, China

Yue-E Zhang, Department of Pathology, Fudan University, 136 Yixue Road, Shanghai 200032, China

Supported by the National Natural Science Foundation of China, N0. 39770292

Correspondence to: Nian-Song Wang, Department of Nephrology, the Sixth Affiliated Hospital of Shanghai Jiaotong University, 600 Yushan Road, Shanghai 200233, China. wangniansong@yahoo.com.cn

Telephone: +86-21-64369181 Ext. 8393 **Fax:** +86-21-64701361

Received: 2004-04-24 **Accepted:** 2004-05-08

Wang NS, Wu ZL, Zhang YE, Liao LT. Existence and significance of hepatitis B virus DNA in kidneys of IgA nephropathy. *World J Gastroenterol* 2005; 11(5): 712-716 <http://www.wjgnet.com/1007-9327/11/712.asp>

INTRODUCTION

IgA nephropathy is one of the most common glomerular diseases worldwide. Its prevalence varies considerably among and within countries, and its pathogenetic mechanisms still remain largely uncertain^[1-3]. Coexistence of mesangial proliferative glomerulonephritis with predominant mesangial IgA deposits and persistent hepatitis B virus surface antigenemia was first reported in five patients by Nagy *et al*^[4], and later by some other studies^[5-9]. In 1996 Zhang *et al*^[5] investigated HBV DNA in renal biopsies from fifty patients with many kinds of glomerulonephritis using *in situ* hybridization, and found that 72% (36/50) cases were HBV DNA positive detected by *in situ* hybridization, and 82% (17/23) cases were proved to be HBV DNA positive in Southern blot analysis. Moreover, among the five patients with IgAN, four and two patients were HBV DNA positive using *in situ* hybridization and Southern blot analysis, respectively. Wang *et al*^[6,9] reported the integrated form of positive HBV DNA in renal biopsies from one of two patients with IgAN in 1996 by using Southern blot analysis, 12 of 20 patients with IgAN by using *in situ* hybridization and 8 of 10 patients with IgAN were the integrated form of positive HBV DNA using Southern blot analysis in 2003. Since China is an endemic area of hepatitis B virus (HBV) infection, and has an incidence of 32% IgA nephropathy in primary glomerulonephritis, according to a clinical analysis of 1001 cases by Li *et al*^[10]. Hence, the relationship between IgA nephropathy and HBV infection is attracting increasing attention. In order to clarify the role of HBV DNA in the pathogenesis of IgA nephropathy, we took advantages of the sensitivity and specificity of molecular techniques using both *in situ* hybridization and Southern blot analysis to detect HBV DNA in kidney tissues from patients with IgA nephropathy.

MATERIALS AND METHODS

Patients

Fifty patients with IgA nephropathy who were admitted to our hospital with positive serum HBV infectious markers and/or HBsAg detected in renal biopsy by immunohistochemistry were enrolled in this study. Of the 50 patients in this study, 27 were males and 23 were females, aged 18-66 years (average 34.6 years). Their clinical data were complete and pathological diagnoses were confirmed by light microscopy and immunofluorescence examination. The criteria for selection of patients included no history of jaundice or liver disease, blood transfusion, or intravenous drug addiction; normal liver functions; absence of cryoglobulinemia; and no clinical and laboratory evidence of secondary renal lesions such as lupus nephritis and Henoch-Schonlein purpura glomerulonephritis. None had liver biopsies.

Abstract

AIM: To investigate the existence and significance of hepatitis B virus (HBV) DNA in the pathogenesis of IgA nephropathy (IgAN).

METHODS: Fifty cases of IgAN with HBV antigenaemia and/or hepatitis B virus antigens (HBsAg, or HBcAg, HBcAg) detected by immunohistochemistry in renal tissues were enrolled in our study. The distribution and localization of HBV DNA were observed using *in situ* hybridization. Southern blot analysis was performed to reveal the state of renal HBV DNA.

RESULTS: Among the 50 patients with IgAN, HBs antigenemia was detected in 17 patients (34%). HBsAg in renal tissues was detected in 48 patients (96%), the positive rate of HBsAg, HBcAg, and HBcAg was 82% (41/50), 58% (29/50), and 42% (21/50) in glomeruli, respectively; and was 94% (47/50), 56% (28/50) and 78% (39/50) in tubular epithelia, respectively. Positive HBV DNA was detected in 72% (36/50) and 82% (41/50) cases in tubular epithelia and glomeruli respectively by *in situ* hybridization, and the positive signals were localized in the nuclei of tubular epithelial cells and glomerular mesangial cells as well as infiltrated interstitial lymphocytes. Moreover, 68% (34/50) cases were proved to be HBV DNA positive by Southern blot analysis, and all were the integrated form.

CONCLUSION: HBV infection might play an important role in occurrence and progress of IgAN. In addition to humoral immune damages mediated by HBsAg-HBAb immune complex, renal tissues of some IgAN are directly infected with HBV and express HBsAg *in situ*, and the cellular mechanism mediated by HBV originating from renal cells *in situ* may also be involved in the pathogenesis of IgAN.

© 2005 The WJG Press and Elsevier Inc. All rights reserved.

Key words: Hepatitis B virus; DNA; IgA nephropathy

Five cases without any HBV infectious markers in both serum or renal tissue were used as controls.

Serologic tests for HBV

Tests for HBV antigens and antibodies were performed before renal biopsy and regularly thereafter. Double antibody sandwich ELISA was used for detecting HBsAg and HbeAg, while double antigen ELISA was used for detecting anti-HBs and antibody competitive ELISA for detecting anti-HBe and anti-HBc. The test reagent kits were purchased from Shanghai Medical Laboratory.

Immunohistochemistry

The biopsy tissue was divided into three to four pieces. One piece was fixed in 95% ethanol and cut into 3 μ m thick sections and stained with hematoxylin and eosin (HE) and periodic acid silver methanamine (PASM). The second piece was embedded in ornithine carbamoyltransferase (OCT) compound (Miles Inc. Elkhart, In, USA), cut into 5 μ m thick sections for detecting IgG, IgA, IgM and C₃ with direct immunofluorescence. The relevant antibodies were labelled with fluorescein (FITC) (Dako Corporation, Santa Barbara, CA, USA). The third piece was prefixed with 2.5 g/L glutaldehyde and postfixed with 10 g/L osmium and cut into ultrathin sections with conventional methods for electron microscopic observation. The fourth piece was freshly preserved at -70 °C for Southern blot analysis.

Detection of HBVAg in renal tissue

Immunohistochemical methods were used to detect the distribution of immunoglobulin, HbsAg and HBcAg. The 4 μ m thick sections were digested with 0.5 g/L trypsin for 15 min at 37 °C to expose the epitopes of HBsAg and HBcAg. Rabbit anti-HBcAg and peroxidase-antiperoxidase (PAP) complex were purchased from Dako Company (Dakopatts, Denmark, USA.). PAP kit for HBcAg, horseradish peroxidase-labelled goat anti-human IgG, IgA and IgM for immunofluorescence examination, and other antibodies were prepared by the Department of Pathology, Shanghai Medical University. The first antibodies for HBV antigens were goat anti-HBs and rabbit anti-HBcAg. The specificity of staining for HBV antigens was checked by blocking and absorption procedures as previously described by Lai *et al*^[11] and Zhang *et al*^[12]. No cross reactivities of anti-HBV antigen (s) with each other and with immunoglobulins, complements, fibrinogen, normal and sclerosed glomerular tissues from HBsAg-negative controls were found. Primary antibodies were replaced by normal sheep and rabbit sera as negative controls.

In situ hybridization

Paraffin-embedded 4 μ m thick sections were used for *in situ* hybridization. The digoxigenin labeled full-length HBV DNA probe was prepared from a HBV plasmid clone of pBR322 and labeled with digoxigenin by random labelling using a detection kit^[13] (Beijing Hepatitis Research Institute). The main procedures of *in situ* hybridization were the same as reported previously^[5-9].

Southern blot analysis

Fresh specimens preserved at -70 °C were processed for the detection of renal HBV DNA state by Southern blot analysis. The ³²P(a)-dCTP- labelled HBV DNA probe and the procedures used were the same as reported previously^[5-9].

Statistical analysis

To analyze the seropositivity of HBV marker or the presence of

HBAg and HBV DNA in renal biopsies in IgAN patients, Fisher's exact test or chi-square test was used as appropriate. $P < 0.05$ was considered statistically significant.

RESULTS

Serologic findings

Seventeen patients (34%) were found to be HBsAg positive in their sera, serum HBeAg was detected in 3 patients (6%), anti-HBe was positive in 10 patients (20%), HBcAb was positive in 26 patients (52%), and HBsAb was positive in 10 patients (20%).

Detection of HBAg in renal tissue

HBAg (HBsAg and/or HBcAg) in renal tissues was detected in 48 patients (96%) by immunohistochemistry. The distribution of positive HBAg on glomeruli was found in 41 cases (82%), including HBsAg in 58% (29/50) cases and HBcAg in 42% (21/50) cases. The distribution of HBAg on glomeruli was found either on capillary loops or in mesangial region or both. The expression of HBAg in tubular epithelial cells was detected in 47 cases (94%). HBsAg and HBcAg in tubular epithelial cells were also found in 56% (28/50) and 78% (39/50) cases. The positive rate of tubular HBcAg (78%) was higher than that of tubular HBsAg (56%), glomerular HBsAg (58%) and HBcAg (42%). Both HBsAg and HBcAg were located in cytoplasm of tubular epithelial cells. Occasionally, HBcAg could be visualized in the nuclei of tubular cells.

Detection of HBV DNA in renal tissue by in situ hybridization

Forty-six of the 50 cases (92%) were HBV DNA positive in renal tissues by *in situ* hybridization. Seventeen of them were found to be HBsAg positive in their sera, HBeAg was detected in 3 patients, HBeAb was positive in 10 patients, HBcAb was positive in 25 patients and HBsAb was positive in 10 patients. All these 46 patients were HBVAg positive in the renal tissue, while HBcAg was positive in glomerular cells and tubular cells in 21 and 39 cases, respectively and HBsAg was positive in 29 and 28 cases, respectively. Of these 50 cases, 41 (82%) were HBV DNA positive in tubular epithelial cells. HBV DNA was detected in glomeruli in 72% cases (36/50). The positive signals of hybridization were localized within the nuclei of tubular epithelial cells and glomerular mesangial cells as well as infiltrated interstitial lymphocytes.

Detection of HBV DNA in renal tissue by Southern blot

Of the 50 cases, 34 (68%) were HBV DNA positive by Southern blot analysis, all these positive specimens were the integrated form of HBV DNA, and none was a non-replicating free form of HBV DNA with a single signal band of 3.2 kb. The integrated state of HBV DNA by Southern blot analysis showed a high molecular weight single band before digestion and revealed irregular multiple bands after *E. coli* restrictive enzyme treatment.

Relationship among HBV infectious markers in sera, and HBAg and HBV DNA in renal tissues

The relationship among HBV infectious markers in sera, and HBAg and HBV DNA in renal tissues of the 50 cases with IgAN are shown in Table 1. Neither HBAg nor HBV DNA was found in the renal tissues from the five control cases of mesangioproliferative glomerulonephritis.

DISCUSSION

The association between chronic hepatitis B virus infection, characterized by persistent hepatitis B surface antigenemia and glomerular disease was first described in 1971^[14].

Table 1 Relationship among HBV infectious markers in sera, and HBsAg and HBV DNA in renal tissue in 50 cases with IgA nephropathy

Case	Age (yr)	Sex	Course	Serum HBV markers					Renal HBsAg				Renal HBV DNA		
				HBsAg		HBsAb			T		G		ISH	Southern bolt	
				HBsAg	HBeAg	HBsAb	HBeAb	HbCAb	HBsAg	HbCAg	HBsAg	HbCAg	T	G	
1	30	F	4 yr	+	-	-	-	+	-	+	+	+	+	+	+
2	32	M	8 mo	+	-	-	-	-	-	+	+	-	+	+	+
3	35	M	2 yr	-	-	-	-	+	-	+	+	-	+	+	+
4	38	M	13 yr	+	-	-	+	+	-	+	-	+	+	+	+
5	35	F	5 yr	-	-	+	-	-	+	-	-	-	+	-	-
6	36	F	7 mo	+	-	-	-	+	+	-	+	+	+	+	+
7	32	M	2 mo	-	-	-	+	-	-	+	-	-	+	-	-
8	26	M	6 yr	-	-	-	-	+	-	+	+	-	+	+	+
9	22	M	5 mo	+	-	-	-	-	+	-	-	+	+	+	+
10	47	F	4 yr	+	-	-	-	+	-	+	+	-	+	+	+
11	24	M	6 yr	-	-	-	+	+	-	+	-	-	+	+	-
12	43	M	9 mo	-	-	-	-	+	+	-	-	+	+	+	+
13	26	F	1 yr	-	+	-	-	-	+	+	+	-	+	+	+
14	28	M	2 yr	-	-	+	-	+	-	+	-	+	+	-	+
15	45	M	3 mo	-	-	-	-	+	-	+	-	+	-	+	-
16	38	F	2 mo	-	-	+	-	-	+	+	+	-	+	-	+
17	53	F	4 yr	+	-	-	-	+	+	+	+	+	+	+	+
18	59	M	1 yr	-	-	-	+	+	+	+	+	-	+	+	+
19	64	M	11 mo	-	-	+	-	-	+	-	+	-	-	+	-
20	58	F	7 mo	-	-	+	-	-	-	+	-	+	-	+	+
21	66	M	2 yr	-	+	-	-	-	+	+	+	+	+	+	+
22	21	F	4 mo	-	-	-	-	-	+	-	+	-	-	+	-
23	30	M	1 yr	-	-	-	+	+	+	+	+	-	+	+	+
24	29	F	4 mo	-	-	-	-	+	-	-	-	-	-	-	-
25	43	F	3 y	+	-	-	-	-	+	+	+	-	+	+	+
26	36	M	1 mo	-	-	+	-	+	-	+	+	-	+	+	+
27	27	M	2 mo	-	-	-	-	-	-	+	-	-	+	-	-
28	53	F	2 yr	-	-	-	-	+	+	+	+	+	+	+	+
29	49	F	5 mo	-	-	+	-	-	-	-	+	-	-	-	-
30	16	M	3 mo	-	-	-	-	+	+	+	+	-	+	+	+
31	28	F	6 mo	-	-	-	+	+	-	+	+	-	+	-	+
32	33	F	4 mo	+	-	-	-	-	+	+	+	-	+	+	+
33	41	M	7 mo	+	-	-	-	-	+	+	+	+	+	+	+
34	20	F	1 mo	-	-	-	-	+	-	+	-	+	+	-	-
35	18	F	2 mo	-	-	-	-	-	-	+	-	-	-	-	-
36	31	M	6 mo	+	-	-	-	-	+	+	+	+	+	+	+
37	29	M	1 yr	-	-	-	+	+	+	+	+	-	+	+	+
38	42	F	3 mo	-	-	+	-	-	+	-	-	-	+	-	-
39	21	F	2 mo	-	-	-	-	+	-	-	-	-	-	-	-
40	36	M	1 yr	+	-	-	-	-	+	+	+	-	+	+	+
41	60	F	2 yr	+	-	-	-	-	-	+	+	-	+	+	+
42	25	M	3 mo	-	-	-	-	+	-	+	-	+	+	-	-
43	19	M	2 mo	-	-	+	-	-	+	-	-	-	+	-	-
44	56	F	7 mo	+	-	-	-	-	+	+	+	+	+	+	+
45	22	M	3 mo	-	-	-	+	+	+	+	+	-	+	+	-
46	43	F	2 yr	+	-	-	-	+	+	+	-	+	+	+	+
47	39	M	6 mo	-	-	-	+	-	+	+	-	+	-	+	+
48	25	M	7 mo	+	+	-	-	-	+	+	+	+	+	+	+
49	36	F	8 mo	-	-	+	+	+	-	+	-	+	+	+	+
50	32	M	3 yr	+	-	-	-	+	+	+	-	+	+	+	+
Total				17	3	10	10	26	28	39	29	21	41	36	34

T: tubules; G: glomeruli; ISH: *in situ* hybridization; +: positive; -: negative.

Hepatitis B virus associated glomerulonephritis (HBVGN) has been traditionally regarded as a typical immune complex glomerulonephritis mediated by hepatitis B antigen (HBsAg) and hepatitis B virus antibody (HBsAb) immune complexes deposited on glomeruli^[14-18]. Various morphological patterns, including membranous nephropathy, membranoproliferative glomerulonephritis (MN), mesangial proliferative glomerulonephritis (MPGN), minimal change nephropathy, and IgA nephropathy have been reported^[18-22,24-30]. IgA nephropathy has been confirmed to be an immune complex-mediated glomerulonephritis, which is morphologically defined by mesangial deposition of IgA^[1-3]. The etiologic role of HBV antigenemia and HBV antigen deposition in IgA nephropathy remains speculative^[5-9]. It most likely involves mesangial and subendothelial trapping of circulating immune complexes (CICs), and the observation that CICs primarily result in mesangial and subendothelial deposits supports this mechanism^[1-3]. The possible role of HBV antigens is highly suspected, especially in endemic areas of HBV infection, such as in Southeastern Asia^[5-9,23]. Many efforts have been contributed to this field^[12,23,27,31-34], yet there are only scattered and incomplete data because of the difficulty in obtaining tissue specimens, complicated clinical settings, less specific and sensitive detection techniques. Humoral immune responses triggered by HBsAg-HBsAb immune complexes are traditionally regarded as the mechanism of tissue injury resulting in HBV-glomerulonephritis (GN). HBsAg, HBcAg and HBeAg with immunoglobulins and complement deposits in the glomeruli of HBV-GN have been demonstrated in many investigations^[4,30-33,35-38]. It remains perplexing why some chronic HBsAg carriers develop IgAN, while others develop membranous glomerulonephritis (MGN) or mesangiocapillary glomerulonephritis (MCGN). This is well related to HBV antigen status as well as the size and charge properties of HBV antigens and their antibodies. The larger size of HBsAg and HBcAg favors the mesangial localization of HbsAg-anti-HBs or /and HBcAg-anti-HBc complexes in HBV-IgAN^[11,12,23].

The demonstration of HBV DNA within the glomeruli in patients with glomerulonephritis^[33-35] and the identification of both free and integrated HBV DNA in kidneys of chronic HBsAg carrier, may favor the notion that HBV might also infect resident glomerular cells leading to immune complex formation. Detection of HBV DNA has been reported in kidneys of chronic HBsAg carriers with different glomerulonephritis^[33-35], yet the consistency of these findings remains controversial, since some investigators were unable to detect similar findings in chronic HBV carriers with coexisting membranous nephropathy^[36]. This issue is of importance in understanding the pathogenesis of HBV-related glomerulonephritis. In 1992 Fang *et al.*^[30] identified the non-replicating free form and the integrated form of HBV DNA in children's membranous glomerulonephritis by Southern blot analysis of renal DNA. Lin^[31] investigated HBV DNA by *in situ* hybridization with ³H-dCTP-labeled full-length HBV DNA probes in 20 child cases of membranous glomerulonephritis, and found that the positive rate of HBV DNA was 87.5% within 6 mo after the disease onset, and only 21% in tubular epithelial cells and none in glomeruli, while the course of glomerulonephritis lasted for more than 6 mo. In 1996, Zhang *et al.*^[5] investigated the HBV DNA in renal biopsies from fifty patients and found that 72% (36/50) cases were HBV DNA positive by using *in situ* hybridization and 73.9% (17/23) cases were HBV DNA positive in Southern blot analysis. Wang *et al.*^[9] reported that HBV DNA was positive in 100% renal biopsies from patients with IgAN by using *in situ* hybridization and 80% (8/10) patients with IgAN were the integrated form of positive HBV DNA by Southern blot analysis. Thereafter, the questions that whether the existence of HBV DNA in renal tissue of glomerulonephritis patients is a general phenomenon and what

role HBV DNA plays in the pathogenesis of renal injury are raised. Therefore, with the help of *in situ* hybridization (ISH) and Southern blot analysis for HBV DNA, and highly sensitive and specific biological techniques, we have found the evidence for the presence of viral transcription in glomerular cells and renal tubular epithelial cells, which supports an etiologic role of HBV in some chronic HBsAg carriers who develop coexisting glomerulonephritis. Since the presence of HBcAg in glomeruli might be not only from the HBV DNA positive glomerular cells, but also from the circulation, the detectable rate of HBcAg in glomeruli has a close correlation with serum HBV antigenaemia and the state of HBV DNA both in serum and renal tissue. The presence of HBcAg and HBV DNA in tubular epithelial might indicate HBV replication in epithelial cells^[39,40]. Southern blot analysis, could identify the state of HBV DNA^[30]. In our study, 34 of 50 cases (68%) were HBV DNA positive by Southern blot analysis, and all were the integrated form. Since the number and molecular weight of the bands of HBV DNA signals of integrated form varied, it is suggested that HBV DNA integration is random. The infected cells with free forms of HBV DNA, consisting of full genome of HBV, may theoretically express HBsAg. However, if only some fragments of HBV DNA randomly integrate into chromosomes of the host cells, whether the cells expressing HBsAg would depend on the integrated part consisted of certain intact HBsAg genomes and their matched promoters as the elements of franking sequence of HBV DNA. Therefore, the kidney might carry dormant HBV DNA after HBV infection^[5,6,28] or express HBsAg triggering immune reaction resulting in tissue injury, which might be mediated by HBsAg-HBsAb immune complexes together with complements. Meanwhile, another possibility is that HBV-infected renal cells with the target HBcAg expression might activate T lymphocytes with relevant lymphokines resulting in increase of the permeability of glomerular epithelial cells and glomerular basement membrane^[41].

In conclusion, the presence of HBV DNA in renal tissues of patients with IgAN, especially with coexisting HBV antigenaemia, appears to be a general phenomenon among IgAN patients in Shanghai, China. The host tissue tropism of HBV is not limited to hepatocytes, and active viral transcription is present in glomerular and tubular epithelial cells. Hepatitis B virus might be the etiologic agent for some chronic HBsAg carriers with coexisting IgA nephropathy. The cellular mechanism mediated by HBV originating from renal cells *in situ* may also be involved in the pathogenesis of IgAN. These concepts might enrich our understanding of the pathogenesis of HBV related IgAN both theoretically and clinically.

REFERENCES

- 1 Endo Y, Kanbayashi H. Etiology of IgA nephropathy syndrome. *Pathol Int* 1994; **44**: 1-13
- 2 Galla JH. IgA nephropathy. *Kidney Int* 1995; **47**: 377-387
- 3 Barratt J, Feehally J, Smith AC. Pathogenesis of IgA nephropathy. *Semin Nephrol* 2004; **24**: 197-217
- 4 Nagy J, Bajtai G, Brasch H, Sule T, Ambrus M, Deak G, Hamori A. The role of hepatitis B surface antigen in the pathogenesis of glomerulopathies. *Clin Nephrol* 1979; **12**: 109-116
- 5 Zhang YE, Ma XL, Fang LJ, Lin SY, Wu ZL, Gu JR. The existence and significance of hepatitis B virus DNA in glomerulonephritis. *Nephrology* 1996; **2**: 119-125
- 6 Wang NS, Wu ZL, Zhang YE, Liao LT, Guo MY. Is there relationship between IgA nephropathy (IgAN) and hepatitis B virus (HBV)? *Zhonghua Shenzangbing Zazhi* 1996; **12**: 276-278
- 7 Wu ZL, Wang NS, Xu XH, Qiu LQ, Zhou Q, Zhang YE. Positive and negative hepatitis B virus in renal biopsies of IgA nephropathy: An 85-case clinicopathological analysis. *Nephrology* 2001; **6**: 185-189

- 8 **Wang NS**, Wu ZL, Zhang YE, Guo MY, Liao LT. Role of hepatitis B virus infection in pathogenesis of IgA nephropathy. *World J Gastroenterol* 2003; **9**: 2004-2008
- 9 **Wang NS**, Wu ZL, Zhang YE, Liao LT. Study on HBV DNA state in renal tissue of IgA nephropathy. *Linchuan Gandanbing Zazhi* 2003; **19**: 27-28
- 10 **Li L**, Li LS, Chen HP, Zhou HZ, Ji DX, Tang Z, Yu YS, Bai XY, Zhou H, Zhang JH. Primary glomerulonephritis in China. Analysis of 1001 cases. *Chin Med J (Engl)* 1989; **102**: 159-164
- 11 **Lai KN**, Lai FM, Chan KW, Chow CB, Tong KL, Vallance-Owen J. The clinico-pathologic features of hepatitis B virus-associated glomerulonephritis. *Q J Med* 1987; **63**: 323-333
- 12 **Zhang YE**, Guo MY, Ying YY. Further study on the immunopathology of hepatitis B virus associated glomerulonephritis. *Zhonghua Neike Zazhi* 1990; **29**: 526-529, 574
- 13 **Yan HP**, Lang ZW, Huang DZ. Preparation of digoxigenin labelled probe and detection of HBV DNA in liver and extrahepatic tissue with *in situ* hybridization. *Zhonghua Neike Zazhi* 1994; **33**: 168-171
- 14 **Combes B**, Shorey J, Barrera A, Stastny P, Eigenbrodt EH, Hull AR, Carter NW. Glomerulonephritis with deposition of Australia antigen-antibody complexes in glomerular basement membrane. *Lancet* 1971; **2**: 234-237
- 15 **Knieser MR**, Jenis EH, Lowenthal DT, Bancroft WH, Burns W, Shalhoub R. Pathogenesis of renal disease associated with viral hepatitis. *Arch Pathol* 1974; **97**: 193-200
- 16 **Brzosko WJ**, Krawczynski K, Nazarewicz T, Morzycka M, Nowoslawski A. Glomerulonephritis associated with hepatitis B surface antigen immune complexes in children. *Lancet* 1974; **2**: 477-482
- 17 **Takekoshi Y**, Tanaka M, Miyakawa Y, Yoshizawa H, Takahashi K, Mayumi M. Free "small" and IgG-associated "large" hepatitis B e antigen in the serum and glomerular capillary walls of two patients with membranous glomerulonephritis. *N Engl J Med* 1979; **300**: 814-819
- 18 **Ito H**, Hattori S, Matusda I, Amamiya S, Hajikano H, Yoshizawa H, Miyakawa Y, Mayumi M. Hepatitis B e antigen-mediated membranous glomerulonephritis. Correlation of ultrastructural changes with HBeAg in the serum and glomeruli. *Lab Invest* 1981; **44**: 214-220
- 19 **Furuse A**, Hattori S, Terashima T, Karashima S, Matsuda I. Circulating immune complex in glomerulonephropathy associated with hepatitis B virus infection. *Nephron* 1982; **31**: 212-218
- 20 **Hirose H**, Udo K, Kojima M, Takahashi Y, Miyakawa Y, Miyamoto K, Yoshizawa H, Mayumi M. Deposition of hepatitis B e antigen in membranous glomerulonephritis: Identification by F(ab')₂ fragments of monoclonal antibody. *Kidney Int* 1984; **26**: 338-341
- 21 **Zhang YE**, Guo MY, Yin JF, Weng NP, Zhang XR, Wang YX, Qiu CL. Immunopathological study of hepatitis B virus immune complex glomerulonephritis. *Zhonghua Shenzangbing Zazhi* 1986; **2**: 127-130
- 22 **Takeda S**, Kida H, Katagiri M, Yokoyama H, Abe T, Hattori N. Characteristics of glomerular lesions in hepatitis B virus infection. *Am J Kidney Dis* 1988; **11**: 57-62
- 23 **Lai KN**, Lai FM, Tam JS, Vallance-Owen J. Strong association between IgA nephropathy and hepatitis B surface antigenemia in endemic areas. *Clin Nephrol* 1988; **29**: 229-234
- 24 **Thyagarajan SP**, Thirunalasundari T, Subramanian S, Panchanadam M, Nammalwar BR, Prabha V, Vijayakumar M. Serum and tissue positivity for hepatitis B virus markers in histopathologically proven glomerulonephropathies. *J Med Microbiol* 1989; **29**: 243-249
- 25 **Zhou WZ**, Zhang WL, Geng L. Glomerulonephropathy associated with hepatitis B virus (HBV) infection. *Zhonghua Neike Zazhi* 1990; **29**: 530-533, 574
- 26 **Zhang YE**, Fang LJ, Ma XL, Guo MY, Du WD, Zhai WR, Wu ZL, Lin SY, Gu JR. Hepatitis B virus infection and pathogenesis of glomerulonephritis. *Zhonghua Binglixue Zazhi* 1995; **24**: 341-344
- 27 **Johnson RJ**, Couser WG. Hepatitis B infection and renal disease: clinical, immunopathogenetic and therapeutic considerations. *Kidney Int* 1990; **37**: 663-676
- 28 **Fang LJ**, Sheng FY, Guo YQ, Wu ZL, Lu FM, Zhang YE, Guo MY, Zhang XR. Hepatitis B virus associated nephritis in adults and children. *Zhonghua Chuanranbingxue Zazhi* 1996; **14**: 92-95
- 29 **Magil A**. IgA nephropathy and membranous nephropathy associated with hepatitis B surface antigenemia. *Hum Pathol* 1988; **19**: 615
- 30 **Fang LJ**, Guo YQ, Zhang YE, Gu JR, Jiang HQ. The study on HBV DNA state in renal tissue of children HBV associated glomerulonephritis. *Zhonghua Shenzangbing Zazhi* 1992; **8**: 65-67
- 31 **Lin CY**. Hepatitis B virus deoxyribonucleic acid in kidney cells probably leading to viral pathogenesis among hepatitis B virus associated membranous nephropathy patients. *Nephron* 1993; **63**: 58-64
- 32 **Lai KN**, Ho RT, Tam JS, Lai FM. Detection of hepatitis B virus DNA and RNA in kidneys of HBV related glomerulonephritis. *Kidney Int* 1996; **50**: 1965-1977
- 33 **Ma XL**, Zhang XR, Du WD, Zhu TF, Zhao ZH, Zhang YE. Detection of HBV DNA and HBsAg in renal tissue of IgA nephropathy by using double staining technology. *Shanghai Yike Daxue Xuebao* 1997; **24**: 293-294
- 34 **He XY**, Fang LJ, Zhang YE, Sheng FY, Zhang XR, Guo MY. *In situ* hybridization of hepatitis B DNA in hepatitis B-associated glomerulonephritis. *Pediatr Nephrol* 1998; **12**: 117-120
- 35 **Lin CY**. Treatment of hepatitis B virus-associated membranous nephropathy with recombinant alpha-interferon. *Kidney Int* 1995; **47**: 225-230
- 36 **Yu YP**, Wang HY, Chen ML. An *in situ* hybridization and immunofluorescent double staining study on the pathogenesis of HBV in kidney disease. *Zhonghua Neike Zazhi* 1990; **29**: 538-540, 575
- 37 **Lai KN**, Tam JS, Lin HJ, Lai FM. The therapeutic dilemma of the usage of corticosteroid in patients with membranous nephropathy and persistent hepatitis B virus surface antigenaemia. *Nephron* 1990; **54**: 12-17
- 38 **Ishihara T**, Akamatsu A, Takahashi M, Yamashita Y, Yokota T, Nagasawa T, Gondo T, Kawano H, Kawamura S, Uchino F. Ultrastructure of kidney from three patients with HBeAg-associated nephropathy with special reference to virus-like particles in the glomerular tufts. *Acta Pathol Jpn* 1988; **38**: 339-350
- 39 **Farza H**, Hadchouel M, Scotto J, Tiollais P, Babinet C, Pourcel C. Replication and gene expression of hepatitis B virus in a transgenic mouse that contains the complete viral genome. *J Virol* 1988; **62**: 4144-4152
- 40 **Araki K**, Miyazaki J, Hino O, Tomita N, Chisaka O, Matsubara K, Yamamura K. Expression and replication of hepatitis B virus genome in transgenic mice. *Proc Natl Acad Sci USA* 1989; **86**: 207-211
- 41 **Nolasco FE**, Cameron JS, Hartley B, Coelho A, Hildreth G, Reuben R. Intraglomerular T cells and monocytes in nephritis: study with monoclonal antibodies. *Kidney Int* 1987; **31**: 1160-1166

Pharmacokinetics of C-1027 in mice as determined by TCA-RA method

You-Ping Liu, Quan-Sheng Li, Yu-Rong Huang, Mao-Jin Zhou, Chang-Xiao Liu

You-Ping Liu, Quan-Sheng Li, Yu-Rong Huang, Mao-Jin Zhou, Chang-Xiao Liu, National Key Laboratory of Pharmacokinetics and Pharmacodynamics, Tianjin Institute of Pharmaceutical Research, Tianjin 300193, China

You-Ping Liu, Mao-Jin Zhou, Laboratory of Drug Metabolism and Pharmacokinetics, Shenyang Pharmaceutical University, Shenyang 110016, Liaoning Province, China

Supported by the National "863" Project of China, No. 2003AA2Z347D

Correspondence to: Academician Chang-Xiao Liu, Tianjin Institute of Pharmaceutical Research, 308 An-Shan West Road, Tianjin 300193, China. liuchangxiao@163.com

Telephone: +86-22-23006863 **Fax:** +86-22-23006860

Received: 2004-02-21 **Accepted:** 2004-03-18

Abstract

AIM: To validate a radioactivity assay, the TCA-RA method, for the measurement of C-1027 in serum and to evaluate its application in determination of pharmacokinetics of C-1027 in mice.

METHODS: ^{125}I -C-1027 was prepared by the Iodogen method and separated by HPLC. The radioactivity assay was established and used to determine ^{125}I -C-1027 in mice at doses of 10, 50 and 100 $\mu\text{g}/\text{kg}$ after precipitation with 20% trichloroacetic acid (TCA-RA method). Several pharmacokinetic parameters were determined after intravenous injection of ^{125}I -C-1027 to mice.

RESULTS: After intravenous injection of ^{125}I -C-1027 to mice, at doses of 10, 50 and 100 $\mu\text{g}/\text{kg}$; the apparent distribution volumes (V_d) were 0.26, 0.31 and 0.33 L/kg; the biological half-lives ($T_{1/2}$) were 3.10, 3.40 and 3.90 h; the areas under curve (AUC) were 18.41, 103.69 and 202.74 ng/h/mL; the elimination rate constants (K) were 1.04, 1.26 and 0.58/h; and the total body clearance (C) were 0.54, 0.48 and 0.49 L/kg/h, respectively.

CONCLUSION: TCA-RA is a sensitive, reliable and suitable method for the determination of ^{125}I -C-1027 in mouse serum.

© 2005 The WJG Press and Elsevier Inc. All rights reserved.

Key words: C-1027; TCA-RA method; Pharmacokinetics

Liu YP, Li QS, Huang YR, Zhou MJ, Liu CX. Pharmacokinetics of C-1027 in mice as determined by TCA-RA method. *World J Gastroenterol* 2005; 11(5): 717-720

<http://www.wjgnet.com/1007-9327/11/717.asp>

INTRODUCTION

Lidamycin (C-1027), produced by *Streptomyces globisporus* in soil, consists of a non-covalently bound apoprotein, and a labile chromophore that is responsible for most of the biological

activities^[1-7]. The structure of C-1027 has been studied by several methods^[8-10]. C-1027 shows a remarkable inhibition on the growth of human liver cancer, colon cancer and epithelial tumor cells^[11-18], and exhibits highly potent cytotoxicity to cultured cancer cells and marked DNA cleaving ability^[19-27]. The protein moiety of C-1027 has a single polypeptide chain cross-linked by two disulfide bonds with a molecular weight of 10 500 Da^[28,29]. The protein protects the stability of the chromophore. Like other enediyne agents, antibiotic C-1027 is believed to exert its biological activity through the induction of cellular DNA and RNA damage^[30-35]. The pre-clinical studies on the pharmacodynamics, pharmacokinetics and toxicology have demonstrated that C-1027 appears to be a very promising anticancer candidate, and has been used in clinical trial in China. The aim of this study was to validate a radioactivity assay after precipitation with 20% trichloroacetic acid (the TCA-RA method) for the measurement of serum C-1027 and to evaluate its application in determination of pharmacokinetics of C-1027 in mice.

MATERIALS AND METHODS

Chemicals and instruments

C-1027 (Lot: 20020525, purity 95.0%) was produced by the Institute of Medicinal Biotechnology, Chinese Academy of Medical Sciences and Peking Union Medical University (Beijing, China). ^{125}I -C-1027, which was radio-iodinated by the Iodogen method^[36], had a specific radioactivity of 7.45 mCi (275.65 MBq)/mg. The radiochemical purity was more than 95%. Iodogen was from Academy of Military Medical Sciences (Beijing, China). Trichloroacetic acid (TCA, analytical grade) was provided by the Chemical Company (Beijing, China), and 0.9% sodium chloride was purchased from Dazhong Pharmaceutical Company (Tianjin, China). Distilled water, prepared from demineralized water, was used throughout the study. Gamma counter (FJ630G/12 model) was produced by Beijing Nuclear Company (Beijing, China). The chromatographic system (LC-6A, Shimadzu, Japan) consisted of a pump (LC-6AT), temperature box and variable wavelength UV detector (Spectra 100, Shimadzu, Japan). Sephadex G-50 column (300 mm \times 7.8 mm I.D) was purchased from Pharmacia Company (USA).

Animals

Kunming mice, male and female, with body weights from 17 to 24 g, were purchased from the Center of Experimental Animals of Tianjin Institute of Pharmaceutical Research (Certificate No: 20020804, Tianjin, China).

Preparation of ^{125}I -C-1027

Iodogen (100 μg) in 100 μL of chloroform was placed in a sample tube, and evaporated to dryness with nitrogen gas. C-1027 (50 μg), and 50 μL of Na^{125}I (74 MBq) were pipetted, mixed, and allowed to react at 15 $^\circ\text{C}$ for 30 min^[36]. The mixture was chromatographed on Sephadex G-50 column. The mobile phase consisted of 0.05 mol/L sodium dodecyl sulfate phosphate buffer solution (pH 7.0) at a flow rate of 0.8 mL/min. The eluted

fractions, detected by gamma counter as the same chromatographic behavior as standard C-1027 and Na¹²⁵I, were components of ¹²⁵I-C-1027 and Na¹²⁵I, respectively (Figure 1). The fraction, collected from 10 min to 12.5 min, was a single radioactive peak of ¹²⁵I-C-1027, and was concentrated to a specific activity and applied for pharmacokinetic study.

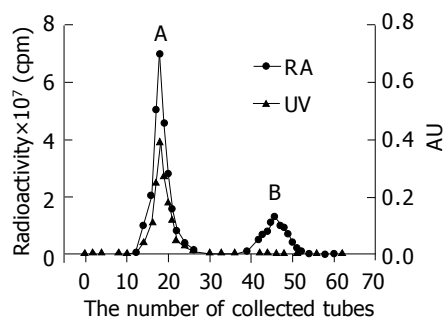


Figure 1 Chromatograms of the separation of ¹²⁵I-C-1027 assayed by UV and radioactivity. A: ¹²⁵I-C-1027; B: Decomposed materials of ¹²⁵I-C-1027 and ¹²⁵I.

Radiochemical purity

The radiochemical purity of ¹²⁵I-C-1027 was calculated from the ratio of radioactivity of ¹²⁵I-C-1027 to the collected total radioactivity. The biological activity of ¹²⁵I-C-1027 was assayed in mice as previously described^[37], and the biological activity was compared with C-1027. Only the ¹²⁵I-C-1027, whose biological activity remained unchanged, was used to study the pharmacokinetics of ¹²⁵I-C-1027.

Solution preparation and quality control samples

Stock solution (10.0 µg/mL) of the ¹²⁵I-C-1027 (275.65 KBq/mL) was prepared in water, and stored at -20 °C. The stock solution was prepared into the serial concentrations of standard solution of 0.5, 1.0, 2.0, 5.0, 10.0, 20.0, 50.0 and 100.0 ng/mL in 0.9% sodium chloride solution. The standard solution was used to prepare standard curves. The serial concentrations of calibration curves were prepared with mouse blank serum instead of 0.9% sodium chloride solution as mentioned above. Quality control (QC) samples were prepared into low, middle and high concentrations (0.5, 5.0 and 50 ng/mL) in mouse serum.

Sample preparation

To 100 µL of mouse serum samples, 100 µL of 20% TCA was added. The mixture was vortexed for 2 min, and the supernatant was removed. Then, radioactivity of the precipitate was determined by the gamma counter.

Specificity, precision, accuracy and stability

Specificity of the assay was demonstrated by comparison between the radioactivity of the mouse serum spiked with ¹²⁵I-C-1027 and the mouse blank serum.

QC samples of low, middle and high concentration levels (0.5, 5.0, and 50 ng/mL) were prepared for the determination of the precision and accuracy of intra- and inter-day. Precision, which was evaluated by one-way analysis (ANOVA), was defined as the relative standard deviation (RSD). Accuracy was defined as the relative errors (RE) between the measured and the nominal value on each of the three concentration levels.

Bench top stability was experimented at room temperature over 12 h. The QC samples in 6 replicates were analyzed at room temperature on the same day. Three freeze-thaw cycles were done on the QC samples.

Application for mouse pharmacokinetics

Each sampling time was randomly distributed in 6 mice. Blood samples (0.4 mL) were collected at 0 min (pre-dose) and 2, 5, 15, 30 min and 1, 2, 4, 6, 8, 12, and 24 h after intravenous administration of ¹²⁵I-C-1027 at doses of 10, 50, and 100 µg/kg. Serum samples were obtained by centrifuging at 2 000 g for 10 min, and stored at -20 °C until analysis.

Pharmacokinetic datum analysis

The concentration-time data were computed using a 3p97 Pharmacokinetic Calculation Program developed by the Mathematic Pharmacological Committee, Chinese Pharmacological Society (Beijing, China). The following pharmacokinetic parameters were calculated: biological half-life ($T_{1/2}$), area under concentration-time curve (AUC), apparent distribution volume (V_d), the total body clearance (Cl), elimination rate constant (K), and other parameters.

RESULTS

Validation of the bioanalytical method

The standard and calibration curve equations of ¹²⁵I-C-1027 showed that the concentrations and their own radioactivity had a good linear correlation. The typical curve equations and correlation coefficients were as follows: $y = 49.5 + 1235.9x$ ($n = 8$, $r = 0.9994$) for the standard solution of ¹²⁵I-C-1027 at the concentration from 0.5 to 100.0 ng/mL, and $y = 127.6 + 969.5x$ ($n = 7$, $r = 0.9999$) for serum samples from 0.5 to 100.0 ng/mL.

Precision and accuracy of the assay were evaluated by analyzing QC samples (0.5, 5.0 and 50.0 ng/mL) in 6 replicates on 3 different days. The relative standard deviation (RSD) was less than 5.0% for intra-day assay and less than 10.1% for inter-day assay at 0.5-100.0 ng/mL. The accuracy was between 96.0% and 99.0% (Table 1). The limit of quantitation was the lowest concentration on the calibration curve if the following conditions were met. (1) There was no interference present in blanks at the retention time of the analyte, or the determination response was at least 10 times greater than any interference in blank sample at the retention time; (2) Analyte peak should be identifiable, discrete and reproducible with a precision of less or equal to 15% and accuracy within $\pm 15\%$. The limit of quantitation of ¹²⁵I-C-1027 for the TCA-RA method was 0.5 ng/mL.

Table 1 Precision and accuracy for determination of ¹²⁵I-C-1027 by TCA-RA method in mouse serum (mean \pm SD, $n = 5$)

Added (ng/mL)	Within-day			Between-day		
	Found	RSD (%)	Accuracy (%)	Found	RSD (%)	Accuracy (%)
1.0	0.98 \pm 0.05	5.0	98.0	0.96 \pm 0.04	4.6	96.0
2.5	2.47 \pm 0.05	1.9	98.6	2.45 \pm 0.25	10.1	98.2
20.0	9.81 \pm 0.14	0.7	99.0	19.65 \pm 1.00	5.1	98.4

Stability

The bench top stability of ¹²⁵I-C-1027 in mouse serum was determined over 12 h at room temperature. The results showed that ¹²⁵I-C-1027 was stable at the concentrations (0.5, 5.0 and 50.0 ng/mL) at room temperature (more than 92.0%, 91.0% and 90.0%, respectively). Similarly when ¹²⁵I-C-1027 underwent 3 freeze-thaw cycles, the percentage differences were 8.9%, 7.3% and 8.2% at 3 different concentrations, respectively.

Specificity

The comparison of blank serum samples and serum samples spiked with ¹²⁵I-C-1027 showed no endogenous interference

with the measurement of ^{125}I -C-1027.

The validation of the TCA-RA method satisfied the requirements for bioanalysis^[38-42].

Pharmacokinetics

After intravenous injection of 10, 50 and 100 $\mu\text{g}/\text{kg}$ ^{125}I -C-1027 to mice, the serum concentrations of ^{125}I -C-1027 were determined by the TCA-RA method. Figure 2 shows the serum concentration-time curve of ^{125}I -C-1027 after intravenous administration ($n=6$). The results of this experiment showed that the pharmacokinetic parameters: $T_{1/2}$, Cl , V_d and K did not exhibit statistically significant differences ($P>0.05$) among the three doses, and the AUC values depended on the administration dose (Table 2).

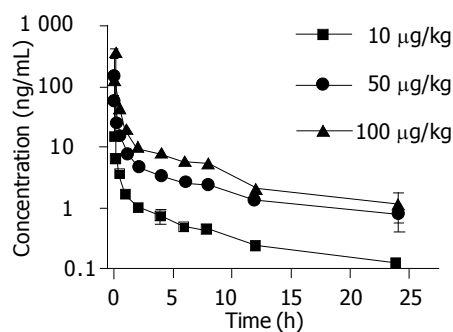


Figure 2 Mean serum concentration-time curves of C-1027 after IV administration to mice at three different doses by TCA-RA method.

Table 2 Mean pharmacokinetic parameters of ^{125}I -C-1027 measured by TCA-RA method at three doses in mice ($n=6$)

Parameters	Unit	Doses ($\mu\text{g}/\text{kg}$)			P
		10	50	100	
A	ng/mL	34.62	142.98	277.02	
α	/h	9.61	9.64	4.92	
B	ng/mL	3.31	18.10	26.02	
β	/h	0.22	0.20	0.18	
$V_{(d)}$	L/kg	0.26	0.31	0.33	>0.05
$T_{1/2\alpha}$	h	0.07	0.07	0.14	
$T_{1/2\beta}$	h	3.10	3.40	3.90	>0.05
K_{21}	/h	1.04	1.26	0.58	
K_{10}	/h	2.06	1.55	1.49	>0.05
K_{12}	/h	6.73	7.03	3.02	
AUC	ng·h/mL	18.41	103.69	202.74	
$CL_{(s)}$	L/(kg·h)	0.54	0.48	0.49	>0.05

$V_{(d)}$: Apparent distribution volume; $T_{1/2}$: Half-life; K : Elimination rate constant; AUC : Area under curve; $CL_{(s)}$: Clearance.

DISCUSSION

Biotechnological pharmaceuticals can be analyzed by many methods, such as bioassays, immunoassays, enzyme-linked immunosorbent assay and solid-phase radioimmunoassay. However, these methods are limited due to the interference of endogenous substances. On the other hand, isotope labeling methods used to analyze pharmacokinetic properties of biotechnological products, can eliminate the interference of endogenous substances, and improve the specificity, accuracy, limit of quantitation, and the speed of analysis.

The method of ^{125}I labeling C-1027 is simple, quick and acceptable. The highly purified ^{125}I -C-1027 (with purity of more

than 95.0%) is obtained by the Sephadex G-50 gel filtration, indicating that Sephadex G-50 gel filtration is an effective procedure to yield the high quality ^{125}I -labeled C-1027. Only the ^{125}I -C-1027 with purity and biological activity in accordance with the regulation can be used for the pharmacokinetic experiments in mice.

The TCA-RA method has been considered to be an accepted method for assay of the precipitated ^{125}I -C-1027^[43]. In this study, the mouse serum determination and pharmacokinetic profiles of ^{125}I -C-1027 were measured by the TCA-RA method after intravenous injection of 10, 50, and 100 $\mu\text{g}/\text{kg}$ ^{125}I -C-1027 to mice. The pharmacokinetic results show that the areas under curves of three doses (10, 50, and 100 $\mu\text{g}/\text{kg}$) depend on the doses. The biological half-lives ($T_{1/2}$) do not change with the doses. The limit of quantitation indicates that this method is a sensitive method for analysis of C-1027.

ACKNOWLEDGEMENTS

The authors are indebted to the Institute of Medicinal Biotechnology (Beijing, China) for their financial support during the course of the study.

REFERENCES

- Hu JL, Xue YC, Xie MY, Zhang R, Otani T, Minami Y, Yamada Y, Marunaka T. A new macromolecular antitumor antibiotic, C-1027. I. Discovery, taxonomy of producing organism, fermentation and biological activity. *J Antibiot (Tokyo)* 1988; **41**: 1575-1579
- Otani T, Minami Y, Marunaka T, Zhang R, Xie MY. A new macromolecular antitumor antibiotic, C-1027. II. Isolation and physico-chemical properties. *J Antibiot (Tokyo)* 1988; **41**: 1580-1585
- Zhen YS, Ming XY, Yu B, Otani T, Saito H, Yamada Y. A new macromolecular antitumor antibiotic, C-1027. III. Antitumor activity. *J Antibiot (Tokyo)* 1989; **42**: 1294-1298
- Otani T, Yasuhara T, Minami Y, Shimazu T, Zhang R, Xie MY. Purification and primary structure of C-1027-AG, a selective antagonist of antitumor antibiotic C-1027, from *Streptomyces globisporus*. *Agric Biol Chem* 1991; **55**: 407-417
- Liu W, Shen B. Genes for production of the enediyne antitumor antibiotic C-1027 in *Streptomyces globisporus* are clustered with the *cagA* gene that encodes the C-1027 apoprotein. *Antimicrob Agents Chemother* 2000; **44**: 382-392
- Matsumoto T, Okuno Y, Sugiura Y. Specific interaction between a novel enediyne chromophore and apoprotein in macromolecular antitumor antibiotic C-1027. *Biochem Biophys Res Commun* 1993; **195**: 659-666
- Otani T. Conformation studies on and assessment by spectral analysis of the protein-chromophore interaction of the macromolecular antitumor antibiotic C-1027. *J Antibiot (Tokyo)* 1993; **46**: 791-802
- Chen Y, Shao R, Bartlam M, Li J, Jin L, Gao Y, Liu Y, Tang H, Zhen Y, Rao Z. Crystallization and preliminary X-ray crystallographic studies of a macromolecular antitumor antibiotic, C1027. *Acta Crystallogr D Biol Crystallogr* 2002; **58**: 173-175
- Tanaka T, Fukuda-Ishisaka S, Hiramata M, Otani T. Solution structures of C-1027 apoprotein and its complex with the aromatized chromophore. *J Mol Biol* 2001; **309**: 267-283
- Semmelhack MF, Jiang Y, Ho D. Synthesis of the amino sugar from C-1027. *Org Lett* 2001; **3**: 2403-2406
- Xu YJ, Li DD, Zhen YS. Mode of action of C-1027, a new macromolecular antitumor antibiotic with highly potent cytotoxicity, on human hepatoma BEL-7402 cells. *Cancer Chemother Pharmacol* 1990; **27**: 41-46
- He QY, Liang YY, Wang DS, Li DD. Characterization of cell death induced by anticancer antibiotic lidamycin in human hepatoma BEL-7402 cells. *Yaoxue Xuebao* 2001; **36**: 174-178
- Cui DP, Wang Z, Li DD. Effect of lidamycin on the expression of genes involved in invasion regulation in HCT-8 human colon

- cancer cells. *Yaouxue Xuebao* 2001; **36**: 246-249
- 14 **He QY**, Jiang B, Li DD, Zhen YS. Effects of lidamycin on apoptotic gene expressions and cytoskeleton in human hepatoma bel-7402 cells. *Aizheng* 2002; **21**: 351-355
- 15 **He QY**, Jiang B, Li DD. Effects of lidamycin on genomic DNA in human hepatoma BEL-7402 cells. *Acta Pharmacol Sin* 2002; **23**: 253-256
- 16 **He QY**, Liang YY, Wang DS, Li DD. Characteristics of mitotic cell death induced by enediyne antibiotic lidamycin in human epithelial tumor cells. *Int J Oncol* 2002; **20**: 261-266
- 17 **Zhen H**, Xue Y, Zhen Y. Inhibition of angiogenesis by antitumor antibiotic C1027 and its effect on tumor metastasis. *Zhonghua Yixue Zazhi* 1997; **77**: 657-660
- 18 **Li J**, Zhen Y, Yang Z. Biodistribution of monoclonal antibody and Fab fragment and antitumor effect of their conjugates on hepatoma xenografts. *Zhongguo Yixuekexueyuan Xuebao* 1994; **16**: 328-333
- 19 **Sugiura Y**. Molecular mechanisms of DNA recognition and function by bioactive compounds. *Yakugaku Zasshi* 2000; **120**: 1409-1418
- 20 **Hiraku Y**, Oikawa S, Kawanishi S. Distamycin A, a minor groove binder, changes enediyne-induced DNA cleavage sites and enhances apoptosis. *Nucleic Acids Res Suppl* 2002: 95-96
- 21 **Wang Z**, He Q, Liang Y, Wang D, Li YY, Li D. Non-caspase-mediated apoptosis contributes to the potent cytotoxicity of the enediyne antibiotic lidamycin toward human tumor cells. *Biochem Pharmacol* 2003; **65**: 1767-1775
- 22 **Dziegielewski J**, Beerman TA. Cellular responses to the DNA strand-scission enediyne C-1027 can be independent of ATM, ATR, and DNA-PK kinases. *J Biol Chem* 2002; **277**: 20549-20554
- 23 **McHugh MM**, Yin X, Kuo SR, Liu JS, Melendy T, Beerman TA. The cellular response to DNA damage induced by the enediynes C-1027 and neocarzinostatin includes hyperphosphorylation and increased nuclear retention of replication protein a (RPA) and trans inhibition of DNA replication. *Biochemistry* 2001; **40**: 4792-4799
- 24 **McHugh MM**, Beerman TA. C-1027-induced alterations in Epstein-Barr viral DNA replication in latently infected cultured human Raji cells: relationship to DNA damage. *Biochemistry* 1999; **38**: 6962-6970
- 25 **Kirk CA**, Goodisman J, Beerman TA, Gawron LS, Dabrowiak JC. Kinetics of cleavage of intra- and extracellular simian virus 40 DNA with the enediyne anticancer drug C-1027. *Biophys Chem* 1997; **63**: 201-209
- 26 **Matsumoto T**, Sugiura Y. Alterations of binding mode and cutting site by G->I replacement in preferred cleavage sequences 5'-AGG of chromoprotein C-1027. *Biochem Biophys Res Commun* 1994; **205**: 1533-1538
- 27 **Xu YJ**, Zhen YS, Goldberg IH. C1027 chromophore, a potent new enediyne antitumor antibiotic, induces sequence-specific double-strand DNA cleavage. *Biochemistry* 1994; **33**: 5947-5954
- 28 **Zhou CS**, Xu LN, Jiang M, Zhen YS. A monoclonal antibody directed against an enediyne antitumor antibiotic and its preliminary application. *Yaouxue Xuebao* 1997; **32**: 28-32
- 29 **Shao RG**, Zhen YS. Relationship between the molecular composition of C1027, a new macromolecular antibiotic with enediyne chromophore, and its antitumor activity. *Yaouxue Xuebao* 1995; **30**: 336-342
- 30 **Liu JS**, Kuo SR, Yin X, Beerman TA, Melendy T. DNA damage by the enediyne C-1027 results in the inhibition of DNA replication by loss of replication protein A function and activation of DNA-dependent protein kinase. *Biochemistry* 2001; **40**: 14661-14668
- 31 **Xu YJ**, Xi Z, Zhen YS, Goldberg IH. Mechanism of formation of novel covalent drug DNA interstrand cross-links and monoadducts by enediyne antitumor antibiotics. *Biochemistry* 1997; **36**: 14975-14984
- 32 **Sugiura Y**, Totsuka R, Araki M, Okuno Y. Selective cleavages of tRNAPhe with secondary and tertiary structures by enediyne antitumor antibiotics. *Bioorg Med Chem* 1997; **5**: 1229-1234
- 33 **McHugh MM**, Beerman TA, Burhans WC. DNA damaging enediyne C-1027 inhibits initiation of intracellular SV40 DNA replication in trans. *Biochemistry* 1997; **36**: 1003-1009
- 34 **Xu YJ**, Xi Z, Zhen YS, Goldberg IH. A single binding mode of activated enediyne C1027 generates two types of double-strand DNA lesions: deuterium isotope-induced shuttling between adjacent nucleotide target sites. *Biochemistry* 1995; **34**: 12451-12460
- 35 **Totsuka R**, Aizawa Y, Uesugi M, Okuno Y, Matsumoto T, Sugiura Y. RNA cleavage by C-1027 chromophore, an enediyne antitumor antibiotic: high selectivity to an anticodon arm. *Biochem Biophys Res Commun* 1995; **208**: 168-173
- 36 **Tang ZM**, Liu XW, Xu LP, Shan CW, Song QS. Pharmacokinetics and tissue distribution of human recombinant interleukin-2 in mice. *Zhongguo YaoLi XueBao* 1994; **15**: 51-56
- 37 **Sugimoto Y**, Otani T, Oie S, Wierzba K, Yamada Y. Mechanism of action of a new macromolecular antitumor antibiotic, C-1027. *J Antibiot (Tokyo)* 1990; **43**: 417-421
- 38 **Liu CX**, Wei GL, Li QS. Methodology study of validation for bioanalysis in studies on pharmacokinetics and bioavailability. *Asian J Drug Metab Pharmacokinet* 2001; **1**: 279-286
- 39 **Shah VP**, Midha KK, Dighe S, McGilveray IJ, Skelly JP, Yacobi A, Layloff T, Viswanathan CT, Cook CE, McDowall RD. Analytical methods validation: bioavailability, bioequivalence and pharmacokinetic studies. Conference report. *Eur J Drug Metab Pharmacokinet* 1991; **16**: 249-255
- 40 **Gao J**. Bioanalytical method validation for studies on pharmacokinetics, bioavailability and bioequivalence: Highlights of the FDA's Guidance. *Asian J Drug Metab Pharmacokinet* 2004; **4**: 5-13
- 41 **Xia JH**. Validation of analytical methods for pharmacokinetics, bioavailability and bioequivalence studies. *Asian J Drug Metab Pharmacokinet* 2001; **1**: 95-100
- 42 **Liu YP**, Zhou MJ. Effect of polyethylene glycol derivation on pharmacokinetic properties of biotechnical drugs. *Asian J Drug Metab Pharmacokinet* 2002; **2**: 127-131
- 43 **Pannell R**, Gurewich V. Pro-urokinase: a study of its stability in plasma and of a mechanism for its selective fibrinolytic effect. *Blood* 1986; **67**: 1215-1223

Edited by Xia HHX and Wang XL Proofread by Chen WW

Correlation between expression of gastrin, somatostatin and cell apoptosis regulation gene bcl-2/bax in large intestine carcinoma

Jia-Ding Mao, Pei Wu, Xiang-Hou Xia, Ji-Qun Hu, Wen-Bin Huang, Guo-Qiang Xu

Jia-Ding Mao, Pei Wu, Xiang-Hou Xia, Ji-Qun Hu, Department of General Surgery, The First Affiliated Yijishan Hospital of Wannan Medical College, Wuhu 241001, Anhui Province, China

Wen-Bin Huang, Guo-Qiang Xu, Department of Pathology, The First Affiliated Yijishan Hospital of Wannan Medical College, Wuhu 241001, Anhui Province, China

Supported by National Natural Science Foundation of China, No. 39270769, and Natural Science Foundation of Anhui Province, No. 03043704, and Natural Science Foundation of Education Bureau of Anhui Province, No.2002kj307

Correspondence to: Professor Pei Wu, Department of General Surgery, The First Affiliated Yijishan Hospital of Wannan Medical College, Wuhu 241001, Anhui Province, China. wp5708@sina.com
Telephone: +86-553-5738856-2343

Received: 2004-02-28 **Accepted:** 2004-03-18

Abstract

AIM: To explore the correlation between expression of somatostatin (SS), gastrin (GAS) and cell apoptosis regulation gene bcl-2/bax in large intestine carcinoma.

METHODS: Sixty-two large intestine cancer tissue samples were randomly and retrospectively selected from patients with large intestine carcinoma. Immunohistochemical staining for bcl-2, bax, GAS, SS was performed according to the standard streptavidin-biotin-peroxidase (S-P) method. According to the semi-quantitative integral evaluation, SS and GAS were divided into three groups as follows. Scores 1-3 were defined as the low expression group, 4-8 as the intermediate expression group, 9-16 as the high expression group. Bax and bcl-2 protein expressions in different GAS and SS expression groups of large intestine carcinoma were assessed.

RESULTS: The positive expression rate of bax had a prominent difference between SS and GAS high, intermediate and low expression groups ($P < 0.05$, $\chi^2_{SS} = 9.246$; $P < 0.05$, $\chi^2_{GAS} = 6.981$). The positive expression rate of bax in SS high (80.0%, 8/10) and intermediate (76.5%, 13/17) expression groups was higher than that in low expression group (40.0%, 14/35) ($P < 0.05$, $\chi^2_{high\ vs\ low} = 5.242$; $P < 0.05$, $\chi^2_{middle\ vs\ low} = 6.097$). The positive expression rate of bax in GAS high expression group (27.3%, 3/8) was lower than that in low expression group (69.4%, 25/36) ($P < 0.05$, $\chi^2 = 4.594$). However, bax expression in GAS intermediate expression group (46.7%, 7/15) was lower than that in low expression group, but not statistically significant. The positive expression rate of bcl-2 had a prominent difference between SS and GAS high, intermediate and low expression groups ($P < 0.05$, $\chi^2_{SS} = 7.178$; $P < 0.05$, $\chi^2_{GAS} = 13.831$). The positive expression rate of bcl-2 in GAS high (90.9%, 10/11) and intermediate (86.7%, 13/15) expression groups was higher than that in low expression group (44.4%, 16/36) ($P < 0.05$, $\chi^2_{high\ vs\ low} = 5.600$; $P < 0.05$, $\chi^2_{middle\ vs\ low} = 7.695$). However, the positive expression rate of bcl-2 in SS high (40.0%, 4/10) and intermediate (47.1%, 8/9) expression groups was lower than that in low expression group (77.1%, 27/35)

($P < 0.05$, $\chi^2_{high\ vs\ low} = 4.710$; $P < 0.05$, $\chi^2_{middle\ vs\ low} = 4.706$). There was a significant positive correlation between the integral ratio of GAS to SS and the integral of bcl-2 ($P < 0.01$, $r = 0.340$). However, there was a negative correlation between the integral ratio of GAS to the SS and bax the integral of ($P < 0.05$, $r = -0.299$).

CONCLUSION: The regulation and control of gastrin, somatostatin in cell apoptosis of large intestine carcinoma may be directly related to the abnormal expression of bcl-2, bax.

© 2005 The WJG Press and Elsevier Inc. All rights reserved.

Key words: Large intestine carcinoma; Gastrin; Somatostatin; bcl-2 gene; Bax gene; Apoptosis

Mao JD, Wu P, Xia XH, Hu JQ, Huang WB, Xu GQ. Correlation between expression of gastrin, somatostatin and cell apoptosis regulation gene bcl-2/bax in large intestine carcinoma. *World J Gastroenterol* 2005; 11(5): 721-725

<http://www.wjgnet.com/1007-9327/11/721.asp>

INTRODUCTION

Large intestine cancer is one of the commonest malignancies in the world including china. Although early diagnosis and treatment have somewhat improved outcomes of patients, large intestine carcinoma still remains the major killer among Chinese^[1-4]. Previous studies have demonstrated that the occurrence of large intestine cancer is directly related to the abnormal expression of gastrointestinal hormones such as gastrin, somatostatin, etc^[5]. Mean while, somatostatin is able to induce cell apoptosis of large intestine cancer and inhibit cell proliferation, but the function of GAS is opposite^[6-8]. However, the detailed mechanism of gastrin and somatostatin in regulation and control of cell apoptosis of large intestine carcinoma remains unknown. We used immunohistochemical staining S-P method to detect the expression of GAS, SS, bcl-2, bax proteins in large intestine cancer tissue. The aim of this study was to explore whether GAS, SS could regulate and control cell apoptosis mainly via influencing the expression of bcl-2/bax proteins in large intestine cancer.

MATERIALS AND METHODS

Large intestine carcinoma specimens

Sixty-two large intestine cancer tissue samples were randomly and retrospectively selected from patients with large intestine carcinoma in the First Affiliated Yijishan Hospital of Wannan Medical College from 2000 to 2002. Among them, 41 were cases of rectal cancer, 21 were cases of colorectal carcinoma. Twenty-two were females, 40 were males. The median age was 50.9±7.8 years, with a range of 28-77 years. The clinical stage was determined according to Dukes' stage. Thirty-four were Dukes' stages A, B and 28 were Dukes' stages C, D. Histological grade of tumors was determined according to the WHO criteria, and 21 patients were grade I, 25 grade II, 16 grade III.

Main reagents

The polyclonal rabbit antibodies against human SS and GAS, monoclonal mouse antibodies against human bcl-2 and bax, and immunohistochemical staining kits were all purchased from Beijing Zhongshan Biological Technology Co, Ltd.

Immunohistochemical staining

Specimens obtained at surgery were routinely fixed in 10% neutral formalin and embedded in paraffin. Serial 4 μm thick sections were cut. Immunohistochemical staining for bcl-2, bax, GAS, SS was performed according to the standard streptavidin-biotin-peroxidase (S-P) method. The detailed manipulation was conducted according to the introductions for users. A previously known positive pancreatic tissue, stomach antrum mucous membrane, amygdala tissue, Hodgkin's disease tissue were used as positive controls for GAS, SS, bcl-2, bax, respectively. PBS 0.01M was used as a negative control to replace the primary antibody.

Evaluation of scores

The standard positive SS and GAS expressions were stained brown-yellow mainly in cell plasma, partly in cell membranes. Both the extent and intensity of immunopositivity of SS and GAS expressions were scored according to Wu *et al*^[8]. The intensity of positivity was scored as follows: 1, no staining; 2, light-yellow; 3, brown-yellow; 4, brown-black. The extent of positivity was scored as follows (one hundred cells were counted by two independent observers, who did not know the clinicopathological features of these large intestine cancers.): 1, $\leq 5\%$, 2, $>5-10\%$, 3, $>10-20\%$, 4, $>20\%$ of the tumor cells in the respective lesions. The final score was determined by multiplying the intensity with extent of positivity scores, yielding a range from 1 to 16. According to the semi-quantitative integral evaluation, SS and GAS were divided into three groups as follows. Scores 1-3 were defined as the low expression group, 4-8 as the intermediate expression group, 9-16 as the high expression group.

The standard positive bcl-2 and bax expressions were stained brown-yellow mainly in cell plasma. Both the extent and intensity of immunopositivity of bcl-2 and bax expressions were scored according to Fromowitz *et al*^[9]. The intensity of positivity was scored as follows: 0, negative; 1, light-yellow; 2, brown-yellow; 3, brown-black. The extent of positivity was scored as follows: 1, $\leq 25\%$; 2, $>25-50\%$; 3, $>50-75\%$; 4, $>75\%$. The final score was determined by adding the intensity to extent of positivity scores, yielding a range from 0 to 12. Scores 1-2 were defined as negative expression (-), 3 as weak staining pattern (+), 4 as moderate staining (++) , ≥ 5 as strong staining (+++).

Statistical analysis

Statistical evaluation was performed using chi-square test to differentiate the rates of different groups and using Spearman test to analyze the correlation between the ratio of GAS to SS and the integral of bcl-2 and bax. $P < 0.05$ was considered statistically significant. SPSS 10.0 software for Windows was employed to analyze all data.

RESULTS

Bax expression in GAS, SS high, intermediate, and low expression groups of large intestine carcinoma

The positive expression rate of bax had a prominent difference in SS and GAS high, intermediate and low expression groups of large intestine cancer ($P < 0.05$, $\chi^2_{\text{SS}} = 9.246$; $P < 0.05$, $\chi^2_{\text{GAS}} = 6.981$). The positive expression rate of bax in SS high (80.0%, 8/10) and intermediate (76.5%, 13/17) expression groups was higher than that in low expression group (40.0%, 14/35) ($P < 0.05$, $\chi^2_{\text{high vs low}} = 5.242$; $P < 0.05$, $\chi^2_{\text{middle vs low}} = 6.097$). The positive expression rate of bax in GAS high expression group (27.3%, 3/8) was lower than that in low expression group (69.4%, 25/36) ($P < 0.05$, $\chi^2 = 4.594$). Bax expression in GAS intermediate expression group (46.7%, 7/15) was lower than that in low expression group, but without statistical significance (Table 1, Figure 1: A-C).

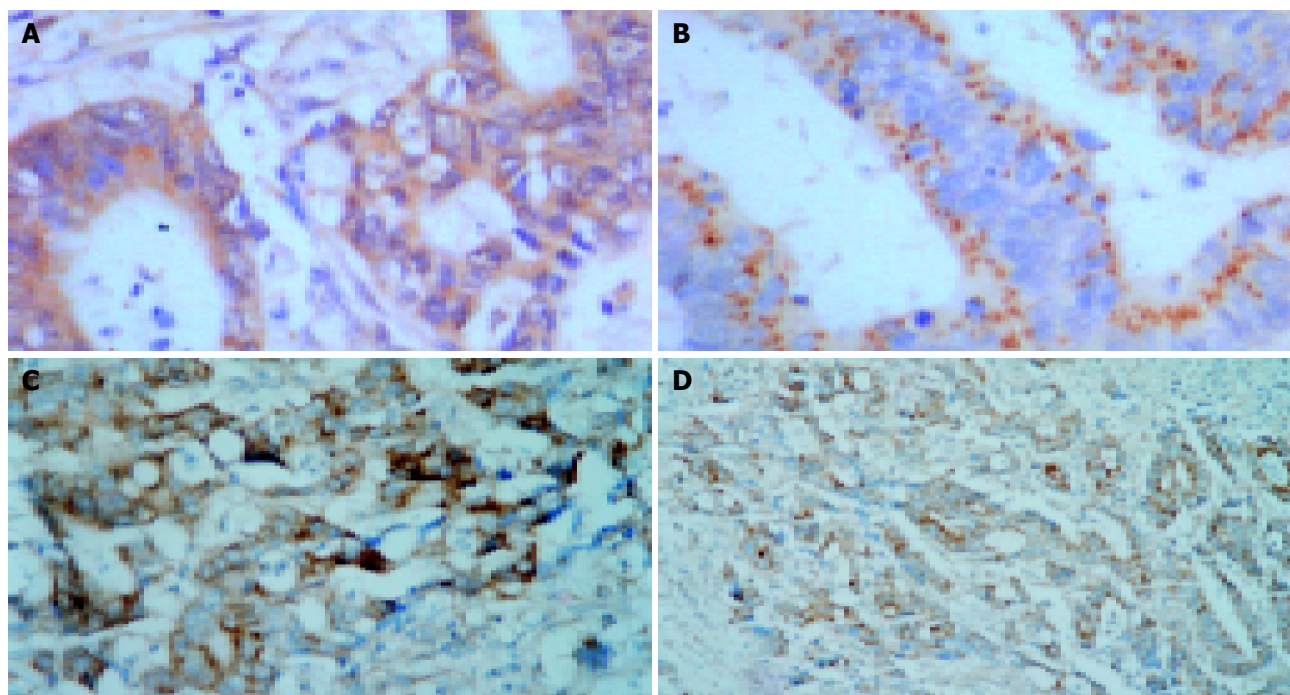


Figure 1 Strong expressions of GAS, SS, bcl-2 and bax in large intestine carcinoma tissue. A: Strong GAS expression in large intestine carcinoma tissue. S-P $\times 400$; B: Strong SS expression in large intestine carcinoma tissue. S-P $\times 400$; C: Strong bax expression in SS high expression group of large intestine carcinoma tissue. S-P $\times 200$; D: Strong bcl-2 expression in GAS high expression group of large intestine carcinoma tissue. S-P $\times 200$.

Table 1 Bax expression in SS and GAS high, intermediate, and low expression groups of large intestine carcinoma

Groups	n	Bax		Positive rate (%)
		Positive	Negative	
SS				
High	10	8	2	80.0 (8/10) ^a
Intermediate	17	13	4	76.5 (13/17) ^a
Low	35	14	21	40.0 (14/35)
GAS				
High	11	3	8	27.3 (3/11) ^c
Intermediated	15	7	8	46.7 (7/15)
Low	36	25	11	69.4 (25/36)

^a $P < 0.05$ vs the SS low expression group; ^c $P < 0.05$ vs GAS low expression group.

Bcl-2 expression in GAS, SS high, intermediate, and low expression groups of large intestine carcinoma

The positive expression rate of bcl-2 had a prominent difference in SS and GAS high, intermediate and low expression groups of large intestine cancer ($P < 0.05$, $\chi^2_{SS} = 7.178$; $P < 0.05$, $\chi^2_{GAS} = 13.831$). The positive expression rate of bcl-2 in GAS high (90.9%, 10/11) and intermediated (86.7%, 13/15) expression groups was higher than that in low expression group (44.4%, 16/36) ($P < 0.05$, $\chi^2_{high\ vs\ low} = 5.600$; $P < 0.05$, $\chi^2_{middle\ vs\ low} = 7.695$). However, the positive expression rate of bcl-2 in SS high (40.0%, 4/10) and intermediate (47.1%, 8/9) expression groups was lower than that in low expression group (77.1%, 27/35) ($P < 0.05$, $\chi^2_{high\ vs\ low} = 4.710$; $P < 0.05$, $\chi^2_{middle\ vs\ low} = 4.706$) (Table 2, Figure 1: D).

Table 2 Bcl-2 expression in SS and GAS high, intermediate, and low expression groups of large intestine carcinoma

Groups	n	Bcl-2		Positive rate (%)
		Positive	Negative	
SS				
High	10	4	6	40.0 (4/10) ^a
Intermediated	17	8	9	47.1 (8/17) ^a
Low	35	27	8	77.1 (27/35)
GAS				
High	11	10	1	90.9 (10/11) ^c
Intermediated	15	13	2	86.7 (13/15) ^c
Low	36	16	20	44.4 (16/36)

^a $P < 0.05$ vs the SS low expression group; ^c $P < 0.05$ vs the GAS low expression group.

Correlation between the integral ratio of GAS to SS and the integral of bcl-2, bax

There was a significant positive correlation between the integral ratio of GAS to SS and the integral of bcl-2 ($P < 0.01$, $r = 0.340$). However, there was a negative correlation between the integral ratio of GAS to SS and the integral of bax ($P < 0.05$, $r = -0.299$).

DISCUSSION

Previous studies have shown that tissue growth is regulated by hormones, and their tumor growth and development are still controlled by hormones^[10]. Gastrointestinal hormones such as gastrin and somatostatin regulate the secretion, motility, absorption, blood flow and cell nutrition of the digestive tract. Abnormality of their secretion often affects the normal functions of digestive tract, even causes clinical symptoms or

syndromes^[11,12]. Some studies have demonstrated that there is a high correlation between the abnormal expressions of GAS, SS and the occurrence and development of large intestine cancer^[13-15]. Recent studies have shown that the abnormal expressions of GAS and SS are closely related to cell apoptosis of large intestine cancer. Gastrin could promote cell proliferation and inhibit cell apoptosis. However, the action of somatostatin is opposite in large intestine carcinoma^[8,16,17].

Apoptosis can not only maintain the body in well stable condition, but also plays an important role in regulating and controlling tumor occurrence, development and treatment^[18]. It has been proved that occurrence of cancer is due to the loss of control of normal apoptosis and the disturbance of balance between cell proliferation and apoptosis^[19,20]. Apoptosis related genes such as bcl-2 family are divided into two categories: pro-apoptosis genes and anti-apoptosis genes. Bcl-2 is an important apoptosis repressor, while Bax is one of the most important apoptosis promoters. The protein it encodes could combine with Bcl-2 to form compounds, which resist the action of apoptosis repression. But it has a positive regulatory action^[21-24]. Recent data indicate that the regulation and control of cell apoptosis by bax and bcl-2 genes are not only based on the level of the two regulatory proteins but also based on their ratio. When the ratio is high, cells undergo apoptosis, otherwise, they proliferate^[19,25,26].

Gastrin is mainly secreted from gastrin secreting cells (G cells) in antrum mucosa or upper small intestine, large intestine. Medulla oblongata and dorsal nuclei of vagus nerves in central nervous system also secrete gastrin^[27]. Some studies indicate that external gastrin is able to inhibit apoptosis of MKN45 cells by inducing over-expression of anti-apoptosis gene bcl-2, and proglumide could block these effects of gastrin^[28]. Zhang *et al.*^[29] found that gastrin was able to increase the threshold of apoptosis by upregulating bcl-2 gene expression in human cholangiocarcinoma cells, but it had no effect on the expression of bax gene. However, Hartwich *et al.*^[30] found that gastrin was able to restrain the apoptosis of tumor cells by inducing over-expression of bcl-2 and inhibiting the bax gene activity. Whether gastrin can regulate and control cell apoptosis mainly by affecting the bax gene expression, needs further studies. In this study, we found that GAS protein expression and the positive expression rate of bcl-2 were higher in large intestine carcinoma, however the expression of bax protein was opposite. These results accord with those of foreign reports and indicate that GAS regulation and control of cell apoptosis and proliferation of large intestine cancer can induce over-expression of bcl-2 protein and down-regulate bax gene activity.

Somatostatin is distributed in human hypothalamus and other sites of the brain, peripheral nerve and gastrointestinal tract. In the digestive system, for example, somatostatin is secreted from somatostatin secreting cells (D cells). D cells are distributed mainly in intestinal nerve plexus, stomach and pancreas. Somatostatin acts as an inhibitory peptide of various secretory and proliferative responses. It has been found that its effects are mediated by a family of G-protein-coupled receptors (sst1-5)^[31-34]. The mechanisms of the inhibition are the combined interaction of somatostatin and its analogs with SST1-5R in tumor tissues, either inhibiting division and proliferation of tumor cells or the activities of growth factors such as vascular endothelial growth factor (VEGF), insulin-like growth factor (IGF), *etc.*^[35-37], thus counteracting tumorigenesis and tissue proliferation^[38]. Recent data have shown that somatostatin is not only able to restrain cell proliferation, but also to induce tumour cell apoptosis. However, the underlying mechanisms have not been elucidated. Sharma *et al.*^[39] reported that somatostatin analogs (SSa) octreotide (OCT) could elicit cytotoxic response in MCF-7 human breast cancer cells, leading to apoptosis which is associated with a rapid, time-dependent induction of wild-type

p53 and an increase of bax. Kang *et al*^[40] demonstrated that apoptosis by somatostatin might occur due to bax- and NO-independent p53 accumulation, and through Fas and caspase-8 activation pathways in peritoneal macrophages. Yuan *et al*^[41] found that somatostatin analogs (SSa) were able to induce the apoptosis of pancreatic acinar cells. The mechanisms of apoptosis are probably correlated with the expression of apoptosis-regulated gene bax, but have no relationship with the expression of p53. In a word, somatostatin and its analogues could induce cell apoptosis. In this study, we found that the higher the integral of SS was, the higher expression of bax protein, but the expression of bcl-2 protein was lower. Our data indicate that SS can promote cell apoptosis and restrain cell proliferation of large intestine carcinoma. The mechanism is through up-regulation of bax gene expression and inhibition of the activity of anti-apoptosis gene bcl-2.

In the present study, we found that the ratio of GAS to SS had an effect on biological characteristics such as malignant type, tissue differentiation and clinical stages of large intestine cancer. The ratio of GAS to SS was increased, which is of significance in large intestine cancer occurrence and development^[10]. Our results show that there is a positive correlation between the ratio of GAS to SS and the semi-quantitative integral of bcl-2 expression, and a negative correlation between GAS/SS and bax. Furthermore, the expression of GAS and SS proteins has a direct relation with the expression of bax and bcl-2.

In conclusion, abnormal expression of GAS and SS can lead to abnormal expression of bcl-2 and bax in large intestine carcinoma.

REFERENCES

- Zhang ZS, Zhang YL. To study evolvement of the large intestine cancer in china. *Shijie Huaren Xiaohua Zazhi* 2001; **9**: 489-494
- Greenlee RT, Murray T, Bolden S, Wingo PA. Cancer statistics, 2000. *CA Cancer J Clin* 2000; **50**: 7-33
- Greenlee RT, Hill-Harmon MB, Murray T, Thun M. *Cancer statistics, 2001*. *CA Cancer J Clin* 2001; **51**: 15-36
- Konturek PC, Bielanski W, Konturek SJ, Hartwich A, Pierzchalski P, Gonciarz M, Marlicz K, Starzynska T, Zuchowicz M, Darasz Z, Gotze JP, Rehfeld JF, Hahn EG. Progastrin and cyclooxygenase-2 in colorectal cancer. *Dig Dis Sci* 2002; **47**: 1984-1991
- Saga T, Tamaki N, Itoi K, Yamazaki T, Endo K, Watanabe G, Maruno H, Machinami R, Koizumi K, Ichikawa T, Takami H, Ishibashi M, Kubo A, Kusakabe K, Hirata Y, Murata Y, Miyachi Y, Tsubuku M, Sakahara H, Katada K, Tonami N, Yamamoto K, Konishi J, Imamura M, Doi R, Shimatsu A, Noguchi S, Hasegawa Y, Ishikawa O, Watanabe Y, Nakajo M. Phase III additional clinical study of 111In-pentetreotide (MP-1727): diagnosis of gastrointestinal hormone producing tumors based on the presence of somatostatin receptors. *Kaku Igaku* 2003; **40**: 185-203
- Sadji-Ouatas Z, Lasfer M, Julien S, Feldmann G, Reyl-Desmars F. Doxorubicin and octreotide induce a 40 kDa breakdown product of p53 in human hepatoma and tumoral colon cell lines. *Biochem J* 2002; **364**: 881-885
- Watson SA, Morris TM, McWilliams DF, Harris J, Evans S, Smith A, Clarke PA. Potential role of endocrine gastrin in the colonic adenoma carcinoma sequence. *Br J Cancer* 2002; **87**: 567-573
- Wu P, Tu JS, Riu J, Hang H, Hang WB, Yuan P. To study the correlation between expression of gastrin, somatostatin and cell proliferation, apoptosis in colorectal carcinoma. *Zhonghua Shiyuan Waikē Zaizhi* 2003; **20**: 947
- Fromowitz FB, Viola MV, Chao S, Oravez S, Mishriki Y, Finkel G, Grimson R, Lundy J. ras p21 expression in the progression of breast cancer. *Hum Pathol* 1987; **18**: 1268-1275
- Sereti E, Gavrili A, Agnantis N, Golematis VC, Voloudakis-Baltatzis IE. Immunoelectron study of somatostatin, gastrin and glucagon in human colorectal adenocarcinomas and liver metastases. *Anticancer Res* 2002; **22**: 2117-2123
- Larsson LI. Developmental biology of gastrin and somatostatin cells in the antropyloric mucosa of the stomach. *Microsc Res Tech* 2000; **48**: 272-281
- Portela-Gomes GM, Albuquerque JP, Ferra MA. Serotonin and gastrin cells in rat gastrointestinal tract after thyroparathyroidectomy and induced hyperthyroidism. *Dig Dis Sci* 2000; **45**: 730-735
- Glover SC, Tretiakova MS, Carroll RE, Benya RV. Increased frequency of gastrin-releasing peptide receptor gene mutations during colon-adenocarcinoma progression. *Mol Carcinog* 2003; **37**: 5-15
- Carroll RE, Matkowskyj K, Sauntharajah Y, Sekosan M, Battey JF, Benya RV. Contribution of gastrin-releasing peptide and its receptor to villus development in the murine and human gastrointestinal tract. *Mech Dev* 2002; **113**: 121-130
- Tejeda M, Gaal D, Barna K, Csuka O, Keri G. The antitumor activity of the somatostatin structural derivative (TT-232) on different human tumor xenografts. *Anticancer Res* 2003; **23**: 4061-4066
- Yu HG, Schrader H, Otte JM, Schmidt WE, Schmitz F. Rapid tyrosine phosphorylation of focal adhesion kinase, paxillin, and p130Cas by gastrin in human colon cancer cells. *Biochem Pharmacol* 2004; **67**: 135-146
- Wu H, Rao GN, Dai B, Singh P. Autocrine gastrins in colon cancer cells Up-regulate cytochrome c oxidase Vb and down-regulate efflux of cytochrome c and activation of caspase-3. *J Biol Chem* 2000; **275**: 32491-32498
- Heinke MY, Yao M, Chang D, Einstein R, dos Remedios CG. Apoptosis of ventricular and atrial myocytes from pacing-induced canine heart failure. *Cardiovasc Res* 2001; **49**: 127-134
- Kanzler S, Galle PR. Apoptosis and the liver. *Semin Cancer Biol* 2000; **10**: 173-184
- Park YN, Chae KJ, Kim YB, Park C, Theise N. Apoptosis and proliferation in hepatocarcinogenesis related to cirrhosis. *Cancer* 2001; **92**: 2733-2738
- Bold RJ, Virudachalam S, McConkey DJ. BCL2 expression correlates with metastatic potential in pancreatic cancer cell lines. *Cancer* 2001; **92**: 1122-1129
- Lowe SL, Rubinchik S, Honda T, McDonnell TJ, Dong JY, Norris JS. Prostate-specific expression of Bax delivered by an adenoviral vector induces apoptosis in LNCaP prostate cancer cells. *Gene Ther* 2001; **8**: 1363-1371
- Chan SL, Yu VC. Proteins of the bcl-2 family in apoptosis signalling: from mechanistic insights to therapeutic opportunities. *Clin Exp Pharmacol Physiol* 2004; **31**: 119-128
- Kim LH, Nadarajah VS, Peh SC, Poppema S. Expression of Bcl-2 family members and presence of Epstein-Barr virus in the regulation of cell growth and death in classical Hodgkin's lymphoma. *Histopathology* 2004; **44**: 257-267
- Jo EH, Hong HD, Ahn NC, Jung JW, Yang SR, Park JS, Kim SH, Lee YS, Kang KS. Modulations of the Bcl-2/Bax family were involved in the chemopreventive effects of licorice root (Glycyrrhiza uralensis Fisch) in MCF-7 human breast cancer cell. *J Agric Food Chem* 2004; **52**: 1715-1719
- Nakamura H, Kumei Y, Morita S, Shimokawa H, Ohya K, Shinomiya K. Antagonism between apoptotic (Bax/Bcl-2) and anti-apoptotic (IAP) signals in human osteoblastic cells under vector-averaged gravity condition. *Ann N Y Acad Sci* 2003; **1010**: 143-147
- Swatek J, Chibowski D. Endocrine cells in colorectal carcinomas. Immunohistochemical study. *Pol J Pathol* 2000; **51**: 127-136
- Wang HM, Cao XF, Huang SQ, Li YS, Yuan AH, Zhang QH, Zhang YL. Effect of external gastrin on apoptosis and expression of bcl-2 gene in gastric cancer cells. *Aizheng* 2002; **21**: 171-173
- Zhang FS, He ZP, Ma KS, Wang SG, Dong JH. Effects of gastrin on apoptotic pathways in human cholangiocarcinoma cell line QBC939. *Zhonghua Putong Waikē Zaizhi* 2002; **17**: 588-589
- Hartwich J, Konturek SJ, Pierzchalski P, Zuchowicz M, Konturek PC, Bielanski W, Marlicz K, Starzynska T, Lawniczak M. Molecular basis of colorectal cancer-role of gastrin and cyclooxygenase-2. *Med Sci Monit* 2001; **7**: 1171-1181
- Zatelli MC, Piccin D, Tagliati F, Ambrosio MR, Margutti A, Padovani R, Scanarini M, Culler MD, degli Uberti EC. Soma-

- tostatin receptor subtype 1 selective activation in human growth hormone (GH)- and prolactin (PRL)-secreting pituitary adenomas: effects on cell viability, GH, and PRL secretion. *J Clin Endocrinol Metab* 2003; **88**: 2797-2802
- 32 **Guillemet J**, Saint-Laurent N, Rochaix P, Cuvillier O, Levade T, Schally AV, Pradayrol L, Buscail L, Susini C, Bousquet C. Somatostatin receptor subtype 2 sensitizes human pancreatic cancer cells to death ligand-induced apoptosis. *Proc Natl Acad Sci USA* 2003; **100**: 155-160
- 33 **Faiss S**, Pape UF, Bohmig M, Dorffel Y, Mansmann U, Golder W, Riecken EO, Wiedenmann B. Prospective, randomized, multicenter trial on the antiproliferative effect of lanreotide, interferon alfa, and their combination for therapy of metastatic neuroendocrine gastroenteropancreatic tumors-the International Lanreotide and Interferon Alfa Study Group. *J Clin Oncol* 2003; **21**: 2689-2696
- 34 **Benali N**, Ferjoux G, Puente E, Buscail L, Susini C. Somatostatin receptors. *Digestion* 2000; **62** Suppl 1: 27-32
- 35 **Hortala M**, Ferjoux G, Estival A, Bertrand C, Schulz S, Pradayrol L, Susini C, Clemente F. Inhibitory role of the somatostatin receptor SST2 on the intracrine-regulated cell proliferation induced by the 210-amino acid fibroblast growth factor-2 isoform: implication of JAK2. *J Biol Chem* 2003; **278**: 20574-20581
- 36 **Buscail L**, Vernejoul F, Faure P, Torrisani J, Susini C. Regulation of cell proliferation by somatostatin. *Ann Endocrinol (Paris)* 2002; **63**: 2S13-2S18
- 37 **Puente E**, Saint-Laurent N, Torrisani J, Furet C, Schally AV, Vaysse N, Buscail L, Susini C. Transcriptional activation of mouse sst2 somatostatin receptor promoter by transforming growth factor-beta. Involvement of Smad4. *J Biol Chem* 2001; **276**: 13461-13468
- 38 **Ferjoux G**, Bousquet C, Cordelier P, Benali N, Lopez F, Rochaix P, Buscail L, Susini C. Signal transduction of somatostatin receptors negatively controlling cell proliferation. *J Physiol Paris* 2000; **94**: 205-210
- 39 **Sharma K**, Srikant CB. Induction of wild-type p53, Bax, and acidic endonuclease during somatostatin-signaled apoptosis in MCF-7 human breast cancer cells. *Int J Cancer* 1998; **76**: 259-266
- 40 **Kang BN**, Jeong KS, Park SJ, Kim SJ, Kim TH, Kim HJ, Ryu SY. Regulation of apoptosis by somatostatin and substance P in peritoneal macrophages. *Regul Pept* 2001; **101**: 43-49
- 41 **Yuan Y**, Gong Z, Lou K, Tu S, Di Z, Xu J. Effects and mechanisms of somatostatin analogs on apoptosis of pancreatic acinar cells in acute pancreatitis in mice. *J Gastroenterol Hepatol* 2001; **16**: 683-688

Edited by Wang XL and Zhu LH

Effect of mutated I κ B α transfection on multidrug resistance in hilar cholangiocarcinoma cell lines

Ru-Fu Chen, Zhi-Hua Li, Xian-He Kong, Ji-Sheng Chen

Ru-Fu Chen, Xian-He Kong, Ji-Sheng Chen, Department of Hepatobiliary Surgery, The Second Affiliated Hospital of Zhongshan University, Guangzhou 510120, Guangdong Province, China

Zhi-Hua Li, Department of Oncology, The Second Affiliated Hospital of Zhongshan University, Guangzhou 510120, Guangdong Province, China

Supported by China Postdoctoral Science Foundation, No. 2002031291

Correspondence to: Professor Ru-Fu Chen, PhD, Department of Hepatobiliary Surgery, The Second Affiliated Hospital of Zhongshan University, Guangzhou 510120, Guangdong Province, China. chenrf63@163.com

Telephone: +86-20-88333035

Received: 2004-05-31 **Accepted:** 2004-06-28

Abstract

AIM: To explore the expression effect of mutated I κ B α transfection on multidrug resistance gene (MDR-1) in hilar cholangiocarcinoma cells by inhibiting the activity of nuclear transcription factor- κ B (NF- κ B).

METHODS: We used the mutated I κ B α plasmid to transfect QBC939HCVC+ cells and QBC939 cells, and electrophoretic gel mobility shift assay (EMSA) to detect the binding activity of NF- κ B DNA and the effect of the transfecting mutated I κ B α plasmid on multidrug resistance gene (MDR-1) in hilar cholangiocarcinoma cells and its expression protein (P-GP).

RESULTS: Plasmid DNA was digested by restriction enzymes XbaI and Hind III, and its product after electrophoresis showed two bands with a big difference in molecular weight, with a size of 4.9 kb and 1.55 kb respectively, which indicated that the carrier was successfully constructed and digested with enzymes. The radioactivity accumulation of QBC939HCVC+ and QBC939 cells transfected with mutated I κ B α plasmid was significantly lower than that of the control group not transfected with mutated I κ B α plasmid. Double densitometer scanning showed that the relative signal density between the transfection group and non-transfection group was significantly different, which proved that the mutated I κ B α plasmid could inhibit the binding activity of NF- κ B DNA in hilar cholangiocarcinoma cells. Compared to control group not transfected with m I κ B α plasmid, the expression level of MDR-1 mRNA in the QBC939 and QBC939HCVC+ cells transfected with mutated I κ B α plasmid was lower. The expression intensity of P-GP protein in QBC939 and QBC939HCVC+ cells transfected with mutated I κ B α was significantly lower than that of the control group not transfected with mutated I κ B α plasmid.

CONCLUSION: The mutated I κ B α plasmid transfection can markedly reverse the multidrug resistance of hilar cholangiocarcinoma cells. Interruption of NF- κ B activity may become a new target in gene therapy for hilar cholangiocarcinoma.

Key words: Hilar cholangiocarcinoma; I κ B α ; NF- κ B; MDR-1 gene; Transfection

Chen RF, Li ZH, Kong XH, Chen JS. Effect of mutated I κ B α transfection on multidrug resistance in hilar cholangiocarcinoma cell lines. *World J Gastroenterol* 2005; 11(5): 726-728

<http://www.wjgnet.com/1007-9327/11/726.asp>

INTRODUCTION

With the discovery of the anti-apoptosis effects of nuclear transcription factor- κ B (NF- κ B) and the research on the activity inhibition of NF- κ B, especially the breakthrough progress in the study on the phosphorylation and degradation mechanism of the I κ B α of NF- κ B, a new way to diagnose and treat hilar cholangiocarcinoma has been explored by inhibiting the activity of NF- κ B through gene therapy^[1-3]. Mutated I κ B α means that the amino acid residues of I κ B α at the sites of 32 and 36 are substituted by alanines (S_{32,36}→A), which block the phosphorylation and degradation of I κ B α by IKKs, and exclusively bind to the activated NF- κ B and subsequently suppress the inappropriate or excessive activation of NF- κ B^[4-6]. In this paper, we used mutated I κ B α to block the activation pathway of NF- κ B to explore the effect of mutated I κ B α transfection on multidrug resistance (MDR-1) in hilar cholangiocarcinoma cell lines.

MATERIALS AND METHODS

Materials

QBC939 cells were provided by Professor Wang Shuguang of Southwest Hospital, Third Military Medical University. QBC939HCVC+ cells were prepared by us and stored in our laboratory. *E. coli* DH5 α was stored in our laboratory by general methods. Mutated I κ B α (S32, 36→A) plasmid was presented by Professor Baldwin of North Carolina State University. CLONfectin (Clontech), Trizol (promega), access RT-PCR system (Promega), RNAzol (TEST INC), sense and anti-sense primers of MDR-1 and β 2-M, were synthesized by Shanghai Sangon Bioengineering and Technology Service Co., Ltd.

Methods

Transformation, identification and maxi preps of mutated I κ B α plasmid We used mutated I κ B α plasmid to transform the calcified *E. coli* DH5 α , screen the positive clones, amplify and extract and purify the plasmid DNA. The plasmid was stored at -20 °C, for transfection use.

Cell culture and transfection QBC939 cells were incubated in DMEM supplemented with 10% fetal bovine serum (FBS), and mutated I κ B α plasmid was transfected to QBC939 and QBC939HCVC+ cell lines in log phase using the liposome-mediated method, and compared with the control group.

EMSA test QBC939 and QBC939HCVC+ cell lines transfected with mutated I κ B α plasmid were examined by electrophoretic gel mobility shift assay (EMSA). Extraction of nuclear protein was referred to the method of Ichikawa *et al*^[7]. The method of Coomassie brilliant blue G250 was used to determine the protein concentration of supernatant. EMSA test was performed

according to operation manual of Promega Company provided with the gel shift assay kit.

Detection of expression of MDR-1 gene in transfected cells with RT-PCR The single-step method of guanidine thiocyanate was used to extract the total RNA, which was then quantitated by an UV spectrophotometer and identified by agarose gel electrophoresis. Reverse transcription-PCR reaction was performed in a sensitive single-tube two-enzyme system, (Promega Company). The reaction volume of 50 μ L contained 20 μ L special RNAase free water, 10 μ L AMV/Inf 5, 1 μ L dNTP mixture (2.5 mmol/L), 10 μ L sense/anti-sense primer mixture, 2 μ L MgSO₄ (25 mmol/L), 1 μ L AMV reverse transcriptase (5 u/ μ L), 1 mL Tfi DNA polymerase (5u/ μ L), 3 μ g RNA sample, MDR-1 sense primer (5'-GTACCCATCATTGCAQATAGC), anti-sense primer (5'-CAAACCTTCTGCTCCTGAGTC-3'). PCR reaction conditions were at 94 $^{\circ}$ C for 40 s, at 56 $^{\circ}$ C for 45 s; at 72 $^{\circ}$ C for 1min for 30 cycles. PCR products were identified by 2% agarose gel electrophoresis, and stained with ethidium bromide (EB). Electrophoresis bands of DNA were analyzed with a gel scanner for determining the photon intensity. The ratio of MDR-1 to β -2-M was regarded as the reference data of expression levels to determine the relative quantity of MDR-1 to PCR products.

Immunohistochemistry determination of the expression of P-GP protein in transfected cells The general immunohistochemistry adopted labeled-streptavidin biotin system (LSAB), and the positive and negative control groups were set up. When over 5% cytoplasm or cell membrane showed brown-yellow in color, the staining was regarded as the positive P-GP.

RESULTS

Identification of mutated I κ B α plasmid

Plasmid DNA was digested by restriction enzymes XbaI and HandIII, and its product after electrophoresis showed two bands with a big difference in molecular weight (Figure 1), with a size of 4.9 kb and 1.55 kb respectively, which indicated the carrier was successfully constructed and digested with enzymes.

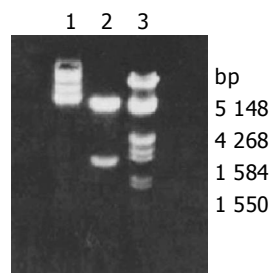


Figure 1 Macrorestriction map of mutated I κ B α Plasmid. Lane 1: Plasmid DNA; lane 2: Plasmid DNA cut by XbaI and HandIII; lane 3: DNA marker.

Inhibition of mutated I κ B α plasmid transfection on NF- κ B DNA binding activity

The radioactivity accumulation of QBC₉₃₉HCVC+ and QBC939 cells transfected with mutated I κ B α plasmid was significantly lower than that of the control group not transfected with mutated I κ B α plasmid. Double densimeter scanning showed that the relative signal density between the transfection group and non-transfection group was significantly different, which proved that the mutated I κ B α plasmid had the function of inhibiting the binding activity of NF- κ B DNA in hilar cholangiocarcinoma cells.

In order to examine the specificity of EMSA technology, this experiment set up a negative control and a competitive reaction control. The reaction solution of the negative control without addition of the labeled probe showed no band after electrophoresis (Band 3 in Figure 2). The reaction solution of

the competitive reaction control after adding the 30 \times non-labeled probe showed no avidity band of NF- κ B after electrophoresis (Band 1 in Figure 1). The experiment indicated that the non-labeled probes bound to NF- κ B competitively, causing the labeled probes to decrease remarkably or almost completely. These two experiments proved that the activity detection of NF- κ B in this research had a specificity.

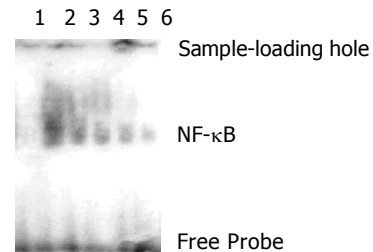


Figure 2 EMSA of QBC₉₃₉ and QBC₉₃₉HCVC+ cells transfected with mutated I κ B α plasmid. Lane 1: Control group; lane 2: QBC₉₃₉HCVC+ cells without transfected with mutated I κ B α ; lane 3: QBC939 cells not transfected with mutated I κ B α ; lanes 4 and 5: QBC₉₃₉HCVC+ cells transfected with mutated I κ B α ; lane 6: QBC939 cells transfected with mutated I κ B α .

Effect of mutated I κ B α plasmid transfection on the expression of MDR-1 and P-GP in hilar cholangiocarcinoma cells

Compared with control group, the expression level of MDR-1 mRNA in QBC939 and QBC939HCVC+ cells transfected with mutated I κ B α plasmid was lower (Figure 3). The expression intensity of P-GP protein in QBC939 and QBC939HCVC+ cells transfected with mutated I κ B α was significantly lower than that in the control group not transfected with mutated I κ B α plasmid (Figures 4A, B).

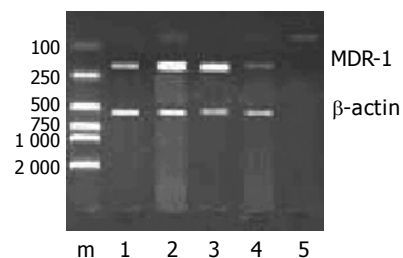


Figure 3 Expression of MDR-1 mRNA in the QBC939 cells transfected with mutated I κ B α . M: DNA marker. Lane 1: The QBC₉₃₉HCVC+ cells transfected with mutated I κ B α , lane 2: The QBC₉₃₉HCVC+ cells not transfected with mutated I κ B α ; lane 3: The QBC₉₃₉ cells not transfected with mutated I κ B α ; lane 4: The QBC₉₃₉ cells transfected with mutated I κ B α .

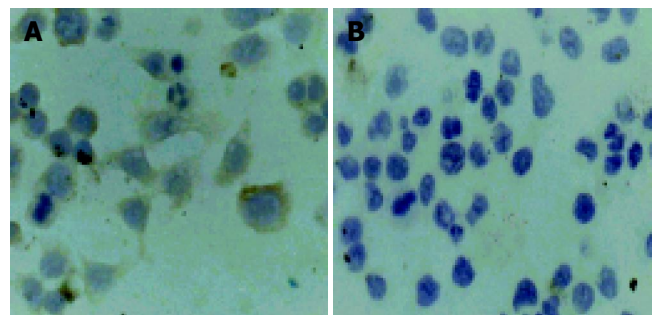


Figure 4 Expression intensity of P-GP protein in QBC939 and QBC939HCVC+ cells transfected with mutated I κ B α . A: Expression of P-GP in the non-transfection Group, LSAB \times 400; B: Expression of P-GP after transfection of mutated I κ B α , LSAB \times 400.

DISCUSSION

I κ B α with a molecular weight of 37KD can be divided into three parts. N-terminal domain can be phosphorylated under signal stimulation and is the basic construction to regulate and control the activity of NF- κ B. In the core of N-terminal domain, there is a repeat sequence comprised of 5 anchored proteins, which are the binding sites of NF- κ B. The C-terminal domain is composed of Pro-Glu-Ser-Thr sequence, which involves in the basic conversion of proteins^[8,9].

In 1995 and 1996, the studies on the mechanism of I κ B α phosphorylation and degeneration made a breakthrough progress, showing that Ser32 and Ser36 play a vital role in the I κ B α phosphorylation and the activation of NF- κ B. Ser32 and Ser36 after mutation are not phosphorylated and degenerated, so that they combine firmly with NF- κ B to stop NF- κ B from entering into the cell nuclei for nuclear transcription^[10]. Therefore, some researchers constructed I κ B α with site mutations at Ser32 and Ser36, which could be used as the super inhibitors. Compared with the I κ B α of wild type, the Ser32 and Ser36 the I κ B α of mutated type are replaced by alanines, the mutated I κ B α is out of the control of I κ B α , continually producing mutated I κ B α , and combines with NF- κ B to form a trimer, reducing the activation level of NF- κ B, which provides a perfect tool for studying the regulation and control of NF- κ B.

The expression of multidrug resistance (MDR) gene in tumor cells is the most crucial obstacle for successful chemical therapy. Once cancer cells express the multidrug resistance gene, drugs with different structures used for chemical therapy would produce drug resistance. MDR-1 is a kind of transmembrane protein P-GP (P-glycoprotein) with a molecular weight of 170kD^[11]. P-GP spreads in tissues. It has been reported that 60% tissues of hilar cholangiocarcinoma could express MDR-1. There are NF- κ B binding sites in the promoter sequence of MDR-1 gene, MDR-1 is under the regulation and control of NF- κ B, which could activate the expression of MDR gene. Therefore, it could be supposed that inhibition of NF- κ B activity may increase the accumulation of poisonous drugs between cells to improve the therapeutic effect.

We have proved that the super activation state of NF- κ B exists in tissues and cells of hilar cholangiocarcinoma. There is evidence that the function of numerous chemical therapeutic drugs for tumor cells is achieved by promoting apoptosis. However, the drugs for chemical therapy can at the same time activate NF- κ B in tumor cells, and activated NF- κ B can motivate the expression of various anti-apoptosis genes, and reduce the

effect of chemical therapeutic drugs. Consequently, people presume that inhibition of NF- κ B can act as an enhancer of chemical therapeutic drugs. Mutated I κ B α plasmid, a inhibitor of NF- κ B, can markedly reduce the expression of MDR-1. The expression of MDR-1 after transfected with mutated I κ B α plasmid is significantly decreased.

REFERENCES

- 1 **Stroh C**, Held J, Samraj AK, Schulze-Osthoff K. Specific inhibition of transcription factor NF-kappaB through intracellular protein delivery of I kappaBalpha by the Herpes virus protein VP22. *Oncogene* 2003; **22**: 5367-5373
- 2 **Mi J**, Li ZY, Ni S, Steinwaerder D, Lieber A. Induced apoptosis supports spread of adenovirus vectors in tumors. *Hum Gene Ther* 2001; **12**: 1343-1352
- 3 **Ross JS**, Kallakury BV, Sheehan CE, Fisher HA, Kaufman RP, Kaur P, Gray K, Stringer B. Expression of nuclear factor-kappa B and I kappa B alpha proteins in prostatic adenocarcinomas: correlation of nuclear factor-kappa B immunoreactivity with disease recurrence. *Clin Cancer Res* 2004; **10**: 2466-2472
- 4 **Fujioka S**, Sclabas GM, Schmidt C, Niu J, Frederick WA, Dong QG, Abbruzzese JL, Evans DB, Baker C, Chiao PJ. Inhibition of constitutive NF-kappa B activity by I kappa B alpha M suppresses tumorigenesis. *Oncogene* 2003; **22**: 1365-1370
- 5 **Xiong HQ**, Abbruzzese JL, Lin E, Wang L, Zheng L, Xie K. NF-kappaB activity blockade impairs the angiogenic potential of human pancreatic cancer cells. *Int J Cancer* 2004; **108**: 181-188
- 6 **Wang JH**, Huang QK, Chen MX. Nuclear factor kappa B activity and cell viability of SMMC-7721 inhibited by mutated inhibitor kappa B alpha. *Zhonghua Ganzangbing Zazhi* 2003; **11**: 222-224
- 7 **Ichikawa K**, DeGroot LJ, Refetoff S, Horwitz AL, Pollak ER. Nuclear thyroid hormone receptors in cultured human fibroblasts: improved method of isolation, partial characterization, and interaction with chromatin. *Metabolism* 1986; **35**: 861-868
- 8 **Gilmore T**, Gapuzan ME, Kalaitzidis D, Starczynowski D. Rel/NF-kappa B/I kappa B signal transduction in the generation and treatment of human cancer. *Cancer Lett* 2002; **181**: 1-9
- 9 **Chen Y**, Vallee S, Wu J, Vu D, Sondek J, Ghosh G. Inhibition of NF-kappaB activity by IkappaBbeta in association with kappaB-Ras. *Mol Cell Biol* 2004; **24**: 3048-3056
- 10 **Kabouridis PS**, Hasan M, Newson J, Gilroy DW, Lawrence T. Inhibition of NF-kappa B activity by a membrane-transducing mutant of I kappa B alpha. *J Immunol* 2002; **169**: 2587-2593
- 11 **Tian WH**, Feng HL, Gao JS, Jiang WQ. Expression and clinical significance of mdr-1 gene in lymphoma. *Aizheng* 2002; **21**: 910-913

Assistant Editor Guo SY Edited by Wang XL

Treatment of pancreatic pseudocysts in line with D'Egidio's classification

Ai-Bin Zhang, Shu-Sen Zheng

Ai-Bin Zhang, Shu-Sen Zheng, Department of Hepatobiliary Surgery, First Hospital College of Medicine, Zhejiang University, Hangzhou 310003, Zhejiang Province, China

Correspondence to: Ai-Bin Zhang, Department of Hepatobiliary Pancreatic Surgery, First Hospital, College of Medicine, Zhejiang University, Hangzhou 310003, Zhejiang Province, China. cheung163@163.com

Telephone: +86-571-87236570 **Fax:** +86-571-87236570

Received: 2004-04-24 **Accepted:** 2004-04-29

Abstract

AIM: To explore the implications of underlying diseases in treatment of pancreatic pseudocysts (PPC).

METHODS: Clinical data of 73 cases of pancreatic pseudocyst treated in a 12-year period were reviewed comprehensively. Pancreatic pseudocysts were classified according to the etiological criteria proposed by D'Egidio. The correlation between the etiological classification, measure of treatment and clinical outcome of the patients was analyzed.

RESULTS: According to the etiological criteria proposed by D'Egidio, 73 patients were divided into three groups. Group I was comprised of 37 patients with type I pseudocyst, percutaneous drainage was successful in the majority (9/11, 82%) while external or internal drainage was not satisfactory with a low success rate (8/16, 50%). Group II was comprised of 24 patients with type II pseudocyst, and internal drainage was curative for most of the cases (11/12, 92%), but the success rate of percutaneous or external drainage was unacceptably low (4/9, 44%). Group III consisted of 12 patients with type III pseudocyst. Internal drainage or pancreatic resection performed in 10 of these patients produced a curative rate of 80% (8/10) with the correction of the ductal pathology as a prerequisite.

CONCLUSION: The classification of pancreatic pseudocyst based on its underlying diseases is meaningful for its management. Awareness of the underlying diseases of pancreatic pseudocyst and detection of the ductal pathology in type II and III pancreatic pseudocysts with endoscopic retrograde cholangiopancreatography may help make better decisions of treatment to reduce the rate of complications and recurrence.

© 2005 The WJG Press and Elsevier Inc. All rights reserved.

Key words: Pancreatic pseudocysts; D'Egidio's classification

Zhang AB, Zheng SS. Treatment of pancreatic pseudocysts in line with D'Egidio's classification. *World J Gastroenterol* 2005; 11(5): 729-732

<http://www.wjgnet.com/1007-9327/11/729.asp>

INTRODUCTION

Pancreatic pseudocyst is the most common complication of acute or chronic pancreatitis^[1]. In an attempt to help decide the timing and choice of surgical intervention, several classifications have been proposed. According to the Atlanta classification^[2], an acute pseudocyst is a collection of pancreatic juice enclosed by a wall of fibrous or granulation tissue, arising as a consequence of acute pancreatitis or pancreatic trauma, whereas a chronic pseudocyst is a collection of pancreatic juice enclosed by a wall of fibrous or granulation tissue, arising as a consequence of chronic pancreatitis and lacking of an antecedent episode of acute pancreatitis. But in clinic, some pseudocysts are usually associated with chronic pancreatitis and may develop after an episode of acute pancreatitis. There is also a classification based entirely on pancreatic duct anatomy proposed by Nealon *et al*^[3]. This system defines the categories of ductal abnormalities seen in patients with pseudocyst and relates the authors' experience with different types of treatment. The classification of pseudocysts proposed by D'Egidio *et al*^[4] takes into account all the aspects mentioned above. They identified three distinct types of pseudocysts: Type I or acute "post-necrotic" pseudocysts that occur after an episode of acute pancreatitis and are associated with normal duct anatomy and rarely communicate with the pancreatic duct, Type II, or post-necrotic pseudocysts which occur after an episode of acute or chronic pancreatitis (the pancreatic duct is diseased but not strictured, and there is often a duct-pseudocyst communication) and Type III, defined as "retention" pseudocysts, which occur in chronic pancreatitis and are uniformly associated with duct stricture and pseudocyst-duct communication.

Based on a review of the literature and 12-year clinical experiences with 73 patients with pancreatic pseudocyst, we analyzed the correlation between the underlying diseases of pancreatic pseudocyst, methods of treatment and the clinical outcome of the patients.

MATERIALS AND METHODS

Clinical data

This study included 43 male and 30 female patients with pancreatic pseudocyst, whose age ranged from 16 to 78 years with an average age of 39 years. All patients were confirmed to have fibrous encapsulation on ultrasonography, computed tomography (CT) or at operation. Patients with acute peripancreatic fluid collection or without evidence of encapsulation were excluded^[2-5]. According to their underlying diseases, the patients were divided into 3 groups on the basis of etiologic criteria for classification proposed by D'Egidio^[4]. Group I consisted of 37 patients with D'Egidio type I pseudocyst, which occurred following an episode of acute pancreatitis in all cases. Patients were categorized as having acute pancreatitis on the clinical basis in conform to Atlanta criteria^[2]. These patients having a clinical diagnosis of acute pancreatitis lacked of any of the findings typically seen in chronic pancreatitis. Endoscopic retrograde cholangiopancreatography (ERCP) or sinography was performed in 12 of these 37 patients, and no pancreatic

duct stricture was identified, only one patient was found to have cyst-duct communication. Group II was comprised of 24 patients with D'Egidio type II pancreatic pseudocyst, 12 of them had definable acute pancreatitis and 19 had various chronic pancreatitis. The diagnosis of chronic pancreatitis was established clinically^[6,7]. Fifteen of these patients received ERCP or sinography, and were confirmed to have chronic pathological changes in the pancreatic duct. Confirmatory imaging of ERCP or sinogram in this group displayed a tortuously or irregularly dilated main pancreatic duct, calcification of pancreas, and no duct stricture. Seven of them were found to have cyst-ductal communication. Group III included 12 patients with chronic pancreatitis, and 8 of them received ERCP or sinography for confirmation of the diagnosis. The evidence for a diagnosis of chronic pancreatitis included structural abnormalities in the pancreas identifiable on the images, and a main pancreatic duct stricture and ductal irregularity, areas of dilation and narrowing (the sign of "chain of lakes").

Table 1 Size of pseudocyst and anatomy of the pancreatic duct of patients

Group	Number of Patients (n)	Average size of cyst (cm)	Duct stricture ¹	Cyst-duct communication ¹
I	37	7.2 (2-23)	0/12	1/12
II	24	4.4 (2-12)	0/15	7/15
III	12	10.5 (5-25)	8/8	7/8

¹ The number before the slash indicates the number of cases receiving ERCP or sonogram, and that after the slash is the positive cases identified.

Treatment

Patients were considered to be candidates for intervention (surgical or radiological) when they were diagnosed as having a pseudocyst 5 cm or greater in diameter with no sign of spontaneous resolution over a period of evaluation varying in length based on specific clinical criteria. Sixty patients were subjected to percutaneous catheter drainage or surgical therapy. The other patients were treated conservatively for relieving their symptoms. The decision to employ percutaneous or surgical drainage was made on the basis of the circumstances. Percutaneous drainage was applied to the patients whose pseudocysts arose as a consequence of acute pancreatitis and were superficial so that there was a suitable route for catheterization. All pseudocysts treated with percutaneous drainage were confirmed with low-density content in CT scan. Some patients were treated with percutaneous drainage because of an unacceptably high risk for surgical intervention. The other patients were treated surgically. The treatment approaches are listed in Table 2.

Table 2 Treatment approaches for pancreatic pseudocysts

Group	Methods of treatment (n)			
	Percutaneous drainage	External drainage	Internal drainage	Distal pancreatectomy
I	11	10	6	0
II	5	4	10	2
III	0	2	5	5

Following-up

After surgical or percutaneous management, patients were followed up regularly by ultrasound for 6 mo to 12 years with an average of 73 mo. Where feasible, follow-up CT scans were

performed to assess recurrence of pseudocyst. All patients were evaluated for complications and recurrence. For percutaneous management, patients who needed to cross over to surgical management were also evaluated.

RESULTS

The incidence of complications in this patient cohort as a whole was 22% (13/60), with a recurrence rate of 12% (7/60) and a mortality rate of 1% (1/73).

Group I

Twenty-seven of the 37 patients I received surgical interventions. Eleven patients were treated by percutaneous drainage for 4 to 24 d with an average of 11 d, and 2 of them experienced episodes of infections that were subsequently cured. Ten patients underwent surgical external drainage, and 2 of them developed pancreatic fistulae and another two had hemorrhage. All the 4 patients were cured by conservative treatment. Pseudocyst recurred in 2 of the remaining 6 patients who received surgical external drainage and were cured after cyst-jejunostomy. Six patients underwent surgical internal drainage, one of them experienced gastric hemorrhage that was cured by conservative treatment, and another developed fatal infections.

Group II

Twenty-one patients were subjected to drainage or surgery, including two patients who were treated surgically after failure of conservative treatment. Five patients underwent percutaneous drainage, one of them developed pancreatic fistulae and was cured by conservative management, and two of them had recourse to surgery, during which cyst-jejunostomy was performed, after 30-d drainage when a cyst-duct communication was identified on the sinogram. Four patients underwent surgical external drainage, and one of them developed a pancreatic fistula that was cured eventually by conservative management, with another having recurrence cured by cyst-jejunostomy. Ten patients underwent surgical internal drainage, and only one of them had recurrence and received cyst-jejunostomy for the cure. The remaining two patients were cured with distal pancreatectomy plus cystectomy.

Table 3 Rate of recurrence of pseudocyst and complications after treatment in 3 groups

Group	Methods of treatment			
	Percutaneous drainage	External drainage	Internal drainage	Distal pancreatectomy
I	2, 0	4, 2	2, 0	-, -
II	3, 0	1, 1	0, 1	0, 0
III	-, -	1, 1	0, 1	0, 1

In each pair of numbers listed in the table, the former indicates the number of patients who had complications, and the latter is the number of patients who had recurrence.

Group III

Twelve patients were subjected to drainage or surgery. Two patients had surgical external drainage and pancreatic fistula occurred in one case to require cyst-jejunostomy and the other had recurrence to necessitate distal pancreatectomy. Five patients received surgical internal drainage, and one of them had pseudocyst recurrence and was cured by pancreatic resection. The remaining 5 patients had distal pancreatectomy plus cystectomy, one of them had recurrence probably attributable to pancreatic fistula and was cured by reoperation for pancreatic resection.

The complications and recurrence in this whole patient cohort are summarized in Table 3.

DISCUSSION

A better definition of pseudocyst that clearly separates it from acute fluid collection, improvements in imaging modalities, and a better understanding of the natural course of pseudocysts have changed the concepts regarding their management. The old teaching that the presence of cysts of more than 6 cm in diameter for 6 wk should be drained is no longer true^[8]. The outcome of pseudocysts, which either spontaneously resolve or require operation, and the rate of complications and recurrence, are similar regardless of the size (be it less than 6 cm in diameter or larger) and the course of disease^[9-12], for the etiology of pancreatitis is a more important determinant of the outcome rather than the size of pseudocyst or course of disease. The indications for drainage are now the presence of symptoms, enlargement of cysts, and complications (infection, hemorrhage, rupture, and obstruction)^[8-13]. From our experience, D'Egidio type I pseudocyst has a greater chance of spontaneous resolution than the other types because of the normal anatomy of pancreatic duct retained in the former. As for D'Egidio types II and III pseudocysts, more active treatment measures should be taken for a smaller chance of spontaneous resolution due to the pathological changes in the pancreatic duct.

The therapeutic approaches currently available for pancreatic pseudocysts include percutaneous drainage, transendoscopic approach, and surgery. The choice of treatment depends on a number of factors, including the size, number, and location of the cysts, presence of communication of the cyst with the pancreatic duct, and presence of infections^[8-15]. Although progress has been made with alternative methods such as endoscopic drainage through the contiguous intestine, through the transpapillary route, or using endoscopic ultrasound, a higher complication and recurrence rate was reported in some documents^[16,17]. All patients in this cohort were treated with percutaneous and surgical approach. The present study also assessed the implications of the underlying diseases as well as pancreatic ductal anatomy in the choice of treatment for pancreatic pseudocysts.

D'Egidio type I pseudocysts occur after an episode of acute pancreatitis, characterized by a shorter disease course and a greater diameter of the pseudocyst, and the patients often have noticeable symptoms^[18], which requires intervention with drainage as soon as possible^[19,20]. External drainage is effective for the pseudocysts without cyst-duct communication. We performed percutaneous drainage with catheter insertion under ultrasound guidance in 11 case of type I pseudocysts. A pigtail catheter greater than 8F gauge in size was left *in situ* until the drainage was completed, which was defined as the total volume of drainage less than 10 mL in 24 h. A sinogram was then taken through the catheter before its removal to exclude a persistent communication with the pancreatic duct. In four cases, the total volume of drainage in 24 h exceeded 1 000 mL, and we treated these patients with octreotide. The drainage was reduced after treatment. Simultaneously, we performed surgical external or internal drainage in 16 cases of type I pseudocyst, with a higher rate of complications or recurrence. We therefore suggest that percutaneous drainage should be performed primarily for D'Egidio type I pancreatic pseudocysts.

D'Egidio type II pseudocysts often occur after an episode of acute pancreatitis associated with chronic pancreatitis. Cyst-duct communication has been identified in about 40% of patients with this type of pseudocysts. The communication between the cyst and pancreatic duct results in a persistent pancreatic fistula. In some cases, the fistula can heal spontaneously after

external drainage^[21]. But a considerable amount of pancreatic juice is lost in long-term of drainage, which leads to electrolyte and acid-base imbalance. In this cohort, percutaneous or surgical external drainage performed in 9 patients with type II pseudocysts resulted in pancreatic fistulae in 4 patients and recurrence in 1 patient. Another 12 patients with type II pseudocysts had surgical internal drainage or resection, and only one patient had recurrence, showing a lower rate of complications or recurrence in comparison with the patients receiving external drainage. Hence we suggest that patients with D'Egidio type II pseudocysts with a cyst-duct communication should be managed by surgical internal drainage or pancreatic resection in order to decrease the rate of complications or recurrence^[22,23]. ERCP and other radiological imaging modalities should be used to better understand the anatomy of the pancreatic duct before treatment.

D'Egidio type III pseudocyst is thought to occur in chronic pancreatitis. Long-term infection of the pancreas results in stricture and even obstruction of the pancreatic duct, leading to rupture of the distal pancreatic duct, extravasation of the pancreatic juice, and subsequently pseudocyst formation. The chance for spontaneous healing of the cyst-duct communication is lower than that of other types of pseudocysts due to the fibrosis of pancreatic tissue as a result of infection^[24,25]. Percutaneous drainage is therefore contraindicated^[5,26-28] and surgical external drainage would also fail^[3,13] because of the abnormal anatomy of pancreatic duct. We performed percutaneous drainage in two patients but neither of them was successful, and ten patients had surgical internal drainage or resection. All these patients were cured except for two who had recurrence but eventually cured by surgical correction of the pathological ductal anatomy. Judging from the results of this present study, it seems that simple drainage or cystectomy could lead to an unacceptably high rate of complications and recurrence^[29-31]. We suggest that surgical maneuvers for this type of pseudocysts should address the specific ductal pathology in addition to complete drainage. Pancreatic resection or cyst-enterostomy plus ductal drainage should be more suitable for this type of pseudocysts.

In conclusion, the choice of treatment of pancreatic pseudocysts depends on a number of factors, including the size, number, and location of cysts, presence of complications, to name a few. But the etiology of pancreatitis is a more important determinant of the choice. The procedure of management should be individualized on the basis of a comprehensive evaluation of these factors. Percutaneous drainage is safe and effective for D'Egidio type I pseudocysts, while appropriate treatment for type II pseudocysts, should be chosen according to the pancreatic anatomy. Surgical internal drainage is adequate for patients with cyst-duct communication. In type III pancreatic pseudocysts, serious pathological changes are often present in the duct and surgical internal drainage or pancreatic resection is needed to address the ductal pathology.

REFERENCES

- 1 Naoum E, Zavos A, Goudis K, Sarros C, Pitsargiotis E, Karamouti M, Tsikrikis P, Karantanis A. Pancreatic pseudocysts: 10 years of experience. *J Hepatobiliary Pancreat Surg* 2003; **10**: 373-376
- 2 Bradley EL. A clinically based classification system for acute pancreatitis. Summary of the International Symposium on Acute Pancreatitis, Atlanta, Ga, September 11 through 13, 1992. *Arch Surg* 1993; **128**: 586-590
- 3 Nealon WH, Walser E. Main pancreatic ductal anatomy can direct choice of modality for treating pancreatic pseudocysts (surgery versus percutaneous drainage). *Ann Surg* 2002; **235**: 751-758
- 4 D'Egidio A, Schein M. Pancreatic pseudocysts: a proposed

- classification and its management implications. *Br J Surg* 1991; **78**: 981-984
- 5 **Neff R**. Pancreatic pseudocysts and fluid collections: percutaneous approaches. *Surg Clin North Am* 2001; **81**: 399-403, xii
- 6 **Apte MV**, Keogh GW, Wilson JS. Chronic pancreatitis: complications and management. *J Clin Gastroenterol* 1999; **29**: 225-240
- 7 **Nealon WH**, Thompson JC. Progressive loss of pancreatic function in chronic pancreatitis is delayed by main pancreatic duct decompression. A longitudinal prospective analysis of the modified puestow procedure. *Ann Surg* 1993; **217**: 458-466; discussion 466-468
- 8 **Cooperman AM**. An overview of pancreatic pseudocysts: the emperor's new clothes revisited. *Surg Clin North Am* 2001; **81**: 391-397, xii
- 9 **Soliani P**, Ziegler S, Franzini C, Dell'Abate P, Del Rio P, Di Mario F, Cavestro M, Sianesi M. The size of pancreatic pseudocyst does not influence the outcome of invasive treatments. *Dig Liver Dis* 2004; **36**: 135-140
- 10 **Pitchumoni CS**, Agarwal N. Pancreatic pseudocysts. When and how should drainage be performed? *Gastroenterol Clin North Am* 1999; **28**: 615-639
- 11 **Cheruvu CV**, Clarke MG, Prentice M, Eyre-Brook IA. Conservative treatment as an option in the management of pancreatic pseudocyst. *Ann R Coll Surg Engl* 2003; **85**: 313-316
- 12 **Vitas GJ**, Sarr MG. Selected management of pancreatic pseudocysts: operative versus expectant management. *Surgery* 1992; **111**: 123-130
- 13 **Cooperman AM**. Surgical treatment of pancreatic pseudocysts. *Surg Clin North Am* 2001; **81**: 411-419, xii
- 14 **Andren-Sandberg A**, Dervenis C. Pancreatic pseudocysts in the 21st century. Part II: natural history. *JOP* 2004; **5**: 64-70
- 15 **Ahearne PM**, Baillie JM, Cotton PB, Baker ME, Meyers WC, Pappas TN. An endoscopic retrograde cholangiopancreatography (ERCP)-based algorithm for the management of pancreatic pseudocysts. *Am J Surg* 1992; **163**: 111-115; discussion 115-116
- 16 **Lehman GA**. Pseudocysts. *Gastrointest Endosc* 1999; **49**: S81-S84
- 17 **Chak A**. Endosonographic-guided therapy of pancreatic pseudocysts. *Gastrointest Endosc* 2000; **52**: S23-S27
- 18 **Baron TH**, Morgan DE. The diagnosis and management of fluid collections associated with pancreatitis. *Am J Med* 1997; **102**: 555-563
- 19 **Behrman SW**, Melvin WS, Ellison EC. Pancreatic pseudocysts following acute pancreatitis. *Am J Surg* 1996; **172**: 228-231
- 20 **Lillemoe KD**, Yeo CJ. Management of complications of pancreatitis. *Curr Probl Surg* 1998; **35**: 1-98
- 21 **Wilson C**. Management of the later complications of severe acute pancreatitis-pseudocyst, abscess and fistula. *Eur J Gastroenterol Hepatol* 1997; **9**: 117-121
- 22 **Yemos K**, Laopodis B, Yemos J, Scouras K, Rissoti L, Lainas A, Patsalos C, Tzardis P, Tierris E. Surgical management of pancreatic pseudocyst. *Minerva Chir* 1999; **54**: 395-402
- 23 **Lillemoe KD**, Kaushal S, Cameron JL, Sohn TA, Pitt HA, Yeo CJ. Distal pancreatectomy: indications and outcomes in 235 patients. *Ann Surg* 1999; **229**: 693-698; discussion 698-700
- 24 **Rosso E**, Alexakis N, Ghaneh P, Lombard M, Smart HL, Evans J, Neoptolemos JP. Pancreatic pseudocyst in chronic pancreatitis: endoscopic and surgical treatment. *Dig Surg* 2003; **20**: 397-406
- 25 **Usatoff V**, Brancatisano R, Williamson RC. Operative treatment of pseudocysts in patients with chronic pancreatitis. *Br J Surg* 2000; **87**: 1494-1499
- 26 **Adams DB**, Srinivasan A. Failure of percutaneous catheter drainage of pancreatic pseudocyst. *Am Surg* 2000; **66**: 256-261
- 27 **Heider R**, Meyer AA, Galanko JA, Behrns KE. Percutaneous drainage of pancreatic pseudocysts is associated with a higher failure rate than surgical treatment in unselected patients. *Ann Surg* 1999; **229**: 781-787; discussion 787-789
- 28 **Barthet M**, Bugallo M, Moreira LS, Bastid C, Sastre B, Sahel J. Management of cysts and pseudocysts complicating chronic pancreatitis. A retrospective study of 143 patients. *Gastroenterol Clin Biol* 1993; **17**: 270-276
- 29 **Nealon WH**, Walser E. Duct drainage alone is sufficient in the operative management of pancreatic pseudocyst in patients with chronic pancreatitis. *Ann Surg* 2003; **237**: 614-620; discussion 620-622
- 30 **Grace PA**, Williamson RC. Modern management of pancreatic pseudocysts. *Br J Surg* 1993; **80**: 573-581
- 31 **Adams DB**, Anderson MC. Percutaneous catheter drainage compared with internal drainage in the management of pancreatic pseudocyst. *Ann Surg* 1992; **6**: 571-576; discussion 576-578

Assistant Editor Guo SY Edited by Chen WW and Wang XL

Effect of glutamate on inflammatory responses of intestine and brain after focal cerebral ischemia

Lei Xu, Jie Sun, Ran Lu, Qing Ji, Jian-Guo Xu

Lei Xu, Jie Sun, Ran Lu, Qing Ji, Jian-Guo Xu, Department of Anesthesiology, Jinling Hospital, Medical School of Nanjing University, Nanjing 210002, Jiangsu Province, China

Correspondence to: Professor Jian-Guo Xu, Department of Anesthesiology, Jinling Hospital, 305 East Zhongshan Road, Nanjing 210002, Jiangsu Province, China. xulei99md@yahoo.com

Telephone: +86-25-80860149 **Fax:** +86-25-84806839

Received: 2004-04-10 **Accepted:** 2004-05-13

Abstract

AIM: To study the modulation of glutamate on post-ischemic intestinal and cerebral inflammatory responses in a ischemic and excitotoxic rat model.

METHODS: Adult male rats were subjected to bilateral carotid artery occlusion for 15 min and injection of monosodium glutamate intraperitoneally, to decapitate them at selected time points. Tumor necrosis factor alpha (TNF- α) level and nuclear factor kappa B (NF- κ B) activity were determined by enzyme-linked immunosorbant assay (ELISA) and electrophoretic mobility shift assay (EMSA), respectively. Hemodynamic parameters were monitored continuously during the whole process of cerebral ischemia and reperfusion.

RESULTS: Monosodium glutamate (MSG) treated rats displayed statistically significant high levels of TNF- α in cerebral and intestinal tissues within the first 6 h of ischemia. The rats with cerebral ischemia showed a minor decrease of TNF- α production in cerebral and intestinal tissues. The rats with cerebral ischemia and treated with MSG displayed statistically significant low levels of TNF- α in cerebral and intestinal tissues. These results correlated significantly with NF- κ B production calculated at the same intervals. During experiment, the mean blood pressure and heart rates in all groups were stable.

CONCLUSION: Glutamate is involved in the mechanism of intestinal and cerebral inflammation responses. The effects of glutamate on cerebral and intestinal inflammatory responses after ischemia are up-regulated at the transcriptional level, through the NF- κ B signal transduction pathway.

© 2005 The WJG Press and Elsevier Inc. All rights reserved.

Key words: Cerebral ischemia; Glutamate; Intestine inflammatory responses; Cerebral inflammatory responses; NF- κ B

Xu L, Sun J, Lu R, Ji Q, Xu JG. Effect of glutamate on inflammatory responses of intestine and brain after focal cerebral ischemia. *World J Gastroenterol* 2004; 11(5): 733-736
<http://www.wjgnet.com/1007-9327/11/733.asp>

INTRODUCTION

Cerebral ischemia, a major threatening pathologic process in many brain diseases, such as gastrointestinal ischemia and hemorrhage^[1]

is complicated by multiple organ dysfunction. In this process, proinflammatory cytokines, such as TNF- α , are elevated in the injured areas^[2].

During an early stage of cerebral ischemia, glutamate, a ubiquitous excitatory amino acid in mammalian brains, is released from neurons and cumulated in intercellular space^[3,4]. Glutamate and its receptors play key roles in pathology of ischemia injury^[5], leading to the glutamate-calcium overload hypothesis^[6,7]. According to this hypothesis, glutamate is implicated in the pathology in two ways: excessive accumulation of glutamate in the extracellular spaces during ischemia, and subsequent activation of glutamate receptors in postsynaptic cells^[8,9].

Thousands of agents are intentionally added into the food we consume. Monosodium glutamate (MSG) is one of the widely-used food additives in our daily diet^[10]. MSG treatment provokes hormonal alterations and specific intestinal changes in smooth muscle reactivity to agonists^[11]. Oral or intestinal stimulation with isotonic MSG solution could increase the discharge rate of gastric branches of the vagus nerve^[12]. In addition, excitotoxic injury could also result in a marked stimulation of TNF- α mRNA expression in forebrain structure lesions^[13]. Although intestinal inflammatory response is activated after the elevation of intracellular glutamate concentrations^[14], the effect of glutamate on the gastrointestinal system after cerebral ischemia still remains unclear.

In the present study, we used a post-ischemic and excitotoxic animal model to investigate the effect of glutamate on inflammatory response of intestine and brain after cerebral ischemia. The involvement of glutamate in the mechanism of post-ischemic inflammatory response and was discussed.

MATERIALS AND METHODS

The rat TNF- α kit was purchased from DIACLONE (Besancon, France). [³²P]ATP was purchased from Free Biotech (Beijing, China). A commercial kit for EMSA was purchased from PROMEGA (Madison, WI). All other reagents were of molecular biology grade and purchased from SIGMA. All reagents and plasticwares used throughout the experiments were pyrogen-free.

Animal and experimental protocol

Adult male Sprague-Dawley rats, purchased from the Animal Center of the Chinese Academy of Sciences (Shanghai, China), were divided into experimental groups in a random manner. All procedures were approved by the Institutional Animal Care Committee. The rats were housed in plexiglass cages at 23±1 °C, and had free access to food and water *ad libitum* for 7 d, and used for experiments when their body weights gained between 300-350 g. The rats were anesthetized with urethane (1 000 mg/kg body weight, intraperitoneally). A polyethylene catheter was implanted in the tail vein for continuous infusion of solutions using a Razel Model WZ-50C syringe pump.

The rats were randomly assigned into 4 groups (6 rats each group). Group A (the control group) accepted a pseudo-operation of cervical incision and was injected with the same volume of physiological saline intraperitoneally. Group B was administered 4 mg/kg body weight MSG after cervical incision.

Group C and group D served as the ischemic groups. An ischaemic model was established by 15-min of bilateral carotid artery occlusion and reperfusion afterwards^[15,16]. Group D, however, accepted an additional MSG (4 mg/kg body weight) at the beginning of carotid artery occlusion.

In the experiments, the right femoral artery was intubated with a 25 G catheter prefilled with heparin solution and hemodynamical parameters were continuously observed by using a Datex monitor. Pre-ischemia was appointed at 0, 10, 20, 30, 60, 120 min after onset of the cerebral ischemia at 10, 20, 30, 60, 120 min, respectively.

The rats were decapitated at 6 h after ischemic insults. Blood plasma, cerebral cortex and small intestine were collected for TNF- α or NF- κ B measurement. All samples were frozen immediately in liquid nitrogen, and stored at -80 °C.

Enzyme-linked immunosorbant assays (ELISA)

TNF- α concentrations in plasma, cerebral and intestinal tissues were quantified by ELISA according to the manufacturer's instructions.

Nuclear protein extracts and electrophoretic mobility shift assay (EMSA)

Nuclear extracts from cerebral and intestinal tissues were prepared by hypotonic lysis followed by high salt extraction as described previously^[17-19]. Intestinal tissue cells were incubated in 0.5 mL ice-cold buffer (10 mmol/L HEPES, pH 7.9, 10 mmol/L KCl, 2 mmol/L MgCl₂, 0.1 mmol/L EDTA, 1 mmol/L dithiothreitol (DTT)), then in 0.5 mmol/L phenylmethylsulfonyl fluoride (PMSF) for 15 min, and 50 μ L NP-40 was added. After 30 s, the mixture was centrifuged at 5 000 g for 10 min at 4 °C, the pellet was suspended in 50 μ L ice-cold buffer (50 mmol/L HEPES, pH 7.9, 50 mmol/L KCl, 300 mmol/L NaCl, 0.1 mmol/L EDTA, 1 mmol/L DTT, 0.5 mmol/L PMSF, with 100 mL/L glycerol) and incubated on ice for 30 min and frequently mixed. After centrifugation at 12 000 g for 15 min at 4 °C, the supernatants were collected and stored at -80 °C until use. Protein concentration was determined as described previously^[20,21].

The NF- κ B consensus oligonucleotide probe (5'-AGT TGA GGG GAC TTT CCC AGG C-3') was end-labeled with [γ -³²P]-ATP with T4-polynucleotide kinase. Nuclear protein (intestine: 80 μ g, cerebra: 60 μ g) was pre-incubated for 10 min at room temperature (RT) in 9 μ L of binding buffer, containing 10 mmol/L Tris-HCl (pH 7.5), 4% glycerol, 1 mmol/L MgCl, and 0.5 mmol/L EDTA, 0.5 mmol/L DTT, 50 mmol/L NaCl, and 0.05 mg/mL poly (di-dc). After the ³²P-labeled oligonucleotide probe was added, the incubation was continued for 20 min at RT. Reaction was stopped by adding 1 μ L gel loading buffer, and the mixture was subjected to non-denaturing 4% polyacrylamide gel electrophoresis in 0.5 \times TBE buffer, pre-run at 300 V for 10 min. Electrophoresis was conducted at 390 V for 1 h. After electrophoresis, gels were transferred to Whatman DE-81 paper, dried and exposed to autoradiographic film (Fuji hyperfilm) with an intensifier screen at -70 °C^[22].

Data presentation and statistical analysis

Data were presented as mean \pm SE, and compared by analysis of variance followed by one-way ANOVA and Tukey test (using SPSS 10.0 software equipped with a Pentium 4 computer). $P < 0.05$ was accepted as statistically significant.

RESULTS

Hemodynamical parameters were stable during cerebral ischemia/MSG insults

In the experiments, the mean artery pressure (MAP) fluctuated

at 80-90 mmHg, and the heart rate was 190-210 beats per minute (bpm). TNF- α was not detected in plasma, there was no significant difference in MAP or heart rate among all groups at any time point (Figures 1, 2).

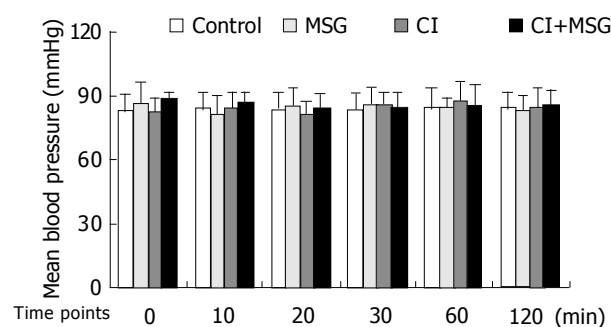


Figure 1 Mean artery pressure (MAP) changes during cerebral ischemia and MSG insults. There were no significant changes between inter-groups or intra-groups.

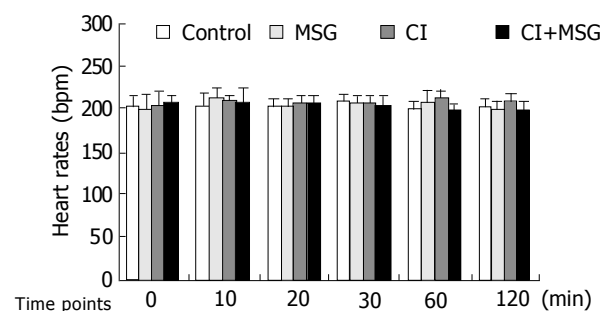


Figure 2 Heart rate changes during cerebral ischemia and MSG insults. There were no significant changes between inter-groups or intra-groups.

MSG provoked TNF- α production both in intestine and in brain

Compared with control animals, the level of TNF- α was elevated 3-fold both in MSG-treated rat intestine (6.08 \pm 0.52 vs 2.03 \pm 0.63 pg/g pro, $P < 0.05$, $n = 6$) and in cerebra (4.94 \pm 0.51 vs 1.85 \pm 0.32 pg/g pro, $P < 0.05$, $n = 6$) (Figure 3).

15-min cerebral ischemia increased TNF- α production in intestine and brain

TNF- α concentrations were elevated both in cerebra and intestine of the ischemic group, but did not differ significantly from the data of control (Figure 3).

Ischemia/MSG treatments increased TNF- α production but attenuated MSG-induced TNF- α elevation in intestine and brain

Cerebral-ischemic rats treated with MSG also had a high level of TNF- α (intestine: 3.02 \pm 0.49 vs 2.03 \pm 0.63 pg/g pro, cerebra: 3.09 \pm 0.69 vs 1.85 \pm 0.32 pg/g pro, $P < 0.05$, $n = 6$). Compared with MSG-treatment, the values were decreased both in intestine and cerebra (intestine: 3.02 \pm 0.49 vs 6.08 \pm 0.52 pg/g pro, cerebra: 3.09 \pm 0.69 vs 4.94 \pm 0.51 pg/g pro, $P < 0.05$, $n = 6$) (Figure 3).

NF- κ B activation in intestine

Both MSG-treatment and cerebral ischemia insults induced a significantly higher intensity of NF- κ B in the intestine than in controls ($P < 0.05$). Compared with MSG-treatment, NF- κ B activity decreased with ischemia-MSG-treatment (Figure 4A).

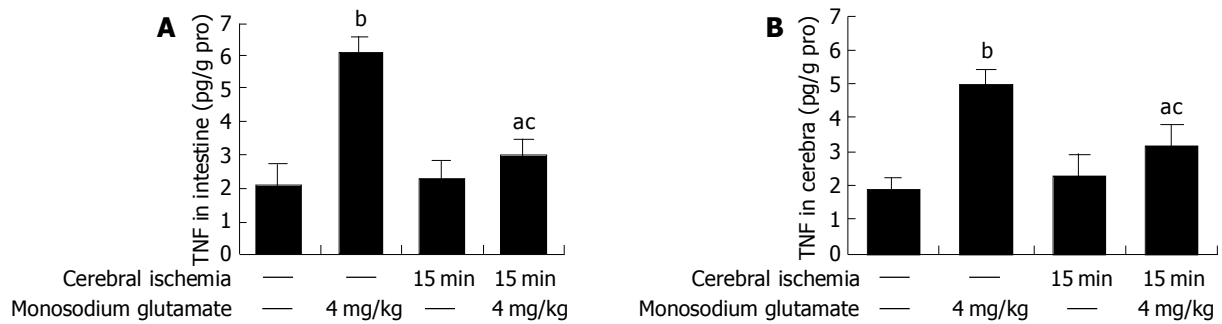


Figure 3 TNF- α production in intestine (A) and cerebra (B). TNF- α concentrations elevated in MSG-treated and ischemia/MSG-treated rats. Compared with that of MSG-treated rats, TNF- α levels decreased one-fold in ischemia/MSG-treated rats. ^a $P < 0.05$ vs control, ^b $P < 0.01$ vs control, ^c $P < 0.05$ vs MSG group.

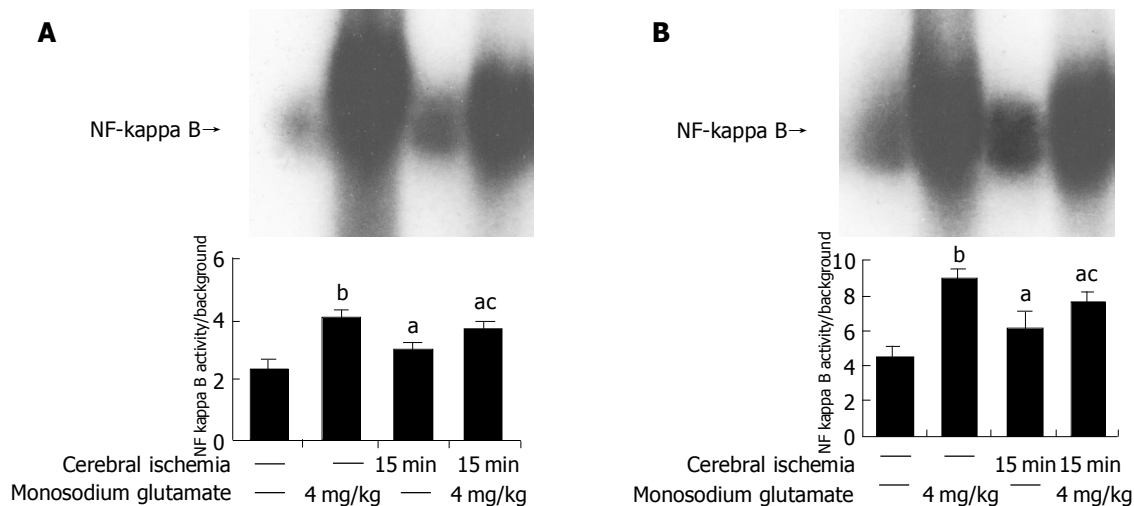


Figure 4 NF- κ B activation in intestinal tissues (A) and in cerebral tissue (B). Lane1: controls, lane 2: MSG-treated rats, lane 3: cerebral-ischemic rats, lane 4: NF- κ B intensity of ischemia/MSG-treated rats ^a $P < 0.05$ vs control, ^b $P < 0.01$ vs control, ^c $P < 0.05$ vs MSG-treatment.

NF- κ B activation in brain

The similar results were found in the brain. MSG-treatment and cerebral ischemia induced a significantly higher intensity of NF- κ B in the cerebra than in control ($P < 0.05$). Compared with MSG-treatment, NF- κ B activity decreased significantly in ischemia-MSG-treatment compared with control ($P < 0.05$) (Figure 4B).

DISCUSSION

In the present study, we demonstrated that 15-min cerebral ischemia plus exogenous glutamate or single exogenous glutamate could provoke significant inflammation responses in the central nervous system and gastrointestinal system characterized by an excess production of TNF- α and activation of NF- κ B. However, the inflammatory response either in brain or in intestine was not prominent during cerebral ischemia injury.

It has been reported that TNF- α is the most important proinflammatory cytokine, which is released early after an inflammatory stimulus^[23], contributing to both morbidity and mortality in conditions of ischemia-reperfusion injury. Among the cytokines produced in intestinal mucosae during inflammation, TNF- α is particularly important because of its biological effects on intestine and other systems^[24].

In cytoplasm, NF- κ B is associated with its inhibitory subunits, inhibitory kappa B (I κ B), which prevents it from translocating into nuclei^[25]. Many stimuli including endotoxin, induce the phosphorylation and degradation of I κ B, freeing NF- κ B from NF- κ B/I κ Bs complexes and enabling it to translocat

into nuclei^[25,26], where it regulates gene transcription. Many effector genes, including those encoding cytokines and adhesion molecules, are in turn regulated by NF- κ B. Some anti-inflammatory agents (e.g., salicylates, dexamethasone) can inhibit NF- κ B, suggesting that it is an important molecular target for the modulation of inflammatory diseases^[27,28].

Cytokines and inflammation in the central nervous system (CNS) have been primarily studied in the context of autoimmune and infectious diseases. In this study, we found that the production of TNF- α in the central nervous system and gastrointestinal system was increased and NF- κ B activity was increased after MSG treatment, indicating that the inflammatory responses in the central nervous and gastrointestinal systems can be enhanced by glutamate after cerebral ischemia. Glutamate could induce gene transcription in numerous physiological and pathological conditions. Among the glutamate-responsive transcription factors, NF-kappaB has been mainly implicated in neuronal survival and death. Glutamate could induce a rapid reduction of I kappaB alpha levels and nuclear translocation of the NF-kappaB subunit p65. The glutamate-induced reduction of I kappaB alpha levels is blocked by the N-methyl-D-aspartate inhibitor MK801^[29]. Inflammatory mediators are involved in the pathogenesis of focal ischemic brain damage and regulated at transcriptional level^[30].

It seems that cerebral ischemia can attenuate the intestinal inflammatory response during an exogenous glutamate challenge. Cerebral ischemia might protect intestinal tissues against exogenous glutamate insults. The intestine may be more

resistant to glutamate-induced toxic effects after cerebral ischemic injury. Perhaps this effect is associated with the distinctive role of glutamate and its receptors in the brain-gut axis^[31]. Excitatory amino acid (EAA) transmission is in the center of the brain-gut axis, the dorsal vagal complex. However, further investigations need to be carried out.

However, we do not advocate administering glutamate, because we found that exogenous glutamate exacerbated inflammation of the central nervous system after cerebral ischemia injury. After all, glutamate is the most important toxic EAA in the pathogenesis of cerebral ischemia-reperfusion injury, and systemic glutamate can be absorbed from portal vein system and may penetrate the blood-brain-barrier (BBB) during or after cerebral ischemia, since the BBB is destroyed after cerebral ischemia-reperfusion injury^[23].

In conclusion, exogenous glutamate can provoke inflammatory responses in brain and intestine. The effect of glutamate on inflammatory response after ischemia is regulated at transcriptional level. Ischemic treatment can attenuate glutamate-induced TNF- α production both in brain and in intestine.

ACKNOWLEDGEMENTS

The authors thank Drs. Gen-Bao Feng, Zhi-Qiang Zhou, Wei-Yan Li, Man-Lin Duan, Si-Hai Zhu, Hong-Yan Liu and Jing Chen for their technical assistance and friendly help.

REFERENCES

- Chen DC, Jing BW. Acute stress-induced neurogenic gastrointestinal mucosa lesions. *Chin J Practical Internal Med* 1997; **17**: 641-642
- Li JS, Zhao JM, Guo SD, Zhang WH, Zhao J, Gao AS, Li JG. Changes and significance of prostaglandin and tumorous necrotic factor in aged rats with gastrointestinal injury after brain ischemia ia reperfusion. *Chin J Gerontol* 2001; **21**: 354-356
- Yusa T. Increased extracellular ascorbate release reflects glutamate re-uptake during the early stage of reperfusion after forebrain ischemia in rats. *Brain Res* 2001; **897**: 104-113
- Tang XC, Rao MR, Hu G, Wang H. Alterations of amino acid levels from striatum, hippocampus, and cerebral cortex induced by global cerebral ischemia in gerbil. *Acta Pharmacol Sin* 2000; **21**: 819-823
- Nakane H, Yao H, Ibayashi S, Kitazono T, Ooboshi H, Uchimura H, Fujishima M. Protein kinase C modulates ischemia-induced amino acids release in the striatum of hypertensive rats. *Brain Res* 1998; **782**: 290-296
- Yamamoto H, Mitani A, Cui Y, Takechi S, Irita J, Suga T, Arai T, Kataoka K. Neuroprotective effect of mild hypothermia cannot be explained in terms of a reduction of glutamate release during ischemia. *Neuroscience* 1999; **91**: 501-509
- Guo J, Meng F, Fu X, Song B, Yan X, Zhang G. N-methyl-D-aspartate receptor and L-type voltage-gated Ca²⁺ channel activation mediate proline-rich tyrosine kinase 2 phosphorylation during cerebral ischemia in rats. *Neurosci Lett* 2004; **355**: 177-180
- Monnerie H, Shashidhara S, Le Roux PD. Effect of excess extracellular glutamate on dendrite growth from cerebral cortical neurons at 3 days *in vitro*: Involvement of NMDA receptors. *J Neurosci Res* 2003; **74**: 688-700
- Pellegrini-Giampietro DE. The distinct role of mGlu1 receptors in post-ischemic neuronal death. *Trends Pharmacol Sci* 2003; **24**: 461-470
- Walker R, Lupien JR. The safety evaluation of monosodium glutamate. *J Nutr* 2000; **130**: 1049S-1052S
- Sukhanov SN, de Andrade IS, Dolnikoff MS, Ferreira AT. Neonatal monosodium glutamate treatment alters rat intestinal muscle reactivity to some agonists. *Eur J Pharmacol* 1999; **386**: 247-252
- Niijima A. Effects of oral and intestinal stimulation with umami substance on gastric vagus activity. *Physiol Behav* 1991; **49**: 1025-1028
- Szaflarski J, Burtrum D, Silverstein FS. Cerebral hypoxia-ischemia stimulates cytokine gene expression in perinatal rats. *Stroke* 1995; **26**: 1093-1100
- Kocdor H, Kocdor MA, Astarcioglu H, Fadiloglu M. Serum tumor necrosis factor-alpha, glutamate and lactate changes in two different stages of mechanical intestinal obstruction. *Turk J Gastroenterol* 2003; **14**: 115-120
- Homi HM, Mixco JM, Sheng H, Grocott HP, Pearlstein RD, Warner DS. Severe hypotension is not essential for isoflurane neuroprotection against forebrain ischemia in mice. *Anesthesiology* 2003; **99**: 1145-1151
- Pei L, Li Y, Zhang GY, Cui ZC, Zhu ZM. Mechanisms of regulation of tyrosine phosphorylation of NMDA receptor subunit 2B after cerebral ischemia/reperfusion. *Acta Pharmacol Sin* 2000; **21**: 695-700
- Shimada T, Watanabe N, Ohtsuka Y, Endoh M, Kojima K, Hiraishi H, Terano A. Polaprezinc down-regulates proinflammatory cytokine-induced nuclear factor-kappaB activation and interleukin-8 expression in gastric epithelial cells. *J Pharmacol Exp Ther* 1999; **291**: 345-352
- Sun J, Wang XD, Liu H, Xu JG. Ketamine suppresses intestinal NF-kappa B activation and proinflammatory cytokine in endotoxic rats. *World J Gastroenterol* 2004; **10**: 1028-1031
- Tian J, Lin X, Guan R, Xu JG. The effects of hydroxyethyl starch on lung capillary permeability in endotoxic rats and possible mechanisms. *Anesth Analg* 2004; **98**: 768-774, table of contents
- Bradford MM. A rapid and sensitive method for the quantitation of microgram quantities of protein utilizing the principle of protein-dye binding. *Anal Biochem* 1976; **72**: 248-254
- Yuksel M, Okajima K, Uchiba M, Okabe H. Gabexate mesilate, a synthetic protease inhibitor, inhibits lipopolysaccharide-induced tumor necrosis factor-alpha production by inhibiting activation of both nuclear factor-kappaB and activator protein-1 in human monocytes. *J Pharmacol Exp Ther* 2003; **305**: 298-305
- Vancurova I, Miskolci V, Davidson D. NF-kappa B activation in tumor necrosis factor alpha-stimulated neutrophils is mediated by protein kinase Cdelta. Correlation to nuclear Ikappa Balpha. *J Biol Chem* 2001; **276**: 19746-19752
- Yang GY, Gong C, Qin Z, Liu XH, Lorris Betz A. Tumor necrosis factor alpha expression produces increased blood-brain barrier permeability following temporary focal cerebral ischemia in mice. *Brain Res Mol Brain Res* 1999; **69**: 135-143
- Chen LW, Egan L, Li ZW, Greten FR, Kagnoff MF, Karin M. The two faces of IKK and NF-kappaB inhibition: prevention of systemic inflammation but increased local injury following intestinal ischemia-reperfusion. *Nat Med* 2003; **9**: 575-581
- Butcher BA, Kim L, Johnson PF, Denkers EY. Toxoplasma gondii tachyzoites inhibit proinflammatory cytokine induction in infected macrophages by preventing nuclear translocation of the transcription factor NF-kappa B. *J Immunol* 2001; **167**: 2193-2201
- Helmer KS, Chang L, Cui Y, Mercer DW. Induction of NF-kappaB, IkappaB-alpha, and iNOS in rat gastric mucosa during endotoxemia. *J Surg Res* 2002; **104**: 46-52
- Xia L, Pan J, Yao L, McEver RP. A proteasome inhibitor, an antioxidant, or a salicylate, but not a glucocorticoid, blocks constitutive and cytokine-inducible expression of P-selectin in human endothelial cells. *Blood* 1998; **91**: 1625-1632
- Hideshima T, Chauhan D, Richardson P, Mitsiades C, Mitsiades N, Hayashi T, Munshi N, Dang L, Castro A, Palombella V, Adams J, Anderson KC. NF-kappa B as a therapeutic target in multiple myeloma. *J Biol Chem* 2002; **277**: 16639-16647
- Scholzke MN, Potrovita I, Subramaniam S, Prinz S, Schwaninger M. Glutamate activates NF-kappaB through calpain in neurons. *Eur J Neurosci* 2003; **18**: 3305-3310
- Ginis I, Jaiswal R, Klimanis D, Liu J, Greenspon J, Hallenbeck JM. TNF-alpha-induced tolerance to ischemic injury involves differential control of NF-kappaB transactivation: the role of NF-kappaB association with p300 adaptor. *J Cereb Blood Flow Metab* 2002; **22**: 142-152
- Hornby PJ. Receptors and transmission in the brain-gut axis. II. Excitatory amino acid receptors in the brain-gut axis. *Am J Physiol Gastrointest Liver Physiol* 2001; **280**: G1055-G1060

Effects of psychological stress on small intestinal motility and expression of cholecystokinin and vasoactive intestinal polypeptide in plasma and small intestine in mice

Shu-Guang Cao, Wan-Chun Wu, Zhen Han, Meng-Ya Wang

Shu-Guang Cao, Wan-Chun Wu, Zhen Han, Department of Gastroenterology, Yijishan Hospital, Wuhu 241001, Anhui Province, China

Meng-Ya Wang, Department of Physiology, Wannan Medical College, Wuhu 241001, Anhui Province, China

Correspondence to: Wan-Chun Wu, Department of Gastroenterology, Yijishan Hospital, Wuhu 241001, Anhui Province, China. letous2002@163.com

Telephone: +86-553-5738401

Received: 2004-02-02 **Accepted:** 2004-02-26

Abstract

AIM: To investigate the effects of psychological stress on small intestinal motility and expression of cholecystokinin (CCK) and vasoactive intestinal polypeptide (VIP) in plasma and small intestine, and to explore the relationship between small intestinal motor disorders and gastrointestinal hormones under psychological stress.

METHODS: Thirty-six mice were randomly divided into psychological stress group and control group. A mouse model with psychological stress was established by housing the mice with a hungry cat in separate layers of a two-layer cage. A semi-solid colored marker (carbon-ink) was used for monitoring small intestinal transit. CCK and VIP levels in plasma and small intestine in mice were measured by radioimmunoassay (RIA).

RESULTS: Small intestinal transit was inhibited ($52.18 \pm 19.15\%$ vs $70.19 \pm 17.79\%$, $P < 0.01$) in mice after psychological stress, compared to the controls. Small intestinal CCK levels in psychological stress mice were significantly lower than those in the control group ($0.75 \pm 0.53 \mu\text{g/g}$ vs $1.98 \pm 1.17 \mu\text{g/g}$, $P < 0.01$), whereas plasma CCK concentrations were not different between the groups. VIP levels in small intestine were significantly higher in psychological stress mice than those in the control group ($8.45 \pm 1.09 \mu\text{g/g}$ vs $7.03 \pm 2.36 \mu\text{g/g}$, $P < 0.01$), while there was no significant difference in plasma VIP levels between the two groups.

CONCLUSION: Psychological stress inhibits the small intestinal transit, probably by down-regulating CCK and up-regulating VIP expression in small intestine.

© 2005 The WJG Press and Elsevier Inc. All rights reserved.

Key words: Small intestine; Psychological stress; Cholecystokinin; Vasoactive intestinal polypeptide; Intestinal motility

Cao SG, Wu WC, Han Z, Wang MY. Effects of psychological stress on small intestinal motility and expression of cholecystokinin and vasoactive intestinal polypeptide in plasma and small intestine in mice. *World J Gastroenterol* 2005; 11(5): 737-740 <http://www.wjgnet.com/1007-9327/11/737.asp>

INTRODUCTION

In recent years, with rapid development of society and increasing competition pressure, psychological stress, which originates in society has imposed impacts on human health, and has become an important stressor. Psychological stress is widely believed to play a major role in gastrointestinal motor disorders, especially in irritable bowel syndrome (IBS) and functional dyspepsia (FD), by precipitating exacerbation of symptoms^[1,2]. Available data clearly demonstrate that in experimental animals the most consistent patterns of gastrointestinal motor alternations induced by psychological stress are delayed gastric emptying^[3,4] and accelerated colon transit^[5,6]. However, almost no valid data are available on small intestinal motility disorders. Previous studies of psychological stress^[7-9] (cold stress, restraint stress, foot-shock stress and swim stress), were all focused on somatic stress. In common, both central and peripheral nervous pathways are involved in the release of gastrointestinal hormones due to psychological stress, thus modulating gastrointestinal motility^[10]. A large body of evidence derived from experiments suggest that CCK could accelerate small intestinal transit^[11,12], while VIP could inhibit it^[13]. However, there are few studies on whether gut hormones are involved in modulating small intestinal motility under psychological stress.

In the present study, experimental animals were obtained to test the relationship between small intestinal motility and release of gastrointestinal hormones during psychological stress. Furthermore, small intestinal motility disorders in response to CCK and VIP due to psychological stress were studied.

MATERIALS AND METHODS

Experimental animals and materials

Thirty-six healthy male mice (provided by Qinglongshan Experimental Animal Center) weighing 20-30 g were used in this study. Mice were housed individually in cages at constant room temperature with a 12-h light/dark cycle and had free access to laboratory chow and water. CCK kit was purchased from Neurobiological Department of Second Military Medical University. VIP kit was purchased from Beijing Haikerui Biological Technology Center.

Establishment of animal models

Thirty-six mice were randomly divided into psychological stress group and control group. Each contained 18 mice. Mice in psychological stress group were housed in the bottom of two-layer cage, with a hungry cat housed in the upper layer of the cage for 10 min each day for 10 d, but mice and the cat had no physical contact^[14]. Procedure for the control group mice were the same as psychological stress group except for no contact with the cat.

Measurement of small intestinal transit

The carbon-ink transit test was modified as described. Mice

were deprived of food for 24 h and water for 12 h prior to experiment, and 0.25 mL carbon-ink was administered into their stomachs by orogastric gavage. Twenty-five minutes later, the mice were killed, abdomen was opened and small intestine was dissected. The total length of the small intestine (pylorus-cecum) and the distance traveled by carbon-ink were measured. Results were expressed as ratio (percentage) of the distance traveled by carbon-ink to the total length of the small intestine. Small intestine was washed with normal saline after measuring. Water was absorbed by filter paper and small intestine was kept in a dry bottle.

Plasma and tissue preparation

Immediately after the mice were killed, blood samples were collected into chilled tubes containing 0.3 μ L ethylenediamine tetraacetic acid (EDTA) and 1000 KIU aprotinin. The blood was centrifuged at 3 000 r/min at 4 $^{\circ}$ C for 10 min. The plasma was stored at -70 $^{\circ}$ C until assayed.

Samples of small intestine were placed in saline and boiled for 10 min. Water was absorbed by filter paper. Small intestine was weighed by analytical balance and then dissolved in 1 mmol/L ice-cold acetic acid (0.3 mL/100 g), homogenized and the same volume 1 mmol/L sodium hydroxide was added and then they were left at room temperature for 20 min, and centrifuged at 3 000 r/min at 4 $^{\circ}$ C for 10 min. The supernatants were stored at -70 $^{\circ}$ C until assayed.

CCK radioimmunoassay

Plasma and small intestine CCK levels were measured using radioimmunoassay (RIA). Briefly, samples and standards diluted in the perfusion medium were incubated with CCK antiserum in tubes for 24 h at 4 $^{\circ}$ C. After addition of 125 I-CCK, all samples were further incubated for 24 h at 4 $^{\circ}$ C to reach equilibrium. Antibody-bound and free tracers were separated by addition of 0.4 mL of activated charcoal.

VIP radioimmunoassay

VIP was determined by radioimmunoassay. Samples and standards diluted in the perfusion medium were incubated with VIP antiserum in tubes for 48 h at 4 $^{\circ}$ C. After addition of 125 I labeled VIP, all samples were further incubated for 48 h at 4 $^{\circ}$ C. After incubation, antibody-bound and free tracers were separated by addition of 0.4 mL of activated charcoal.

Statistical analysis

Data were expressed as mean \pm SD. Experimental results were analyzed by *t* test, $P < 0.05$ was considered statistically significant.

RESULTS

Small intestinal transit

After 25 min of intragastric carbon-ink administration, the overall mean ratio of small intestinal transit ($P < 0.01$) under psychological stress was lower than that of the control (52.18 \pm 19.15% vs 70.19 \pm 17.79%), indicating that psychological stress could inhibit small intestinal transit. Figure 1 presents individual data for the ratio of small intestinal transit (percentage of the distance traveled by carbon-ink to the total length of the small intestine).

CCK concentrations in plasma and small intestine

CCK levels in small intestine of experimental psychological stress mice were significantly lower than those of the control (0.75 \pm 0.53 μ g/g vs 1.98 \pm 1.17 μ g/g, $P < 0.01$). However, no significant changes in plasma CCK levels were observed in experimental psychological stress mice compared to the control

(53.88 \pm 33.17 ng/L vs 52.70 \pm 20.10 ng/L, $P > 0.05$) (Table 1).

Table 1 Changes of CCK in plasma and small intestine (mean \pm SD)

Group	No. of animals	Small intestine μ g/g)	Plasma (ng/L)
Control	18	1.98 \pm 1.17	52.70 \pm 20.10
Stress	18	0.75 \pm 0.53 ^b	53.88 \pm 33.17

^b $P < 0.01$ vs the control.

VIP concentrations in plasma and small intestine

VIP levels in small intestine of experimental psychological stress mice were significantly higher than those of the control (8.45 \pm 1.09 μ g/L vs 7.03 \pm 2.36 μ g/L, $P < 0.01$). However, plasma VIP levels showed no significant difference between the two groups (201.58 \pm 103.23 μ g/L vs 190.05 \pm 90.08 μ g/L, $P > 0.05$).

Table 2 Changes of VIP in small intestine plasma (mean \pm SD)

Group	No. of animals	Small intestine (μ g/g)	Plasma (ng/L)
Control	18	7.03 \pm 2.36	190.05 \pm 90.08
Stress	18	8.45 \pm 1.09 ^b	201.58 \pm 103.23

^b $P < 0.01$ vs the control.

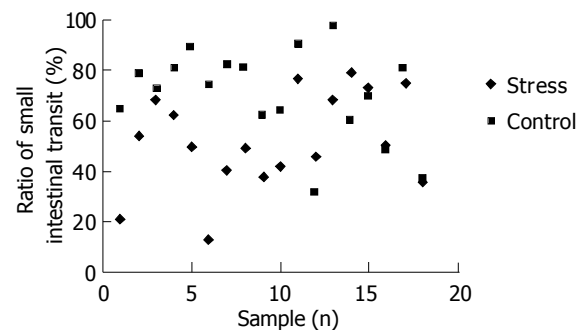


Figure 1 Effect of psychological stress on small intestinal transit.

DISCUSSION

The association between psychological stress and small intestinal motility has been postulated for about twenty years. Some studies in experimental animals indicate contradictory results, and the mechanism by which psychological stress affects small intestinal motility is not well understood. Ditto *et al*^[15] recently reported that stress enhanced small intestinal transit and produced a statistically significant reduction in the mean small intestinal transit time. However, Tsukada *et al*^[16] demonstrated that psychological stress induced inhibition of small intestinal transit. In the present study, our results were similar to Tsukada's. After 25 min of intragastric carbon-ink administration, the ratio of small intestinal transit significantly decreased during psychological stress. Previous studies show that patients with gastrointestinal motility disorders, especially irritable bowel syndrome (IBS), symptoms of abdominal pain and bloating are precipitated after psychological stress (life events or trauma). The mechanism may be that psychological stress induces decrease in small intestinal transit. Intestinal gas could not be evacuated effectively leading to gas retention, which evokes a series of symptoms, especially pain and bloating^[17].

In this study, we showed that CCK levels in small intestine of psychological stress mice were significantly lower than those of the controls, while they did not alter in plasma. CCK, a peptide secreted from I cells of gastrointestinal responds to the presence of nutrients in the small intestine. It is also synthesized in

brain^[18]. Two CCK receptor subtypes that differ markedly in their pharmacological profiles and anatomical distribution have been identified and characterized^[19]. CCK-A receptors exist predominantly at the peripheral level where they are responsible for the digestive effects of CCK^[20]. However, high densities of brain CCK-B receptors are present in cortical and limbic blood. Endogenous CCK appears to act in part by paracrine and endocrine mechanisms to affect gut motility^[21]. It is well established that endogenous CCK regulates gastrointestinal motility, including delay of gastric emptying^[22], acceleration of small intestinal transit^[23] and enhancement of colon motor^[24]. Various studies have provided evidence for the mechanism of CCK underlying small intestinal motility through involvement of CCK-A receptors in small intestine. The selective CCK-A receptor antagonists (devazepide and lorglumide) effectively attenuate this effect while CCK-B receptor antagonists have no effect on it^[25]. Furthermore, both afferent and efferent nerves are implicated in CCK motor actions in the gastrointestinal tract. Patterson *et al*^[27] performed immunohistochemistry using an antibody directed to the C-terminal region of the CCK-A receptor, and found that intestinal cells of Cajal (ICC) in the sphincter muscle and the circular muscle of proximal duodenum displayed strong CCK-A receptor immunoreactivity; at the same time, selection neurons in the myenteric ganglia and a few of single neurons in the submucosa near the proximal duodenum, also expressed strong CCK-A receptor immunoreactivity. In view of these results, we can conclude that the effect of psychological stress on intestinal motility and transit may be partially mediated by decreasing intraluminal concentrations of CCK, which leads to reduced migrating myoelectric complex (MMC) activity of the small intestine, prolonging MMC cycle length, reducing contraction frequency and decreasing propagation velocity.

VIP, which is released from D₁ cells of gut through exocrine into the lumen, has an established role in the regulation of gastrointestinal motor function. VIP is widely distributed in gut. In addition to GI mucosa^[28], it is also found in submucous and myenteric plexus, central and peripheral nervous systems^[29,30]. Furthermore, a large number of VIP receptors are expressed in those regions^[31-33]. Sayadi *et al*^[34] analyzed the distribution of VIP receptors using autoradiographic techniques, and found that the density of VIP receptors was greatest in duodenal mucosa but was lower in jejunal and ileal mucosa. Moreover, previous studies have provided evidence that VIP acts via two receptors (VIP1 and VIP2). In the intestine, VIP1 receptor is significantly higher than VIP2 receptor^[35]. A great number of data demonstrate that VIP has various physiologic functions on small intestinal motility. First, VIP exerts direct stimulatory effect on intestinal smooth muscle, reduces the percentage motor index of pressure waves. This effect of VIP could be partially antagonized by VIP receptor antagonists^[36]. Second, intraduodenal infusion of VIP in rats disrupts the MMC, prolongs MMC cycle length and decreases propagation velocity, while VIP receptor antagonists could reverse this effect^[37-39]. Third, the effect of VIP on intestinal motility involves both myenteric and submucosal neurons, resulting in increased contraction of longitudinal smooth muscle^[40]. Naslund *et al*^[41] demonstrated that intraduodenal but not plasma concentrations of VIP showed an association with the MMC. In the present study, we showed that VIP levels in small intestine were significantly higher than those of the control, but had no difference in plasma. It indicates that small intestine VIP plays an important role in the inhibition of small intestinal transit caused by psychological stress.

The results of this study suggest that gastrointestinal motility disorders during psychological stress may be partially mediated by release of gut hormones from small intestine. But

the following questions need to be answered in future: how does psychological stress modulate gut hormone release from small intestine and how are gastrointestinal motility disorders caused by gut hormones in small intestine.

In summary, psychological stress does induce changes in the small intestinal motility. Changes of CCK and VIP levels in the small intestine of mice may be closely related with the inhibition of small intestine transit. However, there is no relationship between gastrointestinal dysmotility and gut hormones in plasma during psychological stress.

REFERENCES

- 1 **Mayer EA**, Naliboff BD, Chang L, **Coutinho SV. V.** Stress and irritable bowel syndrome. *Am J Physiol Gastrointest Liver Physiol* 2001; **280**: G519-G524
- 2 **Mayer EA**, Craske M, Naliboff BD. Depression, anxiety, and the gastrointestinal system. *J Clin Psychiatry* 2001; **62** Suppl 8: 28-36; [discussion 37](#)
- 3 **Tsukada F**, Nagura Y, Abe S, Sato N, Ohkubo Y. Effect of restraint and footshock stress and norepinephrine treatment on gastric emptying in rats. *Biol Pharm Bull* 2003; **26**: 368-370
- 4 **Mistiaen W**, Blockx P, Van Hee R, Bortier H, Harrisson F. The effect of stress on gastric emptying rate measured with a radionuclide tracer. *Hepatogastroenterology* 2002; **49**: 1457-1460
- 5 **Martinez V**, Tache Y. Role of CRF receptor 1 in central CRF-induced stimulation of colonic propulsion in rats. *Brain Res* 2001; **893**: 29-35
- 6 **Maillot C**, Million M, Wei JY, Gauthier A, Tache Y. Peripheral corticotropin-releasing factor and stress-stimulated colonic motor activity involve type 1 receptor in rats. *Gastroenterology* 2000; **119**: 1569-1579
- 7 **Tsukada F**, Sugawara M, Kohno H, Ohkubo Y. Evaluation of the effects of restraint and footshock stress on small intestinal motility by an improved method using a radionuclide, ⁵¹Cr, in the rat. *Biol Pharm Bull* 2001; **24**: 488-490
- 8 **Dai Y**, Liu JX, Li JX, Xu YF. Effect of pinaverium bromide on stress-induced colonic smooth muscle contractility disorder in rats. *World J Gastroenterol* 2003; **9**: 557-561
- 9 **Curtis AL**, Pavcovich LA, Valentino RJ. Long-term regulation of locus ceruleus sensitivity to corticotropin-releasing factor by swim stress. *J Pharmacol Exp Ther* 1999; **289**: 1211-1219
- 10 **Monnikes H**, Tebbe JJ, Hildebrandt M, Arck P, Osmanoglou E, Rose M, Klapp B, Wiedenmann B, Heymann-Monnikes I. Role of stress in functional gastrointestinal disorders. Evidence for stress-induced alterations in gastrointestinal motility and sensitivity. *Dig Dis* 2001; **19**: 201-211
- 11 **Gaige S**, Abysique A, Bouvier M. Effects of leptin on cat intestinal motility. *J Physiol* 2003; **546**: 267-277
- 12 **Feinle C**, O'Donovan D, Doran S, Andrews JM, Wishart J, Chapman I, Horowitz M. Effects of fat digestion on appetite, APD motility, and gut hormones in response to duodenal fat infusion in humans. *Am J Physiol Gastrointest Liver Physiol* 2003; **284**: G798-G807
- 13 **Chang FY**, Doong ML, Chen TS, Lee SD, Wang PS. Vasoactive intestinal polypeptide appears to be one of the mediators in misoprostol-enhanced small intestinal transit in rats. *J Gastroenterol Hepatol* 2000; **15**: 1120-1124
- 14 **Wang QS**, Zhang JH. Effects of predator stress on emotional behavior and spatial learning and memory of rats. *Chin J psychiatry* 2001; **34**: 180-183
- 15 **Ditto B**, Miller SB, Barr RG. A one-hour active coping stressor reduces small bowel transit time in healthy young adults. *Psychosom Med* 1998; **60**: 7-10
- 16 **Tsukada F**, Sawamura K, Kohno H, Ohkubo Y. Mechanism of inhibition of small intestinal motility by restraint stress differs from that with norepinephrine treatment in rats. *Biol Pharm Bull* 2002; **25**: 122-124
- 17 **Serra J**, Azpiroz F, Malagelada JR. Impaired transit and tolerance of intestinal gas in the irritable bowel syndrome. *Gut* 2001; **48**: 14-19
- 18 **Bohme GA**, Blanchard JC. Cholecystokinins and their receptors.

- Functional aspects. *Therapie* 1992; **47**: 541-548
- 19 **Patterson LM**, Zheng H, Berthoud HR. Vagal afferents innervating the gastrointestinal tract and CCKA-receptor immunoreactivity. *Anat Rec* 2002; **266**: 10-20
- 20 **Sayegh AI**, Ritter RC. CCK-A receptor activation induces fos expression in myenteric neurons of rat small intestine. *Regul Pept* 2000; **88**: 75-81
- 21 **Reidelberger RD**, Kelsey L, Heimann D, Hulce M. Effects of peripheral CCK receptor blockade on gastric emptying in rats. *Am J Physiol Regul Integr Comp Physiol* 2003; **284**: R66-R75
- 22 **Hidalgo L**, Clave P, Estorch M, Rodriguez-Espinosa J, Rovati L, Greeley GH, Capella G, Lluís F. Effect of cholecystokinin-A receptor blockade on postprandial insulinaemia and gastric emptying in humans. *Neurogastroenterol Motil* 2002; **14**: 519-525
- 23 **Lin HC**, Zaidel O, Hum S. Intestinal transit of fat depends on accelerating effect of cholecystokinin and slowing effect of an opioid pathway. *Dig Dis Sci* 2002; **47**: 2217-2221
- 24 **Chey WY**, Jin HO, Lee MH, Sun SW, Lee KY. Colonic motility abnormality in patients with irritable bowel syndrome exhibiting abdominal pain and diarrhea. *Am J Gastroenterol* 2001; **96**: 1499-1506
- 25 **Wu CL**, Hung CR, Chang FY, Pau KY, Wang PS. Involvement of cholecystokinin receptor in the inhibition of gastrointestinal motility by estradiol in ovariectomized rats. *Scand J Gastroenterol* 2002; **37**: 1133-1139
- 26 **Giralt M**, Vergara P. Both afferent and efferent nerves are implicated in cholecystokinin motor actions in the small intestine of the rat. *Regul Pept* 1999; **81**: 73-80
- 27 **Patterson LM**, Zheng H, Ward SM, Berthoud HR. Immunohistochemical identification of cholecystokinin A receptors on interstitial cells of Cajal, smooth muscle, and enteric neurons in rat pylorus. *Cell Tissue Res* 2001; **305**: 11-23
- 28 **Mao YK**, Barnett W, Coy DH, Tougas G, Daniel EE. Distribution of vasoactive intestinal polypeptide (VIP) binding in circular muscle and characterization of VIP binding in canine small intestinal mucosa. *J Pharmacol Exp Ther* 1991; **258**: 986-991
- 29 **King SC**, Slater P, Turnberg LA. Autoradiographic localization of binding sites for galanin and VIP in small intestine. *Peptides* 1989; **10**: 313-317
- 30 **Mao YK**, Tougas G, Barnett W, Daniel EE. VIP receptors on canine submucosal synaptosomes. *Peptides* 1993; **14**: 1149-1152
- 31 **Karacay B**, O'Dorisio MS, Kasow K, Hollenback C, Krahe R. Expression and fine mapping of murine vasoactive intestinal peptide receptor 1. *J Mol Neurosci* 2001; **17**: 311-324
- 32 **Chaudhary P**, Baumann TK. Expression of VPAC2 receptor and PAC1 receptor splice variants in the trigeminal ganglion of the adult rat. *Brain Res Mol Brain Res* 2002; **104**: 137-142
- 33 **You S**, Hsu CC, Kim H, Kho Y, Choi YJ, El Halawani ME, Farris J, Foster DN. Molecular cloning and expression analysis of the turkey vasoactive intestinal peptide receptor. *Gen Comp Endocrinol* 2001; **124**: 53-65
- 34 **Sayadi H**, Harmon JW, Moody TW, Korman LY. Autoradiographic distribution of vasoactive intestinal polypeptide receptors in rabbit and rat small intestine. *Peptides* 1988; **9**: 23-30
- 35 **Ussdin TB**, Bonner TI, Mezey E. Two receptors for vasoactive intestinal polypeptide with similar specificity and complementary distributions. *Endocrinology* 1994; **135**: 2662-2680
- 36 **Yamamoto H**, Kuwahara A, Fujimura M, Maeda T, Fujimiya M. Motor activity of vascularly perfused rat duodenum. 2. Effects of VIP, PACAP27 and PACAP38. *Neurogastroenterol Motil* 1999; **11**: 235-241
- 37 **Hellstrom PM**, Ljung T. Nitroergic inhibition of migrating myoelectric complex in the rat is mediated by vasoactive intestinal peptide. *Neurogastroenterol Motil* 1996; **8**: 299-306
- 38 **Ljung T**, Hellstrom PM. Vasoactive intestinal peptide suppresses migrating myoelectric complex of rat small intestine independent of nitric oxide. *Acta Physiol Scand* 1999; **165**: 225-231
- 39 **Espat NJ**, Cheng G, Kelley MC, Vogel SB, Sninsky CA, Hocking MP. Vasoactive intestinal peptide and substance P receptor antagonists improve postoperative ileus. *J Surg Res* 1995; **58**: 719-723
- 40 **Hens J**, Gajda M, Scheuermann DW, Adriaensen D, Timmermans JP. The longitudinal smooth muscle layer of the pig small intestine is innervated by both myenteric and submucous neurons. *Histochem Cell Biol* 2002; **117**: 481-492
- 41 **Naslund E**, Backman L, Theodorsson E, Hellstrom PM. Intraduodenal neuropeptide levels, but not plasma levels, vary in a cyclic fashion with the migrating motor complex. *Acta Physiol Scand* 1998; **164**: 317-323

Edited by Wang XL and Zhu LH

Tumor angiogenesis and its clinical significance in pediatric malignant liver tumor

Xiao-Yi Sun, Zai-De Wu, Xiao-Feng Liao, Ji-Yan Yuan

Xiao-Yi Sun, Zai-De Wu, Xiao-Feng Liao, Ji-Yan Yuan, Department of Pediatric Surgery, Tongji Hospital Affiliated to Tongji Medical College, Huazhong University of Science and Technology, Wuhan 430030, Hubei Province, China

Correspondence to: Dr. Xiao-Yi Sun, Department of Pediatric Surgery, Tongji Hospital, 1095 Jiefang Avenue, Wuhan 430030, Hubei Province, China. xysun@tjh.tjmu.edu.cn

Telephone: +86-27-83663808

Received: 2004-04-22 **Accepted:** 2004-05-09

Abstract

AIM: To investigate the expression of vascular endothelial growth factor (VEGF) and microvascular density (MVD) count in pediatric malignant liver tumor and their clinical significances.

METHODS: Fourteen children with malignant liver tumors including seven hepatocellular carcinomas (HCCs), five hepatoblastomas, one malignant mesenchymoma and one rhabdomyosarcoma were studied. Twelve adult HCC samples served as control group. All samples were examined with streptavidin-biotin peroxidase (SP) immunohistochemical staining for VEGF expression and MVD count.

RESULTS: VEGF positive expression in all pediatric malignant liver tumors was significantly higher than that in adult HCC (0.4971 ± 0.14 vs 0.4027 ± 0.03 , $P < 0.05$). VEGF expression in pediatric HCC group was also markedly higher than that in adult HCC group (0.5665 ± 0.10 vs 0.4027 ± 0.03 , $P < 0.01$) and pediatric non-HCC group (0.5665 ± 0.10 vs 0.4276 ± 0.15 , $P < 0.05$). The mean value of MVD in pediatric malignant liver tumors was significantly higher than that in adult HCC (33.66 ± 12.24 vs 26.52 ± 4.38 , $P < 0.05$). Furthermore, MVD in pediatric HCC group was significantly higher compared to that in adult HCC group (36.94 ± 9.28 vs 26.52 ± 4.38 , $P < 0.05$), but there was no significant difference compared to the pediatric non-HCC group (36.94 ± 9.28 vs 30.37 ± 14.61 , $P > 0.05$). All 7 children in HCC group died within 2 years, whereas the prognosis in pediatric non-HCC group was better, in which two patients survived more than 5 years.

CONCLUSION: Children with malignant liver tumors, especially with HCC, may have extensive angiogenesis that induces a rapid tumor growth and leads to a poor prognosis.

© 2005 The WJG Press and Elsevier Inc. All rights reserved.

Key words: Liver tumor; Angiogenesis; Vascular endothelial growth factor; Microvascular density

Sun XY, Wu ZD, Liao XF, Yuan JY. Tumor angiogenesis and its clinical significance in pediatric malignant liver tumor. *World J Gastroenterol* 2005; 11(5): 741-743

<http://www.wjgnet.com/1007-9327/11/741.asp>

INTRODUCTION

We reported a group of 26 children with primary liver malignant

tumor during a ten year period, in which hepatocellular carcinoma (HCC) was in the majority^[1]. These patients had a very poor prognosis due to frequent metastases and rapid recurrence, and died in a short time no matter what kind of therapeutic procedures was taken. The characteristics of pediatric malignant liver tumor, especially HCC, are worthwhile to be studied. Recently, the roles of vascular endothelial growth factor (VEGF) in the growth and metastasis of tumors have drawn extensive attention. We presume there is an unusual angiogenesis that might be related with VEGF expression in pediatric liver malignant tumor. In this study, we investigated the VEGF expression and microvascular density (MVD) in primary liver malignant tumor in children, and elucidated the possible reasons and correlative factors responsible for the high malignant behaviors of these tumors.

MATERIALS AND METHODS

Patients

Among 26 children with malignant liver tumor who were treated during 1992 to 2001, 14 cases (10 boys and 4 girls with an average age of 68.6 mo and range 0.8-182 mo) underwent surgery and were pathologically diagnosed as HCC (7 cases, 50%), hepatoblastoma (HB, 5 cases, 35.7%), malignant mesenchymoma (1 case, 7.14%) and rhabdomyosarcoma (1 case, 7.14%). In HCC group, 4 had multiple tumors and 3 had a single tumor in liver, but the patients with HB, malignant mesenchymoma or rhabdomyosarcoma had only single tumor in liver. Alpha-fetoprotein (AFP) and HBsAg in all patients were measured before operation.

Immunohistochemistry of VEGF and MVD

The specimens obtained from normal liver, tumor and tumor surrounding tissues were fixed in 100 mL/L formalin, embedded in paraffin and serially sectioned (4 μ m thick). Routine histopathologic evaluation of the tumor was performed using hematoxylin and eosin staining, streptavidin-biotin peroxidase (SP_{TM} kit, ZYMED, USA) procedure was used for immunohistochemical staining of VEGF and MVD. The first antibodies were rabbit anti-human VEGF polyclonal antibody (1:20, Santa Cruz Biotechnology, Inc) and mouse anti-human CD34 (endothelial cell marker for measuring MVD) monoclonal antibody (1:50, NeoMarkers), respectively. Another 12 specimens obtained from adult HCC (ranging in age from 36 to 59 years) were used as control. All steps of manipulation were carried out according to the manufacturer's instructions of the kit. Positive VEGF staining appeared as brown in cytoplasm was analyzed with microscopy and computer-image system (HPIAS-1000, QianPing Co.). The areas of positively stained cells in five visual fields were measured by HPIAS-1000 in each section. According to the criteria of Weidner *et al*^[2], the number of capillaries and microvessels which were endothelial-lined within tumor was measured by MVD count. The distribution of microvessels in each section was observed primarily under a low-power microscope, and then 5 fields with abundant microvessels were selected for counting under a high power microscope (400 magnification), and a mean value was calculated.

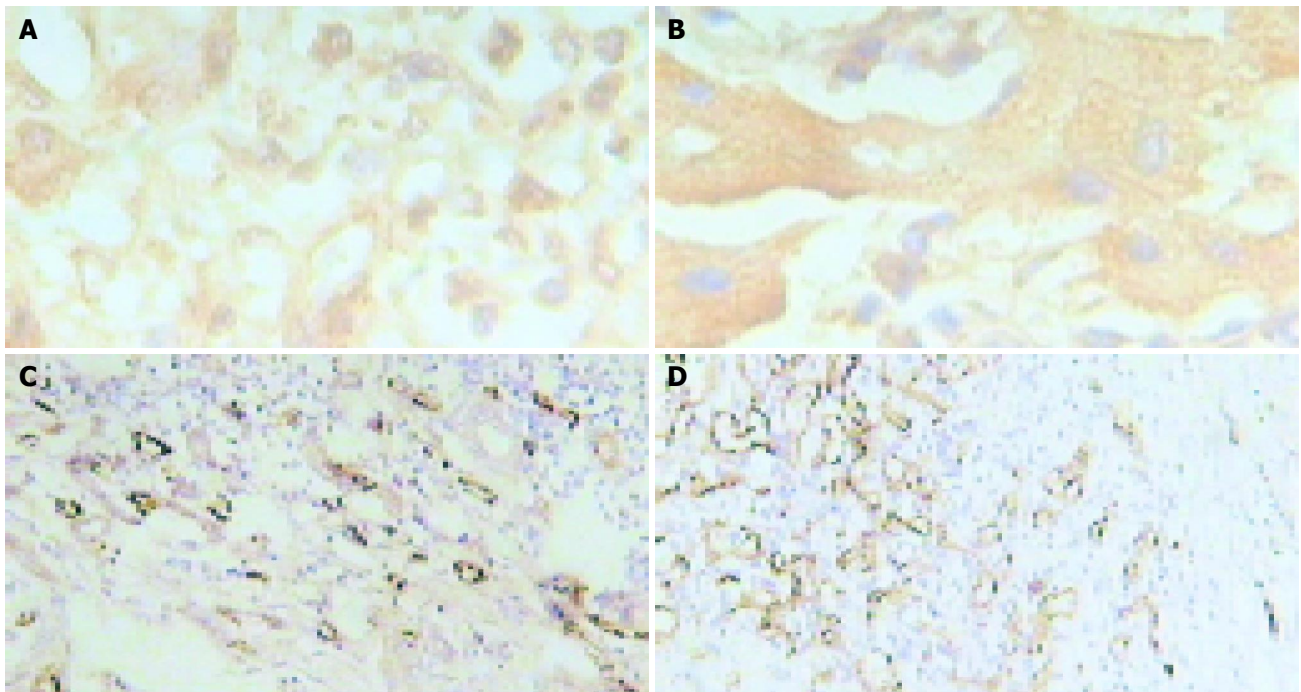


Figure 1 Immunohistochemical staining for VEGF expression ($\times 400$) and MVD ($\times 100$). A, B: Immunohistochemical staining for VEGF expression in HCC (A) and HB (B); C, D: Immunohistochemical staining for MVD ($\times 100$) in HCC (C) and HB (D).

Survival follow-up

The survival time of all children in HCC and non-HCC groups was calculated until their death or September of 2003, and described with the Kaplan-Meier curve.

Statistical analysis

The values of VEGF positive expression and MVD count were presented as mean \pm SD. Student's *t* test was used to analyse the data. $P < 0.05$ was considered statistically significant.

RESULTS

Clinical examination

In children with HCC, HB and two cases of malignant mesenchymoma or rhabdomyosarcoma, the positive rate of AFP was 71.2% (5/7), 100% (5/5) and 0%, respectively. The positive rate of HBsAg was 43% (3/7), 0% and 0%, respectively.

Table 1 VEGF expression and MVD count in each group (mean \pm SD)

Groups	VEGF	MVD
Pediatric malignant liver tumor group ($n = 14$)	0.4971 \pm 0.14 ^a	33.66 \pm 12.24 ^a
Pediatric HCC group ($n = 7$)	0.5665 \pm 0.10 ^b	36.94 \pm 9.28 ^a
Pediatric non-HCC group ($n = 7$)	0.4276 \pm 0.15 ^c	30.37 \pm 14.61
Adult HCC group ($n = 12$)	0.4027 \pm 0.03	26.52 \pm 4.38

^a $P < 0.05$, ^b $P < 0.01$ vs adult HCC group; ^c $P < 0.05$ vs pediatric HCC group.

VEGF expression and MVD count

VEGF positive expression was brown in sections of tumor tissue (Figures 1A, B). It was significantly higher in all pediatric malignant liver tumors than in adult HCC (0.4971 \pm 0.14 vs 0.4027 \pm 0.03, $P < 0.05$). VEGF expression in pediatric HCC group was also markedly higher than that in adult HCC group (0.5665 \pm 0.10 vs 0.4027 \pm 0.03, $P < 0.01$) and pediatric non-HCC group (0.5665 \pm 0.10 vs 0.4276 \pm 0.15, $P < 0.05$, Table 1). The distribution of microvessels

was asymmetric in tumor tissue and the densest distribution was in the edge of the tumor (Figures 1C, D). The mean value of MVD in pediatric malignant liver tumor was significantly higher than that in adult HCC (33.66 \pm 12.24 vs 26.52 \pm 4.38, $P < 0.05$, Table 1). Furthermore, MVD in pediatric HCC group was markedly higher compared to the adult HCC group (36.94 \pm 9.28 vs 26.52 \pm 4.38, $P < 0.05$), but there was no significant difference compared to the pediatric non-HCC group (36.94 \pm 9.28 vs 30.37 \pm 14.61, $P > 0.05$, Table 1).

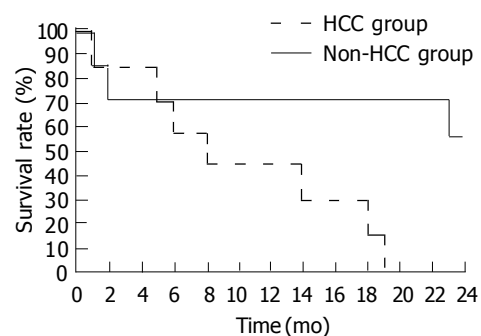


Figure 2 Survival rate described by Kaplan-Meier curve in children with HCC and non-HCC.

Survival rate

All patients were followed-up. All children in HCC group died within two years after operation. The patients in non-HCC group had a better prognosis. Among the survivors, two cases survived for over 5 years. Kaplan-Meier curve showed that although all patients underwent surgery procedures, there was a significant difference in survival rate between patients with HCC and without HCC, the survival rate of non-HCC group was notably higher than that of HCC group (Figure 2).

DISCUSSION

In this study, the clinical characteristics of pediatric primary

malignant liver tumor were as follows: (1) HCC cases outnumbered HB cases. This result was different from previous reports that the incidence of HB was the highest in pediatric malignant liver tumors^[3]. (2) HBsAg was positive in 43%(3/7) of all HCC cases, and negative in all HB cases, implying that hepatitis B virus (HBV) infection might be responsible for HCC in children. (3) AFP was positive in all HB and most HCC cases, but HBsAg and AFP were negative in patients with mesenchymoma or rhabdomyosarcoma. (4) The resection rate of pediatric malignant liver tumor was low, accounting for 38.5% (10/26) during the same period, and the resection rate of HCC was only 21.05% in this study.

Clinical results have shown pediatric malignant liver tumors grow rapidly and are often at the late stage when found or diagnosed. Furthermore, pediatric malignant liver tumors, especially HCC, have a very poor prognosis even if treated. In pediatric HCC group of our study, none survived for over two years. This poor prognosis might be due to the rapid recurrence and metastasis of pediatric malignant liver tumor even after surgical resection.

A more recent research indicates that the growth and metastasis of solid tumors are dependent on the formation of new blood vessels^[4]. The onset of angiogenesis is believed to be an early event in tumorigenesis and may facilitate tumor progression and metastasis^[5]. Several growth factors with angiogenic activity have been described, including fibroblast growth factor (FGF), platelet derived growth factor (PDGF) and VEGF. Among the angiogenesis factors, VEGF is the most important one and a hot spot of study at present. It has been reported that VEGF is a dimeric glycoprotein with a structural homology with PDGF^[6,7], and also a highly specific mitogen for blood vessel endothelial cells, which can stimulate endothelial cells of microvessels to proliferate and increase permeability, resulting in tumor angiogenesis^[8]. On the other hand, tumor MVD is not only the criterion for evaluating angiogenesis, but also has a close relation with malignant behaviors of tumor, such as recurrence and metastasis^[9]. The higher the density of the new blood vessels is in tumor, the worse the prognosis of patients is. Thus VEGF and MVD were chosen to measure and understand the angiogenesis event in pediatric liver malignant tumor in this study.

The VEGF expression and MVD count in pediatric malignant liver tumor, especially in pediatric HCC group, were significantly higher than those in adult HCC group. The results indicate there is stronger angiogenesis in pediatric liver malignant tumor which might be an important reason why tumor growth is faster and prognosis is poorer in children than in adults. Among the children with malignant liver tumor, VEGF positive expression and MVD count in HCC group were also higher than those in

non-HCC group. On the other hand, there were also significant differences in survival rate between HCC and non-HCC groups. Almost all patients in HCC group died within two years after operation, but more patients in non-HCC group survived for over two years. Two possibilities might be accountable for this outcome. First, since this study consisted of a small number of patients, the cases were not sufficient to reflect the different characteristics of angiogenesis of pediatric HCC and non-HCC. Second, except for angiogenesis, other factors, such as types of tumor, differentiation degree, course of disease, location and metastasis, might be responsible for the prognosis. In the non-HCC group, two patients with malignant mesenchymoma or rhabdomyosarcoma are still alive. Interestingly, although without statistical significance, their VEGF expression was negative.

The strong angiogenesis features in pediatric malignant liver tumor can predict the rapid growth, easy metastasis and recurrence, and extremely poor prognosis after operation. All these findings indicate that antiangiogenic therapy could prolong the survival time of malignant liver tumor patients after operation. The cause of the strong expression of VEGF and increased MVD in malignant liver tumor in children is still unclear, thus further studies are needed.

REFERENCES

- 1 Sun XY, Yuan JY, Chen XP. Diagnosis and treatment for liver malignant tumor in children. *J Hepatobiliary Surg* 2000; **8**: 180-182
- 2 Weidner N, Folkman J, Pozza F, Bevilacqua P, Allred EN, Moore DH, Meli S, Gasparini G. Tumor angiogenesis: a new significant and independent prognostic indicator in early-stage breast carcinoma. *J Natl Cancer Inst* 1992; **84**: 1875-1887
- 3 Chen JC, Chen CC, Chen WJ, Lai HS, Hung WT, Lee PH. Hepatocellular carcinoma in children: clinical review and comparison with adult cases. *J Pediatr Surg* 1998; **33**: 1350-1354
- 4 Du JR, Jiang Y, Zhang YM, Fu H. Vascular endothelial growth factor and microvascular density in esophageal and gastric carcinomas. *World J Gastroenterol* 2003; **9**: 1604-1606
- 5 Folkman J, Watson K, Ingber D, Hanahan D. Induction of angiogenesis during the transition from hyperplasia to neoplasia. *Nature* 1989; **339**: 58-61
- 6 Ferrara N, Houck KA, Jakeman LB, Winer J, Leung DW. The vascular endothelial growth factor family of polypeptides. *J Cell Biochem* 1991; **47**: 211-218
- 7 Plate KH, Breier G, Weich HA, Risau W. Vascular endothelial growth factor is a potential tumour angiogenesis factor in human gliomas *in vivo*. *Nature* 1992; **359**: 845-848
- 8 Bussolino F, Mantovani A, Persico G. Molecular mechanisms of blood vessel formation. *Trends Biochem Sci* 1997; **22**: 251-256
- 9 Acenero MJ, Gonzalez JF, Gallego MG, Ballesteros PA. Vascular enumeration as a significant prognosticator for invasive breast carcinoma. *J Clin Oncol* 1998; **17**: 1684-1688

Edited by Wang XL and Kumar M Proofread by Zhu LH

Association of cyclin D1, p16 and retinoblastoma protein expressions with prognosis and metastasis of gallbladder carcinoma

Hong-Bing Ma, Hai-Tao Hu, Zheng-Li Di, Zuo-Ren Wang, Jing-Sen Shi, Xi-Jing Wang, Yi Li

Hong-Bing Ma, Xi-Jing Wang, Yi Li, Department of Cancer Surgery, Second Hospital of Xi'an Jiaotong University, Xi'an 710004, Shaanxi Province, China

Hai-Tao Hu, Department of Human Anatomy, Medical College of Xi'an Jiaotong University, Xi'an 710068, Shaanxi Province, China

Zheng-Li Di, Department of Neurology, Xi'an Center Hospital, Xi'an 710003, Shaanxi Province, China

Zuo-Ren Wang, Jing-Sen Shi, Department of Hepatobiliary Surgery, First Hospital of Xi'an Jiaotong University, Xi'an 710061, Shaanxi Province, China

Correspondence to: Dr. Hong-Bing Ma, Department of Oncology, Second Hospital, Xi'an Jiaotong University, Xi'an 710004, Shaanxi Province, China. mhbmali@yahoo.com.cn

Telephone: +86-29-87679789

Received: 2004-02-27 **Accepted:** 2004-04-13

correlated with Nevin staging and pathologic grading in gallbladder carcinoma.

© 2005 The WJG Press and Elsevier Inc. All rights reserved.

Key words: Gallbladder carcinoma; Cyclin D1; p16 protein; Retinoblastoma protein; Tumor metastasis

Ma HB, Hu HT, Di ZL, Wang ZR, Shi JS, Wang XJ, Li Y. Association of cyclin D1, p16 and retinoblastoma protein expressions with prognosis and metastasis of gallbladder carcinoma. *World J Gastroenterol* 2005; 11(5): 744-747
<http://www.wjgnet.com/1007-9327/11/744.asp>

Abstract

AIM: To investigate the role of cyclin D1, p16 and retinoblastoma in cancerous process of gallbladder carcinomas and to assess the relation between cyclin D1, p16, Rb and the biological characteristics of gallbladder carcinoma.

METHODS: Forty-one gallbladder carcinoma, 7 gallbladder adenoma and 14 chronic cholecystitis specimens were immunohistochemically and histopathologically investigated for the relation of cyclin D1, p16 and Rb with Nevin staging and pathologic grading.

RESULTS: The expression rates of abnormal cyclin D1 in gallbladder carcinoma (68.3%) and gallbladder adenoma (57.1%) were significantly higher than those in chronic cholecystitis (7.1%) ($P < 0.05$). No significant difference was found both among the pathological grades G_1 , G_2 and G_3 and among Nevin stagings S_1 - S_2 , S_3 and S_4 - S_5 of gallbladder carcinoma. The positive rates of p16 (48.8%) and Rb (58.5%) in gallbladder carcinoma were significantly lower compared to those in adenoma (100.0%) and cholecystitis (100.0%) ($P < 0.05$). The positive rates of p16 and Rb in Nevin stagings S_1 - S_2 (80.0% and 90.0%) and S_3 (46.2% and 61.5%) gallbladder carcinomas were significantly higher than those in S_4 - S_5 (33.3% and 38.8%) ($P < 0.05$), and those in pathologic grades G_1 (54.5% and 81.8%) and G_2 (50.0% and 62.5%) gallbladder carcinoma were significantly higher than those in G_3 (28.6% and 35.7%) ($P < 0.05$). The protein expression of p16 and Rb had a negative-correlation in gallbladder carcinoma ($r = -0.2993$, $P < 0.05$), and this negative-correlation was correlated with Nevin staging ($P < 0.05$). Moreover, the protein expression of p16 and cyclin D1 had a negative-correlation in gallbladder carcinoma ($r = -0.9417$, $P < 0.05$).

CONCLUSION: Cyclin D1 may play a role in the early stage of gallbladder carcinoma. Mutation of p16 and Rb genes might be correlated with progression of gallbladder carcinoma. Analysis of p16 and Rb can estimate the prognosis of gallbladder carcinoma. Expression of p16 and Rb may be

INTRODUCTION

Primary carcinoma of gallbladder is a very lethal malignant tumor because of its early metastasis, strong invasion and poor prognosis. It is very important to estimate the malignant degree and invasion tendency in order to guide clinical diagnosis and treatment of gallbladder carcinoma^[1,2]. Cyclin D1 is considered as an oncogene and can promote progression of the cell cycle to S by cyclin D-dependent kinases (CDK4/CDK6)-mediated phosphorylation of the retinoblastoma (Rb) protein^[3,4]. The activities of CDK4/CDK6 are constrained by p16^[4,5]. The onset and progression of gallbladder carcinoma are accompanied with multiple genetic changes that result in qualitative and quantitative alterations in individual gene expression^[3-6]. By immunohistochemical methods, we analyzed cyclin D1, p16 and Rb expression levels in gallbladder carcinomas, adenomas and cholecystitis to evaluate their relationships with the pathogenesis, development and metastasis of gallbladder carcinoma.

MATERIALS AND METHODS

Materials

Sixty-two randomly chosen cholecystectomy specimens included 41 gallbladder carcinomas, 7 gallbladder adenomas and 14 chronic cholecystitis. The Nevin staging of gallbladder carcinoma, and pathologic grading of all cases were determined based on clinical materials. Ten cases were determined as S_1 - S_2 , 13 cases as S_3 and 18 cases as S_4 - S_5 , by Nevin staging. Eleven cases were determined as G_1 , 16 cases as G_2 and 14 cases as G_3 by pathologic grading. The polyclonal p16 antibody was rabbit antiserum against human p16 protein (Dako co, USA). The polyclonal Rb antibody was rabbit antiserum against human Rb protein (Santa Cruz, USA). The monoclonal cyclin D1 antibody was mouse antiserum against human cyclin D1 protein (Santa Cruz, USA).

Methods

Tissue specimens of gallbladder carcinoma were formalin-fixed and paraffin-embedded, and cut into 5 μ m thick sections for staining. The working concentrations of p16, cyclin D1 and Rb antibodies were 1:40, 1:80 and 1:100, respectively. Paraffin-embedded sections of gallbladder carcinoma tissue were dewaxed and dehydrated with ethanol. The sections were incubated with

3 mL/L H₂O₂-methyl alcohol for 30 min. The slides were incubated overnight with appropriate dilutions of monoclonal antibodies/polyclonal antibodies (McAbs/PcAbs) in PBS (pH 7.8) at 4 °C. After several washing steps, the reactivity was visualized using streptavidin/horseradish peroxidase-conjugated horse anti-mouse or goat anti-rabbit immunoglobulin (Zymed Co) diluted at 1:500 in PBS. Diaminobenzidine and hydrogen peroxide were used as substrates. Control slides were incubated with pre-immune sera or PBS. The protein expression was then scored arbitrarily according to the following scales: -, <25% positive cells; +, 25-50% positive cells; ++, >50-75% positive cells; and +++, >75% positive cells. All steps were carried out at room temperature. All reagents were equilibrated at room temperature.

Statistical analysis

Two×two contingency table, chi-square test, and correlation analysis were performed. SPSS 8.0 statistical software was used for calculation. $P<0.05$ was considered statistically significant.

RESULTS

Expression of p16, Rb and cyclin D1 gene in gallbladder carcinoma

The positive staining for p16 and Rb gene expressed as brown granules, was mainly located in nuclei of tumor cells, partly in cytoplasm (Figure 1: A, B). The positive staining for cyclin D1 gene expressed as brown granules, was distributed mainly in cell nuclei (Figure 1C).

The positive expression rates of cyclin D1, p16 and Rb are shown in Table 1. The abnormal cyclin D1 expression rate in gallbladder carcinoma and gallbladder adenoma was significantly higher than that in chronic cholecystitis ($P<0.05$). No significant difference was found between gallbladder carcinoma and adenoma, and in pathologic grades G₁, G₂ and G₃, and in Nevin stagings S₁-S₂, S₃ and S₄-S₅ of gallbladder carcinoma.

Table 1 Positive expression rates of Rb, p16 and cyclin D1

Disease	n	Rb		Cyclin D1		p16	
		+	%	+	%	+	%
Gallbladder carcinoma	41	24	58.7	28	68.3	20	48.8
Adenoma	7	7	100.0	4	57.1	7	100.0
Cholecystitis	14	14	100.0	1	7.1	13	92.8

The positive expression rates of p16 and Rb in gallbladder carcinomas were significantly higher than those in adenomas and cholecystitis ($P<0.05$). The positive expression rates of p16 and Rb in Nevin stagings S₁-S₂ and S₃ of gallbladder carcinoma were significantly higher than those in S₄-S₅ ($P<0.05$).

There was also a significant difference ($P<0.05$) in p16 and Rb expression between pathologic grades G₁ and G₃ of gallbladder carcinoma ($P<0.05$) (Table 2).

Table 2 Correlation between expression rates of Rb, p16 and cyclin D1, and carcinoma staging

Stages	n	Rb		Cyclin D1		p16		
		+	%	+	%	+	%	
Pathologic grading	G ₁	11	9	81.8	8	72.7	6	54.5
	G ₂	16	10	62.5	11	68.8	8	50.0
	G ₃	14	5	35.7	11	78.6	4	28.6
Nevin staging	S ₁ -S ₂	10	9	90.0	6	60.0	8	80.0
	S ₃	13	8	61.5	8	61.5	6	46.2
	S ₄ -S ₅	18	7	38.8	14	77.8	6	33.3

Correlation among Rb, cyclin D1 and p16 protein expression in gallbladder carcinoma

Among the 20 cases of p16-positive gallbladder cancer, 8 were Rb positive. Of the 24 cases of Rb-positive gallbladder cancer, 8 were p16 positive. Tumor suppressor gene p16 was correlated with Rb ($\chi^2 = 5.53$, $P<0.05$; $r = -0.2993$, $P<0.05$). There was a negative correlation between p16 and cyclin D1 ($\chi^2 = 6.03$, $P<0.05$; $r = -0.9417$, $P<0.05$), but no correlation between Rb and cyclin D1 ($\chi^2 = 1.20$) (Table 3).

Table 3 Relationship between expressions of Rb, cyclin D1 and p16 in gallbladder carcinoma

p16	Rb		Cyclin D1		Total
	+	-	+	-	
+	8	12	10	10	20
-	16	5	18	3	21
Total	24	17	28	13	41

DISCUSSION

It has been accepted that there is a restriction point in cell-cycle progression, the restriction point of G₁-S is important. Rb, p16 and cyclin D1 are major restriction factors in the restriction point. The cyclin D1/p16/Rb pathway plays a critical role in tumorigenesis and each component of this pathway may be affected by various malignancies^[7-11]. Cell-cycle progression is normally regulated by cyclins and cyclin inhibiting proteins. Progression of cells from G₁ to S phase is regulated via pRb phosphorylation by cyclin D complexed with cyclin-dependent kinases (CDK) 4 and 6, which are in turn regulated by CDK inhibitors, such as p16^{INK4} protein^[12]. pRb is underphosphorylated throughout G₁ phase and phosphorylated just before S phase^[12,13]. Hypophosphorylated pRb arrests cells in G₁ phase, and

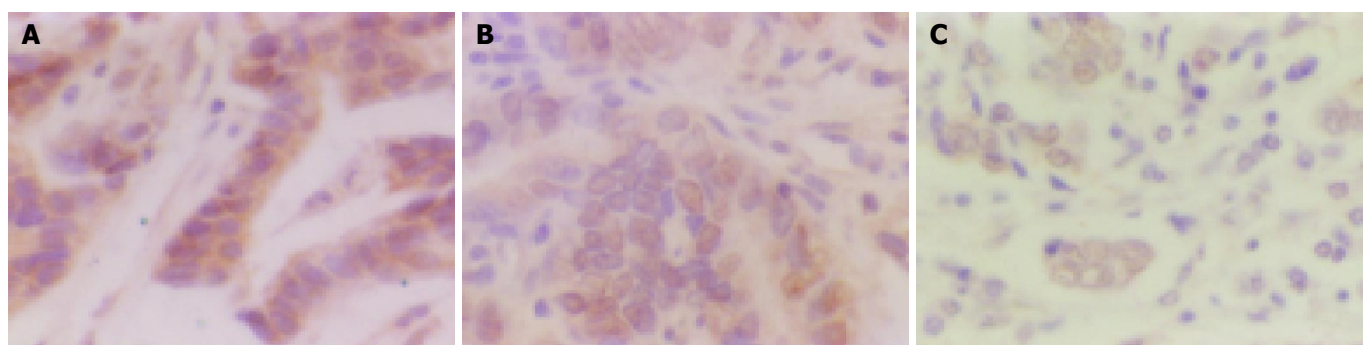


Figure 1 Immunohistochemical staining for Rb, p16 and cyclin D1 (×400). A: Rb-positive expression; B: p16-positive expression; C: cyclin D1-positive expression.

phosphorylation relieves this inhibition resulting in S phase entry^[12-14]. p16^{INK4} is associated with the cyclin D-CDK4 complex, preventing pRb phosphorylation and consequently, S phase entry^[15-18]. Dysregulation of the p16^{INK4}/pRb/cyclin D1 pathway has been reported in numerous tumor types^[19,20]. Inactivation of tumor suppressor gene products pRb and p16^{INK4} protein is a common event in human cancers^[9].

P16 gene located on chromosome 9p21, is a new tumor suppressor gene, which was identified by an American molecular geneticist in 1995 and is also called multiple tumor suppressor 1 (MTS1) for its suppressing function on multiple tumors^[16]. Rb gene is the first tumor suppressor gene located at chromosome 13q14 identified by the location cloning method. The product of Rb is a nuclear phosphoprotein. Loss of pRb has been demonstrated in a variety of cancers, including gastric, pancreatic and bladder cancers, small cell lung and colorectal carcinomas^[21-25].

Our study showed that the positive expression rates of p16 and Rb in gallbladder carcinoma were significantly lower than those in adenoma and cholecystitis. The positive expression rates of p16 and Rb in Nevin stagings S₁-S₂ and S₃ of gallbladder carcinoma were significantly higher than those in S₄-S₅. There was also a significant difference in p16 and Rb expressions between pathologic grades G₁ and G₃ of gallbladder carcinoma. These results suggest that loss and mutation of p16 play an important role in gallbladder carcinoma progression, and there is a consanguineous relation between p16 and invasion and metastasis of gallbladder carcinoma. p16 gene can inhibit the development of gallbladder carcinoma.

The overexpression of cyclin D1 has been reported in a wide range of human cancers^[26-28]. In our study the abnormal cyclin D1 expression rates in gallbladder carcinoma and adenoma were significantly higher than those in chronic cholecystitis. No significant difference was found in cyclin D1 expression between gallbladder carcinoma and adenoma. Similarly, there was no marked difference among the pathologic grades G₁, G₂ and G₃ and among Nevin stagings S₁-S₂, S₃ and S₄-S₅ of gallbladder carcinoma. Hui *et al*^[29] have suggested that cyclin D1 overexpression is an early event in gallbladder carcinogenesis and could independently predict the prognosis for patients with resectable gallbladder carcinoma.

Among the 20 cases of p16-positive gallbladder cancer, 8 were Rb positive. Of 24 cases of Rb-positive gallbladder cancer, 8 were p16 positive. Tumor suppressor gene p16 is correlated with Rb. Therefore, inactivation of pRb may stimulate cells to increase p16^{INK4} expression, which inhibits the activity of CDK4 and inactivates cyclin D1-CDK4 complex. On the contrary, pRb overexpression stimulates cells to increase p16^{INK4} protein loss, which enhances the activity of CDK4, thus inactivating excrescent pRb.

There is a negative correlation between p16 and cyclin D1. A close association of cyclin D1 overexpression with p16^{INK4} protein loss has been found in bladder cancer^[30] and hepatocellular carcinoma^[31,32]. Negative expression of p16^{INK4} protein and positive expression of cyclin D1 protein are significantly correlated to the high invasion and metastasis of tumor and the poor survival of patients.

In conclusion, disruption of the cyclin D1/p16^{INK4}-pRb pathway plays an important role in the progression of gallbladder carcinoma. Loss or decreased expression of p16 and pRb has an obvious correlation with malignant degree and metastasis of gallbladder carcinoma. Cyclin D1 overexpression is an early event in gallbladder carcinogenesis.

REFERENCES

- 1 Fan YZ, Zhang JT, Yang HC, Yang YQ. Expression of MMP-2, TIMP-2 protein and the ratio of MMP-2/TIMP-2 in gallbladder carcinoma and their significance. *World J Gastroenterol* 2002; **8**: 1138-1143
- 2 Taner CB, Nagorney DM, Donohue JH. Surgical treatment of gallbladder cancer. *J Gastrointest Surg* 2004; **8**: 83-89; discussion 89
- 3 Lerma E, Esteller M, Herman JG, Prat J. Alterations of the p16/Rb/cyclin-D1 pathway in vulvar carcinoma, vulvar intraepithelial neoplasia, and lichen sclerosus. *Hum Pathol* 2002; **33**: 1120-1125
- 4 Sdek P, Zhang Z, Cao J. Influence of HPV16 on expression of Rb, p16 and cyclin D1 in oral epithelial cell. *Zhonghua Kouqiang Yixue Zazhi* 2002; **37**: 84-86
- 5 Kramer A, Schultheis B, Bergmann J, Willer A, Hegenbart U, Ho AD, Goldschmidt H, Hehlmann R. Alterations of the cyclin D1/pRb/p16 (INK4A) pathway in multiple myeloma. *Leukemia* 2002; **16**: 1844-1851
- 6 Gerdes B, Ramaswamy A, Ziegler A, Lang SA, Kersting M, Baumann R, Wild A, Moll R, Rothmund M, Bartsch DK. p16INK4a is a prognostic marker in resected ductal pancreatic cancer: an analysis of p16INK4a, p53, MDM2, an Rb. *Ann Surg* 2002; **235**: 51-59
- 7 Hwang CF, Cho CL, Huang CC, Wang JS, Shih YL, Su CY, Chang HW. Loss of cyclin D1 and p16 expression correlates with local recurrence in nasopharyngeal carcinoma following radiotherapy. *Ann Oncol* 2002; **13**: 1246-1251
- 8 Cho NH, Kim YT, Kim JW. Alteration of cell cycle in cervical tumor associated with human papillomavirus: cyclin-dependent kinase inhibitors. *Yonsei Med J* 2002; **43**: 722-728
- 9 Ortega S, Malumbres M, Barbacid M. Cyclin D-dependent kinases, INK4 inhibitors and cancer. *Biochim Biophys Acta* 2002; **1602**: 73-87
- 10 Guner D, Sturm I, Hemmati P, Hermann S, Hauptmann S, Wurm R, Budach V, Dorken B, Lorenz M, Daniel PT. Multigene analysis of Rb pathway and apoptosis control in esophageal squamous cell carcinoma identifies patients with good prognosis. *Int J Cancer* 2003; **103**: 445-454
- 11 Choi YL, Park SH, Jang JJ, Park CK. Expression of the G1-S modulators in hepatitis B virus-related hepatocellular carcinoma and dysplastic nodule: association of cyclin D1 and p53 proteins with the progression of hepatocellular carcinoma. *J Korean Med Sci* 2001; **16**: 424-432
- 12 Beasley MB, Lantuejoul S, Abbondanzo S, Chu WS, Hasleton PS, Travis WD, Brambilla E. The P16/cyclin D1/Rb pathway in neuroendocrine tumors of the lung. *Hum Pathol* 2003; **34**: 136-142
- 13 Yoo J, Park SY, Kang SJ, Shim SI, Kim BK. Altered expression of G1 regulatory proteins in human soft tissue sarcomas. *Arch Pathol Lab Med* 2002; **126**: 567-573
- 14 Kang YK, Kim WH, Jang JJ. Expression of G1-S modulators (p53, p16, p27, cyclin D1, Rb) and Smad4/Dpc4 in intrahepatic cholangiocarcinoma. *Hum Pathol* 2002; **33**: 877-883
- 15 Kamb A, Gruis NA, Weaver-Feldhaus J, Liu Q, Harshman K, Tavtigian SV, Stockert E, Day RS, Johnson BE, Skolnick MH. A cell cycle regulator potentially involved in genesis of many tumor types. *Science* 1994; **264**: 436-440
- 16 Serrano M, Hannon GJ, Beach D. A new regulatory motif in cell-cycle control causing specific inhibition of cyclin D/CDK4. *Nature* 1993; **366**: 704-707
- 17 Bartkova J, Thullberg M, Slezak P, Jaramillo E, Rubio C, Thomassen LH, Bartek J. Aberrant expression of G1-phase cell cycle regulators in flat and exophytic adenomas of the human colon. *Gastroenterology* 2001; **120**: 1680-1688
- 18 Azechi H, Nishida N, Fukuda Y, Nishimura T, Minata M, Katsuma H, Kuno M, Ito T, Komeda T, Kita R, Takahashi R, Nakao K. Disruption of the p16/cyclin D1/retinoblastoma protein pathway in the majority of human hepatocellular carcinomas. *Oncology* 2001; **60**: 346-354
- 19 Shi YZ, Hui AM, Li X, Takayama T, Makuuchi M. Overexpression of retinoblastoma protein predicts decreased survival and correlates with loss of p16INK4 protein in gallbladder carcinomas. *Clin Cancer Res* 2000; **6**: 4096-4100
- 20 Feakins RM, Nickols CD, Bidd H, Walton SJ. Abnormal expression of pRb, p16, and cyclin D1 in gastric adenocarcinoma

- and its lymph node metastases: relationship with pathological features and survival. *Hum Pathol* 2003; **34**: 1276-1282
- 21 **Raghavan D.** Molecular targeting and pharmacogenomics in the management of advanced bladder cancer. *Cancer* 2003; **97**: 2083-2089
- 22 **Zhang R, Zhang JJ, He ZG, Cheng SJ, Gao YN.** Research advances on bladder cancer associated genes. *Aizheng* 2003; **22**: 104-107
- 23 **Gregorc V, Ludovini V, Pistola L, Darwish S, Floriani I, Bellezza G, Sidoni A, Cavaliere A, Scheibel M, De Angelis V, Bucciarelli E, Tonato M.** Relevance of p53, bcl-2 and Rb expression on resistance to cisplatin-based chemotherapy in advanced non-small cell lung cancer. *Lung Cancer* 2003; **39**: 41-48
- 24 **Pan MH, Chen WJ, Lin-Shiau SY, Ho CT, Lin JK.** Tangeretin induces cell-cycle G1 arrest through inhibiting cyclin-dependent kinases 2 and 4 activities as well as elevating Cdk inhibitors p21 and p27 in human colorectal carcinoma cells. *Carcinogenesis* 2002; **23**: 1677-1684
- 25 **Peiro G, Diebold J, Lohrs U.** CAS (cellular apoptosis susceptibility) gene expression in ovarian carcinoma: Correlation with 20q13.2 copy number and cyclin D1, p53, and Rb protein expression. *Am J Clin Pathol* 2002; **118**: 922-929
- 26 **Kumar RV, Kadkol SS, Daniel R, Shenoy AM, Shah KV.** Human papillomavirus, p53 and cyclin D1 expression in oropharyngeal carcinoma. *Int J Oral Maxillofac Surg* 2003; **32**: 539-543
- 27 **Lim SC, Zhang S, Ishii G, Endoh Y, Kodama K, Miyamoto S, Hayashi R, Ebihara S, Cho JS, Ochiai A.** Predictive markers for late cervical metastasis in stage I and II invasive squamous cell carcinoma of the oral tongue. *Clin Cancer Res* 2004; **10**: 166-172
- 28 **Cheung TH, Yu MM, Lo KW, Yim SF, Chung TK, Wong YF.** Alteration of cyclin D1 and CDK4 gene in carcinoma of uterine cervix. *Cancer Lett* 2001; **166**: 199-206
- 29 **Hui AM, Li X, Shi YZ, Takayama T, Torzilli G, Makuuchi M.** Cyclin D1 overexpression is a critical event in gallbladder carcinogenesis and independently predicts decreased survival for patients with gallbladder carcinoma. *Clin Cancer Res* 2000; **6**: 4272-4277
- 30 **Yang CC, Chu KC, Chen HY, Chen WC.** Expression of p16 and cyclin D1 in bladder cancer and correlation in cancer progression. *Urol Int* 2002; **69**: 190-194
- 31 **Huang GX, Cheng RX, Feng DY.** p16 and cyclinD1 protein expression and p16 gene mutation in primary human hepatocellular carcinoma. *Hunan Yike Daxue Xuebao* 2001; **26**: 527-530
- 32 **Ito Y, Matsuura N, Sakon M, Miyoshi E, Noda K, Takeda T, Umeshita K, Nagano H, Nakamori S, Dono K, Tsujimoto M, Nakahara M, Nakao K, Taniguchi N, Monden M.** Expression and prognostic roles of the G1-S modulators in hepatocellular carcinoma: p27 independently predicts the recurrence. *Hepatology* 1999; **30**: 90-99

Edited by Kumar M and Wang XL

Metastasis of primary gallbladder carcinoma in lymph node and liver

Han-Ting Lin, Gui-Jie Liu, Dan Wu, Jian-Ying Lou

Han-Ting Lin, Gui-Jie Liu, Dan Wu, Jian-Ying Lou, Department of General Surgery, the Second Affiliated Hospital of Medical College, Zhejiang University, Hangzhou 310009, Zhejiang Province, China
Correspondence to: Professor Han-Ting Lin, Department of General Surgery, the Second Affiliated Hospital of Medical College, Zhejiang University, Hangzhou 310009, Zhejiang Province, China. zjulgj@163.com

Telephone: +86-571-87783581

Received: 2004-04-09 **Accepted:** 2004-05-13

Abstract

AIM: To evaluate the patterns with metastasis of gallbladder carcinoma in lymph nodes and liver.

METHODS: A total of 45 patients who had radical surgery were selected. The patterns with metastasis of primary gallbladder carcinoma in lymph nodes and liver were examined histopathologically and classified as TNM staging of the American Joint Committee on Cancer.

RESULTS: Of the 45 patients, 29 (64.4%) had a lymph node positive disease and 20 (44.4%) had a direct invasion of the liver. The frequency of involvement of lymph nodes was strongly influenced by the depth of the primary tumor ($P = 0.0001$). The postoperative survival rate of patients with negative lymph node metastasis was significantly higher than that of patients with positive lymph node metastasis ($P = 0.004$), but the postoperative survival rate of patients with N1 lymph node metastasis was not significantly different from that of patients with N2 lymph node metastasis ($P = 0.3874$). The postoperative survival rate of patients without hepatic invasion was significantly better than that of patients with hepatic invasion ($P = 0.0177$).

CONCLUSION: Complete resection of the regional lymph nodes is important in advanced primary gallbladder carcinoma (PGC). The initial sites of liver spread are located mostly in segments IV and V. It is necessary to achieve negative surgical margins 2 cm from the tumor. In patients with hepatic hilum invasion, extended right hepatectomy with or without bile duct resection or portal vein resection is necessary for curative resection.

© 2005 The WJG Press and Elsevier Inc. All rights reserved.

Key words: Gallbladder carcinoma; Liver cancer; Lymph node metastasis

Lin HT, Liu GJ, Wu D, Lou JY. Metastasis of primary gallbladder carcinoma in lymph node and liver. *World J Gastroenterol* 2005; 11(5): 748-751

<http://www.wjgnet.com/1007-9327/11/748.asp>

INTRODUCTION

Primary gallbladder carcinoma (PGC) is one of the most common malignancies of the biliary tract with poor prognosis^[1,2], because

it is usually detected at an advanced stage due to no specific symptoms^[3]. The only potentially curative therapy for gallbladder carcinoma is surgical resection. The spread modes of gallbladder carcinoma are direct, lymphatic, vascular, neural, intraperitoneal, and intraductal. Liver and lymph nodes are the two most common sites of metastasis of gallbladder carcinoma^[4,5]. The purpose of the present study was to assess the spread patterns of gallbladder carcinoma and to discuss the related radical resection methods.

MATERIALS AND METHODS

Patients

From April 1994 to October 2003, a total of 138 patients with primary gallbladder carcinoma were treated in our hospital. Patients without surgery ($n = 36$) and patients with palliative surgery ($n = 57$) were excluded from the study. Forty-five patients undergone radical surgery were included in this study, 22 were men and 23 women, with a mean age of 61.22 years (range: 33-85 years).

Radical resection procedures

Radical resection was defined as the complete removal of a regional tumor with free surgical margins and positive lymph node metastasis restricted to the dissected area, as seen on postoperative histological examination.

The operative procedures are shown in Table 1. Simple cholecystectomy was performed in 3 patients, other patients underwent lymphadenectomy. The operative procedures included wedge resection ($n = 8$), resection of segments IV a and V ($n = 20$), resection of the bile duct ($n = 8$), extended right hepatectomy ($n = 2$), hepatopancreaticoduodenectomy ($n = 5$), and other organ tissue resection ($n = 6$), portal vein resection ($n = 2$), proper hepatic artery resection ($n = 1$). The resected specimens were examined histopathologically. Hepatic and lymph node specimens were especially concerned. The TNM system of the American Joint Committee on Cancer (AJCC) was used for staging.

Table 1 Radical procedures performed in 45 patients with gallbladder carcinoma

Type of resection	Patients (n)	Percent (%)	I	II	III	IV A	IV B
C	3	6.7	2	1			
C+N	7	15.6	2	3	2		
C+WR+N	8	17.8	1	2	2	1	2
C+S4aS5+N	6	13.3				4	2
C+S4aS5+BD+N	8	17.8				5	3
C+ERH+N	2	4.4				1	1
HPD+N	5	11.1				1	4
C+S4aS5+Other+N	6	13.3			1	2	3
Total	45	100	5	6	5	14	15

Abbreviations: C, cholecystectomy; N, lymphadenectomy; WR, wedge resection of the liver bed; S4aS5, liver resection of segments IV a and V; BD, resection of the bile duct; ERH, extended right hepatic resection; HPD, hepatopancreaticoduodenectomy; Other, other organ tissue resection.

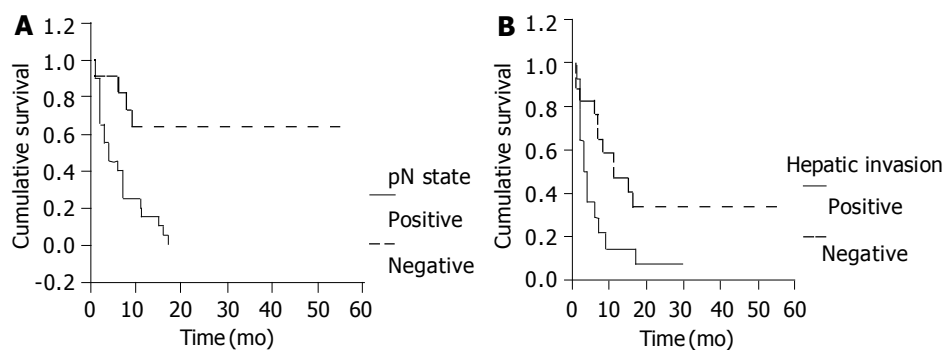


Figure 1 Postoperative survival rate depending on lymph node metastasis (A) and hepatic invasion (B).

Statistical analysis

Cumulative survival rate was determined with the Kaplan-Meier method. Differences in the survival curves were compared with the Log-rank test. $P < 0.05$ was considered statistically significant.

RESULTS

Pathologic features

The 29 patients (64.4%) with a lymph node-positive disease had N1 ($n = 15$) and N2 ($n = 14$) stages of primary gallbladder carcinoma. Of these patients, 7 had positive cystic nodes, 22 had positive pericholedochal nodes, 10 had positive hepatic hilum nodes, 2 had positive retroportal nodes, 3 had positive nodes along the common hepatic artery, 12 had positive posterosuperior pancreaticoduodenal nodes, 1 had positive celiac nodes, 1 had positive superior mesenteric nodes, 3 had positive nodes at the greater curvature of the stomach, 4 had positive para-aortic nodes. All patients with positive para-aortic nodes had N2 stage of primary gallbladder carcinoma. The relationship between N stage and T stage is shown in Table 2. The frequency of lymph node involvement was strongly influenced by the invasion depth of the primary tumor ($P = 0.0001$).

Primary lesions were located in the fundus ($n = 14$), body ($n = 12$), neck ($n = 7$), both in the fundus and in the body ($n = 2$), both in the fundus and in the neck ($n = 2$) of the gallbladder, and in the whole gallbladder ($n = 8$). In 31 patients, the primary lesions were extended out of the gallbladder into the surrounding tissues.

Tumors of gallbladder invaded into the liver ($n = 20$), segment IV ($n = 1$), segment V ($n = 2$), segments IV and V ($n = 15$), segments IV, V and VIII ($n = 2$). Tumors invaded into the bile duct ($n = 12$). There were 3 cases in the third stage. Locations of tumors were in the pancreatic head ($n = 4$), nerve ($n = 3$), portal vein ($n = 2$), proper hepatic artery ($n = 1$), duodenum ($n = 3$) and right transverse colon invasion ($n = 2$).

There were 2 patients with right hepatic metastasis, 2 with abdominal peritoneum metastasis, 1 with ileum metastasis. All metastatic lesions were completely resected.

Based on AJCC TNM staging system, the distributions were in T1 ($n = 6$), T2 ($n = 8$), T3 ($n = 5$), T4 ($n = 26$), N0 ($n = 16$), N1 ($n = 15$), N2 ($n = 14$), M0 ($n = 39$), M1 ($n = 6$). Five cases were stage I, six cases stage II, five cases stage III, fourteen cases stage IVA, and fifteen cases stage IVB.

Survival

Three cases died in hospital of postoperative hepatic failure. Postoperative morbidity and mortality rates of 45 patients were 33.3% and 6.7%, respectively. A total of 31 patients were followed up. Postoperative survival rate was poor in our series as compared to others, with an 1-year survival rate of 32.3% and 3-year survival rate of 9.7%. The postoperative survival rate of patients without lymph node metastasis was significantly

better than that of patients with lymph node metastasis ($P = 0.004$, Figure 1A), but the postoperative survival rate of patients with N1 lymph node metastasis was not significantly different from that of patients with N2 lymph node metastasis ($P = 0.3874$). The postoperative survival rate of patients without hepatic invasion was significantly better than that of patients with hepatic invasion ($P = 0.0177$, Figure 1B).

DISCUSSION

The prognosis of patients with gallbladder carcinoma remains dismal especially in advanced cases. The role of surgery in the treatment of gallbladder carcinoma is still controversial. The pattern and outcome of prospective radical surgery depend on the mode and degree of tumor spread^[6].

Lymph node spread

Shirai *et al*^[7] reported that gallbladder lymph circulated through the pericholedochal lymph nodes to the posterosuperior pancreaticoduodenal lymph nodes, and intraaortic lymph nodes. Ito *et al*^[8] have proposed three pathways of lymphatic drainage from the gallbladder: the cholecystoretropancreatic pathway, the cholecystoceliac pathway and the cholecystomesenteric pathway. But this does not concern the modes of flows to the hepatic hilum lymph nodes. This study also shows that the hepatic hilum lymph node metastasis is a common lymph node metastasis position (10 patients, 34.5%). The cystic and pericholedochal lymph nodes are the initial spreading sites from PBC.

The prognosis of PGC is strongly affected by their lymph node status^[9,10]. Some authors indicate that there is no difference in survival between N0 and N1 patients, while patients with a N2 disease have a significantly worse prognosis^[11]. Some authors indicate that there is no difference in survival between N1 and N2 patients, while patients with a N0 disease have a significantly better prognosis^[12]. This study shows that N0 patients have a significantly better survival than N1 patients, but there is no difference in survival between N1 and N2 patients. The different conclusions may be due to the different radical procedures. After a complete resection of the posterosuperior pancreaticoduodenal nodes, superior mesenteric nodes and celiac nodes, even para-aortic lymph nodes, N2 patients could get a survival rate as N1 patients.

Conflicting radical resection of lymph node metastasis was reported. Benoist *et al*^[1] advocate that radical resection should only be considered in the absence of regional lymph node metastasis, while Chijiwa *et al*^[9] believe that radical resection should be done for patients with involvement confined to the hepatoduodenal ligaments, posterosuperior pancreaticoduodenal area, and the common hepatic artery, but do not advocate radical resection for patients with superior mesenteric node, celiac node, and para-aortic lymph node

metastases. Tsukada *et al*^[11] suggest a more extensive dissection even with pancreaticoduodenectomy and resection of the para-aortic lymph nodes in selected patients. This study also shows that N2 patients with a more extensive dissection could get a better prognosis than N1 patients.

Some authors advocate that there is no lymph node metastasis in T1 patients^[11,13,14]. One T1 patient had pN1 lymph node metastasis (the primary lesion invaded muscle layer) (Table 2), 1 patient had N1 lymph node metastasis and 1 had both N2 and para-aortic lymph node metastases in T2 patients. Complete removal of regional lymph nodes is important in advanced PGC, only patients with tumor lesions lying in mucosae could be treated with simply cholecystectomy^[15]. Radical resection is comprised of resection of the lymph nodes around the head of pancreas, including the lymph nodes along the common hepatic artery, celiac nodes, retroportal lymph nodes, and para-aortic lymph nodes in the aorticocaval space^[16]. A sampling biopsy of para-aortic nodes may be useful before starting a radical resection^[17]. If hepatic hilum lymph nodes are positive, resection of segments IV a and V would be necessary to prevent lymphatic hepatic metastasis^[18].

Table 2 Comparison of depth of invasion of the tumor (T) and lymph node metastases (N)

Depth of tumor	No. of patients with lymph node metastasis			
	N0	N1	N2	Para-aortic lymph node
T1 (n = 6)	5	1	0	0
T2 (n = 8)	6	1	1	1
T3 (n = 5)	1	2	2	0
T4 (n = 26)	4	11	11	3
Total (n = 45)	16	15	14	4

T and N were based on TNM staging of the American Joint Committee on Cancer (AJCC).

Hepatic spread

Shirai *et al*^[19] reported three patterns of direct hepatic invasion. Some authors indicate that venous blood from the gallbladder is drained into segments IV and V by short direct communicating veins or by veins accompanying the extrahepatic ducts into the liver^[20]. This explains why the initial location of liver metastasis is to the portions adjacent to the gallbladder, mostly in segments IV and V, rather than the distant sites of the liver. According to Yoshimitsu *et al*^[21], 96% of gallbladder veins end in the intrahepatic portal branches of segment V, 93% of gallbladder veins end in the intrahepatic portal branches of segment IV. The portal tract lymphatic retrograde spread may be a reason of gallbladder metastasis. This study shows that the most common hepatic spread position is segments IV and V (15 patients, 75%).

Ogura *et al*^[22] reported two patterns of hepatic infiltration, the extensive pattern and the infiltrating pattern. Two modes of tumor invasion have been noted in the infiltrating pattern, the most common site of the main tumor is located in hepatic parenchyma, the front of carcinoma involving vascular infiltration invades the hepatic hilum along the Glisson's sheath. Localized hepatic metastases from gallbladder carcinoma near the gallbladder bed are also reported^[19]. The most important route of early hepatic metastasis from gallbladder carcinoma seems to be the portal tracts^[23].

Hepatic resection for advanced carcinoma of the gallbladder must be decided on the basis of the modes of tumor spread to the liver. Wedge resection or resection of segments IV a and V should be considered as an adequate hepatectomy for patients

with subserosal invasion^[24,25], because early metastasis foci have been detected not only in patients with direct invasion of the liver but also in those without direct invasion. Various degrees of hepatic resection are needed to comply with the depth of direct invasion. It is necessary to achieve negative surgical margins 2 cm from the tumor. In patients with hepatic hilum invasion, extended right hepatectomy with or without bile duct resection or portal vein resection would be necessary for curative resection because the front of carcinoma invasion along the Glisson's sheath is often longer than the extensive pattern tumors. A caudate lobectomy is often needed for this type of radical resection^[22,26]. Central bisegmentectomy plus caudate lobectomy is a useful procedure for infiltrating type of gallbladder carcinoma^[27].

In conclusion, complete excision of regional lymph nodes is important in advanced PGC, only patients with tumors lying in mucosae can be treated with simpl cholecystectomy. In patients with hepatic hilum invasion, extended right hepatectomy with or without bile duct resection or portal vein resection is necessary for curative resection.

REFERENCES

- 1 **Benoist S**, Panis Y, Fagniez PL. Long-term results after curative resection for carcinoma of the gallbladder. French University Association for Surgical Research. *Am J Surg* 1998; **175**: 118-122
- 2 **Ishikawa T**, Horimi T, Shima Y, Okabayashi T, Nishioka Y, Hamada M, Ichikawa J, Tsuji A, Takamatsu M, Morita S. Evaluation of aggressive surgical treatment for advanced carcinoma of the gallbladder. *J Hepatobiliary Pancreat Surg* 2003; **10**: 233-238
- 3 **Donohue JH**. Present status of the diagnosis and treatment of gallbladder carcinoma. *J Hepatobiliary Pancreat Surg* 2001; **8**: 530-534
- 4 **Kokudo N**, Makuuchi M, Natori T, Sakamoto Y, Yamamoto J, Seki M, Noie T, Sugawara Y, Imamura H, Asahara S, Ikari T. Strategies for surgical treatment of gallbladder carcinoma based on information available before resection. *Arch Surg* 2003; **138**: 741-750; discussion 750
- 5 **Ohtani T**, Shirai Y, Tsukada K, Muto T, Hatakeyama K. Spread of gallbladder carcinoma: CT evaluation with pathologic correlation. *Abdom Imaging* 1996; **21**: 195-201
- 6 **Noshiro H**, Chijiwa K, Yamaguchi K, Shimizu S, Sugitani A, Tanaka M. Factors affecting surgical outcome for gallbladder carcinoma. *Hepatogastroenterology* 2003; **50**: 939-944
- 7 **Shirai Y**, Yoshida K, Tsukada K, Ohtani T, Muto T. Identification of the regional lymphatic system of the gallbladder by vital staining. *Br J Surg* 1992; **79**: 659-662
- 8 **Ito M**, Mishima Y, Sato T. An anatomical study of the lymphatic drainage of the gallbladder. *Surg Radiol Anat* 1991; **13**: 89-104
- 9 **Chijiwa K**, Noshiro H, Nakano K, Okido M, Sugitani A, Yamaguchi K, Tanaka M. Role of surgery for gallbladder carcinoma with special reference to lymph node metastasis and stage using western and Japanese classification systems. *World J Surg* 2000; **24**: 1271-1277
- 10 **Shimada H**, Endo I, Togo S, Nakano A, Izumi T, Nakagawara G. The role of lymph node dissection in the treatment of gallbladder carcinoma. *Cancer* 1997; **79**: 892-899
- 11 **Tsukada K**, Kurosaki I, Uchida K, Shirai Y, Ohashi Y, Yokoyama N, Watanabe H, Hatakeyama K. Lymph node spread from carcinoma of the gallbladder. *Cancer* 1997; **80**: 661-667
- 12 **Shimada H**, Endo I, Fujii Y, Kamiya N, Masunari H, Kunihiro O, Tanaka K, Misuta K, Togo S. Appraisal of surgical resection of gallbladder cancer with special reference to lymph node dissection. *Langenbecks Arch Surg* 2000; **385**: 509-514
- 13 **Wakai T**, Shirai Y, Yokoyama N, Nagakura S, Watanabe H, Hatakeyama K. Early gallbladder carcinoma does not warrant radical resection. *Br J Surg* 2001; **88**: 675-678

- 14 **Toyonaga T**, Chijiwa K, Nakano K, Noshiro H, Yamaguchi K, Sada M, Terasaka R, Konomi K, Nishikata F, Tanaka M. Completion radical surgery after cholecystectomy for accidentally undiagnosed gallbladder carcinoma. *World J Surg* 2003; **27**: 266-271
- 15 **Waghlikar GD**, Behari A, Krishnani N, Kumar A, Sikora SS, Saxena R, Kapoor VK. Early gallbladder cancer. *J Am Coll Surg* 2002; **194**: 137-141
- 16 **Noie T**, Kubota K, Abe H, Kimura W, Harihara Y, Takayama T, Makuuchi M. Proposal on the extent of lymph node dissection for gallbladder carcinoma. *Hepatogastroenterology* 1999; **46**: 2122-2127
- 17 **Kondo S**, Nimura Y, Hayakawa N, Kamiya J, Nagino M, Uesaka K. Regional and para-aortic lymphadenectomy in radical surgery for advanced gallbladder carcinoma. *Br J Surg* 2000; **87**: 418-422
- 18 **Uesaka K**, Yasui K, Morimoto T, Torii A, Yamamura Y, Kodera Y, Hirai T, Kato T, Kito T. Visualization of routes of lymphatic drainage of the gallbladder with a carbon particle suspension. *J Am Coll Surg* 1996; **183**: 345-350
- 19 **Shirai Y**, Tsukada K, Ohtani T, Watanabe H, Hatakeyama K. Hepatic metastases from carcinoma of the gallbladder. *Cancer* 1995; **75**: 2063-2068
- 20 **Boerma EJ**. Towards an oncological resection of gall bladder cancer. *Eur J Surg Oncol* 1994; **20**: 537-544
- 21 **Yoshimitsu K**, Honda H, Kaneko K, Kuroiwa T, Irie H, Chijiwa K, Takenaka K, Masuda K. Anatomy and clinical importance of cholecystic venous drainage: helical CT observations during injection of contrast medium into the cholecystic artery. *AJR Am J Roentgenol* 1997; **169**: 505-510
- 22 **Ogura Y**, Tabata M, Kawarada Y, Mizumoto R. Effect of hepatic invasion on the choice of hepatic resection for advanced carcinoma of the gallbladder: histologic analysis of 32 surgical cases. *World J Surg* 1998; **22**: 262-266; discussion 266-267.
- 23 **Ohtsuka M**, Miyazaki M, Itoh H, Nakagawa K, Ambiru S, Shimizu H, Nakajima N, Akikusa B, Kondo Y. Routes of hepatic metastasis of gallbladder carcinoma. *Am J Clin Pathol* 1998; **109**: 62-68
- 24 **Suzuki S**, Yokoi Y, Kurachi K, Inaba K, Ota S, Azuma M, Konno H, Baba S, Nakamura S. Appraisal of surgical treatment for pT2 gallbladder carcinomas. *World J Surg* 2004; **28**: 160-165
- 25 **Chijiwa K**, Nakano K, Ueda J, Noshiro H, Nagai E, Yamaguchi K, Tanaka M. Surgical treatment of patients with T2 gallbladder carcinoma invading the subserosal layer. *J Am Coll Surg* 2001; **192**: 600-607
- 26 **Kondo S**, Nimura Y, Kamiya J, Nagino M, Kanai M, Uesaka K, Hayakawa N. Mode of tumor spread and surgical strategy in gallbladder carcinoma. *Langenbecks Arch Surg* 2002; **387**: 222-228
- 27 **Ogura Y**, Matsuda S, Sakurai H, Kawarada Y, Mizumoto R. Central bisegmentectomy of the liver plus caudate lobectomy for carcinoma of the gallbladder. *Dig Surg* 1998; **15**: 218-223

Edited by Wang XL and Ren SR

Role of PGI₂ in the formation and maintenance of hyperdynamic circulatory state of portal hypertensive rats

Zhi-Yong Wu, Xue-Song Chen, Jiang-Feng Qiu, Hui Cao

Zhi-Yong Wu, Xue-Song Chen, Jiang-Feng Qiu, Hui Cao, Department of General Surgery, Renji Hospital, Shanghai Second Medical University, Shanghai 200127, China

Correspondence to: Dr. Zhi-Yong Wu, Department of General Surgery, Renji Hospital, 1630 Dongfang Road, Shanghai 200127, China. zhengwk@online.sh.cn

Telephone: +86-21-50905336

Received: 2004-04-24 Accepted: 2004-05-09

Abstract

AIM: To investigate the role of prostacyclin (PGI₂) and nitric oxide (NO) in the development and maintenance of hyperdynamic circulatory state of chronic portal hypertensive rats.

METHODS: Ninety male Sprague-Dawley rats were divided into three groups: intrahepatic portal hypertension (IHPH) group by injection of CCl₄, prehepatic portal hypertension (PHPH) group by partial stenosis of the portal vein and sham-operation control (SO) group. One week after the models were made, animals in each group were subdivided into 4 groups: saline controlled group ($n = 23$), N α -nitro-L-arginine (L-NNA) group ($n = 21$), indomethacin (INDO) group ($n = 22$) and high-dose heparin group ($n = 24$). The rats were administrated 1 mL of saline, L-NNA (3.3 mg/kg·d) and INDO (5 mg/kg·d) respectively through gastric tubes for one week, then heparin (200 IU/Kg/min) was given to rats by intravenous injection for an hour. Splanchnic and systemic hemodynamics were measured using radioactive microsphere techniques. The serum nitrate/nitrite (NO₂/NO₃) levels as a marker of production of NO were assessed by a colorimetric method, and concentration of 6-keto-PGF_{1 α} , a stable hydrolytic product of PGI₂, was determined by radioimmunoassay.

RESULTS: The concentrations of plasma 6-keto-PGF_{1 α} (pg/mL) and serum NO₂/NO₃ (μ mol/L) in IHPH rats (1123.85±153.64, 73.34±4.31) and PHPH rats (891.88±83.11, 75.21±6.89) were significantly higher than those in SO rats (725.53±105.54, 58.79±8.47) ($P < 0.05$). Compared with SO rats, total peripheral vascular resistance (TPR) and splanchnic vascular resistance (SVR) decreased but cardiac index (CI) and portal venous inflow (PVI) increased obviously in IHPH and PHPH rats ($P < 0.05$). L-NNA and indomethacin could decrease the concentrations of plasma 6-keto-PGF_{1 α} and serum NO₂/NO₃ in IHPH and PHPH rats ($P < 0.05$). Meanwhile, CI, FPP and PVI lowered but MAP, TPR and SVR increased ($P < 0.05$). After deduction of the action of NO, there was no significant correlation between plasma PGI₂ level and hemodynamic parameters such as CI, TPR, PVI and SVR. However, after deduction of the action of PGI₂, NO still correlated highly with the hemodynamic parameters, indicating that there was a close correlation between NO and the hemodynamic parameters. After administration of high-dose heparin, plasma 6-keto-

PGF_{1 α} concentrations in IHPH, PHPH and SO rats were significantly higher than those in rats administrated vehicle ($P < 0.05$). On the contrary, levels of serum NO₂/NO₃ in IHPH, PHPH and SO rats were significantly lower than those in rats administrated Vehicle ($P < 0.05$). Compared with those rats administrated vehicle, the hemodynamic parameters of portal hypertensive rats, such as CI and PVI, declined significantly after administration of high-dose heparin ($P < 0.05$), while TPR and SVR increased significantly ($P < 0.05$).

CONCLUSION: It is NO rather than PGI₂ that is a mediator in the formation and maintenance of hyperdynamic circulatory state of chronic portal hypertensive rats.

© 2005 The WJG Press and Elsevier Inc. All rights reserved.

Key words: Portal hypertension; Prostacyclin; Nitric oxide; Hyperdynamic circulatory

Wu ZY, Chen XS, Qiu JF, Cao H. Role of PGI₂ in the formation and maintenance of hyperdynamic circulatory state of portal hypertensive rats. *World J Gastroenterol* 2005; 11(5): 752-755

<http://www.wjgnet.com/1007-9327/11/752.asp>

INTRODUCTION

It is well established that systemic and splanchnic hyperdynamic circulatory state plays an important role in maintaining and aggravating the high portal venous pressure. However, the underlying mechanisms have not been completely understood. Recent studies suggest that vasodilators such as nitric oxide (NO) and prostacyclin (PGI₂) contribute much to hyperdynamic circulation^[1,2].

NO may be a mediator in the pathogenesis of hyperdynamic circulatory state, but whether PGI₂ plays the same role is still controversial^[3,4]. In order to elucidate the relative contribution of PGI₂, NO and the possible interaction between these two vasodilators in the development of hyperdynamic circulatory state of chronic portal hypertensive rats, we designed the experiment to detect the plasma PGI₂, NO level and hemodynamic effects of NO inhibitor (L-NNA), COX₂ inhibitor (indomethacin) and high-dose heparin on IHPH, PHPH and SO rats.

MATERIALS AND METHODS

Experimental model

Ninety adult male Sprague-Dawley rats (weighing 300±50 g) were used in all experiments. Animals were housed in an environmentally controlled vivarium with light control (12 h light-dark cycle) and allowed free access to standard pellet diet and water. Survival surgery and hemodynamic studies were performed in strict sterile conditions under ketamine hydrochloride anesthesia (100 mg/kg, im). The temperature of rats was maintained at 37±0.5 °C by a heating lamp and

monitored by a rectal probe. Experimental animals were randomly divided into three groups: IHPH, PHPH and SO.

IHPH was induced in 22 rats by injection of CCl₄ according to a previously reported method^[5]. Briefly, the rats were injected 15 times intramuscularly with (0.3 mL/100 g, first time injection of 0.5 mL/100 g) 60% CCl₄ in mineral oil, once every four days, and were given 10% alcohol instead of water. PHPH was induced in 20 rats by partial portal vein ligation according to a previously reported method^[6]. In brief, the portal vein was isolated and a calibrated stenosis was performed with a single 3-0 silk ligature around a 20-gauge blunt-tipped needle. The needle was then removed, and the portal vein was allowed to reexpand. The viscera were placed back into the abdomen, and the incision was closed in two layers with suture. Antibiotic ointment was applied to the surgical wound. SO was made in 24 rats.

Experimental scheme

One week after the models were made, animals in each group were subdivided into 4 groups: saline controlled group ($n = 23$), N ω -nitro-L-arginine (L-NNA) group ($n = 21$), indomethacin (INDO) group ($n = 22$) and high-dose heparin group ($n = 24$). Rats were administered 1 mL of saline, L-NNA (dissolved in 1 mL saline at the dose of 3.3 mg/kg·d) and INDO (dissolved in 1 mL saline at the dose of 5 mg/kg·d) respectively through gastric tubes for one week, then 1 mL heparin solution at the dose of 200 IU/Kg/min and 1 mL saline were given to high-dose heparin group rats and saline controlled rats respectively by intravenous injection for an hour.

Hemodynamic study

Splanchnic and systemic hemodynamic parameters including mean arterial blood pressure (MAP), free portal pressure (FPP), cardiac index (CI), portal venous inflow (PVI), total peripheral

vascular resistance (TPR) and splanchnic vascular resistance (SVR) were measured using radioactive microsphere techniques^[7].

Assay of 6-keto-PGF_{1 α} and NO₂/NO₃⁻

The concentration of 6-keto-PGF_{1 α} in the plasma, a stable metabolite of PGI₂, was measured by radioimmunoassay as described previously, and NO₂⁻/NO₃⁻ were determined in serum by a colorimetric method according to a previous method^[8].

Statistical analysis

All data were expressed as mean \pm SD. Statistical analysis was performed using SPSS10.0 package of statistical programs. Comparisons of means in three models and subgroups were performed by one-way ANOVA. Pearson's correlation analysis was performed for selected variables. $P < 0.05$ was taken as statistically significant.

RESULTS

Effects of L-NNA and INDO on plasma PGI₂ and NO concentrations

The concentrations of plasma 6-keto-PGF_{1 α} (pg/mL) and NO₂⁻/NO₃⁻ in both IHPH and PHPH rats were significantly higher than those in SO rats ($P < 0.05$). Compared with controlled group, both L-NNA and indomethacin reduced the plasma 6-keto-PGF_{1 α} (pg/mL) and NO₂⁻/NO₃⁻ concentrations (Table 1) ($P < 0.05$).

Effects of L-NNA and INDO on systemic and splanchnic hemodynamics

In basal state, MAP and TPR were significantly decreased but CI was increased in IHPH and PHPH rats when compared with SO rats ($P < 0.05$). Compared with controlled group, the CI decreased while the MAP and TPR in IHPH and PHPH rats elevated after L-NNA or INDO was given (Table 2) ($P < 0.05$).

Table 1 Effects of L-NNA and INDO on plasma PGI₂ and NO concentrations (mean \pm SD)

Group	Vehicle ($n = 23$)	L-NNA ($n = 21$)	Indo ($n = 22$)	Heparin ($n = 24$)
6-keto-PGF _{1α} (pg/mL)				
SO	725.53 \pm 105.54	748.48 \pm 67.68	336.91 \pm 37.05 ^c	3 965.96 \pm 976.82 ^c
IHPH	1 123.85 \pm 153.64 ^a	494.74 \pm 145.98 ^{ac}	342.86 \pm 104.79 ^{ac}	2 930.61 \pm 1 400.38 ^c
PHPH	891.88 \pm 83.11 ^a	386.54 \pm 98.44 ^{ac}	266.94 \pm 57.63 ^c	2 766.47 \pm 506.95 ^c
NO ₂ ⁻ /NO ₃ ⁻ (μ mol/L)				
SO	58.79 \pm 8.47	21.31 \pm 1.76 ^c	55.72 \pm 5.33	45.28 \pm 4.398 ^c
IHPH	73.34 \pm 4.31 ^a	40.17 \pm 10.32 ^{ac}	46.42 \pm 7.43 ^{ac}	54.02 \pm 11.89 ^{ac}
PHPH	75.21 \pm 6.89 ^a	30.45 \pm 3.28 ^{ac}	54.74 \pm 4.39 ^c	62.06 \pm 3.56 ^{ac}

^a $P < 0.05$ vs SO; ^c $P < 0.05$ vs control.

Table 2 Effects of L-NNA and INDO on systemic hemodynamics (mean \pm SD)

Group	Vehicle ($n = 23$)	L-NNA ($n = 21$)	Indo ($n = 22$)	Heparin ($n = 24$)
MAP (mmHg)				
SO	141.86 \pm 3.02	159.29 \pm 1.98 ^c	145.86 \pm 3.72	157.33 \pm 3.77 ^c
IHPH	134.00 \pm 1.83 ^a	161.50 \pm 6.14 ^c	161.14 \pm 4.45 ^{ac}	137.88 \pm 2.17 ^a
PHPH	130.29 \pm 1.89 ^a	142.50 \pm 4.37 ^{ac}	147.71 \pm 2.75 ^c	138.29 \pm 4.39 ^{ac}
CI (mL/min)				
SO	28.46 \pm 0.58	25.34 \pm 2.22 ^c	27.20 \pm 0.61	23.52 \pm 0.72 ^c
IHPH	32.03 \pm 1.34 ^a	25.03 \pm 1.76 ^c	28.66 \pm 1.63 ^c	28.39 \pm 2.25 ^a
PHPH	33.19 \pm 0.66 ^a	28.13 \pm 0.51 ^{ac}	29.62 \pm 1.16 ^{ac}	26.67 \pm 0.66 ^{ac}
TPR (mmHg/mL·min)				
SO	4.99 \pm 0.13	6.33 \pm 0.60 ^c	5.36 \pm 0.13	6.70 \pm 0.33 ^c
IHPH	4.19 \pm 0.18 ^a	6.48 \pm 0.53 ^c	5.64 \pm 0.42 ^c	4.88 \pm 0.36 ^a
PHPH	3.93 \pm 0.06 ^a	5.07 \pm 0.19 ^{ac}	5.00 \pm 0.33 ^{ac}	5.18 \pm 0.21 ^{ac}

^a $P < 0.05$ vs SO; ^c $P < 0.05$ vs control.

Table 3 Effects of L-NNA and INDO on systemic and splanchnic hemodynamics (mean±SD)

Group	Vehicle (n = 23)	L-NNA (n = 21)	Indo (n = 22)	Heparin (n = 24)
FPP (mmHg)				
SO	6.93±0.35	7.29±0.39	7.07±0.35	7.06±0.39
IHPH	10.29±0.39 ^a	8.75±0.46 ^{ac}	9.28±0.57 ^{ac}	9.25±0.65 ^{ac}
PHPH	13.71±0.49 ^a	10.05±0.45 ^{ac}	11.57±0.53 ^{ac}	11.07±0.79 ^a
PVI (mL/min)				
SO	2.35±0.27	1.06±0.20 ^c	1.63±0.17 ^c	1.57±0.31 ^c
IHPH	3.83±0.64 ^a	2.34±0.50 ^{ac}	2.16±0.59 ^c	2.05±0.62 ^{ac}
PHPH	7.37±1.56 ^a	3.71±0.53 ^{ac}	3.77±0.81 ^{ac}	2.35±0.25 ^{ac}
SVR (mmHg/mL·min)				
SO	58.06±6.95	96.18±13.71 ^c	85.56±8.13 ^c	99.36±20.26 ^c
IHPH	32.96±5.09 ^a	67.83±14.33 ^{ac}	74.75±19.34 ^c	68.51±22.26 ^{ac}
PHPH	16.39±3.23 ^a	36.21±5.21 ^{ac}	37.52±8.10 ^{ac}	54.85±6.71 ^{ac}

^a*P*<0.05 vs SO; ^c*P*<0.05 vs control.

Table 4 Pearson partial correlations between PGI₂, NO levels and hemodynamic parameters

Hemodynamic parameters	PGI ₂ (deduction of the action of NO)		NO (deduction of the action of PGI ₂)	
	<i>R</i>	<i>p</i>	<i>R</i>	<i>P</i>
CI	-0.0259	0.8218	0.5520	0.0001
MAP	-0.1335	0.2436	-0.4572	0.0001
TPR	0.0122	0.9154	-0.6053	0.0001
FPP	0.2598	0.0216	0.4659	0.0001
PVI	0.1536	0.1794	0.3579	0.0013
PVR	-0.0523	0.6493	-0.2280	0.0446
SVR	-0.1216	0.2889	-0.4325	0.0001

INDO had no impacts on the CI and TPR in SO rats.

In basal state, FPP and PVI were significantly increased but SVR was lowered in IHPH and PHPH rats when compared with those in SO rats. Both L-NNA and INDO reduced the PVI but enhanced the SVR in IHPH, PHPH and SO rats (Table 3) (*P*<0.05).

Effects of high-dose heparin on plasma PGI₂ and NO concentrations and systemic and splanchnic hemodynamics

After administration of high-dose heparin, plasma 6-keto-PGF_{1α} concentrations (pg/mL) in IHPH, PHPH and SO rats were significantly higher than those in rats administrated vehicle. On the contrary, serum NO₂⁻/NO₃⁻ (μmol/L) concentrations in IHPH, PHPH and SO rats were significantly lower than those in rats administrated vehicle (Table 1) (*P*<0.05). Compared with the rats administrated vehicle, the hemodynamic parameters of portal hypertensive rats such as CI and PVI were declined significantly after the administration of high-dose heparin, while TPR and SVR were increased significantly (Tables 2, 3) (*P*<0.05).

Correlation analysis

There was a significant positive correlation between plasma 6-keto-PGF_{1α} and NO₂⁻/NO₃⁻ (*r*=0.3939, *P*<0.01). There were no significant correlations between plasma PGI₂ level and hemodynamics parameters such as CI, TPR, PVI and SVR after deduction of the action of NO, but after deduction of the action of PGI₂, NO still correlated highly with those hemodynamic parameters (Table 4).

DISCUSSION

Whether PGI₂ plays a role in formation and development of hyperdynamic circulatory state in portal hypertensive rats has not been specifically verified. Hamilton *et al*^[9] found that the plasma concentration of 6-keto-PGF_{1α}, a stable hydrolytic

product of PGI₂, was markedly elevated in PHPH rats by partial stenosis of the portal vein and was positively correlated to portal venous pressure (PVP). Sitzmann *et al*^[10] found that the concentration of PGI₂ in systemic artery circulation had a close relationship to the enhanced PVP, the increased mesenteric artery flow (MAF) and the decreased resistance of mesenteric artery in portal hypertensive rats. The hyperdynamic circulatory state in portal hypertensive rats was significantly alleviated after administration of COX inhibitor (indomethacin), which could be reversed after infusion of extrinsic PGI₂, thus postulating that PGI₂ contributes to the formation of hyperdynamics as a systemic mediator via escaping the hepatic hydrolysis through portal systemic shunt. The following findings that PGI₂ is positively related to PVP in portal hypertension and Budd-chiari syndrome patients and COX-1 mRNA transcription is elevated in superior mesenteric artery and thoracic aortic artery in PHPH rats also support the above hypothesis^[11].

However, Blanchart *et al*^[4] did not find the above-mentioned effects of INDO on hyperdynamics of portal hypertensive rats, considering that the formation of collateral circulation in PHPH rats was a result of vascular dilation adapted to the high PVP. Our previous studies have shown that the magnitude of systemic and splanchnic hyperdynamics as well as portal systemic shunt was in the order of PCS>PHPH>IHPH, whereas the concentration of 6-keto-PGF_{1α} is in the order of PHPH>IHPH>PCS. Moreover, the concentration of 6-keto-PGF_{1α} was higher in PCS rats than in SO rats, but was lower than in PHPH and IHPH rats, namely the dynamics in PCS rats increased most but PGI₂ elevated least. After administration of NOS inhibitors, hyperdynamic state in PCS, PHPH and IHPH rats was reversed to the basic state of SO rats while PGI₂ level was ascended, especially in PCS and SO rats (there was no statistic difference when compared with PHPH and IHPH rats).

In our previous experiments, we also found that 3 and 7 d after orthotopic liver transplantation in IHPH rats, plasma PGI₂ concentration was obviously lower, but was still higher than in normal controlled rats 3 d after operation and so did the PVP. Seven days after operation, there was no difference in PGI₂ concentration between PHPH and normal controlled rats. Nevertheless, 3 and 7 d after orthotopic liver transplantation in IHPH rats, hyperdynamics still existed, verifying that it is the enhanced PVP that causes the increase of PGI₂, and PGI₂ does not play a role in hyperdynamic circulatory state. Recent data also show that PGI₂ could not modulate the vascular tension to the normal level in eNOS deleted mice^[12].

The findings of this study demonstrate that there are some hyperdynamic characteristics in IHPH and PHPH rats such as the increase of cardiac output, PVI, and the decrease of SVR and MAP. L-NNA and INDO could lower the CI and PVI, but elevate the MAP and TPR in both IHPH and PHPH rats, thereby improving the hyperdynamic circulatory state, which seems that both NO and PGI₂ are mediators in the pathogenesis of hyperdynamics. However, Hardy *et al.*^[13] found that while INDO inhibited the synthesis of PGI₂, it could simultaneously inhibit the release of NO, which is consistent with our results in this study (Table 1). In another word, when INDO reduces the plasma PGI₂ level in IHPH and PHPH rats, it decreases the serum NO level as well. Pearson partial correlation analysis between PGI₂, NO levels and hemodynamic parameters manifests that after deduction of the action of NO, there is no significant correlation between plasma PGI₂ level and hemodynamic parameters such as CI, TPR, PVI and SVR. However, after deduction of the action of PGI₂, NO still correlates highly with those hemodynamic parameters. Therefore, it is NO rather than PGI₂ that is a mediator in the formation and development of hyperdynamic circulatory state in chronic portal hypertensive rats.

It was reported that high-dose heparin could make physical changes of endothelial cell membranes to enhance intracellular PLA₂ activity, thus increasing the production of PGI₂^[14,15]. Meanwhile, high-dose heparin could decrease the production of NO in endothelial cells by decreasing expression of eNOS or NOS activity as an effect on cell signaling pathways^[16,17]. These results are consistent with our results in this study that after administration of high-dose heparin, plasma 6-keto-PGF1 α concentrations (pg/mL) in IHPH, PHPH and SO rats were significantly higher than those in rats administered vehicle while serum NO₂/NO₃⁻ (μ mol/L) concentrations in IHPH, PHPH and SO rats were significantly lower than those in rats administered vehicle (Table 1). However, the most important finding after application of high-dose heparin is that heparin attenuates the hyperdynamic circulatory state of portal hypertensive rats while facilitate the production of PGI₂. After administration of high-dose heparin, the CI and PVI in IHPH, PHPH and SO rats attenuated significantly while TPR and SVR significantly increased (Tables 2, 3). These results indicate that high-dose heparin can attenuate the hyperdynamic circulation in portal hypertensive rats by decreasing the production of NO which further supports that PGI₂ is not a mediator of hyperdynamic circulation in portal hypertensive rats.

REFERENCES

1 Cahill PA, Redmond EM, Hodges R, Zhang S, Sitzmann JV.

- Increased endothelial nitric oxide synthase activity in the hypere-remic vessels of portal hypertensive rats. *J Hepatol* 1996; **25**: 370-378
- 2 Casadevall M, Panes J, Pique JM, Marroni N, Bosch J, Whittle BJ. Involvement of nitric oxide and prostaglandins in gastric mucosal hyperemia of portal-hypertensive anesthetized rats. *Hepatology* 1993; **18**: 628-634
- 3 Oberti F, Sogni P, Cailmail S, Moreau R, Pipy B, Lebrec D. Role of prostacyclin in hemodynamic alterations in conscious rats with extrahepatic or intrahepatic portal hypertension. *Hepatology* 1993; **18**: 621-627
- 4 Blanchart A, Hernando N, Fernandez-Munoz D, Hernando L, Lopez-Novoa JM. Lack of effect of indomethacin on systemic and splanchnic haemodynamics in portal hypertensive rats. *Clin Sci (Lond)* 1985; **68**: 605-607
- 5 Chojkier M, Groszmann RJ. Measurement of portal-systemic shunting in the rat by using gamma-labeled microspheres. *Am J Physiol* 1981; **240**: G371-G375
- 6 Wu Y, Burns RC, Sitzmann JV. Effects of nitric oxide and cyclooxygenase inhibition on splanchnic hemodynamics in portal hypertension. *Hepatology* 1993; **18**: 1416-1421
- 7 Pizcueta MP, Pique JM, Bosch J, Whittle BJ, Moncada S. Effects of inhibiting nitric oxide biosynthesis on the systemic and splanchnic circulation of rats with portal hypertension. *Br J Pharmacol* 1992; **105**: 184-190
- 8 Guarner C, Soriano G, Such J, Teixido M, Ramis I, Bulbena O, Rosello J, Guarner F, Gelpi E, Balanzo J. Systemic prostacyclin in cirrhotic patients. Relationship with portal hypertension and changes after intestinal decontamination. *Gastroenterology* 1992; **102**: 303-309
- 9 Hamilton G, Phing RC, Hutton RA, Dandona P, Hobbs KE. The relationship between prostacyclin activity and pressure in the portal vein. *Hepatology* 1982; **2**: 236-242
- 10 Sitzmann JV, Campbell K, Wu Y, St Clair C. Prostacyclin production in acute, chronic, and long-term experimental portal hypertension. *Surgery* 1994; **115**: 290-294
- 11 Hou MC, Cahill PA, Zhang S, Wang YN, Hendrickson RJ, Redmond EM, Sitzmann JV. Enhanced cyclooxygenase-1 expression within the superior mesenteric artery of portal hypertensive rats: role in the hyperdynamic circulation. *Hepatology* 1998; **27**: 20-27
- 12 Brandes RP, Schmitz-Winnenthal FH, Feletou M, Godecke A, Huang PL, Vanhoutte PM, Fleming I, Busse R. An endothelium-derived hyperpolarizing factor distinct from NO and prostacyclin is a major endothelium-dependent vasodilator in resistance vessels of wild-type and endothelial NO synthase knockout mice. *Proc Natl Acad Sci USA* 2000; **97**: 9747-9752
- 13 Hardy P, Abran D, Hou X, Lahaie I, Peri KG, Asselin P, Varma DR, Chemtob S. A major role for prostacyclin in nitric oxide-induced ocular vasorelaxation in the piglet. *Circ Res* 1998; **83**: 721-729
- 14 Nakamura H, Kim DK, Philbin DM, Peterson MB, Debros F, Koski G, Bonventre JV. Heparin-enhanced plasma phospholipase A2 activity and prostacyclin synthesis in patients undergoing cardiac surgery. *J Clin Invest* 1995; **95**: 1062-1070
- 15 Itoh F, Kaji T, Hayakawa Y, Oguma Y, Sakuragawa N. Heparin enhances thrombin-stimulated prostaglandin I2 production by cultured endothelial cells. *Thromb Res* 1990; **57**: 481-488
- 16 Upchurch GR, Welch GN, Freedman JE, Fabian AJ, Pigazzi A, Scribner AM, Alpert CS, Keaney JF, Loscalzo J. High-dose heparin decreases nitric oxide production by cultured bovine endothelial cells. *Circulation* 1997; **95**: 2115-2121
- 17 Boitano S, Dirksen ER, Sanderson MJ. Intercellular propagation of calcium waves mediated by inositol trisphosphate. *Science* 1992; **258**: 292-295

Knockdown of survivin gene expression by RNAi induces apoptosis in human hepatocellular carcinoma cell line SMMC-7721

Sheng-Quan Cheng, Wen-Liang Wang, Wei Yan, Qing-Long Li, Li Wang, Wen-Yong Wang

Sheng-Quan Cheng, Department of Pediatrics, Xijing Hospital, Fourth Military Medical University, Xi'an 710032, Shaanxi Province, China

Wen-Liang Wang, Wei Yan, Qing-Long Li, Li Wang, Wen-Yong Wang, Department of Pathology, Faculty of Preclinical Medicine, Fourth Military Medical University, Xi'an 710032, Shaanxi Province, China

Correspondence to: Professor Wen-Liang Wang, Department of Pathology, Faculty of Preclinical Medicine, Fourth Military Medical University, Xi'an 710032, Shaanxi Province, China. wlwang@fmmu.edu.cn

Telephone: +86-29-83374595

Received: 2004-04-09 **Accepted:** 2004-05-09

Abstract

AIM: To investigate the survivin gene expression in human hepatocellular carcinoma cell line SMMC-7721 and the effects of survivin gene RNA interference (RNAi) on cell apoptosis and biological behaviors of SMMC-7721 cells.

METHODS: Eukaryotic expression vector of survivin gene RNAi and recombinant plasmid pSuppressorNeo-survivin (pSuNeo-SVV), were constructed by ligating into the vector, pSuppressorNeo (pSuNeo) digested with restriction enzymes *Xba* I and *Sal* I and the designed double-chain RNAi primers. A cell model of SMMC-7721 after treatment with RNAi was prepared by transfecting SMMC-7721 cells with the lipofectin transfection method. Strept-avidin-biotin-complex (SABC) immunohistochemical staining and RT-PCR were used to detect survivin gene expressions in SMMC-7721 cells. Flow cytometry was used for the cell cycle analysis. Transmission electron microscopy was performed to determine whether RNAi induced cell apoptosis, and the method of measuring the cell growth curve was utilized to study the growth of SMMC-7721 cells before and after treatment with RNAi.

RESULTS: The eukaryotic expression vector of survivin gene RNAi and pSuNeo-SVV, were constructed successfully. The expression level of survivin gene in SMMC-7721 cells was observed. After the treatment of RNAi, the expression of survivin gene in SMMC-7721 cells was almost absent, apoptosis index was increased by 15.6%, and the number of cells was decreased in G2/M phase and the cell growth was inhibited.

CONCLUSION: RNAi can exert a knockdown of survivin gene expression in SMMC-7721 cells, and induce apoptosis and inhibit the growth of carcinoma cells.

© 2005 The WJG Press and Elsevier Inc. All rights reserved.

Key words: Hepatocellular carcinoma; Survivin; RNA interference; Apoptosis; Gene expression

Cheng SQ, Wang WL, Yan W, Li QL, Wang L, Wang WY. Knockdown of survivin gene expression by RNAi induces apoptosis

in human hepatocellular carcinoma cell line SMMC-7721. *World J Gastroenterol* 2005; 11(5): 756-759

<http://www.wjgnet.com/1007-9327/11/756.asp>

INTRODUCTION

Survivin gene is a new member of inhibitors of the apoptosis protein (IAP) family, and the most powerful apoptosis inhibitory factor as far as we know. Its distribution characteristics in tissues are different from other apoptosis inhibitory factors. It is selectively overexpressed in embryonic and fetal development, as well as in transformed cells and human carcinoma tissues, but not in adult differentiated tissues (with the exception of thymus and genital gland), and is associated with the aggressiveness of diseases and unfavorable outcomes^[1-13]. The expression of survivin gene directly relates to the histological classification of carcinoma, its relapse, metastasis, and growth index and inversely relates to apoptotic index^[1-4,6-8,11]. In contrast, some studies have demonstrated that the expression of survivin gene is not related to the histological classification of carcinoma, its size, infiltration depth, relapse, metastasis and prognosis^[8-10].

RNA interference (RNAi) is a genetic interference phenomenon directed by the double-stranded RNA (dsRNA). It could specifically and efficiently degrade mRNA, resulting in post-transcriptional gene silencing (PTGS)^[14-16], which is a natural mechanism in organisms underlying the resistance to virus invasion and inhibition of transposon mobility. Its blocking action on gene expression has been successfully observed in rat and human cells cultured *in vitro*, and the knockdown of genes in cells has been achieved^[15,16]. A latest study^[17] has shown that 21-25 nt small interference RNA (siRNA) can mediate specific gene silencing in mammal cells. Being effective and highly specific, RNAi probably becomes a new technique in knocking gene down and plays an important role in gene function study and gene therapy of diseases. We constructed the survivin gene eukaryotic expression vector of dsRNAi, and transfected SMMC-7721 cells, to observe the survivin gene expression following RNAi and its effects on cell apoptosis and growth, which has laid a foundation for further studies on the functions of survivin gene and genetic therapy involved in human hepatocellular carcinoma (HCC).

MATERIALS AND METHODS

Main reagents

Trizol reagent and M-MLV were purchased from Gibco BRL. Taq DNA polymerase and dNTPs were obtained from Promega. DNA Marker DL-2000 and DL-15000, T4 DNA ligase, *Bam*H, *Xho* I, *Xba*, *Sal* I and *Sca* I were bought from Takara. Lipofectamine 2000 was purchased from Invitrogen. Competent bacteria (*E. coli* DH5 α) were preserved in our laboratory. Polyclonal rabbit anti-human survivin antibody (sc-10811) was purchased from Santa Cruz. pSuppressorNeo (pSuNeo) was a gift of YAN-Yan (New York University, USA).

Primer design

A survivin sense primer corresponding to nucleotides, 5'-TA GGATCCATGGGTGCCCGACG-3' was added to compatible restriction sites *Bam*H I at the 5' end of the primer sequences. A survivin antisense primer complementary to nucleotides, 5'-ACCTCGAGCTCAATCCATGGCAGCC-3' was added to compatible restriction sites *Xho* I at the 3' end of the primer sequences. The length of amplified fragments was 445 bp.

A forward primer of dsRNAi corresponding to nucleotides was 5'-T CGAG g a g a a c g a g c c a g a c t t g g c c G A G T A C T G ggccaagtctgctgtctcTTTT-3'. The *Xho* I and *Sca* I overhang sites were underlined. A reverse primer of dsRNAi corresponding to nucleotides was 3'-cctcttctcgtctctga accggCTCATGAC cgggttcagaccagcaagagAAAAAGATC-5'. The *Sca* I and *Xba* I overhang sites were underlined. The primers designed were synthesized by Shanghai Sangon Biological Co. (China).

Cell lines and culture

Human hepatocellular carcinoma cell line SMMC-7721 was maintained in our laboratory. The cells were grown in Dulbecco's modified Eagle's medium (DMEM) supplemented with 100 mL/L fetal bovine serum (FBS) and incubated in a humidified incubator containing 50 mL/L CO₂ in at 37 °C.

Construction of recombinant pSuNeo-SVV

Primer annealing (siRNA insert) Forward primer, reverse primer and annealing buffer were incubated at 95 °C for 10 min, and the tube was gradually cooled to room temperature.

Ligation and insertion of vector pSuNeo One microliter of linearized vector pSuNeo (completely digested with *Xba* I and *Sal* I), 1 μL of insert DNA, 1 μL of T4 DNA ligase, and 2 μL of 10×ligase buffer were incubated at 16 °C overnight. Following the ligation reaction, the ligated plasmid DNA was transformed into 200 μL of competent cells of an appropriate host strain (*DH5α*), and then plated on LB plates containing 40 ng/mL of kanamycin.

Transfection of pSuNeo-SVV

The gene transfection mediated by lipofectin was used to introduce the plasmid pSuNeo-SVV and empty the vector pSuNeo into human hepatocellular carcinoma cell line SMMC-7721, respectively. After selected with G418, resistant colonies were obtained. Immunohistochemical staining and RT-PCR were performed to confirm the transfection.

Immunohistochemical staining

Immunohistochemical staining was performed by the a SABC method using SABC kit (Wuhan Boster Biological Co., China). Adherent cell sections were treated with 3 mL/L H₂O₂ in methanol for 30 min to abolish the endogenous peroxidase activity. Sections were blocked with normal goat serum for 30 min at room temperature, and incubated with anti-survivin antibody (1:200) overnight at 4 °C. The sections were incubated with biotinylated anti-rabbit IgG antibody, followed by avidin-biotin-peroxidase complex. Color was developed in a substrate solution of 0.1 mL/L diaminobenzidine-hydrogen peroxide and counterstained with hematoxylin.

RT-PCR analysis

Total RNA was extracted from human hepatocellular carcinoma cell line SMMC-7721 using the Trizol reagent according to the manufacturer's instructions. Complementary DNA (cDNA) was

generated from total RNA using M-MLV. PCR of the cDNA was performed in a final volume of 50 μL containing 4 μL of 4×dNTPs, 2 units of Taq DNA polymerase, and 20 mmol/L of each primer. The samples were amplified 28 cycles at 95 °C for 1 min, at 58 °C for 30 s, and at 72 °C for 40 s, and finally at 72 °C for 10 min. The PCR products were separated by electrophoresis on 10 g/L agarose gels and visualized by ethidium bromide staining. Amplification of human β-actin served as a control for a sample loading and integrity. A β-actin sense primer corresponding to nucleotides was 5'-ACACTGTGCCCATCTACGAGG-3', and an antisense primer complementary to nucleotides was 5'-AGGGGCCGGACTCG-CATTACT-3', the length of amplified fragments was 621 bp.

Transmission electron microscopy assay

The SMMC-7721 cells were digested with 2.5 g/L trypsinase and collected. After rinsed with PBS, the cells were prefixed with 30 g/L glutaraldehyde for 30 min, post-fixed with 10 mL/L osmic acid, dehydrated in graded ethanol, embedded in Epon 812 mixture, and cut into 0.05 μm thick sections on an ultramicrotome. The cells were observed under Hitachi JEM-2000EX electron microscopy.

Flow cytometric analysis

Cell cycle distributions were determined by measuring the cellular DNA content using flow cytometry. Cells were washed with PBS, fixed with 700 mL/L ethanol for 20 min and stored at 4 °C overnight, then washed with PBS, and stained with 100 μL of 50 mg/L PI at 4 °C for 30 min. Apoptotic cells were assayed using the Elite ESP flow cytometer at 488 nm, and data were analyzed with the CELLQuest software.

Assay of cell proliferation

A total of 2×10⁴ cells from transfected plasmid pSuNeo-SVV, vector pSuNeo and SMMC-7721 cell line were seeded in triplicate in 24-well plates and cultured in DMEM supplemented with 100 mL/L FBS. At each time point, cells were trypsinized to a single cell suspension and counted on a Coulter counter set at >10 μm in diameter.

Statistical analysis

Data were expressed as mean±SD. Statistical significance was determined by the Students' *t*-test. *P*<0.05 was considered statistically significant.

RESULTS

Analysis of pSuNeo-SVV digested with restriction enzymes

Digested results of the empty vector pSuNeo and recombinant plasmid pSuNeo-SVV showed 2 to 3 bands in pSuNeo, pSuNeo-SVV, and pSuNeo-SVV digested by *Sal* I. After pSuNeo was digested by *Sal* I and pSuNeo-SVV was digested by *Sca* I, a 3.4 kb band appeared in both of them (Figure 1A).

Expression of survivin gene in SMMC-7721 cells

The RT-PCR findings revealed that the SMMC-7721 cells in the control groups (SMMC-7721 and SMMC-7721 transfected with empty vector pSuNeo) presented a bright strip at 445 bp, while SMMC-7721 transfected with pSuNeo-SVV did not (Figure 1B). By SABC immunohistochemical staining, we found that the cell nuclei of SMMC-7721 and SMMC-7721 transfected with empty vector pSuNeo were yellow colored, while the cell nuclei of SMMC-7721 transfected with pSuNeo-SVV were not colored (Figure 2).

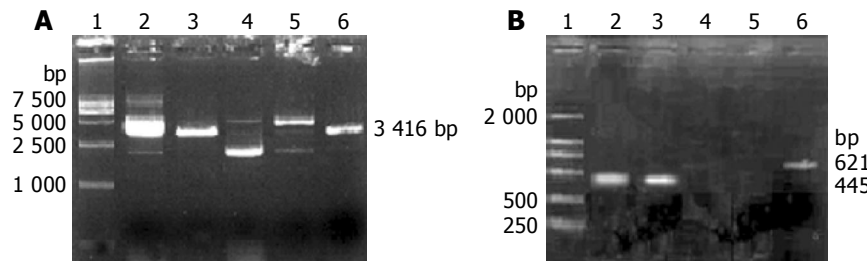


Figure 1 Degested results of the empty rector pSuNeo and recombinant pSuNeo-SVV. A: Electrophoretic profile of pSuNeo-SVV digested with restriction enzymes. Lane 1: DNA marker DL-15000, lane 2: pSuNeo, lane 3: pSuNeo/*Sal* I, lane 4: pSuNeo-SVV, lane 5: pSuNeo-SVV/*Sal* I, lane 6: pSuNeo-SVV/*Sca* I. B: Electrophoretic profile survivin gene by RT-PCR. Lane 1: DNA marker DL-2000, lane 2: untransfected survivin gene, lane 3: pSuNeo, lane 4: pSuNeo-SVV, lane 5: empty control, lane 6: β -actin.

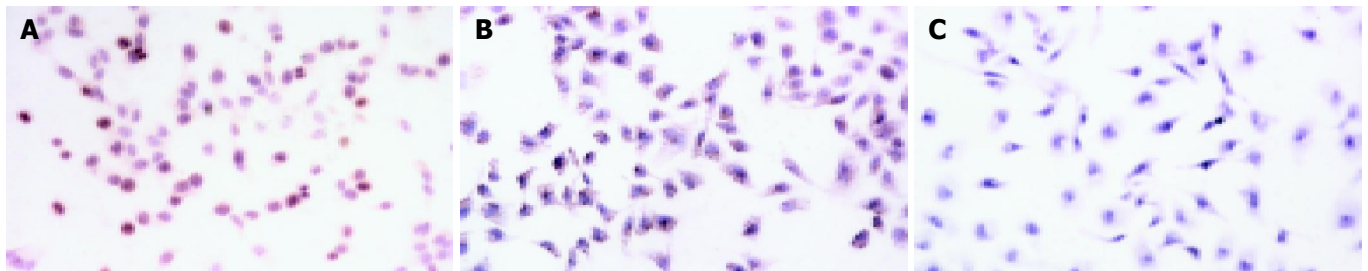


Figure 2 Immunohistochemical staining of survivin in SMMC-7721 cells. A: SMMC-7721 cells, B: SMMC-7721 cells transfected with pSuNeo, C: SMMC-7721 cells transfected with pSuNeo-SVV.

Transmission electron microscopic observation

Transmission electron microscopy revealed that in SMMC-7721 cells transfected with pSuNeo-SVV, dense chromatin appeared near the nucleus membranes, which presented some typical manifestations of cell apoptosis (Figure 3A), while no typical manifestation of cell apoptosis was observed in the control groups and the nuclei appeared to undergo karyokinesis, which showed a vigorous cell proliferation (Figure 3B).

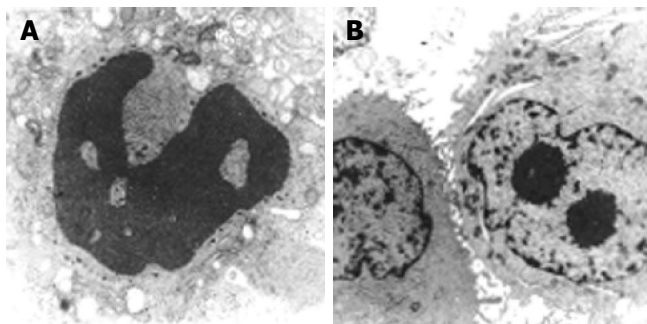


Figure 3 SMMC-7721 cells transfected with pSuNeo-SVV (A) and pSuNeo (B).

Flow cytometry analysis

Flow cytometry analysis of cell cycle revealed that SMMC-7721 cells transfected with pSuNeo-SVV showed a marked reduction in G2/M phase by 9.5%, the apoptosis index was as high as 15.6%, 17.1% and 17.1% in the control groups respectively.

Assay of cell proliferation

The cell growth curve shows that SMMC-7721 cells transfected with pSuNeo-SVV grew slowly, reached a stage of platform on the 7th d, and the number of cells was much less than that of the two control groups, while SMMC-7721 cells in the control groups proliferated rapidly on the 6th d and reached a stage of platform on the 8th d (Figure 4).

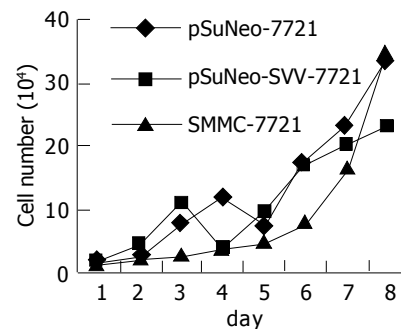


Figure 4 Growth curve of SMMC-7721 cells.

DISCUSSION

In recent years, researches on the functions of gene and gene therapeutic technologies for cancers, have been designed to identify these functions with gene transduction, antisense technology, transgene and gene knockout, and artificial chromosome transduction to deprive the functions of particular genes. RNAi possesses a high ability to specifically silence particular genes. Therefore, it can be used as a powerful tool in researches on the functions of genes and genetic therapy for carcinoma^[15,16]. Attention has been paid to RNAi in the field of researches on gene functions.

Our study demonstrated that the recombinant pSuNeo-SVV was not linearized when digested with *Xba* I, *Xho* I, or *Sal* I, but was linearized only with *Sca* I. SABC immunohistochemical staining showed that the nuclei of SMMC-7721 cells and SMMC-7721 cells transfected with empty vector pSuNeo revealed positive staining for survivin, while the nuclei of SMMC-7721 cells transfected with pSuNeo-SVV were almost not stained, suggesting that survivin gene is blocked at the level of protein. RT-PCR findings demonstrated that survivin gene was blocked in SMMC-7721 cells transfected with pSuNeo-SVV at the level of transcription. Flow cytometry analysis revealed that the

SMMC-7721 cells transfected with pSuNeo-SVV presented a marked reduction in G2/M phase, an obvious AP peak, and an increase in apoptosis index compared to the control groups. Transmission electron microscopy showed that in SMMC-7721 cells transfected with pSuNeo-SVV, dense chromatin appeared near the nuclei membranes which presents some typical manifestations of cell apoptosis, while no typical manifestation of cell apoptosis was observed in the control groups and the nuclei underwent karyokinesis, indicating a vigorous cell proliferation. We also observed that SMMC-7721 cells transfected with pSuNeo-SVV grew slowly, as compared with the control groups.

The above-mentioned findings confirm that chemically synthesized siRNAs can specifically block survivin gene expression, induce cell apoptosis, and inhibit the growth of carcinoma cells. Therefore, our study has laid a foundation for further studies on the use of RNAi in treating liver cancer.

It has been reported that the possible anti-apoptosis mechanisms of survivin gene include the direct inhibitory effect of survivin gene on the activities of caspases, especially caspase-3 and caspase-7 to block cell apoptosis; interactions of survivin gene with cyclin-dependent kinase 4 (CDK4), leading to CDK2/cyclin E activation and Rb phosphorylation; the release of p21 waf1/cip from survivin-CDK4 complex and its combination with the procaspase-3 of mitochondria, leading to the inhibition of its activity and the blockage of cell apoptosis blocked^[18,19]. Survivin is characterized by cell cycle-dependent expression, that is, it is expressed only in G2/M. Ito *et al.*^[4] transfected survivin into 4 human hepatocellular carcinoma cell lines and found that the number of cells in G0/G1 was remarkably reduced, and the number of cells in S or G2/M increased. It has been reported that survivin is involved in the formation of blood vessels, as a possible protective gene induced by growth factor in the formation of blood vessels to protect the normal proliferation of endothelial cells^[20]. In the formation of blood vessels, the action of angiopoietin-1 (the key factor to maintain the vascular stability and to form the cavity) depends on the up-regulation of survivin gene expression^[21]. In the carcinoma cell lines transfected with antisense oligonucleotide target survivin, cell apoptosis is increased and cell proliferation is inhibited^[22,23]. A study reported that apoptosis induced by tumor necrosis factors-related apoptosis inducing ligand (TRAIL) was related to its inhibitory action on survivin gene expression. Survivin expression might resist apoptosis induced by chemotherapy agents in cholangiocarcinomas.

The results of our study confirm that the inhibitory activity of survivin gene on the growth of liver cancer cells could be realized by inducing cell apoptosis. Besides, RNAi alone could block survivin gene expression to induce a remarkable increase in cell apoptosis. This unique effect of survivin provides new evidence for its antiapoptotic effects on liver cancer cells.

In summary, survivin gene can be regarded as a very good target gene in genetic therapy for carcinomas. RNAi of survivin gene is a promising approach in treating carcinomas.

REFERENCES

- 1 Sarela AI, Macadam RC, Farmery SM, Markham AF, Guillou PJ. Expression of the antiapoptosis gene, survivin, predicts death from recurrent colorectal carcinoma. *Gut* 2000; **46**: 645-650
- 2 Mori A, Wada H, Nishimura Y, Okamoto T, Takemoto Y, Kakishita E. Expression of the antiapoptosis gene survivin in human leukemia. *Int J Hematol* 2002; **75**: 161-165
- 3 Das A, Tan WL, Teo J, Smith DR. Expression of survivin in primary glioblastomas. *J Cancer Res Clin Oncol* 2002; **128**: 302-306
- 4 Ito T, Shiraki K, Sugimoto K, Yamanaka T, Fujikawa K, Ito M, Takase K, Moriyama M, Kawano H, Hayashida M, Nakano T, Suzuki A. Survivin promotes cell proliferation in human hepatocellular carcinoma. *Hepatology* 2000; **31**: 1080-1085
- 5 Sarela AI, Verbeke CS, Ramsdale J, Davies CL, Markham AF, Guillou PJ. Expression of survivin, a novel inhibitor of apoptosis and cell cycle regulatory protein, in pancreatic adenocarcinoma. *Br J Cancer* 2002; **86**: 886-892
- 6 Wakana Y, Kasuya K, Katayanagi S, Tsuchida A, Aoki T, Koyanagi Y, Ishii H, Ebihara Y. Effect of survivin on cell proliferation and apoptosis in gastric cancer. *Oncol Rep* 2002; **9**: 1213-1218
- 7 Cohen C, Lohmann CM, Cotsonis G, Lawson D, Santoianni R. Survivin expression in ovarian carcinoma: correlation with apoptotic markers and prognosis. *Mod Pathol* 2003; **16**: 574-583
- 8 Lu CD, Altieri DC, Tanigawa N. Expression of a novel antiapoptosis gene, survivin, correlated with tumor cell apoptosis and p53 accumulation in gastric carcinomas. *Cancer Res* 1998; **58**: 1808-1812
- 9 Kawasaki H, Altieri DC, Lu CD, Toyoda M, Tenjo T, Tanigawa N. Inhibition of apoptosis by survivin predicts shorter survival rates in colorectal cancer. *Cancer Res* 1998; **58**: 5071-5074
- 10 Tanaka K, Iwamoto S, Gon G, Nohara T, Iwamoto M, Tanigawa N. Expression of survivin and its relationship to loss of apoptosis in breast carcinomas. *Clin Cancer Res* 2000; **6**: 127-134
- 11 Trieb K, Lehner R, Stulnig T, Sulzbacher I, Shroyer KR. Survivin expression in human osteosarcoma is a marker for survival. *Eur J Surg Oncol* 2003; **29**: 379-382
- 12 Sui L, Dong Y, Ohno M, Watanabe Y, Sugimoto K, Tokuda M. Survivin expression and its relationship with cell proliferation and prognosis in epithelial ovarian tumors. *Int J Oncol* 2002; **21**: 315-320
- 13 Zhu XD, Lin GJ, Qian LP, Chen ZQ. Expression of survivin in human gastric carcinoma and gastric carcinoma model of rats. *World J Gastroenterol* 2003; **9**: 1435-1438
- 14 Fire A, Xu S, Montgomery MK, Kostas SA, Driver SE, Mello CC. Potent and specific genetic interference by double-stranded RNA in *Caenorhabditis elegans*. *Nature* 1998; **391**: 806-811
- 15 Konnikova L, Kotecki M, Kruger MM, Cochran BH. Knockdown of STAT3 expression by RNAi induces apoptosis in astrocytoma cells. *BMC Cancer* 2003; **3**: 23
- 16 Tuschl T, Borkhardt A. Small interfering RNAs: a revolutionary tool for the analysis of gene function and gene therapy. *Mol Interv* 2002; **2**: 158-167
- 17 Elbashir SM, Lendeckel W, Tuschl T. RNA interference is mediated by 21- and 22-nucleotide RNAs. *Genes Dev* 2001; **15**: 188-200
- 18 Suzuki A, Ito T, Kawano H, Hayashida M, Hayasaki Y, Tsutomi Y, Akahane K, Nakano T, Miura M, Shiraki K. Survivin initiates procaspase 3/p21 complex formation as a result of interaction with Cdk4 to resist Fas-mediated cell death. *Oncogene* 2000; **19**: 1346-1353
- 19 Shin S, Sung BJ, Cho YS, Kim HJ, Ha NC, Hwang JI, Chung CW, Jung YK, Oh BH. An anti-apoptotic protein human survivin is a direct inhibitor of caspase-3 and -7. *Biochemistry* 2001; **40**: 1117-1123
- 20 O'Connor DS, Schechner JS, Adida C, Mesri M, Rothermel AL, Li F, Nath AK, Pober JS, Altieri DC. Control of apoptosis during angiogenesis by survivin expression in endothelial cells. *Am J Pathol* 2000; **156**: 393-398
- 21 Papapetropoulos A, Fulton D, Mahboubi K, Kalb RG, O'Connor DS, Li F, Altieri DC, Sessa WC. Angiopoietin-1 inhibits endothelial cell apoptosis via the Akt/survivin pathway. *J Biol Chem* 2000; **275**: 9102-9105
- 22 Ambrosini G, Adida C, Sirugo G, Altieri DC. Induction of apoptosis and inhibition of cell proliferation by survivin gene targeting. *J Biol Chem* 1998; **273**: 11177-11182
- 23 Grossman D, McNiff JM, Li F, Altieri DC. Expression of the apoptosis inhibitor, survivin, in nonmelanoma skin cancer and gene targeting in a keratinocyte cell line. *Lab Invest* 1999; **79**: 1121-1126

Effect of bone marrow-derived monocytes transfected with RNA of mouse colon carcinoma on specific antitumor immunity

Xiao-Yuan Chu, Long-Bang Chen, Jing Zang, Jing-Hua Wang, Qun Zhang, Huai-Cheng Geng

Xiao-Yuan Chu, Long-Bang Chen, Jing Zang, Jing-Hua Wang, Qun Zhang, Huai-Cheng Geng, Department of Oncology, Nanjing General Hospital of PLA, Nanjing 210002, Jiangsu Province, China

Correspondence to: Dr. Xiao-Yuan Chu, Department of Oncology, Nanjing General Hospital of PLA, Nanjing 210002, Jiangsu Province, China. zxy_6906@tom.com

Telephone: +86-25-80860072

Received: 2004-02-02 **Accepted:** 2004-03-04

Abstract

AIM: To investigate the effect of bone marrow-derived monocytes transfected with RNA of CT-26 (a cell line of mouse colon carcinoma) on antitumor immunity.

METHODS: Mouse bone marrow-derived monocytes were incubated with mouse granulocyte macrophage colony stimulating factor (mGM-CSF) *in vitro*, and the purity of monocytes was detected by flow cytometry. Total RNA of CT-26 was obtained by TRIzol's process, and monocytes were transfected by TransMessenger *in vitro*. The activity of cytotoxic T lymphocytes (CTL) *in vivo* was estimated by the modified lactate dehydrogenase (LDH) release assay. Changes of tumor size in mice and animal's survival time were observed in different groups.

RESULTS: Monocytes from mouse bone marrow were successfully incubated, and the positive rate of CD11b was over 95%. Vaccination of the monocytes transfected with total RNA induced a high level of specific CTL activity *in vivo*, and made mice resistant to the subsequent challenge of parental tumor cells. *In vivo* effects induced by monocytes transfected with total RNA were stronger than those induced by monocytes pulsed with tumor cell lysates.

CONCLUSION: Antigen presenting cells transfected with total RNA of CT-26 can present endogenous tumor antigens, activate CTL, and effectively induce specific antitumor immunity.

© 2005 The WJG Press and Elsevier Inc. All rights reserved.

Key words: Colon carcinoma; RNA; Bone marrow-derived monocytes; Cytotoxic T lymphocytes

Chu XY, Chen LB, Zang J, Wang JH, Zhang Q, Geng HC. Effect of bone marrow-derived monocytes transfected with RNA of mouse colon carcinoma on specific antitumor immunity. *World J Gastroenterol* 2005; 11(5): 760-763
<http://www.wjgnet.com/1007-9327/11/760.asp>

INTRODUCTION

With the development of immunology, molecular biology, and genetic engineering technology, cancer immunotherapy has become the fourth mode following surgery, chemical therapy and radiotherapy. One of the hot spots in the field of tumor

immunotherapy research is to develop a simple and effective specific tumor immunity^[1]. Monocytes are important antigen presenting cells (APCs) in the body with the function of antigen processing and presenting. Monocytes activated by the antigen, mitogens and cytokines can transform into activated macrophages, and make the body produce a specific ability against tumors through activating T cells^[2-5]. In this study, we observed the effects of bone marrow-derived monocytes transfected with total RNA of mice CT-26 on specific antitumor immunity *in vivo*.

MATERIALS AND METHODS

Animals and cell strain

Balb/c male mice, 6-8 wk old, were bought from Shanghai B and K Experimental Animal Co, Ltd. Mice colon carcinoma cell strain CT-26 was passaged routinely in our laboratory.

Reagents

Reagents and suppliers were RPMI1640 (Gibco Company), fetal calf serum (Sijiqing Company of Hangzhou), IL-2 and mGM-CSF (Sigma Company), TransMessenger transfected reagent (Qiagen Company), CD11b-FITC fluorescent antibody (Pharmingen Company), LDH test reagent (Nanjing Jiancheng Reagent Company).

Incubation of mice bone marrow-derived monocytes

Mice femurs were taken in aseptic conditions and marrow cells were washed out, erythrocytes were dissolved with Tris-NH₄Cl and washed twice with PBS. Then RPMI1640 culture medium with 10% fetal calf serum was added and its density was regulated to 1×10⁶/mL, mGM-CSF 10 ng/mL was added and incubated in a cultural vial. On every fourth day the culture medium and floating cells were discarded, fresh medium and 10 ng/mL mGM-CSF were added. On the ninth day of culture *in vitro*, the supernate and floating cells were removed, the density was regulated and then the culture was added to a 6-well plate on the 6×10⁶/well, replenished with 2 mL fresh culture medium and 10 ng/mL mGM-CSF for each well and incubated overnight. The next step was to slightly blow its surface, and to discard all the culture medium and floating cells. Monocytes attached to the wall were harvested.

FACS analysis of monocytes

Monocytes harvested were added to 100 μL anti-CD11b antibody (its density 5 μg/mL) and incubated in darkness at 4 °C for 45 min. Monocytes were irrigated twice with PBS, then analyzed by a flow cytometer (FACS caliber, B.D Company).

Extraction and identification of total RNA of CT-26 cells

After incubated for 24 h, total RNA of CT-26 cells was obtained by Trizol process when cells became confluent at 80%. The A₂₆₀ and A₂₈₀ values of total RNA were measured by spectrophotometer, and formaldehyde denatural electrophoresis was used to test its purity and integrity.

Preparation of tumor cell lysates

CT-26 cells were collected *in vitro* through passage culture for

24 h and washed twice with PBS, the density of which was regulated to $1 \times 10^7/\text{mL}$. The cells were frozen and thawed 4 times, centrifuged at 12 000 g in low temperature for 30 min and prepared for use after the supernatant was removed and filtered.

Monocytes transfected with RNA *in vitro*

Monocytes were transfected with total RNA *in vitro* according to the protocol of TransMessenger. The whole culture medium and floating cells in the 6-well plates were discarded. The monocytes attached to the wall were left and washed twice with PBS, 4 μL enhancer R was instilled to EPP tube with 94 μL buffer EC-R and then added to 2 μL RNA (RNA density 1 ng/ μL), turned over and mixed evenly for 10 s. After keeping at room temperature for 5 min, the culture was centrifuged for 5 s, and then the supernate was removed and 8 μL TransMessenger reagent was added and again turned over and mixed evenly for 10 s. The culture was kept at room temperature for 10 min, then added to RPMI 1640 culture liquid without any calf serum and antibiotics. It was then vibrated twice and the tumor RNA-TransMessenger compounds were quickly instilled into the spare monocytes and the culture plate was lightly shaken. It was incubated at 37 °C in 50 mL/L CO₂ for 3 h and then the supernate was removed, RPMI 1640 culture liquid was added and incubated for 24 h in an incubator. The next step was to add 10 mL EDTA and to assimilate the culture at room temperature for 5 min, and then monocytes were collected, and washed twice with PBS. Normal saline was added to regulate the monocyte density to $5 \times 10^7/\text{mL}$ and immediately re-transfused to mice by injection into the abdominal cavity at 100 $\mu\text{L}/\text{mouse}$.

Monocytes pulsed with tumor cell lysates *in vitro*

Monocytes were obtained by incubation as above, 20 μL tumor cell lysate was added and incubated at 37 °C in an incubator containing 50 mL/L CO₂ for 24 h. After assimilated with EDTA, the monocytes were collected and washed twice with PBS. Normal saline was added to regulate the monocyte density to $5 \times 10^7/\text{mL}$, and then re-transfused to mice immediately by injection into the abdominal cavity at 100 $\mu\text{L}/\text{mouse}$.

Experiment *in vivo*

The mice were randomly divided into 5 groups with 8 mice in each group. Abdominal cavity injection was performed at the dosage of $5 \times 10^6/\text{mouse}$. Group 1: monocytes transfected with tumor RNA by TransMessenger *in vitro*; group 2: monocytes pulsed with tumor RNA directly; group 3: monocytes pulsed with tumor lysates; group 4: monocytes; group 5: PBS. Subjects were inoculated with CT-26 cells at the dosage of $2 \times 10^5/\text{mouse}$ under the costal regions subcutaneously after 10 d of re-transfusion, and then the growth of tumor and the animal survival time were observed.

Test of cytotoxic activity

Cytotoxic activity was tested by LDH release assay^[6]. Eight days after retransfusion of monocytes, 3 mice from each group were randomly selected and their spleens were taken to prepare cell suspension. Then 2×10^7 spleen cells were taken and added to 2×10^6 CT-26 cells that underwent inactivation for 40 min with mitomycin, 10 mL RPMI 1640, 10% fetal calf serum and IL-II 50 U/mL, and then incubated for 5 d at 37 °C 50 mL/L CO₂. We collected live cells as the effector cells, mixed them with CT-26 target cells according to the effect/target ratios 100:1, 50:1 and 25:1, put in a 96 well-round bottom culture plate with its total volume reached to 200 μL , and incubated for 4 h. After incubation, 0.9% NaCl was added to stop effector/target reaction, and then centrifuged at 1 500 r/min for 5 min and 100 μL supernate was taken to test LDH release rate. The killing activity of CTL cells against tumor cells was calculated with the following formula.

$$\text{Killing activity (\%)} = \frac{\text{Sample release group } A \text{ value} - \text{natural release group } A \text{ value}}{\text{The greatest release group } A \text{ value} - \text{natural release group } A \text{ value}} \times 100\%$$

RESULTS

Monocytes cultivated *in vitro*

A lot of proliferated cell colonies attached to the wall could be obtained after mGM-CSF 10 ng/mL was added to mice bone marrow cells *in vitro* and incubated for 3-5 d. There were dead T and, B cells, erythrocytes and granulocytes in the supernate, which was removed when the liquid was changed. After culturing for 9 d, an abundance of proliferated cells was scattered in the supernate. These cells were removed and put into a new culture plate. After culturing overnight, granulocytes and dendritic cells were suspended in supernate with only monocytes attached to the wall. Only monocytes remained after the supernate was removed (Figure 1). Plenty of monocytes (over 10^8 cells) in the form of typical irregular stretching adherent cells were collected after culturing for 9 d in mouse bone marrow. These cells were sensitive to assimilation of EDTA and pancreatin, the specific mark of monocytes tested by flow cytometry was CD11b, and the positive rate of CD11b in monocytes was over 95% (Figure 2), which indicated that the purity of cultivated monocytes was quite high.

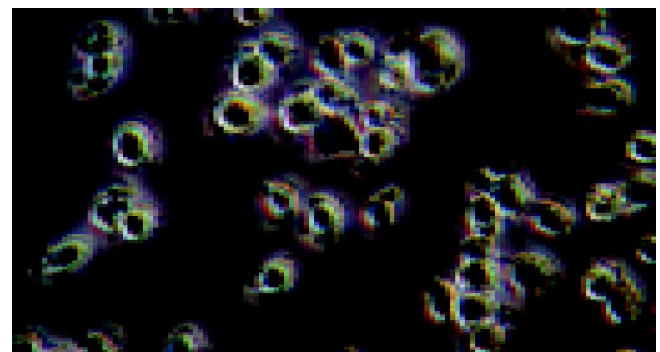


Figure 1 Expansion of monocytes from murine bone marrow cells *in vitro* cultured with mGM-CSF.

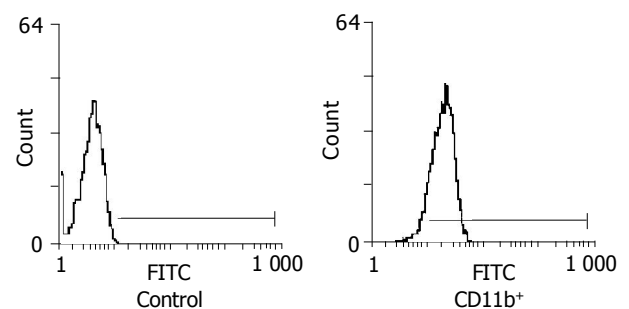


Figure 2 Detection of the surface marker (CD11b) presented on the bone marrow-derived monocytes by flow cytometry.

Quality of extracted tumor RNA

A_{260/280} of total RNA of CT-26 cells tested by spectrophotometer was 1.83, indicating that the purity of RNA was high. The results of formaldehyde denaturalization electrophoresis showed that the total RNA was free from DNA pollution. There were two bright bands, 28S and 18S, the proportion was 2:1 with no degradation band, indicating that the RNA had sound integrity and less degradation (Figure 3).

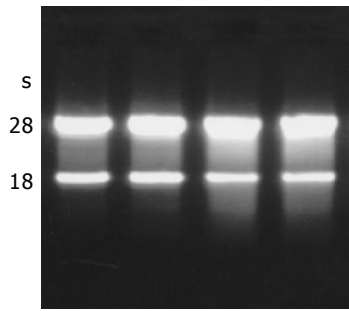


Figure 3 Ethidium bromide-stained formaldehyde agarose gel of total RNA isolated from 1×10^7 CT-26 tumor cells.

Activity of specific CTL *in vivo*

As shown in Figure 4, after monocytes transfected with total RNA of CT-26 cells *in vitro* by TransMessenger were re-transfused into the mice, the mice could be induced to generate high levels of activity of specific CTL. Monocytes impacted with CT-26 cell lysates *in vitro* could induce a moderate CTL activity *in vivo*. These results showed that monocytes transfected with tumor RNA *in vitro* by TransMessenger had a higher ability to activate CD8⁺CTL than those pulsed with tumor cell lysates *in vitro*.

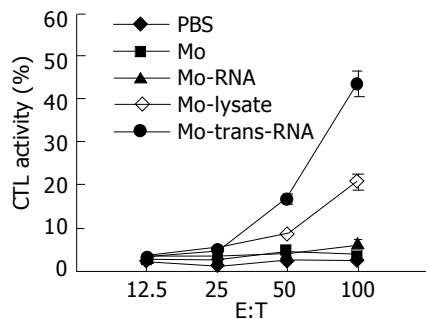


Figure 4 Induction of specific CTL activity *in vivo* by vaccination with tumor antigen-pulsed monocytes.

Antitumor effects *in vivo*

As shown in Figure 5, monocytes transfected with total RNA of CT-26 cells by TransMessenger could generate a stronger protecting immunity against attack by parent CT-26 tumor cells lately vaccinated. All mice could live longer and produce a completely protective effect because their immunologic function was raised *in vivo*. Retransfusion of monocytes pulsed with tumor cell lysates also generated a protective effect, but it was lower than that of the monocytes transfected with tumor total RNA, as only 60% of mice could survive for a long time.

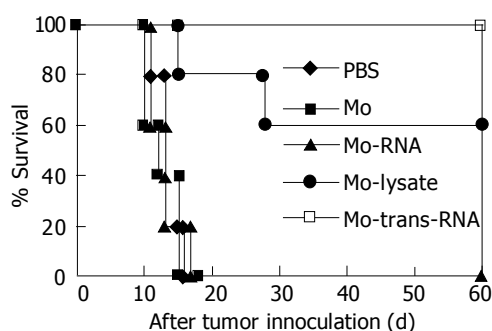


Figure 5 Resistance of mice to the subsequent challenge of parental tumor cells induced by tumor antigen-pulsed monocytes.

DISCUSSION

T lymphocytes receive a specific antigen signal through TCR on its surface. That is, T lymphocytes receive a specific antigen signal through recognizing the compounds of MHC-I and MHC-II molecules on the surface of antigen presenting cells and tumor antigen peptide, which activate T lymphocytes with a specific subsidiary signal of antigen presenting cells stimulating molecules (B7, ICAM-1 and CD40) to bring the killing effect on tumor cells into play^[7-9]. One of the main reasons for immune evasion in tumor cells is the lower ability of antigen presenting cells to present tumor antigen to T cells, which enable the body to generate effective antitumor immune reaction.

At present, tumor antigens include tumor cell lysates, withered corpuscles, irradiated and inactivated tumor vaccine, tumor antigen polypeptide, RNA coded tumor antigens and anti-specific tumor vaccines^[10,11]. After these impacted antigen presenting cells *in vitro* are re-transfused to the subject mice, a strong antitumor immunological function can be produced^[12-15], which demonstrates the clinical values for antitumor treatment. Monocytes transfected *in vitro* with tumor RNA that is taken as a kind of antigens could get endogenous expression antigens, and present MHC-I molecules to monocyte's surface, which could activate CD8⁺T cells, and when they are re-transfused to animals, the activity of lymphocytes on killing tumor in the body could be enhanced. As the professional antigen presenting cells, monocytes/macrophages play an important role in anti-tumor immune reaction^[16]. But at present, it is a very complicated process to separate a large number of monocytes from peripheral blood and it is hard to meet the needs of clinical application. We took small amounts of bone marrow cells out of body and added cytokines for culturing and proliferating, and finally we obtained a large number of monocytes, which could be retransfused to the body to protect against tumor *in vivo*.

This study shows that when monocytes transfected with CT-26 cell total RNA by TransMessenger *in vitro* are re-transfused, they could induce a strong specific antitumor immune protection *in vivo*, demonstrating that tumor RNA extracted by TRIzol possesses good antigenic traits and pulsed monocytes *in vitro* could stimulate the body to produce antitumor ability markedly. Compared with other types of tumor antigens, the advantage of tumor RNA extracted by TRIzol is that it is easily prepared and could be used for every patient whose tumor cells could be obtained through operation or puncture. The extracted tumor RNA covers all the tumor antigens. TRIzol could also extract the RNA of specific tumor antigen effectively. Using the method of transfected medium, tumor RNA can be expressed endogenously as tumor antigens in antigen presenting cells, which could effectively activate the antitumor effect of T cells in the body.

In brief, monocytes transfected with tumor RNA *in vitro* by TransMessenger can be used as a new type of tumor vaccine, and they can induce a specific antitumor immunological function *in vivo*.

REFERENCES

- Rosenberg SA. Progress in human tumour immunology and immunotherapy. *Nature* 2001; **411**: 380-384
- Bonnotte B, Larmonier N, Favre N, Fromentin A, Moutet M, Martin M, Gurbuxani S, Solary E, Chauffert B, Martin F. Identification of tumor-infiltrating macrophages as the killers of tumor cells after immunization in a rat model system. *J Immunol* 2001; **167**: 5077-5083
- Toujas L, Delcros JG, Diez E, Gervois N, Semana G, Corradin G, Jotereau F. Human monocyte-derived macrophages and dendritic cells are comparably effective *in vitro* in presenting

- HLA class I-restricted exogenous peptides. *Immunology* 1997; **91**: 635-642
- 4 **Yoshida R**, Yoneda Y, Kuriyama M, Kubota T. IFN-gamma and cell-to-cell contact-dependent cytotoxicity of allograft-induced macrophages against syngeneic tumor cells and cell lines: an application of allografting to cancer treatment. *J Immunol* 1999; **163**: 148-154
 - 5 **Reiter I**, Krammer B, Schwamberger G. Cutting edge: differential effect of apoptotic versus necrotic tumor cells on macrophage antitumor activities. *J Immunol* 1999; **163**: 1730-1732
 - 6 **Chen BY**, Ma JY, Huang QT, You LF. Simply natural killing experiment DA kind of modified LDH release assay. *Shanghai Mianyixue Zazhi* 1989; **9**: 218-219
 - 7 **Zhan Y**, Corbett AJ, Brady JL, Sutherland RM, Lew AM. CD4 help-independent induction of cytotoxic CD8 cells to allogeneic P815 tumor cells is absolutely dependent on costimulation. *J Immunol* 2000; **165**: 3612-3619
 - 8 **Tamura H**, Dong H, Zhu G, Sica GL, Flies DB, Tamada K, Chen L. B7-H1 costimulation preferentially enhances CD28-independent T-helper cell function. *Blood* 2001; **97**: 1809-1816
 - 9 **Bai XF**, Bender J, Liu J, Zhang H, Wang Y, Li O, Du P, Zheng P, Liu Y. Local costimulation reinvigorates tumor-specific cytolytic T lymphocytes for experimental therapy in mice with large tumor burdens. *J Immunol* 2001; **167**: 3936-3943
 - 10 **Koido S**, Kashiwaba M, Chen D, Gendler S, Kufe D, Gong J. Induction of antitumor immunity by vaccination of dendritic cells transfected with MUC1 RNA. *J Immunol* 2000; **165**: 5713-5719
 - 11 **Gatza E**, Okada CY. Tumor cell lysate-pulsed dendritic cells are more effective than TCR Id protein vaccines for active immunotherapy of T cell lymphoma. *J Immunol* 2002; **169**: 5227-5235
 - 12 **Henry F**, Boisteau O, Bretaudeau L, Lieubeau B, Meflah K, Grégoire M. Antigen-presenting cells that phagocytose apoptotic tumor-derived cells are potent tumor vaccines. *Cancer Res* 1999; **59**: 3329-3332
 - 13 **Gong J**, Avigan D, Chen D, Wu Z, Koido S, Kashiwaba M, Kufe D. Activation of antitumor cytotoxic T lymphocytes by fusions of human dendritic cells and breast carcinoma cells. *Proc Natl Acad Sci USA* 2000; **97**: 2715-2718
 - 14 **Ota S**, Ono T, Morita A, Uenaka A, Harada M, Nakayama E. Cellular processing of a multibranch lysine core with tumor antigen peptides and presentation of peptide epitopes recognized by cytotoxic T lymphocytes on antigen-presenting cells. *Cancer Res* 2002; **62**: 1471-1476
 - 15 **Strome SE**, Voss S, Wilcox R, Wakefield TL, Tamada K, Flies D, Chapoval A, Lu J, Kasperbauer JL, Padley D, Vile R, Gastineau D, Wettstein P, Chen L. Strategies for antigen loading of dendritic cells to enhance the antitumor immune response. *Cancer Res* 2002; **62**: 1884-1889
 - 16 **Mortarini R**, Anichini A, Di Nicola M, Siena S, Bregni M, Belli F, Molla A, Gianni AM, Parmiani G. Autologous dendritic cells derived from CD34+ progenitors and from monocytes are not functionally equivalent antigen-presenting cells in the induction of melan-A/Mart-1(27-35)-specific CTLs from peripheral blood lymphocytes of melanoma patients with low frequency of CTL precursors. *Cancer Res* 1997; **57**: 5534-5541

Edited by Wang XL Proofread by Chen WW

Acquired hepatocerebral degeneration: A case report

Wei-Xing Chen, Ping Wang, Sen-Xiang Yan, You-Ming Li, Chao-Hui Yu, Ling-Ling Jiang

Wei-Xing Chen, Ping Wang, Sen-Xiang Yan, You-Ming Li, Chao-Hui Yu, Ling-Ling Jiang, Department of Gastroenterology, First Affiliated Hospital, College of Medicine, Zhejiang University, Hangzhou 310003, Zhejiang Province, China

Correspondence to: Mr. Ping Wang, Department of Gastroenterology, First Affiliated Hospital, College of Medicine, Zhejiang University, 261 Qingchun Road, Hangzhou 310003, Zhejiang Province, China. structxing@163.com

Telephone: +86-571-87230354 **Fax:** +86-571-87978444

Received: 2004-03-23 **Accepted:** 2004-04-29

Abstract

AIM: Acquired hepatocerebral degeneration (AHD) is an exceptional type of hepatic encephalopathies (HE). It is characterized by neuropsychiatric and extrapyramidal symptomatology similar to that seen in hepatolenticular degeneration (Wilson's disease). In this paper, we report a case of AHD with unusual presenting features.

METHODS: A 28-year-old man with AHD was described and the literature was reviewed.

RESULTS: The man had a history of HBV-related liver cirrhosis. He was admitted to our hospital with apathy, dysarthria, mild consciousness impairment and extrapyramidal symptoms after hematemesis. By review of the literature, cases with AHD often did not present consciousness impairment. So our case was once diagnosed incorrectly as Wilson's disease.

CONCLUSION: AHD is a rare syndrome and its variable clinical manifestations make it difficult to be diagnosed. But we believe that extensive examination and thorough understanding of the disease are beneficial to a correct diagnosis. Moreover, biocoene is effective in treating the case.

© 2005 The WJG Press and Elsevier Inc. All rights reserved.

Key words: Acquired hepatocerebral degeneration

Chen WX, Wang P, Yan SX, Li YM, Yu CH, Jiang LL. Acquired hepatocerebral degeneration: A case report. *World J Gastroenterol* 2005; 11(5): 764-766

<http://www.wjgnet.com/1007-9327/11/764.asp>

INTRODUCTION

Acquired hepatocerebral degeneration (AHD) is a rare syndrome characterized by neuropsychiatric and extrapyramidal symptomatology in patients with portocaval shunt. The pathophysiology of this disorder is still unknown, but hyperammonemia and/or brain manganese overload may play a role. Medical treatment is often disappointing. We reported a case of AHD whose clinical features led us to a misdiagnosis at one time.

CASE REPORT

The patient was a 28-year-old man. He had a history of HBV-related liver cirrhosis. No familial hepatic or neurological diseases

were reported. Two weeks ago, he had an episode of tarry stool and was cured. But he developed apathy, dysarthria, mild consciousness impairment and involuntary abnormal movements after some days. Physical examination revealed splenomegaly and shifting dullness. Abdominal ultrasonic examination suggested portal hypertension and a great deal of ascites. Cranial magnetic resonance imaging (MRI) revealed increased signal intensity in basal ganglia bilaterally on T2-weighted images similar to hepatolenticular degeneration (Wilson's disease) (Figure 1). Electroencephalogram (EEG) disclosed diffuse slow wave activity (Figure 2A). Slit lamp examination found no Kayser-Fleischer (K-F) ring of the cornea associated with Wilson's disease. Copper balance and cerebrospinal fluid examinations gave normal results. Liver failure was grade B-9 of the Child-Pugh classification. The level of serum ammonia was measured several times, and was above the reference range (132 $\mu\text{mol/L}$) one time. He was treated with hepatic protector tablets, ammonia lowering agents, bowel relaxants and branched chain amino acid infusion. But therapeutic effect was not so good. Then naloxone and anaxate (Flumazenil) were added, but the symptoms did not relieve obviously. Finally, after administration of biocoene (coenzyme complex injection), his neuropsychiatric abnormalities and the presentation of EEG markedly improved (Figure 2B). By 3 mo follow-up, we found that he recovered well and could take care of himself after leaving hospital.

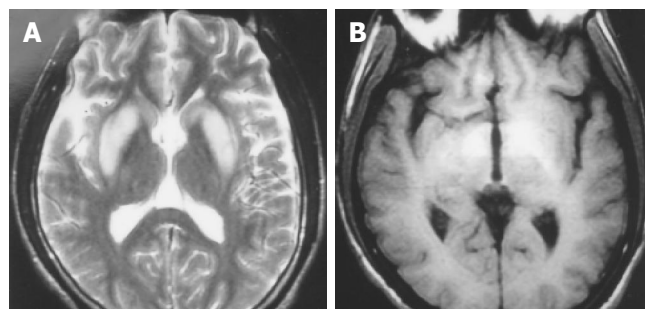


Figure 1 Cranial MRI in the patient with similar hepatolenticular degeneration (Wilson's disease). A: increased signal intensity in basal ganglia bilaterally on T2WI; B: increased signal intensity in basal ganglia bilaterally on T1WI.

DISCUSSION

AHD is an exceptional type of hepatic encephalopathies (HE). It has been described in patients with severe liver disease of many causes, and notably in patients with surgically or spontaneously induced porto-systemic shunts. But many questions remain unanswered. Its frequency and pathogenesis remain largely uncertain. The clinical, neuroradiological, and biological characteristics of AHD have not yet been fully determined. The response to treatment is also incompletely understood. Our review of the literature (including MEDLINE, from 1981 to April 2003) yielded 36 similar cases^[1-13], among them, 8 (22.2%) were Chinese and 28 (77.8%) were from Western countries.

Studies have indicated that the disease is associated with multiple metabolic insults, such as ammonia, manganese, etc. Especially, the toxic effects of manganese might be the major determinant^[1-3,14]. It has been proved that manganese is cleared by the hepatobiliary system and whole blood and cerebrospinal

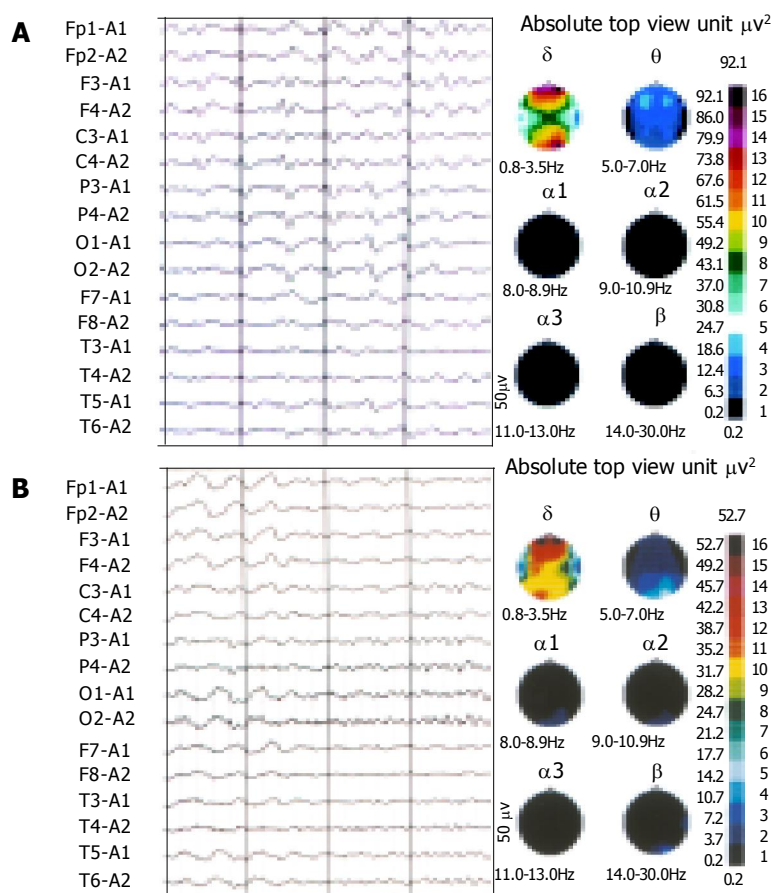


Figure 2 θ wave intermixed with δ wave, triphasic wave and spike and wave on EEG before treatment(A). and waves reduction on EEG after treatment(B).

fluid manganese concentrations in some patients with AHD are several fold above the reference range. This deposition of manganese in the brain is postulated in patients with AHD, which may induce diffuse degeneration in parenchymal brain. Microscopically, neuronal loss, Alzheimer type II astrocytes and cytoplasmic glycogen granules in basal ganglia are characteristic^[3-6,14,15]. The spectrum of clinical presentations can be neuropsychiatric (apathy, lethargy, excessive somnolence, secondary dementia, *etc.*), extrapyramidal symptoms (focal dystonia, postural tremor, myoclonus, rigidity, dysarthria, choreoathetosis, *etc.*), or both^[1-5,7-9,14]. But no consciousness impairment has been reported. MR imaging scans showed a hyperintense T1 signal in the basal ganglia^[1-3]. But it was also reported that some patients showed increased signal intensity in the dentate nuclei bilaterally on T2-weighted images indistinguishable from Wilson's disease. The clinical symptoms, neuropathological features and MR imaging appearance of AHD are rather uniform and similar to those seen in Wilson's disease, so it is also named pseudo-Wilson disease. The discrimination depends on the following aspects: (1) Morbidity age: Wilson's disease is a genetic disease, which rarely starts after the age of thirty, whereas AHD occurs in those with severe liver disease of many causes at different ages. (2) Copper metabolism: copper metabolism *in vivo* in Wilson's disease is out of balance so that overload copper deposits in the liver, brain, kidney, cornea, *etc.* Thus the concentration of ceruloplasmin is under 200 $\mu\text{g/L}$, the contents of copper in liver and urine are respectively over 250 μg per gram dry weight tissue and 100 $\mu\text{g}/24\text{ h}$. But copper metabolizes normally in patients with AHD. (3) Wilson's disease is characterized by Kayser-Fleischer ring of the cornea as a result of abnormal copper deposition in the cornea. But this change is not seen in AHD^[4,5,10]. Moreover, the disease is

also distinct from the more acute and transient episodes of HE. The neurological symptoms of HE disappear when the disease relieves, and there is no organic damage in HE^[11]. The disease develops gradually and the symptoms become progressively worse. Medical treatment is often disappointing. But it has been reported that some patients with AHD are responsive to branched chain amino acids or levodopa therapy. It has also been reported that endovascular occlusion of a porto-systemic shunt is temporarily effective. Moreover, liver transplantation in selected cases could be curative. Is that AHD might be a reversible and treatable disorder partly^[1,2,10,14].

As described above, the disease is characterized by neuropsychiatric and extrapyramidal symptoms developing from chronic hepatic encephalopathies. By review of similarly published cases at home and abroad, there has been no consciousness impairment reported. The case was exceptional for the presentation of mild consciousness impairment. Therefore, we hold that the symptoms of AHD might be overlapped partly with those of hepatic encephalopathies. The patient was irresponsive to the routine therapy of anti-hepatic encephalopathies (such as branched chain amino acids, *etc.*), but responsive to biocoene. The reason might be that biocoene contains glutathione, which can play the role in detoxicating and nourishing the liver.

REFERENCES

- 1 Burkhard PR, Delavelle J, Du Pasquier R, Spahr L. Chronic parkinsonism associated with cirrhosis: a distinct subset of acquired hepatocerebral degeneration. *Arch Neurol* 2003; **60**: 521-528
- 2 Condat B, Dusoleil A, Bernardeau M, Roche A, Pelletier G, Buffet C. Chronic acquired hepatocerebral degeneration: the role of manganese and treatment by endovascular occlusion

- of a porto-systemic shunt. *Gastroenterol Clin Biol* 1999; **23**: 268-270
- 3 **Jog MS**, Lang AE. Chronic acquired hepatocerebral degeneration: case reports and new insights. *Mov Disord* 1995; **10**: 714-722
 - 4 **Levy VG**, Cameron E, Ollat H, Opolon P, Darnis F, Contamin F. Chronic hepatic encephalopathies. Acquired cerebral degeneration not due to Wilson's disease. *Sem Hop* 1983; **59**: 1369-1373
 - 5 **Spencer DC**, Forno LS. February 2000: Dementia with motor dysfunction in a patient with liver disease. *Brain Pathol* 2000; **10**: 315-316, 319
 - 6 **Soffer D**, Sherman Y, Tur-Kaspa R, Eid A. Acquired hepatocerebral degeneration in a liver transplant recipient. *Acta Neuropathol* 1995; **90**: 107-111
 - 7 **Spitaleri DL**, Vitolo S, Fasanaro AM, Valiani R. Choreoathetosis. Uncommon manifestation during chronic liver disease with portocaval shunt. *Riv Neurol* 1983; **53**: 293-299
 - 8 **Thobois S**, Giraud P, Debat P, Gouttard M, Maurizi A, Perret-Liaudet A, Kopp N, Broussolle E. Orofacial dyskinesias in a patient with primary biliary cirrhosis: a clinicopathological case report and review. *Mov Disord* 2002; **17**: 415-419
 - 9 **Stracciari A**, Guarino M, Pazzaglia P, Marchesini G, Pisi P. Acquired hepatocerebral degeneration: full recovery after liver transplantation. *J Neurol Neurosurg Psychiatry* 2001; **70**: 136-137
 - 10 **Ueki Y**, Isozaki E, Miyazaki Y, Koide R, Shimizu T, Yagi K, Hirai S. Clinical and neuroradiological improvement in chronic acquired hepatocerebral degeneration after branched-chain amino acid therapy. *Acta Neurol Scand* 2002; **106**: 113-116
 - 11 **Wang DY**. Clinical analysis of hepatic cirrhosis with chronic hepatocerebral: Clinical analysis of 8 cases. *Shanxi Yixue Zazhi* 1997; **26**: 406-407
 - 12 **de Santi MM**, Lungarella G, Luzi P, Miracco C, Tosi P. Ultrastructural features in active chronic hepatitis with changes resembling Wilson's disease. *Am J Clin Pathol* 1986; **85**: 365-369
 - 13 **Lee J**, Lacomis D, Comu S, Jacobsohn J, Kanal E. Acquired hepatocerebral degeneration: MR and pathologic findings. *AJNR Am J Neuroradiol* 1998; **19**: 485-487
 - 14 **Layrargues GP**. Movement dysfunction and hepatic encephalopathy. *Metab Brain Dis* 2001; **16**: 27-35
 - 15 **Finlayson MH**, Superville B. Distribution of cerebral lesions in acquired hepatocerebral degeneration. *Brain* 1981; **104**: 79-95

Edited by Kumar M and Wang XL Proofread by Zhu LH

• CASE REPORT •

Hematemesis as the initial complication of pancreatic adenocarcinoma directly invading the duodenum: A case report

Yueh-Hung Lin, Chih-Yen Chen, Chih-Ping Chen, Tien-Yin Kuo, Full-Young Chang, Shou-Dong Lee

Yueh-Hung Lin, Chih-Yen Chen, Tien-Yin Kuo, Full-Young Chang, Shou-Dong Lee, Division of Gastroenterology, Department of Medicine, Taipei Veterans General Hospital and School of Medicine, National Yang-Ming University, Taipei, Taiwan

Chih-Ping Chen, Department of Health, Tao-Yuan General Hospital Tao-Yuan, Taiwan

Correspondence to: Chih-Yen Chen, M.D., Division of Gastroenterology, Taipei Veterans General Hospital, 12F, 201, Sec. 2, Shih-Pai Road, Taipei 112, Taiwan. chency@vghtpe.gov.tw

Telephone: +886-2-28757308 **Fax:** +886-2-28711058

Received: 2004-05-25 **Accepted:** 2004-06-29

Abstract

Pancreatic carcinoma is a debilitating disease and carries a poor prognosis. It is a rare cause of upper gastrointestinal bleeding, even though pancreas, stomach, duodenum and jejunum are adjacent organs. The incidence of pancreatic adenocarcinoma directly invading the gastrointestinal tract leading to gastrointestinal hemorrhage is very low, and most of them present with melena and hematochezia. Here, we describe one unique case manifesting characteristically severe and unremitting hematemesis as an initial presentation of pancreatic adenocarcinoma. This tumor directly invaded the duodenal mucosa as a bleeding protruding tumor mass. Our MEDLINE search has confirmed that this is the first reported case with an initial manifestation of hematemesis from pancreatic adenocarcinoma in Asians. Pancreatic adenocarcinoma directly invading duodenum complicated by hemorrhage can be a rare cause of hematemesis, and clinicians should be reminded of it while they are making differential diagnosis.

© 2005 The WJG Press and Elsevier Inc. All rights reserved.

Key words: Pancreatic adenocarcinoma; Duodenum tumor; Hematemesis; Neoplasm invasiveness

Lin YH, Chen CY, Chen CP, Kuo TY, Chang FY, Lee SD. Hematemesis as the initial complication of pancreatic adenocarcinoma directly invading the duodenum: A case report. *World J Gastroenterol* 2005; 11(5): 767-769

<http://www.wjgnet.com/1007-9327/11/767.asp>

INTRODUCTION

Pancreatic carcinoma is very common in developed countries. This tumor carries a poor prognosis, behaves devastatingly, and often invades the contiguous organs, which in turn results in 4 major symptoms: obstructive jaundice, duodenal obstruction, weight loss, and cancer pain^[1-8]. The main symptoms usually result from external compression of duodenal serosal side or common bile duct by pancreatic carcinoma, frequently requiring palliative management clinically. However, direct invasion to gastrointestinal tract by pancreatic adenocarcinoma, while rare, has been reported^[9,10]. The incidence was 2.6% in an American retrospective series, and the commonest symptoms were tarry stool passage and hematochezia^[9]. Up to

date, only one case manifesting hematemesis as the initial presentation of pancreatic adenocarcinoma has been reported^[9]. Herein, we reported the first case in Orientals.

CASE REPORT

A 77-year-old man suffered from nausea, epigastric fullness and pain, dizziness, and body weight loss of 15 kg over a three-month period. Physical examination was otherwise unremarkable, except for moderate tenderness over the epigastrium. Abdominal sonography showed mild dilatation of the pancreatic duct and multiple hepatic masses over both lobes. Computed tomography of the abdomen disclosed a 3 cm×3 cm mass over the pancreatic head that could not be distinguished from the adjacent duodenal wall, and multiple liver metastases (Figure 1). The upper gastrointestinal endoscopy revealed a polypoid mass, protruding over the anterior wall of the duodenal bulb with partial obstruction of the duodenal lumen (Figure 2). During this examination, endoscopy-assisted contrast medium infusion was performed through the stricture segment of duodenum, which was requested by radiologists to facilitate fine needle biopsy of pancreatic tumor later. Endoscopically biopsied tissues revealed adenocarcinoma (Figure 3A). The patient next received a computed tomography-guided biopsy for pancreatic lesion which was proved to be a moderately differentiated adenocarcinoma (Figure 3B). The morphology was quite compatible with the previous endoscopic specimen. Thus, the diagnosis of pancreatic adenocarcinoma with invasion of duodenal mucosa was virtually established.

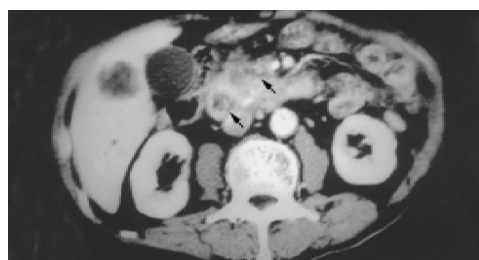


Figure 1 A soft tissue mass (3 cm×3 cm in size) over the pancreatic head (arrow), duodenal infiltration (arrowhead), and superior mesenteric vein encasement shown by abdominal computed tomography.



Figure 2 A soft polypoid mass protruding over the anterior wall of the duodenal bulb with partial obstruction of the second portion of the duodenum shown by upper gastrointestinal endoscopy.

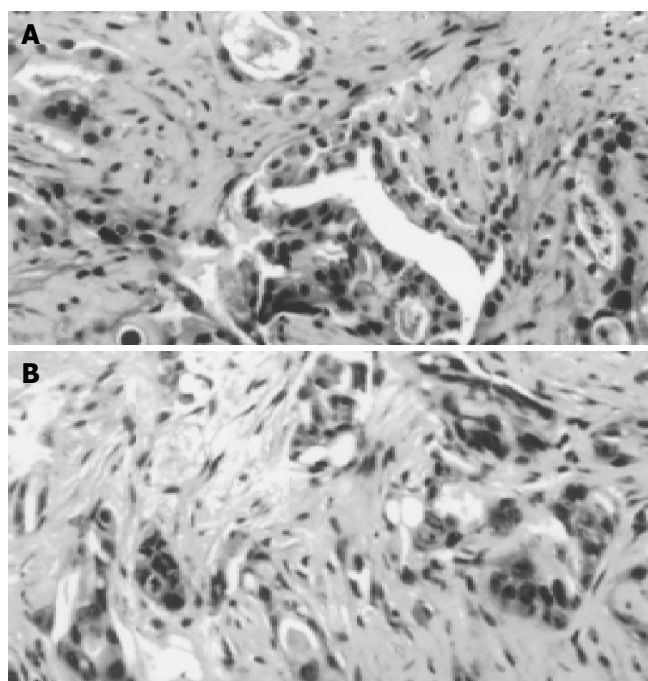


Figure 3 Morphology of adenocarcinoma and pancreatic lesion. A: Biopsy of the duodenal tumor via upper gastrointestinal endoscopy revealed a picture of adenocarcinoma cells in an acinar pattern; B: Biopsy of the pancreatic head tumor via computed tomography-guidance showed moderately differentiated adenocarcinoma cells infiltrating into the collagenous stroma (hematoxylin and eosin stain; magnification $\times 200$).

Unfortunately, hematemesis and tarry stool developed six days after admission. Intravenous fluid resuscitation and blood transfusion with packed red cells were administered. An urgent upper gastrointestinal endoscopy observed a tumor invasion with blood oozing over the anterior wall of the first and second portions of the duodenum. Local epinephrine injection was then employed, and bleeding was temporarily stopped. Approximately three weeks after the episode of upper gastrointestinal bleeding, obstructive jaundice and cholangitis developed. He then received palliative percutaneous transhepatic drainage to relieve obstructive jaundice. In addition, palliative radiotherapy and adjuvant chemotherapy with 5-fluorouracil and gemcitabine were administered for one week. However, finally the patient expired six weeks later due to cachexia, sepsis and multiple organ failure.

DISCUSSION

Pancreatic carcinoma is becoming more and more prevalent in Asia. It has been the tenth leading cause of death from cancer in Taiwan in 2002^[11]. The one-year survival rate is reported to

be about 8%. The clinical course is poor, and the median survival time is about 3-5 mo. About 80% of patients with pancreatic cancer, at the time of diagnosis, were far advanced and unresectable^[12]. Regarding palliative therapeutic strategy in advanced pancreatic carcinoma, gemcitabine is a strongly recommended drug of choice by an updated study^[11]. We also applied this promising drug to our patient. However, the patient still expired due to a poor general condition and relentless disease progress six weeks after diagnosis eventually.

Pancreatic malignancy may have a variety of presentations. The most common clinical manifestations are jaundice, pruritus, abdominal pain, body weight loss, anorexia, and nausea^[3,13,14]. Obstructive symptoms, either obstructive jaundice or duodenal obstruction, are not rare manifestations of pancreatic carcinoma while massive gastrointestinal hemorrhage is seldom encountered^[3,9,10,13,14]. By summarization from literature, there are three mechanisms for the pathogenesis, either by gastric variceal bleeding secondary to splenic vein occlusion^[15-17], a fistula from the blood vessel to duodenum (namely wirsungorrhage)^[18,19], or direct tumor bleeding via the pancreatic duct (namely hemosuccus)^[20,21]. However, in our case, the pancreatic tumor extending to the duodenum was evident from the abdominal CT image, where the patient experienced massive hematemesis. In addition, the pathologic results from both the biopsies of the pancreatic tumor and the duodenal intraluminal protruding mass were quite compatible. Therefore, the diagnosis of pancreatic adenocarcinoma directly invading the duodenum, complicated by upper GI bleeding, was confirmed. In contrast to the clear elucidation of pancreatic parenchymal neoplasms manifesting hematemesis^[20-23], pancreatic ductal carcinoma presenting with upper gastrointestinal bleeding has been rarely reported, and common symptoms are melena and hematochezia. To the best of our knowledge, there has been only one case of pancreatic adenocarcinoma presenting with hematemesis reported^[9]. These two patients' clinical manifestations are shown in Table 1. One of them (our case) presented with a polypoid mass from tumor infiltration of duodenal mucosa, while the other failed to have positive finding from upper gastrointestinal endoscopy due to its deep location in the third portion of duodenum.

The pancreatic tumor was located in the retroperitoneal space, and was somewhat difficult to approach by fine needle biopsy. Using the assistant method of endoscopy-assisted contrast medium infusion through the constrictive segment of duodenum to define the accurate tumor location, we successfully obtained tumor tissue from the pancreas.

In conclusion, pancreatic carcinoma may present with a varying spectrum of gastrointestinal bleeding, including hematemesis, which is easily overlooked by clinicians. Prompt endoscopic examination, including judicious scrutiny of the first and second portions of the duodenum, together with tissue biopsy may provide imperative information for early detection and enable selection of appropriate treatment.

Table 1 Clinical features of patients with pancreatic adenocarcinoma directly invading the duodenum complicated by upper gastrointestinal bleeding

	Our patient	Lee <i>et al.</i> ¹
Age (yr)	78	83
Sex	Male	Female
Clinical manifestation	Massive gastrointestinal bleeding (hematemesis)	Persistent gastrointestinal bleeding (hematemesis)
Endoscopic finding	Polypoid mass	Normal
Location of tumor invasion	The first and second portions of duodenum	The third portion of duodenum
Treatment	Radiotherapy, chemotherapy	Not mentioned
Survival duration	Six weeks	Not mentioned

¹Reference 9.

REFERENCES

- 1 **Storniolo AM**, Enas NH, Brown CA, Voi M, Rothenberg ML, Schilsky R. An investigational new drug treatment program for patients with gemcitabine: results for over 3000 patients with pancreatic carcinoma. *Cancer* 1999; **85**: 1261-1268
- 2 **Mu DQ**, Peng SY, Wang GF. Risk factors influencing recurrence following resection of pancreatic head cancer. *World J Gastroenterol* 2004; **10**: 906-909
- 3 **Selch MT**, Parker RG. Results in the management of locally unresectable pancreatic carcinoma. *Am J Clin Oncol* 1986; **9**: 139-145
- 4 **Bungay K**, Dennistone S, Hunt PS. Duodenal obstruction and carcinoma of the head of pancreas. *Med J Aust* 1980; **2**: 150-151
- 5 **Lichtenstein DR**, Carr-Locke DL. Endoscopic palliation for unresectable pancreatic carcinoma. *Surg Clin North Am* 1995; **75**: 969-988
- 6 **Bakkevold KE**, Kambestad B. Palliation of pancreatic cancer. A prospective multicentre study. *Eur J Surg Oncol* 1995; **21**: 176-182
- 7 **Egrari S**, O'Connell TX. Role of prophylactic gastroenterostomy for unresectable pancreatic carcinoma. *Am Surg* 1995; **61**: 862-864
- 8 **Scott-Mackie P**, Morgan R, Farrugia M, Glynos M, Adam A. The role of metallic stents in malignant duodenal obstruction. *Br J Radiol* 1997; **70**: 252-255
- 9 **Lee P**, Sutherland D, Feller ER. Massive gastrointestinal bleeding as the initial manifestation of pancreatic carcinoma. *Int J Pancreatol* 1994; **15**: 223-227
- 10 **Sharon P**, Stalnikovicz R, Rachmilewitz D. Endoscopic diagnosis of duodenal neoplasms causing upper gastrointestinal bleeding. *J Clin Gastroenterol* 1982; **4**: 35-38
- 11 **Department of Health, Executive Yuan, Republic of China, General Health Statistic, 2002**. Leading causes of death from cancers, Taiwan area, 2002, Health and Vital Statistics.
- 12 **Tepper JE**, Noyes D, Krall JM, Sause WT, Wolkov HB, Dobelbower RR, Thomson J, Owens J, Hanks GE. Intraoperative radiation therapy of pancreatic carcinoma: a report of RTOG-8505. Radiation Therapy Oncology Group. *Int J Radiat Oncol Biol Phys* 1991; **21**: 1145-1149
- 13 **Lillemoe KD**, Pitt HA. Palliation. Surgical and otherwise. *Cancer* 1996; **78**: 605-614
- 14 **Lillemoe KD**. Palliative therapy for pancreatic cancer. *Surg Oncol Clin N Am* 1998; **7**: 199-216
- 15 **Ferguson JM**, Palmer KR, Garden OJ, Redhead DN. Transhepatic venous angioplasty and stenting: a treatment option in bleeding from gastric varices secondary to pancreatic carcinoma. *HPB Surg* 1997; **10**: 173-175
- 16 **McDermott VG**, England RE, Newman GE. Case report: bleeding gastric varices secondary to splenic vein thrombosis successfully treated by splenic artery embolization. *Br J Radiol* 1995; **68**: 928-930
- 17 **Mullan FJ**, McKelvey ST. Pancreatic carcinoma presenting as bleeding from segmental gastric varices: pitfalls in diagnosis. *Postgrad Med J* 1990; **66**: 401-403
- 18 **Thorstad BL**, Keller FS. Fistula from the superior mesenteric artery to duodenum: a rare cause of death from pancreatic carcinoma. *Gastrointest Radiol* 1987; **12**: 200-202
- 19 **Ghaphery AD**, Gupta R, Currie RA. Carcinoma of the head of the pancreas with aortoduodenal fistula. *Am J Surg* 1966; **111**: 580-583
- 20 **Clay RP**, Farnell MB, Lancaster JR, Weiland LH, Gostout CJ. Hemosuccus pancreaticus. An unusual cause of upper gastrointestinal bleeding. *Ann Surg* 1985; **202**: 75-79
- 21 **Baruch Y**, Levy Y, Goldsher D, Munichor M, Eidelman S. Massive haematemesis--presenting symptoms of cystadenocarcinoma of the pancreas. *Postgrad Med J* 1989; **65**: 42-44
- 22 **Goldenberg AM**, Present DH, Bauer J, Gordon R. Islet cell tumor presenting as massive upper gastrointestinal bleeding in pregnancy. *Am J Gastroenterol* 1988; **83**: 873-875
- 23 **Sacks MI**. Pancreatic tumor with repeated gastrointestinal hemorrhage and steatorrhea. *Isr J Med Sci* 1965; **1**: 141-148

Edited by Wang XL Proofread by Zhu LH

• ACKNOWLEDGEMENTS •

Acknowledgements to Reviewers of *World Journal of Gastroenterology*

Many reviewers have contributed their expertise and time to the peer review, a critical process to ensure the quality of *World Journal of Gastroenterology*. The editors and authors of the articles submitted to the journal are grateful to the following reviewers for evaluating the articles (including those were published and those were rejected in this issue) during the last editing period of time.

Janaka de Silva, Professor
University of Kelaniya, Janaka de Silva, Faculty of Medicine,
University of Kelaniya, Ragama 6, Sri Lanka

Sheung-Tat Fan, Professor
Department of Surgery, The University of Hong Kong, Queen
Mary Hospital, 102 Pokfulam Road, Hong Kong, China

Xue-Gong Fan, Professor
Xiangya Hospital, Changsha 410008, China

De-Wu Han, Professor
Shanxi Medical University, 86 Xinjian South Road, Taiyuan
030001, China

Shao-Heng He, Professor
Medical College of Shantou University, 22 Xinling Rd, Shantou,
Guangdong, Shantou 515031, China

Zhi-Qiang Huang, Professor
Abdominal Surgery Institute of General Hospital of PLA, Fuxing
Road, Beijing 100853, China

Hiromi Ishibashi, Professor
Director General, Clinical Research Center, National Hospital
Organization (NHO) Nagasaki Medical Center, Professor,
Department of Hepatology, Nagasaki University Graduate
School of Biomedical Sciences, Kubara 2-1001-1 Kubara Omura,
Nagasaki 856-8562, Japan

Richard A Kozarek, M.D.
Department of Gastroenterology, Virginia Mason Medical
Center, 1100 Ninth Avenue, P.O. Box 900, Seattle 98111-0900,
United States

Wai-Keung Leung, M.D.
The Chinese University of Hong Kong, Department of Medicine
and Therapeutics, Prince of Wales Hospital, Shatin, Hong Kong,
China

Zhi-Hua Liu, Professor
Cancer Institute, Chinese Academy of Medical Sciences, 17
Panjiayuan Nanli, Beijing 100021, China

Ai-Ping Lu, Professor
China Academy of Traditional Chinese Medicine, Dongzhimen

Nei, 18 Beixincang, Beijing 100700, China

Yury Kharitonovich Marakhouski, Professor
Department of Gastroenterology and Nutrition, Byelorussian
Medical Academy Postgraduate Education, Brovki str 3, Minsk
220013, Belarus

Hiroshi Nakagawa, Assistant Professor
Gastroenterology Division, University of Pennsylvania, 415
Curie Blvd. 638B CRB, Philadelphia 19104, United States

Jae-Gahb Park, Professor
Seoul National University College of Medicine, 28 Yongon-
dong, Chongno-gu, Seoul 110-744, Korea, Republic of

Tilman Sauerbruch, M.D.
Department of Internal Medicine I, University of Bonn,
Sigmund-Freud-Strasse 25, 53105 Bonn, Germany

Philip Martin Sherman, Professor
Department of Paediatrics and Microbiology, University of
Toronto, Hospital for Sick Children, University of Toronto, GI/
Nutrition, Room 8409, Hospital for Sick Children, 555 University
Avenue, Toronto M5G 1X8, Canada

Rakesh Tandon, M.D.
Professor and Head, Department of Gastroenterology, All India
Institute of Medical Sciences, Ansari Nagar New Delhi-110029,
India

Frank Ivor Tovey, M.D.
Department of Surgery, University College London, 5
Crossborough Hill, Basingstoke RG21 4AG, United Kingdom

Chun-Yang Wen, M.D.
Department of Molecular Pathology, Atomic Bomb Disease
Institute, Nagasaki University Graduate School of Biomedical
Sciences. 1-12-4 Sakamoto, Nagasaki 852-8523, Japan

Jia-Yu Xu, Professor
Shanghai Second Medical University, Rui Jin Hospital, 197 Rui
Jin Er Road, Shanghai 200025, China

Yuan Yuan, Professor
Cancer Institute of China Medical University, 155 North Nanjing
Street, Heping District, Shenyang 110001, Liaoning Province, China

Man-Fung Yuen, Associate Professor
Department of Medicine, The University of Hong Kong, Queen
Mary Hospital, Hong Kong, China

Shu Zheng, Professor
Scientific Director of Cancer Institute, Zhejiang University,
Secondary Affiliated Hospital, Zhejiang University, 88# Jiefang
Road, Hangzhou 310009, China

Meetings

Major meetings coming up

Digestive Disease Week
106th Annual Meeting of AGA, The American Gastroenterology Association
May 14-19, 2005
www.ddw.org/
Chicago, Illinois

13th World Congress of Gastroenterology
September 10-14, 2005
www.wcog2005.org/
Montreal, Canada

13th United European Gastroenterology Week, UEGW
October 15-20, 2005
www.uegf.org/
Copenhagen, Denmark

American College of Gastroenterology Annual Scientific Meeting
October 28-November 2, 2005
www.acg.gi.org/
Honolulu Convention Center, Honolulu, Hawaii

Events and Meetings in the upcoming 6 months

Canadian Digestive Disease Week Conference
February 26-March 6, 2005
www.cag-acg.org
Banff, AB

International Colorectal Disease Symposium 2005
February 3-5, 2005
info@icds-hk.org
Hong Kong

EASL 2005 the 40th annual meeting
April 13-17, 2005
www.easl.ch/easl2005/
Paris, France

Pediatric Gastroenterology, Hepatology and Nutrition
March 13, 2005
Jakarta, Indonesia

21st annual international congress of Pakistan society of Gastroenterology & GI Endoscopy
March 25-27, 2005
www.psgc2005.com
Peshawar

8th Congress of the Asian Society of HepatoBiliary Pancreatic Surgery
February 10-13, 2005
Mandaluyong, Philippines

World Congress on Gastrointestinal Cancer
June 15-18, 2005
Barcelona

British Society of Gastroenterology Conference (BSG)
March 14-17, 2005
www.bsg.org.uk
Birmingham

Digestive Disease Week DDW 106th Annual Meeting
May 15-18, 2005
www.ddw.org
Chicago, Illinois

Events and meetings in 2005

Canadian Digestive Disease Week Conference
February 26-March 6, 2005
www.cag-acg.org
Banff, AB

2005 World Congress of Gastroenterology
September 12-14, 2005
Montreal, Canada

International Colorectal Disease Symposium 2005
February 3-5, 2005
Hong Kong

13th UEGW meeting United European Gastroenterology Week
October 15-20, 2005
www.webasistent.cz/guarant/uegw2005/
Copenhagen-Malmoe

7th International Workshop on Therapeutic Endoscopy
September 10-12, 2005
www.alfamedical.com
Theodor Bilharz Research Institute

EASL 2005 the 40th annual meeting
April 13-17, 2005
www.easl.ch/easl2005/
Paris, France

Pediatric Gastroenterology, Hepatology and Nutrition
March 13, 2005
Jakarta, Indonesia

21st annual international congress of Pakistan society of Gastroenterology & GI Endoscopy
March 25-27, 2005
www.psgc2005.com
Peshawar

8th Congress of the Asian Society of HepatoBiliary Pancreatic Surgery
February 10-13, 2005
Mandaluyong, Philippines

APDW 2005 - Asia Pacific Digestive Week 2005
September 25-28, 2005
www.apdw2005.org
Seoul, Korea

World Congress on Gastrointestinal Cancer
June 15-18, 2005
Barcelona

British Society of Gastroenterology Conference (BSG)
March 14-17, 2005
www.bsg.org.uk
Birmingham

Digestive Disease Week DDW 106th Annual Meeting
May 15-18, 2005
www.ddw.org
Chicago, Illinois

70th ACG Annual Scientific Meeting and Postgraduate Course
October 28-November 2, 2005
Honolulu Convention Center, Honolulu, Hawaii

Events and Meetings in 2006

EASL 2006 - THE 41ST ANNUAL MEETING
April 26-30, 2006
Vienna, Austria

Canadian Digestive Disease Week Conference
March 4-12, 2006
www.cag-acg.org
Quebec City

XXX pan-american congress of digestive diseases XXX congreso panamericano de enfermedades digestivas
November 25-December 1, 2006
www.gastro.org.mx
Cancun

World Congress on Gastrointestinal Cancer
June 14-17, 2006
Barcelona, Spain

7th World Congress of the International Hepato-Pancreato-Biliary Association
September 3-7, 2006
www.edinburgh.org/conference
Edinburgh

71st ACG Annual Scientific Meeting and Postgraduate Course
October 20-25, 2006
Venetian Hotel, Las Vegas, Nevada

Instructions to authors

GENERAL INFORMATION

World Journal of Gastroenterology (WJG, ISSN 1007-9327) is a weekly journal of more than 48 000 circulation, published on the 7th, 14th, 21st and 28th of every month.

Original Research, Clinical Trials, Reviews, Comments, and Case Reports in esophageal cancer, gastric cancer, colon cancer, liver cancer, viral liver diseases, *etc.*, from all over the world are welcome on the condition that they have not been published previously and have not been submitted simultaneously elsewhere.

Published jointly by

The WJG Press and Elsevier Inc.

SUBMISSION OF MANUSCRIPTS

Manuscripts should be typed double-spaced on A4 (297×210 mm) white paper with outer margins of 2.5 cm. Number all pages consecutively, and start each of the following sections on a new page: Title Page, Abstract, Introduction, Materials and Methods, Results, Discussion, Acknowledgements, References, Tables, Figures and Figure Legends. Neither the Editors nor the Publisher is responsible for the opinions expressed by contributors. Manuscripts formally accepted for publication become the permanent property of The WJG Press and Elsevier Inc., and may not be reproduced by any means, in whole or in part without the written permission of both the Authors and the Publisher. We reserve the right to put onto our website and copy-edit accepted manuscripts. Authors should also follow the guidelines for the care and use of laboratory animals of their institution or national animal welfare committee.

Authors should retain one copy of the text, tables, photographs and illustrations, as rejected manuscripts will not be returned to the author(s) and the editors will not be responsible for the loss or damage to photographs and illustrations.

Online submission

Online submission is strongly advised. Manuscripts should be submitted through the Online Submission System at: <http://www.wjgnet.com/index.jsp>. Authors are highly recommended to consult the ONLINE INSTRUCTIONS TO AUTHORS (<http://www.wjgnet.com/wjg/help/instructions.jsp>) before attempting to submit online. Authors encountering problems with the Online Submission System may send an email describing the problem to wjg@wjgnet.com for assistance. If you submit manuscript online, do not make a postal contribution. A repeated online submission for the same manuscript is strictly prohibited.

Postal submission

Send 3 duplicate hard copies of the full-text manuscript typed double-spaced on A4(297×210 mm) white paper together with any original photographs or illustrations and a 3.5 inch computer diskette or CD-ROM containing an electronic copy of the manuscript including all the figures, graphs and tables in native Microsoft Word format or *.rtf format to:

World Journal of Gastroenterology

Room 1066, Yishou Garden,
No.58, North Langxinzhuang Road,
PO Box 2345, Beijing 100023, China
E-mail: wjg@wjgnet.com
<http://www.wjgnet.com>

MANUSCRIPT PREPARATION

All contributions should be written in English. All articles must be submitted using a word-processing software. All submissions must be typed in 1.5 line spacing and in word size 12 with ample margins. The letter font is Tahoma. For authors originating from China, one copy of the Chinese translation of the manuscript is also required (excluding references). Style should conform to our house format. Required information for each of the manuscript sections is as follows:

Title page

Full manuscript title, running title, all author(s) name(s), affiliations, institution(s) and/or department(s) where the work was accomplished,

disclosure of any financial support for the research, and the name, full address, telephone and fax numbers and email address of the corresponding author should be involved. Titles should be concise and informative (removing all unnecessary words), emphasize what is NEW, and avoid abbreviations. A short running title of less than 40 letters should be provided. List the author(s)' name(s) as follows: initials and/or first name, middle name or initial(s) and full family name.

Abstract

An informative, structured abstract of no more than 250 words should accompany each manuscript. Abstracts for original contributions should be structured into the following sections: AIM: Only the purpose should be included. METHODS: The materials, techniques, instruments and equipments, and the experimental procedures should be included. RESULTS: The observatory and experimental results, including data, effects, outcome, *etc.* should be included. Authors should present *P* value where necessary, and the significant data should accompany. CONCLUSION: Accurate view and the value of the results should be included.

The format of structured abstracts is at: <http://www.wjgnet.com/wjg/help/11.doc>

Key words

Please list 3-10 key words that could reflect content of the study.

Text

For most article types, the main text should be structured into the following sections: INTRODUCTION, MATERIALS AND METHODS, RESULTS and DISCUSSION, and should include appropriate Figures and Tables. Data should be presented in the body text or Figures and Tables, not both.

Illustrations

Figures should be numbered as 1, 2, 3 and so on, and mentioned clearly in the main text. Provide a brief title for each figure on a separate page. No detailed legend should be involved under the figures. This part should add into the text where the figures are applicable. Digital images: black and white photographs should be scanned and saved in TIFF format at a resolution of 300 dpi; color images should be saved as CMYK (print files) and not RGB (screen-viewing files). Place each photograph in a separate file. Print images: supply images of size no smaller than 126×76 mm printed on smooth surface paper; label the image by writing the Figure number and orientation using an arrow. Photomicrographs: indicate the original magnification and stain in the legend. Digital Drawings: supply files in EPS if created by Freehand and Illustrator, or TIFF from Photoshop. EPS files must be accompanied by a version in native file format for editing purposes. Scans of existing line drawings should be scanned at a resolution of 1200 dpi and as close as possible to the size at which they will appear when printed, not smaller. Please use uniform legends for the same subjects. For example: Figure 1 Pathological changes of atrophic gastritis after treatment. A: ...; B: ...; C: ...; D: ...; E: ...; F: ...; G: ...

Tables

Three-line tables should be numbered as 1, 2, 3 and so on, and mentioned clearly in the main text. Provide a brief title for each table. No detailed legend should be involved under the tables. This part should add into the text where the tables are applicable. The information should complement but not duplicate that contained in the text. Use one horizontal line under the title, a second under the column heads, and a third below the Table, above any footnotes. Vertical and italic lines should be omitted.

Notes in tables and illustrations

Data which is not statistically significant should not be noted. ^a*P*<0.05, ^b*P*<0.01 (*P*>0.05 should not be noted). If there are other series of *P* values, ^c*P*<0.05 and ^d*P*<0.01 are used; Third series of *P* values can be expressed as ^e*P*<0.05 and ^f*P*<0.01. Other notes in tables or under illustrations should be expressed as ¹*F*, ²*F*, ³*F*; or some other symbols with a superscript (Arabic numerals) in the upper left corner. In a multi-curve illustration, each curve should be labeled with ●, ○, ■, □, ▲, △, *etc.* in a certain sequence.

Acknowledgments

Brief acknowledgments of persons who have made genuine contributions to the manuscripts and who endorse the data and conclusions are included. Authors are responsible for obtaining written permission to use any copyrighted text and/or illustrations.

References

Cited references should mainly be drawn from journals covered in the Science Citation Index (<http://www.isinet.com>) and/or Index Medicus (<http://www.ncbi.nlm.nih.gov/PubMed>) databases. Mention all references in the text, tables and figure legends, and set off by consecutive, superscripted Arabic numerals. References should be numbered consecutively in the order in which they appear in the text. Abbreviate journal title names according to the Index Medicus style (<http://www.ncbi.nlm.nih.gov/entrez/query.fcgi?db=journals>). Unpublished observations and personal communications are not listed as references. The style and punctuation of the references conform to ISO standard and the Vancouver style (5th edition); see examples below. Reference lists not conforming to this style could lead to delayed or even rejected publication status. Examples:

Standard journal article (list all authors and include the PubMed ID [PMID] where applicable)

- 1 **Das KM**, Farag SA. Current medical therapy of inflammatory bowel disease. *World J Gastroenterol* 2000; 6: 483-489 [PMID: 11819634]
- 2 **Pan BR**, Hodgson HJF, Kalsi J. Hyperglobulinemia in chronic liver disease: Relationships between in vitro immunoglobulin synthesis, short lived suppressor cell activity and serum immunoglobulin levels. *Clin Exp Immunol* 1984; 55: 546-551 [PMID: 6231144]
- 3 **Lin GZ**, Wang XZ, Wang P, Lin J, Yang FD. Immunologic effect of Jianpi Yishen decoction in treatment of Pixu-diarrhoea. *Shijie Huaren Xiaohua Zazhi* 1999; 7: 285-287 [CMFAID:1082371101835979]

Books and other monographs (list all authors)

- 4 **Sherlock S**, Dooley J. Diseases of the liver and biliary system. 9th ed. Oxford: Blackwell Sci Pub, 1993: 258-296

Chapter in a book (list all authors)

- 5 **Lam SK**. Academic investigator's perspectives of medical treatment for peptic ulcer. In: Swabb EA, Azabo S. Ulcer disease: investigation and basis for therapy. New York: Marcel Dekker, 1991: 431-450

Electronic journal (list all authors)

- 6 **Morse SS**. Factors in the emergence of infectious diseases. *Emerg Infect Dis serial online*, 1995-01-03, cited 1996-06-05; 1(1):24 screens. Available from: URL: <http://www.cdc.gov/ncidod/EID/eid.htm>

PMID requirement

From the full reference list, please submit a separate list of those references embodied in PubMed, keeping the same order as in the full reference list, with the following information only: (1) abbreviated journal name and citation (e.g. *World J Gastroenterol* 2003;9(11):2400-2403; (2) article title (e.g. Epidemiology of gastroenterologic cancer in Henan Province, China); (3) full author list (e.g. Lu JB, Sun XB, Dai DX, Zhu SK, Chang QL, Liu SZ, Duan WJ); (4) PMID (e.g. 14606064). Provide the full abstracts of these references, as quoted from PubMed on a 3.5 inch disk or CD-ROM in Microsoft Word format and send by post to the *WJG* Press. For those references taken from journals not indexed by *Index Medicus*, a printed copy of the first page of the full reference should be submitted. Attach these references to the end of the manuscript in their order of appearance in the text.

Inappropriate references

Authors should always cite references that are relevant to their article, and avoid any inappropriate references. Inappropriate references include those that are linked with a hyphen and the difference between the two numbers at two sides of the hyphen is more than 5. For example, [1-6], [2-14] and [1,3,4-10,22] are all considered as inappropriate references. Authors should not cite their own unrelated published articles.

Statistical data

Present as mean±SD and mean±SE.

Statistical expression

Express *t* test as *t*(in italics), *F* test as *F*(in italics), chi square test as χ^2 (in

Greek), related coefficient as *r*(in italics), degree of freedom as γ (in Greek), sample number as *n*(in italics), and probability as *P*(in italics).

Units

Use SI units. For example: body mass, *m*(B) = 78 kg; blood pressure, *p*(B) = 16.2/12.3 kPa; incubation time, *t*(incubation)=96 h, blood glucose concentration, *c*(glucose) 6.4±2.1 mmol/L; blood CEA mass concentration, *p*(CEA) = 8.6 24.5 μg/L; CO₂ volume fraction, 50 mL/L CO₂ not 5% CO₂; likewise for 40 g/L formaldehyde, not 10% formalin; and mass fraction, 8 ng/g, etc. Arabic numerals such as 23,243,641 should be read 23 243 641.

The format about how to accurately write common units and quantum is at: <http://www.wjgnet.com/wjg/help/15.doc>

Abbreviations

Standard abbreviations should be defined in the abstract and on first mention in the text. In general, terms should not be abbreviated unless they are used repeatedly and the abbreviation is helpful to the reader. Permissible abbreviations are listed in Units, Symbols and Abbreviations: A Guide for Biological and Medical Editors and Authors (Ed. Baron DN, 1988) published by The Royal Society of Medicine, London. Certain commonly used abbreviations, such as DNA, RNA, HIV, LD50, PCR, HBV, ECG, WBC, RBC, CT, ESR, CSF, IgG, ELISA, PBS, ATP, EDTA, mAb, can be used directly without further mention.

Italicization

Quantities: *t* time or temperature, *c* concentration, *A* area, *l* length, *m* mass, *V* volume.

Genotypes: *gyrA*, *arg 1*, *c myc*, *c fos*, etc.

Restriction enzymes: *EcoRI*, *HindI*, *BamHI*, *Kbo I*, *Kpn I*, etc.

Biology: *Helicobacter pylori*, *H pylori*, *E coli*, etc.

SUBMISSION OF THE REVISED MANUSCRIPTS AFTER ACCEPTED

Please revise your article according to the revision policies of *WJG*. The revised version including manuscript and high-resolution image figures (if any) should be copied on a floppy or compact disk. Author should send the revised manuscript, along with printed high-resolution color or black and white photos, copyright transfer letter, the final check list for authors, and responses to reviewers by a courier (such as EMS) (submission of revised manuscript by e-mail or on the *WJG* Editorial Office Online System is NOT available at present).

Language evaluation

The language of a manuscript will be graded before sending for revision. (1) Grade A: priority publishing; (2) Grade B: minor language polishing; (3) Grade C: a great deal of language polishing; (4) Grade D: rejected. The revised articles should be in grade B or grade A.

Copyright assignment form

It is the policy of *WJG* to acquire copyright in all contributions. Papers accepted for publication become the copyright of *WJG* and authors will be asked to sign a transfer of copyright form. All authors must read and agree to the conditions outlined in the Copyright Assignment Form (which can be downloaded from <http://www.wjgnet.com/wjg/help/9.doc>).

Final check list for authors

The format is at: <http://www.wjgnet.com/wjg/help/13.doc>

Responses to reviewers

Please revise your article according to the comments/suggestions of reviewers. The format for responses to the reviewers' comments is at: <http://www.wjgnet.com/wjg/help/10.doc>

Proof of financial support

For paper supported by a foundation, authors should provide a copy of the document and serial number of the foundation.

Publication fee

Authors of accepted articles must pay publication fee.

World Journal of Gastroenterology standard of quantities and units

Number	Nonstandard	Standard	Notice
1	4 days	4 d	In figures, tables and numerical narration
2	4 days	four days	In text narration
3	day	d	After Arabic numerals
4	Four d	Four days	At the beginning of a sentence
5	2 hours	2 h	After Arabic numerals
6	2 hs	2 h	After Arabic numerals
7	hr, hrs,	h	After Arabic numerals
8	10 seconds	10 s	After Arabic numerals
9	10 year	10 years	In text narration
10	Ten yr	Ten years	At the beginning of a sentence
11	0,1,2 years	0,1,2 yr	In figures and tables
12	0,1,2 year	0,1,2 yr	In figures and tables
13	4 weeks	4 wk	
14	Four wk	Four weeks	At the beginning of a sentence
15	2 months	2 mo	In figures and tables
16	Two mo	Two months	At the beginning of a sentence
17	10 minutes	10 min	
18	Ten min	Ten minutes	At the beginning of a sentence
19	50% (V/V)	500 mL/L	
20	50% (m/V)	500 g/L	
21	1 M	1 mol/L	
22	10 μM	10 μmol/L	
23	1NHCl	1 mol/L HCl	
24	1NH ₂ SO ₄	0.5 mol/L H ₂ SO ₄	
25	4rd edition	4 th edition	
26	15 year experience	15- year experience	
27	18.5 kDa	18.5 ku, 18 500u or M _r 18 500	
28	25 g.kg ⁻¹ .d ⁻¹	25 g/(kg.d) or 25 g/kg per day	
29	6900	6 900	
30	1000 rpm	1 000 r/min	
31	sec	s	After Arabic numerals
32	1 pg.L ⁻¹	1 pg/L	
33	10 kilograms	10 kg	
34	13 000 rpm	13 000 g	High speed; g should be in italic and suitable conversion.
35	1000 g	1 000 r/min	Low speed. g cannot be used.
36	Gene bank	GenBank	International classified genetic materials collection bank
37	Ten L	Ten liters	At the beginning of a sentence
38	Ten mL	Ten milliliters	At the beginning of a sentence
39	umol	μmol	
40	30 sec	30 s	
41	1 g/dl	10 g/L	10-fold conversion
42	OD ₂₆₀	A ₂₆₀	"OD" has been abandoned.
43	Oneg/L	One microgram per liter	At the beginning of a sentence
44	A _{260 nm}	A _{260nm}	A should be in italic.
	^b P<0.05	^a P<0.05	In Table, no note is needed if there is no significance in statistics: ^a P<0.05, ^b P<0.01 (no note if P>0.05). If there is a second set of P value in the same table, ^c P<0.05 and ^d P<0.01 are used for a third set: ^c P<0.05, ^d P<0.01.
45	*F=9.87, [§] F=25.9, [#] F=67.4	¹ F=9.87, ² F=25.9, ³ F=67.4	Notices in or under a table
46	KM	km	kilometer
47	CM	cm	centimeter
48	MM	mm	millimeter
49	Kg, KG	kg	kilogram
50	Gm, gr	g	gram
51	nt	N	newton
52	l	L	liter
53	db	dB	decibel
54	rpm	r/min	rotation per minute
55	bq	Bq	becquerel, a unit symbol
56	amp	A	ampere
57	coul	C	coulomb
57	HZ	Hz	watt
59	w	W	kilo-pascal
60	KPa	kPa	pascal
61	p	Pa	volt (electronic unit)
62	ev	EV	joule
63	Jonle	J	kilojoule per mole
64	J/mmol	kJ/mol	
65	10×10×10cm ³	10 cm×10 cm×10 cm	
66	N.km	KN.m	moment
67	$\bar{x}\pm s$	mean±SD	In figures, tables or text narration
68	Mean±SEM	mean±SE	In figures, tables or text narration
69	im	im	intramuscular injection
70	iv	intravenous	injection
71	Wang et al	Wang <i>et al</i>	
72	EcoRI	<i>EcoRI</i>	<i>Eco</i> in italic and RI in positive. Restriction endonuclease has its prescript form of writing.
73	Ecoli	<i>E.coli</i>	Bacteria and other biologic terms have their specific expression.
74	Hp	<i>H pylori</i>	
75	Iga	<i>Iga</i>	writing form of genes
76	igA	IgA	writing form of proteins
77	-70 kDa	~70 ku	